THE HONG KONG
POLYTECHNIC UNIVERSITY
香港理工大學
Pao Yue-kong Library
包玉剛圖書館

Copyright Undertaking

This thesis is protected by copyright, with all rights reserved.

By reading and using the thesis, the reader understands and agrees to the following terms:

1. The reader will abide by the rules and legal ordinances governing copyright regarding the use of the thesis.
2. The reader will use the thesis for the purpose of research or private study only and not for distribution or further reproduction or any other purpose.
3. The reader agrees to indemnify and hold the University harmless from and against any loss, damage, cost, liability or expenses arising from copyright infringement or unauthorized usage.

If you have reasons to believe that any materials in this thesis are deemed not suitable to be distributed in this form, or a copyright owner having difficulty with the material being included in our database, please contact lbsys@polyu.edu.hk providing details. The Library will look into your claim and consider taking remedial action upon receipt of the written requests.

Pao Yue-kong Library, The Hong Kong Polytechnic University, Hung Hom, Kowloon, Hong Kong

http://www.lib.polyu.edu.hk

This thesis in electronic version is provided to the Library by the author. In the case where its contents is different from the printed version, the printed version shall prevail.

Ruthenium-Catalyzed *β*-Alkylation of Secondary Alcohols with Primary Alcohols, *α*-Alkylation of Arylacetonitriles with Primary Alcohols and Markovnikov and Anti-Markovnikov Functionalization of Terminal Alkynes

Hung-Wai CHEUNG

Ph.D

The Hong Kong Polytechnic University

2010

The Hong Kong Polytechnic University

Department of Applied Biology and Chemical Technology

Ruthenium-Catalyzed *β*-Alkylation of Secondary Alcohols with Primary Alcohols, *α*-Alkylation of Arylacetonitriles with Primary Alcohols and Markovnikov and Anti-Markovnikov Functionalization of Terminal Alkynes

By

Hung-Wai CHEUNG

A Thesis Submitted in Partial Fulfillment of the Requirements
for the Degree of Doctor of Philosophy

September, 2009

Supervisor: Prof. Chak-Po LAU

This is Blank Page

Declaration

I hereby declare that this thesis is my own work and that, to the best of my knowledge and belief, it reproduces no material previously published or written, nor material that has been accepted for the award of any other degree or diploma, except where due acknowledgement has been made in the text.

_____

Hung-Wai CHEUNG

September, 2009

Abstract of thesis entitled "Ruthenium-Catalyzed β-Alkylation of Secondary Alcohols with Primary Alcohols, α-Alkylation of Arylacetonitriles with Primary Alcohols and Markovnikov and Anti-Markovnikov Functionalization of Terminal Alkynes."

Submitted by Hung-Wai CHEUNG

for the Degree of Doctor of Philosophy

at The Hong Kong Polytechnic University

in September, 2009

Abstract

A one-pot catalytic *β*-alkylation of secondary alcohols with primary alcohols to give higher alcohols with water as the only by-product is a highly desirable process. Cyclopentadienyl (Cp) ruthenium complexes $[CpRu(PPh_3)_2(CH_3CN)]^+BF_4^-$ (**M1**), $CpRu(PPh_3)_2Cl$ (**M2**) and CpRu(dppm)Cl (**M3**) and hydrotris(pyrazolyl)borato (Tp) ruthenium complexes $TpRu(PPh_3)_2Cl$ (**M4**) and $[TpRu(dppm)(CH_3CN)]^+BF_4^-$ (**M5**) are found to be active catalysts for the *β*-alkylation of secondary alcohols with primary alcohols. Mechanistic aspects of the **M1**-**M5**-catalyzed reactions were investigated; the crucial hydrido complexes $CpRu(PPh_3)_2H$ (**M6**), $TpRu(PPh_3)_2H$ (**M8**), CpRu(dppm)H (**M10**) and TpRu(dppm)H (**M11**), which were formed by alkoxide attack at the metal center and subsequent *β*-elimination, were identified. Aldehydes and ketones were generated concomitantly. The reaction pathway is broadly similar to that of the common mechanism for the one-pot catalytic *β*-alkylation of secondary alcohols with primary alcohols involving alcohol oxidation, ketone alkylation and ketone reduction. Carbonyl complexes $CpRu(PPh_3)(CO)Ph$ (**M7**) and $TpRu(PPh_3)(CO)Ph$ (**M9**) resulting from aldehyde decarbonylation were formed in some cases, and surprisingly, they are also found to be active for the catalytic processes. Although not observed, the anionic metal hydride complex is believed to be the key intermediate of the catalytic process.

The aminocyclopentadienyl-ruthenium complexes $[(CpNMe_2)Ru(PPh_3)_2(CH_3CN)]^+BF_4^-$ (**M16**) and $[(CpNEt_2)Ru(PPh_3)_2(CH_3CN)]^+BF_4^-$ (**M17**) were prepared by protonation of the

hydride precursors, $(CpNMe_2)Ru(PPh_3)_2H$ (**M14**) and $(CpNEt_2)Ru(PPh_3)_2H$ (**M15**), with $HBF_4{\cdot}Et_2O$ in the presence of acetonitrile; the hydride complexes **M14** and **M15** were formed by reacting $CpRu(PPh_3)_2Cl$ (**M2**) with $LiNR_2$ (R = CH_3, C_2H_5) in THF. X-ray crystallography study of **M16** shows that the nitrogen atom of the aminocyclopentadienyl ligand is nearly coplanar with its substituents, which indicates delocalization of the lone pair electrons.

M16 and **M17** are found to be moderately active catalysts for α-alkylation of arylacetonitriles with primary alcohols; on the other hand, the analogous unsubstituted cyclopentadienyl ruthenium complex $[CpRu(PPh_3)_2(CH_3CN)]^+BF_4^-$ (**M1**) shows very low catalytic activity. On the basis of experimental results and theoretical calculations, rationalization for the much higher catalytic activity of the aminocyclopentadienyl complexes over that of the unsubstituted Cp complex is provided. In the catalytic systems with the aminocyclopentadienyl-ruthenium complexes **M16** and **M17**, it is possible to regenerate the active solvento species via protonation of the metal hydride intermediate and subsequent ligand substitution; this process is, however nonfacile in the catalytic system with the unsubstituted cyclopentadienyl ruthenium complex **M1**.

Tp-ruthenium (II) diphosphinoamino complex $TpRu(4\text{-}CF_3C_6H_4N(PPh_2)_2)OTf$ (**M24**) is prepared by chloride abstraction from its chloride precursor $TpRu(4\text{-}CF_3C_6H_4N(PPh_2)_2)Cl$ (**M21**) using AgOTf in THF as the solvent; the chloride precursor **M21** is formed by reacting $TpRu(PPh_3)_2Cl$ (**M4**) with $4\text{-}CF_3C_6H_4N(PPh_2)_2$ in toluene. The molecular structures of **M21** and **M22** are determined by X-ray crystallography.

M24 is found to be an active catalyst for the 2-alkenylation of 1,3-dicarbonyl compounds with terminal alkynes in Markovnikov manner. The $^{31}P\{^{1}H\}$NMR monitoring experiment shown that, **M24** reacts with terminal alkyne to give the vinylidene complex $[TpRu(4\text{-}CF_3C_6H_4N(PPh_2)_2)(=C=CHR)]^+OTf^-$. Under the reaction conditions, the vinylidene complex is deprotonated by adventitious water in the substrates to afford the alkynyl complex $TpRu(4\text{-}CF_3C_6H_4N(PPh_2)_2)(C\equiv CR)$, which is the dominant metal-containing species throughout the catalytic process; the alkynyl complex by itself, however, is not the active species as demonstrated by an independent experiment. It is proposed that, triflate acid ($H_3O^+OTf^-$) generated by the deprotonation of the vinylidene moiety of $[TpRu(4\text{-}CF_3C_6H_4N(PPh_2)_2)(=C=CHR)]^+OTf^-$ by H_2O reacts with other species presence in the catalytic system to form a new acidic species suspected to be 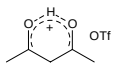 (**B**$^+$). To a very small extent, the alkynyl complex is partially protonated by **B**$^+$ to generate very minute amount of the vinylidene complex, which at the reaction temperature equilibrates with its η^2-alkyne tautomer; the latter is immediately attacked by the 1,3-dicarbonyl compound or its enol form originated from **B**$^+$ and in *close vicinity*. The molecular structures of the intermediates in the **M24**-catalyzed 2-alkenylation of acetylacetone with phenylacetylene are determined by X-ray crystallography.

Secondary amines also add to terminal alkynes yielding the corresponding enamines under the influence of **M24**. Similarly, displacement of the triflate ligand in **M24** by the terminal alkyne affords the vinylidene complex $[TpRu(4\text{-}CF_3C_6H_4N(PPh_2)_2)(=C=CHR)]^+OTf^-$. In the presence of amine the

vinylidene complex is expected to be in equilibrium with the alkynyl complex $TpRu(4\text{-}CF_3C_6H_4N(PPh_2)_2)(C{\equiv}CR)$; the equilibrium lies predominately to the side of the latter, which is the most stable metal-containing species throughout the catalysis. The vinylidene complex undergoes nucleophilic attack by the amine at the α-carbon to afford an α-aminovinylruthenium species. Protonlysis of the intermediate regenerates the catalytic cycle. In contrast to the result of the **M24**-catalyzed 2-alkenylation of 1,3-dicarbonyl compounds with terminal alkynes to yield Markovnikov products, **M24** catalyzes hydroamination of terminal alkynes to enamines in anti- Markovnikov fashion.

Publications

Cheung, H. W., Li, J., Zheng, W., Zhou, Z., Chiu, Y. H., Lin, Z. and Lau, C. P., Dialkylamino Cyclopentadienyl Ruthenium (II) Complex-Catalyzed α-Alkylation of Arylacetonitriles with Primary Alcohols, *Dalton Transactions*, **2010**, 39, 265-274.

Cheung, H. W., Lee, T. Y., Lui, H. Y., Yeung, C. H., and Lau, C. P., Ruthenium-Catalyzed β-Alkylation of Secondary Alcohols with Primary Alcohols, *Advanced Synthesis & Catalysis*, **2008**, 350(18), 2975-2983.

Cheung, H. W., Chiu Y. H., Ng S. M. and Lau, C. P., Dialkylamino Cyclopentadienyl Ruthenium (II) Complexes-Catalyzed α-Alkylation of Benzyl Cyanides with Primary Alcohols, *14th International Symposium on Organometallic Chemistry Directed Towards Organic Synthesis (OMCOS), Nara, Japan*, **2007**, pp P-181.

Cheung, H. W., Poon, K. H. and Lau, C. P., Mechanistic study of the Tp-Ruthenium (II) Diphosphinoamino Complexes-Catalyzed Markovnikov and Anti- Markovnikov Functionalization of Terminal Alkynes, *16th Symposium on Chemistry Postgraduate Research in Hong Kong*, **2009**, pp I-88.

Cheung, H. W. and Lau, C. P., Tp Ruthenium (II) PNP^R (PNP =$Ph_2PN(R)PPh_2$) Complexes-Catalyzed Insertion of Terminal Acetylenes into a C-H bond of Activated Methylene Compounds, *15th Symposium on Chemistry Postgraduate Research in Hong Kong*, **2008**, pp I-57.

Acknowledgements

I would like to express my deepest gratitude to my supervisor Prof. Lau Chak Po for his invaluable advice, supervision, and guidance throughout the course of my study.

Thanks are also expressed to Prof. Lin Zhenyang and his research group in the Department of Chemistry, The Hong Kong University of Science and Technology, for their support on theoretical calculations.

I convey special acknowledgement to Prof. Zhou Zhongyuan for resolving the crystal structures of the complexes.

I also want to thank all my postgraduate colleagues Dr. Leung Chung Wing, Mr. Lee Ting Yan and Mr. So Chau Ming, all of whom have made my study most pleasant and smooth. Special thanks are given to Mr. Ng Siu Man and Mr. Wang Dexian for their valuable discussion, assistance and encouragement from the very early stage of my study.

I am obliged to the staff and technical service crew of the Chemical Technology Section of the Department of Applied Biology and Chemical Technology, The Hong Kong Polytechnic University for their assistance throughout my postgraduate study, especially to Mr. Au Yiu kwok for his help on performing the MS, and Mr. Kwan Wing kong and Dr. Yan Siu Cheong for their assistance in running NMR spectra.

I would like to thank my family and friends for their love and continual support in various ways, especially to Miss Yeung Yi Fung for her concern, understanding, forbearance, and support when I was engaged in the research work.

Finally, I would like to acknowledge the Research Degree Committee of The Hong Kong Polytechnic University for the award a studentship and a grant supporting my conference presentation in the 14th International Symposium on Organometallic Chemistry Directed Towards Organic Synthesis (OMCOS) held in Nara, Japan on 2-6 August 2007.

Table of Contents

List of Figures

List of Tables

List of Schemes

Abbreviations

δ	Chemical shift (NMR)
η	Descriptor for hapticity
μ	Descriptor for bridging
υ	Frequency
e^-	Electron
L	Generalized ligand, in particular a $2e^-$ ligand
L_nM	Generalized metal fragment with n ligands
[]	Encloses complex molecules or ions
ESI-MS	Electro-spray ionization mass spectroscopy
FAB-MS	Fast atom bombardment mass spectroscopy
IR	Infra-red
NMR	Nuclear magnetic resonance spectroscopy
THF	Tetrahydrofuran
MeOH	Methanol
EtOH	Ethanol
Et_2O	Diethyl ether
Tp	Hydrotris(1-pyrazolyl) borate
Cp	Cyclopentadienyl
$CpNR_2$	Aminocyclopentadienyl
Cp*	Pentamethylcyclopentadienyl
OTf	Trifluoromethanesulfonate
BF_4	Tetrafluoroborate
P^iPr_3	Triisopropylphosphine
PPh_3	Triphenylphosphine

PMe_3	Trimethylphosphine
dppm	Bis(diphenylphosphino)methane
R	Generalized alkyl group
Me	Methyl
Et	Ethyl
^{i}Pr	Isopropyl
^{t}Bu	*t*-butyl
^{n}Bu	*n*-butyl
Ph	Phenyl, C_6H_5
br	Broad
sh	Sharp
vs	Very strong
w	weak
s	Singlet
d	Doublet
t	Triplet
q	Quartet
m	Multiplet

$[CpRu(PPh_3)_2(CH_3CN)]^+BF_4^-$ (**M1**)

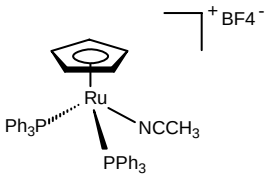

$CpRu(PPh_3)_2Cl$ (**M2**)

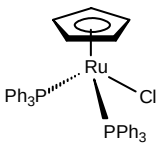

CpRu(dppm)Cl (**M3**)

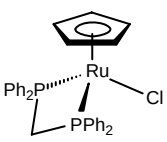

$TpRu(PPh_3)_2Cl$ (**M4**)

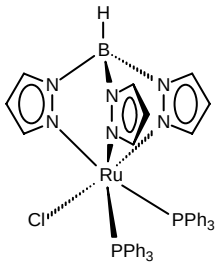

$[TpRu(dppm)(CH_3CN)]^+BF_4^-$ (**M5**)

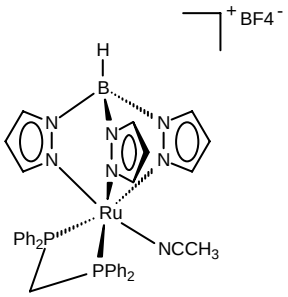

$CpRu(PPh_3)_2H$ (**M6**)

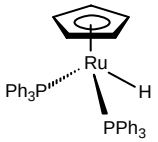

$CpRu(PPh_3)(CO)Ph$ (**M7**)

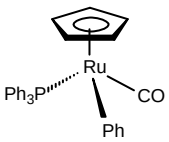

$TpRu(PPh_3)_2H$ (**M8**)

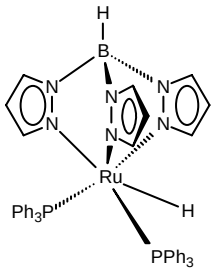

$TpRu(PPh_3)(CO)Ph$ (**M9**)

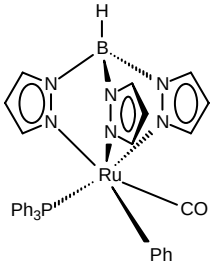

CpRu(dppm)H (**M10**)

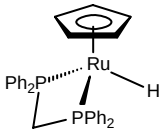

TpRu(dppm)H (**M11**)

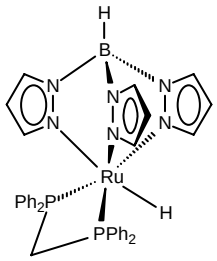

CpRu(PPh_3)(CO)(3,4-Dimethoxyphenyl) (**M12**)

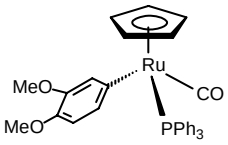

TpRu(PPh_3)(CO)(3,4-Dimethoxyphenyl) (**M13**)

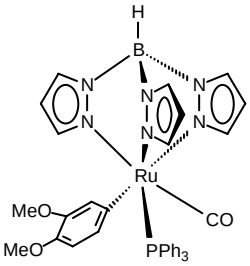

($CpNMe_2$)Ru(PPh_3)$_2$H (**M14**)

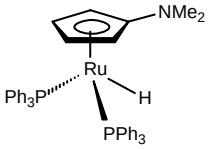

($CpNEt_2$)Ru(PPh_3)$_2$H (**M15**)

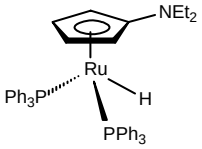

[($CpNMe_2$)Ru(PPh_3)$_2$(CH_3CN)]$^+BF_4^-$ (**M16**)

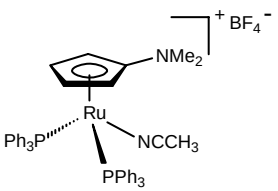

$[(CpNEt_2)Ru(PPh_3)_2(CH_3CN)]^+BF_4^-$ (**M17**)

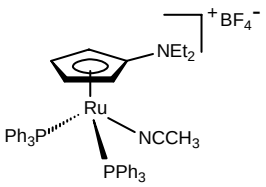

$(CpNMe_2)Ru(PPh_3)(CO)Ph$ (**M18**)

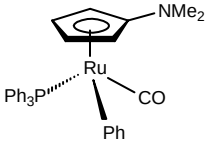

$[(CpNMe_2)Ru(PPh_3)_2H_2]^+BF_4^-$ (**M19**)

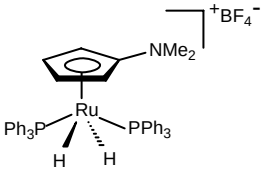

$[CpRu(PPh_3)_2H_2]^+BF_4^-$ (**M20**)

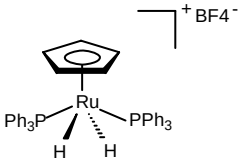

$TpRu(4\text{-}CF_3C_6H_4N(PPh_3)_2)Cl$ (**M21**)

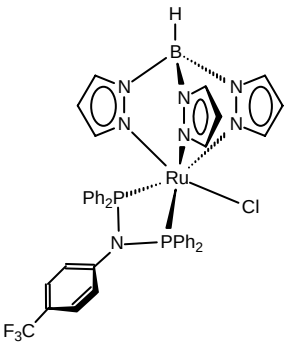

$TpRu(^nBuN(PPh_2)_2)Cl$ (**M22**)

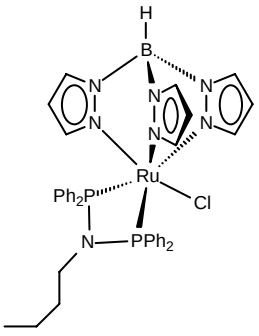

TpRu(^{n}BuN(CH_2PPh_2)$_2$)Cl (**M23**)

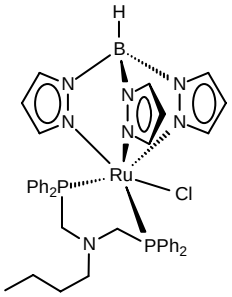

TpRu(4-$CF_3C_6H_4N(PPh_2)_2$)OTf (**M24**)

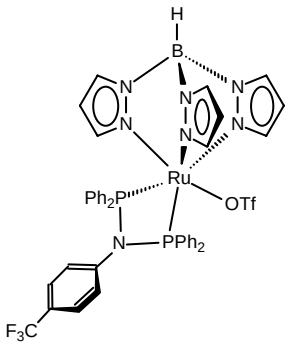

[TpRu(4-$CF_3C_6H_4N(PPh_2)_2$)CH_3CN]$^+$OTf$^-$ (**M25**)

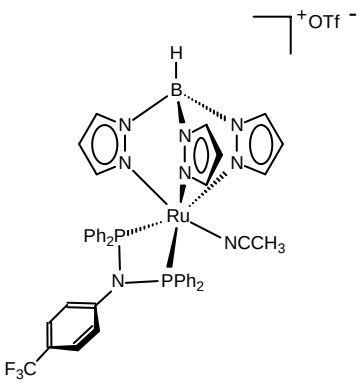

TpRu(^{n}BuN(PPh_2)$_2$) OTf (**M26**)

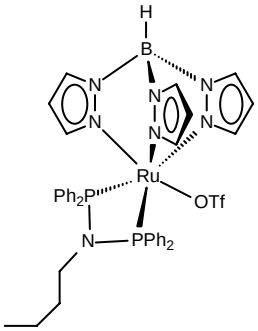

[TpRu(^{n}BuN(PPh_2)$_2$)CH_3CN]$^+$OTf$^-$ (**M27**)

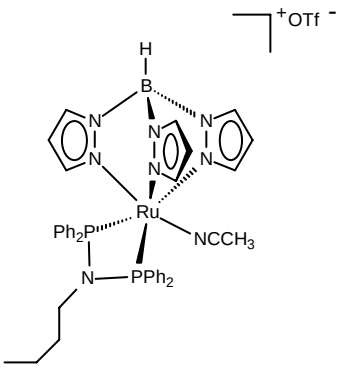

[TpRu(^{n}BuN(CH_2PPh_2)$_2$)CH_3CN]$^+$OTf$^-$ (**M28**)

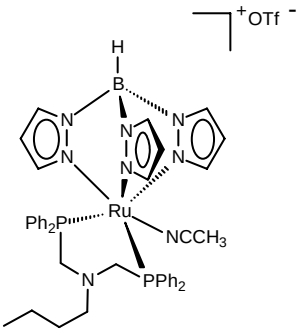

[TpRu(PMe_3)$_2CH_3CN$]$^+PF_6^-$ (**M29**)

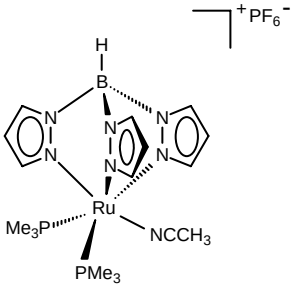

[TpRu(PPh_3)$_2CH_3CN$]$^+BF_4^-$ (**M30**)

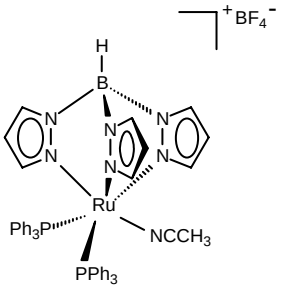

[TpRu(dppm)CH_3CN] $^{+}OTf^{-}$ (**M31**)

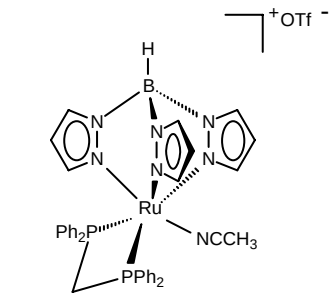

[TpmRu(PPh_3)$_2CH_3CN]^{2+}(BF_4^{-})_2$ (**M32**)

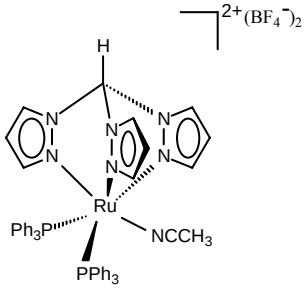

[TpRu(4-$CF_3C_6H_4N(PPh_2)_2$)(=C=CHPh)] $^{+}OTf^{-}$ (**M33**)

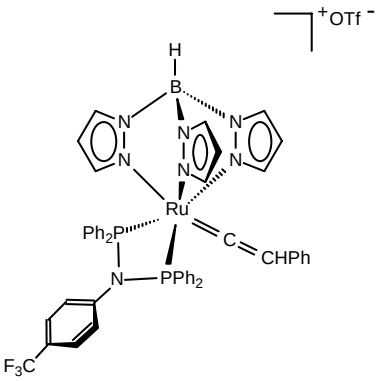

TpRu(4-$CF_3C_6H_4N(PPh_2)_2$)(C≡CPh) (**M34**)

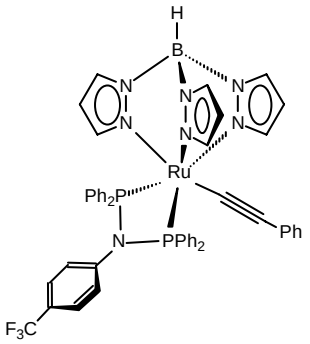

[TpRu(4-$CF_3C_6H_4N(PPh_2)_2$)(CO)]$^+$OTf$^-$ (**M35**)

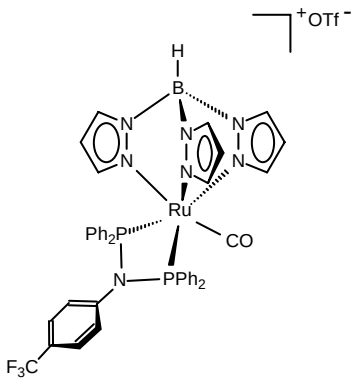

[TpRu(4-$CF_3C_6H_4N(PPh_2)_2$)(=C=$(CH_2)_3CH_3$)]$^+$OTf$^-$ (**M36**)

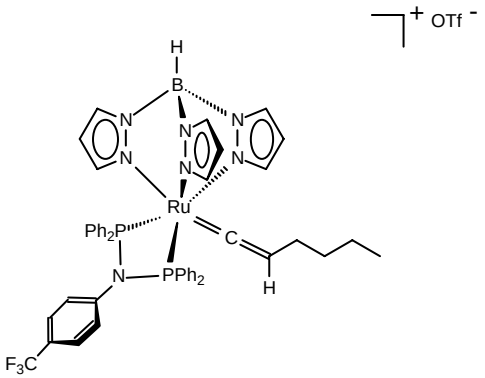

This is Blank Page

Chapter 1 Introduction

1.1 Oxidation as an Activation Process for Alcohols

Alcohols have limited reactivity without certain activation. In general, activation can be either by the addition of a basic reagent to form a nucleophilic alkoxide, or by the addition of an acid to provide an electrophilic species. Carbonyl compounds, on the contrary, usually have a much wider range of reactivity, and are much susceptible to nucleophilic reagent, or acting as nucleophiles themselves (enol or enolate). Therefore, an activation process involving a temporary oxidation of an alcohol into a corresponding carbonyl compound is desirable.

Alcohols can be temporarily converted into carbonyl compounds by metal-catalysed oxidization reaction. The carbonyl compounds show a much wider range of reactivity than the precursor alcohols and can react *in situ* to give various α-functionalized carbonyl derivatives. The metal catalyst borrows the hydrogen atoms and then returns them back to the transformed carbonyl compounds, resulting in an overall process in which the alcohols are converted into higher molecules. Examples involving the utilization of the above activation strategy are identified in **Scheme 1.1**. The additional reactivity of carbonyl compounds over alcohols is illustrated by imine formation followed by reduction (i), alkene formation and reduction to a C-C bond (ii) and enolisation, electrophilic trap and reduction leading to a functionalized alcohol (iii). In all cases, there is ideally no net hydrogen loss during the reaction sequence, thus giving rise to a high atomic efficiency.

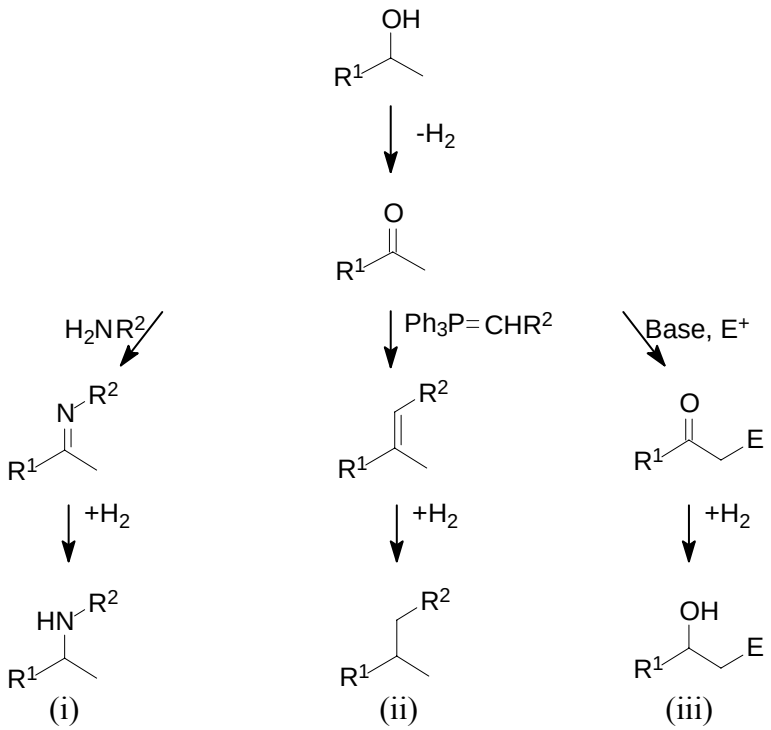

Scheme 1.1 Activation of alcohols by borrowing hydrogen

Recent researches in this area have benefited from the development of transfer hydrogenation chemistry. Late transition metals have been shown to be a catalytic component for imine and alkene reduction using alcohols as hydrogen donors.[1] Transfer hydrogenation reactions,[2] and their asymmetric variants[3] have been well reviewed, along with a detailed analysis of the mechanisms involved in these processes.[4] In the transfer hydrogenation reactions, several mechanisms are proposed depending on the metal-ligands relationship. Metal catalysts may react via mono-hydride or di-hydride complexes, or even react without forming any hydrido species.

The "borrowing hydrogen" strategy has been adopted for the *β*-alkylation of secondary alcohols and 2-alkylation of organic nitriles in this research; we are

herein reviewing various reactions involving the activation of alcohols by temporary oxidation followed by reductive restoration of the alcoholic moiety.

1.1.1 Carbon-Carbon Bond Formation from Alcohols

The direct C-C bond formation via alcohols to give higher alcohols is of fundamental importance. However, the process is generally disfavoured due to the poor leaving ability of the hydroxide group. An alternative activation pathway that involves alkenes formation followed by *in situ* reduction is therefore desirable.

Kaneda *et al.* reported a related α-alkylation reaction of various nitriles with primary alcohols or carbonyl compounds through tandem reactions consisting of oxidation, aldol reaction and reduction promoted by hydrotalcite-supported metal species.[5, 6] A similar system was studied by Grigg and co-workers. A wide range of substituted aryl and heteroaryl nitriles reacted with primary alcohols in the presence of $[IrCp^*Cl_2]_2$ to deliver the α-alkylated derivatives in excellent yield.[7]

Wittig reaction has also been used in this strategy for the synthesis of C-C bond from alcohols. Williams and co-workers reported an indirect Wittig reaction of alcohols using an iridium catalyst, $[IrCl(cod)_2]$. The complex was believed to remove hydrogen atoms from alcoholic substrates to afford intermediate carbonyl compounds, which then underwent *in situ* olefination to give alkenes. The iridium catalyst returned the borrowed hydrogen atoms and provided alkanes as products where a new C-C bond had been generated from

the starting alcohol (**Scheme 1.2**).[8] This domino reaction sequence afforded alkane derivatives directly from alcohol. Only one equiv. of alcohol was required as the hydrogen atoms loaned from the oxidation step would subsequently be returned in the hydrogenation of the alkene intermediates.

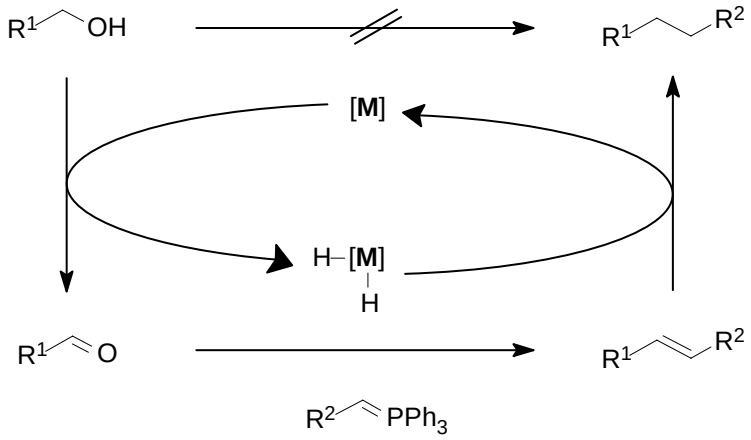

Scheme 1.2 Indirect Wittig reaction of alcohols

The α-alkylation of ketones with primary alcohols has been studied extensively during the past decade. For example, Cho, Shim and co-workers reported an example of ruthenium-catalyzed transfer hydrogenation between an array of ketones and primary alcohols. The reaction proceeded via a successive oxidation, aldol condensation followed by reduction pathway.[9] Later on, they showed that the same reaction was carried out in the presence of a hydrogen acceptor such as 1-dodecene to avoid the formation of α-alkylated alcohols.[10] Alternatively, α-alkylation of ketones could also be accomplished by the phosphine free ruthenium catalyst $Ru(DMSO)_4Cl_2$ as reported by Yus and co-worker. By changing the reaction conditions, either the expected ketones or their related alcohols were produced.[11, 12] Palladium catalyst was also used for the

α-alkylation of ketones by Park *et al*. The heterogeneous palladium catalyst, which is composed of palladium nanopartical entrapped in aluminum hydroxide, was applied in this type of reaction. An important feature of the reaction was that the catalyst was active in the presence of oxygen and produced enones selectively under 1 atm O_2, whereas ketones were the major product under Ar (**eq. 1.1**).[13]

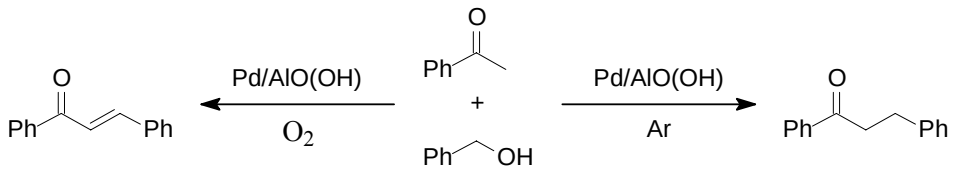

(1.1)

Ishii and co-workers developed an iridium-based catalyst, $[Ir(cod)Cl]_2$, for the C-C bond formation from alcohols. Ketones were directly α-alkylated with primary alcohols under the solvent free condition.[14] All the above mentioned methods provide convenient routes to ketones derivatives to which a carbonyl function can be introduced at the desired position by choosing different combinations of ketones and alcohols substrates.

1.1.2 β-Functionalization of Alcohols

Temporary oxidation of alcohol to a carbonyl compound also provides an opportunity to access to the enol/enolate chemistry. **Scheme 1.3** represents the possibility for the β-functionalization of alcohols. When alcohol is oxidized to the corresponding carbonyl compound, the electronic nature is temporarily enhanced to enable an electrophilic addition to the enol/enolate.

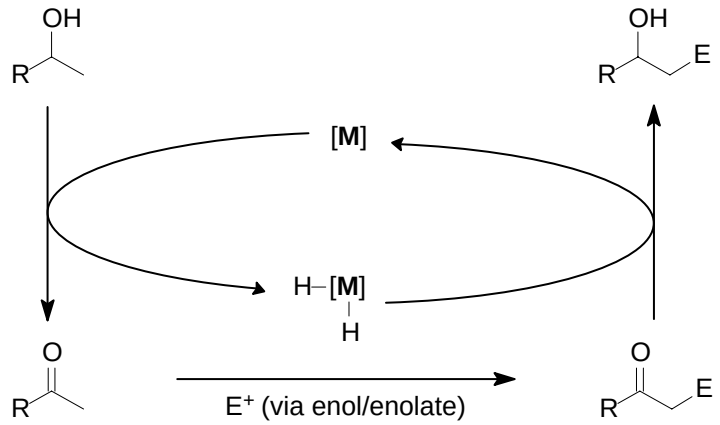

Scheme 1.3 Borrowing hydrogen in the *β*-functionalization of alcohols

Examples of the *β*-functionalization of alcohols via enol/enolate include the bromination of alcohols as reported by Williams and co-workers. In the presence of an aluminum alkoxide, bromination followed by reduction afforded brominated product as described in **eq. 1.2**.[15]

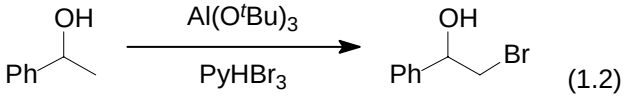

(1.2)

The activation of two primary alcohols by borrowing hydrogen can lead to an interesting coupling reaction. Sbrana and co-workers have reported their achievement in the selective synthesis of isobutanol via the Guerbet condensation of methanol with *n*-propanol using a variety of transition metal catalysts.[16, 17] The *β*-alkylation of secondary alcohols with primary alcohols has also been reported as outlined in **Scheme 1.4**. Typically, such reactions are believed to involve oxidization of both alcohols to form a ketone and an aldehyde, which undergo an aldol concentration giving an *α,β*-unsaturated ketone, and it is reduced to afford *β*-alkylated alcohol.

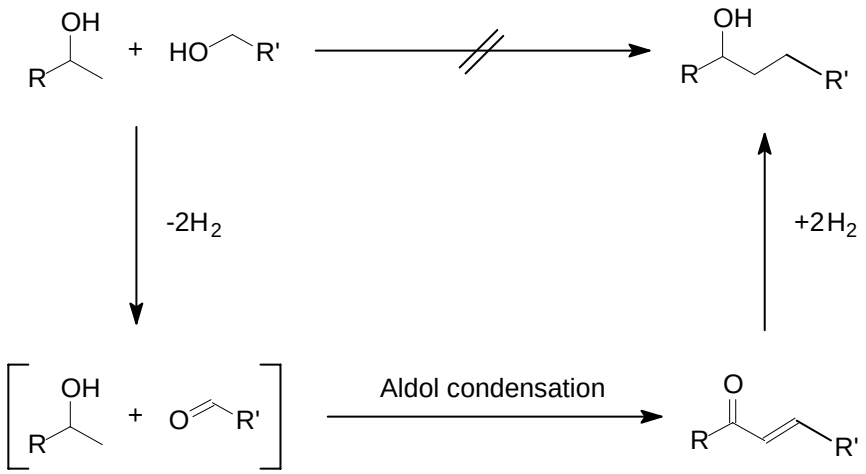

Scheme 1.4 Carbon-Carbon bond formation between alcohols

Following the progress of α-alkylation of ketones,[9] Cho *et al*. designed a ruthenium-catalyzed regioselective β-alkylation of secondary alcohols with primary alcohols where 1-dodecene was added as a sacrificial hydrogen acceptor.[18] The reaction pathway was broadly similar to that outlined in **Scheme 1.4**. The reaction was applicable to a wide range of aryl methyl, alkyl methyl and cyclic carbinol, and with alkyl methyl carbinols. The alkylation took place exclusively at the less-hindered methyl position over β-methylene and β-methine. Yamaguchi *et al.* reported a similar system for the β-alkylation of secondary alcohols with primary alcohols using Cp*Ir complex. The reported system required neither the addition of hydrogen acceptor nor donor. [19]

1.2 Introduction of Diphosphinoamine ligands, $RN(PX_2)_2$, and Related Chemistry

Throughout the development of inorganic and organometallic chemistry, few ligands have been as widely employed as tertiary monophosphines and diphosphines.[20] Diphosphine ligands in which two phosphorous nuclei are linked by a carbon atom or chain have been the subject of numerous investigations during the past three decades.[21-24] The versatility of these ligands arises from their ready coordination to metal centers through the lone pair electrons at both of the phosphorous atoms, and the variety of their coordination modes (monodentate, chelating and bridging).

The major application of metal complexes containing phosphine ligands is in homogeneous catalysis.[25] Since Wilkinson's original work on the catalytic activity of $Rh(PPh_3)_3Cl$ for hydrogenation reaction,[26] phosphine complexes have been extensively developed and are now commonly used in catalysis.[27] More recently, interest in diphosphine ligands, in which the backbone of the molecule comprises a heteroatom or group, is also growing rapidly. Diphosphinoamine ligands, $RN(PX_2)_2$ (**Chart 1.1**), for example, are particular important as they are isoelectronic with $Ph_2PCH_2PPh_2$ [bis(diphenylphosphospino)methane, dppm];[28-32] they offer considerable scope and versatility[33] since the substitutions on both nitrogen and phosphorous can be varied readily with attendant changes in the P-N-P bond angle and the conformation around the phosphorous centers.[34, 35] Furthermore, fairly small differences in these ligands can cause significant changes in their coordination behavior and the structural features of the resulting complex.[36]

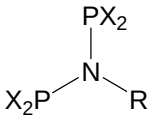

Chart 1.1

Diphosphinoamine ligands plays an important role in the present research; we are herein going to review their synthesis, reactivity, coordination chemistry and their application in catalysis.

1.2.1 Syntheses of Diphosphinoamine Ligands

The synthesis of diphosphinoamine ligands have been achieved via a number of routes. Silylated amines such as hexamethyldisilazane can be used in condensation reactions with chlorodiphenylphosphine to afford bis(diphenylphosphino)amine, $HN(PPh_2)_2$ (dppa), in good yield (**eq. 1.3**).[37] Instead of using silylated amine as a source of nitrogen, reactions employing alkyl or aryl substituted primary amines and chlorodiphenylphosphine also yields ligands of the type $RN(PPh_2)_2$ (**eq. 1.4**).[38] The HCl liberated from the reaction forms a salt with an organic base, for instance triethylamine, which is insoluble in the reaction solvent and therefore leads to facile separation and purification. By similar methods, other derivatives can also be prepared. Ligands of the type $RN(PCl_2)_2$ can be synthesized by a variety of routes. The most common one is the reaction of RNH_3Cl salt with trichlorophosphine;[39] subsequent reaction of the chloro-ligand with antimony trifloride gives the fluoro-derivative $RN(PF_2)_2$ (**eq. 1.5**).

$$HN(SiMe_3)_2 + 2PPh_2Cl \longrightarrow HN(PPh_2)_2 + 2Me_3SiCl \quad (1.3)$$

$$2PPh_2Cl + RNH_2 \longrightarrow RN(PPh_2)_2 + 2HCl \quad (1.4)$$

$$2PCl_3 + RNH_3Cl \longrightarrow RN(PCl_2)_2 + 3HCl \longrightarrow RN(PF_2)_2 + SbCl_3 \quad (1.5)$$

The ligands behave as diphosphines in many reactions. Oxidation occurs with selected chalcogen elements (i.e. oxygen, sulphur or selenium) to afford a range of possible ligands (**Scheme 1.5**). Double oxidization of diphosphinoamine ligands gives another set of ligands, $RNP((E)X_2)_2$ (E= O, S or Se), which have shown an extensive coordination chemistry with numerous metals.

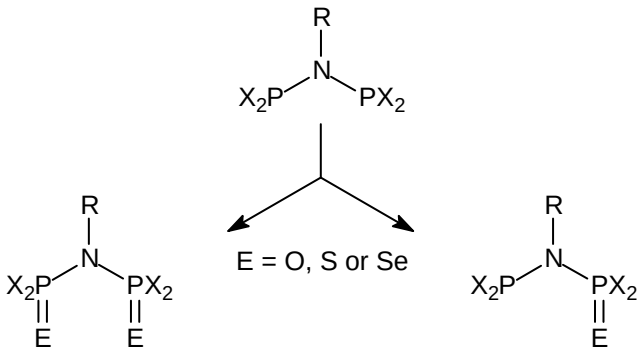

Scheme 1.5 Heteroatom ligands derived from diphosphinoamine ligands

The P-N bonds of diphosphinoamine ligands are relatively unstable. They can be cleaved by gaseous HCl to produce the corresponding alkyl or arylamine hydrochloride and chlorodiphenylphosphine. Whilst dilute aqueous HCl hydrolyses the ligands to the corresponding ammonium ion and diphenylphosphinous acid, the diphenylphosphinous acid is then oxidized to diphenylphosphinic acid. Concentrated aqueous HCl does not hydrolyse the P-N bond, but forms the corresponding hydrochloride. In comparison the alkylamino

bis(difluorophosphines) are more resistant to cleavage, but do react with aqueous HCl with cleavage of both P-N bonds to afford chlorodifluorophosphine.[39]

1.2.2 Coordination Chemistry of Diphosphinoamine Ligands

The versatility of diphosphinoamine ligands is illustrated by the fluoro-derivative, $MeN(PF_2)_2$. Following Nixon's work on Group 6 metal carbonyl derivatives containing $MeN(PF_2)_2$, [40] King *et al.* showed that $MeN(PF_2)_2$ could coordinate to transition metals in a monodentate or bidentate fashion to give rise to mononuclear as well as dinuclear species.[33] Although a monodentate mode of coordination is feasible, the planar geometry of the nitrogen atom in diphosphinoamine ligands permits facile incorporation of the ligands to the transition metal as a chelated or bridged structure[41]. The structures of the transition metal complexes with diphosphinoamine ligands also depend on the other ligands present and the coordination tendency of the particular metal such as Cr(0) octahedral, Fe(0) trigonal and Ni(0) tetrahedral. Accordingly, diphosphinoamine complexes can display several modes of coordination as shown in **Figure 1.1**. The coordination chemistry of diphosphinoamine ligands will be described in the following section which classifyies the complexes in terms of different Groups in the periodic table of elements.

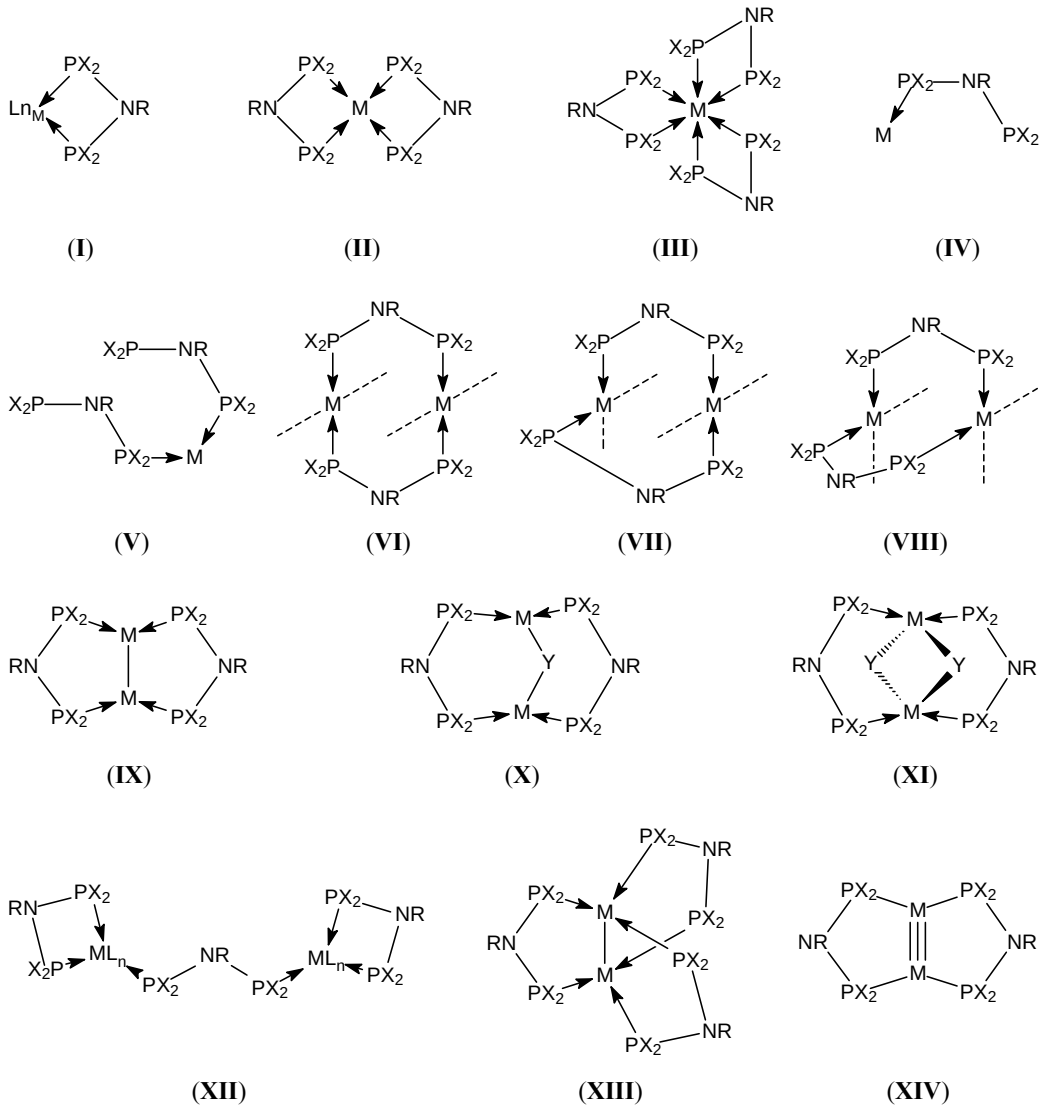

Figure 1.1 Possible coordination modes of diphosphinoamine ligands

Illuminating the metal precursors $CpM(CO)_4$ (M= V or Nb) with $MeN(PF_2)_2$ under ultraviolet irradiation affords mononuclear complexes.[33, 42] These are the first examples in which all four carbonyl groups of the $CpM(CO)_4$ unit have been completely replaced by other ligands (**eq 1.6**).

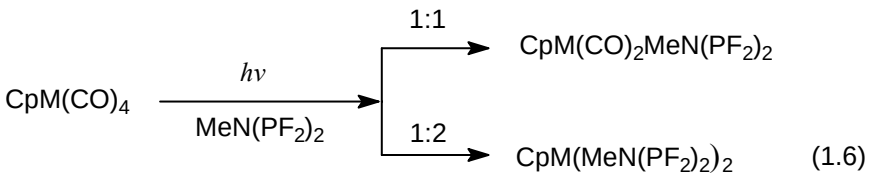

Reactions of diphosphinoamine ligands with Group 6 metals were first reported by Payne *et al*.[43, 44] Krishnamurthy and co-workers also demonstrated the ready formation of the monochelated complexes. An X-ray crystallographic study of the complexes $Mo(CO)_4PhN\{P(OPh)_2\}_2$ and $W(CO)_4{}^{i}PrN(PPh_2)_2$ confirmed that these complexes possessed the expected *cis*-configuration.[45] Photochemical reactions of $M(CO)_6$ (M=Cr, Mo or W) with an excess of $MeN(PF_2)_2$ gave completely substituted complexes, $Mo\{MeN(PF_2)_2\}_3$, which were the first known carbonyl free chelate complexes of Group 6 metals.[46, 47] Such complete substitution of CO groups of Group 6 metal carbonyls by diphosphino alkanes $Ph_2P(CH_2)_nPPh_2$ (n=2-4) could not be achieved either thermally or photochemically.

Only a few diphosphinoamine complexes of Mn are known. Ultraviolet irradiation of $CpMn(CO)_3$ with $MeN(PF_2)_2$ gives $CpMn(CO)MeN(PF_2)_2$ and the carbonyl-free complex $CpMn\{MeN(PF_2)_2\}_2$ containing one bidentate and one monodentate $MeN(PF_2)_2$ ligand (**eq. 1.7**).[48] The triple bonded dirhenium complexes of dppa have been reported by Walton and co-workers. The reactions of dirhenium (III) carboxylates of the type $[Re_2(O_2CMe)_2X_4(H_2O)_2]$ (X= Cl or Br) with dppa afforded mixed phosphine-halide complexes with bridging phosphino and acetato ligands.[49, 50]

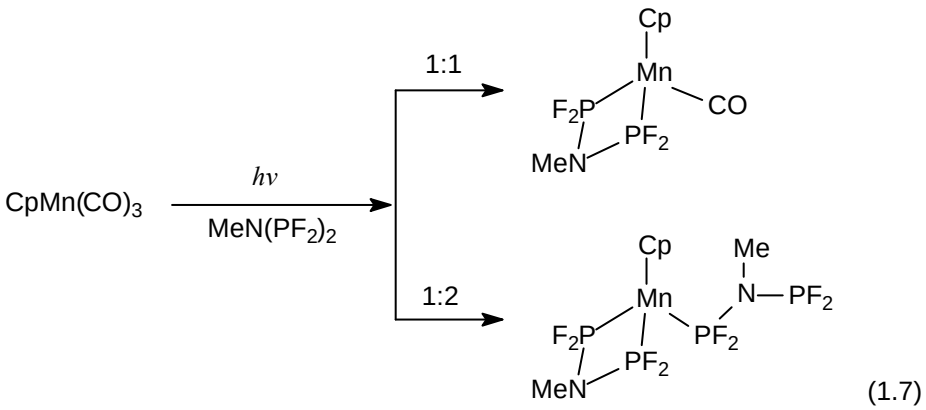

(1.7)

Photochemical reactions of $Fe(CO)_5$ or $Fe(CO)_9$ with $RN(PX_2)_2$ afford products that contain either chelating or bridging diphosphinoamines, depending on the reaction conditions.[51] Ultraviolet irradiation of equimolar quantity of $Fe(CO)_5$ and $RN(PX_2)_2$ in the presence of triethylamine *N*-oxide affords the chelated mononuclear complexes of the type $Fe_2(CO)_3RN(PX_2)$.[45] The reactions of ruthenium clusters and their derivatives with diphosphinoamine ligands have been investigated extensively by Haines and co-workers. In addition to chelated complexes, di-, tri- and even tetranuclear complexes have been isolated.[29, 52, 53] Treatment of $Ru_3(CO)_{12}$ with dppa leads to trinuclear complexes $Ru_3(CO)_{10}$(dppa) or $Ru_3(CO)_8$(dppa)$_2$ quantitatively, depending on the reaction conditions.[54] Reactions of various diphosphinoamine ligands with $CpRu(PPh_3)_2Cl$ leads to the formation of different types of mononuclear complexes depending on the substituents on both of the phosphorus centers and the bridging nitrogen atom. For example, reaction of dppa with $CpRu(PPh_3)_2Cl$ gives a neutral complex CpRu(μ^2-dppa)Cl and two cationic complexes [CpRu(μ^2-dppa)(μ^1-dppa)]Cl and [CpRu(μ^2-dppa)(PPh_3)]Cl. This once again demonstrates the versatility of diphosphinoamine ligands.[55]

Reaction of $MeN(P(OMe)_2)_2$ with $Co_4(CO)_{12}$ affords $Co_2(CO)_4\{MeN(P(OMe)_2)_2\}_2$.[56] The analogous complexes of $R'N(P(OR)_2)_2$ have also been reported. An ionic intermediate $[Co_2(CO)_4\{R'N(P(OR)_2)_2\}]$-$[Co(CO)_6]$ was identified by Haines and co-workers[57]. Protonation of $Co_2(CO)_4\{EtN(P(OR)_2)_2\}_2$ (R = Me or ^{i}Pr) gave a hydrido-bridged complex $[Co_2(\mu\text{-H})(CO)_4\{\mu\text{-}(P(OR)_2)_2NEt\}_2]^+$ (**eq. 1.8**).[58] Werner *et al.* reported that the reaction of $Co(\eta^5\text{-}C_5Me_4H)(PMe_3)_2]$ with $MeN(PPh_2)_2$ yielded the unstable chelated complex $[Co(\eta^5\text{-}C_5Me_4H)\{MeN(PPh_2)_2\}]$ upon treating with NH_4PF_6; it was isolated as a stable hydrido complex $[Co(H)(\eta^5\text{-}C_5Me_4H)\{MeN(PPh_2)_2\}]^+PF_6^-$.[59] The reaction of $RN(PX_2)_2$ (R = Et, Ph; X = OPh; R = Me, X = F) with $[RhX'diene]_2$ (diene = COD or NBD; X' = Cl, Br or I) leads to the successive replacement of diene ligands and the formation of complexes of the types $Rh_2X'_2(diene)\{RN(PX_2)_2\}$ and $[Rh\{RN(PX_2)_2\}X']_2$.[60] The reactions of dialkoxyphosphinoamine, $RN\{P(OR')_2\}_2$ with rhodium and iridium derivatives afford a range of mono- and bimetallic complexes.[61] Heterobimetallic complexes containing diphosphinoamines have been reported by Mague and co-workers. Reactions of $[FeCp\{MeN(PF_2)_2\}_2Cl]$ with $[IrCl(CO)(PMe_2Ph)_2]$ and $[RhCl(CO)_2]_2$ afforded the bimetallic complexes $[CpFeIrCl_2(PMe2Ph)\{MeN(PF_2)_2\}_2]$ and $[CpFeRhCl_2\{MeN(PF_2)_2\}_2]$, respectively.[62, 63]

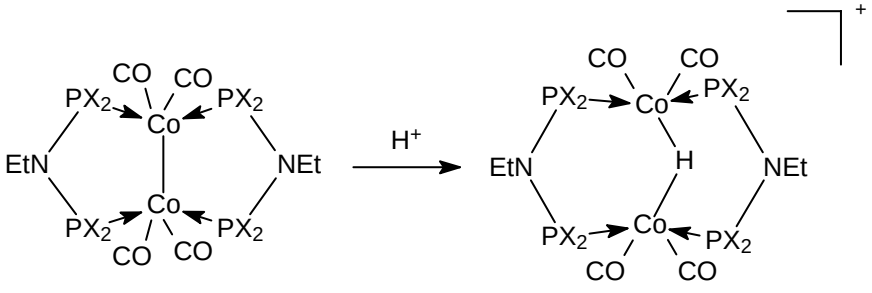

X = OMe or O^{i}Pr (1.8)

Nickel(II) halides or thiocyanates react with $PhN(PPh_2)_2$ to give $NiX_2\{PhN(PPh_2)_2\}$(X = Cl, Br, I or NCS). Treating nickel perchlorate with the same ligand gives the perchlorate complex $[Ni\{PhN(PPh_2)_2\}_2]$ $(ClO_4)_2$ which contains two chelating diphosphinoamines.[64] Reactions of $RN(PPh_2)_2$ with $[NiCp(NBD)]BF_4$ afford the cationic complexes $[NiCp\{RN(PPh_2)_2\}]BF_4$ (R= Me, Ph); a neutral complex $NiCp\{\eta^1\text{-}(PPh_2)_2NPh\}CN$ in which the diphosphinoamine ligand displaying a monodentate coordination can be obtained by treating $[NiCp\{PhN(PPh_2)_2\}]BF_4$ with NaCN.[65] Reactions of $RN(PX)_2$ with palladium or platinium derivatives such as $[K_2PdCl_4]$ or *cis*-$[PtCl2(SEt_2)_2]$ give chelated complexes of the type *cis*-$[MCl_2RN(PX_2)_2]$.[66, 67] In contrast, reactions of platinium derivatives with $\{P(OEt)_2\}_2O$ afford an dinuclear complex, $Pt_2Cl_4[\{P(OEt)_2\}_2O]_2$, in which the ligand bridges two metal centers because of the lower flexibility of the P-O-P backbone.[67] Treating $[Pd_2(dba)_3 . CHCl_3]$ with excess $MeN(P(OPh)_2)_2$ affords the dinuclear complex, $[Pd_2\{MeN(P(OPh)_2)_2\}_3]$, connected by three bridging diphosphinoamine ligands. Under similar conditions, the phenyl- derivative, $PhN(P(OPh)_2)_2$ does not afford an easily identifiable dinuclear complex. The $^{31}P\{^1H\}$NMR spectrum suggests that presumably a bis-chelated mono-nuclear complex $[Pd\{PhN(P(OPh)_2)_2\}_2]$ is formed in the reaction.[68]

1.2.3 Application of Diphosphinoamine Ligands in Catalysis

The application of diphosphinoamine ligands in catalysis has not been explored in detail. Wass *et al.* reported that palladium (II) complexes containing ligands of the type $MeN(PAr_2)_2$ (Ar = *ortho*-substituted phenyl group) were efficient catalysts for ethylene/CO copolymerization.[69] Furthermore, nickel (II)

complexes with these ligands were found to be highly active and poison-tolerant catalysts for the ethylene polymerization reactions.[70] In addition, these ligands bearing *ortho*-methoxy-substituted aryl groups, together with a chromium source and an aluminoxane activator, were reported to be extremely active and selective ethylene trimerization catalysts.[71]

Recently, Kuhlmann *et al.* reported an unprecedented ethylene tetramerization that produced 1-ocetene in good yield. A variety of diphosphinoamine ligands, in combination with Cr(III) compounds activated by aluminoxanes, were found to be very active and efficient catalysts for the purpose.[72] Following the first report of ethylene tetramerization, numerous studies on the effect of ligand structure on the outcome of the catalysis were launched. These studies highlighted the relationship between some key ligand structures and reaction selectivity.[73, 74] A systematic study of the effect of various structures of diphosphinoamine ligands was reported by Wasserscheid *et al*.[75] They demonstrated that steric bulk effects of each *N*-substituent on diphosphinoamine ligands were the dominant parameter influencing the reaction selectivity and concluded that α-branching was essential for obtaining highly selective tetramerisation catalysts. These demonstrated the growing utility of diphosphinoamine ligands in catalysis.

1.3 Catalytic Markovnikov and Anti-Markovnikov functionalization of Terminal Alkynes

Regioselective functionalization of terminal alkynes is of utmost importance for the synthesis of a wide variety of organic products. Among

various chemical transformation methods, the addition of E-Nu (E = H, BR_2, Si, Hg, Sn, etc.; Nu = halogen, CN, CHO, OH, CO, COOR, NR_2, etc.) across the multiple bond is simple and the most efficient in terms of atom utilization due to the avoidance of stoichiometric amounts of by-products. Based on the original observation by Vladimir Markovnikov, the possible regioisomeric products are classified as Markovnikov or anti-Markovnikov products. In general, most of the electrophilic addition reactions follow the Markovnikov rule. However, it is nowadays possible to control the regiochemistry of various additions of nucleophiles to alkynes by applying different transition metal catalysts.

The reaction pattern of terminal alkynes in the coordination sphere of transition metals is illustrated in **Scheme 1.6**. When a terminal alkyne molecule approaches a transition metal center, the initial interaction between them occurs either through the C≡C triple bond or C-H σ-bond. The metal-CH interaction is normally less stable and leads to an oxidative addition (*i*) product MH(C≡CR), which rearranges through 1,3-hydride migration (*ii*) to give metal vinylidene. Nevertheless, the metal vinylidene can also be derived from the 1,2-hydride migration (*iii*) over the η^2-alkyne.[76-81] The regioselectivity of the reaction is determined by the coordination modes. For the Markovnikov manner, alkynes are activated by the η^2-cooridnation, which renders it susceptible to nucleophilic attack (*iv*). Subsequent protolytic cleavage (*v*) of the metal-carbon bone provides Markovnikov products; this selectivity contrasts with that of metal vinylidene, where the α-carbon linked to the metal centre is an electrophilic site. Nucleophilic attack (*iv*) followed by protolytic cleavage (*v*) affords products in anti-Markovnikov fashion.

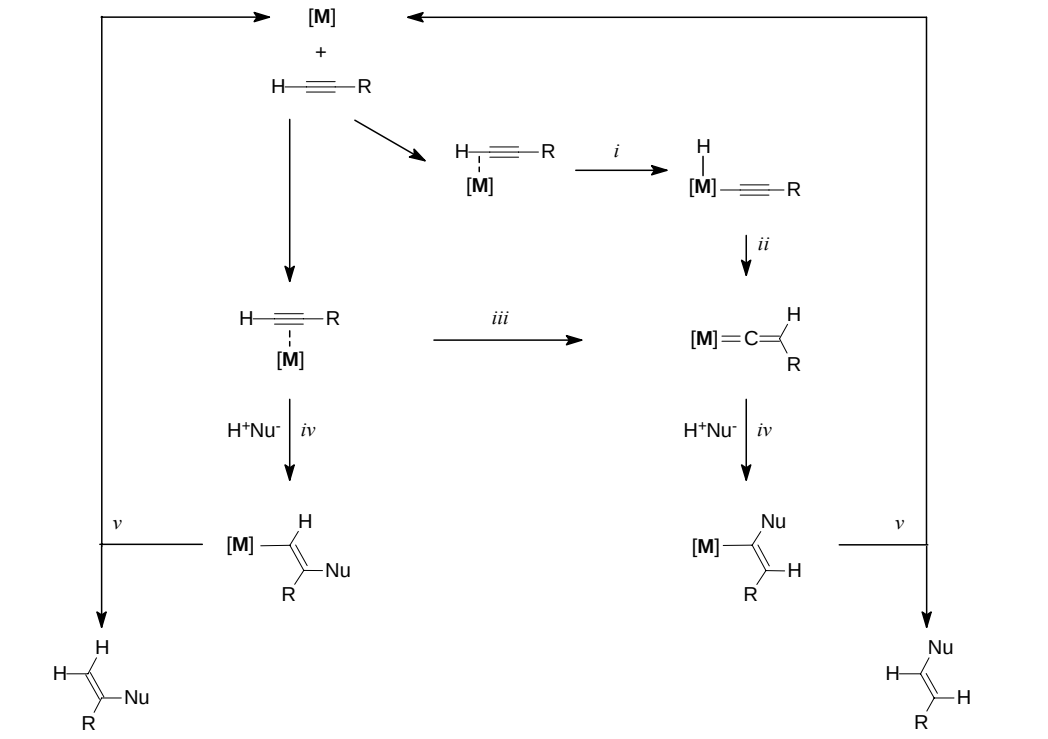

Scheme 1.6 Reaction pattern of 1-alky-metal complexes

Terminal alkynes have been functionalized in both Markovnikov and anti- Markovnikov fashions in this research; we herein review the recent development in this area with special focus on the control of regioselectivity. This review focuses on the addition of H-Nu across C≡C bond of alkynes. We have structured the content according to different addition reactions. In most cases, reported mechanisms are presented to facilitate the understanding of the reactions.

1.3.1 Carbonylation

Carbonylation of alkynes involves the insertion of >C=O moiety across the C≡C triple bond (**eq. 1.9**).

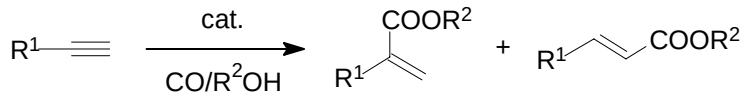

(1.9)

This class of reactions is one of the most useful transformations using transition metal complex catalysts. During the past several decades, palladium and platinum-based catalysts have been extensively used for the purpose. For example, Knifton *et al.* reported the $[PdCl_2(P(p\text{-}MeC_6H_4)_3)_2]$-SnCl and $[PdCl_2(Me_2PPh)_2]$-SnCl-catalyzed regioselective carbonylation of terminal alkynes. Linear α,β-unsaturated acid esters were obtained in up to 96% selectivity under mild condition.[82] Carbonylation of alkynes under the catalytic system consisting of $Pd(OAc)_2$, a monophosphine, *p*-toluene sulphonic acid and semilabile anionic bidentate ligands such as pyridine or piperdine carboxylic acid was also reported by Jayasree *et al.* (Scheme 2).[83] In contrast to Knifton's work, branched isomers were obtained in up to 98% selectivity.

Similarly, the platinum-based systems, which are exemplified by $[PtCl_2(PPh_3)_2]/SnCl_2$ and $[PtH(SnCl_3)(PPh_3)_2]$, have been found to catalyze the carbonylnation of terminal as well as internal alkynes; the product distribution depends on the catalyst system used.[84] For instance, 1-octyne is selectively carbonylated to branch ether with 59% yielding under the influence of $[PtH(SnCl_3)(PPh_3)_2]$, while the $[PtCl_2(PPh_3)_2]/SnCl_2$ system is also active but exhibits a lower selectivity (*n : iso* = 1.2:1). When triphenylphosphite is added to the $[PtCl_2(PPh_3)_2]/SnCl_2$ system, only linear α,β-unsaturated acid esters is obtained. The reason for this selectivity difference is not fully understood.

1.3.2 Addition of Active Methylene Compounds

The addition of active methylene compounds to terminal alkynes is one of the most common methods to form carbon-carbon bond. The direct α-functionalization of active methylene compounds without prior enolate formation represents a more efficient approach. Recently, Toste and co-workers have reported a phosphinegold(I)-catalyzed intramolecular addition of β-ketoesters to an unactivated alkynes under neutral conditions at room temperature.[85] A series of alkynic β-ketoesters reacted in the presence of catalytic amounts of $(PPh_3)AuCl$ and AgOTf to afford the cycloisomerization products (**eq. 1.10**). In most cases, the reaction required low catalyst loadings, short reaction times and proceeded under open atmosphere.

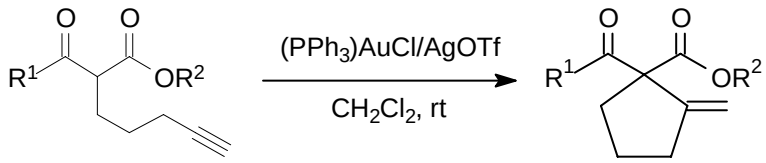

(1.10)

The Au-catalyzed Conia-ene reaction of deutroacetylene afforded cycloisomer selectively deuterated (90%) syn to the ketoester (**eq. 1.11**). This implied that the mechanism involved nucleophilic attack on a Au(I)-alkyne complex by the enol form of the ketoesters, affording vinyl-Au intermediate which was then protonated to furnish the corresponding cycloisomer as shown in **Scheme 1.7**.

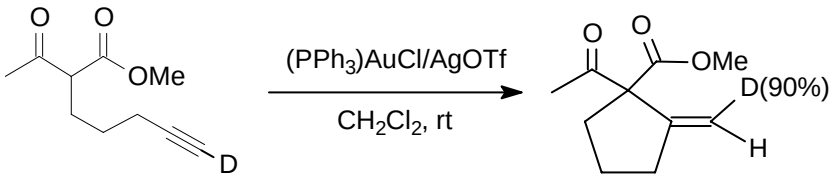

(1.11)

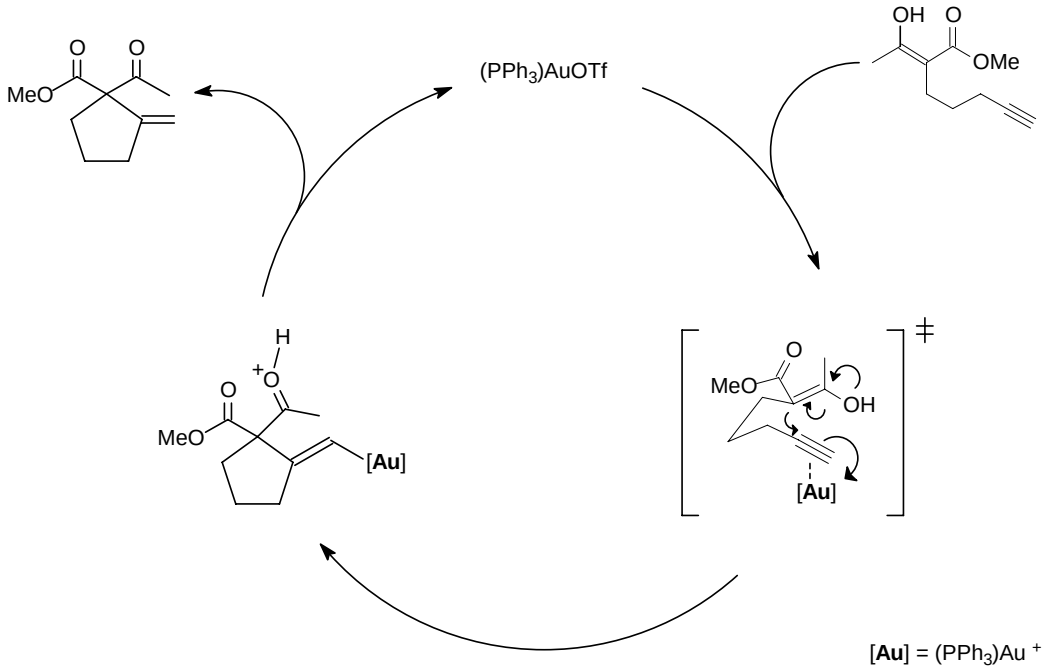

Scheme 1.7 Mechanism of Au(I)-catalyzed Conia-ene reaction of *β*-ketoesters with alkynes

In addition to the phosphineAu(I)/AgOTf system, Ni(II) complex was also applied in the Conia-ene reaction of 1,3-dicarbonyl compounds with alkynes.[86] In the presence of $Ni(acac)_2$ and $Yb(OTf)_3$, a wide range of alkynic 1,3-dicarbonyl substrates underwent Conia-ene reaction to give the corresponding olefinic cyclopentane derivatives. Surprisingly, the deuterium labeling experiment is counter to those obtained by Toste *et al.* which suggested that the Ni(II)-catalyzed reaction proceeded in a completely different mechanism. The reported mechanism depicted in **Scheme 1.8** operates by the formation of a enol-yne-Ni complex. The insertion of Ni enolate to the alkyne generated a Ni(II) vinyl species. Protonlysis of the C-Ni bond gave the cyclized product.

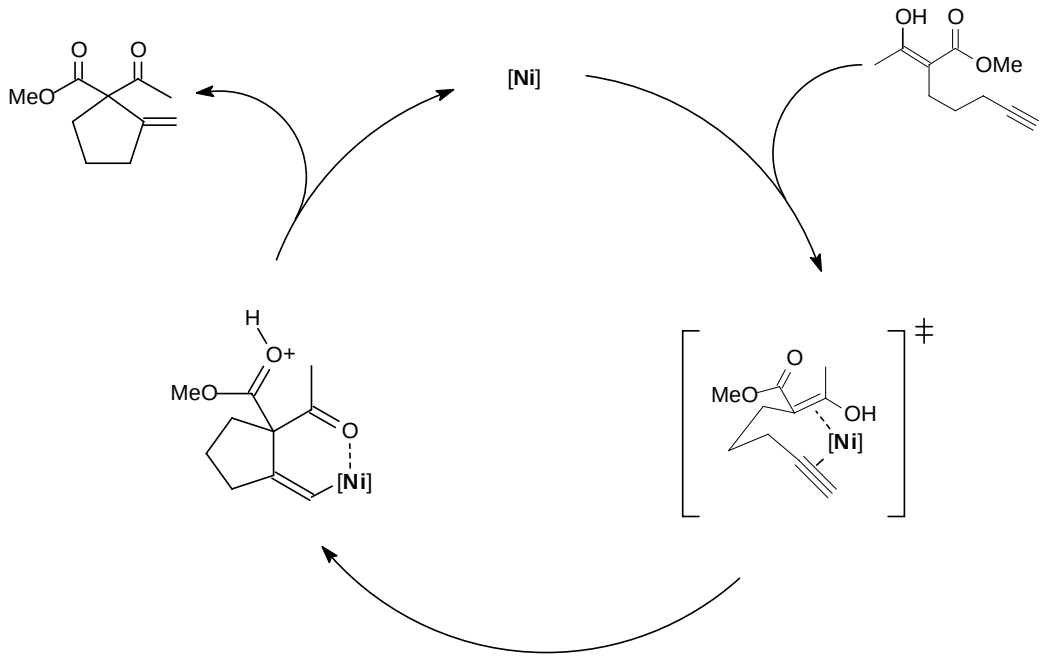

Scheme 1.8 Mechanism of Ni(II)-catalyzed Conia-ene reaction of *β*-ketoesters with alkynes

Even though examples of several metal-catalyzed intramolecular addition of activated methylene compounds to terminal alkynes have been reported there are only a few reports on the intermolecular version of the addition reaction. For example, Endo *et al.* reported the indium-catalyzed intermolecular addition reaction of active methylene compounds to alkynes; 1,3-dicarbonyl compounds were added to terminal alkynes in the presence of a catalytic amount of $In(OTf)_3$ to give 2-alkenylated 1,3-dicarbonyl in Markovnikov fashion, with carbon-carbon bond formation on the acetylene moiety (**eq. 1.12**).[87, 88]

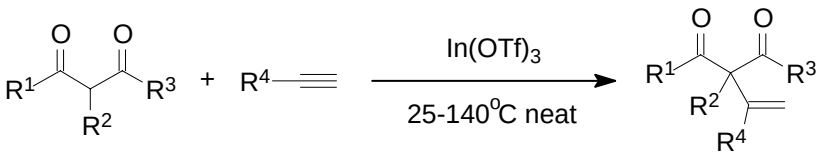

(1.12)

Experimental and theoretical studies on the mechanism indicated that the key step in the catalytic cycle involved a concerted carbometalation of the indium (III) enolate to the alkyne to afford an alkenyl indium (III) intermediate. Protonation of the alkenyl indium(III) intermediate by the dicarbonyl compound completed the catalytic cycle (**Scheme 1.9**).

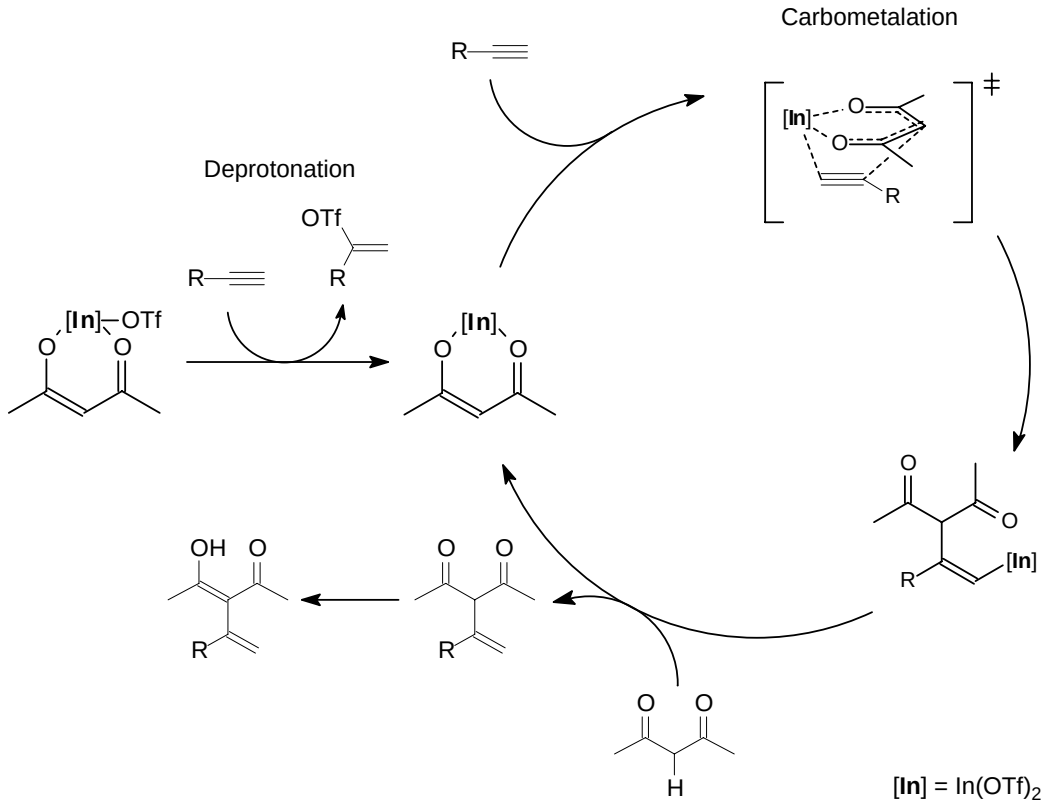

Scheme 1.9 Mechanism of In(III)-catalyzed 2-alkenylation of dicarbonyl compounds with terminal alkyne

A rhenium complex $[ReBr(CO)_3(THF)]_2$-catalyzed intermolecular addition of an active methylene compounds to terminal alkynes was reported by Kuninobu.[89] The mechanism involving the formation of enol-yne-Re intermediate, which was substantially similar to that outlined by Gao *et al.*[86] was reported, it was supported by deuterium-labeling experiments. To our

knowledge anti- Markovnikov addition of active methylene compounds to terminal alkynes is basically not known. Thus, metal-catalyzed insertion of terminal alkynes into a C-H bond of the active methylene with anti-Markovnikov regioselectivity has been regarded as one of the major challenges of catalysis for decades.

1.3.3 Hydroamination

Introducing an N-H bond to C-C multiple bonds, which is known as hydroamination, offers an attractive route for the synthesis of highly substituted nitrogen-containing organic molecules (**eq. 1.13**).

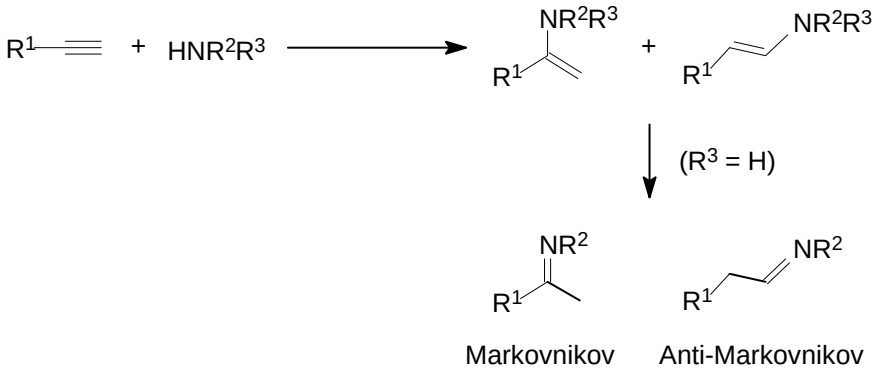

(1.13)

Hydroamination offers a promising route to various amines, enamines and imines. In general, a wide variety of metal complexes have been employed in catalytic hydroamination of terminal or even internal alkynes to yield Markovnikov products. For example, Wakatsuki and co-workers demonstrated that the $[Ru_3(CO)_{12}]/NH_4PF_6$ or $HBF_4{\cdot}Et_2O$ catalytic system permitted high-yielding conversion of anilines with terminal phenylacetylenes to give the corresponding branched imines.[90] Advantageously, the reactions could be run

under an air atmosphere and a solvent-free condition. Similarly, intermolecular hydroamination of alkynes with both aromatic and aliphatic amines occurred regiospecifically in the presence of silver-exchanged tungstophosphoric acid (AgTPA) and formed the corresponding ketimine.[91] The reported mechanism envisaged the formation of a η^2-coordinated alkyne; an amine coordinated to the Ag center prior to the C-N bond formation (**Scheme 1.10**).

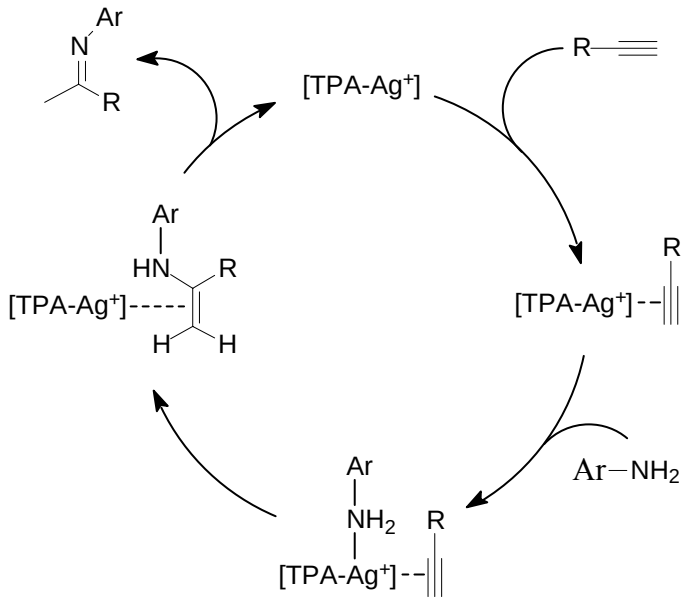

Scheme 1.10 Mechanism of AgTPA-catalyzed intermolecular hydroamination of alkynes

Even though hydroamination of functionalized phenylacetylene derivatives is efficient; a similar process for aliphatic alkynes remains underdeveloped and only a few examples have been reported. Hartung *et al.* reported the hydroamination of aliphatic alkynes with anilines using the commercially available rhodium catalyst $[Rh(cod)_2]BF_4/PR_3$ under very mild reaction conditions to yield the corresponding imines in Markovnikov

fashion.[92] This is the first example of rhodium-catalyzed hydroamination of alkynes which proceeds at room temperature.

Apparently, in all the hydroaminations of alkynes with late transition-metal catalysts mentioned, electronic factors govern the regioselective attack of the nucleophile at the internal carbon atom to afford Markovnikov products; hydroamination of alkynes in an anti-Markovnikov fashion is relatively rare. The first anti-Markovnikov hydroamination of terminal alkynes with primary amines was realized by Haskel *et al.* using organoactinide complexes $Cp^*_2AnMe_2$ ($Cp^* = C_5Me_5$, An = Th or U) as catalysts (**eq. 1.14**).[93, 94]

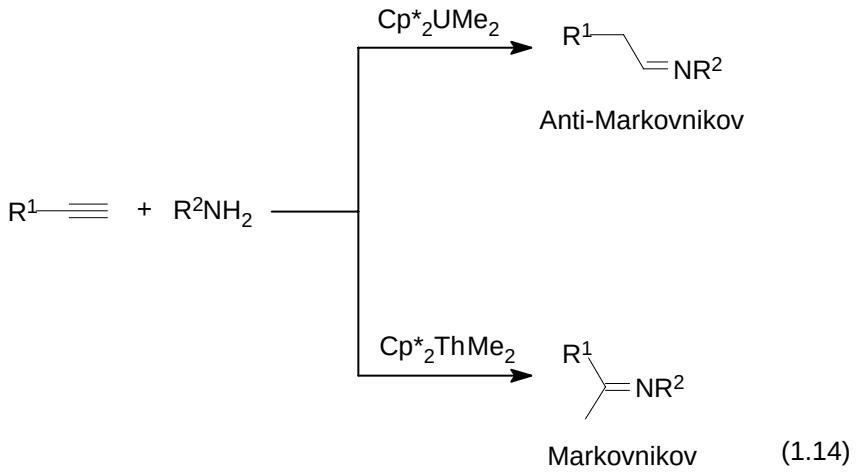

(1.14)

The regioselectivity of the reaction was found to be highly dependent on the nature of the catalysts and the bulkiness of the amines but almost did not depend on the nature of alkynes. The complex $Cp^*_2UMe_2$ catalyzed the formation of anti-Markovnikov imines; however, a similar reaction with $Cp^*_2ThMe_2$ as the catalyst reversed the regioselectivity completely. Haskel and coworkers reported a mechanism which involved the formation of an actinide imido complex (**A**).

The intermediate **A** underwent a rapid double bond metathesis with an incoming alkyne to yield a metallacycle (**B**). Protonolytic ring opening of **B** by an amine yielded an actinide-enamine amido complex (**C**). **C** then isomerized to an actinide-alkyl (imine) amido complex via an intramolecular 1,3-sigmatropic hydrogen shift, which upon a subsequent protonolysis by an addition amine affords the imine as product (**Scheme 1.11**).

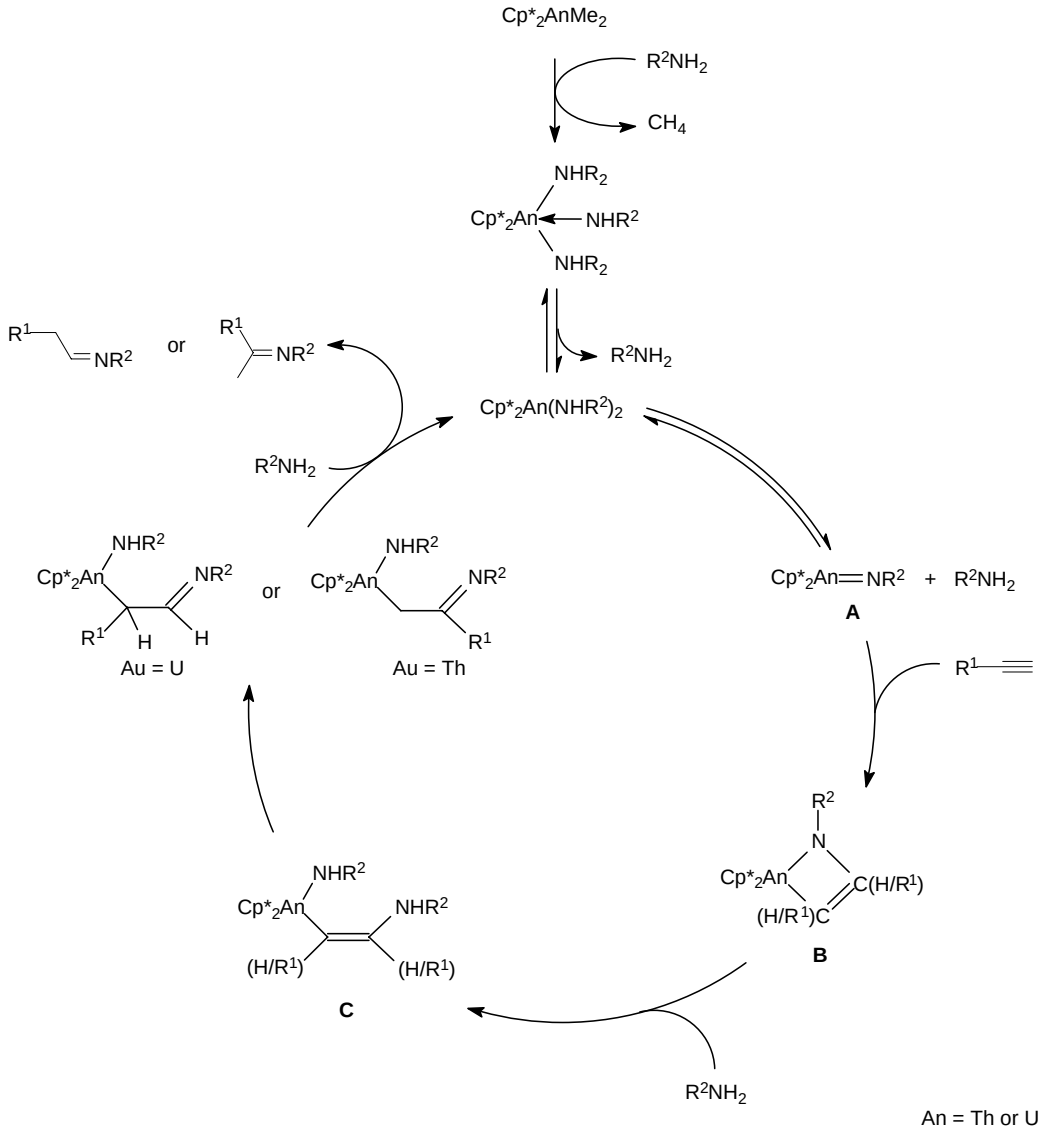

Scheme 1.11 Mechanism of organoactinide-catalyzed intermolecular hydroamination of terminal alkynes

The product distinction between the two catalysts was achieved by a contrasting stereochemistry in the metathesis of alkynes, toward the imido complex (**Scheme 1.12**).

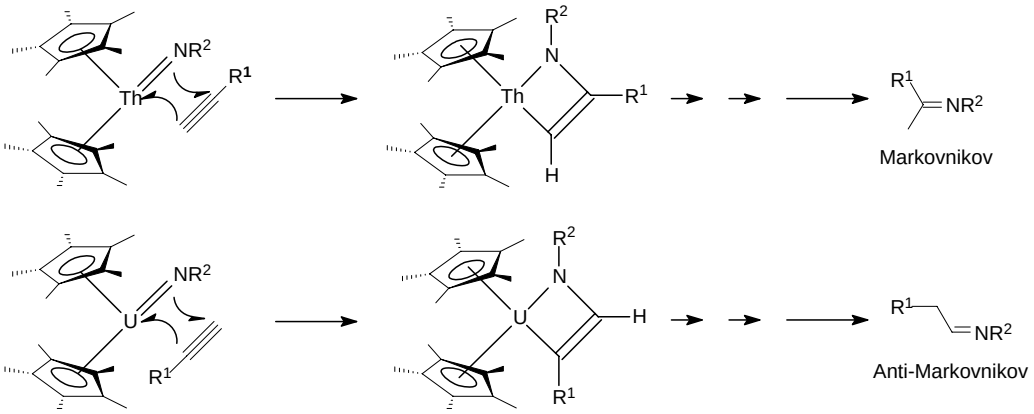

Scheme 1.12 Opposite reactivity exhibited in the reaction of organoactinide-imido complexes with terminal alkynes

In addition to the advancement in the area of organoactinide-based catalytic system, some progresses with titanocene derivatives have also been reported. Tillack *et al.* reported the [$Cp_2Ti(\eta^2$-$Me_3SiC{\equiv}CSiMe_3)$] and [$Cp_2Ti(\eta^2$-$Me_3SiC{\equiv}CPh)$]-catalyzed hydroamination of internal and terminal alkynes; high selectivity to give the corresponding anti-Markovnikov functionlized imines was observed.[95, 96] The reported titanocene complexes are easily available, stable, and can be used in a safe and practical manner. Although details of the reaction mechanism have not been reported, it seems likely that the formation of azatitanacyclobutene (**Chart 1.2**), a metallacycle, is important in the reaction mechanism.

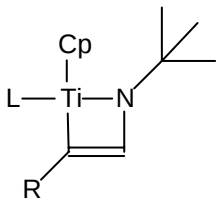

Chart 1.2

Subsequently, Schafer *et al.* revealed the highly regioselective anti-Markovnikov hydroamination of a wide range of terminal alkyl alkynes with alkylamines using bis(amidata)titanium complexes as catalysts.[97, 98] The proposed catalytic cycle is consistent with the generally accepted imido-based mechanism.

However, the complexes described above are not applicable to hydroaminations with secondary amines, since the formation of the imido intermediate is prohibited. Hydroamination of phenylacetylene with secondary amines using cesium hydroxide as catalyst was briefly mentioned by Tzalis and co-workers.[99] Unfortunately, the reactions were limited to the *N*-substituted anilines and phenylacetylene pairs. The Wilkinson's catalyst was also found to be active for the addition of 2-*N*-methylaminopyridine to 1-decyne, giving the corresponding anti-Markovnikov enamine in 40% yield.[100] The reported mechanism proceeded via a Rh(I)-vinylidene complex (**A**), which was a common intermediate for transition-metal-mediated reaction of terminal alkynes; a direct attack of 2-*N*-methylaminopyridine led to the rhodium(III)-hydride complex (**B**). Reductive elimination of **B** furnished the corresponding anti-Markovnikov enamine (**Scheme 1.13**); in this case, the pyridine ring was essential in order to obtain the product.

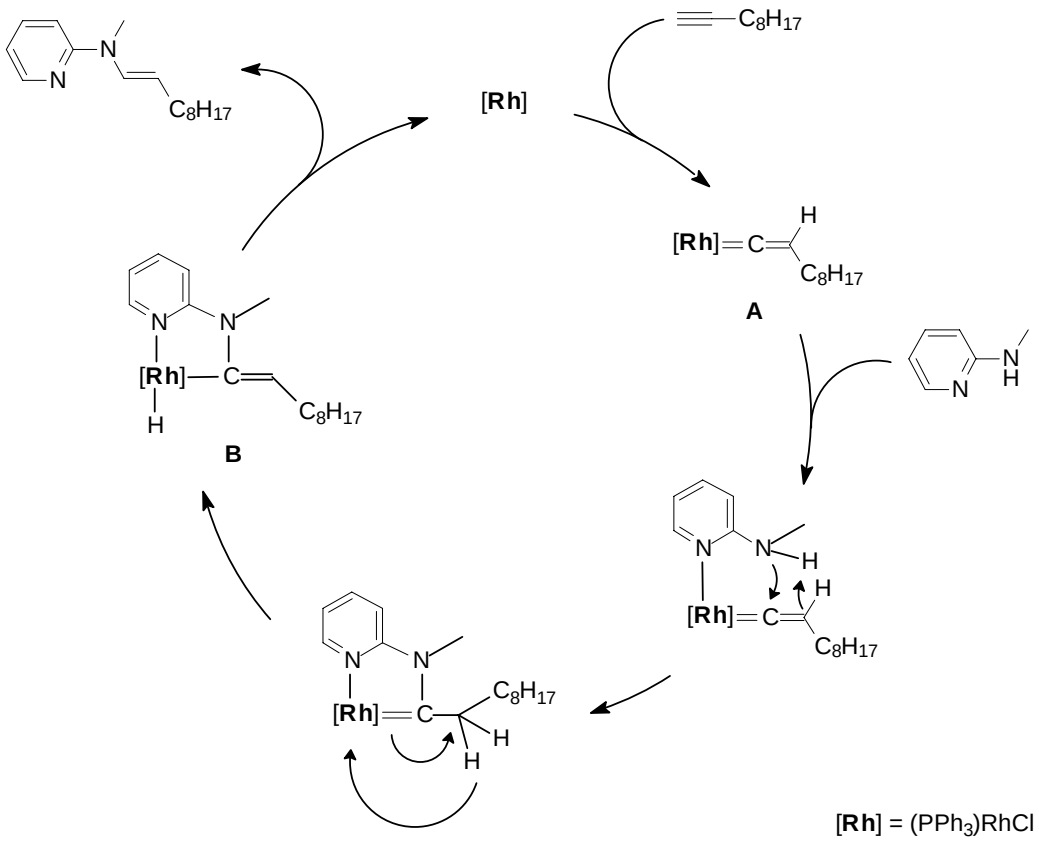

Scheme 1.13 Mechanism of chelation-assisted hydroamination of terminal alkynes

More recently, Fukumoto and co-workers reported the hydroamination of terminal acetylenes with both primary and secondary amines in the presence of catalytic amount of $TpRh(C_2H_4)_2$.[101] This is the first catalytic system that allows both primary and secondary amines to react with terminal alkynes to give anti-Markovnikov products. Similarly, it seems likely that the Rh-vinylidene complex exists as a crucial intermediate in the reaction cycle.

1.3.4 Hydration

Addition of water molecule to C≡C triple bond is again one of the most useful methods for functionalizing alkynes. In general, the reaction leads to the corresponding ketone under electronic control. For example, Hiscox and Jennings reported the platinum (II) complex in the form of Zeise's dimmer, $[PtCl_2(C_2H_4)_2]$ for the hydration of several alkyl-subsituted alkynes.[102] Terminal alkyne was hydrated to the corresponding ketone. In the case of asymmetric substituted alkynes, nucleophilic addition at more hindered side was preferable. The η^2-coordinated acetylene complex is a critical intermediate in the reported mechanistic cycle. Regioselectivity arose when the platinum moiety was forced aside from the alkyne centre that created a partial cationic centre at the distal carbon atom at which the water molecule attacked as shown in **Scheme 1.14**.

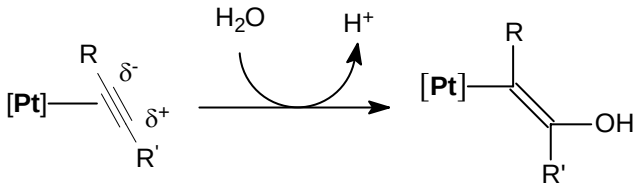

[**Pt**] = PtX_2 (X = Cl, Br and I)
R' is bulkier than R

Scheme 1.14 Regioselective hydration of asymmetric substituted alkynes

Interestingly**,** Francisco et al. recently reported the *cis*-$[PtCl_2(TPPTS)_2]$-catalyzed (TPPTS = $P(m\text{-}C_6H_4SO_3Na)_3$) hydration of 4-pentyn-1-ol and 3-pentyn-1-ol.[103] Both hydration reactions led to the same product, 5-hydroxy-2-pentone. The product of both catalytic hydrations arose through intramolecular

cyclization followed by hydrolysis of the heterocyclic intermediate as shown in **Scheme 1.15**. 5-hydroxy-2-pentone was formed from 4-pentyn-1-ol through a 5-exo-dig mechanism (Markovnikov reaction); while hydration of 3-pentyn-1-ol occurred through a 5-endo-dig mechanism (anti-Markovnikov reaction).

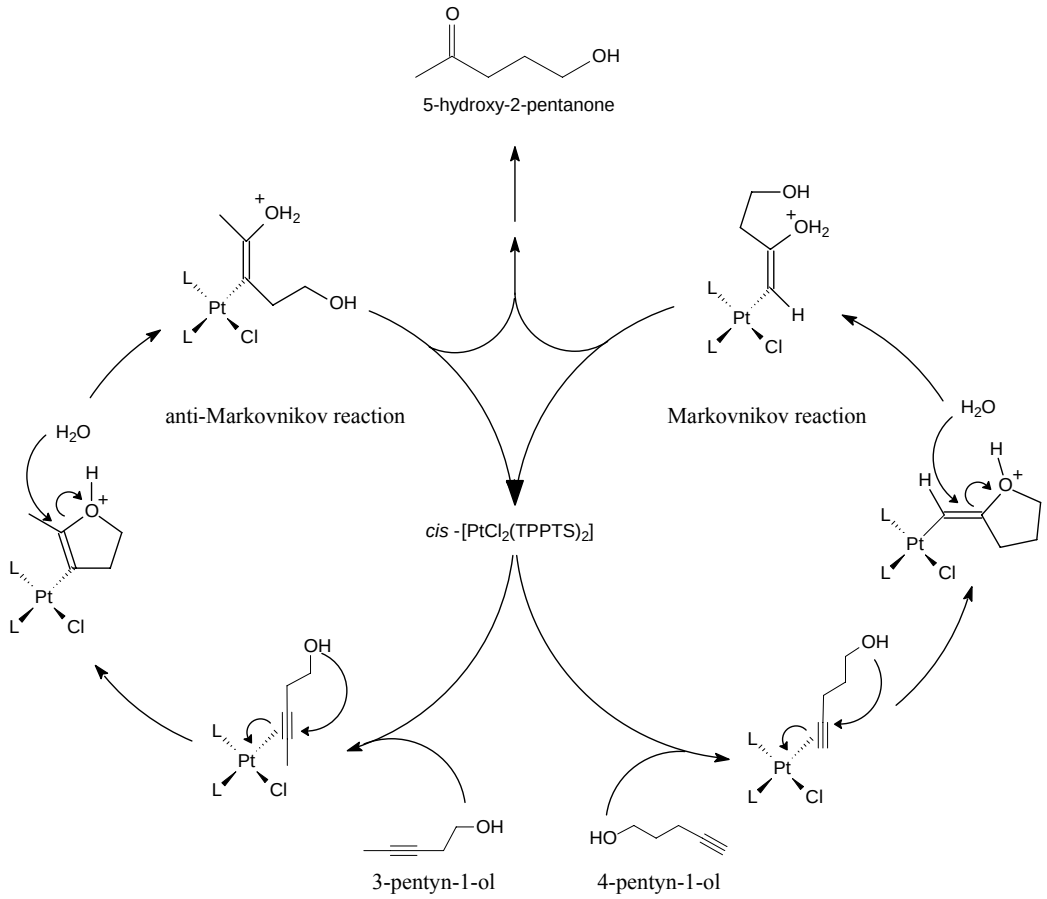

Scheme 1.15 Mechanism of Pt-catalyzed hydration of 4-pentyn-1-ol and 3-pentyn-1-ol

The anti-Markovnikov addition of water to terminal alkynes which gives the aldehydes preferentially using different Ru-based catalyst systems was also reported. The easily available cyclopentadienyl ruthenium complexes of the types CpRu(P-P)Cl and $CpRu(PR_3)_2Cl$ were used for the anti-Markovnikov

hydration of terminal alkynes to give *n*-aldehyde as products.[104] Ruthenium complexes bearing appropriate bidentate phosphine ligands were highly active and allowed regiospecific formation of aldehyde. The activities of ruthenium complexes with monodentate phosphine ligands were also satisfactory. These, in particular $CpRu(PMe_2Ph)_2Cl$, showed high activities for the hydration of 1-hexyne to give hexanal exclusively. It is very likely that the hydration reactions promoted by cyclopentadienyl ruthenium complexes take place via a vinylidene intermediate.

A class of highly efficient ruthenium catalysts was recently developed for the anti-Markovnikov hydration of terminal alkynes by Grotjahn *et al*.[105, 106] In the presence of phosphanylimidazole or phosphanylpyridine Ru catalysts the anti-Markovnikov hydrations of terminal alkynes occurred, giving the corresponding aldehydes as products. The bifunctional catalysts exhibited an enzyme–like rate of acceleration and selectivity. Other advantages claimed for the system included a high toleration of several important functional groups. The 2-imidazoleyl and 2-pyridyl group on a phosphine moiety enabled the formation of vinylidene, and subsequently the addition of water to α-carbon of vinylidene was mediated by the hydrogen bonding (**Scheme 1.16**). The protonated pendant base moiety donated a hydrogen bond to the acyl oxygen.[107]

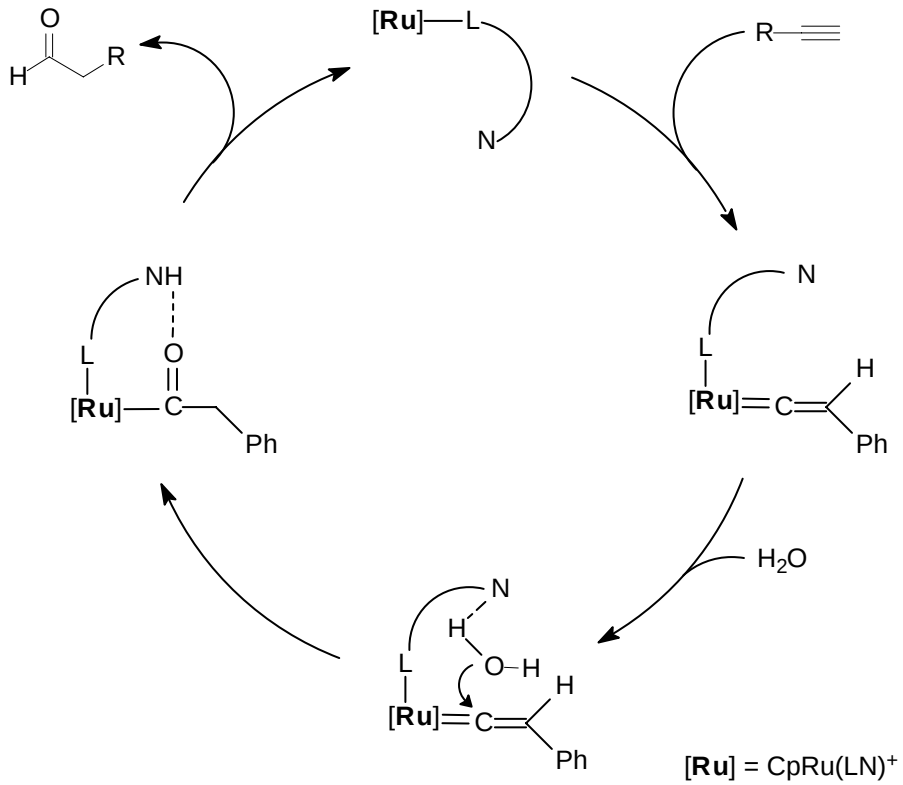

Scheme 1.6 Mechanism of Ru-catalyzed hydration of terminal alkynes

Chapter 2 Ruthenium-Catalyzed *β*-Alkylation of Secondary Alcohols with Primary Alcohols

2.1 Introduction

β-alkylation of secondary alcohols to give higher alcohols is a rather tedious multi-step process that involves alcohol oxidation, ketone alkylation and ketone reduction and produces a lot of waste. A one-pot catalytic *β*-alkylation of secondary alcohols with primary alcohols to give higher alcohols with water as the only by-product (**eq. 2.1**) is therefore a highly desirable process.

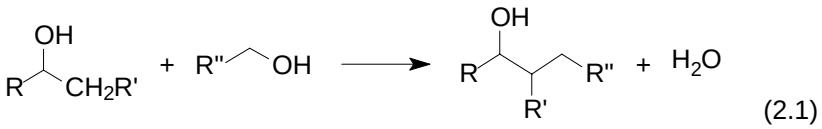

(2.1)

Despite its obvious merits, the number of catalytic systems known to affect this reaction is surprisingly small. On the other hand, alkylation of a range of nucleophilic agents with primary alcohols has been reported.[108, 109] The first reported one-pot catalytic reaction based on the $RuCl_2(PPh_3)_3$/KOH system was reported by Cho and Shim.[18] The reported mechanism proceeded via the oxidations of both primary and secondary alcohols to the corresponding aldehyde and ketone, which underwent an aldol concentration to afford an *α,β*-unsaturated ketone. Subsequent hydrogenation of the *α,β*-unsaturated ketone gave the desired product (**Scheme 2.1**). The reaction, unfortunately, required the addition of large amount of sacrificial hydrogen acceptor (5 equiv. of 1-dodecene); addition of 1-dodecene seems to be considered as a faster regeneration of [Ru] from [Ru]H_2 generated in the initial oxidation stages by reducing 1-dodecene to dodecane.

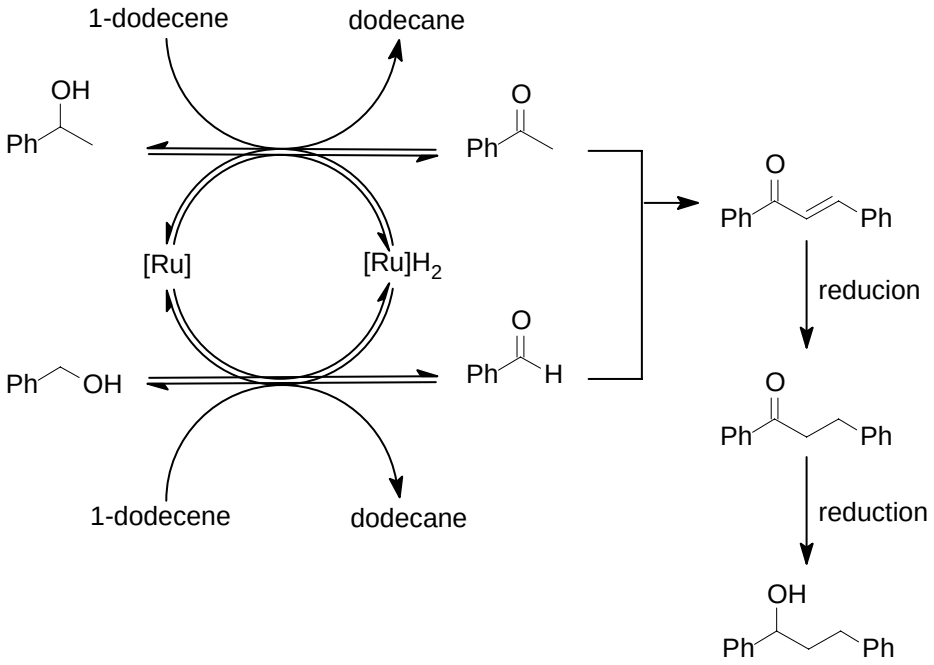

Scheme 2.1 Mechanism of Ru-catalyzed one-pot *β*-alkylation of secondary alcohols with primary alcohols

It was briefly mentioned in a paper on the ruthenium-catalyzed dehydrogenation of alcohols that the Grubb's catalyst $PhCH=Ru(PCy_3)_2Cl_2$ and the other ruthenium complex $[(p\text{-Cymene})RuCl_2]_2$ were able to catalyze *β*-alkylation of 1-phenylethanol with benzyl alcohol; considerable amount of 1,3-diphenylpropan-1-one was formed in addition to the alkylation product 1,3-diphenylpropan-1-ol. No other substrates other than the 1-phenylethanol/benzyl alcohol pair were studied. The major catalytic pathway is supposed to be similar to those proposed by Cho, Shim and co-workers.[110] The solvento complex $[RuCl_2(DMSO)_4]$ was found to be an active catalyst for the *β*-alkylation of secondary alcohols with primary alcohols, giving high yields of higher alcohols; however, a relatively high catalyst loading (2 mol%) and an exceedingly long

reaction time (7 days) were required.[111] The iridium complex $(Cp^*IrCl_2)_2$ has also been shown to be an efficient catalyst for the reaction; this complex is, however, very expensive.[19] It has been learned very recently that the two ruthenium Janus-Head complexes (one dinuclear, the other tetranuclear, **Chart 2.1**) with a triazolediylidene ligand exhibit high catalytic activity for both aliphatic and aromatic alcohols.[112]

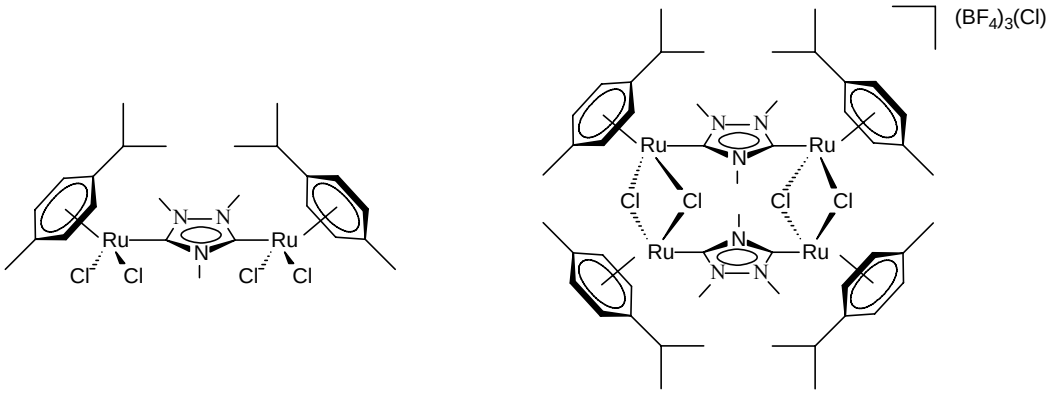

Chart 2.1

Reported here are a number of catalytic systems based on ruthenium complexes for the *β*-alkylation of secondary alcohols with primary alcohols without any sacrificial additives. More information on the mechanism of the catalytic reaction is provided.

2.2 Experimental Section

2.2.1 Materials and Instrumentation

All manipulations were carried out under nitrogen atmosphere using standard Schlenk techniques. Solvents were freshly distilled under nitrogen from sodium-benzophenone (tetrahydrofuran), sodium (diethyl ether, hexane and toluene), calcium hydride (dichloromethane, chloroform and acetonitrile), magnesium-iodine (methanol and ethanol) or P_2O_5 (C_6D_6 and $CDCl_3$); they were degassed prior to use. Elemental analyses were performed by M-H-W Laboratories, Phoenix, AZ (USA). ^{1}H NMR spectra were obtained from a Bruker DPX-400 spectrometer at 400.13 MHz; chemical shifts were reported relative to residual peaks of the deuterated solvents used ($CDCl_3$ δ 7.26 ppm, C_6D_6 δ 7.24 ppm). $^{13}C\{^1H\}$NMR spectra were recorded with a Bruker DPX-400 spectrometer at 100.61 MHz; chemical shifts were internally referenced to $CDCl_3$ (δ = 77.7 ppm) or C_6D_6 (δ = 128.1 ppm). $^{31}P\{^1H\}$NMR spectra were recorded on a Bruker DPX-400 spectrometer at 161.70 MHz; chemical shifts were externally referenced to 85% H_3PO_4 in D_2O (δ 0.00 ppm). Infrared spectra were obtained from a Bruker Vector 22 FT-IR spectrophotometer. Mass spectrometry was carried out with a Finnigan MAT 95S mass spectrometer with the samples dissolved in dichloromethane or acetone. HRMS was carried out with Waters Micromass Q-Tof-2. The complexes $[CpRu(PPh_3)_2(CH_3CN)]^+BF_4^-$ (**M1**),[113] $CpRu(PPh_3)_2Cl$ (**M2**),[114] CpRu(dppm)Cl (**M3**),[115] $TpRu(PPh_3)_2Cl$ (**M4**),[116] $[TpRu(dppm)(CH_3CN)]^+BF_4^-$ (**M5**),[117] and $TpRu(PPh_3)(CO)Ph$ (**M7**)[118] were prepared according to methods provided in literature.

2.2.2 Syntheses and Reactions

2.2.2.1 $CpRu(PPh_3)(CO)Ph$ (M7)

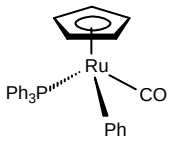

A sample of $CpRu(PPh_3)_2Cl$ (0.50g, 0.69mmol) and NaOH (0.55g, 0.014mol) were loaded into a two-necked round bottom flask, which was then evacuated and flushed with nitrogen for four cycles. Freshly degassed toluene (20 mL) and benzyl alcohol (0.21mL, 2.07mmol) were added to a flask and the resulting mixture was refluxed with stirring for 16h. At the end of this period, the solution was cooled to room temperature and filtered through Celite. The solvent of the filtrate was removed under reduced pressure to yield a pale yellow paste. Hexane (5 mL) was added to the residue, with stirring, to produce a pale yellow solid. The solid was filtered out and washed with diethyl ether (2 × 5 mL). It was collected and dried under vacuum at room temperature. Yield: 0.15 g (41 %). Anal. Calcd (%) of $C_{30}H_{25}OPRu$: C 67.53, H 4.72. Found: C 67.45, H 4.61. IR. (KBr, cm^{-1}): $\upsilon_{(C\equiv O)}$ 1919 (vs). ^1H NMR (400.13 MHz, C_6D_6, 25°C): δ 7.64–7.66 (m, 2H; Ph–*H*), δ 7.45–7.49 (m, 6H; PPh_3–*H*), δ 7.06–7.08 (m, 9H; PPh_3–*H*), δ 7.06–7.08 (m, 3H; Ph–*H*), δ 4.81 (s, 5H; Cp–*H*). $^{31}P\{^1H\}$NMR (161.7MHz, $CDCl_3$, 25°C): δ 59.70 (s). $^{13}C\{^1H\}$NMR (100.61 MHz, C_6D_6, 25 °C): δ 207.67 (d, $^2J_{PC}$ = 20.9 Hz, Ru-*C*O); δ 149.58 (d, $^2J_{PC}$ = 13.8 Hz, ipso C of Ru-C_6H_5). ESI-MS: *m/z* 533.93, $[M]^+$.

2.2.2.2 $CpRu(PPh_3)(CO)$(3,4-dimethoxyphenyl) (M12)

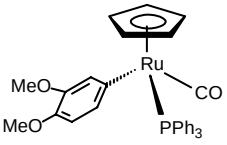

A procedure similar to that for the synthesis of the complex $CpRu(PPh_3)(CO)Ph$ was followed, except that 3,4-Dimethoxybenzyl alcohol (0.30 ml, 2.07 mmol) was used in

place of the benzyl alcohol. Yield: 0.15 g (37 %). Anal. Calcd (%) of $C_{32}H_{29}O_3PRu$: C 64.75, H 4.92. Found: C 63.25, H 4.70. IR. (KBr, cm^{-1}): $\upsilon_{(C\equiv O)}$ 1917 (vs). ^1H NMR (400.13 MHz, C_6D_6, 25°C): δ 7.44-7.49 **(**m, 6H; PPh_3-*H*), δ 7.07-7.08 **(**m, 9H; PPh_3 PPh_3-*H*)**,** δ 7.07-7.08 (m, 1H; 3,4-dimethoxyphenyl-*H*)**,** δ 6.99 (s, 1H; 3,4- dimethoxyphenyl-*H*), δ 6.72 (d, 1H**;** 3,4-dimethoxyphenyl-*H*), δ 4.87 (s, 5H; Cp-*H*), δ 3.64 (s, 3H; 3,4-dimethoxyphenyl-CH_3), δ 3.47 (s, 3H**;** 3,4-dimethoxyphenyl-CH_3), $^{31}P\{^1H\}$NMR (161.7MHz, $CDCl_3$, 25°C): δ 60.02 (s). $^{13}C\{^1H\}$NMR (100.61 MHz, C_6D_6, 25 °C): δ 207.45 (d, $^2J_{PC}$ = 20.9 Hz, Ru-*C*O). ESI-MS: *m/z* 594.09, $[M]^+$.

2.2.2.3 TpRu(PPh_3)(CO)(3,4-dimethoxyphenyl) (M13)

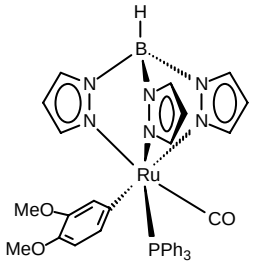

A sample of TpRu(PPh_3)$_2$Cl (0.5g, 0.57mmol) and NaOH (0.46g, 0.011mol) were loaded into a two-necked round bottom flask, which was then evacuated and flushed with nitrogen for four cycles. Freshly degassed toluene (20 mL) and 3,4-Dimethoxybenzyl alcohol (0.25 ml, 1.71mmol) were added to a flask and the resulting mixture was refluxed with stirring for 16h. At the end of this period, the solution was cooled to room temperature and then filtered through Celite. The solvent of the filtrate was removed under reduced pressure and a white paste was precipitated out. Hexane (5 mL) was added to the residue, with stirring, to produce a white solid. The solid was filtered out and washed with diethyl ether (2 × 5 mL). It was then collected and dried under vacuum at room temperature. Yield: 0.31 g (73%). Anal. Calcd (%) of $C_{36}H_{34}BN_6O_3PRu$: C 58.31, H 4.62. Found: C 58.12, H 4.58. IR. (KBr, cm^{-1}): $\upsilon_{(B-H)}$ 2487 (br), $\upsilon_{(C\equiv O)}$ 1935 (vs). ^1H NMR (400.13 MHz, C_6D_6, 25°C): δ 7.75 (d, 1H;

Tp-*H*), δ 7.65 (d, 1H; Tp-*H*), δ 7.59 (d, 1H; Tp-*H*), δ 7.31–7.34 (m, 3H; PPh_3-*H*), δ 7.15–7.19 (m, 6H; PPh_3-*H*), δ 7.09 (d, 1H; Tp-*H*), δ 6.85–6.89 (m, 6H; PPh_3-*H*), δ 6.82 (d, 1H; Tp-*H*), δ 6.63 (d, 1H; Tp-*H*), δ 6.47 (s, 1H; 3,4-dimethoxyphenyl-*H*)**,** δ 6.45 (s, 1H; 3,4-dimethoxyphenyl-*H*), δ 6.36 (s, 1H**;** 3,4-dimethoxyphenyl-*H*)**,** δ 6.02 (t, 1H; Tp-*H*), δ 5.92 (t, 1H; Tp-*H*), δ 5.88 (t, 1H; Tp-*H*), δ 3.81 (s, 3H; 3,4-dimethoxyphenyl-CH_3)**,** δ 3.34 **(**s, 3H; methoxyl group of ,4-dimethoxyphenyl-CH_3)**,** $^{31}P\{^1H\}$NMR (161.7MHz, $CDCl_3$, 25°C): δ 50.32 (s). $^{13}C\{^1H\}$NMR (100.61 MHz, C_6D_6, 25 ˚C): δ 207.77 (d, $^2J_{PC}$ = 15.7 Hz, Ru-*C*O), δ 152.23 (d, $^2J_{PC}$ = 12.5 Hz, ipso C of Ru-3,4-dimethoxyphenyl). ESI-MS: *m/z* 742.15, $[M]^+$.

2.2.2.4 General Procedure for Catalytic *β*-Alkylation of Secondary Alcohols

The reactions were carried out in 11 mm Schlenk tubes equipped with Teflon screw caps. In a typical run, ruthenium complex (0.005 mmol) and NaOH (0.25 mmol) were loaded into the tube equipped with a magnetic stirrer. The system was evacuated and filled with nitrogen for four cycles. Secondary alcohol (1.25 mmol) and primary alcohol (1.5 mmol) were then added to the tube via syringes and needles. The tube was sealed with the screw cap and the solution was stirred in a silicon oil bath at 120°C for 24 h. At the end of this period, the tube was cooled to room temperature; a 0.1 mL aliquot of the solution was removed and analyzed by ^1H NMR spectroscopy (in $CDCl_3$). Comparison of the integrations of the characteristic peaks of the product and the unreacted secondary alcohol gave the conversions of the reactions. The organic products **3a, 3c, 3h-3k, 3s**;[19] **3m**, **3t**;[18] **3n**;[119] **3p**;[120] **3q**[121] and **3r**[12] described in **Table 2.2** are known and were characterized by comparing their ^1H and

$^{13}C\{^{1}H\}$NMR data with the reported ones. In cases where the organic products are new compounds (**3b**, **3d-3g**, **3l**), they were isolated by flash column chromatography on silica gel or by preparative thin layer chromatography (silica gel) and were characterized by ^{1}H, $^{13}C\{^{1}H\}$NMR, mass spectrometry and HRMS analysis.

2.2.2.5 3-(2-methoxyphenyl)-1-phenylpropan-1-ol (3b)

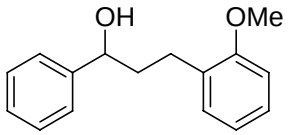

Pale yellow oil; ^{1}H NMR (400 MHz, $CDCl_3$): δ 7.38-6.87 (m, 9H; Ar–*H*), δ 4.64 (t, *J* = 6 Hz, 1H; Ph–C*H*(OH)), δ 3.84 (s, 3H; Ph–OCH_3), δ 2.80-2.76 (t, *J* = 8 Hz, 2H; –CH_2CH_2Ar), δ 2.49 (s, 1H; Ph–CH(O*H*)), δ 2.11-2.01 (m, 2H; –CH_2CH_2Ar); $^{13}C\{^{1}H\}$NMR (100 MHz, $CDCl_3$): δ 157.4, 144.7, 130.1, 128.4, 127.4, 127.3, 126.0, 120.7, 110.4, 73.6, 55.4, 39.4, 26.5; HRMS (+ESI): *m*/*z*: calcd for $C_{16}H_{18}O_2Na^+$: 265.1204; found: 265.1216 $[M+Na]^+$.

2.2.2.6 3-(3,4-dimethoxyphenyl)-1-phenylpropan-1-ol (3d)

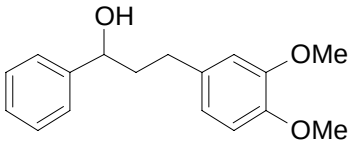

Pale yellow oil; ^{1}H NMR (400 MHz, $CDCl_3$): δ 7.38-7.30, 6.82-6.76 (m, 8H; Ar–*H*), δ 4.68 (t, J = 6 Hz, 1H; Ph–C*H*(OH)), δ 3.86 (s, 6H; Ph–OCH_3), δ 2.90 (s, 1H; Ph–CH(O*H*)), δ 2.74-2.65 (m, 2H; –CH_2CH_2Ar), δ 2.15-2.04 (m, 2H; –CH_2CH_2Ar); $^{13}C\{^{1}H\}$NMR (100 MHz, $CDCl_3$): δ 148.8, 147.1, 144.8, 134.5, 128.4, 127.5, 126.0, 120.3, 111.9, 111.4, 73.7, 55.9, 55.8, 40.7, 31.7; HRMS (+ESI): *m*/*z*: calcd for $C_{17}H_{20}O_3Na^+$: 295.1310; found: 295.1313 $[M+Na]^+$.

2.2.2.7 3-(4-fluorophenyl)-1-phenyl-propan-1-ol (3e)

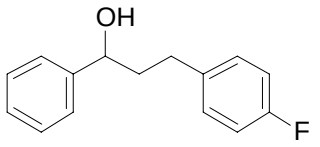

Colorless oil; ^{1}H NMR (400 MHz, $CDCl_3$): δ 7.37-6.94 (m, 9H; Ph–*H*), δ 4.61 (t, *J* = 6Hz, 1H; Ph–C*H*(OH)), δ 2.69-2.60 (m, 2H; –CH_2CH_2Ar), δ 2.48 (s, 1H; Ph–C*H*(OH)), δ 2.08-1.95 (m, 2H; –CH_2CH_2Ar); ^{13}C{^{1}H}NMR (100 MHz, $CDCl_3$): δ 162.5, 160.1, 144.5, 137.5, 137.4, 129.8, 128.6, 127.7, 126.0, 115.2, 115.0, 73.7, 40.6, 31.2; HRMS (+ESI): *m*/*z*: calcd for $C_{15}H_{15}OFNa^{+}$: 253.1005; found: 253.1017 $[M+Na]^{+}$.

2.2.2.8 3-(furan-2-yl)-1-phenylpropan-1-ol (3f)

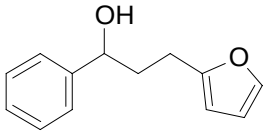

Pale yellow oil; ^{1}H NMR (400 MHz, $CDCl_3$): δ 7.34-7.27 (m, 6H; Ph–*H* + 5-furyl–*H*), δ 6.28 (d, *J* = 2 Hz, 1H; 4-furyl–*H*), δ 5.99 (d, *J* = 2 Hz; 1H, 3-furyl–*H*), δ 4.65 (t, *J* = 6 Hz, 1H; Ph–C*H*(OH)), δ 2.72-2.67 (m, 2H; –CH_2CH_2(2-furyl)), δ 2.40 (s, 1H; Ph–CH(O*H*)), δ 2.09-2.02 (m, 2H; –CH_2CH_2(2-furyl)). ^{13}C{^{1}H}NMR (100 MHz, $CDCl_3$): δ 155.6, 144.4, 141.0, 128.5, 127.7, 126.0, 110.2, 105.1, 73.6, 37.1, 24.4. HRMS (+ESI): *m*/*z*: calcd for $C_{13}H_{14}O_2Na^{+}$: 225.3903; found: 225.3907 $[M+Na]^{+}$

2.2.2.9 1-phenyl-(3-thiophen-2-yl)-propan-1-ol (3g)

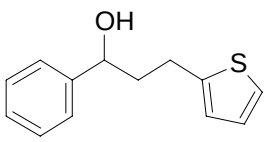

Colorless oil; ^{1}H NMR (400 MHz, $CDCl_3$): δ 7.35-7.27 (m, 5H; Ph–*H*), δ 7.13 (d, *J* = 5 Hz, 1H; thiophen-5-yl–*H*), δ 6.93 (dd, *J* = 5, 3 Hz, 1H; thiophen-4-yl–*H*), δ 6.81 (d, J = 3 Hz, 1H; thiophen-3-yl–*H*), δ 4.67 (t, *J* = 6 Hz, 1H; Ph–C*H*(OH)), δ

2.94-2.88 (m, 2H; –CH_2CH_2(thiophen-2-yl)), δ 2.46 (s, 1H; Ph–CH(O*H*)), δ 2.18-2.05 (m, 2H; –CH_2CH_2(thiophen-2-yl)). $^{13}C\{^1H\}$NMR (100 MHz, $CDCl_3$): δ 144.7, 144.4, 128.6, 127.7, 126.9, 126.0, 124.4, 123.2, 73.5, 40.7, 26.3. HRMS (+ESI): *m*/*z*: calcd for $C_{13}H_{14}ONaS^+$: 241.0663; found: 241.0663 $[M+Na]^+$.

2.2.2.10 3-cyclohexyl-1-phenylpropan-1-ol (3l)

White solid; ^1H NMR (400 MHz, $CDCl_3$): δ 7.36-7.25 (m, 5H, Ph–*H*), δ 4.62 (t, *J* = 6 Hz, 1H; Ph–C*H*(OH)), δ1.88 (s, 1H; Ph–CH(O*H*)), δ1.73-1.67 (m, 6H; Ph–CH(OH)CH_2CH_2 + Cy–*H*), δ1.26-1.13 (m, 7H; Ph–CH(OH)CH_2CH_2 + Cy–*H*), δ0.87-0.85 (m, 2H; Cy–*H*); $^{13}C\{^1H\}$NMR (100 MHz, $CDCl_3$): δ 145.6, 129.1, 127.9, 126.6, 75.7, 38.3, 37.0, 34.1, 34.0, 27.3, 27.0. HRMS (+ESI): *m*/*z*: calcd for $C_{15}H_{22}ONa^+$: 241.1568; found: 241.1559 $[M+Na]^+$.

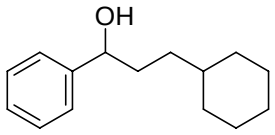

2.2.2.11 NMR Monitoring of Ru(II)–Catalyzed *β*-Alkylation of 1-Phenylethanol with Benzyl Alcohol

The reactions were carried out in 5 mm NMR tubes capped with rubber septa. In a typical run, ruthenium complex (0.01 mmol, 1 mol %) and NaOH (0.2 mmol, 20 mol %) were loaded to a NMR tube. The system was then evacuated and filled with nitrogen for four cycles. Toluene (0.2 mL), 1-phenylethanol (1 mmol) and benzyl alcohol (1.2 mmol) were then added to the NMR tube via syringes and needles. The resulting solution was heated in a silicon oil bath at 120^{o}C. At different time intervals, the NMR tube was rapidly cooled down to room temperature and $^{31}P\{^1H\}$NMR spectra of the solution were taken. The relative concentrations of the species present were obtained by comparing the integrations of their signals in the $^{31}P\{^1H\}$NMR spectra.

2.2.2.12 Crystallographic Structures Analysis of $CpRu(PPh_3)(CO)$(3,4-dimethoxyphenyl) (M12) and $TpRu(PPh_3)(CO)$(3,4-dimethoxyphenyl) (M13)

Crystals suitable for X-ray diffraction study for **M12** and **M13** were obtained by layering of hexane onto saturated dichloromethane solutions of the complexes. A suitable crystal of each of the complexes was mounted on a Bruker CCD area detector diffractomer and subjected to Mo Kα radiation (λ = 0.71073 Å) from a generator operating at 50 kV and 30 mA. The intensity data of **M12** and **M13** were collected in the range θ = 2.31 – 27.49° and 2.01 – 27.50°, respectively, with oscillation frames of ψ and ω in the range 0 – 180°. A total of 1216 frames in **M12** and 380 frames in **M13** were taken in four shells. An empirical absorption correction of the SADABS (Sheldrick, 1996) program based on Fourier coefficient fitting was applied. The crystal structures were solved by Patterson function methods and expanded by difference Fourier synthesis, then refined by full-matrix least-squares on F^2 using the Bruker Smart and Bruker SHELXTL program packages. All non-hydrogen atoms were refined anisotropically. Hydrogen atoms were placed in ideal positions and refined as riding atoms. The R and R_w values of **M12** are 0.0270 and 0.0685, respectively, and those of **M13** are 0.0228 and 0.0600, respectively. Further crystallographic details and selected bond distances and angles for **M12** and **M13** can be found in the results and discussion section.

2.3 Results and Discussion

2.3.1 CpRu(dppm)Cl (M3)-Catalyzed *β*-Alkylation of 1-Phenylethanol with Benzyl Alcohol

The alkylation of 1-phenylethanol (**1a**) with benzyl alcohol (**2a**) to give the corresponding alcohol, 1,3-diphenyl-propan-ol (**3a**), was chosen as the model reaction in order to optimize the various parameters (**Table 2.1**, **eq. 2.2**). When the reaction of **1a** (1.25 mmol) and **2a** (1.5 mmol) was carried out in the presence of CpRu(dppm)Cl (**M3**) (0.005 mmol) and NaOH (0.25 mmol) at 120^{o}C for 24 h, 1,3-diphenyl-propan-ol (**3a**) was formed in a conversion of 94% along with a small amount of benzylacetophenone (entry 1). KOH and KO^{t}Bu were also effective for the reaction (entries 2, 3). But the reaction failed when other bases such as DBU and Na_2CO_3 were used (entries 4, 5). Decrease in temperature also gave lower yields (entries 6, 7 & 8). In addition, reactions in different solvent systems were also tested, in all cases unsatisfactory results were obtained (entries 9-12).

Table 2.1. **Optimization of *β*-alkylation of Secondary Alcohols with Primary Alcohols**[a]

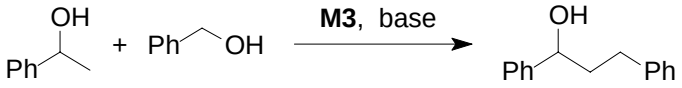

1a **2a** **3a** (2.2)

entry	base	solvent (mL)	temperature (^{o}C)	% conversion[b]
1	NaOH	none	120	94 (3)
2	KOH	none	120	70 (3)
3	KO^{t}Bu	none	120	80 (4)
4	DBU	none	120	0 (1)
5	Na_2CO_3	none	120	0 (0)
6	NaOH	none	60	0 (0)
7	NaOH	none	80	4 (0)
8	NaOH	none	100	40 (1)
9	NaOH	Toluene (0.3)	120	60 (2)
10	NaOH	Benzene (0.3)	120	38 (1)
11	NaOH	Dioxane (0.3)	120	20(0)
12	NaOH	THF (0.3)	120	12 (0)

[a]Reaction conditions: catalyst **M3** (0.005 mmol), 1-phenylethanol (1.25 mmol), benzyl alcohol (1.5 mmol), base (0.25 mmol, 20 mol% w.r.t. 1-phenylethanol), 24h.

[b]Conversion (based on 1-phenylethanol) determined by ^{1}H NMR spectroscopy. Values in parenthesis indicate the conversion of corresponding ketone.

2.3.2 Ru(II)-Catalyzed *β*-Alkylation of Secondary Alcohols with Primary Alcohols

On the basis of the above results, we next examined the reaction of various secondary alcohols with primary alcohols under optimized conditions. A number of ruthenium complexes supported by cyclopentadienyl (Cp) and hydrotris(pyrazolyl)borato (Tp) ligands were found to be active catalysts for the *β*-alkylation of secondary alcohols with primary alcohols (**Table 2.2**). The controlled experiment, in which no complex was present, shows that *β*-alkylation

of 1-phenylethanol (**1a**) with benzyl alcohol (**2a**) only proceeds to a small extend (entry 1, foot note c). The Cp and Tp complexes are in general of similar activity. In a few cases (entries 2, 4-7, 12) where the *β*-alkylation products are new compounds, they were isolated and characterized. Aryl methyl carbinols can be alkylated with many primary alcohols. The reactions with benzyl alcohols derivatives and heterocyclic alcohols (entries 1-7) give higher conversions than with primary aliphatic alcohols (entries 8-12). Lowering of conversion in alkylation reactions with primary alkyl alcohol is not attributable to self-condensation of these alcohols as no self-condensation products were detected in the reactions; it is probably due to diminished electrophilicity of the carbonyl carbon atoms of the aldehydes generated via oxidation of the primary alkyl alcohols. Alkyl methyl carbinols seem to be less active than their aryl analogues toward *β*-alkylation (entries 15-17). 1-phenyl-1-propanol, however, does not undergo alkylation. All of the complexes **M1-M5** are basically inactive for the *β*-alkylation of alkyl methyl carbinols with primary alkyl alcohol (entries 20, 21); other known ruthenium catalysts do not seem to be active for the coupling of alkyl methyl carbinols with primary alkyl alcohols as well.[18, 110-112] Alkylation of 1,2,3,4-tetrahydro-1-naphthol (**1g**) gives mixtures of diastereomers (entries 18-19).

Table 2.2 Ru(II)-catalyzed *β*-alkylation of Secondary Alcohols with Primary Alcohols[a]

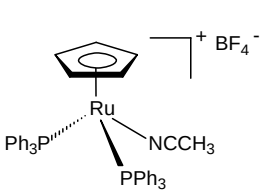

M1

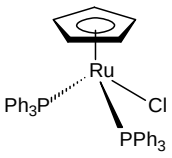

M2

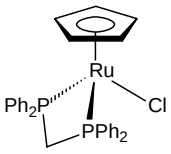

M3

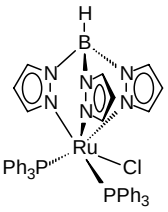

M4

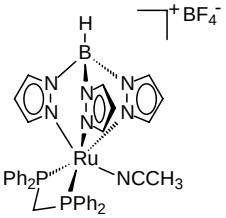

M5

entry	2° alcohol	1° alcohol	product	% conversion[b]				
			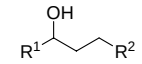	**M1**	**M2**	**M3**	**M4**	**M5**
1	**1a** R^1 = Ph	**2a** R^2 = Ph	**3a**	11(1)[c]	88(7)	71(3)	94(3)	73(13)	74(13)
2	**1a**	**2b** R^2 = 2-$MeOC_6H_4$	**3b**		77(6)	84(6)	81(7)	74(10)	78(8)
3	**1a**	**2c** R^2 = 4-$MeOC_6H_4$	**3c**		78(5)	84(6)	85(5)	88(6)	83(8)
4	**1a**	**2d** R^2 = 3,4-$(MeO)_2C_6H_3$	**3d**		91(7)	85(8)	84(3)	88(6)	80(10)
5	**1a**	**2e** R^2 = 4-FC_6H_4	**3e**		61(3)	66(2)	71(2)	77(9)	77(9)
6	**1a**	**2f** R^2 = 2-furyl	**3f**		83(7)	82(5)	82(0)	73(10)	79(4)
7	**1a**	**2g** R^2 = thiophen-2-yl	**3g**		79(2)	88(0)	80(2)	77(10)	91(5)
8	**1a**	**2h** R^2 = phenethyl	**3h**		65(9)	48(5)	57(0)	60(4)	56(5)
9	**1a**	**2i** R^2 = benzyl	**3i**		30(0)	8(0)	8(0)	21(3)	29(4)
10	**1a**	**2j** R^2 = Pr	**3j**		30(8)	40(3)	26(3)	29(3)	28(3)
11	**1a**	**2k** R^2 = ^{i}Pr	**3k**		37(8)	23(4)	15(0)	20(0)	14(0)
12	**1a**	**2l** R^2 = Cy	**3l**		52(5)	40(4)	13(0)	29(2)	32(2)
13	**1b** R^1 = 4-$MeOC_6H_4$	**2a**	**3m**		78(17)	60(20)	74(17)	70(25)	68(20)
14	**1c** R^1 = 4-ClC_6H_4	**2a**	**3n**		75(0)	72(0)	87(4)	93(3)	92(6)
15	**1d** R^1 = phenethyl	**2a**	**3p**		57(0)	31(0)	54(9)	31(0)	46(0)
16	**1e** R^1 = Cy	**2a**	**3q**		59(6)	50(5)	35(3)	60(6)	41(5)
17	**1f** R^1 = *n*-pentyl	**2a**	**3r**		46(4)	49(5)	51(3)	31(4)	25(0)
18	 **1g**	**2j**	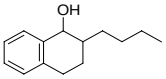 **3s**		46(17) (*Z*:*E* = 70:30)	50(15) (*Z*:*E* = 76:24)	24(3) (*Z*:*E* = 67:33)	46(18) (*Z*:*E* = 74:26)	30(14) (*Z*:*E* = 77:23)
19	**1g**	**2a**	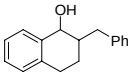 **3t**		42(9) (*Z*:*E* = 40:60)	47(6) (*Z*:*E* = 53:47)	54(3) (*Z*:*E* = 46:54)	30(11) (*Z*:*E* = 57:43)	53(13) (*Z*:*E* = 47:53)
20	**1d**	**2j**	**3u**		Trace[d]	Trace[d]	Trace[d]	Trace[d]	Trace[d]
21	**1f**	**2j**	**3v**		Trace[d]	Trace[d]	Trace[d]	Trace[d]	Trace[d]

[a]Reaction conditions: catalyst (0.005 mmol), 2° alcohol (1.25 mmol), 1° alcohol (1.5 mmol), NaOH (0.25 mmol, 20 mol% w.r.t. 2° alcohol), 120°C, 24 h.

[b]Conversion (based on 2° alcohol) determined by ^{1}H NMR spectroscopy. Values in parenthesis indicate the conversion of corresponding ketone.

[c]Controlled experiment, no complex was present.

[d]Trace amount of the ketone product.

2.3.3 NMR Monitoring of Ru(II)–Catalyzed *β*-Alkylation of 1-Phenylethanol with Benzyl Alcohol

To gain more insight into the mechanism of the catalytic reactions, the 1-phenylethanol/benzyl alcohol alkylation reactions catalyzed by the Cp and Tp complexes were monitored with $^{31}P\{^{1}H\}$NMR spectroscopy. For the catalytic reaction with the Cp bis(triphenylphosphine) complex **M2** (**Figure 2.1**), it was observed that the complex completely disappeared and was converted to a mixture of the hydride species $CpRu(PPh_3)_2H$ (**M6**) and the phenyl carbonyl complex $CpRu(PPh_3)(CO)Ph$ (**M7**) in a 7:3 ratio within 30 min. The ratio changed to 13:7 after 12h and it remained unchanged at the end of the monitoring (24h). In the **M4**-catalyzed reaction (**Figure 2.2**), the Tp bis(triphenylphosphine) complex was completely converted to a mixture of $TpRu(PPh_3)_2H$ (**M8**) and $TpRu(PPh_3)(CO)Ph$ (**M9**) (in a 17:3 ratio) after 30 min; the ratio became 3:17 after 12h, and **M9** became the only observable species after 24h. In the catalytic reactions with the Cp dppm complexes (**M3**), it was shown by $^{31}P\{^{1}H\}$NMR spectroscopy that **M3** was rapidly converted to the hydride species CpRu(dppm)H (**M10**) (**Figure 2.3**), and it remained the only ruthenium complex detected throughout the catalysis (24h); similar results were observed in the **M5**-catalyzed reaction. In the **M1**-catalyzed reaction, the complexes recovered at the end of the reaction were an 87:13 mixture of **M6** and **M7**. **Table 2.3** summarizes the distribution of the organometallic species at the end of the catalytic reactions.

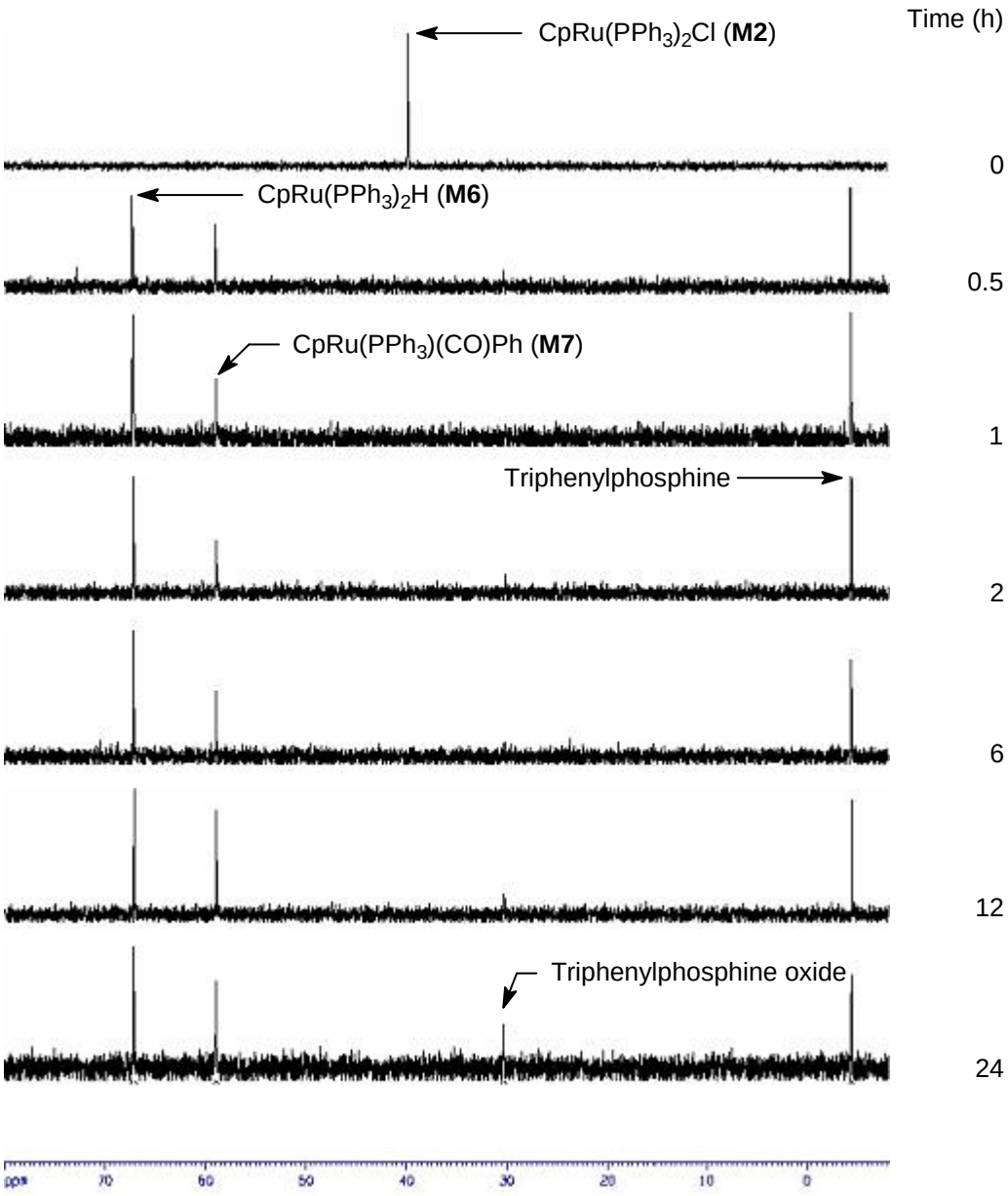

Figure 2.1 $^{31}P\{^{1}H\}$NMR study of $CpRu(PPh_3)_2Cl$ (M2)-catalyzed *β*-alkylation of 1-phenylethanol with benzyl alcohol

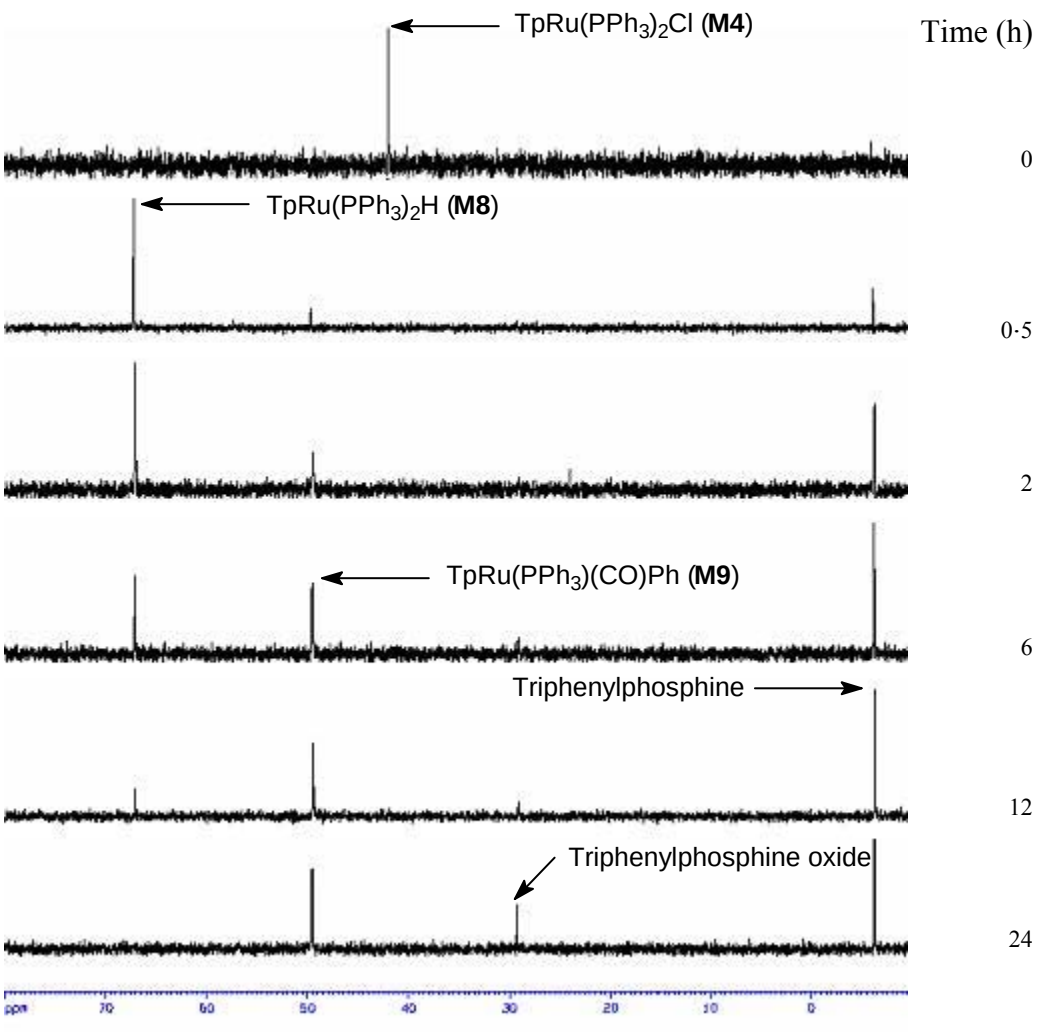

Figure 2.2 $^{31}P\{^{1}H\}$NMR study of $TpRu(PPh_3)_2Cl$ (M4)-catalyzed *β*-alkylation of 1-phenylethanol with benzyl alcohol

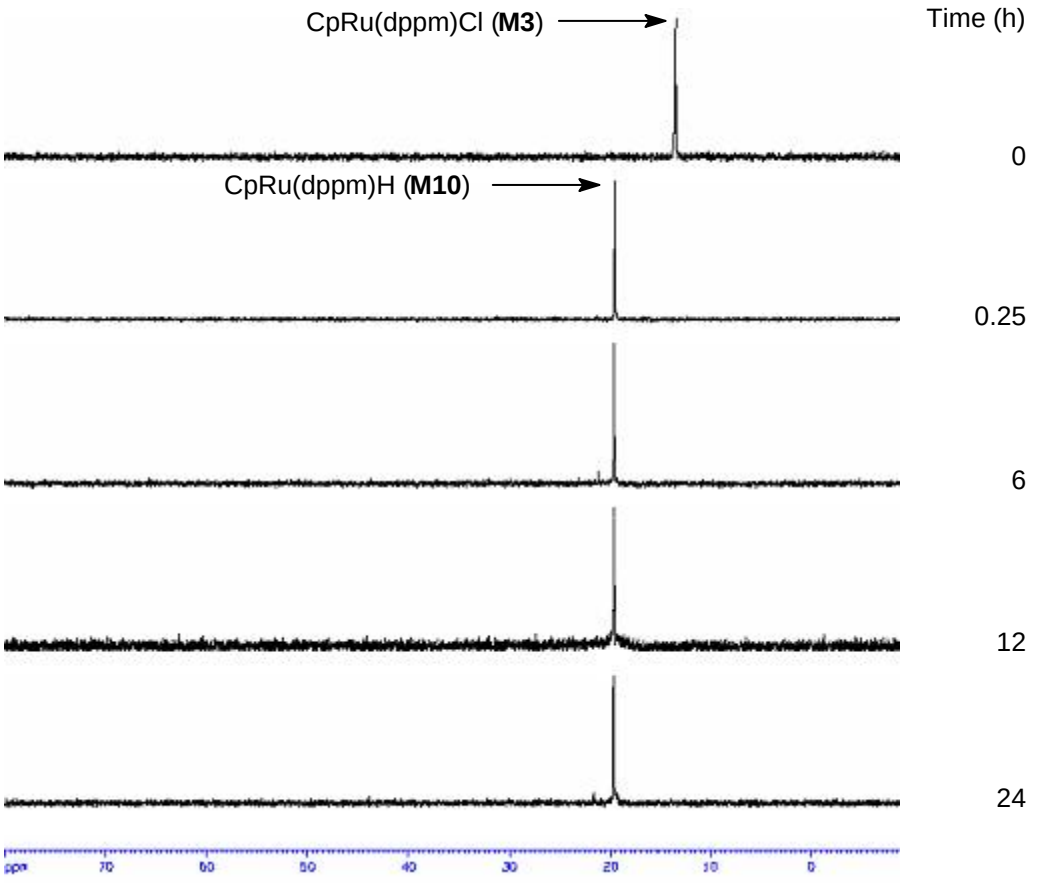

Figure 2.3 $^{31}P\{^{1}H\}$NMR study of CpRu(dppm)Cl (M3)-catalyzed *β*-alkylation of 1-phenylethanol with benzyl alcohol

Table 2.3 Distribution of the Organometallic Species at the end of the Catalytic Reactions with M1-M5[a]

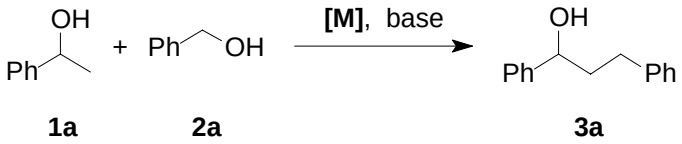

1a **2a** **3a**

Catlyst	Distribution of Ru species[b]
$[CpRu(PPh_3)_2(CH_3CN)]^+BF_4^-$ (**M1**)	**M1** (0%) $CpRu(PPh_3)_2H$ (**M6**) (87%) $CpRu(PPh_3)(CO)Ph$ (**M7**) (13%)
$CpRu(PPh_3)_2Cl$ (**M2**)	**M2** (0%) **M6** (65%) **M7** (35%)
CpRu(dppm)Cl (**M3**)	**M3** (0%) CpRu(dppm)H (**M10**) (100%)
$TpRu(PPh_3)_2Cl$ (**M4**)	**M4** (0%) $TpRu(PPh_3)_2H$ (**M8**) (0%) $TpRu(PPh_3)(CO)Ph$ (**M9**) (100%)
$[TpRu(dppm)(CH_3CN)]^+BF_4^-$ (**M5**)	**M5** (0%) TpRu(dppm)H (**M11**) (100%)

[a]Reaction conditions: toluene (0.2 mL), 1-phenylethanol (1 mmol), benzyl alcohol (1.2 mmol), catalyst (0.01 mmol), NaOH (0.2 mmol), 120˚C, 24 h.

[b]The relative concentrations of the complexes were obtained by the $^{31}P\{^1H\}$NMR integrations.

2.3.4 $CpRu(PPh_3)(CO)Ph$ (M7) and $TpRu(PPh_3)(CO)Ph$ (M9)-Catalyzed *β*-Alkylation of 1-Phenylethanol with Benzyl Alcohol

Quite unexpectedly, the phenyl carbonyl complexes **M7** and **M9** were found to be active catalysts for *β*-alkylation of 1-phenylethanol with benzyl alcohol; **Table 2.4** shows the results of the reactions. Addition of 5 equiv. of triphenylphosphine significantly suppresses the yields (compare entries 1 and 3, 2 and 4), indicating that the dissociation of the phosphine ligand is necessary in the catalysis. The fact that addition of 15-crown-5 and cryptand C221, which are complexing agents for sodium ion, lowers the yields significantly (compare entries 5 with 7 and 9; 6 with 8 and 10) implies that the sodium ion might play a role in the catalytic process. After each of the catalytic process, it was confirmed by $^{31}P\{^1H\}$NMR spectroscopy that the complex remained unchanged.

Table 2.4 $CpRu(CO)(PPh_3)Ph$ (M7) and $TpRu(CO)(PPh_3)Ph$ (M9)-Catalyzed *β*-Alkylation of 1-Phenylethanol with Benzyl Alcohols[a]

1a **2a** **3a** **4a**

entry	catalyst	solvent	additives (mol% w.r.t. **1a**)	% conversion[b]	
				3a	**4a**
1	**M7**	nil	nil	56	2
2	**M9**	nil	nil	48	1
3	**M7**	nil	PPh_3 (2)	23	0
4	**M9**	nil	PPh_3 (2)	18	0
5	**M7**	Toluene (0.5 mL)	nil	43	1
6	**M9**	Toluene (0.5 mL)	nil	38	0
7	**M7**	Toluene[c]	15-crown-5 (40)	25	0
8	**M9**	Toluene[c]	15-crown-5 (40)	21	0
9	**M7**	Toluene[c]	Cryptand C221 (40)	17	0
10	**M9**	Toluene[c]	Cryptand C221 (40)	7	0

[a]Reaction conditions: **1a** (1.25 mmol), **2a** (1.5 mmol), catalyst (0.005 mmol, 0.4 mol% w.r.t. **1a**), base (0.25 mmol, 20 mol% w.r.t. **1a**), 120˚C, 24 h.

[b]Conversion (based on **1a**) determined by ^1H NMR spectroscopy.

[c]Total volume of solvent and additive 0.5mL.

2.3.5 Proposed Mechanism for $CpRu(CO)(PPh_3)Ph$ (M7) and $TpRu(CO)(PPh_3)Ph$ (M9)-Catalyzed *β*-Alkylation of 1-Phenylethanol with Benzyl Alcohol

Scheme 2.2 summarizes the reaction pathways of the **M7** and **M9**-catalyzed *β*-alkylation of 1-phenylethanol with benzyl alcohol consistent with the observed chemistry. Initially, the phosphine ligand is lost to make room for the alkoxide attack; subsequent *β*-elimination yields the anionic metal hydride complex **A**. Although not observed, we propose this species to be the key intermediate of the

catalytic process. Anionic hydrides exhibit hydridic reactivity and have been employed in ketone, aldehyde, alkyl halide, and acyl chloride reduction.[122-126] The initially formed α,β-unsaturated ketone is first reduced in cycle **I**. The reduction might proceed by an associative mechanism in which the Cp ligand or the Tp ligand undergoes ring-slippage or unarming, respectively, to allow substrate coordination to the metal center and subsequent hydride transfer; or the reduction might proceed via an intermolecular hydride transfer process. In both processes, the α,β-unsaturated ketone is activated toward hydride transfer by the sodium ion. The hydride is added to the β-carbon of the substrate probably by virtue of the resonance structure (**Chart 2.2**). It was proposed in the

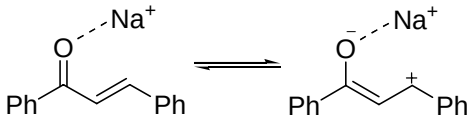

Chart 2.2

hydrogenation of ketones catalyzed by the potassium hydrido(phosphine) ruthenate complexes that the carbonyl group of the ruthenium-coordinated ketone is polarized by the Lewis acid effect of K^+ (**Chart 2.3**). [127] The alternative intermolecular hydride transfer is similar to ionic hydrogenation

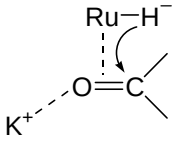

Chart 2.3

of ketones with transition-metal hydride/Brønsted acid (M−H/HA) pair (**Chart 2.4**),[128] with the Na^+ ion playing a similar role as H^+. The saturated ketone produced in cycle **I** is reduced in cycle **II** in a similar manner.

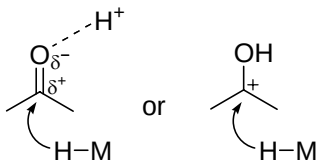

Chart 2.4

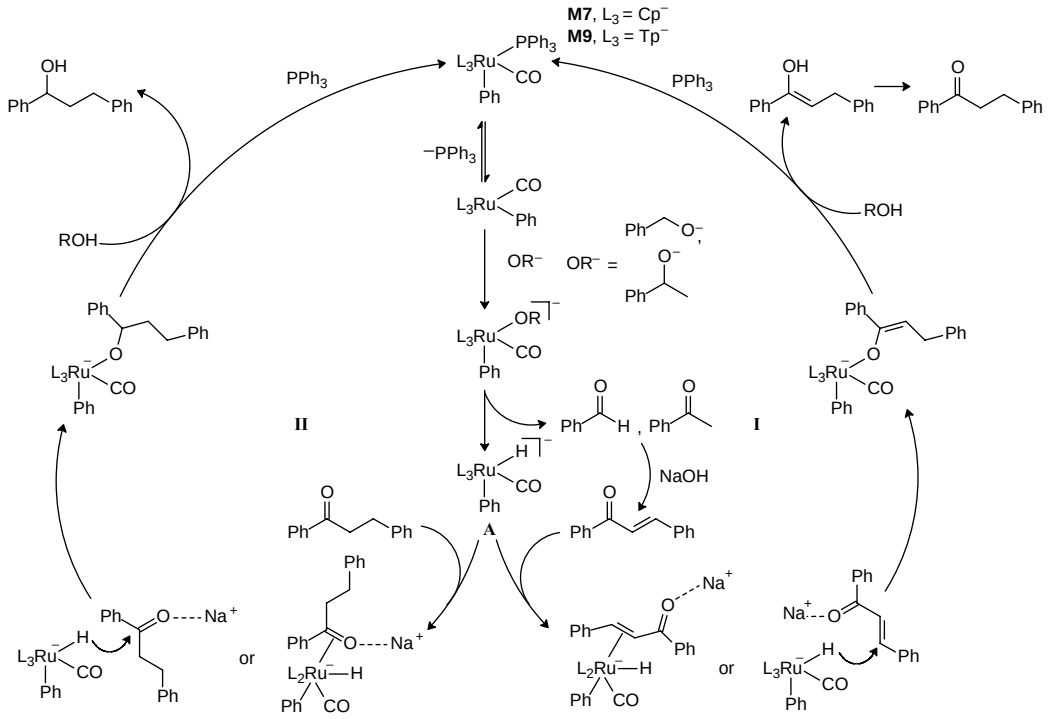

Scheme 2.2 Proposed mechanism of $CpRu(CO)(PPh_3)Ph$ (M7) and $TpRu(CO)(PPh_3)Ph$ (M9)-catalyzed *β*-alkylation of 1-phenylethanol with benzyl alcohol

2.3.6 Preparation and X-ray Crystallographic Studies of $CpRu(PPh_3)(CO)$(3,4-dimethoxyphenyl) (M12) and $TpRu(PPh_3)(CO)$(3,4-dimethoxyphenyl) (M13)

Reaction of 1-phenylethanol (**1a**) and CpRu(dppm)Cl (**M3**) (2 mol%) in the presence of NaOH at 120°C for 4h in C_6D_6 gave CpRu(dppm)H (**M11**) quantitatively. When benzyl alcohol (**2a**) was used in place of **1a**, **M3** was completely converted to **M11** upon 2h of heating. The hydride complexes **M6**, **M8**, **M10**, and **M11** were obviously formed by alkoxide attack at the metal center and subsequent β-elimination; benzaldehyde and acetophenone were then generated concomitantly. Formation of the phenyl carbonyl complexes **M7** and **M9** is probably due to benzaldehyde decarbonylation at the metal center. We had previously reported that $TpRu(PPh_3)(CO)Ph$ (**M10**) could be prepared by reacting $TpRu(PPh_3)(CH_3CN)H$ with benzaldehyde;[118] the analogue $CpRu(PPh_3)(CO)Ph$ (**M8**) was independently prepared in this study. Also the Cp- and Tp-ruthenium carbonyl complexes $CpRu(PPh_3)(CO)$(3,4-dimethoxyphenyl) (**M12**) and $TpRu(PPh_3)(CO)$(3,4-dimethoxyphenyl) (**M13**) were synthesized by reacting the bis(triphenylphosphine)chloro complexes **M2** and **M4** with 3,4-dimethoxybenzyl alcohol in the presence of NaOH (**eq. 2.3**). The structures of **M12** and **M13** were determined by X-ray crystallography. The ORTEP view of the complexes **M12** and **M13** confirms the existence of a 3,4-dimethoxyphenyl moiety as shown in **Figures 2.4** and **2.5**, respectively. Crystal data and structure refinement details are given in **Table 2.5**. Selected bond distances and angles are given in **Tables 2.6** and **2.7** for **M12** and **M1**3, respectively.

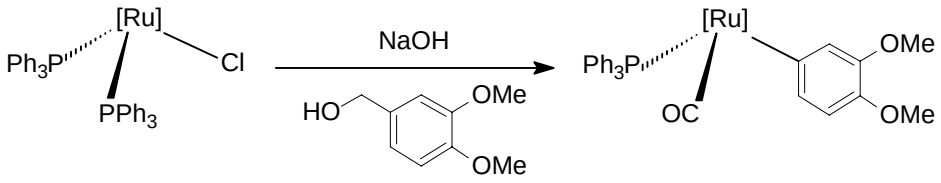

M12 [Ru] = $CpRu^+$
M13 [Ru] = $TpRu^+$ (2.3)

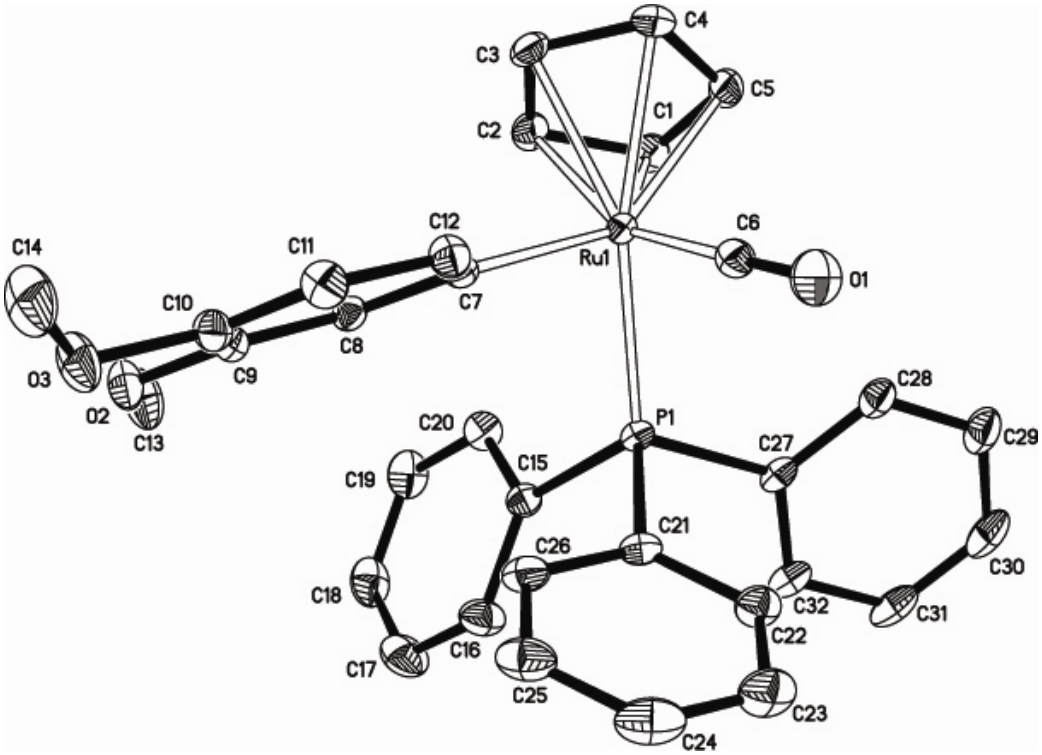

Figure 2.4 ORTEP view (30% probability) of $CpRu(PPh_3)(CO)$(3,4-dimethoxyphenyl) (M12) showing the atom-labeling scheme

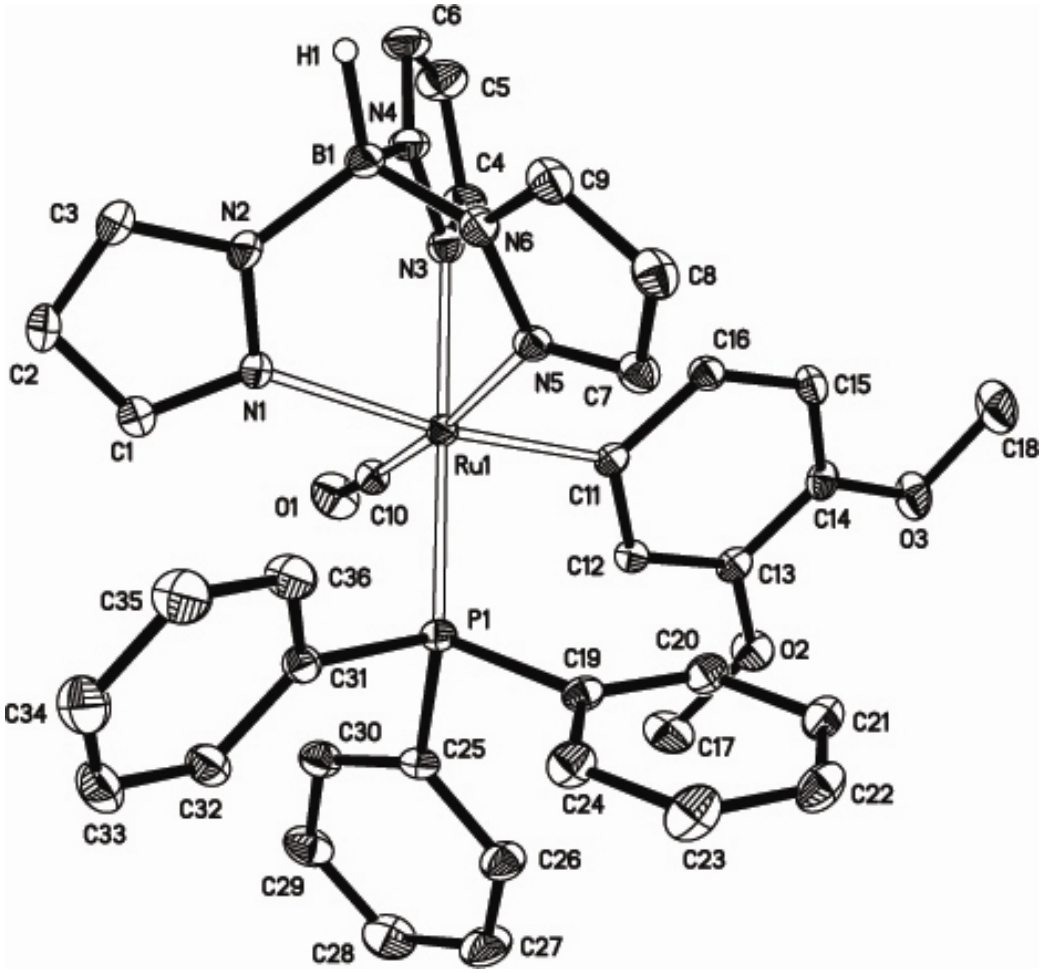

Figure 2.5. **ORTEP view (30% probability) of TpRu(PPh$_3$)(CO)(3,4-dimethoxyphenyl) (M13) showing the atom-labeling scheme**

Table 2.5 Crystal Data and Structure Refinement of $CpRu(PPh_3)(CO)(3,4\text{-dimethoxyphenyl})$ (M12) and $TpRu(PPh_3)(CO)(3,4\text{-dimethoxyphenyl})$ (M13)

Complex	**M12**		**M13**	
Empirical formula	$C_{32}H_{30}O_3PRu$		$C_{36}H_{34}BN_6O_3PRu$	
Formula weight	593.59		741.54	
Temperature	296(2) K		296(2) K	
Wavelength	0.71073 Å		0.71073 Å	
Crystal system	Monoclinic		Triclinic	
Space group	P2(1)/n		P1	
Unit cell dimensions	a = 17.9747(2) Å	α = 90°.	a = 9.09120(10) Å	α = 68.0220(10) °.
	b = 10.26640(10) Å	β =106.5320(10) °.	b = 9.66720(10) Å	β =85.9580(10) °.
	c = 15.6542(2) Å	γ = 90°.	c = 10.9951(2) Å	γ = 80.3790(10) °.
Volume	2769.34(5) $Å^3$		878.75(2) $Å^3$	
Z	4		1	
Density (calculated)	1.424 Mg/m^3		1.401 Mg/m^3	
Absorption coefficient	0.655 mm^{-1}		0.536 mm^{-1}	
F(000)	1216		380	
Crystal size	0.60 x 0.16 x 0.14 mm^3		0.5 x 0.5 x 0.46 mm^3	
Theta range for data collection	2.31 to 27.49°.		2.01 to 27.5°.	
Index ranges	-23<=h<=22, 0<=k<=13, 0<=l<=20		-11<=h<=11, -12<=k<=12, -14<=l<=12	
Reflections collected	6351		9703	
Independent reflections	6351 [R(int) = 0.0000]		5164 [R(int) = 0.174]	
Completeness to theta	= 27.49°, 99.8 %		= 27.50°, 99.7 %	
Absorption correction	multi		Semi-empirical from equivalents	
Max. and min. transmission	1.000 and 0.831		1.000 and 0.794	
Refinement method	Full-matrix least-squares on F^2		Full-matrix least-squares on F^2	
Data / restraints / parameters	6351 / 0 / 334		5164 / 3 / 433	
Goodness-of-fit on F^2	1.007		1.007	
Final R indices [I>2sigma(I)]	R1 = 0.0270, wR2 = 0.0685		R1 = 0.0228, wR2 = 0.0600	
R indices (all data)	R1 = 0.036, wR2 = 0.0713		R1 = 0.0229, wR2 = 0.0601	
Largest diff. peak and hole	0.399 and -0.277 $e.Å^{-3}$		0.354 and -0.596 $e.Å^{-3}$	

Table 2.6 Selected Bond Distances (Å) and Angles (˚) for $CpRu(PPh_3)(CO)$(3,4-dimethoxyphenyl) (M12)

Bond distances (Å)

Ru(1)-C(6)	1.836(2)	Ru(1)-P(1)	2.2885(5)
Ru(1)-C(7)	2.0897(19)	O(1)-C(6)	1.151(3)
C(1)-C(2)	1.420(3)	O(2)-C(9)	1.374(2)
C(1)-C(5)	1.399(4)	O(2)-C(13)	1.404(3)
C(2)-C(3)	1.404(4)	O(3)-C(10)	1.382(3)
C(3)-C(4)	1.402(3)	O(3)-C(14)	1.404(3)
C(4)-C(5)	1.414(3)		

Bond angles (˚)

C(1)-C(5)-C(4)	107.9(2)	C(7)-Ru(1)-P(1)	87.75(5)
C(3)-C(2)-C(1)	107.4(2)	C(8)-C(7)-Ru(1)	119.99(14)
C(3)-C(4)-C(5)	107.9(2)	C(9)-O(2)-C(13)	118.14(18)
C(4)-C(3)-C(2)	108.6(2)	C(10)-O(3)-C(14)	117.1(2)
C(5)-C(1)-C(2)	108.2(2)	C(12)-C(7)-Ru(1)	124.42(15)
C(6)-Ru(1)-C(7)	91.04(9)	O(1)-C(6)-Ru(1)	177.4(2)
C(6)-Ru(1)-P(1)	86.22(7)		

Table 2.7 Selected Bond Distances (Å) and Angles (˚) for TpRu(PPh_3)(CO)(3,4-dimethoxyphenyl) (M13)

Bond distances (Å)			
Ru(1)-C(10)	1.822(2)	O(1)-C(10)	1.145(3)
Ru(1)-C(11)	2.0853(18)	O(2)-C(13)	1.385(2)
Ru(1)-N(1)	2.2037(16)	O(2)-C(17)	1.385(3)
Ru(1)-N(3)	2.136(2)	O(3)-C(14)	1.386(2)
Ru(1)-N(5)	2.1748(16)	O(3)-C(18)	1.413(3)
Ru(1)-P(1)	2.3293(5)		
Bond angles (˚)			
C(10)-Ru(1)-C(11)	87.86(8)	N(3)-Ru(1)-N(1)	83.23(7)
C(10)-Ru(1)-N(1)	92.65(8)	N(3)-Ru(1)-N(5)	83.46(7)
C(10)-Ru(1)-N(3)	89.11(9)	N(3)-Ru(1)-P(1)	175.71(5)
C(10)-Ru(1)-N(5)	172.57(9)	N(5)-Ru(1)-N(1)	86.25(6)
C(10)-Ru(1)-P(1)	94.80(7)	N(5)-Ru(1)-P(1)	92.62(5)
C(11)-Ru(1)-N(1)	171.97(8)	C(12)-C(11)-Ru(1)	123.27(14)
C(11)-Ru(1)-N(3)	88.76(7)	C(14)-O(3)-C(18)	117.58(18)
C(11)-Ru(1)-N(5)	92.21(7)	C(16)-C(11)-Ru(1)	120.94(13)
C(11)-Ru(1)-P(1)	93.14(6)	C(17)-O(2)-C(13)	118.78(17)
N(1)-Ru(1)-P(1)	94.80(5)	O(1)-C(10)-Ru(1)	174.31(19)

The complexes display one strong $\nu_{(C\equiv O)}$ absorption in their IR spectra (**M12** at 1917 cm^{-1}, and **M13** at 1935 cm^{-1}). The ^{1}H NMR spectra show the signal corresponding to the proton on the methoxy groups of the 3,4-dimethoxyphenyl moiety as a pair of singlets (**M12** at δ 3.47 and 3.64 ppm; and **M13** at δ 3.34 and 3.81 ppm). Each of the complexes shows a doublet in the $^{13}C\{^{1}H\}$NMR corresponding to the carbonyl carbon (**M12** at δ 207.45 ppm; and **M13** at δ 207.77 ppm). One singlet was observed in the $^{31}P\{^{1}H\}$NMR spectra of these complexes corresponding to the triphenylphosphine ligand (**M12** at δ 60.02 ppm; and **M13** at δ 50.32 ppm).

The ruthenium carbonyl complexes **M12** and **M13** are isostructural. The coordination geometry of each of the complexes is approximately octahedral, in which the Cp or Tp ligand fills three coordination positions while the other three are occupied by a carbonyl ligand, a phosphorous atom, and an ipso carbon of the 3,4-dimethoxyphenyl moiety. The ruthenium-carbon distances are 1.836(2) Å and 1.822(2) Å in **M12** and **M13**, respectively, which are similar to those of the related ruthenium (II) complexes.[129, 130] The carbonyl C≡O bond distances of **M12** (O(1)-C(6), 1.151 (3) Å) and **M13** (O(1)-C(10), 1.145 (3) Å) are consistent with a C≡O bond distance.[130] The Ru-C≡O group of each of the complexes is virtually linear, having a O(1)-C(6)-Ru(1) angle of 177.4(2)˚ and O(1)-C(10)-Ru(1) angle of 174.31(2)˚ for **M12** and **M13**, respectively. The existence of the 3,4-dimethoxyphenyl moiety in **M12** and **M13** is yet evidence which reveals that the aldehydes are decarbonylated at the metal centre to form the corresponding phenyl carbonyl complexes. Aldehyde decarbonylation forming metal carbonyl species often causes catalyst deactivation.[131-134]

2.3.7 Proposed Mechanism for the Cp and Tp Ruthenium Complexes-Catalyzed *β*-Alkylation of 1-Phenylethanol with Benzyl Alcohol

Based on our observations in the $^{31}P\{^{1}H\}$NMR-monitored catalytic reactions, we propose a mechanism, using the 1-phenylethanol/benzyl alcohol pair as an example, for the Cp and Tp ruthenium complexes-catalyzed alkylation of secondary alcohols with primary alcohols (**Scheme 2.3**). The reaction proceeds via initial oxidation of both substrates to acetophenone and benzaldehyde. The carbonyl compounds then undergo cross-aldol condensation by the action of base to give the *α*,*β*-unsatureted ketone, which is subsequently hydrogenated to give the products. The major catalytic pathway is similar to those proposed by others; these authors, although having suggested the metal hydride as the key intermediate in the catalysis, have never reported identifying it.[18, 19, 110, 111] We have, in our study, unequivocally identified these species. In the **M3**- and **M5**-catalyzed reactions, the dppm complexes were readily converted to the hydride species, and they remained the only observable ruthenium complexes throughout the courses of the catalytic reactions. No carbonyl complex was formed in either case. Probably, the presence of the chelating dppm ligand makes it difficult to create a vacant site at the metal center for the aldehyde attack. In the cases of the bis(triphenylphosphine) complexes, the hydride intermediate can more readily dissociate one of the phosphine ligands to generate unsaturation; aldehyde attack at the metal, H_2 extrusion, and subsequent decarbonylation lead to the formation of the phenyl carbonyl complexes **M7** and **M9**.

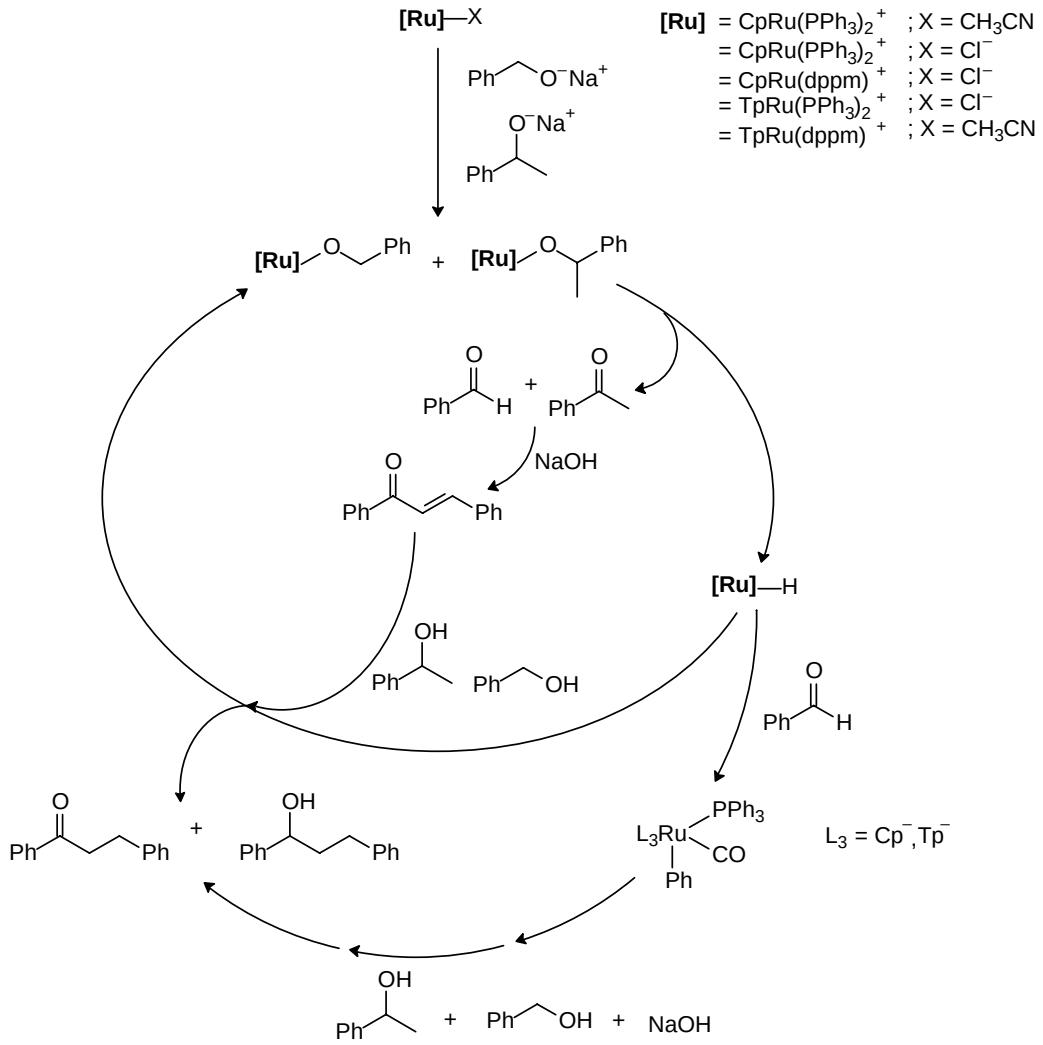

Scheme 2.3 Proposed mechanism of Cp and Tp ruthenium complexes-catalyzed *β*-alkylation of 1-phenylethanol with benzyl alcohol

Chapter 3 Dialkylaminocyclopentadienyl Ruthenium (II) Complex-Catalyzed α-Alkylation of Arylacetonitriles with Primary Alcohols

3.1 Introduction

α-alkylated nitriles are an important class of compounds for their potentials as versatile building blocks in the synthesis of amides, amidines, carboxylic acids, ketones, and biologically active compounds.[135-141] Traditional synthesis of these nitriles requires the usage of alkyl halides and stoichiometric amount of inorganic base; the toxicity of the former constitutes a major drawback of this synthetic method. Direct catalytic alkylation of nitriles thus represents an attractive green reaction from both an economical and environmental point of view. Few examples of direct alkylation of nitriles with alcohols which are catalyzed by transition metals are known. An early one being the Ru- and Rh-catalyzed reactions;[142] more recent ones include reactions catalyzed by the iridium complex $[Cp^*IrCl_2]_2$[7] and a novel Ru-grafted hydrotalcite.[143] In these reactions, aryl- and heteroaryl nitriles were used. Closely related reactions involving the addition of acetonitrile and other alkyl nitriles to aldehydes to yield *β*-hydroxynitriles have been reported; these reactions were catalyzed by ruthenium[144, 145] and rhodium complexes.[146] *β*-hydroxynitriles are potential precursors for pharmaceutically important substances.[147, 148]

In the previous chapter, we have reported that *β*-alkylation of secondary alcohols with primary alcohols are catalyzed by a number of ruthenium complexes, by virtue of their being able to affect oxidation of the primary and secondary alcohols to aldehydes and methyl ketones, respectively, which then undergo aldol condensation under basic conditions.[149] Continuing our interest

on ruthenium-catalyzed C-C bond formation reactions, we studied catalytic α-alkylation of nitriles with primary alcohols with these ruthenium complexes. However, they were found to be inactive or very poor catalysts for the reactions. Fortunately, we later found that a couple of aminocyclopentadienyl-ruthenium complexes are active catalysts for the reactions; we report here the findings on our work with these catalytic systems. We also, with the help of theoretical calculations, provide explanation for the low catalytic activity of the analogous clcyopentadienyl-ruthenium species.

3.2 Experimental Section

3.2.1 Materials and Instrumentation

All manipulations were carried out under nitrogen atmosphere using standard Schlenk techniques. Solvents were freshly distilled under nitrogen from sodium-benzophenone (tetrahydrofuran), sodium (diethyl ether, hexane and toluene), calcium hydride (dichloromethane, and acetonitrile), magnesium-iodine (methanol) or P_2O_5 (C_6D_6 and $CDCl_3$); they were degassed prior to use. Elemental analyses were performed by M-H-W Laboratories, Phoenix, AZ (USA). ^{1}H NMR spectra were obtained from a Bruker DPX-400 spectrometer at 400.13 MHz; chemical shifts (δ, ppm) were reported relative to residual peaks of the deuterated solvents used. $^{13}C\{^1H\}$NMR spectra were recorded with a Bruker DPX-400 spectrometer at 100.61 MHz; chemical shifts were internally referenced to $CDCl_3$ (δ = 77.7 ppm), C_6D_6 (δ = 128.1 ppm), $(CD_3)_2CO$ (δ = 206.26, 29.84ppm) or CD_2Cl_2 (δ = 54.18 ppm). $^{31}P\{^1H\}$NMR spectra were recorded on a Bruker DPX-400 spectrometer at 161.70 MHz; chemical shifts

were externally referenced to 85% H_3PO_4 in D_2O (δ 0.00 ppm). All spectra were obtained at ambient probe temperature unless stated otherwise. Infrared spectra were obtained from a Bruker Vector 22 FT-IR spectrophotometer. Mass spectrometry was carried out with a Finnigan MAT 95S mass spectrometer with the samples dissolved in dichloromethane or acetone. The complexes $[CpRu(PPh_3)_2(CH_3CN)]^+BF_4^-$ (**M1**),[113] and $CpRu(PPh_3)_2Cl$ (**M2**)[114] were prepared according to literature methods.

3.2.2 Syntheses and Reactions

3.2.2.1 $(CpNMe_2)Ru(PPh_3)_2H$ (M14)

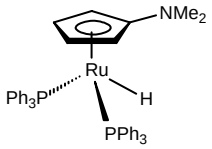

A sample of $CpRu(PPh_3)_2Cl$ (0.50g, 0.69mmol) was added to a two-necked round bottom flask equipped with a dropping funnel, the system was then evacuated and flushed with nitrogen for four cycles. Freshly degassed THF (50mL) was added to the flask. $LiN(Me)_2$ (0.18g, 3.53mmol) was added to the dropping funnel and 20mL of THF was added to dissolve the salt; the resulting solution was then slowly added to the flask. The mixture was stirred at room temperature for 2h. At the end of this period, 0.1mL of H_2O was added to the reaction mixture. It was then evaporated to dryness under reduced pressure to produce a yellow colloidal material. 20mL of freshly degassed toluene was then added, and the insoluble material was filtered out. The solvent of the filtrate was removed under reduced pressure to give a yellow paste; pre-cooled hexane (15 mL) was added to the residue, with stirring, to produce a yellow solid. The solid was collected by filtration and dried under vacuum at room temperature. Yield: 0.41g (82%). ^1H

NMR (400MHz, C_6D_6, 25°C): δ 7.74(m, 12H; PPh_3-*H*), δ 7.15-7.03(m, 18H; PPh_3-*H*), δ 4.80, δ 3.00 (s, 2H, 2H; C_5H_4), δ 2.34 (s, 6H; –N(CH_3)$_2$), δ -10.30 (t, *J* = 32 Hz, 1H; Ru-*H*). $^{31}P\{^1H\}$NMR (161MHz, C_6D_6, 25°C): δ 68.59 (s). $^{13}C\{^1H\}$NMR (100.61 MHz, C_6D_6, 25°C): δ 66.54 (t, *J* = 5 Hz, –*C*-N(CH_3)$_2$), δ 43.88 (s, –N(*C*H_3)$_2$). ESI-MS: *m/z* 734.15, $[M-H]^+$.

3.2.2.2 ($CpNEt_2$)$Ru(PPh_3)_2H$ (M15)

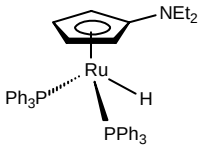

To a solution of diethylamine (0.36mL, 3.45mmol) in freshly degassed THF (10mL) cooled in an ice bath was slowly added *n*-butyllithium (1.7 mL, 2.7mmol, 1.6 M in Hexane). The solution was then allowed to warm to room temperature, and stirring was continued for 30 min. A sample of $CpRu(PPh_3)_2Cl$ (0.50g, 0.69mmol) was added to a two-necked round bottom flask, which was then evacuated and flushed with nitrogen for four cycles. Freshly degassed THF (50mL) was added to the flask. Upon complete dissolution of $CpRu(PPh_3)_2Cl$, the lithium diethylamide solution just prepared was added and the mixture was stirred at room temperature for 2h. At the end of this period, 0.1mL of H_2O was added to the reaction mixture. It was then evaporated to dryness under reduced pressure to produce a yellow colloidal material. 20mL of freshly degassed toluene was added, and the insoluble material was filtered out. The solvent of the filtrate was removed under reduced pressure to give a yellow paste; pre-cooled hexane (15 mL) was added to the residue, with stirring, to produce a yellow solid. The solid was collected by filtration and dried under vacuum at room temperature. Yield: 0.38 g (73 %). ^1H NMR (400MHz, C_6D_6, 25°C): δ 7.85-7.75(m, 12H; PPh_3-*H*), δ 7.11-7.04(m, 18H; PPh_3-*H*), δ 4.69, δ 3.27 (s, 2H, 2H; C_5H_4), δ 2.83 (q, *J* = 7 Hz, 4H; –

N(CH_2CH_3)$_2$), δ 1.09 (t, J = 7 Hz, 6H; –N(CH_2CH_3)$_2$), δ -10.23 (t, J = 33 Hz, 1H; Ru-*H*). $^{31}P\{^1H\}$NMR (161MHz, C_6D_6, 25°C): δ 69.04 (s). $^{13}C\{^1H\}$NMR (100.61 MHz, C_6D_6, 25°C): δ 65.70(t, J = 4 Hz, –*C*-N(CH_2CH_3)$_2$), δ 47.20 (s, –C-N(*C*H_2CH_3)$_2$), δ 13.73 (s, –C-N(CH_2CH_3)$_2$). ESI-MS: *m/z* 762.21, $[M-H]^+$.

3.2.2.3 $[(CpNMe_2)Ru(PPh_3)_2(CH_3CN)]^+BF_4^-$ (M16)

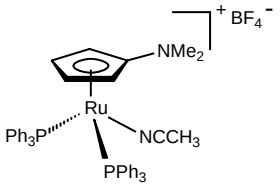

A sample of (CpNMe$_2$)Ru(PPh$_3$)$_2$H (0.10g, 0.14mmol) was added to a two-necked round bottom flask which was degassed and flushed with nitrogen for four times. Freshly degassed THF (20mL) was added to dissolve the complex followed by the addition of $HBF_4{\cdot}Et_2O$ (25μL, 1.5mmol) and CH_3CN (1 mL). The solution was stirred at room temperature for 1h, and evaporated to dryness under reduced pressure to yield a yellow paste. Hexane (5 mL) was added to the residue, with stirring, to produce a yellow solid. The solid was filtered out and washed with diethyl ether (2 × 2 mL). It was collected and dried under vacuum at room temperature. Yield: 89mg (76%). Anal. Calcd (%) of $C_{45}H_{43}BF_4N_2P_2Ru$: C, 62.73; H, 5.03; N, 3.25. Found: C, 62.55; H, 5.09; N, 3.19. ^1H NMR (400MHz, $(CD_3)_2O$, 25°C): δ 7.46-7.39(m, 6H; PPh$_3$-*H*), δ 7.31-7.25 (m, 24H; PPh$_3$-*H*), δ 4.28, δ 3.27 (s, 2H, 2H; C_5H_4), δ 2.88 (s, 6H; N(CH_3)$_2$), δ 2.28 (s, 3H; Ru-NCC*H*$_3$). $^{31}P\{^1H\}$NMR (161MHz, $(CD_3)_2O$, 25°C): δ 46.22 (s). $^{13}C\{^1H\}$NMR (100.61 MHz, $(CD_3)_2O$, 25°C): δ 60.42 (t, J = 6 Hz, –*C*-N(CH_3)$_2$), δ 40.12 (s, –N(*C*H_3)$_2$). ESI-MS: *m/z* 734.15, $[M-CH_3CN]^+$.

3.2.2.4 $[(CpNEt_2)Ru(PPh_3)_2(CH_3CN)]^+BF_4^-$ (M17)

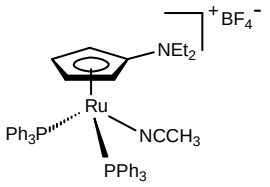

A procedure similar to that for the synthesis of $[(CpNMe_2)Ru(PPh_3)_2(CH_3CN)]^+BF_4^-$ was followed, except that $(CpNEt_2)Ru(PPh_3)_2H$ (0.10g, 0.13mmol) was used in place of $(CpNMe_2)Ru(PPh_3)_2H$. Yellow solid; yield: 83 mg (71 %). Anal. Calcd (%) of $C_{47}H_{47}BF_4N_2P_2Ru$: C, 63.45; H, 5.32; N, 3.15. Found: C, 63.38; H, 5.39; N, 3.11. ^{1}H NMR (400MHz, $CDCl_3$, 25^{o}C): δ 7.37-7.30 (m, 6H; PPh_3-*H*), δ 7.27-7.21(m, 12H; PPh_3-*H*), δ 7.19-7.11(m, 12H; PPh_3-*H*), δ 4.08, δ 3.04 (s, 2H, 2H; C_5H_4), δ 3.15 (q, *J* = 7 Hz, 4H; –N(CH_2CH_3)$_2$), δ 2.20 (s, 3H; Ru-NCC*H*$_3$), δ 1.11 (t, *J* = 7 Hz, 6H; –N(CH_2CH_3)$_2$). ^{31}P{^{1}H}NMR (161MHz, $(CD_3)_2O$, 25^{o}C): δ 46.45 (s). ^{13}C{^{1}H}NMR (100.61 MHz, $(CD_3)_2O$, 25^{o}C): δ 59.95 (t, *J* = 6 Hz, –*C*-N(CH_2CH_3)$_2$), δ 45.85 (s, –C-N(*C*H_2CH_3)$_2$), δ 13.55 (s, –C-N(CH_2C*H*$_3$)$_2$). ESI-MS: *m/z* 762.19, $[M\text{-}CH_3CN]^+$.

3.2.2.5 $(CpNMe_2)Ru(PPh_3)(CO)Ph$ (M18)

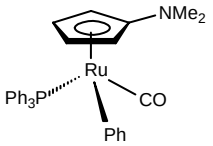

A sample of $[(CpNMe_2)Ru(PPh_3)_2H$ (0.50g, 0.68mmol) was loaded into a two-necked round bottom flask, which was then evacuated and flushed with nitrogen for four cycles. Degassed toluene (10 mL) and benzaldehyde (0.35mL, 2.07mmol) were then added and the resulting mixture was refluxed with stirring for 24h. At the end of this period, the solution was cooled to room temperature and was evaporated to dryness under reduced pressure to yield a pale yellow paste. Hexane (5 mL) was added to the residue, with stirring at -78^{o}C, to produce a yellow solid. The solid was filtered out and throughly dried under vacuum to give **M18** which was contaminated by free triphenylphosphine and phosphine oxide. **M18** was

characterized by NMR spectroscopy. ^{1}H NMR (400MHz, C_6D_6, 25^{o}C): δ 7.79-7.04(m, 20H; PPh_3-*H,* Ru-C_6H_5), δ 4.87, δ 4.53 (d, *J* = 2 Hz, 1H, 1H; C_5H_4), δ 4.18, δ 4.16 (s, 1H, 1H; C_5H_4), δ 2.23 (s, 6H; $N(CH_3)_2$). ^{31}P{^{1}H}NMR (161MHz, C_6D_6, 25^{o}C): δ 59.88 (s) ^{13}C{^{1}H}NMR (100.61 MHz, C_6D_6, 25^{o}C): δ 207.70 (d, $^{2}J_{PC}$ = 19 Hz, Ru-*C*O); δ 152.31 (d, $^{2}J_{PC}$ = 12 Hz, ipso C of Ru-C_6H_5).

3.2.2.6 $[(CpNMe_2)Ru(PPh_3)_2H_2]^{+}BF_4^{-}$ (M19)

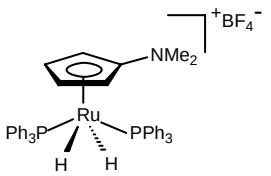

A suspension of $(CpNMe_2)Ru(PPh_3)_2H$ (0.15g, 0.20mmol) in freshly degassed methanol (10mL) was cooled in an ice bath. $HBF_4{\cdot}Et_2O$ (38μL, 0.22mmol) was added; pale yellow microcrystalline solid appeared after 30 min. The reaction mixture was allowed to stir in the ice bath for 2h. At the end of this period, the precipitate was filtered out and washed with pre-cooled methanol (3× 2mL). It was collected and dried under vacuum at room temperature. Yield: 77mg (46%). ^{1}H NMR (400MHz, CD_2Cl_2, 25^{o}C): δ 7.42 – 7.37 (m, 18H; PPh_3-*H*), δ 7.35-7.29(m, 12H; PPh_3-*H*), δ 4.76, δ 3.59 (s, 2H, 2H; C_5H_4), δ 2.30 (s, 6H; –$N(CH_3)_2$), δ -6.58(t, *J* = 25 Hz, 2H; Ru-H_2). ^{31}P{^{1}H}NMR (161MHz, CD_2Cl_2, 25^{o}C): δ 59.56 (s). ^{13}C{^{1}H}NMR (100.61 MHz, CD_2Cl_2, 25^{o}C): δ 71.60 (t, *J* = 4 Hz, –*C*-$N(CH_3)_2$), δ 41.32 (s, –$N(CH_3)_2$). ESI-MS: *m/z* 734.17, $[M-2H]^{+}$.

3.2.2.7 *In Situ* Preparation of $DBUH^{+}BF_4^{-}$

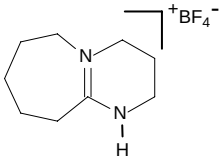

The compound was synthesized according to literature method with slight modification.[150] $HBF_4{\cdot}Et_2O$ (0.58mL, 3.6mmol) was added to an ice-cooled solution of DBU (0.5mL, 3.3mmol) in Et_2O (10mL). The reaction mixture was allowed to stir in the ice

bath for 30min. At the end of this period, the mixture was evaporated to dryness under reduced pressure to give a pale yellow oil. The resulting oil was washed with pentane (2 × 3 mL). It was collected and dried under vacuum at room temperature. Yield: 0.66g (83 %). ^{1}H NMR (400MHz, $CDCl_3$, 25^{o}C): δ 7.97 (s, 1H; N*H*), δ 3.58-3.53 (m, 4H), δ 3.41-3.39 (m, 2H), δ 2.69-2.67(m, 2H), δ 2.09-2.037(m, 2H), δ 1.76-1.70 (m, 6H).

3.2.2.8 General Procedure of Catalytic *α*-Alkylation of Arylacetonitriles

The reactions were carried out in a 10mL round-bottomed flask equipped with a reflux condenser topped with a nitrogen bypass. In a typical run, ruthenium complex (0.02 mmol) was loaded into the flask; it was then evacuated and filled with nitrogen for four cycles. Arylacetonitriles (1 or 2 mmol depending on mol% of cat.), primary alcohol (6 mmol) and DBU (0.4 mmol) were added to the flask via syringes and needles. The flask was heated in a silicon oil bath at 120^{o}C for 24 h. At the end of this period, the system was cooled to room temperature and 25μL 1,1,2,2-tetrachloroethane was added as an internal standard; a 0.1 mL aliquot of the solution was removed and analyzed by ^{1}H NMR spectroscopy (in $CDCl_3$). Conversions of the reactions were obtained by measuring the integrations of the characteristic peaks of the products with reference to the distinct peaks of the internal standard. The organic products **3a**, **3b**, **3i** and **3j** are commercially available; **3c**,[151] **3d**,[152] **3e**,[153] **3f**,[6] **3g**,[154] and **3h**,[152] described in **Table 3.3** are known and were characterized by comparing their ^{1}H NMR data with the reported ones.

3.2.2.9 NMR Monitoring of $[(CpNMe_2)Ru(PPh_3)_2(CH_3CN)]^+BF_4^-$ (M16) and $[CpRu(PPh_3)_2(CH_3CN)]^+BF_4^-$ (M1)-Catalyzed *α*-Alkylation of Benzyl Cyanide with Benzyl Alcohol

The reactions were carried out in 5 mm NMR tubes capped with septa. In a typical run, the ruthenium complex (0.01 mmol, 1 mol %) was loaded into a tube; it was evacuated and filled with nitrogen for four cycles. Benzyl cyanide (1 mmol), benzyl alcohol (3 mmol) and DBU (0.2 mmol) were added to the tube via syringes and needles. The tube was heated in a silicon oil bath at 120^oC. At different time intervals, the NMR tubes were rapidly cooled down to room temperature and $^{31}P\{^1H\}$NMR spectra of the solution were taken. The relative concentrations of the species present were obtained by comparing the integrations of their signals in the $^{31}P\{^1H\}$NMR spectra.

3.2.2.10 Reactions of the Metal Hydrides $(CpNMe_2)Ru(PPh_3)_2H$ (M14) and $CpRu(PPh_3)_2H$ (M6) with $DBUH^+$ in the presence of CH_3CN

A weighted amount of hydride complex (0.01 mmol) was loaded to a 5 mm NMR tube capped with a septum; the tube was then evacuated and filled with nitrogen for four cycles. Freshly prepared $HDBU^+BF_4^-$ (0.12g, 0.5mmol) in THF (0.45 mL) was then added to the tube via syringe and needle. After complete dissolution of the complex, CH_3CN (26μL, 0.5mmol) was added. The resulting solution was heated in a silicon oil bath at 60^oC. At different time intervals, the NMR tube was cooled down to room temperature and $^{31}P\{^1H\}$NMR spectra of the solution were taken. The relative concentrations of the complexes present were obtained by comparing the integrations of their signals in the $^{31}P\{^1H\}$NMR spectra.

3.2.2.11 Crystallographic Structures Analysis of $[(CpNMe_2)Ru(PPh_3)_2(CH_3CN)]^+BF_4^-$ (M16) and $[(CpNMe_2)Ru(PPh_3)_2H_2]^+BF_4^-$ (M19)

Crystals suitable for X-ray diffraction study for **M16** and **M19** were obtained by layering of hexane onto a saturated dichloromethane solution of the complexes. A suitable crystal of each of the complexes was mounted on a Bruker CCD area detector diffractomer and subjected to Mo Kα radiation (λ = 0.71073 Å) from a generator operating at 50 kV and 30 mA. The intensity data of **M16** and **M19** were collected in the range θ = 1.97 – 27.38° and 2.03 – 27.59°, respectively, with oscillation frames of ψ and ω in the range 0 – 180°. A total of 1756 frames in **M16** and 1688 frames in **M19** were taken in four shells. An empirical absorption correction of the SADABS (Sheldrick, 1996) program based on Fourier coefficient fitting was applied. The crystal structure was solved by Patterson function methods and expanded by difference Fourier synthesis, then refined by full-matrix least-squares on F^2 using the Bruker Smart and Bruker SHELXTL program packages. All non-hydrogen atoms were refined anisotropically. Hydrogen atoms were placed in ideal positions and refined as riding atoms expect for the two hydride ligands in **M19**; they were located by difference electron density map. The R and R_w values of **M16** are 0.0493 and 0.0891, respectively, and those of **M19** are 0.0496 and 0.1161, respectively. Further crystallographic details, selected bond distances and angles for **M16** and **M19** can be found in the results and discussion section.

3.2.2.12 Computational Details

In the DFT calculations, PMe_3 was used as a model for PPh_3. Geometry optimizations and frequency calculations were performed for all species involved

in the reaction at the Becke3LYP[155-157] level of density functional theory (no imaginary frequency for an equilibrium structure and one imaginary frequency for a transition structure). The intrinsic reaction coordinate (IRC)[158, 159] analysis was also carried out to confirm that all stationary points are smoothly connected to each other. Gibbs free energy at 298.15 K was obtained on the basis of the frequency calculations. The Ru and P atoms were described using the LANL2DZ basis set, a double-ζ valence basis set with the Hay and Wadt effective core potential (ECP).[160, 161] For all other atoms, the 6-31G basis set was used.[162] Polarization functions were added for N (ζ_d = 0.864) and for P (ζ_d = 0.387). For those H bonded to Ru, polarization functions were also added (ζ_p = 1.100).[163] All calculations were performed with Gaussian 03 packages.[164]

3.3 Results and Discussion

In view of the catalytic activity of ruthenium complexes in *β*-alkylation of secondary alcohols with primary alcohols, we studied the catalytic *α*-alkylation of nitriles with primary alcohols using a number of Cp-Ru (Cp = cyclopentadienyl) and Tp-Ru complexes (Tp = hydrotris(pyrazolyl)borate); however, they were found to be inactive or very lowly active.

We then prepared the aminocyclopentadienyl-Ru complexes $[(CpNMe_2)Ru(PPh_3)_2(CH_3CN)]^+BF_4^-$ (**M16**) and $[(CpNEt_2)Ru(PPh_3)_2(CH_3CN)]^+BF_4^-$ (**M17**) and found that they are active for the nitrile alkylation reactions (**eq. 3.1**).

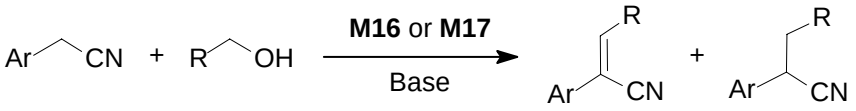

1 **2** **3** **4** (3.1)

3.3.1 Preparation and Characterization of Complexes $[(CpNMe_2)Ru(PPh_3)_2(CH_3CN)]^+BF_4^-$ (M16) and $[(CpNEt_2)Ru(PPh_3)_2(CH_3CN)]^+BF_4^-$ (M17), and X-ray Structure of M16

The aminocyclopentadienyl-ruthenium complexes **M16** and **M17** were prepared by the protonation of the hydride precursors, $(CpNMe_2)Ru(PPh_3)_2H$ (**M14**) and $(CpNEt_2)Ru(PPh_3)_2H$ (**M15**), with $HBF_4{\cdot}Et_2O$ in the presence of acetonitrile; the hydride complexes **M14** and **M15** were formed by reacting $CpRu(PPh_3)_2Cl$ (**M2**) with $LiNR_2$ (R = CH_3, C_2H_5) in THF (**eq. 3.2**).

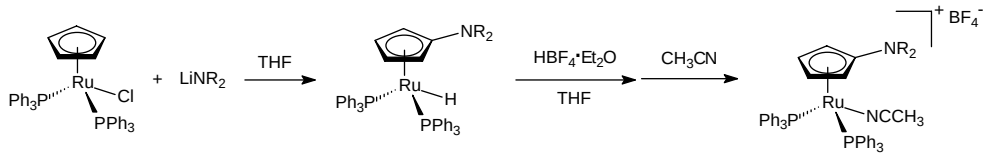

M2

M14, R = Me
M15, R = Et

M16, R = Me
M17, R = Et

(3.2)

Aminocyclopentadienyl-Fe hydride complexes $(CpNR_2)Fe(L_1)(L_2)H$ (R = CH_3, C_2H_5; L_1 = CO, L_2 = PR_3; L_1 = L_2 = PR_3) have been prepared in a similar manner.[165] The ^1H NMR spectra of **M16** and **M17** show signals of the acetonitrile ligands at δ 2.28 and 2.20 ppm, respectively. A singlet that corresponds to the amino methyl groups in **M16** is seen at δ 2.88 ppm; on the other hand, the existence of amino ethyl groups of **M17** is confirmed by the observation of a quartet signal(δ 3.15 ppm) and a triplet one (δ 1.11 ppm) which

are present in a 2:3 ratio. The phosphine ligands of **M16** and **M17** appear as singlets at δ 46.2 and 46.5 ppm, respectively, in their $^{31}P\{^{1}H\}$NMR spectra.

Yellow crystals of **M16** suitable for X-ray diffraction study were obtained by layering hexane onto a saturated CH_2Cl_2 solution of the complex. **Figure 3.1** shows the molecular structure of **M16**. The crystal data and refinement details are given in **Table 3.1**. Selected bond distances and angles are given in **Table 3.2**. The amino moiety is linked to the Cp ring via a short C(1)-N(11) bond (1.351(5) Å) which is shorter than the standard $C(sp^2)$-$N(sp^3)$ single bonds (1.40 – 1.44 Å) but longer than the typical $C(sp^2)$=$N(sp^2)$ double bonds (1.25 – 1.28 Å).[166, 167] The distance from Ru to the $N(CH_3)_2$-substituted Cp carbon (Ru-C(1), 2.363(3) Å) and to the two carbons in *β* positions from C(1) (Ru-C(3), 2.172(4) Å; Ru-C(4), 2.167(4) Å) are significantly longer and shorter, respectively, than those found in the unsubstituted Cp complex $[CpRu(PPh_3)_2(CH_3CN)]^+BF_4^-$ (**M1**) (Ru-C(Cp) ≈ 2.21 Å).[168] The nitrogen atom is nearly coplanar with its substituents (sum of the angles around N, $\Sigma_{N(11)}$ = 356.3°); it sits 0.156 Å above the C_1-C_6-C_7 plane, which makes a small angle of 4.4° with the Cp ring. The structural properties of $\mathbf{M16}^+$ is in line with the structural data reported for the aminocyclopentadienyl-Fe complex $(CpNEt_2)Fe(PPh(OEt)_2)(CO)Br$[165] and for 1,1'-bis(dimethylamino)-titanocene dichloride.[169] The structure of **M16** shows hydrogen-bonding interactions between two of the fluorine atoms of the tetrafluoroborate anion and two of the Cp hydrogen atoms (H(3A)...F(1), 2.34 Å; H(4A)...F(3), 2.66 Å).

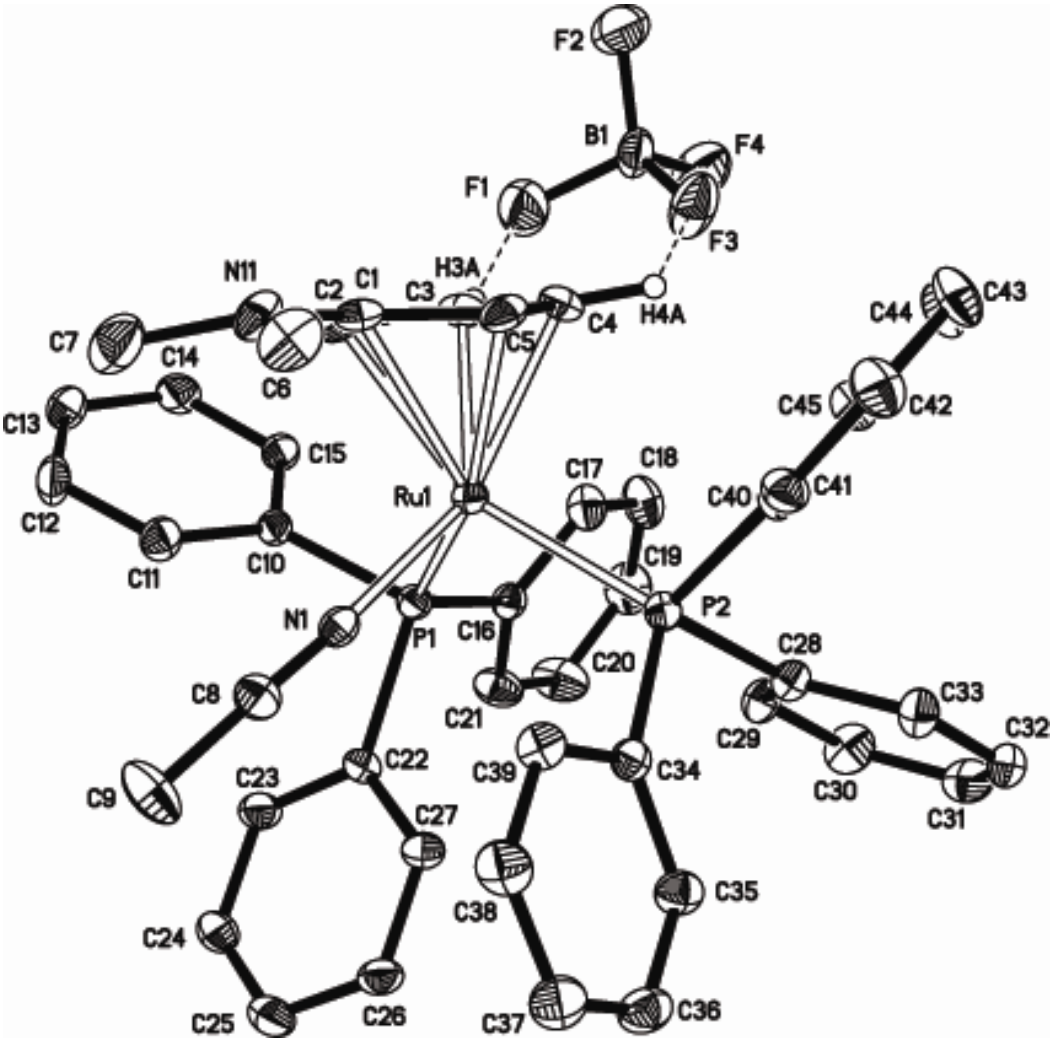

Figure 3.1 ORTEP view (30% probability) of $[(CpNMe_2)Ru(PPh_3)_2(CH_3CN)]^+BF_4^-$ (M16) showing the atom-labeling scheme

Table 3.1 Crystal Data and Structure Refinement of $[(CpNMe_2)Ru(PPh_3)_2(CH_3CN)]^+BF_4^-$ (M16)

Empirical formula	$C_{45}H_{43}BF_4N_2P_2Ru$	
Formula weight	858.61	
Temperature	296(2) K	
Wavelength	0.71073 Å	
Crystal system	Orthorhombic	
Space group	Pca2(1)	
Unit cell dimensions	a = 20.6849(5) Å	$\alpha = 90°$.
	b = 10.1795(2) Å	$\beta = 90°$.
	c = 19.2592(5) Å	$\gamma = 90°$.
Volume	4055.25(16) $Å^3$	
Z	4	
Density (calculated)	1.406Mg/m^3	
Absorption coefficient	0.518 mm^{-1}	
F(000)	1756	
Crystal size	0.28 x 0.24 x 0.20 mm^3	
Theta range for data collection	1.97 to 27.38°.	
Index ranges	-26<=h<=26, -13<=k<=13, -24<=l<=23	
Reflections collected	33629	
Independent reflections	8863 [R(int) = 0.0993]	
Completeness to theta = 27.38°	99.7 %	
Absorption correction	Semi-empirical from equivalents	
Max. and min. transmission	1.000 and 0.736	
Refinement method	Full-matrix least-squares on F^2	
Data / restraints / parameters	8863 / 1 / 496	
Goodness-of-fit on F^2	1.001	
Final R indices [I>2sigma(I)]	R1 = 0.0493, wR2 = 0.0891	
R indices (all data)	R1 = 0.1001, wR2 = 0.1044	
Absolute structure parameter	-0.05(4)	
Largest diff. peak and hole	1.279 and -1.099 e.$Å^{-3}$	

Table 3.2 Selected Bond Distances (Å) and Angles (°) for $[(CpNMe_2)Ru(PPh_3)_2(CH_3CN)]^+BF_4^-$ (M16)

Bond distances (Å)			
Ru(1)-C(1)	2.363(3)	C(1)-C(2)	1.435(4)
Ru(1)-C(2)	2.226(3)	C(1)-C(5)	1.429(6)
Ru(1)-C(3)	2.172(4)	C(2)-C(3)	1.418(5)
Ru(1)-C(4)	2.167(4)	C(3)-C(4)	1.390(5)
Ru(1)-C(5)	2.224(3)	C(4)-C(5)	1.433(5)
Ru(1)-N(1)	2.059(3)	N(1)-C(8)	1.145(5)
Ru(1)-P(1)	2.3413(9)	N(11)-C(1)	1.351(5)
Ru(1)-P(2)	2.3662(9)		

Bond angles (°)			
C(1)-C(5)-C(4)	107.6(3)	C(6)-N(11)-C(7)	116.7(4)
C(1)-N(11)-C(6)	120.6(3)	C(8)-N(1)-Ru(1)	176.3(3)
C(1)-N(11)-C(7)	119.0(3)	N(1)-C(8)-C(9)	178.1(5)
C(3)-C(2)-C(1)	108.3(3)	N(1)-Ru(1)-P(1)	86.52(8)
C(3)-C(4)-C(5)	108.6(3)	N(1)-Ru(1)-P(2)	92.71(8)
C(4)-C(3)-C(2)	108.4(3)	P(1)-Ru(1)-P(2)	105.47(3)
C(5)-C(1)-C(2)	106.5(4)		

Hydrogen bond distances (Å)

D-H...A	d(D-H)	d(H...A)	d(D...A)
C(3)-H(3A)...F(1)	0.98	2.34	3.277(5)
C(4)-H(4A)...F(3)	0.98	2.66	3.202(5)

Hydrogen bond angles (°)

D-H...A	<(DHA)
C(3)-H(3A)...F(1)	158.9
C(4)-H(4A)...F(3)	115.3

3.3.2 Catalytic *α*-Alkylation of Arylacetonitriles with Alcohols

The major products of the reactions are the unsaturated nitriles, and the saturated nitriles in some cases only appear as very minor products (**Table 3.3**). Product distributions in our study are quite different from those of studies carried out by others;[7, 143] in their studies, the saturated nitriles are the overwhelming products.

The Cp complex $[CpRu(PPh_3)_2(CH_3CN)]^+BF_4^-$ (**M1**) shows very low activity. In general, the complex with the diethylamino substituent on the Cp ring (**M17**) is more active than the one in which the Cp ring carries the dimethylamino group (**M16**). Benzyl alcohols with electron-donating substituents give lower overall conversions (entries 3–6), and the one containing the electron-withdrawing fluoro group affords higher conversion (entry 2). Alcohols containing heteroatoms seem to be less active than benzyl alcohol (entries 7-9), and alkyl alcohol is even less reactive (entry 10). Attachment of the electron-withdrawing fluoro group to the arylacetonitrile modestly increases the overall conversion (entry 15); on the other hand, the presence of an electron-donating substituent lowers the activity of the system (entries 11-14).

Table 3.3 Ru(II)-Catalyzed α-Alkylation of Arylacetonitriles with Primary Alcohols[a]

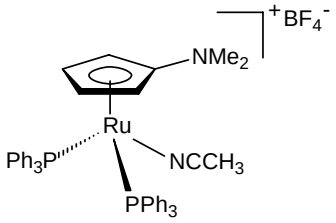

M16

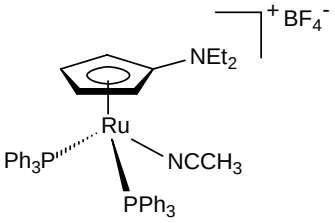

M17

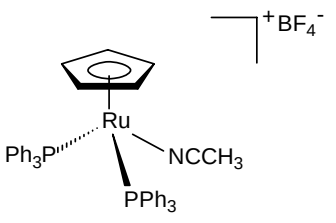

M1

entry	nitrile	alcohol	products	mol % Ru	% conversion[b]		
	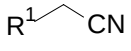 **1**	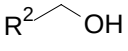 **2**	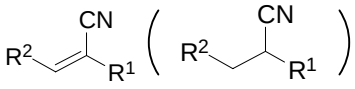 **3** **4**		**M16**	**M17**	**M1**
1	**1a** R^1 = Ph	**2a** R^2 =Ph	**3a** (**4a**)	1%	37(18)	38 (32)	7 (0)
2	**1a**	**2b** R^2 = 4-FC_6H_4	**3b**(**4b**)	1%	50 (19)	58 (21)	4 (0)
3	**1a**	**2c** R^2 = 2-$OMeC_6H_4$	**3c** (**4c**)	1%	16 (0)	27 (10)	4 (0)
4				2%	33(24)	41(14)	15(0)
5	**1a**	**2d** R^2 = 4-$OMeC_6H_4$	**3d** (**4d**)	1%	22 (0)	35 (8)	3 (0)
6				2%	33(11)	37(15)	15(0)
7	**1a**	**2e** R^2 = thiophen-2-yl	**3e** (**4e**)	1%	57 (6)	67 (7)	4 (0)
8	**1a**	**2f** R^2 = 2-furyl	**3f** (**4f**)	1%	40 (5)	49 (9)	3 (0)
9				2%	49 (4)	58 (9)	7(0)
10[c]	**1a**	**2g** R^2 = Pr	**3g** (**4g**)	2%	31(7)	23(33)	11(0)
11	**1b** R^1 = 4-$OMeC_6H_4$	**2a**	**3h** (**4h**)	1%	25(0)	31 (0)	5 (0)
12				2%	36 (0)	40 (0)	16(0)
13	**1b**	**2b**	**3i** (**4i**)	1%	26 (0)	34 (0)	6 (0)
14				2%	35(0)	39 (0)	22(trace)
15	**1c** R^1 = 4-FC_6H_4	**2a**	**3j** (**4j**)	1%	36(31)	40(38)	6 (0)

[a]Reaction conditions: catalyst (0.02 mmol), nitrile (1 or 2 mmol depend on mol % of cat. used), alcohol (6 mmol), DBU (0.4 mmol), 120˚C, 24 h.

[b]Conversion (based on nitrile) determined by ^{1}H NMR spectroscopy with 1,1,2,2-tetrachloroethane as an internal standard. Values in parenthesis indicate the conversion of the corresponding saturated products **4**.

[c]48 h.

We are interested in understanding the large difference in catalytic activity between the systems based on aminocyclopentadienyl complexes **M16**, **M17** and that based on the unsubstituted Cp complex **M1**. We learned in a separate experiment that benzyl cyanide reacts with benzaldehyde in the presence of DBU (40 mol %) to give the unsaturated nitrile **3a** in 88 % conversion; no metal catalyst is needed for the reaction (**eq. 3.3**). The reaction, however, does not proceed in the absence of a base. It therefore seems that in the **M16**- and **M17**-catalyzed arylacetonitrile α-alkylation reactions, the major function of the metal complex is to affect dehydrogenation of the alcohol to yield aldehyde, which then undergoes condensation with the arylacetonitrile under basic conditions. In the presence of DBU, the complex reacts with alcohol to generate metal alkoxide; subsequent β-elimination give the aldehyde and the metal hydride species.

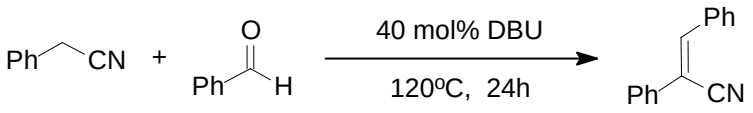

1a **3a**

88 % conversion (3.3)

3.3.3 NMR Monitoring of $[(CpNMe_2)Ru(PPh_3)_2(CH_3CN)]^+BF_4^-$ (M16)- and $[CpRu(PPh_3)_2(CH_3CN)]^+BF_4^-$ (M1)-Catalyzed Alkylation of Benzyl Cyanide with Benzyl Alcohol

We monitored the **M16**- and **M1**-catalyzed alkylation of benzyl cyanide with benzyl alcohol with $^{31}P\{^1H\}$NMR spectroscopy. In the **M16**-catalyzed reaction (**Figure 3.2**), it was found that the metal hydride $(CpNMe_2)Ru(PPh_3)_2H$ (**M14**) was rapidly formed and it remained the major metal-containing species

throughout the experiment. Free phosphine and phosphine oxide due to complex decomposition were detected; their amounts increased with time. In addition, minute amounts of the carbonyl species ($CpNMe_2$)Ru(PPh_3)(CO)Ph (**M18**) and an unknown species were also detected.

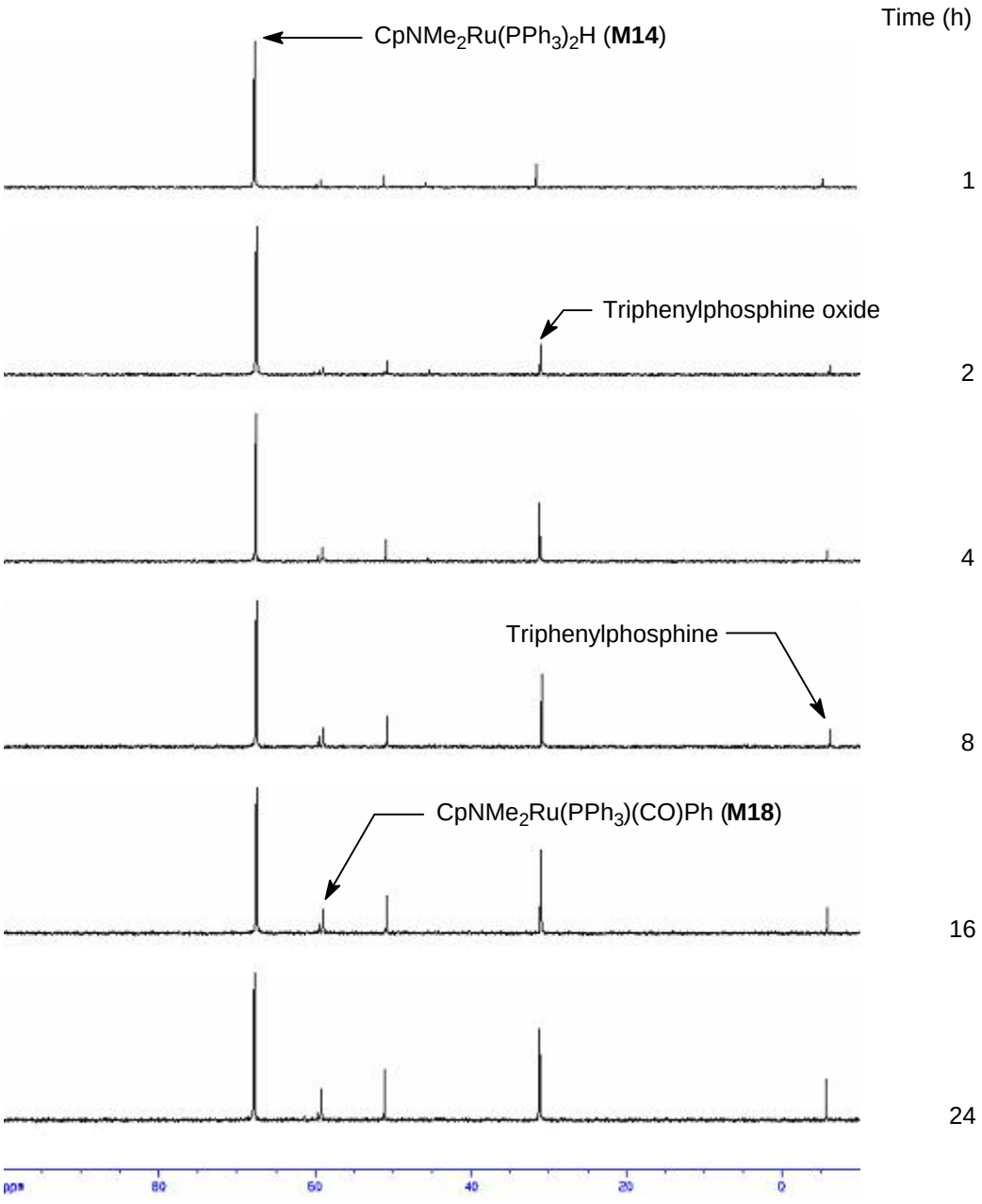

Figure 3.2 $^{31}P\{^1H\}$NMR study of [$CpNMe_2Ru(PPh_3)_2CH_3CN]^+BF4^-$(M16)-catalyzed α-alkylation of benzyl cyanide with benzyl alcohol

In the **M1**-catalyzed alkylation reaction (**Figure 3.3**), in which conversion was very low, the hydride complex $CpRu(PPh_3)_2H$ (**M6)** was the overwhelming species detected during the monitoring process. Small amounts, which remained pretty constant throughout the experiment, of free phosphine and phosphine oxide, indicative of small degree of complex decomposition, were observed. Minute quantities of carbonyl complex $CpRu(PPh_3)(CO)Ph$ (**M7**) and an unknown species were also formed. The formation of phenyl carbonyl complexes **M18** and **M7** is probably due to benzaldehyde decarbonylation at the metal center. Decarbonylation of aldehydes by transition metal complexes to form carbonyl complexes is well-established.[127, 134, 170-174] Aldehyde decarbonylation forming metal carbonyl species often causes catalyst deactivation.[131-134] It seems that in both **M16**- and **M1**-catalyzed alkylation reactions, the resting states of the catalytic systems are the metal hydride complexes. Why then the catalytic activity of **M16** is high and that of **M1** is low? We suspect that in the **M16**-catalyzed reaction, the system is able to regenerate **M16** readily and therefore complete the catalytic cycle (see **Section 3.3.7**, **Scheme 3.2**) by protonation of the hydride complex with $DBUH^+$ to form the η^2-dihydrogen intermediate and subsequent substitution of the dihydrogen ligand with acetonitrile; in the case of the **M1**-catalyzed reaction, this protonation and ligand substitution process is probably not facile.

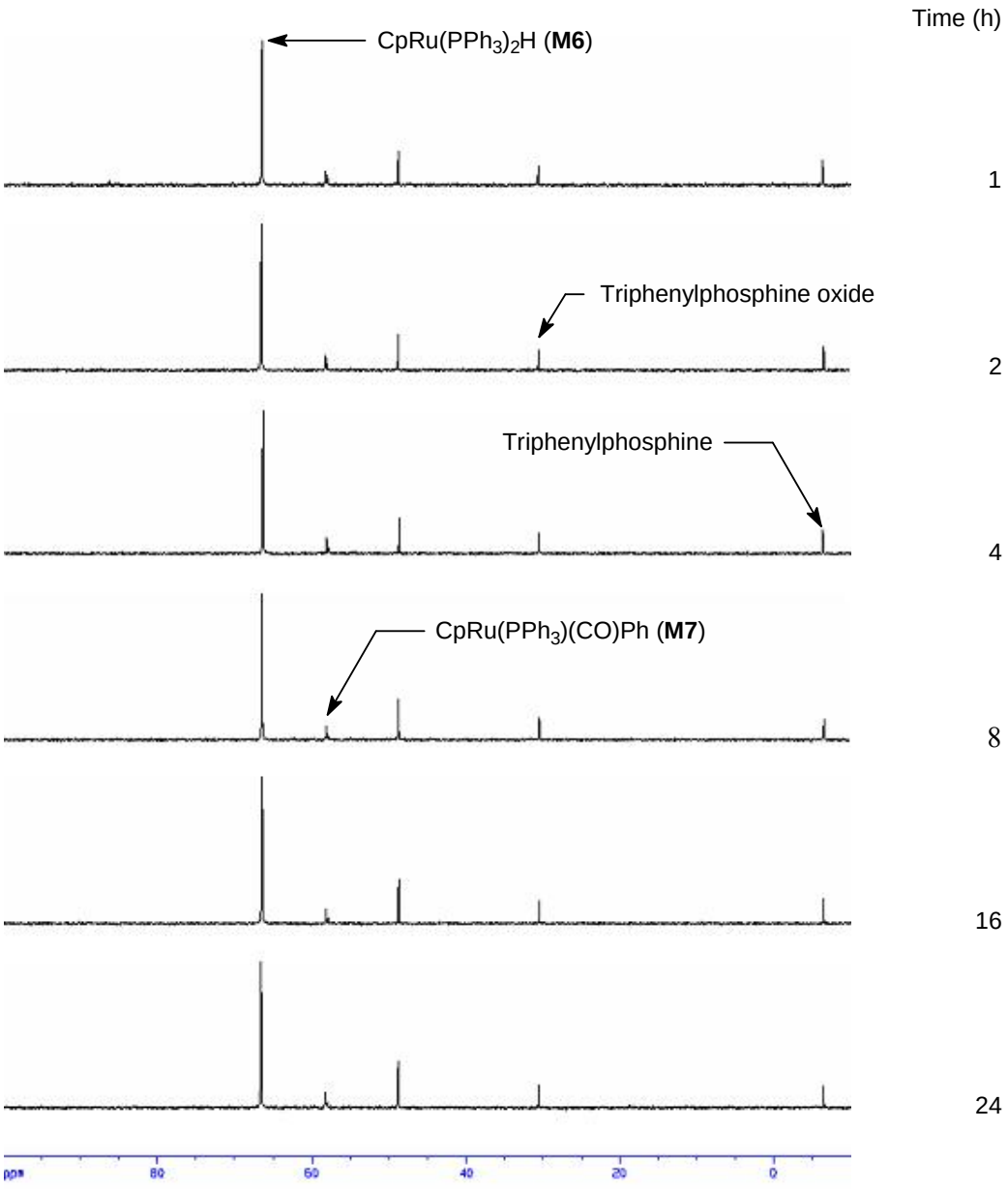

Figure 3.3 $^{31}P\{^{1}H\}$NMR study of $[CpRu(PPh_3)_2CH_3CN]^+BF4^-$(M1)-catalyzed *α*-alkylation of benzyl cyanide with benzyl alcohol

3.3.4 Preparation and Characterization of the Dihydride Complex $[(CpNMe_2)Ru(PPh_3)_2H_2]^+BF_4^-$ (M19), and X-ray Structure of M19

Under an acidic condition (1 equiv of $HBF_4{\cdot}Et_2O$), the complexes **M14** and **M6** can be easily converted to the corresponding dihydrogen complexes through protonation at the hydride ligands. The dihydrogen complexes are thermodynamically unstable and can easily isomerize to dihydride complex $[(CpNMe_2)Ru(PPh_3)_2H_2]^+BF_4^-$ (**M19**) and the known complex $[CpRu(PPh_3)_2H_2]^+BF_4^-$ (**M20**), respectively in which the two hydride ligands are angularly *tran*s to each other (**eq. 3.4**).[175]

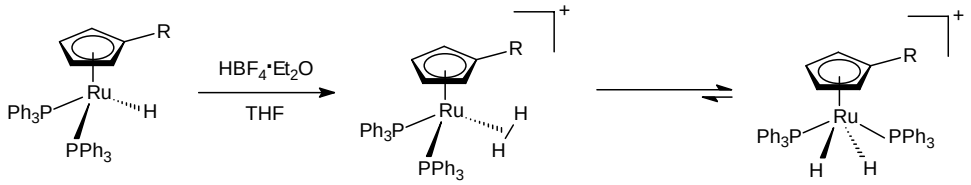

M14, R = NMe_2
M6, R= H

M19, R = NMe_2
M20, R= H (3.4)

The ^1H NMR spectra of **M19** show a signal of two chemically equivalent hydride ligands at δ -6.59 ppm. A singlet that corresponds to the amino methyl groups is seen at δ 2.30 ppm. The phosphine ligands of **M19** appear as a singlet at δ 59.6 ppm in the $^{31}P\{^1H\}$NMR spectrum. Pale yellow crystals of **M19** suitable for X-ray diffraction study were obtained by layering hexane onto a saturated CH_2Cl_2 solution of the complex. **Figure 3.4** shows the molecular structure of $\mathbf{M19}^+$. The crystal data and refinement details are given in **Table 3.4**. Selected bond distances and angles are given in **Table 3.5**. The complex adopts four-legged piano-stool geometry. The amino moiety is linked to the Cp ring via a short N(1)-C(1) bond (1.344(3) Å) which lies between the standard C(sp^2)-

$N(sp^3)$ single bond and $C(sp^2)=N(sp^2)$ double bond. Angles sum around the nitrogen atom $\Sigma_{N(1)}$ equals to 353.7°; it sits 0.155 Å above the C_1-C_6-C_7 plane, which makes an angle of 14.9° with the Cp ring. The two hydride ligands are *trans* to one another with ruthenium-hydride distances equal to 1.578 Å and 1.505 Å for HM1-Ru(1) and HM2-Ru(1), respectively.

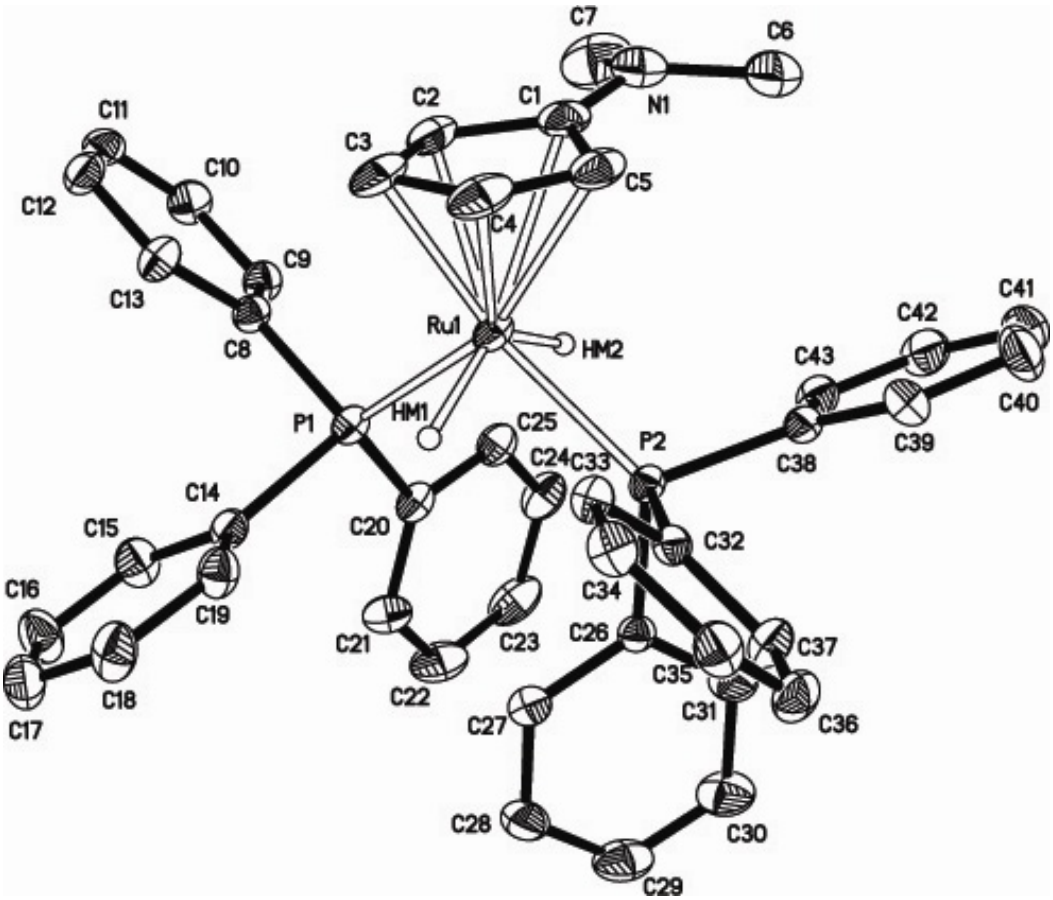

Figure 3.4 ORTEP view (30% probability) of $[(CpNMe_2)Ru(PPh_3)_2H_2]^+$ ($M19^+$) showing the atom-labeling scheme

Table 3.4 Crystal Data and Structure Refinement of $[(CpNMe_2)Ru(PPh_3)_2H_2]^+$ (M19)

Empirical formula	$C_{43}H_{42}BF_4NP_2Ru$	
Formula weight	822.60	
Temperature	296(2) K	
Wavelength	0.71073 Å	
Crystal system	Monoclinic	
Space group	P2(1)/n	
Unit cell dimensions	a = 11.440(2) Å	$\alpha = 90°$.
	b = 21.536(4) Å	$\beta = 96.251(11)°$.
	c = 15.716(5) Å	$\gamma = 90°$.
Volume	3848.9(12) $Å^3$	
Z	4	
Density (calculated)	1.420Mg/m^3	
Absorption coefficient	0.542 mm^{-1}	
F(000)	1688	
Crystal size	0.24 x 0.22 x 0.20 mm^3	
Theta range for data collection	2.03 to 27.59°.	
Index ranges	-14<=h<=14, -27<=k<=27, -20<=l<=20	
Reflections collected	45815	
Independent reflections	8730 [R(int) = 0.0785]	
Completeness to theta = 27.59°	98.0 %	
Absorption correction	Semi-empirical from equivalents	
Max. and min. transmission	1.000 and 0.791	
Refinement method	Full-matrix least-squares on F^2	
Data / restraints / parameters	8730 / 22 / 511	
Goodness-of-fit on F^2	1.002	
Final R indices [I>2sigma(I)]	R1 = 0.0496, wR2 = 0.1161	
R indices (all data)	R1 = 0.0954, wR2 = 0.1370	
Largest diff. peak and hole	0.768 and -0.457 e.$Å^{-3}$	

Table 3.5 Selected Bond Distances (Å) and Angles (˚) for[$(CpNMe_2)Ru(PPh_3)_2H_2]^+$ (M19)

Bond distances (Å)			
Ru(1)-C(1)	2.404(2)	C(1)-C(5)	1.435(3)
Ru(1)-C(2)	2.234(2)	C(2)-C(3)	1.402(4)
Ru(1)-C(3)	2.175(2)	C(3)-C(4)	1.409(3)
Ru(1)-C(4)	2.204(2)	C(4)-C(5)	1.407(4)
Ru(1)-C(5)	2.253(2)	H(M1)-Ru(1)	1.578
Ru(1)-P(1)	2.3292(7)	H(M2)-Ru(1)	1.505
Ru(1)-P(2)	2.3092(6)	N(1)-C(1)	1.344(3)
C(1)-C(2)	1.427(3)		

Bond angles (˚)			
C(1)-N(1)-C(6)	119.6(2)	C(4)-C(5)-C(1)	109.0(2)
C(1)-N(1)-C(7)	118.9(2)	C(7)-N(1)-C(6)	115.2(3)
C(2)-C(1)-C(5)	105.5(2)	P(1)-Ru(1)-HM1	76.2(7)
C(2)-C(3)-C(4)	108.8(2)	P(1)-Ru(1)-HM2	78.6(7)
C(3)-C(2)-C(1)	108.6(2)	P(2)-Ru(1)-HM1	72.9(7)
C(3)-C(4)-C(5)	107.3(2)	P(2)-Ru(1)-HM2	75.0(7)

Upon addition of DBU (1 equiv), both **M19** and **M20** are converted reversibly to **M14** and **M6**, respectively. The equilibra lie at the side of the latter with $DBUH^+BF_4^-$ generated concomitantly (**eq. 3.5**).

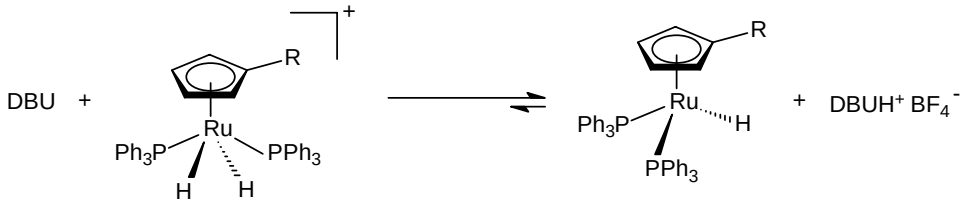

M19, R = NMe_2
M20, R= H

M14, R = NMe_2
M6, R= H (3.5)

3.3.5 Comparison of Rates of Conversion of the Metal Hydrides to $[(CpNMe_2)Ru(PPh_3)_2(CH_3CN)]^+BF_4^-$ (M16) and $[CpRu(PPh_3)_2(CH_3CN)]^+BF_4^-$ (M1)

We have studied the reaction of the hydride species **M14** and **M6** with $DBUH^+BF_4^-$ in the presence of excess CH_3CN, and tried to compare the respective rates of formation of **M16** and **M1**. The experimental investigations revealed that at 60 °C **M14** (0.01 mmol), in a THF solution (0.45 mL) containing 50 equiv of CH_3CN, was partially protonated by $DBUH^+BF_4^-$ (50 equiv) to generate a very minute amount of a transient dihydrogen complex; 70 % of the **M14** was converted to **M16** after 30 min by the rapid H_2/CH_3CN ligand exchange; the pseudo first order rate constant k was determined to be 0.0589 min^{-1}. Meanwhile, under identical conditions, no conversion of **M6** was observed.

It is known that transition-metal hydride might be protonated by acidic alcohols to form η^2-dihydrogen complexes;[176-180]the dihydrogen ligand might then be displaced by the alkoxide. (**eq. 3.6**). We looked into the possibility

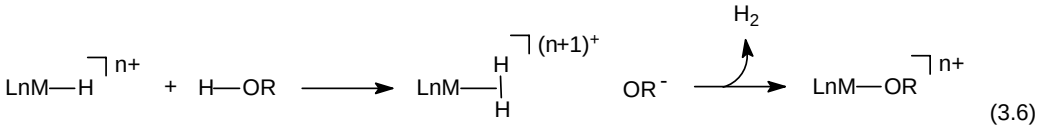

(3.6)

that the metal hydrides **M14** and **M6** would be protonated by benzyl alcohol to form the metal alkoxide which then via β-elimination to generate the metal hydride and benzaldehyde (**Scheme 3.1**). It was found that heating a C_6D_5Cl solution of **M14** in the presence of 50 equiv of benzyl alcohol at 120 °C for 48 h only resulted in the formation of 0.2 equiv of benzaldehyde. $^{31}P\{^1H\}$NMR spectroscopy showed that **M14** basically remained unchanged although minute amounts of free phosphine, phosphine oxide and a couple of unknown species, probably due to **M14** decomposition, were observed. In the case of **M6**, under identical conditions, only trace amount of benzaldehyde was generated; **M6** was recovered unchanged. These experiments seem to indicate that the reaction shown in **Scheme 3.1** occurred to negligibly small extends.

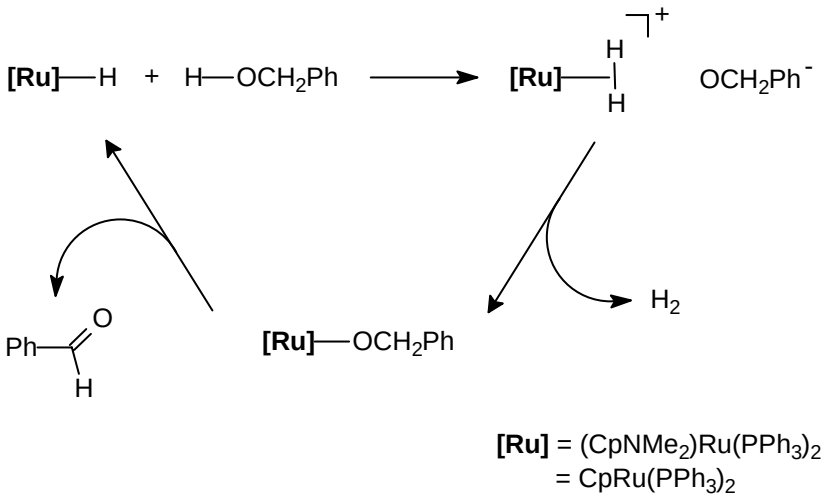

Scheme 3.1 Reaction of metal hydride with benzyl alcohol

3.3.6 Theoretical Calculations on the Displacement of H_2 from the Dihydrogen complexes by CH_3CN

To gain support for the much more facile regeneration of the active solvent complex from the hydride species in the case of the aminocyclopentadienyl complex in comparison to the non-substituted Cp-Ru system, theoretical calculations, performed at the Becke3LYP level of theory, on the displacement of H_2 from the dihydrogen complexes by CH_3CN (**eq. 3.7**) were carried out.

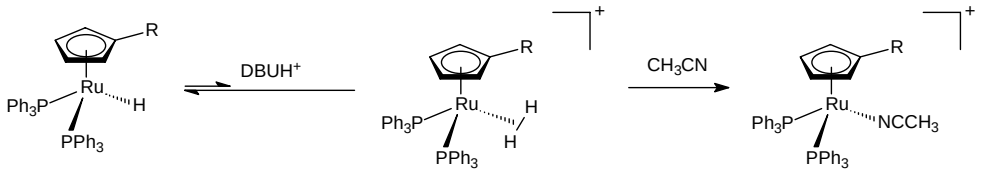

M14, R = NMe_2
M6, R = H

M16, R = NMe_2
M1, R = H (3.7)

In the presence of $DBUH^+$, both **M14** and **M6** can be reversibly converted to the corresponding dihydrogen complexes via protonation of the hydride ligands,[181] although the equilibra would probably lie at the side of the hydrides because after all $DBUH^+$ is a weak acid. We focus at the processes of the H_2/CH_3CN exchange of the two dihydrogen species. In the DFT calculations, PMe_3 is used as a model for PPh_3. Both dihydrogen complexes are 18-electron species and each contains an η^5-cyclopentadienyl ligand. Therefore, the H_2/CH_3CN exchange is expected to occur either via a dissociative mechanism or an associative mechanism involving $\eta^5 \rightarrow \eta^3$ ring slippage of the cyclopentadienyl ligand, which is a well-known phenomenon for η^5-Cp transition metal complexes.[182-184] Our calculations show that the Cp ring slippage for the dihydrogen complexes is much less favorable than H_2 dissociation. The results are understandable because dihydrogen is a weakly-coordinated ligand.

Figure 3.5 shows the energy required to dissociate H_2 from **A** to give (**A'** + H_2) is 17.3 kcal/mol. After H_2 dissociation, **A'** takes in CH_3CN to form **M16'**, which is more stable than **A** by 7 kcal/mol. The activation barrier for the dissociative mechanism was estimated by calculating the H_2 dissociation energy, which is the upper limit for a dissociative ligand substitution reaction. **Figure 3.6** shows the corresponding energy profile calculated for the dihydrogen complex **B**; the H_2 dissociation energy was found to be 21.3 kcal/mol.

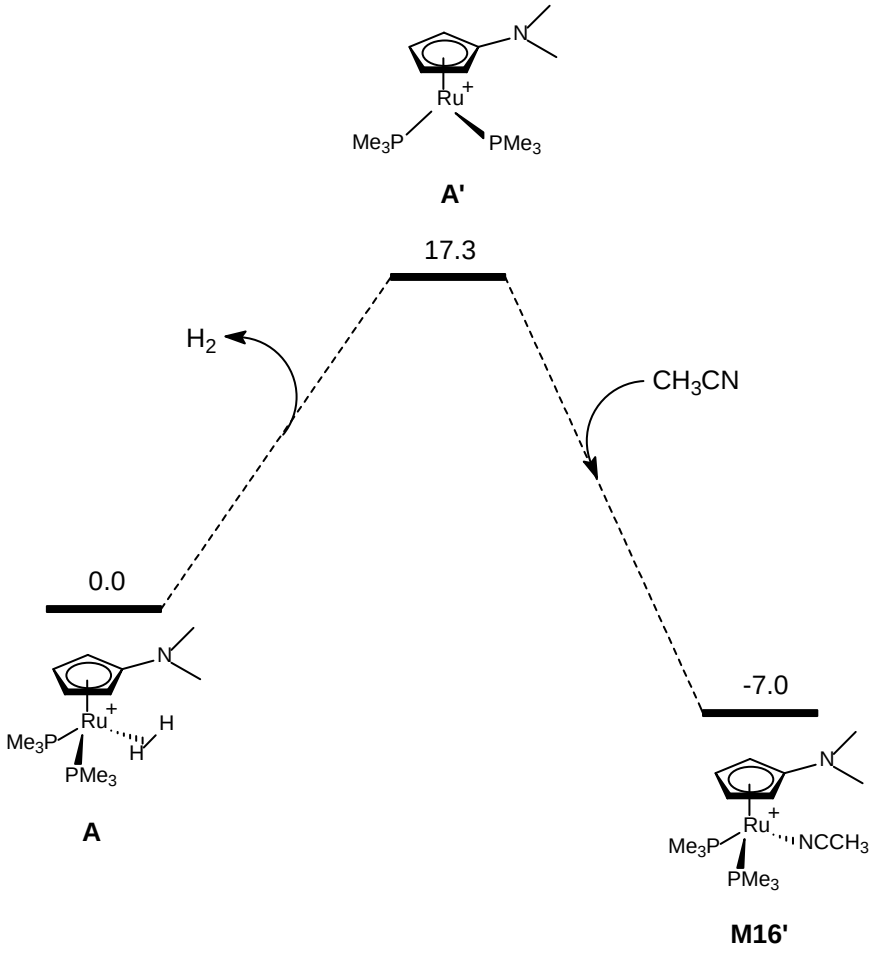

Figure 3.5 Energy profile calculated for the H_2/CH_3CN ligand exchange in the complex A. The calculated relative electronic energies are given in kcal/mol

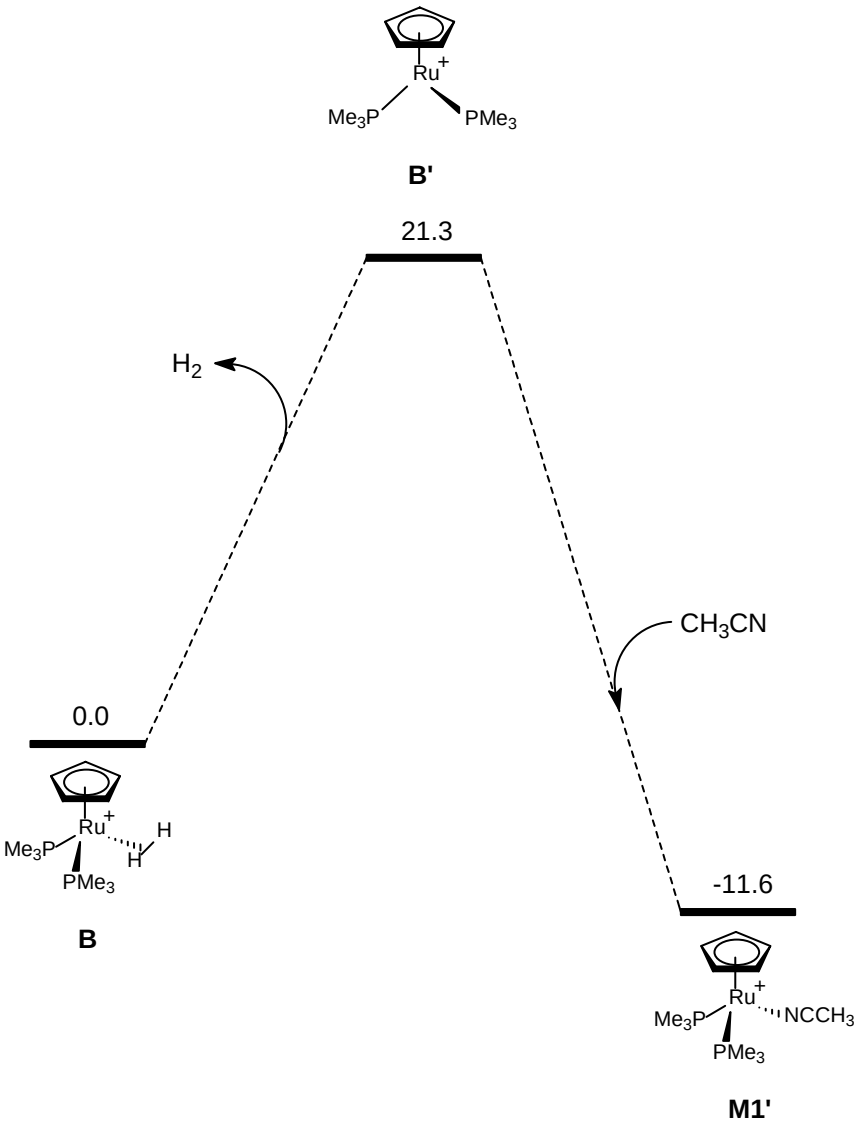

Figure 3.6 Energy profile calculated for the H_2/CH_3CN ligand exchange in the complex B. The calculated relative electronic energies are given in kcal/mol

The metal fragment **A'** derived from H_2 dissociation from **A** is relatively more stable than the metal fragment **B'** generated by H_2 dissociation from **B**. Therefore, the H_2 dissociation process from the complex **A** is more favorable. The electron donating NMe_2 moiety on the Cp ring contributes to stabilize the electron deficient 16-e^- metal fragment **A'**. In complex **B**, absence of an NMe_2

substituent makes H_2 dissociation much less favorable. Brookhart and co-workers has carried out a detailed mechanistic study on $[CpFe(CO)(PPh_3)]^+$-catalyzed silane alcoholysis and revealed that displacement of H_2 ligand of the η^2-dihydrogen intermediate by silane is probably the rate-determining step.[185] Density functional study showed that introduction of an amino substituent at the Cp ring of the catalyst lowers the barrier of the H_2/silane exchange step; it is rationalized by the π-donating capability of the amine group which makes the Cp ring more electron-rich, resulting in better stabilization of the electron-deficient iron center upon H_2 dissociation.[186]

3.3.7 Proposed Mechanism for the Catalytic α-Alkylation of Arylacetonitrile with Primary Alcohol

Taken together, a mechanism is proposed for the **M16**- or **M17**-catalyzed α-alkylation of arylacetonitriles with primary alcohols (**Scheme 3.2**). In the presence of base (DBU) and the metal complex, the alcohol is oxidized to aldehyde while the metal complex is converted to a hydride species $(CpNMe_2)Ru(PPh_3)_2H$ (**M14**) or $(CpNEt_2)Ru(PPh_3)_2H$ (**M15**). The aldehyde, by the action of base, undergoes Knoevenagel condensation with the arylacetonitrile to afford the unsaturated nitrile **3**. The crucial and slow step if the regeneration of the solvent complex **M16** or **M17** via protonation of the hydride species **M14** or **M15** (with $DBUH^+$) and subsequent H_2/CH_3CN exchange. This process is very slow for the analogous Cp hydride species **M6**, and this is probably the major reason for the unsubstituted Cp system **M1** being a poor catalyst for the α-alkylation reactions. In the **M16**- or **M17**-catalyzed reaction, the barrier of the ligand exchange step is lowered with increased electron density at the metal

center; this is probably the reason for **M17**, which contains the more electron-donating diethylamino group, being more active than **M16** bearing the dimethylamino substituent on the Cp ring. Electron-donating nature of the amino group is also illustrated by the nitrogen atom being coplanar with its substituents, as shown in the X-ray structure of **M16**; the sp^2-hybridized nitrogen atom can better donate its lone pair into the ring. The initially formed unsaturated nitrile **3** could be partially reduced by H_2 catalyzed by the hydride complex **M14** or **M15** and via insertion of **3** into the Ru-H bond of **M14** or **M15** and subsequent protoantion by the alcohol.

Benzyl alcohols with electron-withdrawing and electron-donating substituents giving higher and lower conversions, respectively, is in consonance with the fact that aldehyde with more electrophilic carbon center undergoes condensation with arylacetonitrile more readily than the ones with less electrophilic carbon centers. Lower conversion with 4-methoxyphenylacetonitrile is probably attributable to its less readiness to be deprotonated by base to generate the α-cyano carbanion, which is the nucleophile attacking the aldehyde carbon in the condensation reaction.

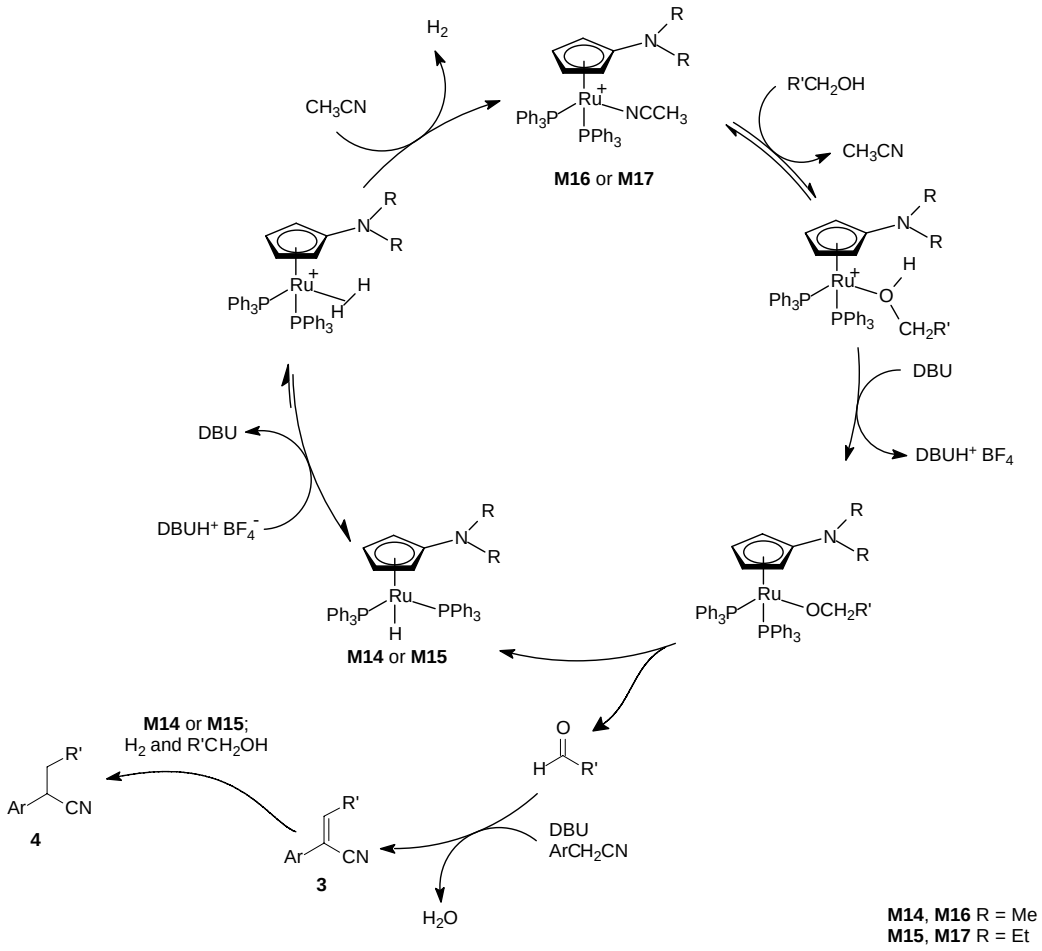

Scheme 3.2 Proposed mechanism of $[(CpNMe_2)Ru(PPh_3)_2(CH_3CN)]^+BF_4^-$ (M16)- and $[(CpNEt_2)Ru(PPh_3)_2(CH_3CN)]^+BF_4^-$ (M17)-catalyzed α-alkylation of arylacetonitrile with primary alcohol

Chapter 4 Tp-Ruthenium (II) Diphosphinoamino Complex-Catalyzed Markovnikov and Anti-Markovnikov Functionalization of Terminal Alkynes

4.1 Introduction

Addition of 1,3-dicarbonyl compounds to unactivated alkynes under neutral conditions without prior enolate formation represents an attractive and atom economical method for the formation of carbon-carbon bonds.[187] Intramolecular addition reaction was exemplified by the gold(I)-catalyzed Conia-ene reaction of *β*-ketoesters with alkynes reported by Toste and co-workers; the reaction proceeds under neutral conditions at room temperature.[85] It has been reported by Yang and co-workers that in the presence of $Ni(acac)_2$ and $Yb(OTf)_3$, various acetylenic 1,3-dicarbonyl compounds undergo Conia-ene reaction to give mono- and bicyclic olefin cyclopentanes; a mechanism involving the intermediacy of an enol-yne-Ni complex and supported by deuterium-labeling experiment was proposed.[86] On the other hand, intermolecular version of the addition reaction was reported by Nakamura to be catalyzed by indium triflate; experimental and theoretical studies suggested that the reaction proceeds via a concerted carbometalation reaction of an indium(III) enolate with the acetylene, where indium-acetylene interaction is important.[87, 88] The rhenium complex $[ReBr(CO)_3(THF)]_2$ was found to be active catalyst for both inter- and intramolecular addition reactions of 1,3-dicarbonyl compounds with terminal acetylenes under mild conditions.[89]

Catalytic intra- and intermolecular addition of N-H bond to alkynes providing cyclic and acyclic enamines/imines, respectively, are important organic transformations as the products are useful intermediates for further synthetic elaboration;[188] these processes are highly atom-economical as no waste is generated.[189-191] The hydroamination of terminal alkynes provides additional challenge in terms of regioselectivity. A variety of metals including early, late transition-metals, lanthanides and actinides are capable of catalyzing intermolecular addition of N-H to terminal alkynes yielding Markovnikov products or mixtures of Markovnikov and anti-Markovnikov products. On the other hand, highly regioselective catalytic systems generating anti-Markovnikov products are relatively rare. The organouranium complex $Cp^*_2UMe_2$ is the first catalyst for the anti-Markovnikov hydroamination of terminal alkynes with primary amines.[93] Beller then learned that some titanocene derivatives catalyzed anti-Markovnikov hydroamination of terminal alkynes with bulky aliphatic amines, while mainly Markovnikov products are obtained with anilines and aryl hydrazines.[95, 96] Unlike the titanocene-based catalyst systems, the bis(amidate)titanium complexes employed by Schafer for terminal alkyne hydroamination demonstrate high regioselectivity in favor of anti-Markovnikov hydroamination of terminal alkynes with primary alkyl amines regardless of the steric bulks in either the amine or the alkyne substrates.[97, 98] The CsOH-catalyzed hydroamination of phenylacetylene with substituted anilines and N-heterocycles was the only known example of anti-Markovnikov addition of secondary amines to terminal alkynes[99] until very recently when it was reported that $TpRh(C_2H_4)_2/PPh_3$ catalyzes anti-Markovnikov hydroamination of terminal alkynes with secondary amines as well as primary ones.[101]

4.2 Experimental Section

4.2.1 Materials and Instrumentation

All manipulations were carried out under nitrogen atmosphere using standard Schlenk techniques. Solvents were freshly distilled under nitrogen from sodium-benzophenone (tetrahydrofuran), sodium (diethyl ether, hexane and toluene), calcium hydride (dichloromethane, chloroform and acetonitrile), magnesium-iodine (methanol and ethanol) or P_2O_5 (C_6D_6 and $CDCl_3$); they were degassed prior to use. Elemental analyses were performed by M-H-W Laboratories, Phoenix, AZ (USA). ^{1}H NMR spectra were obtained from a Bruker DPX-400 spectrometer at 400.13 MHz; chemical shifts (δ, ppm) were reported relative to residual peaks of the deuterated solvents used. $^{13}C\{^1H\}$NMR spectra were recorded with a Bruker DPX-400 spectrometer at 100.61 MHz; chemical shifts were internally referenced to $CDCl_3$ (δ = 77.7 ppm), C_6D_6 (δ = 128.1 ppm) or $(CD_3)_2CO$ (δ = 206.26, 29.84ppm). $^{31}P\{^1H\}$NMR spectra were recorded on a Bruker DPX-400 spectrometer at 161.70 MHz; chemical shifts were externally referenced to 85% H_3PO_4 in D_2O (δ 0.00 ppm). ^{19}F NMR spectra were recorded on a Varian Inova AS 500 NMR spectrometer at 470.22 MHz; chemical shifts were externally referenced to trifluoro-toluene in C_6D_6 (δ = -62.5 ppm). All spectra were obtained at ambient probe temperature unless stated otherwise. High-pressure NMR studies were carried out in commercial 5mm Wilmad pressure-valved NMR Tubes. Infrared spectra were obtained from a Bruker Vector 22 FT-IR spectrophotometer. Mass spectrometry was carried out with a Finnigan MAT 95S mass spectrometer with the samples dissolved in dichloromethane or acetone. HRMS was carried out with Waters Micromass Q-

Tof-2. The ligands *N*,*N*-bis(diphenylphosphino)butylamine (^{n}BuN(PPh$_2$)$_2$),[192] *N*,*N*-bis(diphenylphosphinomethylene)butylamine (^{n}BuN(CH$_2$PPh$_2$)$_2$)[193] and the complexes TpRu(PPh$_3$)$_2$Cl,[116] [TpRu(PMe$_3$)$_2$(CH$_3$CN)]$^{+}$PF$_6^{-}$,[194] [TpRu(PPh$_3$)$_2$(CH$_3$CN)]$^{+}$BF$_4^{-}$,[118] [TpRu(dppm)(CH$_3$CN)]$^{+}$OTf^{-}[117] and [TpmRu(PPh$_3$)$_2$(CH$_3$CN)]$^{2+}$(BF$_4^{-}$)$_2$[195] were prepared according to literature methods.

4.2.2 Syntheses and Reactions

4.2.2.1 4-(trifluoromethyl)-*N*,*N*-bis(diphenylphosphino)benzenamine (4-CF$_3$C$_6$H$_4$N(PPh$_2$)$_2$)

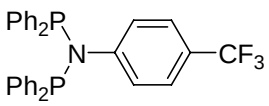

To a stirring solution of 4-(trifluoromethyl)aniline (0.63mL, 5mmol) in toluene (40mL), NEt$_3$ (5mL) was added, followed by dropwise addition of Ph$_2$PCl (2mL, 11mmol). After complete addition, the mixture was heated at 80^{o}C for 16h. At the end of this period, the solution was cooled to room temperature and the insoluble material was filtered out. The solvent of the filtrate was evaporated under reduced pressure and a white paste was obtained. Pre-cooled hexane (5 mL) was added to the residue, with stirring, to produce a white solid. The solid was filtered out and dried under vacuum at room temperature. Yield: 1.27 g (48%). ^{1}H NMR (400.13 MHz, C$_6$D$_6$, 25^{o}C): δ 7.74-7.70 (m, 8H), δ 7.28-7.27 (m, 12H), δ 7.20-7.17 (m, 4H). ^{31}P{^{1}H }NMR (161.7MHz, C$_6$D$_6$, 25^{o}C): δ 68.62 (s).

4.2.2.2 TpRu(4-$CF_3C_6H_4N(PPh_2)_2$)Cl (M21)

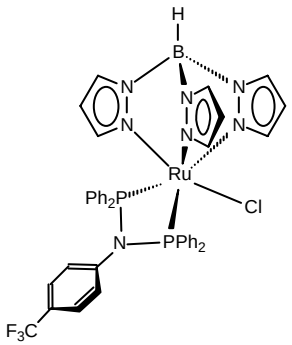

The complex $TpRu(PPh_3)_2Cl$ (2.0g, 2.3mmol) and the ligand 4-$CF_3C_6H_4N(PPh_2)_2$ (1.3g, 2.5mmol) were dissolved in freshly degassed toluene (20 mL). The resulting mixture was refluxed with stirring for 4h. At the end of this period, the mixture was cooled to room temperature and evaporated to dryness under reduced pressure to yield a pale yellow paste. Hexane (15 mL) was added to the residue, with stirring, to produce a pale yellow solid. The solid was filtered out and washed with diethyl ether (2 × 10 mL). It was collected and dried under vacuum at room temperature. Yield: 1.47 g (73 %). Anal. Calcd (%) of $C_{40}H_{34}BClF_3N_7P_2Ru$: C, 54.66; H, 3.90; N, 11.15. Found: C, 54.61; H, 3.97; N, 11.03. IR. (KBr, cm^{-1}): $\upsilon_{(B\text{-}H)}$ 2486 (br). ^1H NMR (400.13 MHz, C_6D_6, 25°C): δ 8.44-8.47 (m, 4H; PPh_2-*H*), δ 7.82 (s, 2H; Tp-*H*), δ 7.59-7.62 (m, 4H; PPh_2-*H*), δ 7.54 (d, 2H; Tp-*H*), δ 7.43 (d, 1H; Tp-*H*), δ 7.28-7.32 (m, 4H; PPh_2-*H*), δ 7.30 (d, 2H; 4-$CF_3C_6H_4$N–), δ 7.16 (d, 2H; 4-$CF_3C_6H_4$N–), δ 6.94-6.96 (m, 4H; PPh_2-*H*), δ 6.81-6.85 (m, 4H; PPh_2-*H*), δ 5.94 (s, 2H; Tp-*H*), δ 5.36 (d, 1H; Tp-*H*), δ 5.22 (t, 1H; Tp-*H*). $^{31}P\{^1H\}$NMR (161.7MHz, C_6D_6, 25°C): δ 88.80 (s). ESI-Ms: *m/z* 879.02, $[M]^+$.

4.2.2.3 TpRu(^{n}BuN(PPh_2)$_2$)Cl (M22)

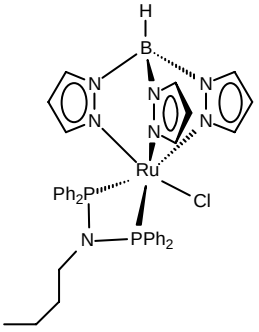

A procedure similar to that for the synthesis of TpRu(4-$CF_3C_6H_4N(PPh_2)_2$)Cl was followed, except that ^{n}BuN$(PPh_2)_2$ (1.1g, 2.5mmol) was used in place of 4-$CF_3C_6H_4N(PPh_2)_2$. Yellow solid; yield: 1.29 g (72 %). Anal. Calcd (%) of $C_{37}H_{39}BClN_7P_2Ru$: C, 56.18; H, 4.97; N,

12.39. Found: C, 55.96; H, 5.05; N, 12.17. IR. (KBr, cm^{-1}): $\upsilon_{(B-H)}$ 2462 (br). ^1H NMR (400.13 MHz, $CDCl_3$, 25°C): δ 8.04-8.05 (m, 4H; PPh_2-*H*), δ 7.68 (s, 2H; Tp-*H*), δ 7.62 (s, 2H; Tp-*H*), δ 7.39-7.44 (m, 6H; PPh_2-*H*), δ 7.38 (d, 1H; Tp-*H*), δ .19-7.23 (m, 6H; PPh_2-*H*), δ 7.09-7.11 (m, 4H; PPh_2-*H*), δ 6.14 (s, 2H; Tp-*H*), δ 5.81 (d, 1H; Tp-*H*), δ 5.17 (t, 1H; Tp-*H*), δ 3.44 (m, 2H; –NC*H*$_2$–), δ 1.44 (m, 2H; –NCH_2CH_2–), δ 1.01 (m, 2H; –$NCH_2CH_2CH_2$–), δ 0.67 (t, 3H; –$NCH_2CH_2CH_2CH_3$). $^{31}P\{^1H\}$NMR (161.7MHz, $CDCl_3$, 25°C): δ 82.97 (s). ESI-M: *m/z* 791, $[M]^+$.

4.2.2.4 TpRu(^{n}BuN(CH_2PPh_2)$_2$)Cl (M23)

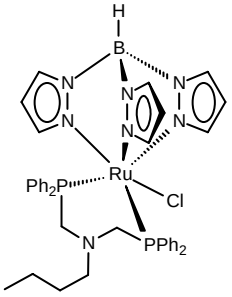

A procedure similar to that for the synthesis of TpRu(4-$CF_3C_6H_4N(PPh_2)_2$)Cl was followed, except that ^{n}BuN(CH_2PPh_2)$_2$ (1.2g, 2.5mmol) was used in place of 4-$CF_3C_6H_4N(PPh_2)_2$. Yellow solid; yield: 1.19 g (63 %). Anal. Calcd (%) of $C_{39}H_{43}BClN_7P_2Ru$: C, 57.19; H, 5.29; N, 11.97. Found: C, 57.03; H, 5.34; N, 11.85. IR. (KBr, cm^{-1}):$\upsilon_{(B-H)}$ 2459 (br). ^1H NMR (400.13 MHz, C_6D_6, 25°C): δ 8.45 (m, 4H; PPh_2-*H*), δ 7.64 (s, 2H; Tp-*H*), δ 7.59 (s, 2H; Tp-*H*), δ 7.34 (d, 1H; Tp-*H*), δ 7.19-7.30 (m, 6H; PPh_2-*H*), δ 6.88-6.94 (m, 10H; PPh_2-*H*), δ 5.84 (s, 2H; Tp-*H*), δ 5.73 (d, 1H; Tp-*H*), δ 5.04 (t, 1H; Tp-*H*), δ 3.86 (m, 2H; –NC*H*$_2$–), δ 3.63 (m, 2H; PPh_2PCH_2–), δ 2.56 (t, 2H; PPh_2PCH_2–), δ 1.36 (m, 2H; –NCH_2CH_2–), δ 1.23 (m, 2H; –$NCH_2CH_2CH_2$–), δ 0.94 (t, 3H; –$NCH_2CH_2CH_2CH_3$). $^{31}P\{^1H\}$NMR (161.7MHz, C_6D_6, 25°C): δ 34.82 (s). ESI-M: *m/z* 819, $[M]^+$.

4.2.2.5 TpRu(4-$CF_3C_6H_4N(PPh_2)_2$)OTf (M24)

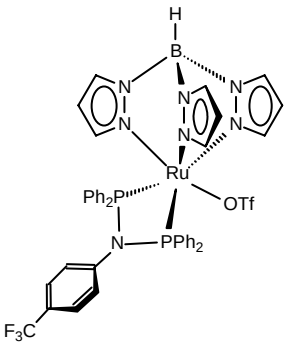

The complex TpRu(4-$CF_3C_6H_4N(PPh_2)_2$)Cl (1.0g, 1.14mmol) and silver triflate (0.36g, 1.4mmol) were dissolved in freshly degassed THF (20 mL). The resulting mixture was refluxed with stirring for 4h. At the end of this period, the mixture was cooled to room temperature and evaporated to dryness under reduced pressure. The residue was extracted with dichloromethane (2 × 10mL). The insoluble material was filtered out. The solvent of the filtrate was removed under reduced pressure and a yellow paste was obtained. Hexane (5 mL) was added to the residue, with stirring, to produce a yellow solid. The solid was filtered out and washed with hexane/ethanol (1:1, 2 × 10 mL). It was then collected and dried under vacuum at room temperature. Yield: 0.81 g (72%). Anal. Calcd (%) of $C_{41}H_{34}BF_6N_7O_3P_2RuS$: C, 49.61; H, 3.45; N, 9.88. Found: C, 49.80; H, 3.57; N, 9.60. IR. (KBr, cm^{-1}): $\upsilon_{(B\text{-}H)}$ 2468 (br). ^1H NMR (400.13 MHz, $(CD_3)_2CO$, 25°C): δ 8.08 (s, 2H; Tp-*H*), δ 7.99-7.98 (m, 4H; PPh_2-*H*), δ 7.70-7.69 (m, 6H; PPh_2-*H*), δ 7.67 (d, 1H; Tp-*H*), δ 7.52 (d, 2H; 4-$CF_3C_6H_4$N–), δ 7.46-7.45 (m, 6H; PPh_2-*H*), δ 7.32-7.30 (m, 4H; PPh_2-*H*), δ 7.21 (d, 2H; 4-$CF_3C_6H_4$N–), δ 6.99 (s, 2H; Tp-*H*), δ 6.33 (d, 2H; Tp-*H*), δ 5.20 (d, 1H; Tp-*H*), δ 5.19 (t, 1H; Tp-*H*). $^{31}P\{^1H\}$NMR (161.7MHz, $(CD_3)_2CO$, 25°C): δ 85.90 (s). ESI-MS: *m/z* 844.22, $[M\text{-}OTf]^+$.

4.2.2.6 [TpRu(4-$CF_3C_6H_4N(PPh_2)_2$)CH_3CN]$^+OTf^-$ (M25)

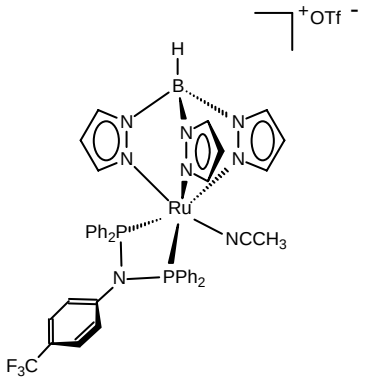

The complex TpRu(4-$CF_3C_6H_4N(PPh_2)_2$)Cl (1.0g, 1.14mmol) and silver triflate (0.36g, 1.4mmol) were dissolved in THF/acetonitrile (20:1, 20 mL). The resulting mixture was refluxed with stirring for 4h. At the end of this period, the mixture was cooled to room temperature and evaporated to dryness under reduced pressure. The residue was extracted with dichloromethane (2 × 10mL). The insoluble material was filtered out. The solvent of the filtrate was removed under reduced pressure and a yellow paste was obtained. Hexane (5 mL) was added to the residue, with stirring, to produce a yellow solid. The solid was filtered out and washed with hexane/ethanol (1:1, 2 × 10 mL). It was then collected and dried under vacuum at room temperature. Yield: 0.77 g (66 %). Anal. Calcd (%) of $C_{43}H_{37}BF_6N_8O_3P_2RuS$: C, 49.96; H, 3.61; N, 10.84. Found: C, 49.60; H, 3.71; N, 10.56. IR. (KBr, cm^{-1}): $\upsilon_{(B-H)}$ 2487 (br). ^1H NMR (400.13 MHz, CD_3CN, 25°C): δ 7.89 (s, 2H; Tp-*H*), δ 7.83-7.84 (m, 4H; PPh_2-*H*), δ 7.74 (s, 2H; Tp-*H*), δ 7.72-7.74 (m, 4H; PPh_2-*H*), δ 7.56 (d, 1H; Tp-*H*), δ 7.41 (t, 4H; PPh_2-*H*), δ 7.28 (q, 4H; PPh_2-*H*), δ 7.13-7.27 (m, 4H; PPh_2-*H*), δ 7.13-7.27 (m, 4H; 4-$CF_3C_6H_4$N–), δ 6.32 (t, 2H; Tp-*H*), δ 5.31 (d, 1H; Tp-*H*), δ 5.20 (t, 1H; Tp-*H*), δ 2.07 (s, 3H; NCCH_3). $^{31}P\{^1H\}$NMR (161.7MHz, CD_3CN, 25°C): δ 87.05 (s). ESI-M: *m/z* 885, $[M]^+$.

4.2.2.7 TpRu(^{n}BuN(PPh$_2$)$_2$) OTf (M26)

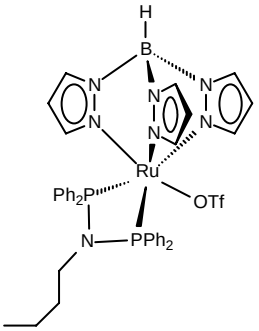

A procedure similar to that for the synthesis of TpRu(4-$CF_3C_6H_4N(PPh_2)_2$)OTf was followed, except that TpRu(^{n}BuN(PPh$_2$)$_2$)Cl (0.9g, 1.14mmol) was used in place of TpRu(4-$CF_3C_6H_4N(PPh_2)_2$)Cl. Yellow solid; yield: 0.84 g (67%). Anal. Calcd (%) of $C_{38}H_{39}BF_3N_7O_3P_2RuS$: C, 50.45; H, 4.35; N 10.84. Found: C, 50.19; H, 4.41; N, 10.61. IR. (KBr, cm^{-1}): $\upsilon_{(B-H)}$ 2478 (br). ^{1}H NMR (400.13 MHz, $CDCl_3$, 25^{o}C): δ 7.77 (d, 2H; Tp-*H*), δ 7.74 (m, 4H; PPh_2-*H*), δ 7.62 (s, 2H; Tp-*H*), δ 7.47-7.53 (m, 6H; PPh_2-*H*), δ 7.28 (t, 2H; PPh_2-*H*), δ 7.17 (s, 1H; Tp-*H*), δ 7.11-7.17 (m, 8H; PPh_2-*H*), δ 6.21 (s, 2H; Tp-*H*), δ 5.82 (s, 1H; Tp-*H*), δ 5.13 (s, 1H; Tp-*H*), δ 3.50 (m, 2H; –NC*H*$_2$–), δ 1.52 (m, 2H; –NCH_2CH_2–), δ 1.06 (m, 2H; –$NCH_2CH_2CH_2$–), δ 0.70 (t, 3H; –$NCH_2CH_2CH_2CH_3$). ^{31}P{^{1}H}NMR (161.7MHz, $CDCl_3$, 25^{o}C): δ 83.32 (s). ESI-M: *m/z* 755, $[M-OTf]^+$.

4.2.2.8 [TpRu(^{n}BuN(PPh$_2$)$_2$)$CH_3CN]^+OTf^-$ (M27)

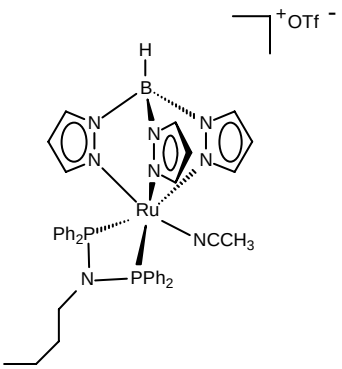

A procedure similar to that for the synthesis of [TpRu(4-$CF_3C_6H_4N(PPh_2)_2$)CH3CN]$^+$OTf$^-$ was followed, except that TpRu(^{n}BuN(PPh$_2$)$_2$)Cl (0.9g, 1.14mmol) was used in place of TpRu(4-$CF_3C_6H_4N(PPh_2)_2$)Cl. Yellow solid; yield: 0.81 g (69%). Anal. Calcd (%) of $C_{40}H_{42}BF_3N_8O_3P_2RuS$: C, 50.80; H, 4.48; N, 11.85. Found: C, 50.64; H, 4.60; N, 11.65. IR. (KBr, cm^{-1}): $\upsilon_{(B-H)}$ 2495 (br). ^{1}H NMR (400.13 MHz, $CDCl_3$, 25^{o}C): δ 7.79 (s, 2H; Tp-*H*), δ 7.59-7.68 (m, 10H; PPh_2-*H*), δ 7.59-7.68 (d, 1H; Tp-*H*), δ 7.34 (t, 2H; PPh_2-*H*), δ

7.23 (s, 2H; Tp-*H*), δ 7.12-7.16 (m, 4H; PPh_2-*H*), δ 7.02-7.03 (m, 4H; PPh_2-*H*), δ 6.28 (d, 1H; Tp-*H*), δ 6.24 (s, 2H; Tp-*H*), δ 5.49 (t, 1H; Tp-*H*), δ 3.74 (m, 2H; –NC*H*$_2$–), δ 2.09 (s, 3H; NCC*H*$_3$), δ 1.63 (m, 2H; –NCH_2C*H*$_2$–), δ 1.22 (m, 2H; –NCH_2CH_2C*H*$_2$–), δ 0.81 (t, 3H; –$NCH_2CH_2CH_2C$*H*$_3$). $^{31}P\{^1H\}$NMR (161.7MHz, $CDCl_3$, 25°C): δ 83.81 (s). ESI-M: *m/z* 797, $[M]^+$.

4.2.2.9 [TpRu(*n*BuN(CH_2PPh_2)$_2$)$CH_3CN]^+OTf^-$ (M28)

A procedure similar to that for the synthesis of $[TpRu(4\text{-}CF_3C_6H_4N(PPh_2)_2)CH_3CN]^+OTf^-$ was followed, except that TpRu(*n*BuN(CH_2PPh_2)$_2$)Cl (0.9g, 1.14mmol) was used in place of TpRu(4-$CF_3C_6H_4N(PPh_2)_2$)Cl. Yellow solid; yield: 0.73 g (61 %). Anal. Calcd (%) of $C_{42}H_{46}BF_3N_8O_3P_2RuS$: C, 51.81; H, 4.76; N, 11.51. Found: C, 51.88; H, 4.88; N, 11.26. IR. (KBr, cm^{-1}): $\upsilon_{(B\text{-}H)}$ 2484 (br). ^1H NMR (400.13 MHz, $CDCl_3$, 25°C): δ 7.90 (d, 1H; Tp-*H*), δ 7.84 (s, 2H; Tp-*H*), δ 7.67 (m, 4H; PPh_2-*H*), δ 7.52-7.58 (m, 4H; PPh_2-*H*), δ 7.33-7.47 (m, 2H; PPh_2-*H*), δ 7.21 (t, 2H; PPh_2-*H*), δ 7.19 (s, 2H; Tp-*H*), δ 6.96 (t, 4H; PPh_2-*H*), δ 6.92 (d, 1H; Tp-*H*), δ 6.35 (m, 4H; PPh_2-*H*), δ 6.11 (s, 2H; Tp-*H*), δ 5.79 (t, 1H; Tp-*H*), δ 4.11 (m, 2H; –NC*H*$_2$–), δ 3.34 (m, 2H; PPh_2PC*H*$_2$–), δ 3.04 (t, 2H; PPh_2PC*H*$_2$–), δ 1.65 (m, 2H; –NCH_2C*H*$_2$–), δ 1.56 (s, 3H; NCC*H*$_3$), δ 1.40 (m, 2H; –NCH_2CH_2C*H*$_2$–), δ 0.97 (t, 3H; –$NCH_2CH_2CH_2C$*H*$_3$). $^{31}P\{^1H\}$NMR (161.7MHz, $CDCl_3$, 25°C): δ 31.01 (s). ESI-M: *m/z* 825, $[M]^+$; 784, $[M\text{-}NCCH_3]^+$.

4.2.2.10 [TpRu(4-$CF_3C_6H_4N(PPh_2)_2$)(=C=CHPh)]$^+$OTf$^-$ (M33)

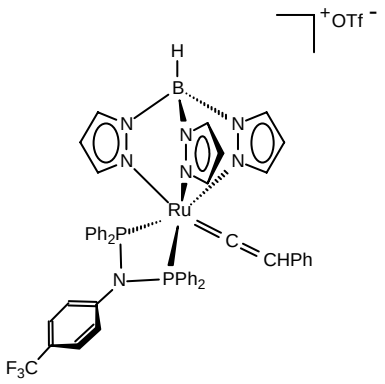

The complex TpRu(4-$CF_3C_6H_4N(PPh_2)_2$)OTf (0.5g, 0.5mmol) was dissolved in freshly degassed chloroform (10 mL) and treated with 3 equiv of phenylacetylene (0.16mL, 1.5mmol) via syringe and needle. The resulting mixture was heated at 60^{o}C for 16h. At the end of this period, the mixture was cooled to room temperature and evaporated to dryness under reduced pressure to yield a pink paste. Hexane (5 mL) was added to the residue, with stirring, to produce a pink solid. The solid was filtered out and washed with hexane/ethanol (3:2, 2 × 5 mL). It was collected and dried under vacuum at room temperature. Yield: 0.43 g (78 %). Anal. Calcd (%) of $C_{49}H_{40}BF_6N_7O_3P_2RuS$: C, 53.76; H, 3.68; N, 8.96. Found: C, 53.64; H, 3.79; N, 8.84. IR. (KBr, cm^{-1}): $\upsilon_{(B\text{-}H)}$ 2486 (br), $\upsilon_{(C=C)}$ 1663 (s). ^{1}H NMR (400.13 MHz, $CDCl_3$, 25^{o}C): δ 7.83 (s, 2H; Tp-*H*), δ 7.79-7.80 (m, 4H; PPh_2-*H*), δ 7.64 (t, 3H; PPh_2-*H*), δ 7.50 (s, 2H; Tp-*H*), δ 7.48 (s, 1H; Tp-*H*), δ 7.46-7.50 (m, 4H; PPh_2-*H*), δ 7.39 (d, 2H; 4-$CF_3C_6H_4$N–), δ 7.24 (t, 3H; =C=CHPh-*H*), δ 7.08-7.23 (m, 10H; PPh_2-*H*), δ 7.01 (d, 2H; 4-$CF_3C_6H_4$N–), δ 6.51 (d, 2H; =C=CHPh-*H*), δ 6.34 (s, 2H; Tp-*H*), δ 5.49 (d, 1H; Tp-*H*), δ 5.36 (t, 1H; Tp-*H*), δ 4.50 (t, 1H; =C=C*H*Ph). ^{31}P{^{1}H}NMR (161.7MHz, $CDCl_3$, 25^{o}C): δ 76.01 (s). ^{13}C{^{1}H}NMR (100.61 MHz, $CDCl_3$, 25 ˚C): δ 375.74 (t, J_{PC} = 18.1 Hz, =*C*=*C*HPh). ESI-MS: *m/z* 945.30, $[M\text{-}PhCCH]^+$.

4.2.2.11 TpRu(4-$CF_3C_6H_4N(PPh_2)_2$)(C≡CPh) (M34)

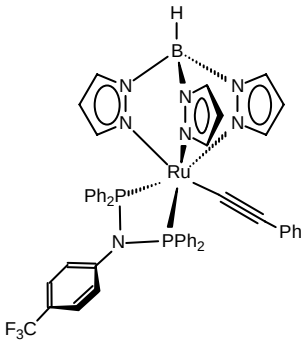

The complex [TpRu(4-$CF_3C_6H_4N(PPh_2)_2$)(=C=CHPh)]OTf (0.5g, 0.45mmol) and NaOH (0.09g, 2.3mol) were dissolved in freshly degassed ethanol (10 mL). The resulting mixture was stirred at room temperature for 30 min. At the end of this period, the solvent of the mixture was evaporated to dryness under reduced pressure. The residue was extracted with toluene (2 × 10mL). The insoluble material was filtered out. The solvent of the filtrate was removed under reduced pressure and a yellow paste was obtained. Hexane (5 mL) was added to the residue, with stirring, to produce a yellow solid. The solid was filtered out and washed with hexane/ethanol (3:2, 2 × 5 mL). It was then collected and dried under vacuum at room temperature. Yield: 0.23 g (55%). Anal. Calcd (%) of $C_{48}H_{39}BF_3N_7P_2Ru$: C, 61.03; H, 4.16; N, 10.38. Found: C, 61.17; H, 4.31; N, 10.16. IR. (KBr, cm^{-1}): $\upsilon_{(B\text{-}H)}$ 2480 (br), $\upsilon_{(C\equiv C)}$ 2086 (vs). ^1H NMR (400.13 MHz, $CDCl_3$, 25°C): δ 8.49-8.51 (m, 4H; PPh_2-*H*), δ 7.78 (s, 2H; Tp-*H*), δ 7.60-7.62 (m, 4H; PPh_2-*H*), δ 7.49 (s, 2H; Tp-*H*), δ 7.49 (s, 1H; Tp-*H*), δ 7.44 (d, 2H; 4-$CF_3C_6H_4$N–), δ 7.25 (m, 4H; PPh_2-*H*), δ 7.17 (q, 3H; –C≡CPh-*H*), δ 7.08 (m, 2H; –C≡CPh-*H*), δ 7.07 (d, 2H; 4-$CF_3C_6H_4$N–), δ 6.94 (m, 4H; PPh_2-*H*), δ 6.88 (m, 4H; PPh_2-*H*), δ 5.92 (d, 2H; Tp-*H*), δ 5.41 (d, 1H; Tp-*H*), δ 5.40 (t, 1H; Tp-*H*). $^{31}P\{^1H\}$NMR (161.7MHz, $CDCl_3$, 25°C): δ 90.66 (s). $^{13}C\{^1H\}$NMR (100.61 MHz, $CDCl_3$, 25 ˚C): δ 132.29 (t, J_{PC} = 23 Hz, –*C*≡CPh). ESI-MS: *m/z* 945.32 $[M]^+$.

4.2.2.12 [TpRu(4-$CF_3C_6H_4N(PPh_2)_2$)(CO)]$^+$OTf$^-$ (M35)

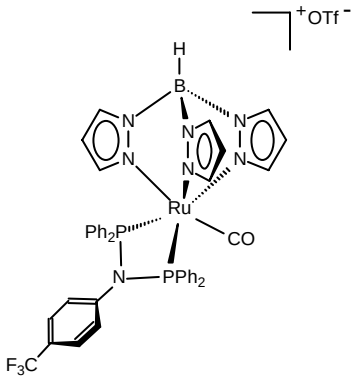

The reaction was carried out in a 250 mL stainless steel autoclave. The complex TpRu(4-$CF_3C_6H_4N(PPh_2)_2$)OTf (0.5g, 0.5mmol) was dissolved in freshly degassed chloroform (10 mL). The solution was heated under 5 bar of CO at 120^{o}C for 30 min. At the end of this period, the mixture was cooled to room temperature and evaporated to dryness under reduced pressure to yield a white paste. Hexane (5 mL) was added to the residue, with stirring, to produce a white solid. The solid was filtered out and washed with diethyl ether (2 × 5 mL). It was collected and dried under vacuum at room temperature. Yield: 0.41 g (80 %). Anal. Calcd (%) of $C_{42}H_{34}BF_6N_7O_4P_2RuS$: C, 49.43; H, 3.36; N, 9.61. Found: C, 50.15; H, 3.49; N, 9.44. IR. (KBr, cm^{-1}): $\upsilon_{(B\text{-}H)}$ 2525 (br), $\upsilon_{(C\equiv O)}$ 1995 (vs). ^{1}H NMR (400.13 MHz, $CDCl_3$, 25^{o}C): δ 7.81 (s, 2H; Tp-*H*), δ 7.77-7.79 (m, 10H; PPh_2-*H*), δ 7.50 (d, 1H; Tp-*H*), δ 7.46-7.50 (t, 2H; PPh_2-*H*), δ 7.40 (d, 2H; 4-$CF_3C_6H_4$N–), δ 7.24-7.28 (m, 4H; PPh_2-*H*), δ 7.11-7.15 (m, 4H; PPh_2-*H*), δ 7.13 (s, 2H; Tp-*H*), δ 6.94 (d, 2H; 4-$CF_3C_6H_4$N–), δ 6.31 (s, 2H; Tp-*H*), δ 5.43 (d, 1H; Tp-*H*), δ 5.35 (t, 1H; Tp-*H*). ^{31}P{^{1}H}NMR (161.7MHz, $CDCl_3$, 25^{o}C): δ 80.66 (s). ^{13}C{^{1}H}NMR (100.61 MHz, $CDCl_3$, 25 ˚C): δ 201.06 (t, J_{PC} = 14.7 Hz, –*C*≡O). ESI-MS: *m/z* 872.24, [M]$^+$.

4.2.2.13 General Procedure for TpRu(4-$CF_3C_6H_4N(PPh_2)_2$)OTf (M24)-Catalyzed 2-Alkenylation of 1,3-Dicarbonyl Compounds with Terminal Alkynes

The reactions were carried out in 11 mm Schlenk tubes equipped with Teflon screw caps. (The reactions in **Table 4.6**, entries 7-9, 11, 13 were carried out in 5mm pressure-valved NMR tubes under 10 bar of Ar). In a typical run, ruthenium complex (0.005 mmol, 0.4mol %) was loaded into the tube; the system was evacuated and filled with nitrogen for four cycles. 1,3-Dicarbonyl compounds (1.25 mmol) and terminal alkynes (1.5 mmol) were then added to the tube via syringes and needles. The tube was sealed with the screw cap and the reaction mixture was heated in a silicon oil bath at 120^oC. At the end of the specific period, the tube was cooled to room temperature. 50μL of 1,1,2,2-tetrachloroethane was added as internal standard; a 0.1 mL aliquot of the solution was removed and analyzed by ^1H NMR spectroscopy (in $CDCl_3$). Conversion of the reaction was obtained by measuring the integrations of the characteristic peaks of the products with reference to distinct peaks of the internal standard. The organic products **3a**,[88] **3i**,[196] **3j**,[197] **3l**,[198] and **3m**[88] described in **Table 4.6** are known and were characterized by comparing their ^1H and $^{13}C\{^1H\}$NMR data with the reported ones. In cases where the organic products are new compounds (**3b**, **3c**, **3d**, **3e**, **3f**, **3g**, **3h** and **3k**), they were isolated by flash column chromatography on silica gel or by preparative thin layer chromatography (silica gel) and were characterized by ^1H, $^{13}C\{^1H\}$NMR spectroscopies, mass spectrometry and HRMS analysis.

4.2.2.14 3-(1-hydroxyethylidene)-4-(4-methoxyphenyl)pent-4-en-2-one (3b)

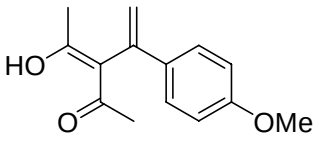

Pale yellow oil; ^{1}H NMR (400 MHz, $CDCl_3$): δ 16.66 (s, 1H; enol-O*H*), δ 7.35 (d, *J* = 9 Hz, 2H; 4-$OCH_3C_6H_4$–), δ 6.85 (d, *J* = 9 Hz, 2H; 4-$OCH_3C_6H_4$–), δ 5.78 (s, 1H; –C=CH_2), δ 5.10 (s, 1H; –C=CH_2), δ 3.77 (s, 3H; 4-O$CH_3C_6H_4$–), δ 1.96 (s, 6H; methyl–CH_3). ^{13}C{^{1}H}NMR (100 MHz, $CDCl_3$): δ 191.52, 160.09, 143.26, 132.55, 127.51, 116.53, 114.42, 114.38, 55.51, 23.798. HRMS (+ESI): *m*/*z*: calcd for $C_{14}H_{16}O_3$: 232.1099; found: 233.1171 $[M+H]^+$.

4.2.2.15 4-hydroxy-3-(1-p-tolylvinyl)pent-3-en-2-one (3c)

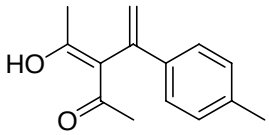

Pale yellow oil; ^{1}H NMR (400 MHz, $CDCl_3$): δ 16.73 (s, 1H; enol-O*H*), δ 7.38 (d, *J* = 8 Hz, 2H; 4-$CH_3C_6H_4$–), δ 7.18 (d, *J* = 8 Hz, 2H; 4-$CH_3C_6H_4$–), δ 5.91 (s, 1H; –C=CH_2), δ 5.21 (s, 1H; –C=CH_2), δ 2.38 (s, 3H; 4-C$H_3C_6H_4$–), δ 2.02 (s, 6H; methyl–CH_3). ^{13}C{^{1}H}NMR (100 MHz, $CDCl_3$): δ 191.59, 143.78, 138.43, 137.26, 129.86, 126.29, 117.74, 114.37, 23.90, 21.48. HRMS (+ESI): *m*/*z*: calcd for $C_{14}H_{16}O_2$: 216.2756; found: 217.1227 $[M+H]^+$.

4.2.2.16 3-(1-(4-bromophenyl)vinyl)-4-hydroxypent-3-en-2-one (3d)

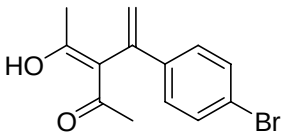

Pale yellow oil; ^{1}H NMR (400 MHz, $CDCl_3$): δ 16.84 (s, 1H; enol-O*H*), δ 7.56 (d, *J* = 8 Hz, 2H; 4-BrC_6H_4–), δ 7.44 (d, *J* = 8 Hz, 2H; 4-BrC_6H_4–), δ 6.04 (s, 1H; –C=CH_2), δ 5.39 (s, 1H; –C=CH_2), δ 2.08 (s, 6H; methyl–CH_3). ^{13}C{^{1}H}NMR (100 MHz, $CDCl_3$): δ 191.71, 143.14, 139.31, 132.47, 128.18, 122.85, 119.68, 113.90, 24.12. HRMS (+ESI): *m*/*z*: calcd for $C_{13}H_{13}BrO_2$: 281.1451; found: 281.0188 $[M]^+$.

4.2.2.17 3-(1-(4-fluorophenyl)vinyl)-4-hydroxypent-3-en-2-one (3e)

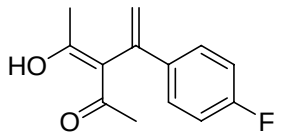

Pale yellow oil; ^{1}H NMR (400 MHz, $CDCl_3$): δ 16.66 (s, 1H; enol-O*H*), δ 7.38 (dd, *J* = 6, 8 Hz, 2H; 4-FC_6H_4–), δ 6.97 (t, *J* = 8 Hz, 2H; 4-FC_6H_4–), δ 5.81 (s, 1H; –C=CH_2), δ 5.18 (s, 1H; –C=CH_2), δ 1.93 (s, 6H; methyl–CH_3). ^{13}C{^{1}H}NMR (100 MHz, $CDCl_3$): δ 191.62, 164.38, 161.92, 142.99, 136.36, 128.09, 118.55, 116.12, 115.91, 114.13, 23.84. HRMS (+ESI): *m*/*z*: calcd for $C_{13}H_{13}FO_2$: 220.2395; found: 221.0975 $[M+H]^+$.

4.2.2.18 4-hydroxy-3-(1-(thiophen-3-yl)vinyl)pent-3-en-2-one (3f)

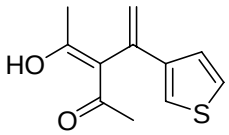

Pale yellow oil; ^{1}H NMR (400 MHz, $CDCl_3$): δ 16.59 (s, 1H; enol-O*H*), δ 7.08 (m, 1H; thiophene-*H*), δ 7.25-7.29 (m, 1H; thiophene-*H*), δ 7.29-7.33 (m, 1H; thiophene-*H*), δ 5.81 (s, 1H; –C=CH_2), δ 5.15 (s, 1H; –C=CH_2), δ 2.00 (s, 6H; methyl–CH_3). ^{13}C{^{1}H}NMR (100 MHz, $CDCl_3$): δ 191.57, 142.85, 139.00, 127.12, 125.52, 122.97, 117.52, 114.51. HRMS (+ESI): *m*/*z*: calcd for $C_{11}H_{12}O_2S$: 208.2768; found: 209.0639 $[M+H]^+$.

4.2.2.19 3-(1-cyclopentylideneethyl)-4-hydroxypent-3-en-2-one (3g)

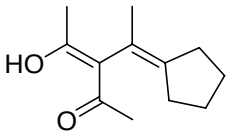

Pale yellow oil; ^{1}H NMR (400 MHz, $CDCl_3$): δ 16.12 (s, 1H; enol-O*H*), δ 2.11 (m, 2H; cyclopentyl–CH_2), δ 1.82 (m, 2H; cyclopentyl–CH_2), δ 1.79 (s, 6H; methyl–CH_3), δ 1.59 (s, 6H; methyl–CH_3), δ 1.53 (m, 2H; cyclopentyl–CH_2), δ 1.44 (m, 2H; cyclopentyl–CH_2). ^{13}C{^{1}H}NMR (100 MHz, $CDCl_3$): δ 190.29, 144.85, 121.53, 116.12, 32.41,

30.97, 27.21, 22.98, 21.18. HRMS (+ESI): *m*/*z*: calcd for $C_{12}H_{18}O_2$: 194.2701; found: 195.1384 $[M+H]^+$.

4.2.2.20 3-(1-hydroxyethylidene)-4,7-dimethyloct-4-en-2-one (3h)

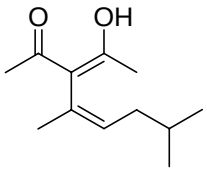

Pale yellow oil; ^{1}H NMR (400 MHz, $CDCl_3$): δ 16.46 (s, 1H; enol-O*H*), δ 5.54 (t, *J* = 7 Hz,1H; =C*H*CH_2–), δ 1.99 (s, 6H; methyl–C*H*$_3$), δ 1.83 (s, 3H; methyl–C*H*$_3$), δ 1.74 (t, *J* = 7 Hz, 2H; =CHC*H*$_2$–), δ 1.61 (m, 1H; –C*H*$(CH_3)_2$), δ 0.86 (d, *J* = 6 Hz, 6H; –CH(C*H*$_3$)$_2$). ^{13}C{^{1}H}NMR (100 MHz, $CDCl_3$): δ 190.77, 132.28, 131.98, 113.46, 39.14, 29.00, 25.82, 23.49, 23.27. HRMS (+ESI): *m*/*z*: calcd for $C_{12}H_{20}O_2$: 196.286; found: 197.1543 $[M+H]^+$.

4.2.2.21 4-hydroxy-6-methyl-3-(1-phenylvinyl)heptan-2-one (3k)

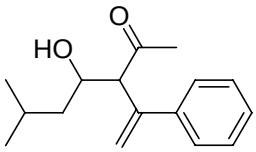

Pale yellow oil; ^{1}H NMR (400 MHz, $CDCl_3$): δ 17.17 (s, 1H; enol-O*H*), δ 7.66 (d, *J* = 7 Hz, 2H; Ph–*H*), δ 7.54 (t, *J* = 7 Hz, 2H; Ph–*H*), δ 7.49 (m, 1H; Ph–*H*), δ 6.14 (s, 1H; –C=C*H*$_2$), δ 5.43 (s, 1H; –C=C*H*$_2$), δ 2.49 (m, 1H; –CH_2C*H*$(CH_3)_2$), δ 2.33 (m, 2H; –C*H*$_2$CH$(CH_3)_2$), δ 2.20 (s, 3H, methyl–C*H*$_3$), δ 1.03-1.71 (m, 6H; –CH_2CH(C*H*$_3$)$_2$). ^{13}C{^{1}H}NMR (100 MHz, $CDCl_3$): δ 193.00, 192.68, 143.72, 140.28, 129.09, 128.55, 126.27, 118.89, 114.48, 44.79, 26.17, 24.31, 22.93. HRMS (+ESI): *m*/*z*: calcd for $C_{16}H_{20}O_2$: 244.3288; found: 245.1540 $[M+H]^+$.

4.2.2.22 NMR Monitoring of TpRu(4-$CF_3C_6H_4N(PPh_2)_2$)OTf (M24)-Catalyzed 2-Alkenylation of Acetylacetone with Phenylacetylene

The reactions were carried out in 11 mm Schlenk tubes equipped with Teflon screw caps. Ruthenium complex TpRu(4-$CF_3C_6H_4N(PPh_2)_2$)OTf (0.005 mmol, 0.4mol %) was loaded into each of the eight tubes equipped with magnetic stirrers. The thbes were evacuated and filled with nitrogen for four cycles. Acetylacetone (1.25 mmol) and phenylacetylene (1.5 mmol) were then added to each tube via syringes and needles. The tubes were sealed with the screw caps and heated in a silicon oil bath at 120^oC. At different time intervals, a tube was withdrawn from the silicon oil bath and rapidly cooled down to room temperature; ^1H, ^{19}F and $^{31}P\{^1H\}$NMR spectra of the mixture were taken. The relative concentrations of the species present were obtained by comparing the integrations of their signals in the $^{31}P\{^1H\}$NMR spectra. Conversion of the reaction was obtained by measuring the integrations of the characteristic peaks of the products with reference to distinct peaks of unreacted acetylacetone in the ^1H NMR spectrum.

4.2.2.23 General Procedure for TpRu(4-$CF_3C_6H_4N(PPh_2)_2$)OTf (M24)-Catalyzed Hydroamination of Terminal Alkynes with Secondary Amines

The reactions were carried out in 11 mm Schlenk tubes equipped with Teflon screw caps. In a typical run, ruthenium complex TpRu(4-$CF_3C_6H_4N(PPh_2)_2$)OTf (0.01 mmol, 1 mol %) was loaded into the tube. The tube was evacuated and filled with nitrogen for four cycles. Methanol (0.1 mL), secondary amine (1 mmol) and terminal alkyne (1.2 mmol) were then added to the tube via syringes and needles. The tube was sealed with the screw cap and the solution was stirred in a silicon oil bath at 120^oC for 24 h. At the end of this

period, the tube was cooled to room temperature and 25μL of 1,1,2,2-tetrachloroethane was added as internal standard; a 0.1 mL aliquot of the solution was removed and analyzed by ^{1}H NMR spectroscopy (in C_6D_6). Conversion of the reaction was obtained by measuring the integrations of the characteristic peaks of the products with reference to distinct peaks of the internal standard. The organic products **5a**, **5b**,[199] **5c**,[200] **5d**, **5e**, **5f**,[199] **5g**,[201] **5h**,[202] **5i**[203] and **5j**[204] described in **Table 4.12** are known compounds and were characterized by comparing their ^{1}H NMR data with the reported ones.

4.2.2.24 NMR Monitoring of TpRu(4-$CF_3C_6H_4N(PPh_2)_2$)OTf (M24)-Catalyzed Hydroamination of Phenylacetylene with Diethylamine

The reaction was carried out in a 5 mm NMR pressure-valved NMR tube. The ruthenium complex TpRu(4-$CF_3C_6H_4N(PPh_2)_2$)OTf (0.01 mmol, 1 mol %) was loaded to the tube; it was evacuated and filled with nitrogen for four cycles. CD_3OD (0.1 mL), diethylamine (1 mmol) and phenylacetylene (1.2 mmol) were then added to the tube via syringes and needles. The tube was heated in a silicon oil bath at 120^{o}C under 10 bar of Ar. At different time intervals, the NMR tube was rapidly cooled down to room temperature and ^{1}H and $^{31}P\{^{1}H\}$NMR spectra of the solution were taken. The relative concentrations of the species present were obtained by comparing the integrations of their signals in the $^{31}P\{^{1}H\}$NMR spectra. Conversion of the reaction was obtained by measuring the integrations of the characteristic peaks of the products with reference to distinct peaks of unreacted diethylamine in the ^{1}H NMR spectrum.

4.2.2.25 Crystallographic Structures Analysis of Ru(II) Complexes M21, M22,M24, M33-M35

Crystals suitable for X-ray diffraction study were obtained by layering of hexane onto saturated benzene solutions, (**M21** and **M34**), chloroform solution (**M24**) and dichloromethane solution (**M33** and **M35**). A suitable crystal of each of the complex was mounted on a Bruker CCD area detector diffractomer and subjected to Mo Kα radiation (λ = 0.71073 Å) from a generator operating at 50 kV and 30 mA. The intensity data of **M21**, **M22**, **M24**, **M33-M35** were collected in the range θ = 1.68 – 27.44^{o}, 1.51-27.45 ^{o}, 1.73 – 27.58^{o}, 1.81-27.44^{o}, 2.09-27.49 ^{o} and 1.73-27.59 ^{o} respectively, with oscillation frames of ψ and ω in the range 0 – 180^{o}. A total of 2288 frames in **M21**, 3416 frames in **M22**, 2240 frames in **M24**, 2264 frames in **M33**, 1928 frames in **M34** and 2064 frames in **M35** were taken in four shells. An empirical absorption correction of the SADABS (Sheldrick, 1996) program based on Fourier coefficient fitting was applied. The crystal structure was solved by Patterson function methods and expanded by difference Fourier synthesis, then refined by full-matrix least-squares on F^2 using the Bruker Smart and Bruker SHELXTL program packages. All non-hydrogen atoms were refined anisotropically. Hydrogen atoms were placed in ideal positions and refined as riding atoms. The R and R_w values of **M21** are 0.0600 and 0.1221, **M22** are 0.0391 and 0.1213, **M24** are 0.0930 and 0.2400, **M33** are 0.0733 and 0.2046, **M34** are 0.0434 and 0.0561 and **M35** are 0.0703, respectively. Further crystallographic details and selected bond distances and angles for **M21**, **M24**, **M33-M35** can be found in results and discussion section.

4.3 Results and Discussion

In continuance of our recent work on the catalytic activities of ruthenium complexes,[149] we studied the 2-alkenylation of 1,3-dicarbonyl compounds with terminal alkynes catalyzed by ruthenium complexes (**eq. 4.1**).

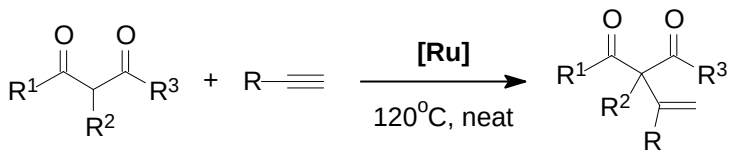

1 **2** **3** (4.1)

Complexes **M29-M32** are well-known hydrotris(pyrazolyl)borate (Tp) ruthenium complexes; complexes **M24-M28** are Tp complexes containing bis(phosphino)amine ligands (**Chart 4.1**). These amine-bridged diphosphines, which offer more opportunities for electronic and steric tuning than the dppm analogue, have played important roles in chromium-catalyzed ethylene trimerization[71] and tetramerization reactions.[72] The amine moiety of bis(phosphino)amine might act as an internal base or as a hydrogen acceptor in hydrogen bonding.

4.3.1 Preparation and characterization of M21-M28, and X-ray structures of M21, M22 and M24

Complexes **M24-M28** were prepared by chloride abstraction from their chloride precursors, TpRu(4-$CF_3C_6H_4N(PPh_2)_2$)Cl (**M21**), TpRu(^{n}BuN$(PPh_2)_2$)Cl (**M22**) and TpRu(^{n}BuN$(CH_2PPh_2)_2$)Cl (**M23**) using Ag^+OTf^- in the absence or presence of acetonitrile; the chloride precursors **M21-M23** were prepared by ligand substitution of TpRu$(PPh_3)_2$Cl (**M4**) in toluene (**Scheme 4.1**).

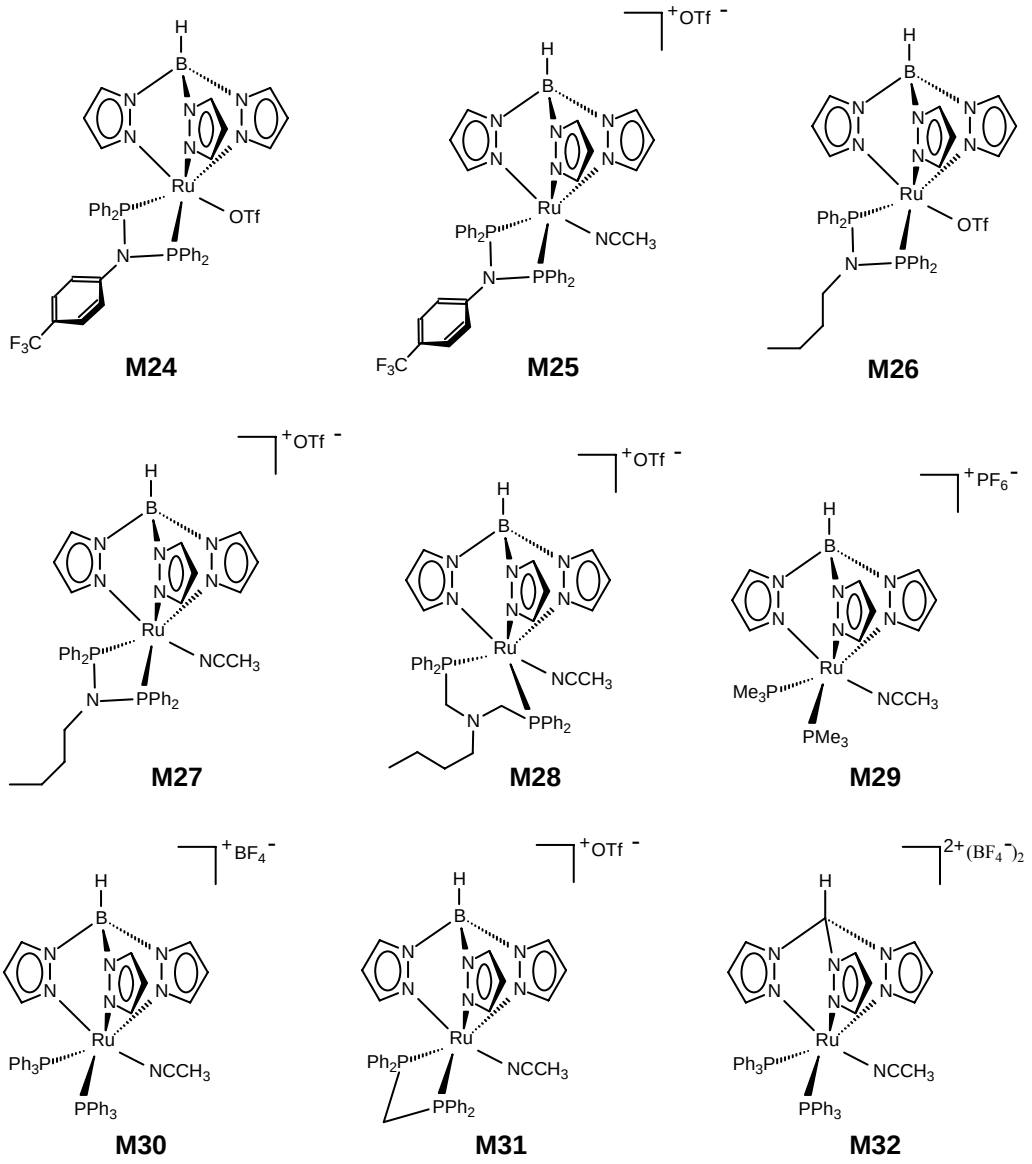

Chart 4.1

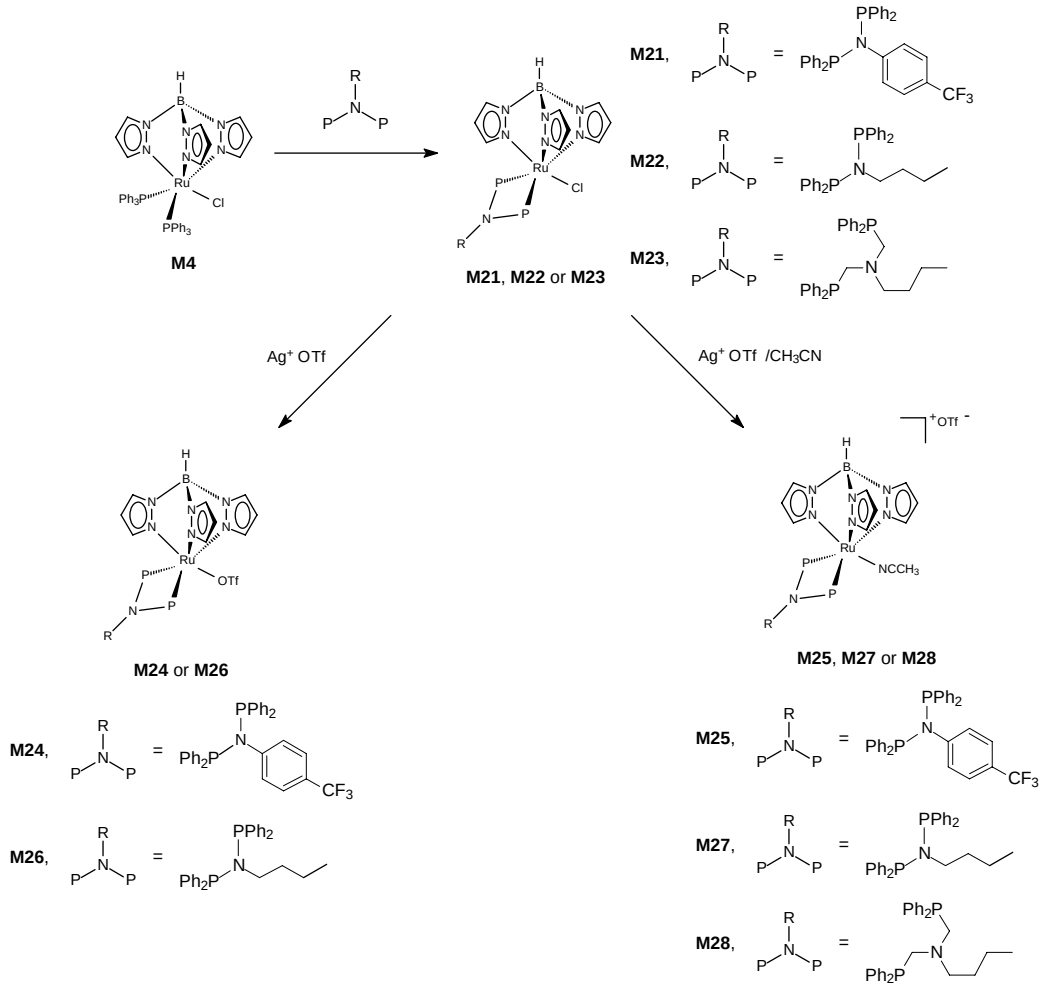

Scheme 4.1 Preparation of M21-M28

The complexes **M21**-**M28** have been characterized by elemental analyses, IR, NMR (^{1}H, ^{31}P{^{1}H} and ^{13}C{^{1}H}) spectroscopies and mass spectroscopy (details are given in **Section 4.2**). The ^{1}H NMR spectra of the chloride complexes **M21**-**M23** exhibit the resonances of Tp and the bis(phosphino)amine ligands in the expected ranges. The methylene hydrogen atoms of the *N*,*N*-bis(diphenylphosphinomethylene)butylamine ligand of **M23** are diasterotopic, which appear as a pair of multiplets at δ 3.63 and 2.56 ppm. The ^{31}P{^{1}H}NMR spectrum of each of the complexes **M21**-**M23** shows a singlet for the bis(phosphino)amine ligand at δ 88.8, 83.0 and 34.8 ppm for **M21**, **M22** and

M23, respectively. Structural views of **M21** and **M22** determined by X-ray crystallography are shown in **Figures 4.1** and **4.2**, respectively. The crystal data and refinement details for the complexes are given in **Table 4.1**. Selected bond distances and angles are given in **Tables 4.2** and **4.3**. The strained 4-membered rings sustain acute chelated angles of P(1)-Ru(1)-P(2) = 70.84(2)° and P(2)-Ru(1)-P(1) = 69.990(12)°, respectively, in **M21** and **M22**. The mean P–N bond distances in **M21** and **M22** are 1.74 Å and 1.71 Å, respectively. The sum of the angles around nitrogen atoms of the bis(phosphino)amine ligands (Σ_N) in both **M21** and **M22** are equal to 360°, clearly indicates that the geometries around nitrogen atoms are strictly planar; this is a characteristic feature of bis(phosphino)amine ligands[205] and their complexes.[68]

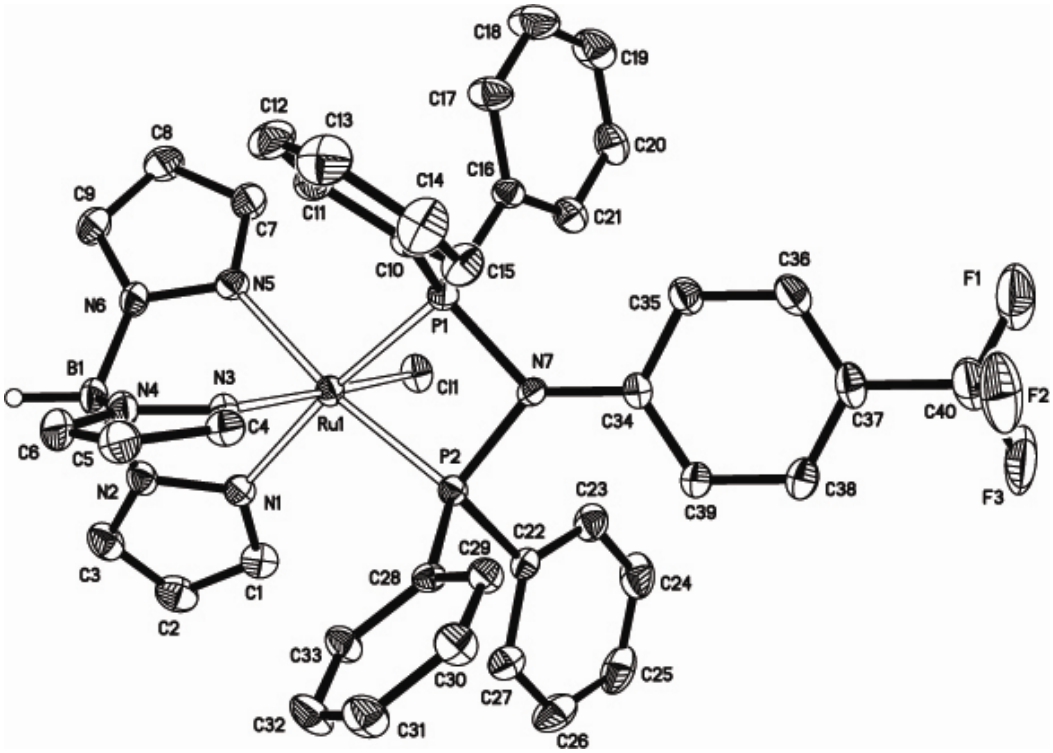

Figure 4.1 ORTEP view (30% probability) of TpRu(4-$CF_3C_6H_4N(PPh_2)_2$)Cl (M21) showing the atom-labeling scheme

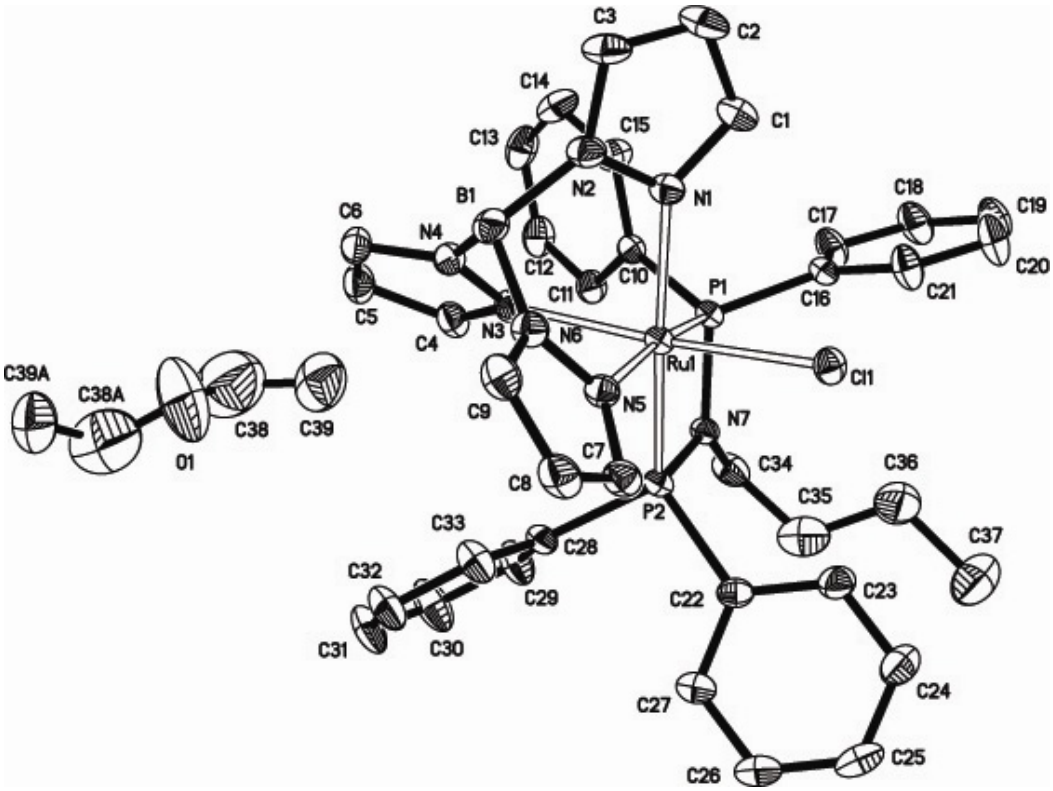

Figure 4.2 ORTEP view (30% probability) of TpRu(^{n}BuN(PPh$_2$)$_2$)Cl ·1/2($C_2H_5OC_2H_5$) (M22 ·1/2($C_2H_5OC_2H_5$)) showing the atom-labeling scheme

Table 4.1 Crystal Data and Structure Refinement of TpRu(4-$CF_3C_6H_4N(PPh_2)_2$)Cl (M21), TpRu(^{n}BuN(PPh_2)$_2$)Cl (M22·1/2($C_2H_5OC_2H_5$)) and TpRu(4-$CF_3C_6H_4N(PPh_2)_2$)OTf (M24·$CHCl_3$)

Complex	**M21**		**M22·1/2($C_2H_5OC_2H_5$)**		**M24·$CHCl_3$**	
Empirical formula	$C_{40}H_{34}BClF_3N_7P_2Ru$		$C_{37}H_{39}BClN_7P_2Ru \cdot 1/2(C_2H_5OC_2H_5)$		$C_{41}H_{34}BF_6N_7O_3P_2RuS \cdot CHCl_3$	
Formula weight	1113.34		828.08		1112.00	
Temperature	296(2) k		296(2) k		296(2) k	
Wavelength	0.71073 Å		0.71073 Å		0.71073 Å	
Crystal system	Monoclinic		Monoclinic		Monoclinic	
Space group	P2(1)/n		C2/c		P2(1)/n	
Unit cell dimensions	a = 14.5535(3) Å	α = 90°.	a = 24.7652(3) Å	α = 90°.	a = 11.0918(3) Å	α = 90°.
	b = 23.0611(4) Å	β = 101.0910(10) °.	b = 17.1575(2) Å	β = 118.1980(10) °.	b = 18.3635(5) Å	β = 91.642(2) °.
	c = 16.7854(3) Å	γ = 90°.	c = 21.1208(4) Å	γ = 90°.	c =23.4991(7) Å	γ = 90°.
Volume	5528.29(18) $Å^3$		7909.3 $Å^3$		4784.4(2) $Å^3$	
Z	4		8		4	
Density (calculated)	1338 Mg/m^3		1.391 Mg/m^3		1.544 Mg/m^3	
Absorption coefficient	0.444 mm^{-1}		0.584 mm^{-1}		0.676 mm^{-1}	
F(000)	2288		3416		2240	
Crystal size	0.42 x 0.38 x 0.32 mm^3		0.50 x 0.38 x 0.36 mm^3		0.48 x 0.40 x 0.36 mm^3	
Theta range for data collection	1.68 to 27.44°.		1.51 to 27.45°.		1.73 to 27.58°.	
Index ranges	-18<=h<=11, -28<=k<=29, -17<=l<=21		-32<=h<=32, -17<=k<=22, -27<=l<=27		-14<=h<=14, -21<=k<=23, -30<=l<=30	
Reflections collected	44183		32648		57260	
Independent reflections	12576 [R(int) = 0.0928]		9033 [R(int) = 0.0299]		10929 [R(int) = 0.2478]	
Completeness to theta	= 27.44°, 99.7 %		= 27.45°, 99.8 %		=27.58°, 98.6 %	
Absorption correction	Semi-empirical from equivalents		Semi-empirical from equivalents		Semi-empirical from equivalents	
Max. and min. transmission	1.000 and 0.768		1.000 and 0.814		1.000 and 0.420	
Refinement method	F ull-matrix least-squares on F^2		F ull-matrix least-squares on F^2		Full-matrix least-squares on F^2	
Data / restraints / parameters	12576 / 33 / 679		9033 / 6 / 464		10929 / 48 / 622	
Goodness-of-fit on F^2	1.003		1.004		1.006	
Final R indices [I>2sigma(I)]	R1 = 0.0600, wR2 = 0.1221		R1 = 0.0391, wR2 = 0.1213		R1 = 0.0930, wR2 = 0.2400	
R indices (all data)	R1 = 0.1405, wR2 = 0.1499		R1 = 0.0561, wR2 = 0.1405		R1 = 0.2356, wR2 = 0.3042	
Largest diff. peak and hole	0.575 and -0.508 e.$Å^{-3}$		0.926 and -0.448 e.$Å^{-3}$		1.011 and -0.938 e.$Å^{-3}$	

Table 4.2 Selected Bond Distances (Å) and Angles (˚) for TpRu(4-$CF_3C_6H_4N(PPh_2)_2$)Cl (M21)

	Bond distances (Å)		
Ru(1)-Cl(1)	2.4011(6)	Ru(1)-P(1)	2.2403(5)
Ru(1)-N(1)	2.1333(16)	Ru(1)-P(2)	2.2468(6)
Ru(1)-N(3)	2.0985(16)	P(1)-N(7)	1.7344(17)
Ru(1)-N(5)	2.1206(17)	P(2)-N(7)	1.7435(16)
	Bond angles (˚)		
C(34)-N(7)-P(1)	131.90(13)	N(3)-Ru(1)-P(2)	97.69(5)
C(34)-N(7)-P(2)	131.32(14)	N(5)-Ru(1)-Cl(1)	87.94(5)
N(1)-Ru(1)-Cl(1)	87.63(5)	N(5)-Ru(1)-N(1)	84.81(6)
N(1)-Ru(1)-P(1)	173.36(5)	N(5)-Ru(1)-P(1)	101.65(5)
N(1)-Ru(1)-P(2)	102.64(5)	N(5)-Ru(1)-P(2)	172.05(5)
N(3)-Ru(1)-Cl(1)	170.37(4)	P(1)-N(7)-P(2)	96.78(8)
N(3)-Ru(1)-N(1)	84.65(6)	P(1)-Ru(1)-Cl(1)	91.043(19)
N(3)-Ru(1)-N(5)	85.65(6)	P(1)-Ru(1)-P(2)	70.84(2)
N(3)-Ru(1)-P(1)	97.27(4)	P(2)-Ru(1)-Cl(1)	89.59(2)

Table 4.3 Selected Bond Distances (Å) and Angles (°) for TpRu(^{n}BuN(PPh$_2$)$_2$)Cl·1/2($C_2H_5OC_2H_5$) (M22·1/2($C_2H_5OC_2H_5$))

Bond distances (Å)			
Ru(1)-Cl(1)	2.4116(4)	Ru(1)-P(1)	2.2767(4)
Ru(1)-N(1)	2.1357(10)	Ru(1)-P(2)	2.2672(3)
Ru(1)-N(3)	2.1040(11)	P(1)-N(7)	1.7065(10)
Ru(1)-N(5)	2.1252(12)	P(2)-N(7)	1.7129(12)
Bond angles (°)			
C(34)-N(7)-P(1)	128.15(9)	N(3)-Ru(1)-P(2)	94.75(3)
C(34)-N(7)-P(2)	132.55(9)	N(5)-Ru(1)-Cl(1)	84.68(3)
N(1)-Ru(1)-Cl(1)	85.38(3)	N(5)-Ru(1)-N(1)	85.56(4)
N(1)-Ru(1)-P(1)	103.06(3)	N(5)-Ru(1)-P(1)	171.32(3)
N(1)-Ru(1)-P(2)	173.05(3)	N(5)-Ru(1)-P(2)	101.39(3)
N(3)-Ru(1)-Cl(1)	1167.21(4)	P(1)-N(7)-P(2)	99.30(6)
N(3)-Ru(1)-N(1)	85.71(4)	P(1)-Ru(1)-Cl(1)	96.818(13)
N(3)-Ru(1)-N(5)	85.50(5)	P(2)-Ru(1)-Cl(1)	95.195(12)
N(3)-Ru(1)-P(1)	94.12(4)	P(2)-Ru(1)-P(1)	69.990(12)

The ^{1}H NMR spectra of the triflate complexes TpRu(4-$CF_3C_6H_4$N(PPh$_2$)$_2$)OTf (**M24**) and TpRu(^{n}BuN(PPh$_2$)$_2$) OTf (**M26**) are similar to those of their chloride precursors **M21** and **M22**, respectively, and are not further discussed here. The bis(phosphino)amine ligands of **M24** and **M26** appear as

singlets at δ 85.9 and 83.3 ppm, respectively, in their $^{31}P\{^{1}H\}$NMR spectra. Other analytical data of **M24** and **M26** support the given formulation. In addition, the structure of **M24** was confirmed by X-ray crystallography as depicted in **Figure 4.3**. The crystal data and refinement details for the complexes are given in **Table 4.1**. Selected bond distances and angles are reported in **Table 4.4**. The geometry at the ruthenium exists as a distorted octachedral. The bite angle of bis(phosphino)amine ligand produces a P(1)-Ru(1)-P(2) angle of 71.05(4)°, which is highly deviated from 90°. The Ru(1)-O(1) distance to the bounded triflate of 2.162(3) Å is significantly shorter than the Ru-OTf distances of 2.227 (mean Ru–O bond distances), 2.239(5) and 2.2377(16) Å seen for *cis-mer*-$Ru(SO_3CF_3)(CO)(Cyttp)$ (Cyttp = $PhP(CH_2CH_2CH_2PCy_2)$,[206] $[Ru(Me)(CO)_2(^{i}Pr\text{-}DAB)]^{+}OTf^{-}$ (^{i}Pr-DAB = $^{i}Pr–N=CHCH=N–^{i}Pr$)[207] and $Ru(SO_3CF_3)\{C_6H_3(CH_2NMe_2)_2\text{-}2,6\}(C_7H_8)$,[208] respectively, implying high electrophilicity of the metal center. The mean P-N distance in **M24** of 1.73 Å is slightly shorter than its chloride precursor **M21**. The angles sum around nitrogen atoms of the bis(phosphino)amine ligands $\Sigma_{N(7)}$ are equal to 359.88°, which is very close to planar.

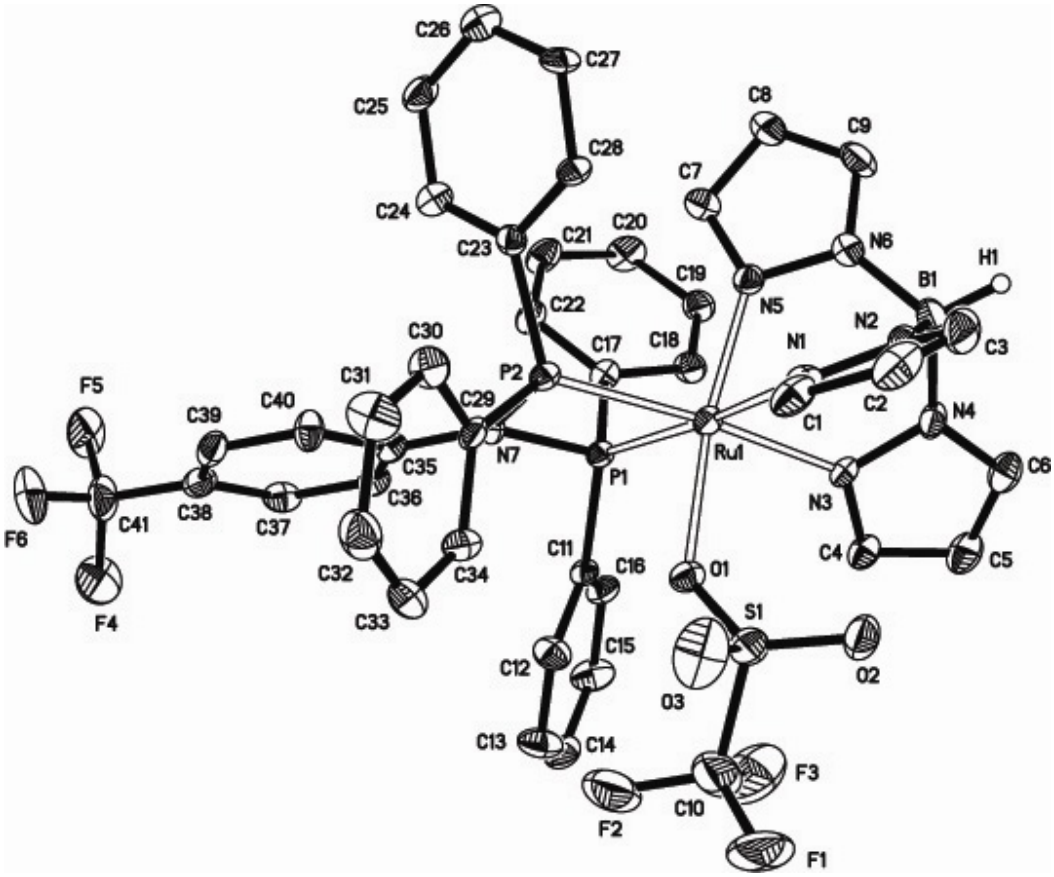

Figure 4.3 ORTEP view (30% probability) of TpRu(4-$CF_3C_6H_4N(PPh_2)_2$)OTf (M24) showing the atom-labeling scheme

Table 4.4 Selected Bond Distances (Å) and Angles (°) for TpRu(4-$CF_3C_6H_4N(PPh_2)_2$)OTf (M24)

Bond distances (Å)			
Ru(1)-N(1)	2.145(3)	Ru(1)-P(1)	2.2537(10)
Ru(1)-N(3)	2.117(3)	Ru(1)-P(2)	2.2641(11)
Ru(1)-N(5)	2.062(3)	P(1)-N(7)	1.740(3)
Ru(1)-O(1)	2.162(3)	P(2)-N(7)	1.723(3)
Bond angles (°)			
C(35)-N(7)-P(1)	128.0(2)	N(5)-Ru(1)-N(1)	84.74(13)
C(35)-N(7)-P(2)	133.3(2)	N(5)-Ru(1)-N(3)	85.94(12)
N(1)-Ru(1)-O(1)	89.34(12)	N(5)-Ru(1)-O(1)	171.69(11)
N(1)-Ru(1)-P(1)	173.52(9)	N(5)-Ru(1)-P(1)	95.92(9)
N(1)-Ru(1)-P(2)	102.47(9)	N(5)-Ru(1)-P(2)	96.51(9)
N(3)-Ru(1)-N(1)	85.90(12)	O(1)-Ru(1)-P(1)	90.63(8)
N(3)-Ru(1)-O(1)	87.82(11)	O(1)-Ru(1)-P(2)	90.45(8)
N(3)-Ru(1)-P(1)	100.57(9)	P(1)-Ru(1)-P(2)	71.05(4)
N(3)-Ru(1)-P(2)	171.43(9)	P(2)-N(7)-P(1)	98.58(15)

The ^{1}H NMR spectra of the solvent complexes [TpRu(4-$CF_3C_6H_4N(PPh_2)_2$)CH_3CN]$^+$OTf$^-$ (**M25**), [TpRu(^{n}BuN$(PPh_2)_2$)CH_3CN]$^+$OTf$^-$ (**M27**) and [TpRu(^{n}BuN$(CH_2PPh_2)_2$)CH_3CN]$^+$OTf$^-$ (**M28**) show signals of the acetonitrile ligands at δ 2.07, 2.09 and 1.56 ppm, respectively. The methylene

resonances of the *N*,*N*-bis(diphenylphosphinomethylene)butylamine ligand of **M28** appear as a pair of multiplets at δ 3.34 and 3.04 ppm. Singlets that correspond to the bis(phosphino)amine ligands are seen at δ 87.1, 83.8 and 31.0 ppm for **M25**, **M27** and **M28**, respectively.

4.3.2 Hydrotris(pyrazolyl)borato (Tp) Ruthenium Complexes-Catalyzed 2-Alkenylation of Acetylacetone with Phenylacetylene

The efficacy of the bis(phosphino)amine as a ligand in the 2-alkenylation of acetylacetone was initially tested in a brief qualitative screening with several metal catalyst candidates **M24**-**M32** (**Chart 4.1**). **Table 4.5** summarizes the results on the 2-alkenylation of acetylacetone with phenylacetylene catalyzed by those Tp ruthenium complexes.

The complexes TpRu(4-$CF_3C_6H_4N(PPh_2)_2$)OTf (**M24**), [TpRu(4-$CF_3C_6H_4N(PPh_2)_2$)CH_3CN]$^+$OTf$^-$ (**M25**), and TpRu(^{n}BuN$(PPh_2)_2$) OTf (**M26**) catalyzes the 2-alkenylation efficiently (entries 3-5). However, the 2-alkenylation reactions result in lower yields at lower temperature (entries 1 & 2). Complex [TpRu(^{n}BuN$(PPh_2)_2$)CH_3CN]$^+$OTf$^-$ (**M27**) displays moderate catalytic activity for the reaction (entries 6 & 12). The *N*,*N*-bis(diphenylphosphinomethylene) analogue [TpRu(^{n}BuN$(CH_2PPh_2)_2$)CH_3CN]$^+$OTf$^-$ (**M28**) of **M27**, shows a low catalytic activity towards the 2-alkenylation reaction (entries 7 & 13). In contrast to the high activity of **M24**-**M26**, complexes [TpRu$(PMe_3)_2CH_3CN$]$^+PF_6^-$ (M**29**), [TpRu$(PPh_3)_2CH_3CN$]$^+BF_4^-$ (**M30**), [TpRu(dppm)CH_3CN] $^+$OTf$^-$ (**M31**) and [TpmRu$(PPh_3)_2CH_3CN$]$^{2+}(BF_4^-)_2$ (**M32**) show very low reactivities even heating for 6 h (entries 8-11, 14-17).

Table 4.5 Tp Ru(II) Complexes-Catalyzed 2-Alkenylation of Acetylacetone with Phenylacetylene[a]

entry	catalyst	Temp. (^oC)	time(h)	% conversion[b]
1	$TpRu(4\text{-}CF_3C_6H_4N(PPh_2)_2)OTf$ (**M24**)	80	3	0
2	**M24**	100	3	3
3	**M24**	120	3	89
4	$[TpRu(4\text{-}CF_3C_6H_4N(PPh_2)_2)CH_3CN]^+OTf^-$ (**M25**)	120	3	64
5	$TpRu(^nBuN(PPh_2)_2)OTf$ (**M26**)	120	3	64
6	$[TpRu(^nBuN(PPh_2)_2)CH_3CN]^+OTf^-$ (**M27**)	120	3	13
7	$TpRu(^nBuN(CH_2PPh_2)_2))CH_3CN]^+OTf^-$ (**M28**)	120	3	7
8	$[TpRu(PMe_3)_2CH_3CN]^+PF_6^-$ (**M29**)	120	3	5
9	$[TpRu(PPh_3)_2CH_3CN]^+BF_4^-$ (**M30**)	120	3	0
10	$[TpRu(dppm)CH_3CN]^+OTf^-$ (**M31**)	120	3	0
11	$[TpmRu(PPh_3)_2CH_3CN]^{2+}(BF_4^-)_2$ (**M32**)	120	3	0
12	**M27**	120	6	46
13	**M28**	120	6	29
14	**M29**	120	6	7
15	**M30**	120	6	4
16	**M31**	120	6	0
17	**M32**	120	6	0

[a]Reaction conditions: catalyst (0.005 mmol), acetylacetone (1.25 mmol), phenylacetylene (1.5 mmol).

[b]Conversion (based on acetylacetone) determined by ^1H NMR spectroscopy.

4.3.3 TpRu(4-$CF_3C_6H_4N(PPh_2)_2$)OTf (M24)-Catalyzed 2-Alkenylation of 1,3-Dicarbonyl Compounds with Terminal Alkynes

The **M24**-catalyzed 2-alkenylation of 1,3-dicarbonyl compounds with terminal alkynes was found to be facile and versatile in the absence of any solvent; we carried out a detailed investigation on the reaction. The results of **M24**-catalyzed 2-alkenylation of 1,3-dicarbonyl compounds with terminal alkynes are summarized in **Table 4.6**. The regioselectivity favors introduction of the 1,3-dicarbonyl moiety to the internal alkynic carbon atom to give 2-alkenyl-1,3-dicarbonyl derivatives.

Acetylacetone reacts is alkenylated with phenylacetylene derivatives with high yields (entries 1-5). Substituents on the phenyl ring of the alkynes do not induce pronounced electronic effect, although electron-withdrawing groups seem to slow down the reactions to a certain extent. The heterocyclic alkyne, 3-ethynylthiophene (**2f**) reacts slower and longer reaction time is needed to achieve quantitative yield (entry 6). Likewise, the alkyl acetylenes and the benzyl derivative are not very reactive but still high-yielding upon 6 and 10 h of heating, respectively (entries 8-10). The sterically bulky dicarbonyl compound, dibenzoylmethane (**1c**) only gives high yield after prolonged heating (entry 12). Substrates with low boiling point do not undergo alkenylation under normal reaction conditions. The reactions have to be proformed inside pressure-valved NMR tubes which are pressurized with 10 bar of Ar to prevent the solutions from boiling too vigorously (entries 7-9, 11, and 13). Isomeric products resulting from C=C bond migration are formed in some cases (entries 7-10, 12).

Table 4.6 TpRu(4-$CF_3C_6H_4N(PPh_2)_2$)OTf (M24)-Catalyzed 2-Alkenylation of 1,3-Dicarbonyl Compounds with Terminal Alkynes[a]

entry	dicarbonyl compound	terminal alkyne	time (h)	product	% conversion[b]
1	**1a** 	**2a** 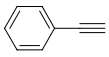	3.5	**3a** 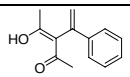	95 [87]
2	**1a**	**2b** 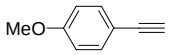	4	**3b** 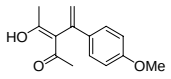	92 [86]
3	**1a**	**2c** 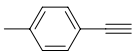	4	**3c** 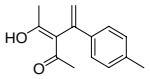	98 [93]
4	**1a**	**2d** 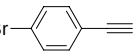	5	**3d** 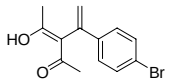	97 [93]
5	**1a**	**2e** 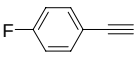	6	**3e** 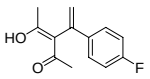	99 [89]
6	**1a**	**2f** 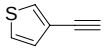	8	**3f** 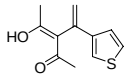	99 [92]
7[c]	**1a**	**2g** 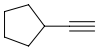	3	**3g** 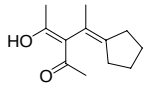	97 [78]
8[c]	**1a**	**2h** 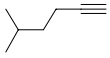	6	**3h** 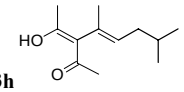 (*Z*:*E* = 47:53)	90 [73]
9[c]	**1a**	**2i** 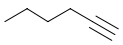	6	**3i** 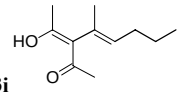 (*Z*:*E* = 54:46)	91 [69]
10	**1a**	**2j** 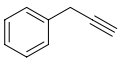	10	**3j** 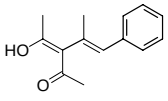 (*Z*:*E* = 35:65)	97 [86]
11[c]	**1b** 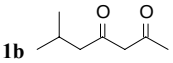	**2a**	4	**3k** 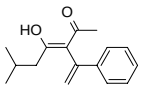	94 [76]
12	**1c** 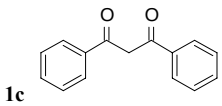	**2a**	24	**3l** 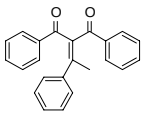	93 [88]
13[c]	**1d** 	**2a**	4	**3m** 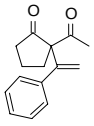	91 [78]

[a]Reaction conditions: catalyst (0.005 mmol), dicarbonyl compound (1.25 mmol), terminal alkyne (1.5 mmol); 120˚C.
[b]Conversion (based on dicarbonyl compound) determined by ^{1}H NMR spectroscopy. Values in bracket indicate isolated yields.
[c]Under 10 bar Ar.

4.3.4 NMR Monitoring of TpRu(4-$CF_3C_6H_4N(PPh_2)_2$)OTf (M24)-Catalyzed 2-Alkenylation of Acetylacetone with Phenylacetylene

To gain more information on the possible reaction mechanism of the catalytic reaction, **M24**-catalyzed 2-alkenylation of acetylacetone with phenylacetylene was monitored by NMR spectroscopy. Several solutions prepared from the same mother solution containing **M24** and the substrates were heated in sealed tubes in the same oil bath at 120 °C. The tubes were removed from the oil bath at different times; an aliquot was taken from each tube and studied by ^1H, ^{19}F and $^{31}P\{^1H\}$NMR spectroscopies. **Figure 4.4** shows the $^{31}P\{^1H\}$ spectra of the samples which had been heated for different periods of time; the percent conversions to the product with time are summarized in **Table 4.7**. The $^{31}P\{^1H\}$ spectrum (in benzene-d_6) of the sample after 5 min of heating showed a signal at δ 75.9 ppm due to the vinylidene complex [TpRu(4-$CF_3C_6H_4N(PPh_2)_2$)(=C=CHPh)]$^+$OTf$^-$ (**M33**). A very minor signal attributing to the alkynyl species TpRu(4-$CF_3C_6H_4N(PPh_2)_2$)(C≡CPh) (**M34**) was also observable; the intensity of this peak grew with time at the expense of that of the signal of **M33**. A minute amount of the carbonyl complex [TpRu(4-$CF_3C_6H_4N(PPh_2)_2$)(CO)]$^+$OTf$^-$ (**M35**) was detected after 1 h. The complexes **M33**-**M35** were identified by comparison with independently prepared samples. ^{19}F NMR spectroscopy revealed the formation of minute amount of phenylacetylene-TfOH adduct, styryl triflate after 5 min, as indicated by the presence of a very small signal at δ -74.4 ppm; this signal, which disappeared after 15 min, was identical to that of an authentic sample of styryl triflate. It should be pointed out that the ^1H NMR spectra taken concurrently with the $^{31}P\{^1H\}$NMR spectra showed that the 2-alkenylation of acetylacetone only

proceeded to a very small extend at 30 min of heating; moderate progress of catalysis was observed after 90min, and approximately 90% of the acetylacetone was converted to the corresponding alkenyl derivative after heating for 3h.

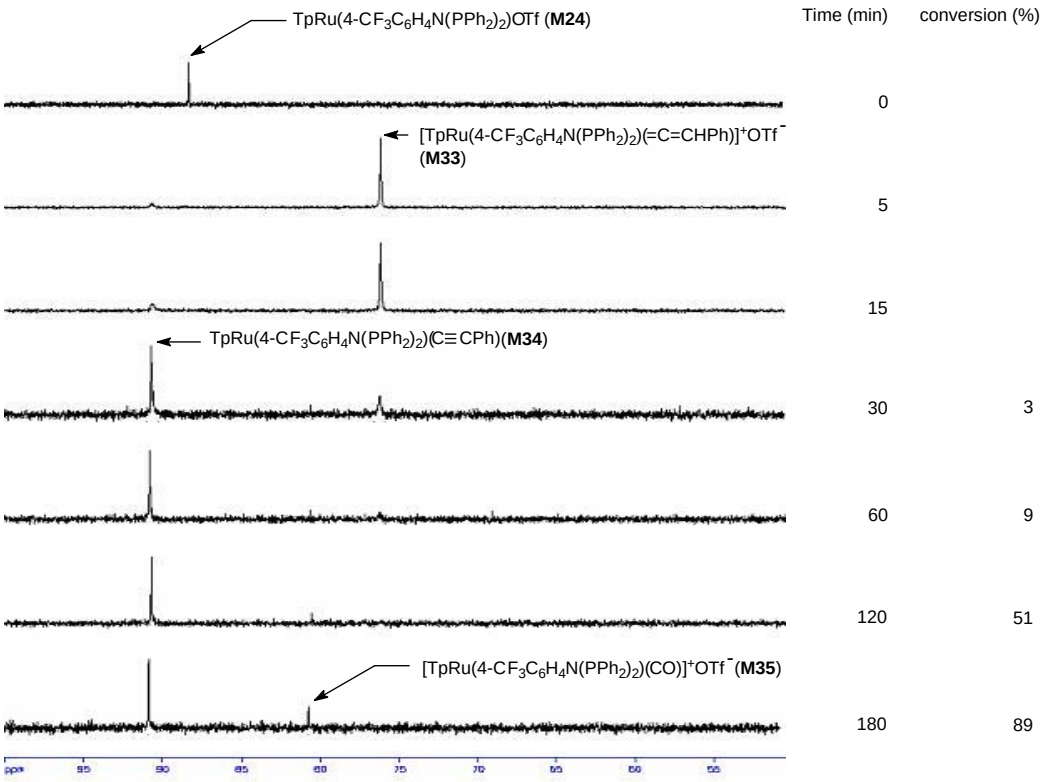

Figure 4.4 $^{31}P\{^{1}H\}$NMR study of TpRu(4-$CF_3C_6H_4N(PPh_2)_2$)OTf (M24)-catalyzed 2-alkenylation of acetylacetone with phenylacetylene

Table 4.7 Conversion of TpRu(4-$CF_3C_6H_4N(PPh_2)_2$)OTf (M24)-Catalyzed 2-Alkenylation of Acetylacetone with Phenylacetylene[a]

Time (min)	Conversion (%)[b]
30	3
60	9
90	31
120	51
150	74
180	89

[a]Reaction conditions: catalyst (0.005 mmol), acetylacetone (1.25 mmol), phenylacetylene (1.5 mmol); 120˚C.

[b] Conversion based on acetylacetone.

4.3.5 NMR Monitoring of TpRu(4-$CF_3C_6H_4N(PPh_2)_2$)OTf (M24)-Catalyzed 2-Alkenylation Reaction using Dried Acetylacetone and Phenylacetylene

The $^{31}P\{^1H\}$NMR monitoring showed that the alkynyl complex **M34** was the dominant metal-containing species throughout the catalytic process and it was probably generated via deprotonation of the vinylidene complex **M33**. The possibility that formation of the phenylacetylene-TfOH adduct (**eq. 4.2**) was the

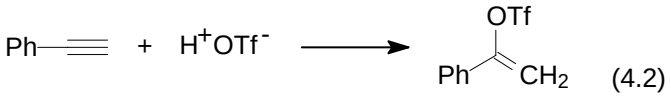

(4.2)

cause of deprotonation of **M33** can be ruled out since the adduct was formed in minute amount and it only existed for a short period of time. We suspect that adventitious water in the substrates, which were not dried, might be the reagent that deprotonated the vinylidene species to give **M34**. We therefore treated the acetylacetone and phenylacetylene with 4 Å molecular sieves and repeated the ^1H and $^{31}P\{^1H\}$NMR montoring experiment with these 'dried' substrates. **Figure 4.5** shows the $^{31}P\{^1H\}$ profile of the 2-alkenylation at different periods of time, the column at the right shows the percent conversions to the product. Obviously, for alkenylation reaction using the 'dried' substrates, the disappearance and the growing in of **M33** and **M34**, respectively, took place at a much slower pace. The latter only became the dominant species after nearly 2 h; minor amount of the carbonyl species **M35** was also detected. It is also noteworthy that only 27 % conversion was obtained with the 'dried' substrates after 3 h, whereas with 'undried' substrates gave 89 % conversion.

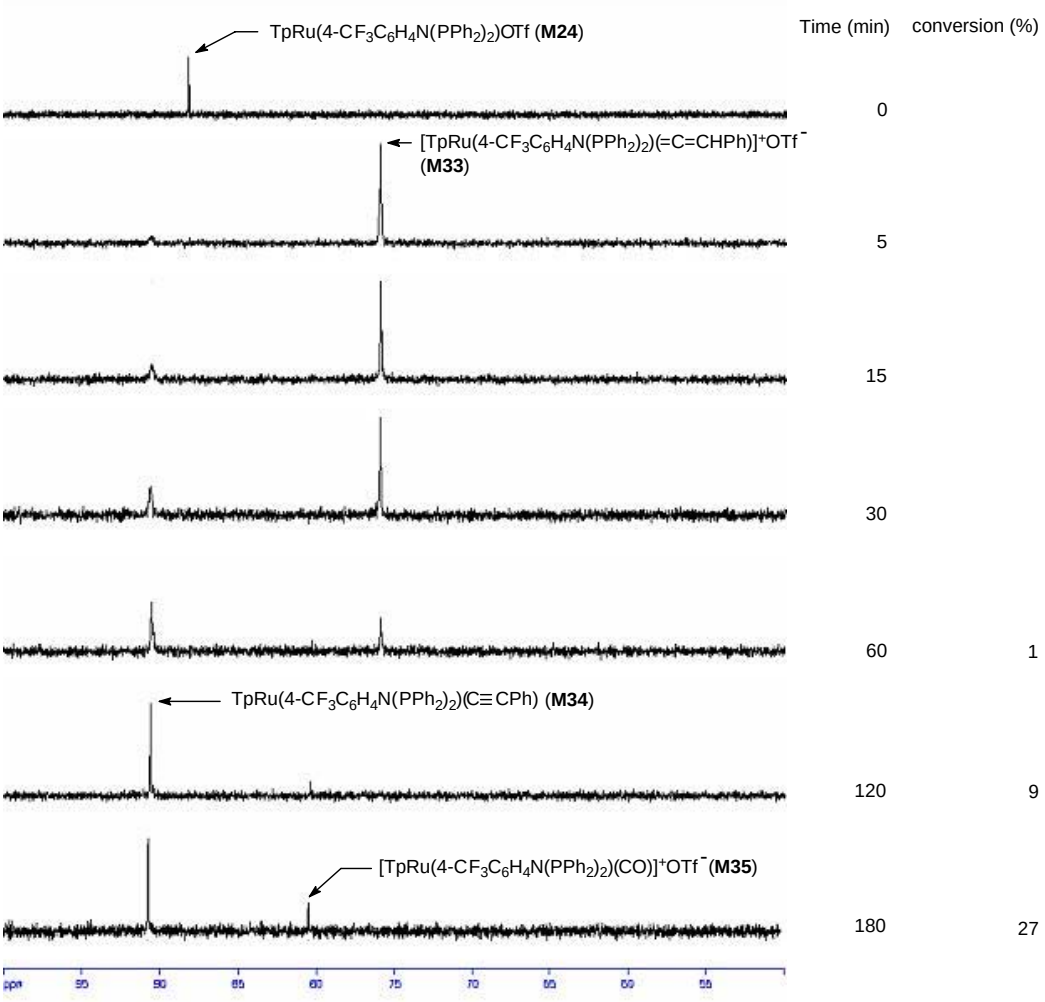

Figure 4.5 $^{31}P\{^{1}H\}$NMR study of TpRu(4-$CF_3C_6H_4N(PPh_2)_2$)OTf (M24)-catalyzed 2-alkenylation reaction using dried substrates

4.3.6 NMR Monitoring of TpRu(4-$CF_3C_6H_4N(PPh_2)_2$)(C≡CPh) (M34)-Catalyzed 2-Alkenylation of Acetylacetone with Phenylacetylene

The alkynyl complex **M34**, which seems to be the resting state of the **M24**-catalyzed 2-alkenylation of acetylacetone with phenylacetylene, was independently prepared. Surprisingly, this independently-prepared **M34** was found to be inactive for the 2-alkenylation reaction; however, upon addition of 1 equiv of $H_3O^+OTf^-$ (6M), it became active, showing a catalytic activity similar to that of **M24**. It can be seen from **Figure 4.6** that upon addition of 1 equiv of

$H_3O^+OTf^-$, **M34** was immediately converted to the vinylidene complex **M33**. After heating at 120 °C for 30 min, **M34** reappeared and became the dominant species throughout the monitoring experiment.

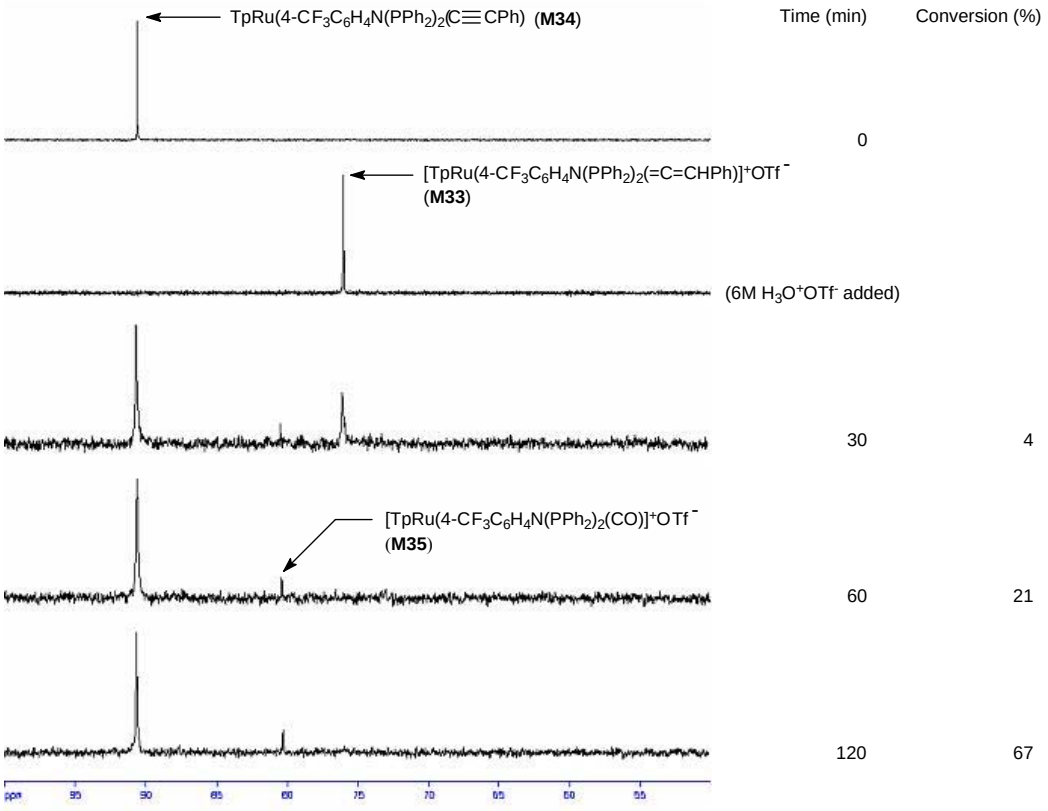

Figure 4.6 $^{31}P\{^1H\}$NMR study of TpRu(4-$CF_3C_6H_4N(PPh_2)_2$)(C≡CPh) (M34)-catalyzed alkenylation of acetylacetone with phenylacetylene

When the observations of the NMR monitoring experiments (**Figures 4.4 - 4.6**) are taken together, it seems that $H_3O^+OTf^-$, which is the conjugate acid formed from the deprotonation of the vinylidene complex **M33** by H_2O in the course of catalysis, readily protonates the alkynyl complex **M34** to regenerate **M33** at room temperature; however, at the reaction temperature (120 °C), it might have reacted with other species present in the catalytic system and form a

new acidic species which would not be able to protonate **M34** to regenerate **M33**. One possibility is the trapping of the proton from $H_3O^+OTf^-$ by the 1,3-dicarbonyl compounds to form $\mathbf{B}^+$ (**eq 4.3**).

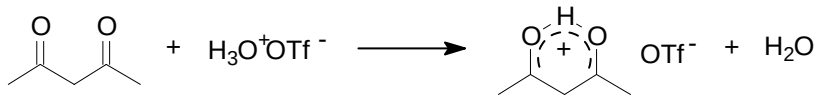

$\mathbf{B}^+$ (4.3)

4.3.7 Preparation, Characterization and X-ray Structure of [TpRu(4-$CF_3C_6H_4N(PPh_2)_2$)(=C=CHPh)]$^+OTf^-$ (M33)

The vinylidene complex **M33** was readily prepared by reacting the triflate complex **M24** with excess phenylacetylene in chloroform at 60 °C. The most relevant spectroscopic feature of **M33** is the characteristic deshielded $^{13}C\{^1H\}$NMR signal for the α-carbon of the vinylidene moiety at δ 375.7 ppm; the C_β resonance falling within the aromatic region. The vinylidene proton of **M33** can be readily identified as a triplet at δ 4.5 ppm in the ^1H NMR spectrum. $^{31}P\{^1H\}$NMR spectroscopy shows a singlet at δ 75.9 ppm, which is consistent with the chemical equivalence of the two phosphorous atoms of the bis(phosphino)amine ligand. Similar to other reported bis(phosphino)amino complexes, the ^{31}P NMR signal of **M33** is considerably deshielded compared to that of the free ligand.

Pink crystals of **M33** suitable for X-ray diffraction study were obtained by layering of hexane onto a saturated dichloromethane solution of the complex. The structure of **M33** is shown as **Figure 4.7**. The crystal data and refinement

details are given in **Table 4.8**. Selected bond lengths and angles are listed in **Table 4.9**. The ruthenium atom appears in a distorted octahedral coordination, where the Tp ligand fills three coordination positions, and the other are occupied by the two phosphorus atoms of the chelating 4-$CF_3C_6H_4N(PPh_2)_2$ ligand and the C_α atom of the vinylidene group. The two Ru-N bond distances *cis* to the vinylidene moiety are significantly shorter (Ru(1)-N(3) = 2.147(2) Å); (Ru(1)-N(5) = 2.134(2) Å) than the one *trans* to vinylidene (Ru(1)-N(1) = 2.198(2) Å). Similar phenomena were observed for the complexes $[TpRu=C=CHPh(pn)]^+OTf^-$ (pn = $Ph_2PCH_2CH_2NMe_2$),[129] $[TpRu=C=CHPh(tmeda)]^+BPh_4^-$ (tmeda = $Me_2NCH_2CH_2NMe_2$)[209] and $[TpRu=C=CHPh(PEt_3)_2]^+BPh_4^-$.[210] This is attributable to the strong π-acceptor ability of vinylidene ligand. The two Ru-P bond distances Ru(1)-P(1) and Ru(1)-P(2) measure 2.3078(7) Å and 2.2804(8) Å, respectively. The Ru(1)-C(10) bond distance of 1.838(3) Å corresponding to a ruthenium-carbon double bond is relatively longer than that in $[TpRu=C=CHPh(pn)]^+OTf^-$ (1.821(5) Å),[129] $[TpRu=C=CHPh(tmeda)]^+BPh_4^-$ (1.820(5) Å),[209] $[TpRu=C=CHPh(PEt_3)_2]^+BPh_4^-$ (1.810(1) Å),[210] and $TpRu=C=CHPh(PPh_3)(Cl)$ (1.801(4) Å).[211] The C(10)-C(11) bond distance, 1.296(5) Å, corresponds to a C=C double bond. The vinylidene group assembles almost linearly with the ruthenium atom, forming a C(11)-C(10)-Ru(1) angle of 171.0(3)˚. The sum of the angles around nitrogen atom $\Sigma_{N(7)}$ that links the phosphorus atoms in the diphosphinoamine ligand is 359.99°.

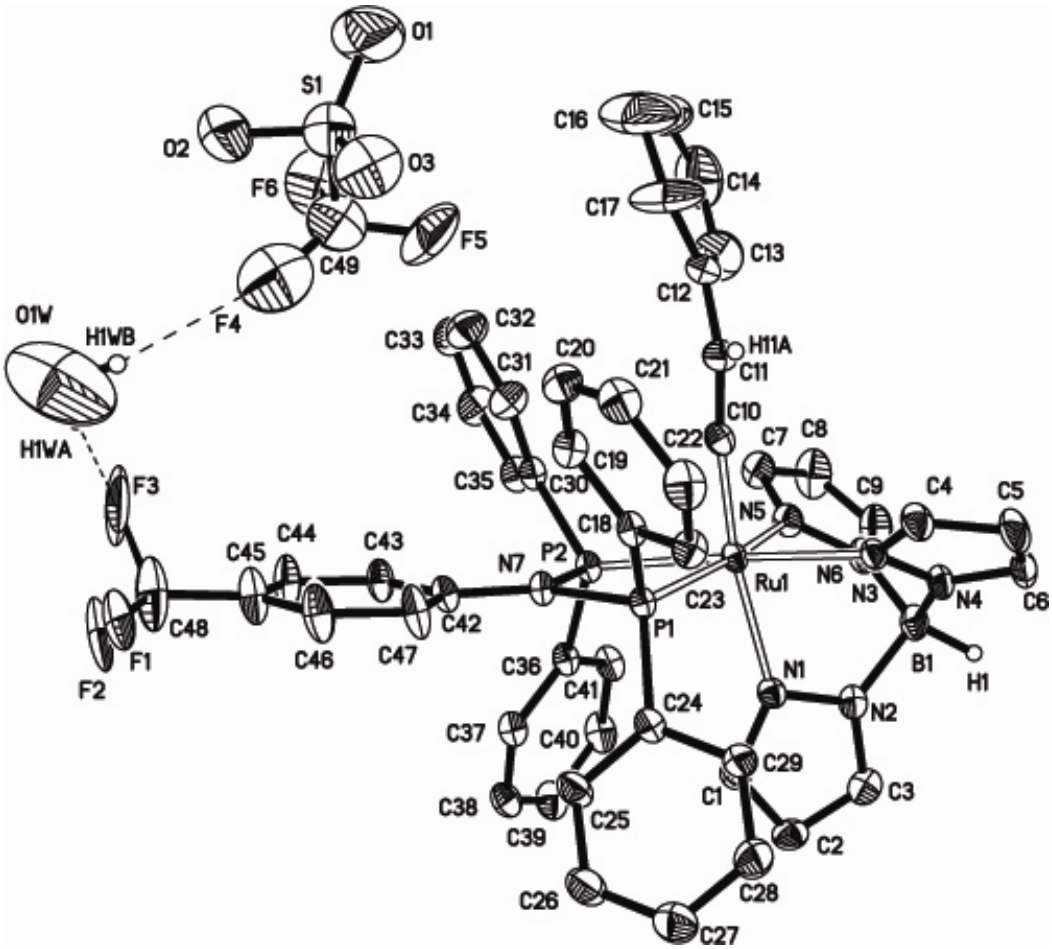

Figure 4.7 ORTEP view (30% probability) of [TpRu(4-$CF_3C_6H_4N(PPh_2)_2$)(=C=CHPh)]$^+$OTf$^-$·H_2O (M33·H_2O) showing the atom-labeling scheme

Table 4.8 Crystal Data and Structure Refinement of [TpRu(4-$CF_3C_6H_4N(PPh_2)_2$)(=C=CHPh)]$^+OTf^-$ (M33·H_2O), TpRu(4-$CF_3C_6H_4N(PPh_2)_2$)(C≡CPh) (M34) and [TpRu(4-$CF_3C_6H_4N(PPh_2)_2$)(CO)]$^+OTf^-$ (M35)

Complex	**M33·H_2O**		**M34**		**M35**	
Empirical formula	$C_{49}H_{40}BF_6N_7O_3P_2RuS·H_2O$		$C_{48}H_{39}BF_3N_7P_2Ru$		$C_{42}H_{34}BF_6N_7O_4P_2RuS$	
Formula weight	1112.78		944.68		1020.64	
Temperature	296(2) K		296(2) K		296(2) K	
Wavelength	0.71073 Å		0.71073 Å		0.71073 Å	
Crystal system	Monoclinic		Monoclinic		Orthorhombic	
Space group	P2(1)/n		P2(1)/n		Pnma	
Unit cell dimensions	a = 11.48330(10) Å	α = 90°.	a = 14.5044(3) Å	α = 90°.	a = 18.4601(7) Å	α = 90°.
	b = 22.5318(2) Å	β = 95.8470(10) °.	b = 18.5417(3) Å	β = 95.7070(10) °.	b = 15.4521(6) Å	β = 90 °.
	c = 19.4927(2) Å	γ = 90°.	c = 16.6001(3) Å	γ = 90°.	c = 15.3426(5) Å	γ = 90°.
Volume	5017.29(8) $Å^3$		4442.24(14) $Å^3$		4376.4(3) $Å^3$	
Z	4		4		4	
Density (calculated)	1.473 Mg/m^3		1.413 Mg/m^3		1.549 Mg/m^3	
Absorption coefficient	0.491 mm^{-1}		0.480 mm^{-1}		0.556 mm^{-1}	
F(000)	2264		1928		2064	
Crystal size	0.38 x 0.30 x 0.28 mm^3		0.38 x 0.16 x 0.04 mm^3		0.22 x 0.18 x 0.06 mm^3	
Theta range for data collection	1.81 to 27.44°.		2.09 to 27.49°.		1.73 to 27.59°.	
Index ranges	-14<=h<=14, -29<=k<=28, -25<=l<=25		-18<=h<=18, -24<=k<=24, -21<=l<=21		-20<=h<=23, -20<=k<=19, -19<=l<=19	
Reflections collected	51235		60436		27758	
Independent reflections	11418 [R(int) = 0.0624]		10184 [R(int) = 0.1740]		5191 [R(int) = 0.1861]	
Completeness to theta	= 27.44°, 99.7 %		= 27.49°, 98.7 %		= 27.59°, 98.7 %	
Absorption correction	Semi-empirical from equivalents		Semi-empirical from equivalents		Semi-empirical from equivalents	
Max. and min. transmission	1.000 and 0.764		1.000 and 0.442		0.9674 and 0.8875	
Refinement method	Full-matrix least-squares on F^2		Full-matrix least-squares on F^2		Full-matrix least-squares on F^2	
Data / restraints / parameters	11418 / 120 / 680		10184 / 18 / 587		5191 / 18 / 364	
Goodness-of-fit on F^2	1.004		0.638		0.998	
Final R indices [I>2sigma(I)]	R1 = 0.0733, wR2 = 0.2046		R1 = 0.0434, wR2 = 0.0561		R1 = 0.0703, wR2 = 0.1235	
R indices (all data)	R1 = 0.1187, wR2 = 0.2375		R1 = 0.1488, wR2 = 0.0693		R1 = 0.1889, wR2 = 0.1578	
Largest diff. peak and hole	0.906 and -0.833 $e.Å^{-3}$		0.763 and -0.292 $e.Å^{-3}$		0.676 and -0.493 $e.Å^{-3}$	

Table 4.9 Selected Bond Distances (Å) and Angles (˚) for [TpRu(4-$CF_3C_6H_4N(PPh_2)_2$)(=C=CHPh)]$^+$OTf$^-$ (M33)

		Bond distances (Å)	
Ru(1)-P(1)	2.3078(7)	Ru(1)-C(10)	1.838(3)
Ru(1)-P(2)	2.2804(8)	C(10)-C(11)	1.296(5)
Ru(1)-N(1)	2.198(2)	C(11)-C(12)	1.426(5)
Ru(1)-N(3)	2.147(2)	P(1)-N(7)	1.720(2)
Ru(1)-N(5)	2.134(2)	P(2)-N(7)	1.717(2)
		Bond angles (˚)	
C(10)-Ru(1)-N(1)	171.86(12)	N(3)-Ru(1)-P(1)	105.85(6)
C(10)-Ru(1)-N(3)	88.84(11)	N(3)-Ru(1)-P(2)	175.61(6)
C(10)-Ru(1)-N(5)	94.71(12)	N(5)-Ru(1)-N(1)	83.65(9)
C(10)-Ru(1)-P(1)	86.89(9)	N(5)-Ru(1)-N(3)	86.05(10)
C(10)-Ru(1)-P(2)	92.19(10)	N(5)-Ru(1)-P(1)	168.05(8)
C(42)-N(7)-P(1)	131.33(16)	N(5)-Ru(1)-P(2)	98.12(8)
C(42)-N(7)-P(2)	128.77(17)	P(2)-N(7)-P(1)	99.89(11)
N(1)-Ru(1)-P(1)	96.37(6)	P(2)-Ru(1)-P(1)	69.96(2)
N(1)-Ru(1)-P(2)	95.93(6)	C(11)-C(10)-Ru(1)	171.0(3)
N(3)-Ru(1)-N(1)	83.10(8)	C(10)-C(11)-C(12)	132.3(4)

4.3.8 Preparation, Characterization and X-ray Structure of TpRu(4-$CF_3C_6H_4N(PPh_2)_2$)(C≡CPh) (M34)

The alkynyl complex **M34** was conveniently prepared by deprotonation of the vinylidene complex **M33** with NaOH in ethanol. The presence of the alknyl moiety was confirmed by the appearance of a $\upsilon_{(C\equiv C)}$ absorption band at 2086 cm^{-1} in the IR spectrum (KBr). The C_α of the alkynyl moiety appear as a triplet at δ 132.3 ppm in the $^{13}C\{^1H\}$NMR spectrum. $^{31}P\{^1H\}$NMR spectroscopy shows a singlet at δ 90.7 ppm attributable to the equivalent phosphorus atoms.

Yellow crystals of **M34** suitable for X-ray diffraction analysis were obtained by layering of hexane onto a saturated solution of the complex in benzene. The ORTEP view of **M34**, shown in **Figure 4.8**, consists of a ruthenium atom coordinated to a Tp ligand, two phosphorus atoms of the chelating 4-$CF_3C_6H_4N(PPh_2)_2$ ligand and a C_α atom of the alkynyl group. The complex is composed of pseudo-octahedral coordination sphere. The crystal data and refinement details are given in **Table 4.8**. Selected bond lengths and angles are listed in **Table 4.10**. The Ru(1)-C(34) bond distance of 2.013(2) Å is similar to those of related Ru(II) complexes TpRu(CO)(PPh3)(C≡CPh) (2.031(3)Å)[194] and $Ru(C\equiv CPh)_2(cym)(PMe_3)$ (cym = η^6-4-methylisopropylbenzene) (2.003(9) Å), (2.026(3) Å).[212] The C(34)-C(35) bond distance, 1.178(3) Å, is in the typical range of transition metal alkynyls.[194, 212, 213] The alkynyl ligand is almost linear, with the C(35)-C(34)-Ru(1) bond angle of 170.1(2) ˚. The angles sum around the nitrogen atom that links the phosphorus atoms is very close to planar ($\Sigma_{N(7)}$ = 359.91°), indicating delocalization of the lone pair electrons.

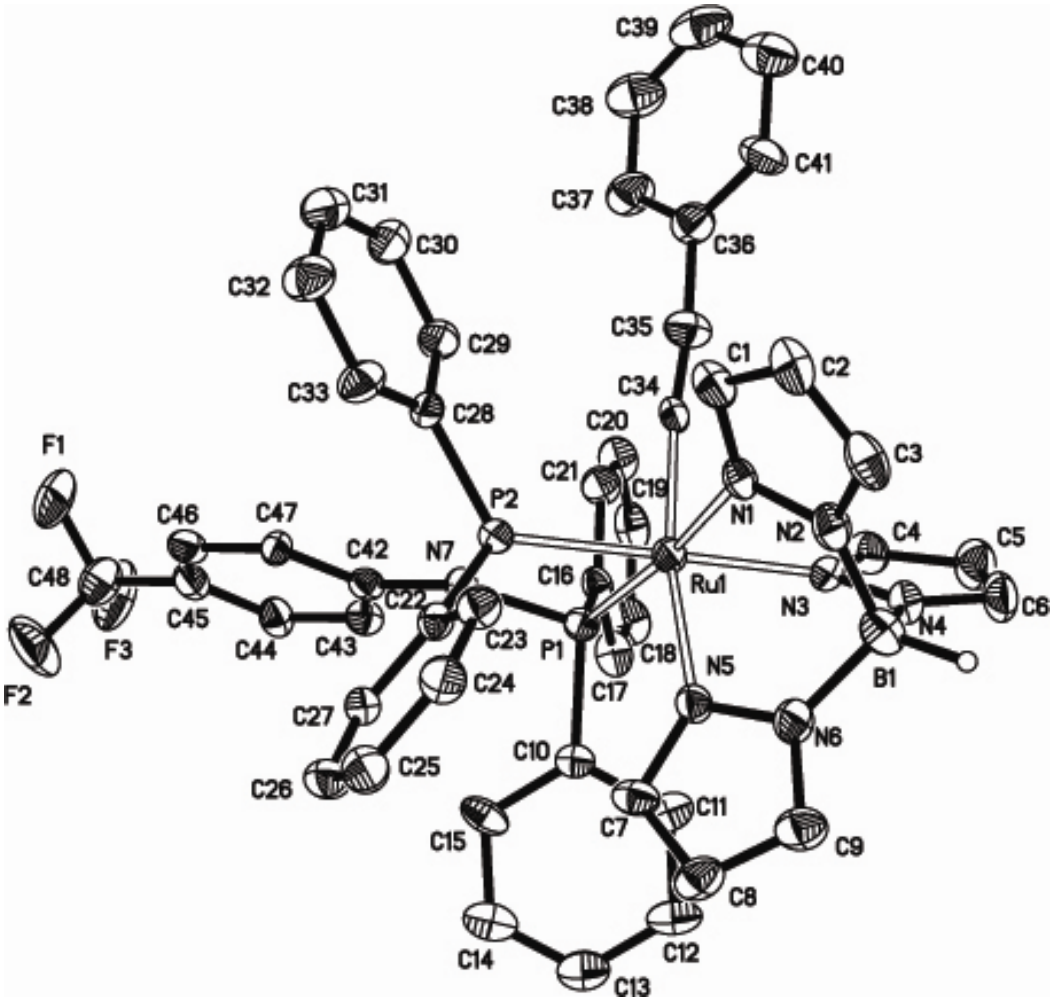

Figure 4.8 ORTEP view (30% probability) of TpRu(4-$CF_3C_6H_4N(PPh_2)_2$)(C≡CPh) (M34) showing the atom-labeling scheme

Table 4.10 Selected Bond Distances (Å) and Angles (˚) for TpRu(4-$CF_3C_6H_4N(PPh_2)_2$)(C≡CPh) (M34)

Bond distances (Å)			
Ru(1)-P(1)	2.2487(7)	Ru(1)-C(34)	2.013(2)
Ru(1)-P(2)	2.2350(7)	C(34)-C(35)	1.178(3)
Ru(1)-N(1)	2.1354(19)	C(35)-C(36)	1.452(4)
Ru(1)-N(3)	2.1202(19)	P(1)-N(7)	1.7431(19)
Bond angles (˚)			
C(34)-Ru(1)-N(1)	85.73(9)	N(3)-Ru(1)-N(1)	84.23(7)
C(34)-Ru(1)-N(3)	87.47(9)	N(3)-Ru(1)-N(5)	85.08(8)
C(34)-Ru(1)-N(5)	168.43(8)	N(3)-Ru(1)-P(1)	103.03(6)
C(34)-Ru(1)-P(1)	94.32(7)	N(3)-Ru(1)-P(2)	173.49(6)
C(34)-Ru(1)-P(2)	90.44(7)	N(5)-Ru(1)-P(1)	95.97(5)
C(42)-N(7)-P(1)	132.33(16)	N(5)-Ru(1)-P(2)	97.89(5)
C(42)-N(7)-P(2)	130.71(16)	P(2)-N(7)-P(1)	96.87(9)
N(1)-Ru(1)-N(5)	84.72(7)	P(2)-Ru(1)-P(1)	70.97(3)
N(1)-Ru(1)-P(1)	172.74(5)	C(34)-C(35)-C(36)	172.5(3)
N(1)-Ru(1)-P(2)	101.77(5)	C(35)-C(34)-Ru(1)	170.1(2)

4.3.9 Preparation, Characterization and X-ray Structure of [TpRu(4-$CF_3C_6H_4N(PPh_2)_2$)(CO)]$^+$OTf$^-$ (M35)

Treatment of the vinylidene complex **M33** in chloroform with excess water at 60 °C for 24 h afforded the carbonyl complex **M35**. The reaction sequence outlined in **Scheme 4.2** is similar to that proposed by Bianchini et al, who found that reaction of *n*-$PrN(CH_2CH_2PPh_2)_2Ru(PPh_3)Cl_2$ with excess phenylacetylene and water led to quantitative formation of the carbonyl species *n*-$PrN(CH_2CH_2PPh_2)_2Ru(CO)Cl_2$ with one equiv of toluene formed as by-product.[214] It is worth to note that in the course of the **M24**-catalyzed 2-alkenylation reaction, water on the one hand might have acted as a base to deprotonate the vinylidene species **M33** to generate the alkynyl complex **M34**, and on the other hand plays the role of a nucleophile attacking the C_α of the vinylidene moiety of **M33** resulting in the formation of the carbonyl species **M35**. Apparently, the role of a base is the major one. Complex **M35** is conveniently characterized by NMR and IR spectroscopies. $^{13}C\{^1H\}$NMR spectroscopy shows a triplet corresponding to the carbonyl carbon in **M35** at δ 201.1 ppm. A singlet corresponding to the equivalent phosphorous atoms of the bis(phosphino)amine ligand is seen at δ 80.7 ppm in the $^{31}P\{^1H\}$NMR spectrum; IR spectroscopy shows the $\upsilon_{(C\equiv O)}$ absorption at 1995 cm^{-1}.

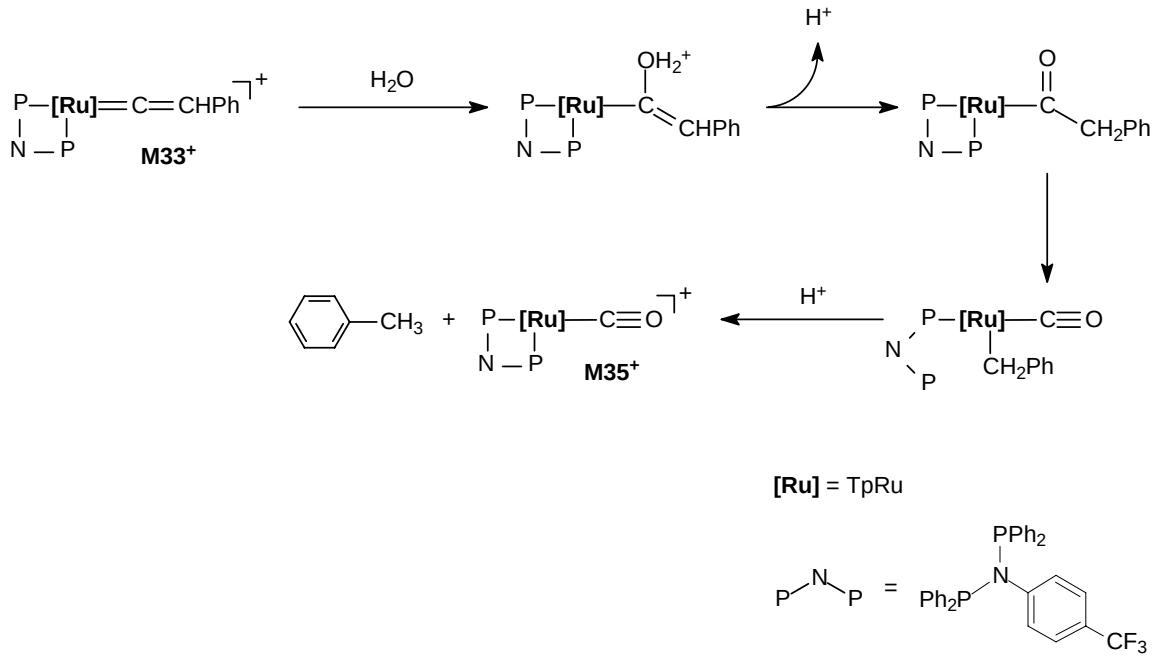

Scheme 4.2 Proposed mechanism of formation of [TpRu(4-$CF_3C_6H_4N(PPh_2)_2$)(CO)]$^+$OTf$^-$ (M35)

White crystals of **M35** suitable for X-ray diffraction analysis were obtained by layering of hexane onto a saturated solution of the complex in dichloromethane. An ORTEP view of **M35**, as determined by X-ray crystallography, is shown in **Figure 4.9**. The crystal data and refinement details are given in **Tables 4.8**. Selected bond lengths and angles are shown in **Table 4.11**. It was observed that the ruthenium-carbon distance Ru(1)-C(24) is 1.840(5) Å. The Ru-C≡O group is virtually linear, having a O(1)-C(24)-Ru(1) angle of 175.6(4)˚. The sum of the angles around nitrogen atom of the diphosphinoamine ligand $\Sigma_{N(5)}$ is 359.92°. Reaction of **M24** with CO in chloroform provides an alternative simple route to **M35**.

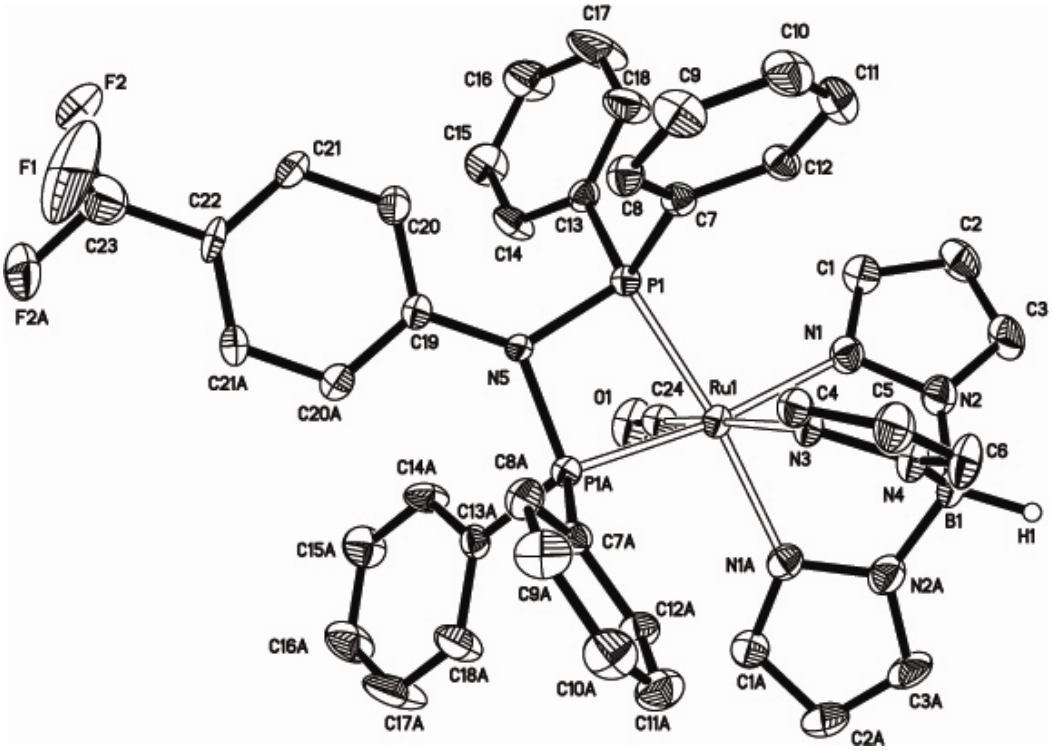

Figure 4.9 ORTEP view (30% probability) of [TpRu(4-$CF_3C_6H_4N(PPh_2)_2$)(CO)]$^+$OTf$^-$ (M35) showing the atom-labeling scheme

Table 4.11 Selected Bond Distances (Å) and Angles (°) for [TpRu(4-$CF_3C_6H_4N(PPh_2)_2$)(CO)]$^+$OTf$^-$ (M35)

Bond distances (Å)			
Ru(1)-C(24)	1.840(5)	Ru(1)-P(1A)	2.2886(9)
Ru(1)-N(1)	2.128(3)	N(5)-P(1A)	1.724(2)
Ru(1)-N(1A)	2.128(3)	P(1)-N(5)	1.724(2)
Ru(1)-N(3)	2.149(4)	O(1)-C(24)	1.161(6)
C(19)-N(5)-P(1)	130.08(9)	N(1)-Ru(1)-P(1)	101.01(7)
C(19)-N(5)-P(1A)	130.08(9)	N(3)-Ru(1)-P(1)	94.21(8)
C(24)-Ru(1)-N(1)	91.09(13)	N(3)-Ru(1)-P(A1)	94.21(8)
C(24)-Ru(1)-N(1A)	91.09(13)	P(1)-Ru(1)-P(1A)	70.33(4)
C(24)-Ru(1)-P(1)	91.76(13)	C(24)-Ru(1)-N(3)	172.69(18)
C(24)-Ru(1)-P(1A)	91.76(13)	N(1A)1-Ru(1)-P(1)	170.96(7)
N(1)-Ru(1)-P(1)	101.01(7)	N(1)1-Ru(1)-P(A)	170.96(7)
N(1A) -Ru(1)-N(1)	87.52(14)	P(1A)1-N(5)-P(1)	99.76(18)
N(1A) -Ru(1)-N(3)	83.65(10)	O(1)-C(24)-Ru(1)	175.6(4)
N(1A)-Ru(1)-P(1A)	101.01(7)		

4.3.10 Reaction of [TpRu(4-$CF_3C_6H_4N(PPh_2)_2$)(=C=CHPh)]$^+$OTf$^-$ (M33) with 1-Hexyne and Acetonitrile

The Markovnikov nature of the alkenylated products shown in **Table 4.6** indicates that they are probably not formed via nucleophilic attack of 1,3-dicarbonyl compound or its enol form at the vinylidene moiety of the vinylidene complex **M33** because such attack would have led to anti-Markovnikov products. On the other hand, attack of 1,3-dicarbonyl compound or its enol form at the η^2-alkyne tautomer of **M33** would give Markovnikov products having the same regioselectivity as the products of the **M24**-catalyzed alkenylation reactions. The reversibility of η^1-vinylidene ─ η^2-alkyne tautermerization is well-established. For ruthenium, it is commonplace that the η^1-vinylidene species is thermodynamically more stable than the η^2-alkyne complex; however, the energy barrier to the η^2-alkyne species from the η^1-vinylidene complex is usually low enough to be overcome under normal experimental reaction conditions. For example, recent kinetic study on the release of terminal alkyne from indenylruthenium(II) vinylidene complexes provides another piece of evidence consistent with the hypothesis that η^2-alkyne tautomer is formed under transient conditions and either returns rapidly to vinylidene complex or is captured by solvent to yield the acetonitrile adduct and free alkyne.[215]

We monitored the displacement of the vinylidene moiety of **M33** with 1-hexyne (5 equiv) by $^{31}P\{^1H\}$NMR spectroscopy. Remarkably, chloroform solution of **M33** reacted with 1-hexyne at 60 ^oC for 4h to afford a 2:3 mixture of **M33** and the substituted vinylidene complex [TpRu(4-$CF_3C_6H_4N(PPh_2)_2$)(=C=$(CH_2)_3CH_3$)]$^+$OTf$^-$ (**M36**) (**eq 4.4**). Although no product other than vinylidene complexes could be detected by $^{31}P\{^1H\}$NMR

spectroscopy (**Figure 4.10**), it is likely that these vinylidene complexs are in equilibrium with their corresponding η^2-alkyne tautomers as shown in **Scheme 4.3**.

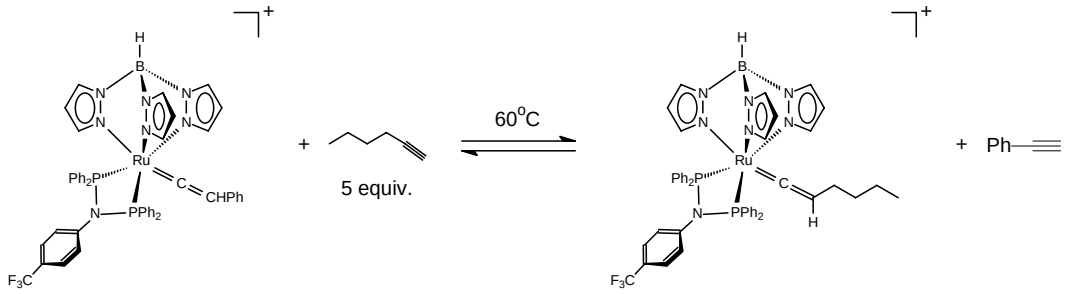

M33 **M36** (4.4)

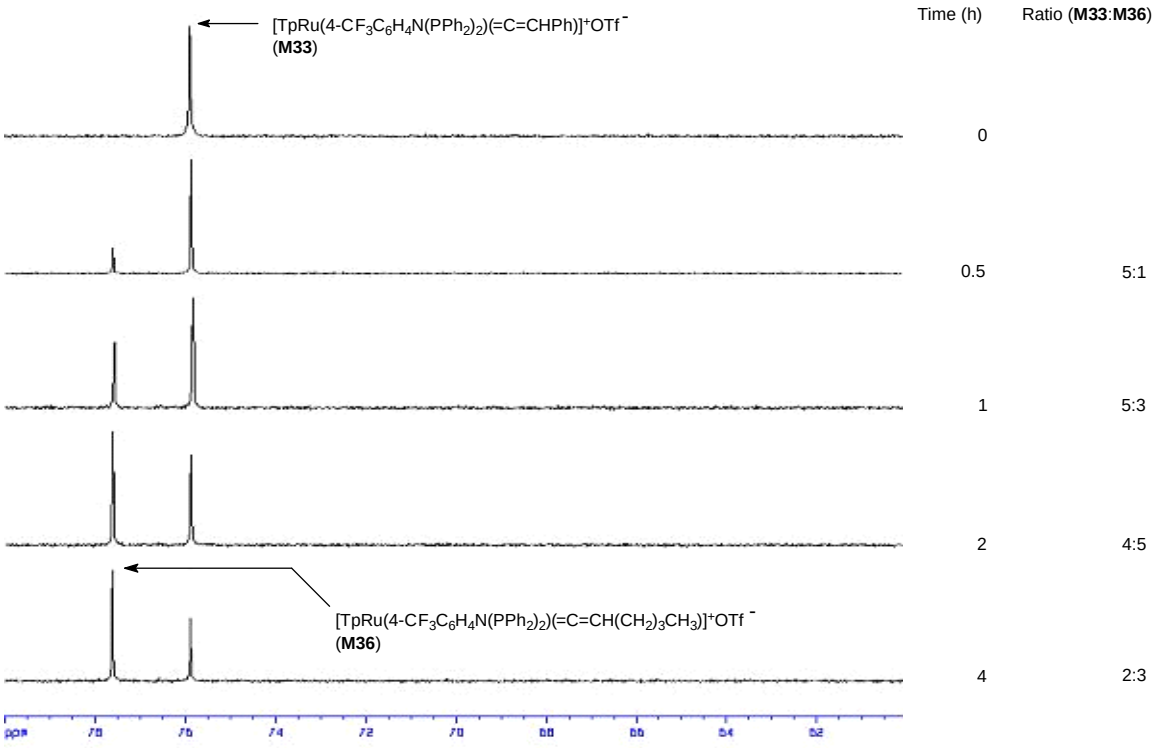

Figure 4.10 $^{31}P\{^1H\}$NMR study of the reaction of [TpRu(4-$CF_3C_6H_4N(PPh_2)_2$)(=C=CHPh)]$^+$OTf$^-$ (M33) with 1-hexyne

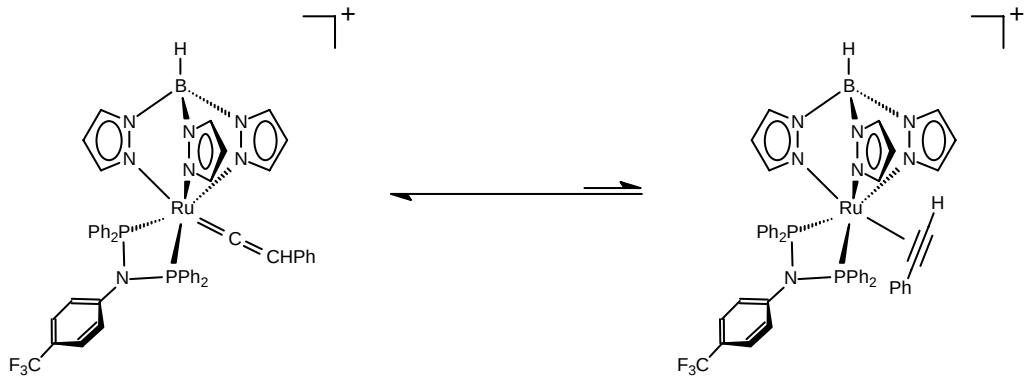

M33

Scheme 4.3 Equilibrium between the vinylidene complex and the η^2-alkyne tautomer

Furthermore, reacting **M33** with excess acetonitrile at 60 ^{o}C gave the the corresponding solvento derivative $[TpRu(4\text{-}CF_3C_6H_4N(PPh_2)_2)CH_3CN]^+OTf^-$ (**M25**) (**eq 4.5**). The analyses of the exponential decay of the relative integrated values, according to the first-order rate equation, give the values of the observed rate constants, k_{obs}. The k_{obs} value calculated from the disappearance of **M33** is exemplified in **Figure 4.11**; the slope gives $-k_{obs}$. The k_{obs} at 60 ^{o}C was determined to be 1×10^{-4} s^{-1} for the ligand exchange of **M33**. Similarly, $^{31}P\{^1H\}$NMR spectra only show the resonance of the starting material **M33** and the corresponding acetonitrile derivative **M25**. Although, the putative intermediate η^2-alkyne tautomer cannot be observed, it is probably true that the vinylidene complex is in equilibrium with the corresponding η^2-alkyne tautomer, although the equilibrium shift toward the side of vinylidene (**Scheme 4.3**).

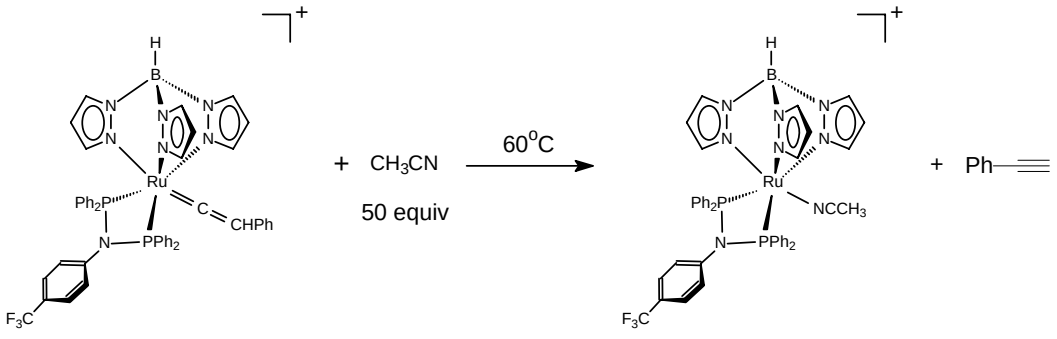

M33 **M25** (4.5)

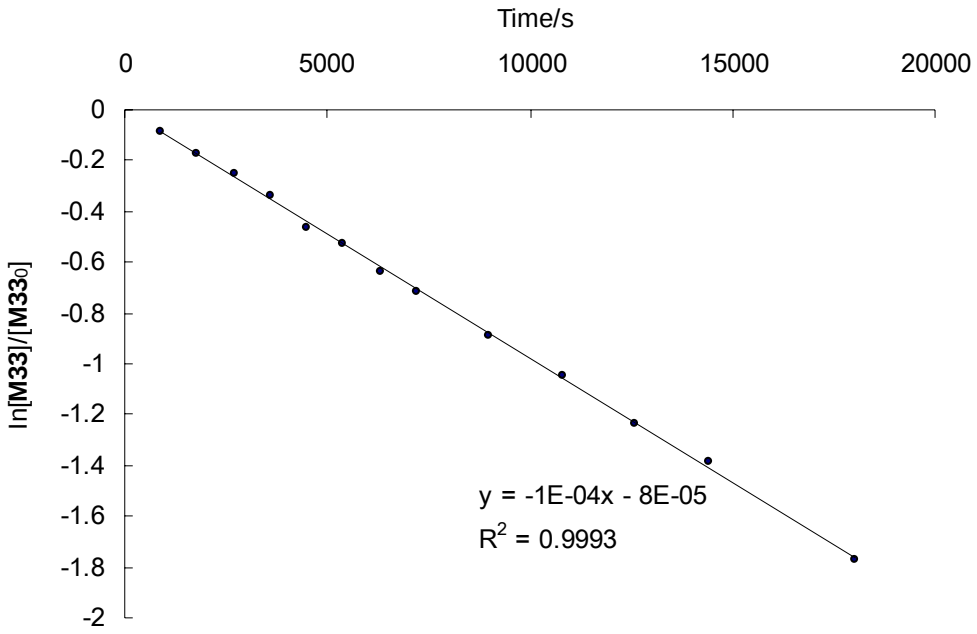

Figure 4.11 Plot of ln [M33]/[M33$_0$] against time for first-order fits of the substrates disappearance; the slope gives -k_{obs}

4.3.11 Proposed Mechanism for the [TpRu(4-$CF_3C_6H_4N(PPh_2)_2$)]$^+$OTf$^-$ (M24)-Catalyzed 2-Alkenylation of 1,3-Dicarbonyl Compounds with Terminal alkynes

The $^{31}P\{^1H\}$NMR monitoring experiment depicted in **Figure 4.4 - 4.6** show that the vinylidene complex exists in the early stage of the catalytic process; however, there is basically no conversion at this stage, indicating that tautormerization of **M33** to its η^2-alkyne tautomer and subsequent attack by the 1,3-dicarbonyl compound or its enol form at the latter might not be a major route for product generation. Alkenylated product only begins to appear after most of the vinylidene species is converted to the alkynyl complex **M34**. However, the alkynyl species **M34** is also not the active species as demonstrated in an independent experiment. We are, however, of the opinion that a combination of **M34** and $\mathbf{B}^+$ might have constituted an active system for the addition reaction. $\mathbf{B}^+$ might, to a very small degree, partially protonate **M34** to generate very minute amount of **M33**,

which at the reaction temperature equilibrates with its η^2-alkyne tautomer; the latter is immediately attacked by the 1,3-dicarbonyl compound or its enol form which originates from $\mathbf{B}^+$ and is in *close vicinity*. We have to admit that the proposed mechanism depicted in **Scheme 4.4** (using acetylacetone and phenylacetylene as substrates) for the **M24**-catalyzed 2-alkenylation of 1,3-dicarbonyl compounds with terminal alkynes contains considable degree of speculation, but it seems to be able to account for the phenomena revealed by the NMR monitoring experiments (**Figure 4.4** - **4.6**).

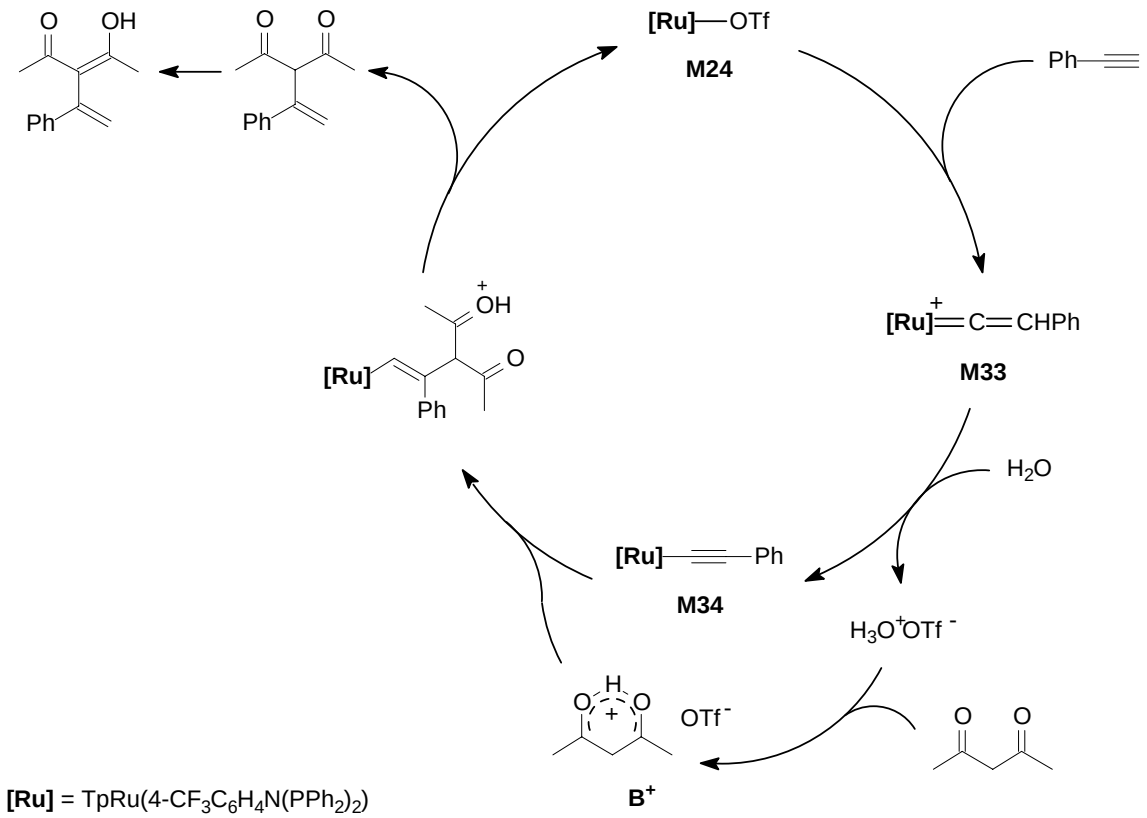

Scheme 4.4 Proposed Mechanism for the TpRu(4-$CF_3C_6H_4N(PPh_2)_2$)OTf (M24)-Catalyzed 2-Alkenylation of 1,3-Dicarbonyl Compounds with Terminal alkynes

4.3.12 TpRu(4-$CF_3C_6H_4N(PPh_2)_2$)OTf (M24)-Catalyzed Hydroamination of Terminal Alkynes with Secondary Amines

Introducing a N-H bond to a C-C multiple bond, known as hydroamination, offers an attractive route for synthesis of highly substituted nitrogen-containing organic molecules. We have demonstrated that terminal alkynes can be activated by **M24** to form the important intermediate, the vinylidene complex. In the continuity of these studies, we document herein a **M24**-catalyzed anti-Markovnikov addition of secondary amines to terminal alkynes, affording the desired enamines (**eq. 4.6**).

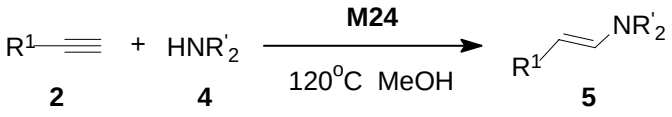

2 **4** **5** (4.6)

We examined the **M24**-catalyzed hydroamination reaction of terminal alkynes with secondary amines. **Table 4.12** summarizes the results for the reactions. The secondary amines react with the functionalized phenylacetylene derivatives to give the corresponding *E*-isomers without the formation of the Markovnikov product. The highest reactivity is displayed by cyclic amines (entries 3 & 4). Morpholine and 1,4-dioxa-8-azaspiro[4.5]decane, whose basicity is strongly reduced because of electrophilic oxygen atoms,[216] also reacts moderately (entries 5 & 6). Despite advanced basicity,[216] reactions of acyclic aliphatic amines with phenylacetylene do not proceed with high conversions (entries 1 & 2). Reactions of phenylacetylene with *N*-methylaniline, aniline and butylamine, however, do not take place, it seem that **M24** is active catalyst only for the hydroamination with secondary amines. Phenylacetylene substituted with electron-donating methyl group or electron-withdrawing halo groups gives similar conversions; the reaction seems to be dependent on the nature of amines but not that of alkynes (entries 7-10).

Table 4.12 TpRu(4-$CF_3C_6H_4N(PPh_2)_2$)OTf (M24)-Catalyzed Hydroamination of Terminal Alkynes with Secondary Amines[a]

entry	terminal alkyne	secondary amine	product	% conversion[b]
1	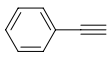 **2a**	 **4a**	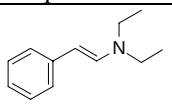 **5a**	56
2	**2a**	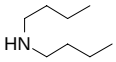 **4b**	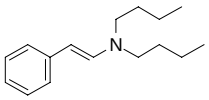 **5b**	43
3	**2a**	 **4c**	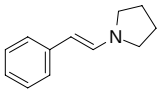 **5c**	63
4	**2a**	 **4d**	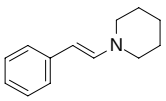 **5d**	76
5	**2a**	 **4e**	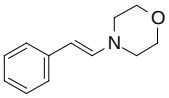 **5e**	33
6	**2a**	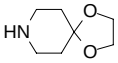 **4f**	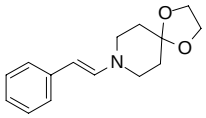 **5f**	43
7	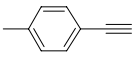 **2c**	**4c**	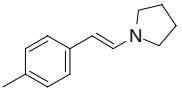 **5g**	44
8	**2c**	**4d**	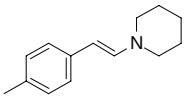 **5h**	50
9	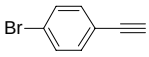 **2d**	**4d**	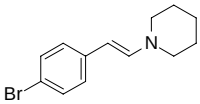 **5i**	56
10	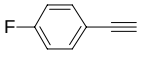 **2e**	**4d**	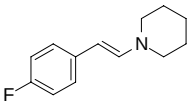 **5j**	49

[a]Reaction conditions: catalyst (0.01 mmol), secondary amine (1 mmol), terminal alkyne (1.2 mmol); in 0.1 mL MeOH, 120˚C, 24 h.

[b]Conversion determined by ^{1}H NMR spectroscopy with 1,1,2,2-tetrachloroethane as an internal standard.

4.3.13 NMR Monitoring of TpRu(4-$CF_3C_6H_4N(PPh_2)_2$)OTf (M24)-Catalyzed Hydroamination of Phenylacetylene with Diethylamine

The **M24**- catalyzed phenylacetylene/diethylamine hydroamination reaction was monitored with ^1H and $^{31}P\{^1H\}$NMR spectroscopy (**Figure 4.12**). Phenylacetylene(1.2 mmol) and diethylamine(1 mmol) were added to a CD_3OD solution of **M24** (0.01 mmol) in a 5mm pressure-valved NMR tube, which was pressurized with 10 bar Ar. After heating for 5 min at 120 ºC, the $^{31}P\{^1H\}$NMR spectrum showed signals corresponding to the alkynyl complex **M34** and the triflate complex **M24** in a ratio approximately equal to 2:1. The vinylidene complex **M33** was not observed in the catalysis. Probably, in the presence of amine, **M33** was readily deprotonated. The ratio changed to 18:5 after 1h; ^1H NMR spectroscopy showed that the hydroamination of phenylacetylene began to occur. Heating the reaction mixture for another 3h led to the complete conversion to **M34**, as reflected by the presence of only one signal, which is due to **M34**, in the $^{31}P\{^1H\}$NMR spectrum; approximately 15% of the diethylamine was converted to the corresponding enamine. **M34** remained the only ruthenium complexes detected throughout the period of monitoring (24h). At the end of this period, the conversion of diethylamine was 45%.

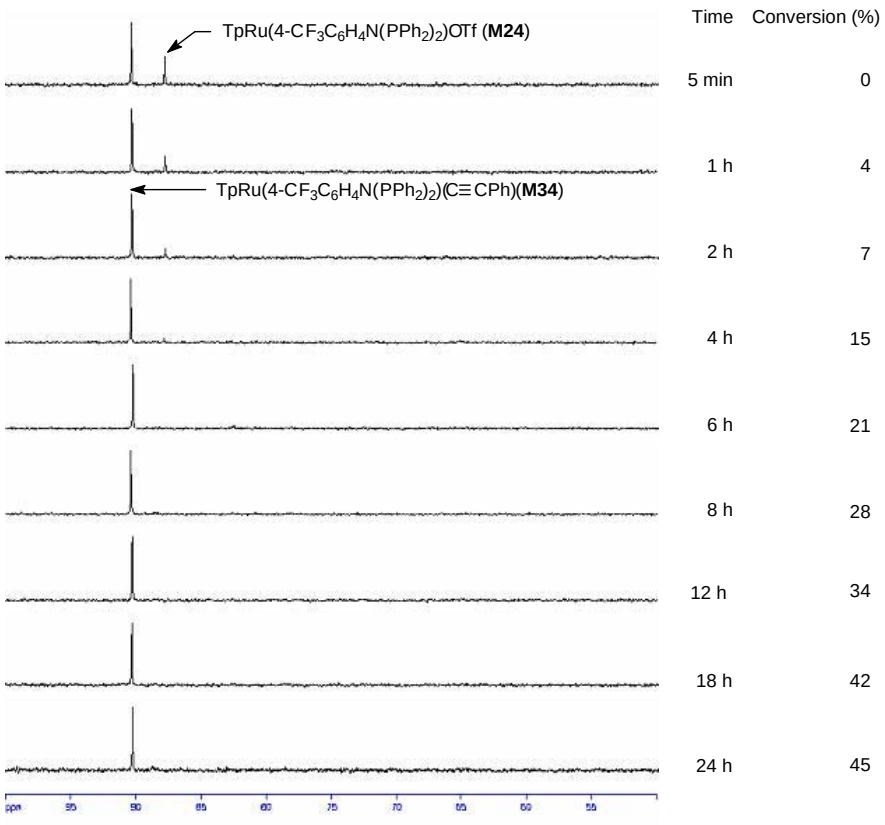

Figure 4.12 $^{31}P\{^{1}H\}$NMR study of TpRu(4-$CF_3C_6H_4N(PPh_2)_2$)OTf (M24)-catalyzed hydroamination of phenylacetylene with diethylamine

4.3.14 Proposed Mechanism for the [TpRu(4-$CF_3C_6H_4N(PPh_2)_2$)]$^{+}$$OTf^{-}$ (M24)-Catalyzed Hydroamination of Termial Alkynes with Secondary Amines

The anti-Markonikov hydroamination of terminal alkynes catalyzed by organouranium and organotitanium complexes are only applicable to primary amines, because in these reactions the metal-imido complexes (M=NR) are the crucial intermediates in the catalytic cycle.[93-98] In contrast to these reactions, the **M24**-catalyzed anti-Markovnikov hydroamination of terminal alkynes only works with secondary amines, implicating the catalytic cycle of this process does not involve the intermediacy of the metal-imido species. We suspect that the metal-vinylidene species (M=C=CHR) might play a crucial role in the catalytic process. A proposed mechanism

for the **M24**-catalyzed hydroamination reaction is shown in **Scheme 4.5** (using phenylacetylene as example). The reaction begins with reaction of **M24** with the terminal alkyne to rapidly generate the vinylidene complex **M33** which, in the presence of excess amine, is in equilibrium with the alkynyl complex **M34**. As shown by the NMR monitoring experiment, the equilibrium lies mainly on the side of the alkynyl species, the equilibrium concentration of the vinylidene speciesis is so low that it is not detectable by NMR spectroscopy. The very minute amount of **M33** is attacked at the α-carbon of the vinylidene moiety by the amine to give the intermediate **C**. Cleavage of the metal-vinyl bond by proton transfer from the quarternary nitrogen in **C** yields the hydroamination product. Alternatively, the quarternary nitrogen in **C** is deprotonated by the amine to give **D**; the ruthenium-vinyl bond of which is then cleaved intermolecularly.

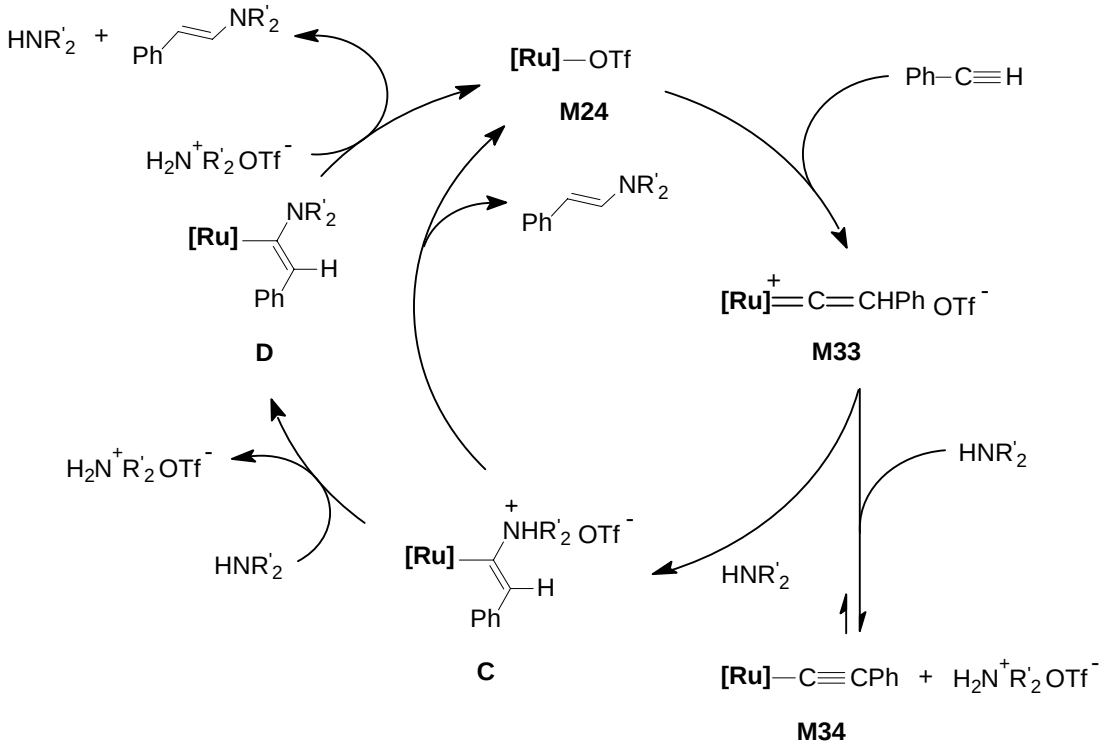

[Ru] = TpRu(4-$CF_3C_6H_4N(PPh_2)_2$)

Scheme 4.5 Proposed mechanism of TpRu(4-$CF_3C_6H_4N(PPh_2)_2$)OTf (M24)-catalyzed Hydroamination of terminal alkynes with secondary amines

Chapter 5

Conclusion

Catalytic *β*-alkylation of secondary alcohols with primary alcohols, although, is an important reaction for the synthesis of higher alcohols with high atom economy, the number of examples reported in literature is surprisingly small. We have here reported that a number of ruthenium complexes are efficient catalysts for the reaction. We have been able to present a clearer picture of the mechanistic aspects of the reaction, and unequivocally identify the key intermediates, metal hydrides, in the catalysis. More interestingly, we have demonstrated that the carbonyl complexes resulting from aldehyde decarbonylation, which is usually regarded as the cause of catalyst deactivation, are also active for the *β*-alkylation reactions of 1-phenylethanol with benzyl alcohol.

Few examples of transition metal-catalyzed α-alkylation of nitriles with primary alcohols, which is a green and atom-economical reaction to yield α-alkylated nitriles, are known to-date. Success of this reaction lies on the ability of the metal to catalyze oxidation of the alcohol to aldehyde. Moreover, readiness of the aldehyde to undergo condensation with the nitrile, which is usually an aryl- or heteroarylacetonitrile, is also important. We have demonstrated in this work that aminocyclopentadienyl ruthenium complexes are reasonably good catalysts for α-alkylation of arylacetonitriles with primary alcohols. The main thrust of our work lies on our being able to provide supports, both experimental and theoretical, for the proposed mechanism which accounts for the much higher catalytic activity of the aminocyclopentadienyl ruthenium complexes over the non-substituted analogous Cp-Ru complexes, and this is important from the point of view of basic organometallic chemistry.

We have found that the Tp-ruthenium (II) diphosphinoamino complex TpRu(4-$CF_3C_6H_4N(PPh_2)_2$)OTf (**M24**) is a good catalyst for the 2-alkenylation of 1,3-dicarbonyl compounds with terminal alkynes. It is also capable of catalyzing the addition of secondary amines to aromatic alkynes, although the conversions are only moderate. Of the two reactions catalyzed by this complex, the former follows the Markovnikov addition pattern, while the regioselectivity of the latter is exclusively anti-Markovnikov. Another interesting point is that the two reactions have identical catalytst resting state, i.e. a ruthenium alkynyl species **[Ru]**-C≡CR. To account for the regioselectivities of the addition reactions, we proposed that in the 2-alkenylation of 1,3-dicarbonyl compounds with terminal alkynes, the active species is the ruthenium η^2-alkyne complex; on the other hand, in the hydroamination reactions, the active species is suspected to be the ruthenium vinylidene complex **[Ru]**=C=CHR. Both active complexes are transient species generated from the ruthenium alkynyl resting state.

Appendix

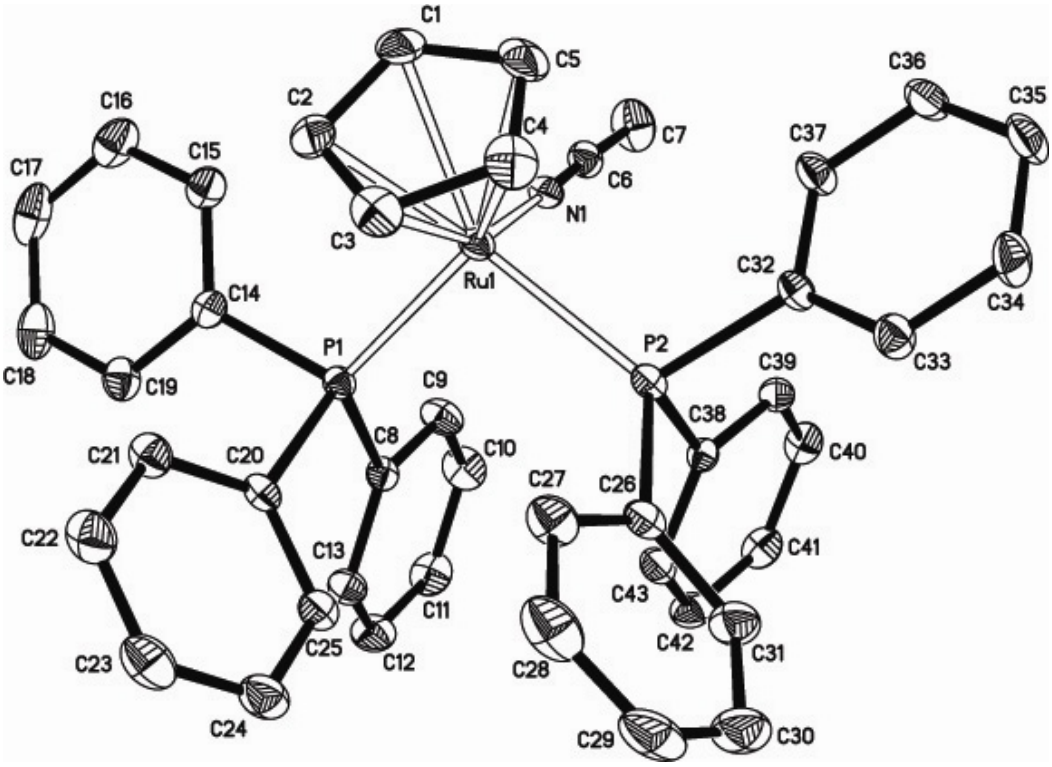

Figure 2.6 ORTEP view (30% probability) of $[CpRu(PPh_3)_2(CH_3CN)]^+BF_4^-$ (M1) showing the atom-labeling scheme

Table 2.8 Crystal Data and Structure Refinement of $[CpRu(PPh_3)_2(CH_3CN)]^+BF_4^-$ (M1)

Empirical formula	$C_{43}H_{38}BF_4NP_2Ru \cdot 1.5C_6H_6$	
Formula weight	935.73	
Temperature	294(2) K	
Wavelength	0.71073 Å	
Crystal system	Monoclinic	
Space group	C2/c	
Unit cell dimensions	a = 24.232(4) Å	= 90°.
	b = 18.121(3) Å	= 117.111(3)°.
	c = 23.195(4) Å	= 90°.
Volume	9066(3) $Å^3$	
Z	8	
Density (calculated)	1.371 Mg/m^3	
Absorption coefficient	0.469 mm^{-1}	
F(000)	3848	
Crystal size	0.38 x 0.28 x 0.26 mm^3	
Theta range for data collection	1.51 to 23.34°.	
Index ranges	-26<=h<=26, -20<=k<=20, -25<=l<=25	
Reflections collected	29510	
Independent reflections	6541 [R(int) = 0.0554]	
Completeness to theta = 23.34°	99.6 %	
Absorption correction	Semi-empirical from equivalents	
Max. and min. transmission	1.000 and 0.774	
Refinement method	Full-matrix least-squares on F^2	
Data / restraints / parameters	6541 / 78 / 552	
Goodness-of-fit on F^2	1.002	
Final R indices [I>2sigma(I)]	R1 = 0.0453, wR2 = 0.1129	
R indices (all data)	R1 = 0.0617, wR2 = 0.1236	
Largest diff. peak and hole	0.517 and -0.555 e.$Å^{-3}$	

Table 2.9 Selected Bond Distances (Å) and Angles (˚) for $[CpRu(PPh_3)_2(CH_3CN)]^+BF_4^-$ (M1)

Bond distances (Å)			
C(1)-C(2)	1.402(5)	Ru(1)-C(2)	2.219(3)
C(1)-C(5)	1.415(5)	Ru(1)-C(3)	2.200(3)
C(2)-C(3)	1.402(5)	Ru(1)-C(4)	2.204(3)
C(3)-C(4)	1.411(5)	Ru(1)-C(5)	2.203(3)
C(4)-C(5)	1.417(5)	Ru(1)-N(1)	2.050(2)
C(6)-C(7)	1.458(5)	Ru(1)-P(1)	2.3304(8)
N(1)-C(6)	1.133(4)	Ru(1)-P(2)	2.3264(8)
Ru(1)-C(1)	2.223(3)		
Bond angles (˚)			
C(1)-C(2)-C(3)	109.0(3)	C(6)-N(1)-Ru(1)	174.7(2)
C(1)-C(5)-C(4)	107.7(3)	N(1)-C(6)-C(7)	177.2(4)
C(2)-C(1)-C(5)	107.6(3)	N(1)-Ru(1)-P(1)	93.60(6)
C(2)-C(3)-C(4)	107.6(3)	N(1)-Ru(1)-P(2)	88.89(7)
C(3)-C(4)-C(5)	108.0(3)	P(2)-Ru(1)-P(1)	98.03(3)

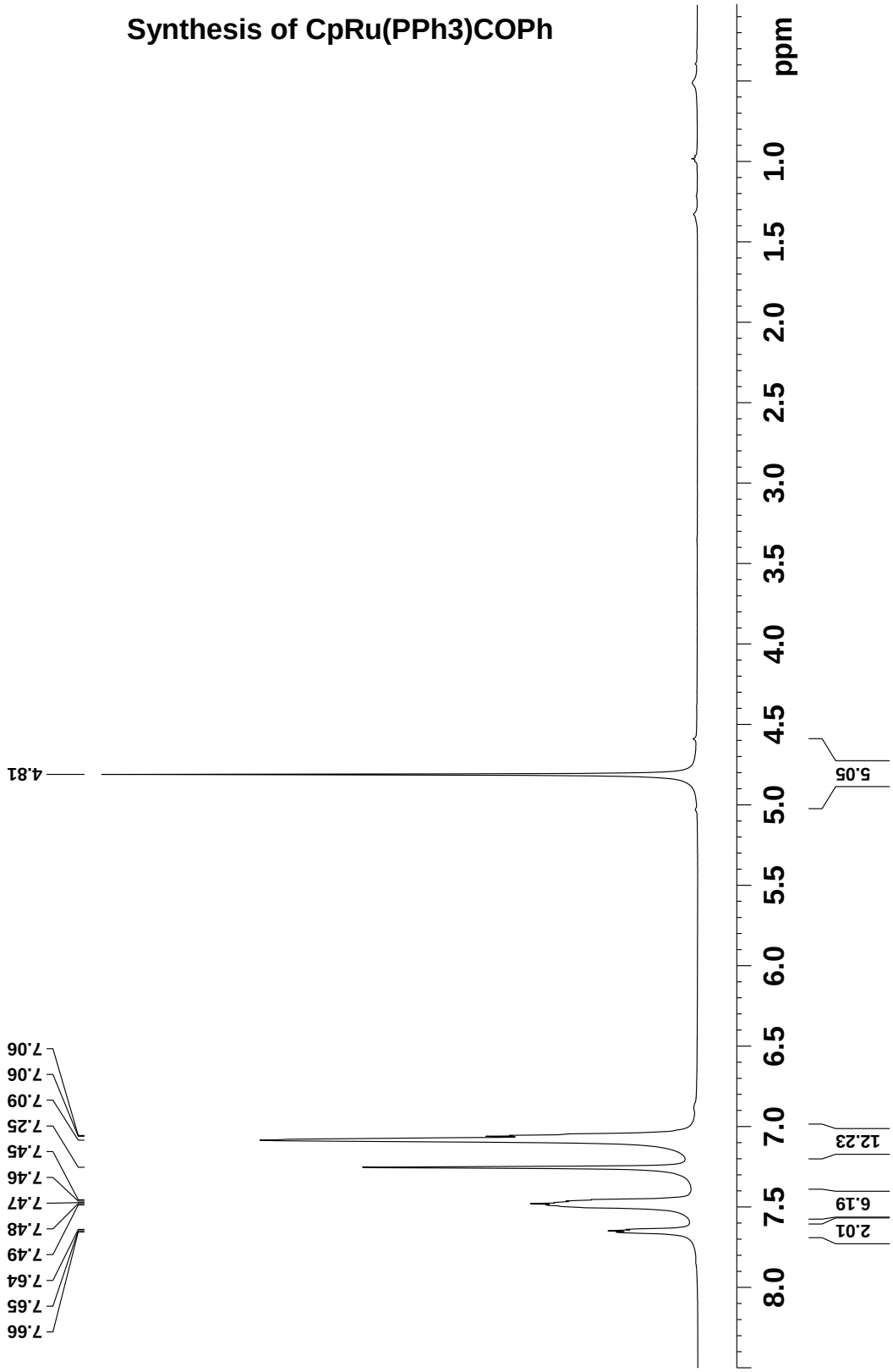

Figure 2.7 ^{1}H NMR spectrium of CpRu(PPh$_3$)(CO)Ph (M7)

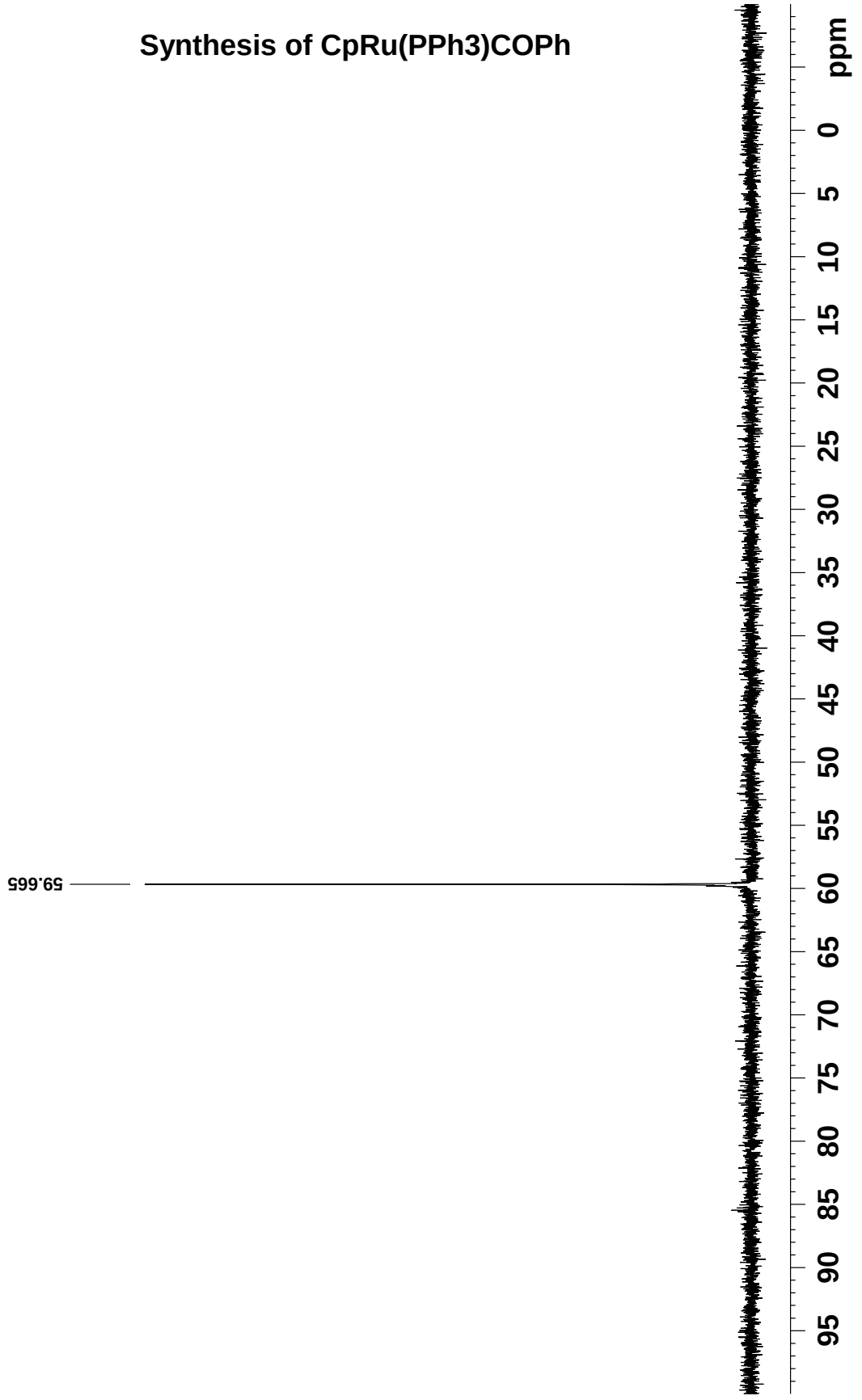

Figure 2.8 $^{31}P\{^{1}H\}$NMR spectrium of $CpRu(PPh_3)(CO)Ph$ (M7)

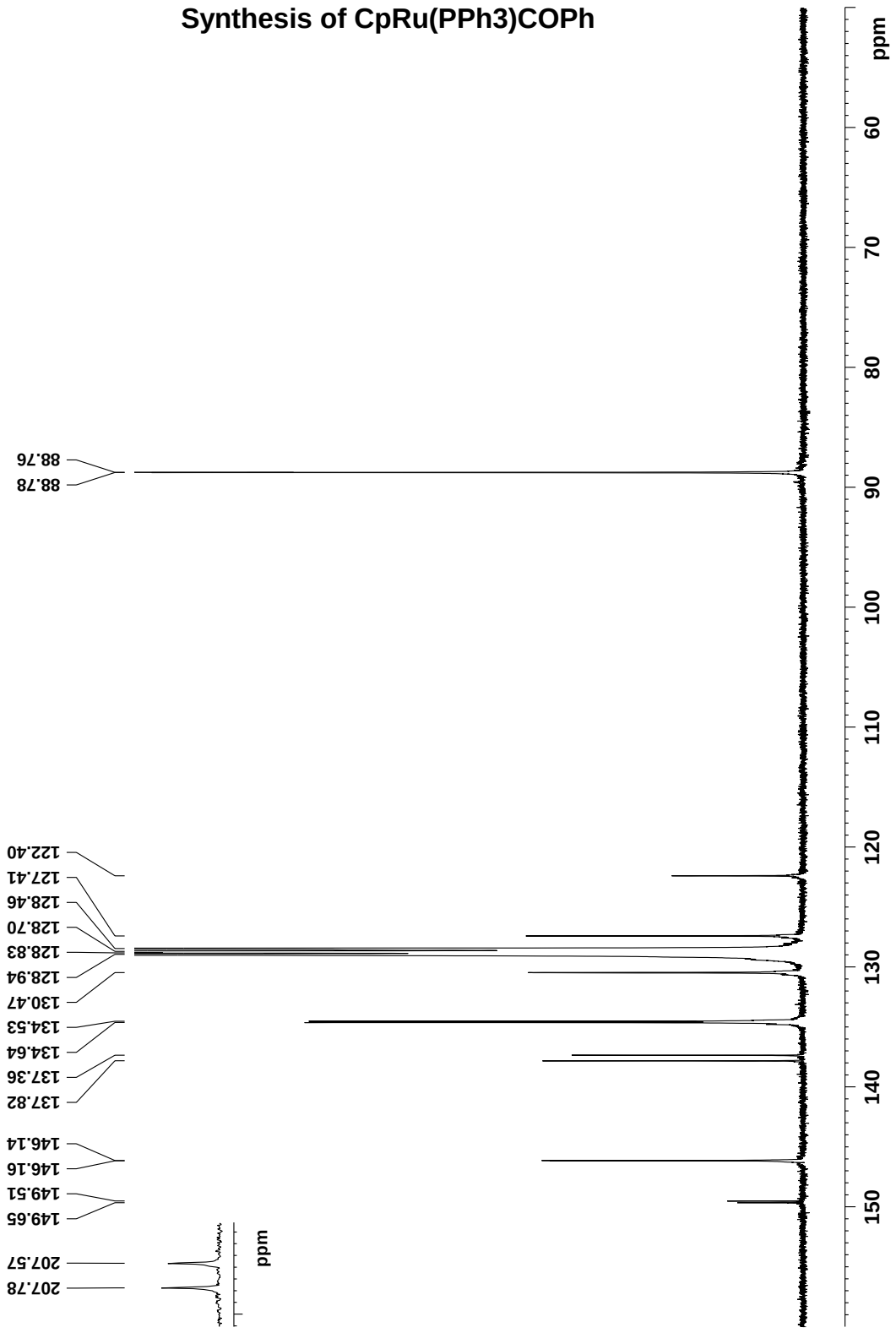

Figure 2.9 $^{13}C\{^{1}H\}$NMR spectrium of $CpRu(PPh_3)(CO)Ph$ (M7)

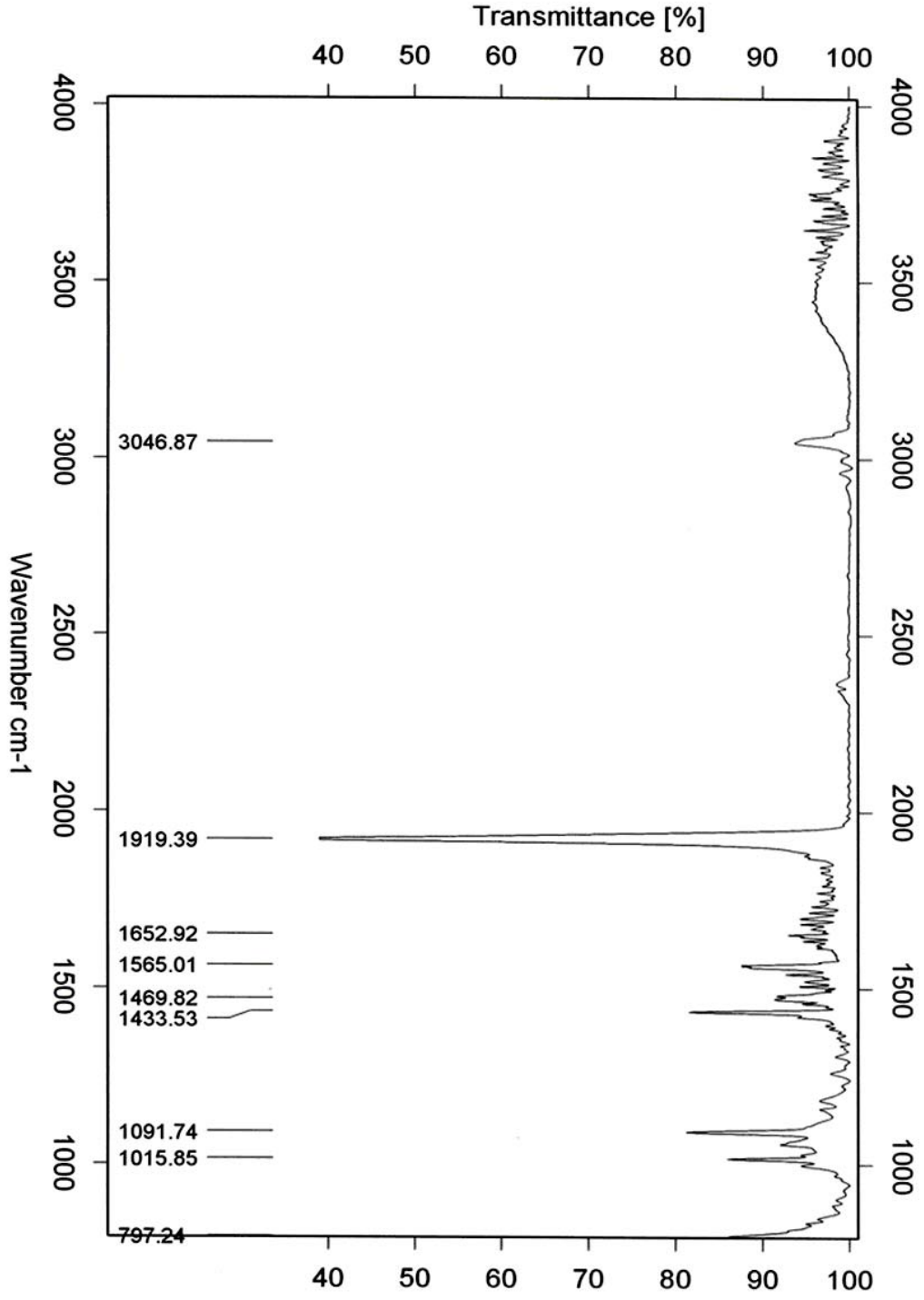

Figure 2.10 Infra-red spectrium of $CpRu(PPh_3)(CO)Ph$ (M7)

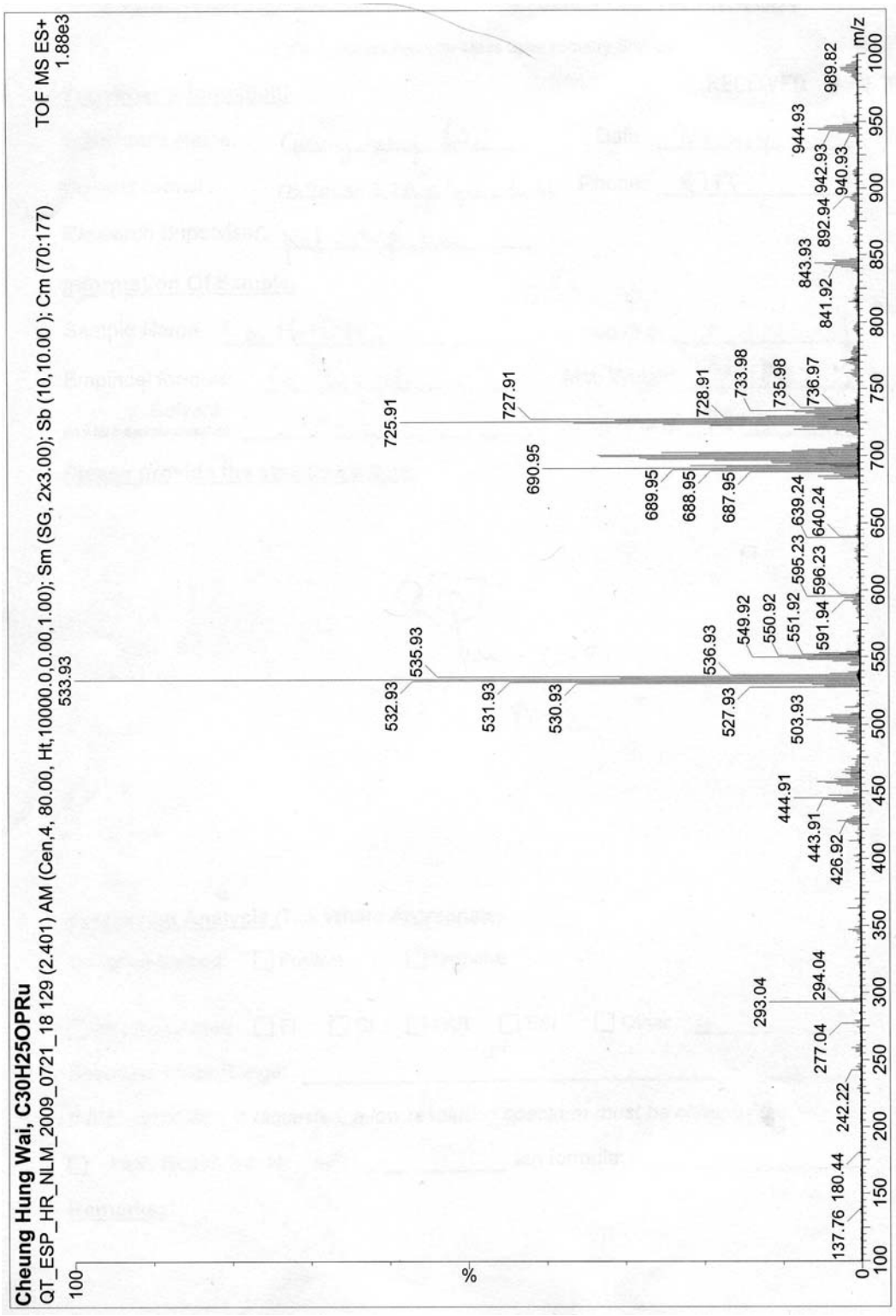

Figure 2.11 Mass spectrium of $CpRu(PPh_3)(CO)Ph$ (M7)

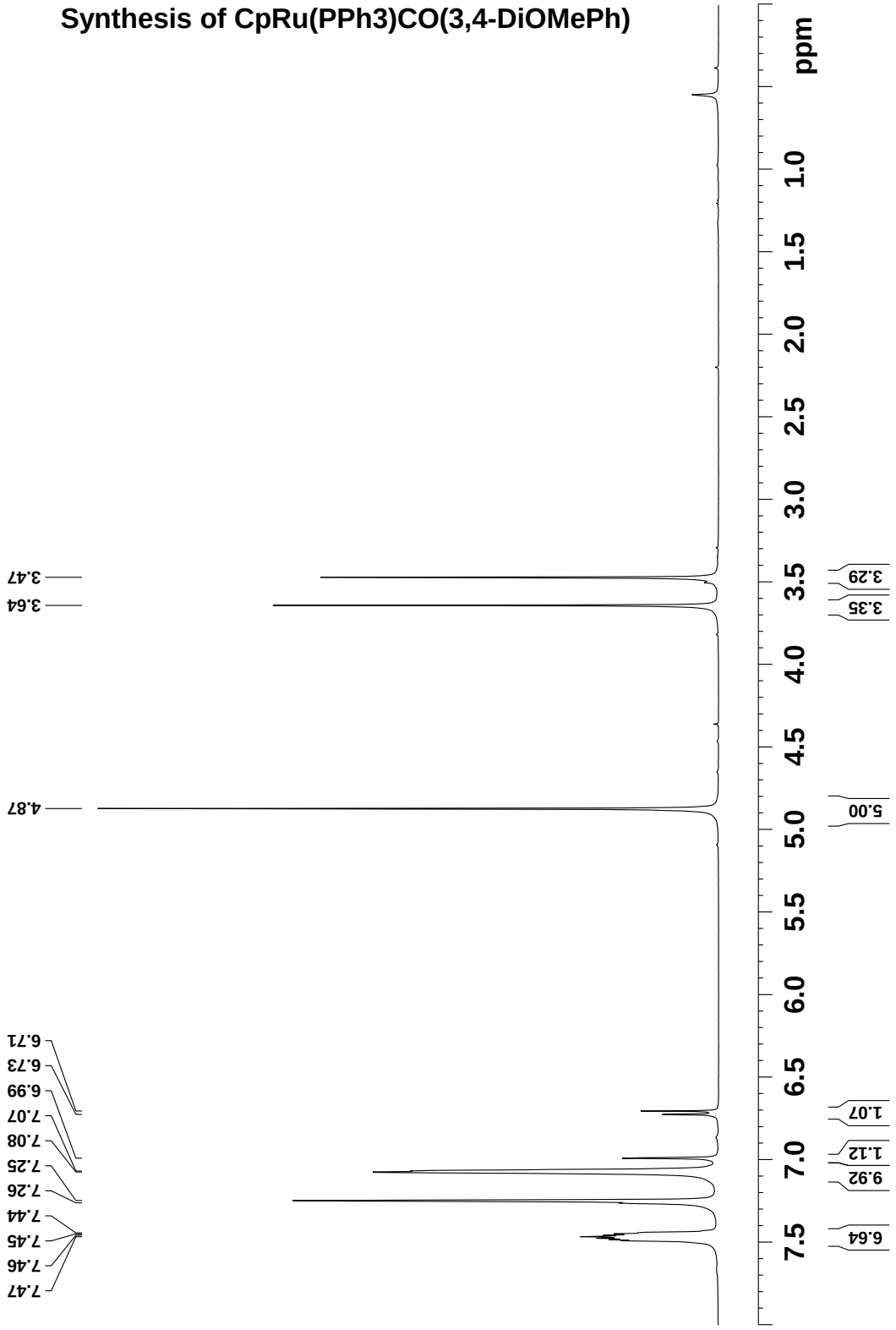

Figure 2.12 ^{1}H NMR spectrium of CpRu(PPh$_3$)(CO)(3,4-Dimethoxyphenyl) (M12)

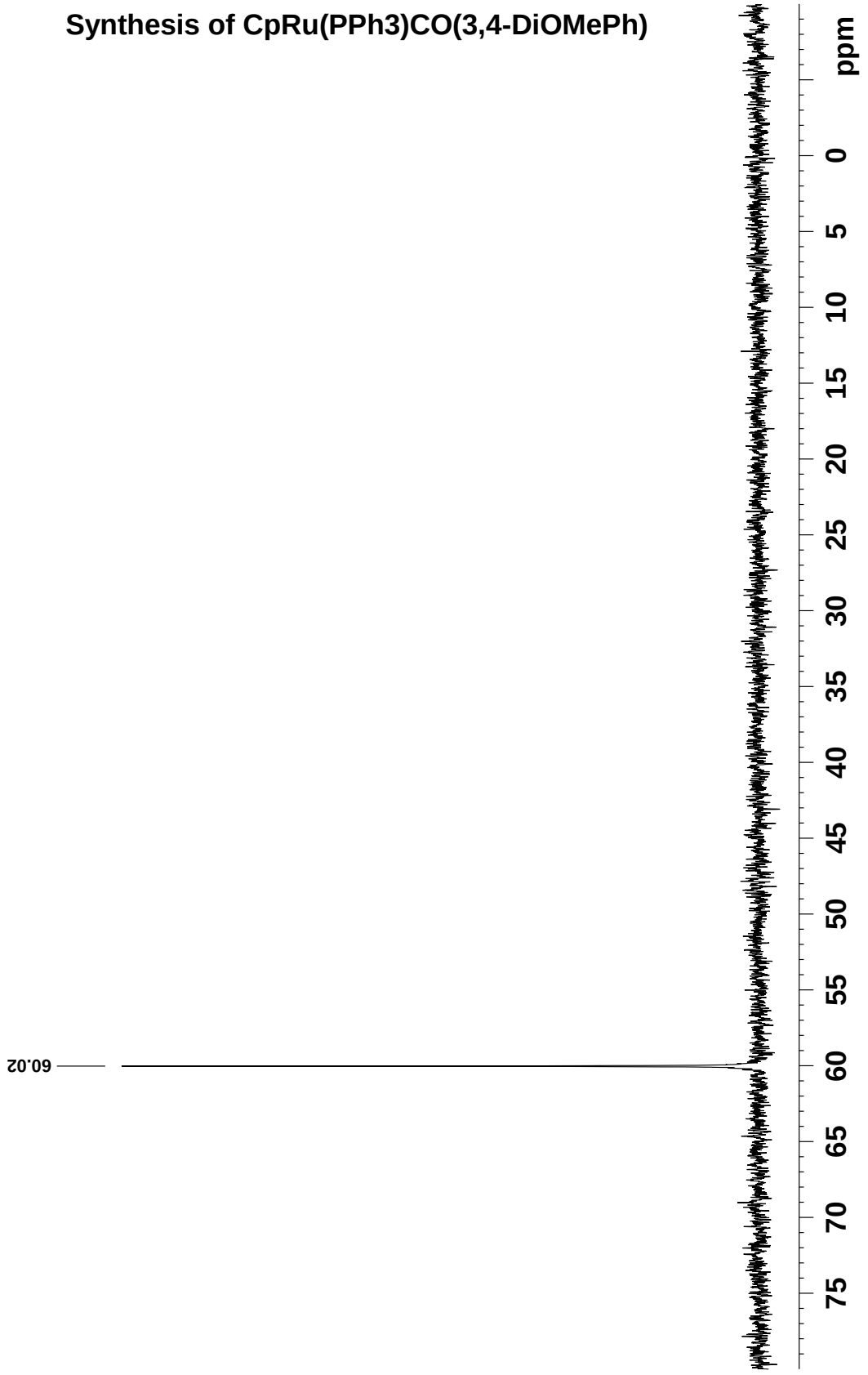

Figure 2.13 $^{31}P\{^{1}H\}$NMR spectrium of CpRu(PPh_3)(CO)(3,4-Dimethoxyphenyl) (M12)

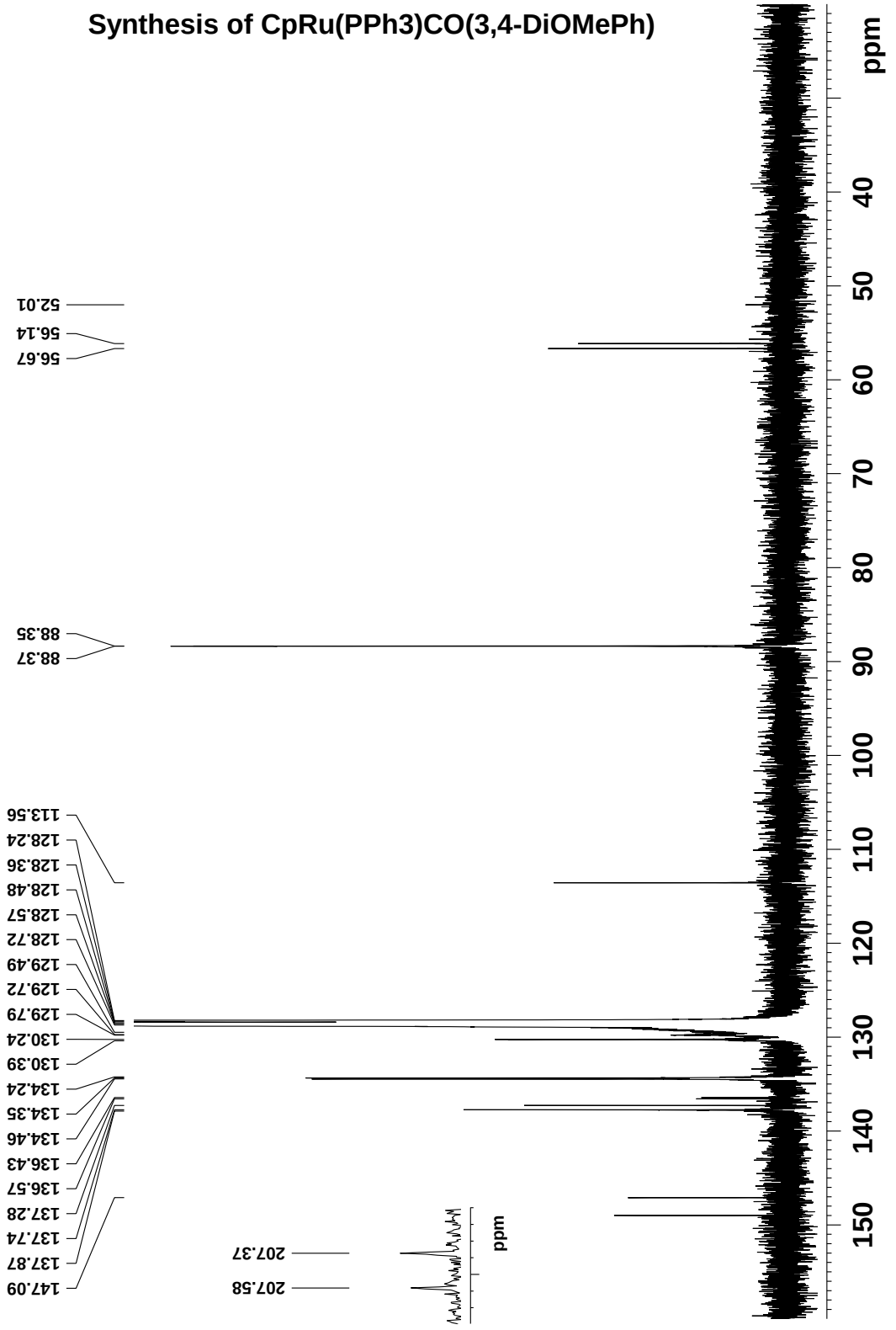

Figure 2.14 $^{13}C\{^{1}H\}$NMR spectrium of CpRu(PPh_3)(CO)(3,4-Dimethoxyphenyl) (M12)

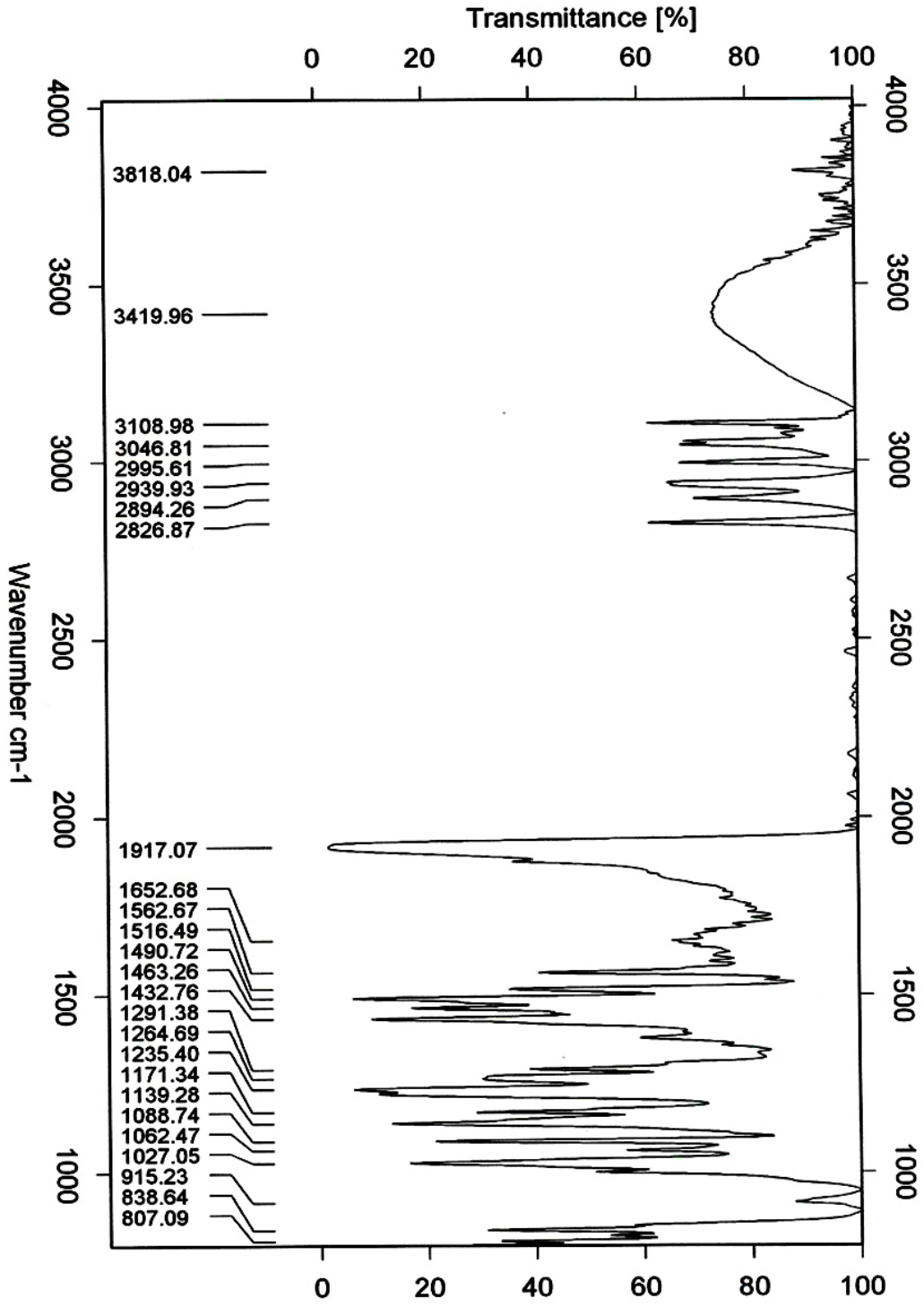

Figure 2.15 Infra-red spectrium of $CpRu(PPh_3)(CO)$(3,4-Dimethoxyphenyl) (M12)

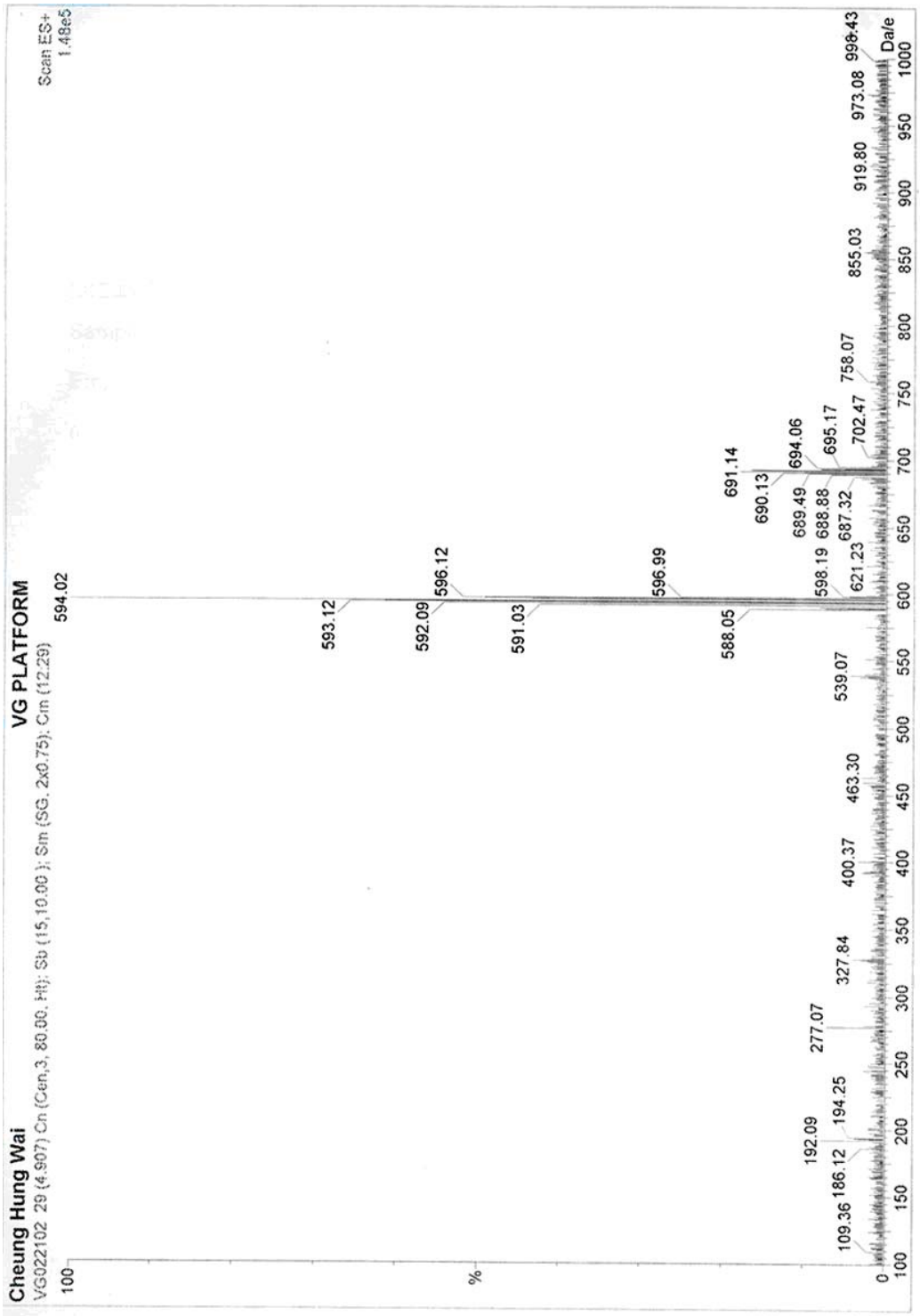

Figure 2.16 Mass spectrum of $CpRu(PPh_3)(CO)$(3,4-Dimethoxyphenyl) (M12)

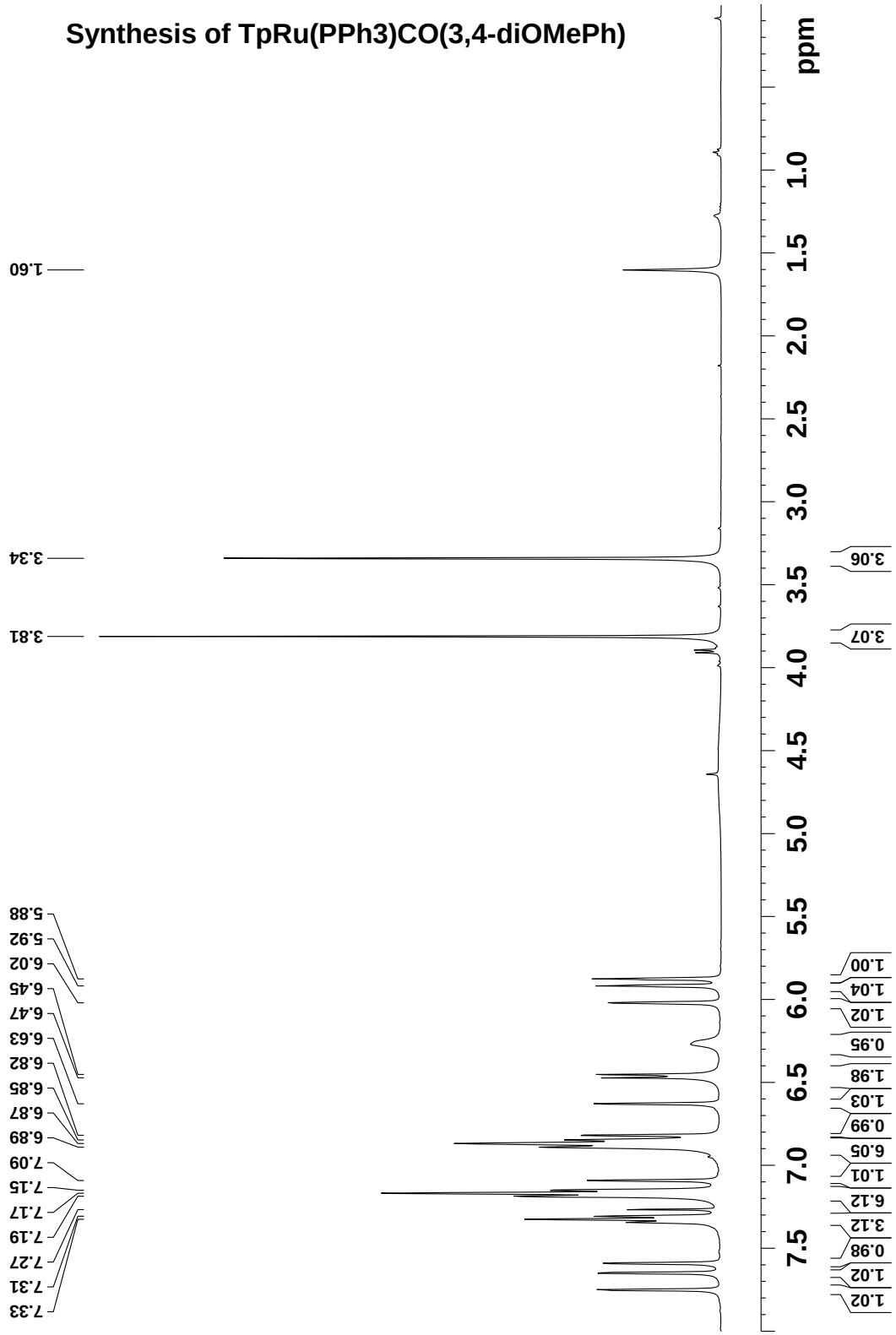

Figure 2.17 ^{1}H NMR spectrium of TpRu(PPh$_3$)(CO)(3,4-Dimethoxyphenyl) (M13)

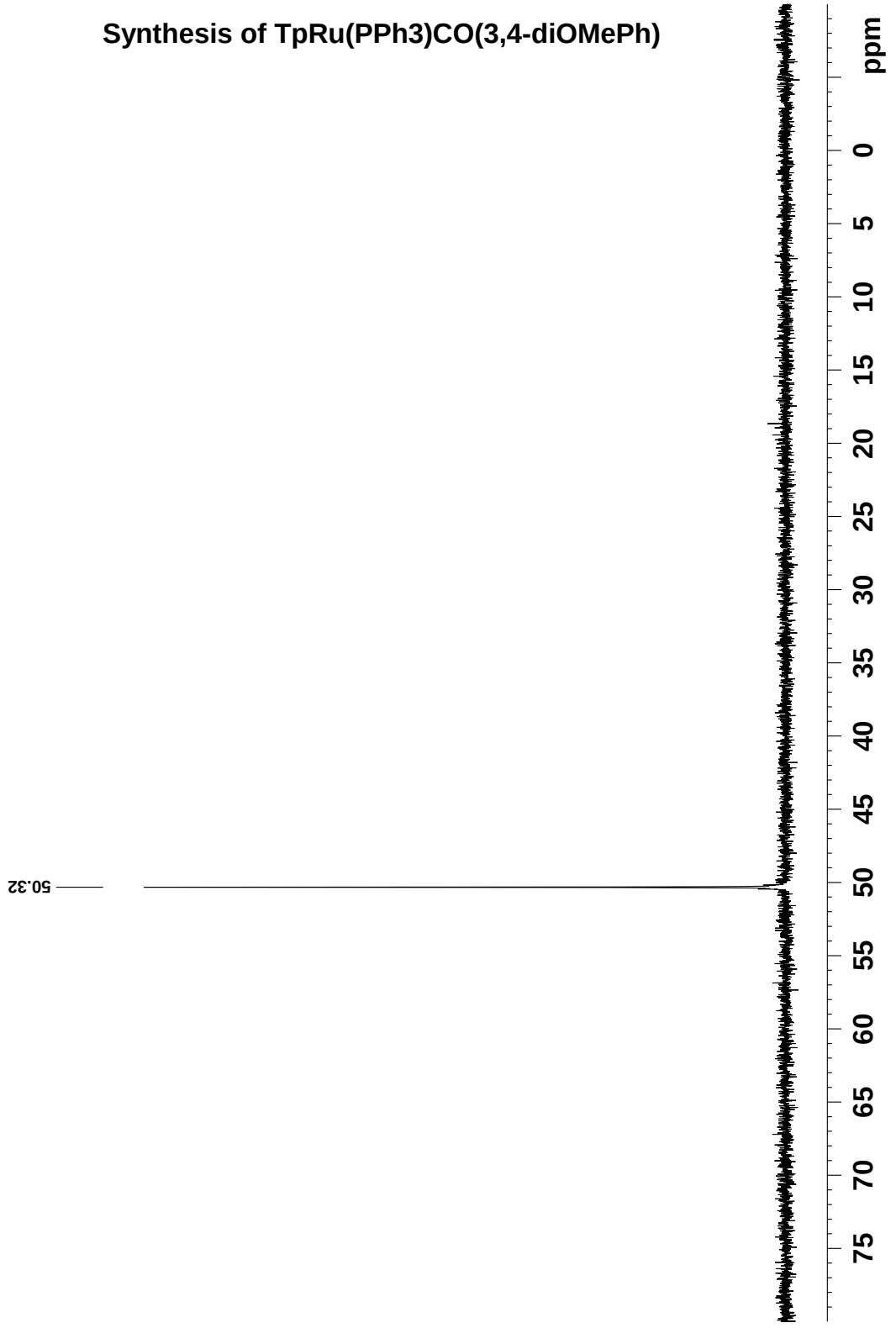

Figure 2.18 $^{31}P\{^{1}H\}$NMR spectrium of TpRu(PPh_3)(CO)(3,4-Dimethoxyphenyl) (M13)

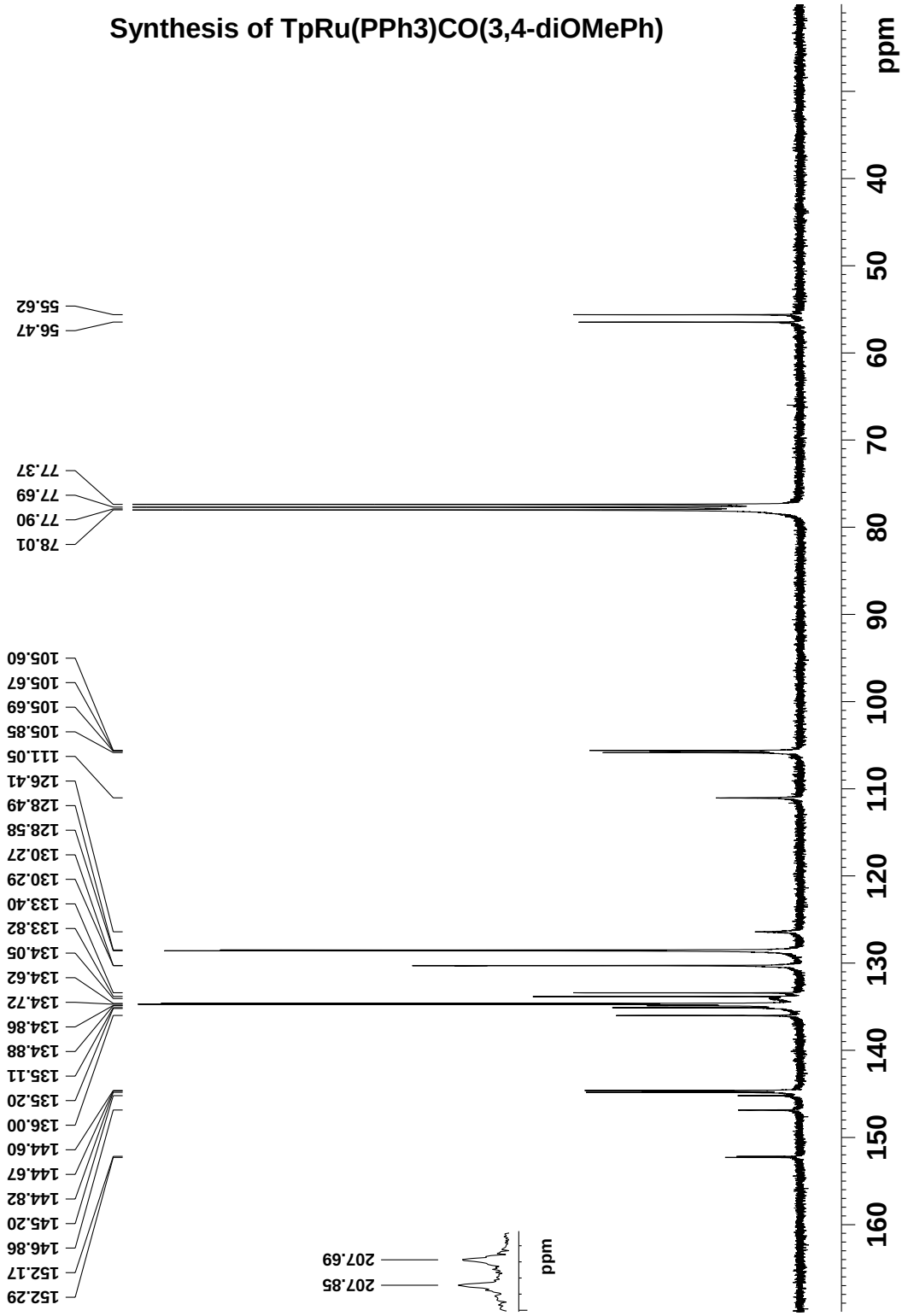

Figure 2.19 $^{13}C\{^{1}H\}$NMR spectrium of TpRu(PPh_3)(CO)(3,4-Dimethoxyphenyl) (M13)

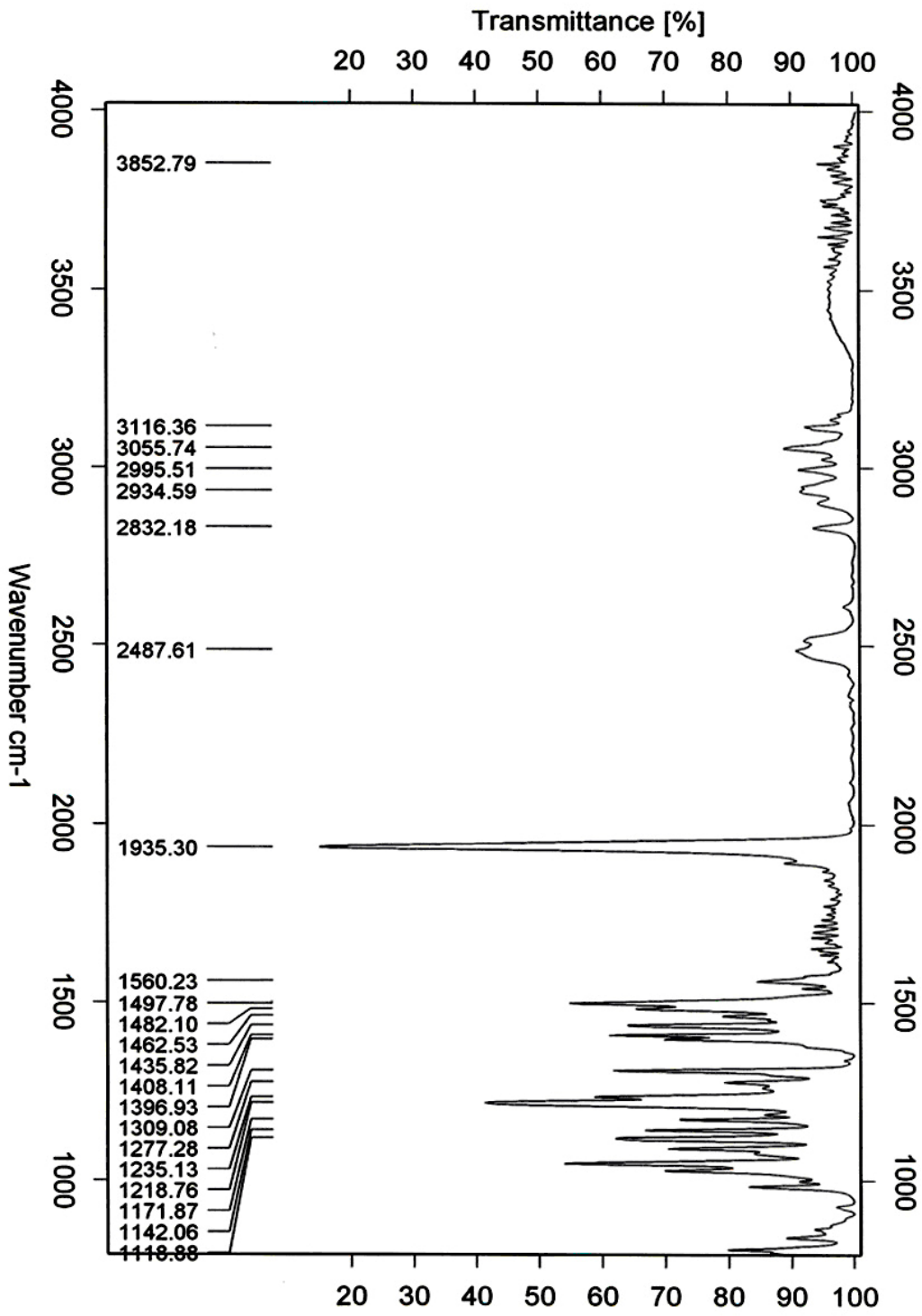

Figure 2.20 Infra-red spectrium of TpRu(PPh_3)(CO)(3,4-Dimethoxyphenyl) (M13)

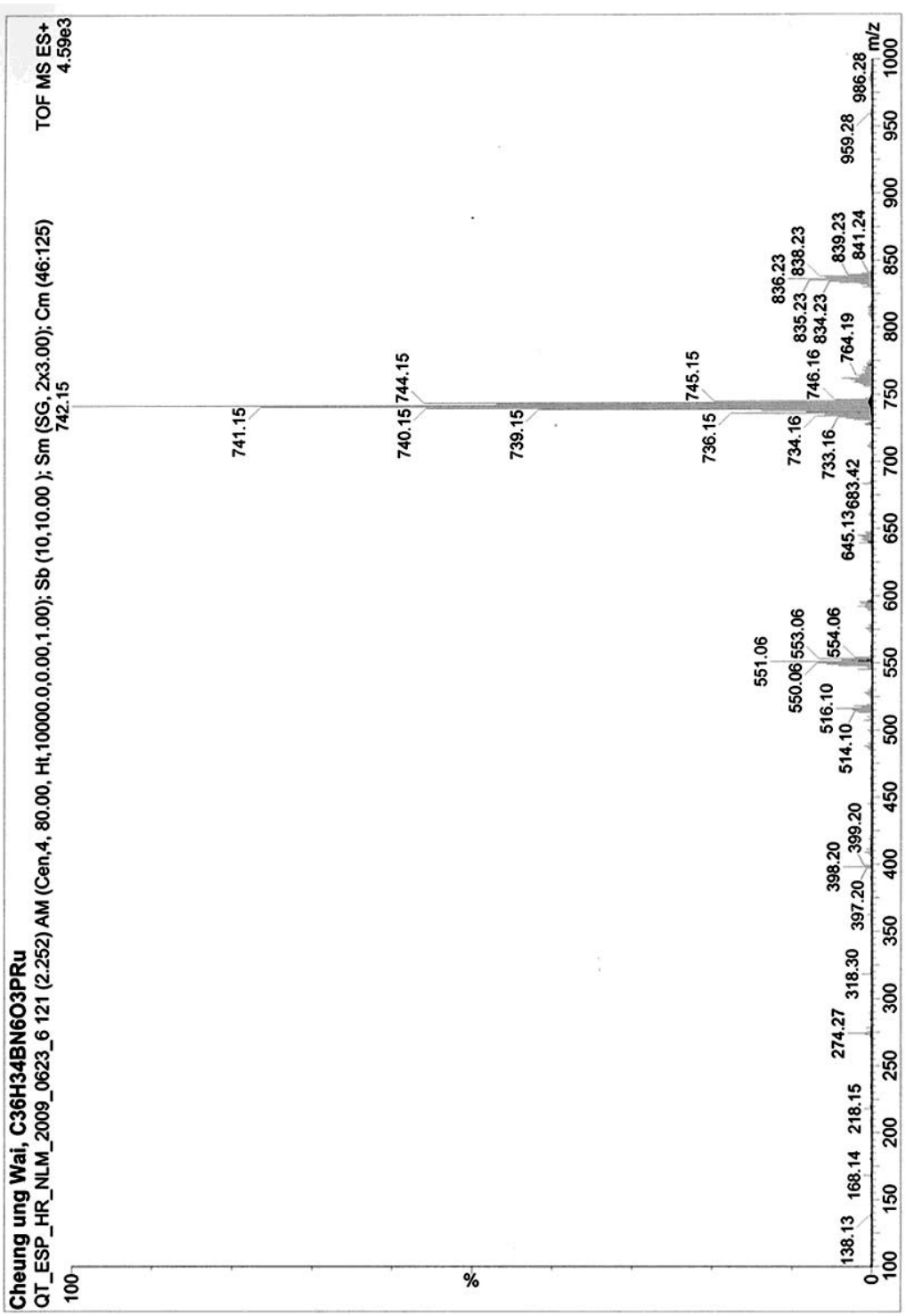

Figure 2.21 Mass spectrium of TpRu(PPh$_3$)(CO)(3,4-Dimethoxyphenyl) (M13)

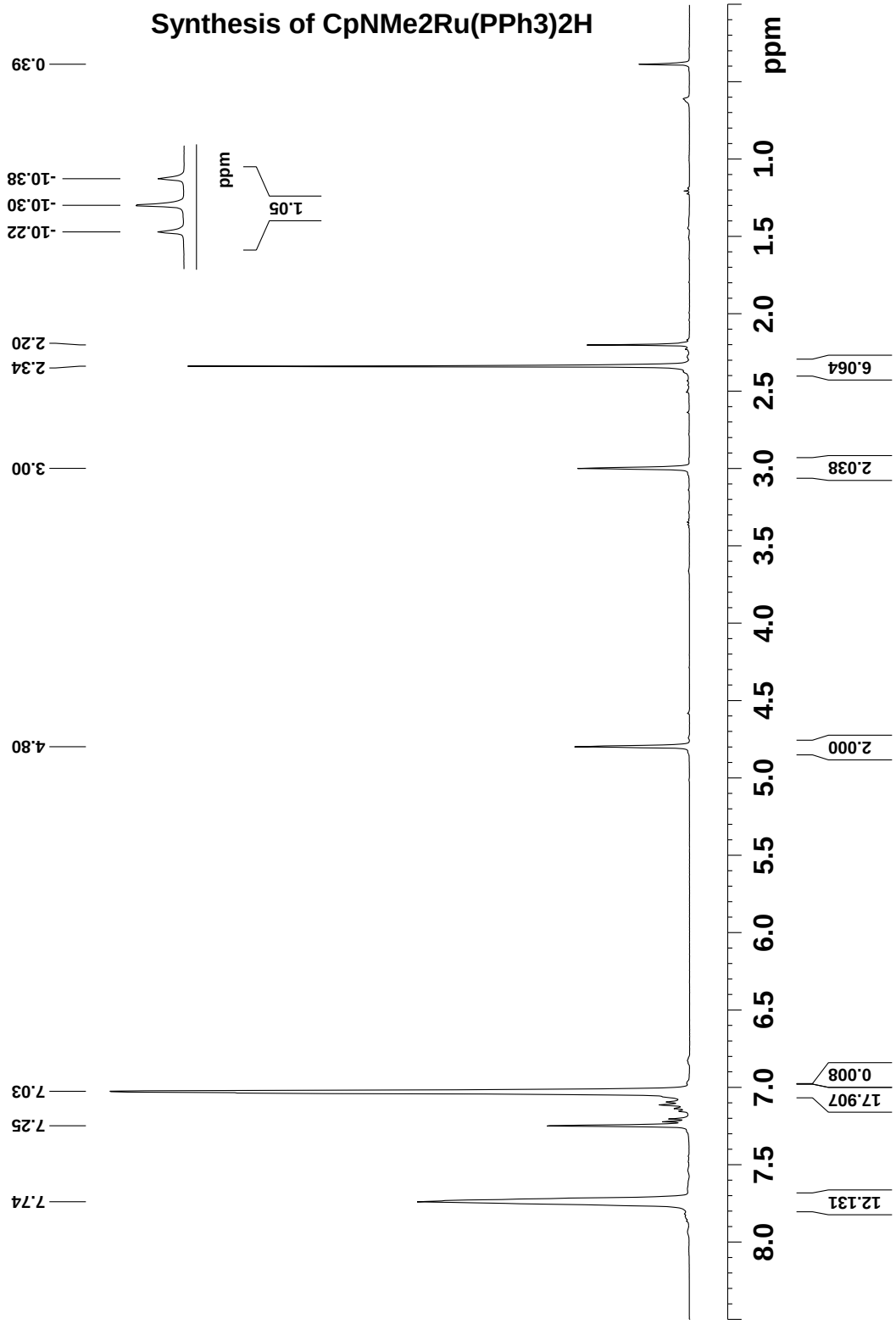

Figure 3.7 ^{1}H NMR spectrium of $(CpNMe_2)Ru(PPh_3)_2H$ (M14)

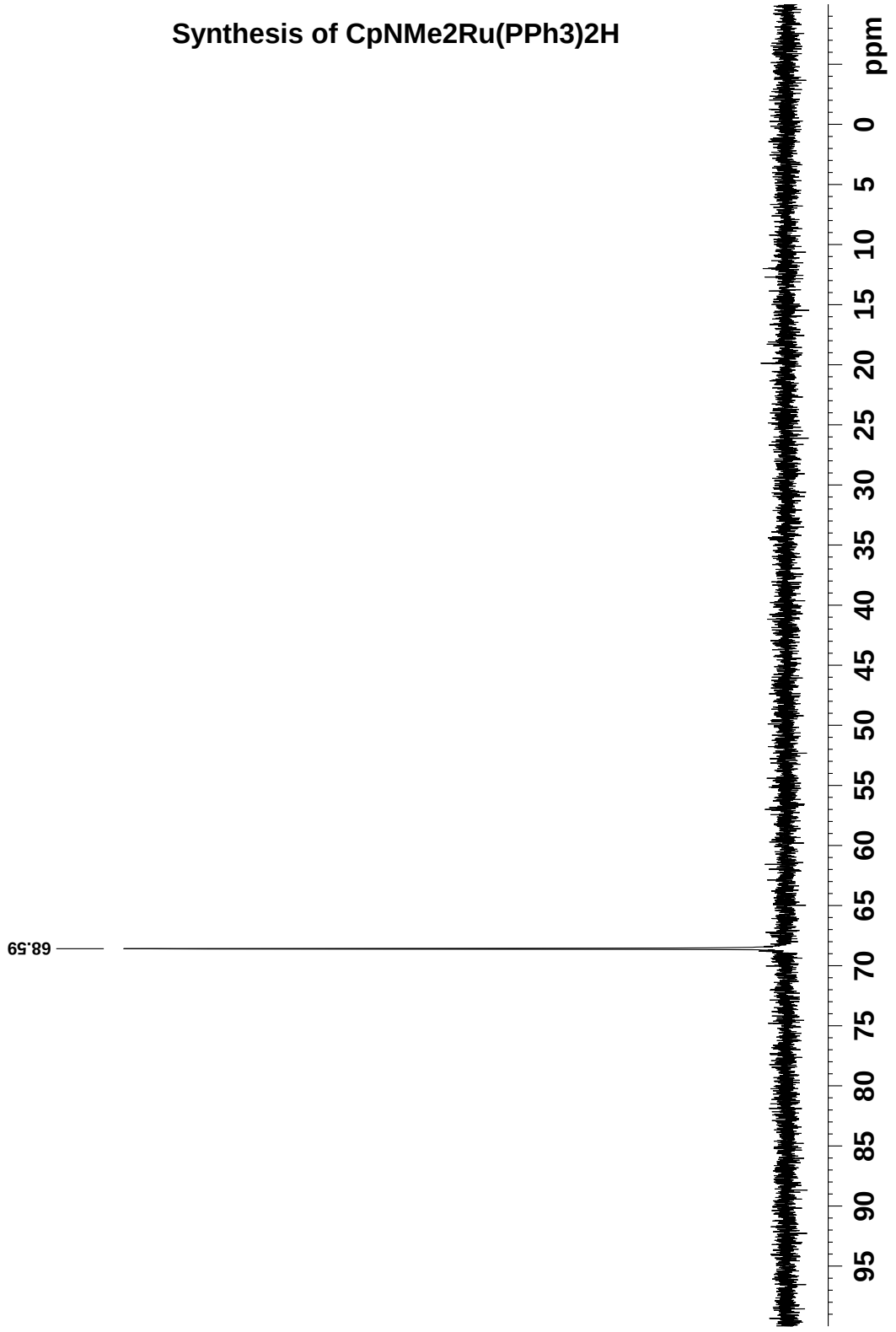

Figure 3.8 $^{31}P\{^{1}H\}$NMR spectrium of $(CpNMe_2)Ru(PPh_3)_2H$ (M14)

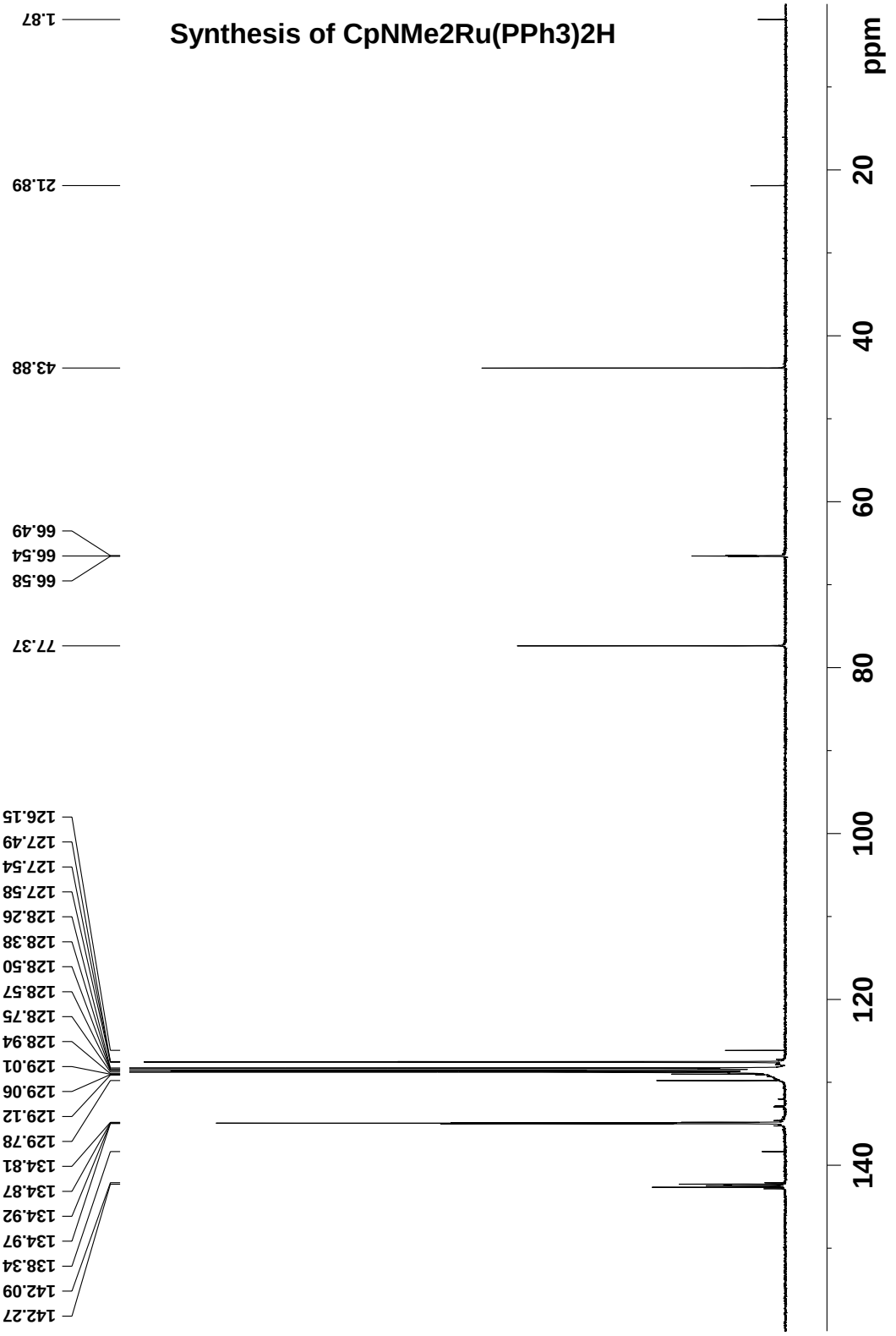

Figure 3.9 $^{13}C\{^{1}H\}$NMR spectrium of $(CpNMe_2)Ru(PPh_3)_2H$ (M14)

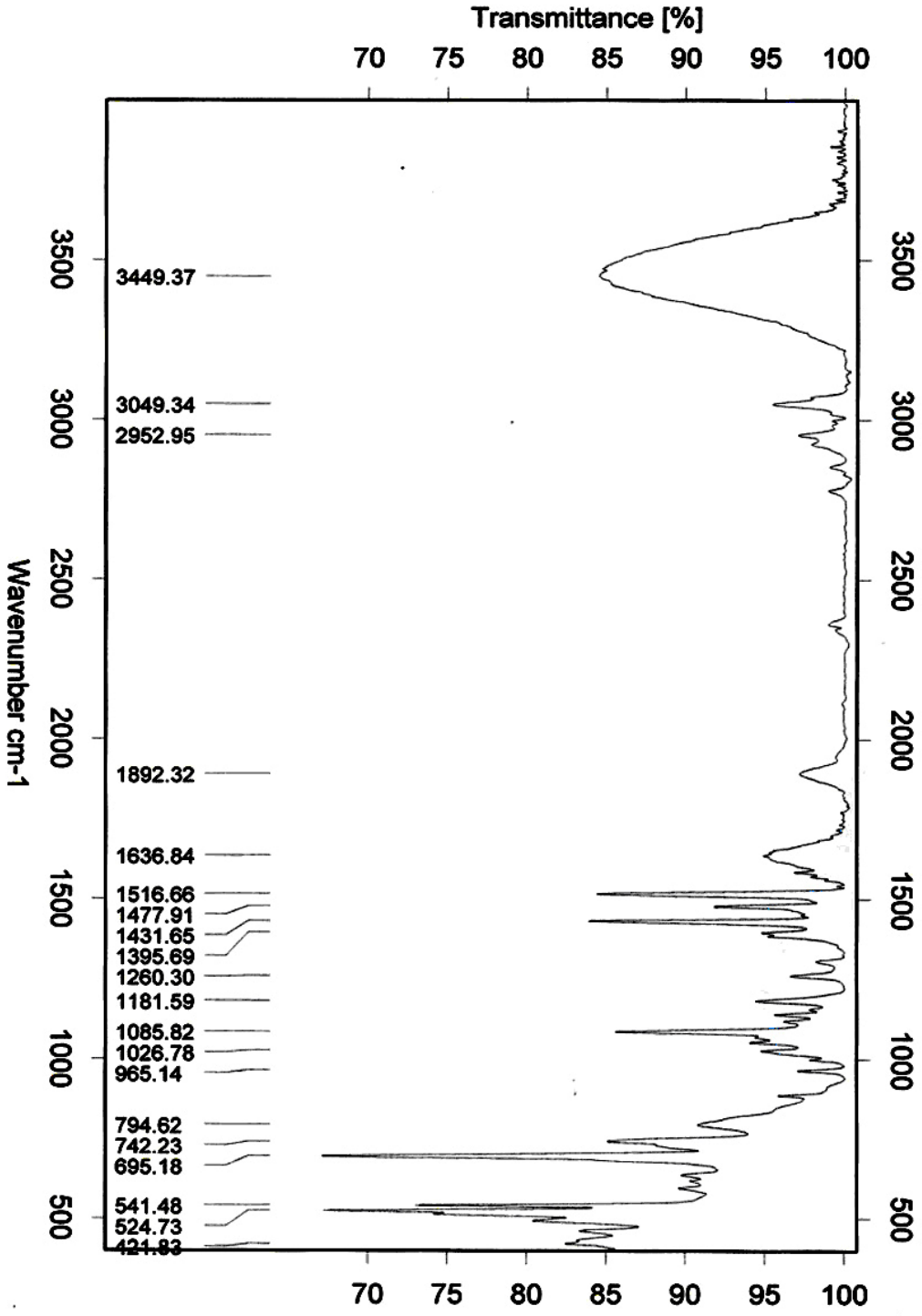

Figure 3.10 Infra-red spectrium of $(CpNMe_2)Ru(PPh_3)_2H$ (M14)

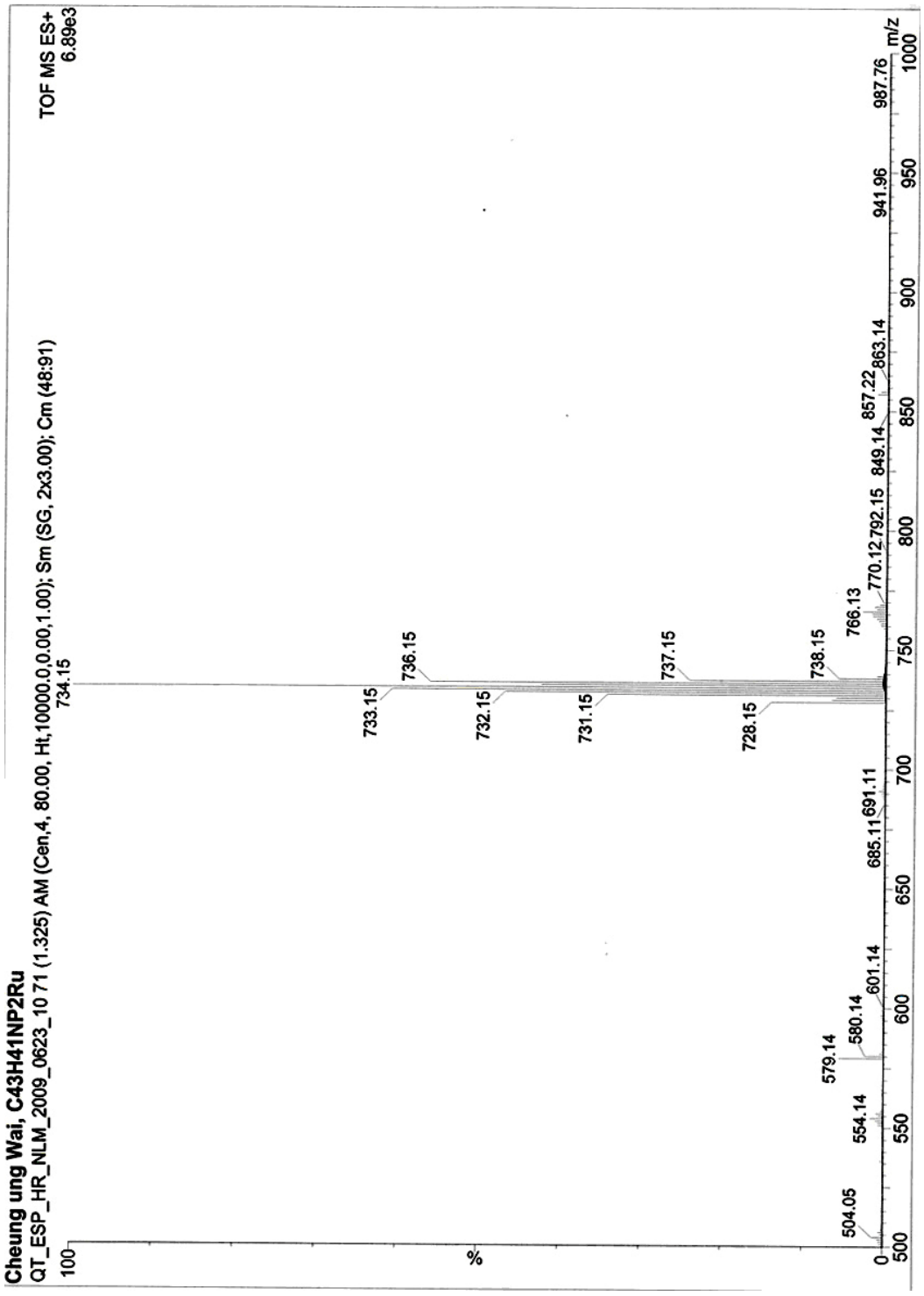

Figure 3.11 Mass spectrium of $(CpNMe_2)Ru(PPh_3)_2H$ (M14)

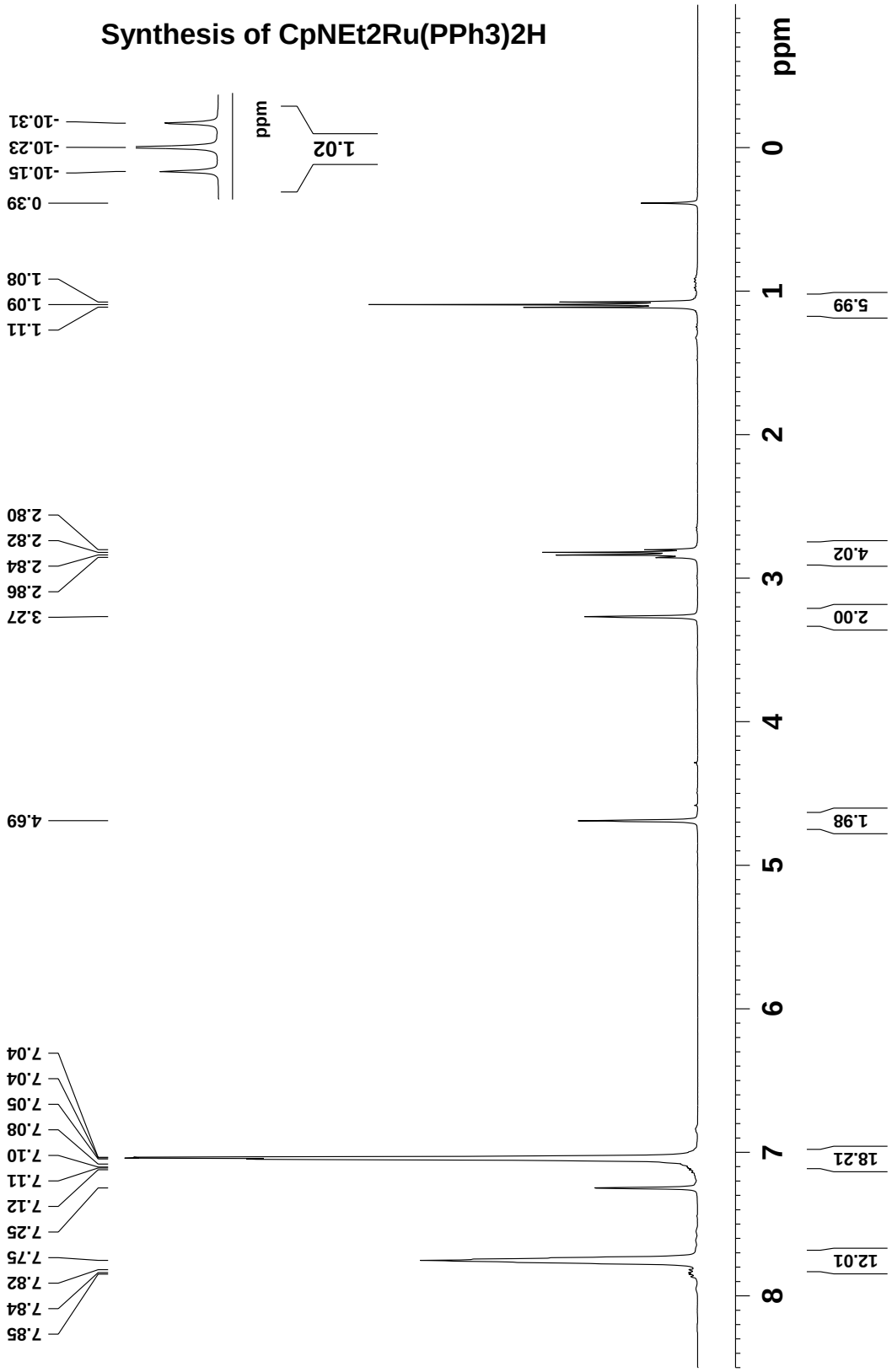

Figure 3.12 ^{1}H NMR spectrium of $(CpNEt_2)Ru(PPh_3)_2H$ (M15)

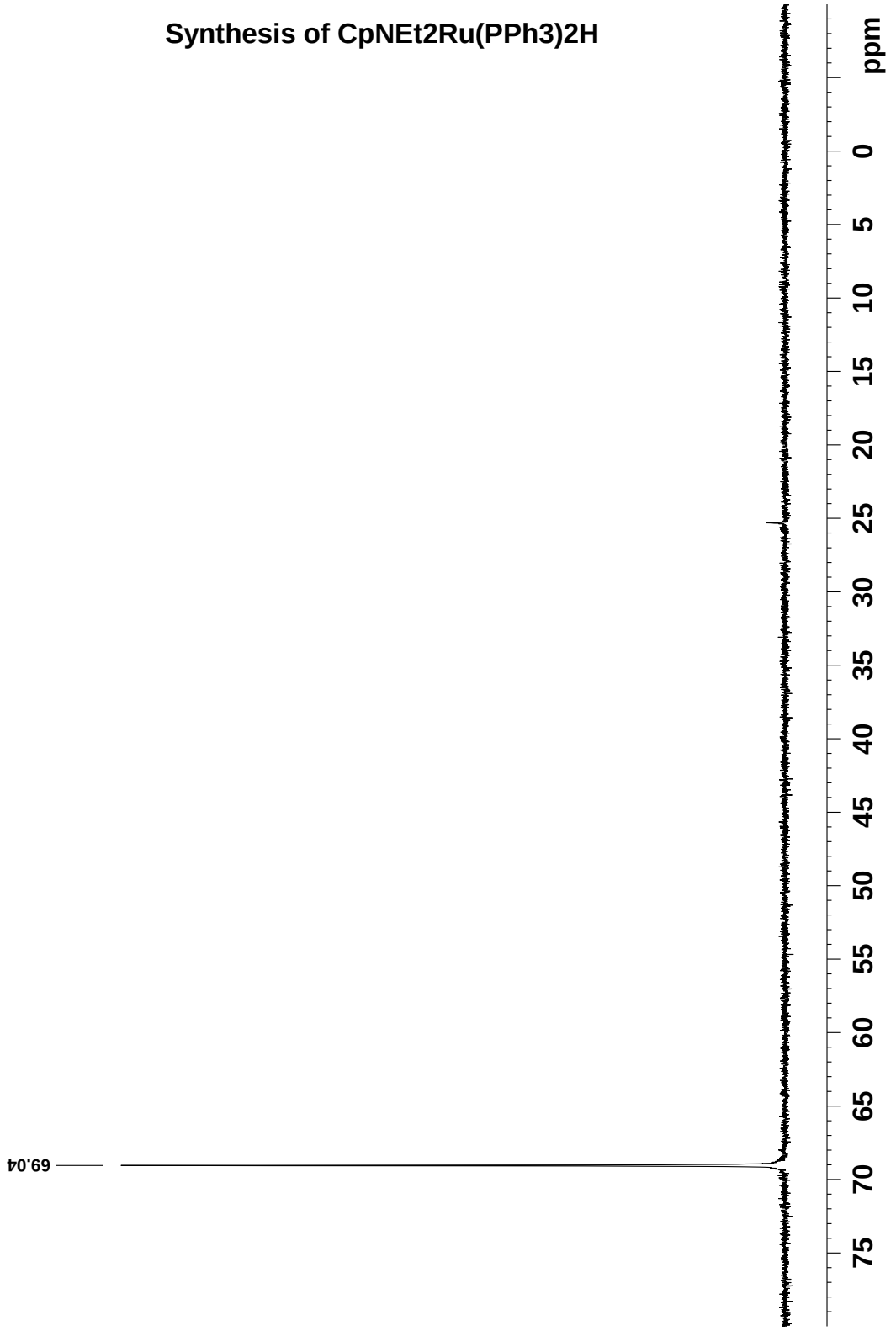

Figure 3.13 $^{31}P\{^{1}H\}$NMR spectrium of $(CpNEt_2)Ru(PPh_3)_2H$ (M15)

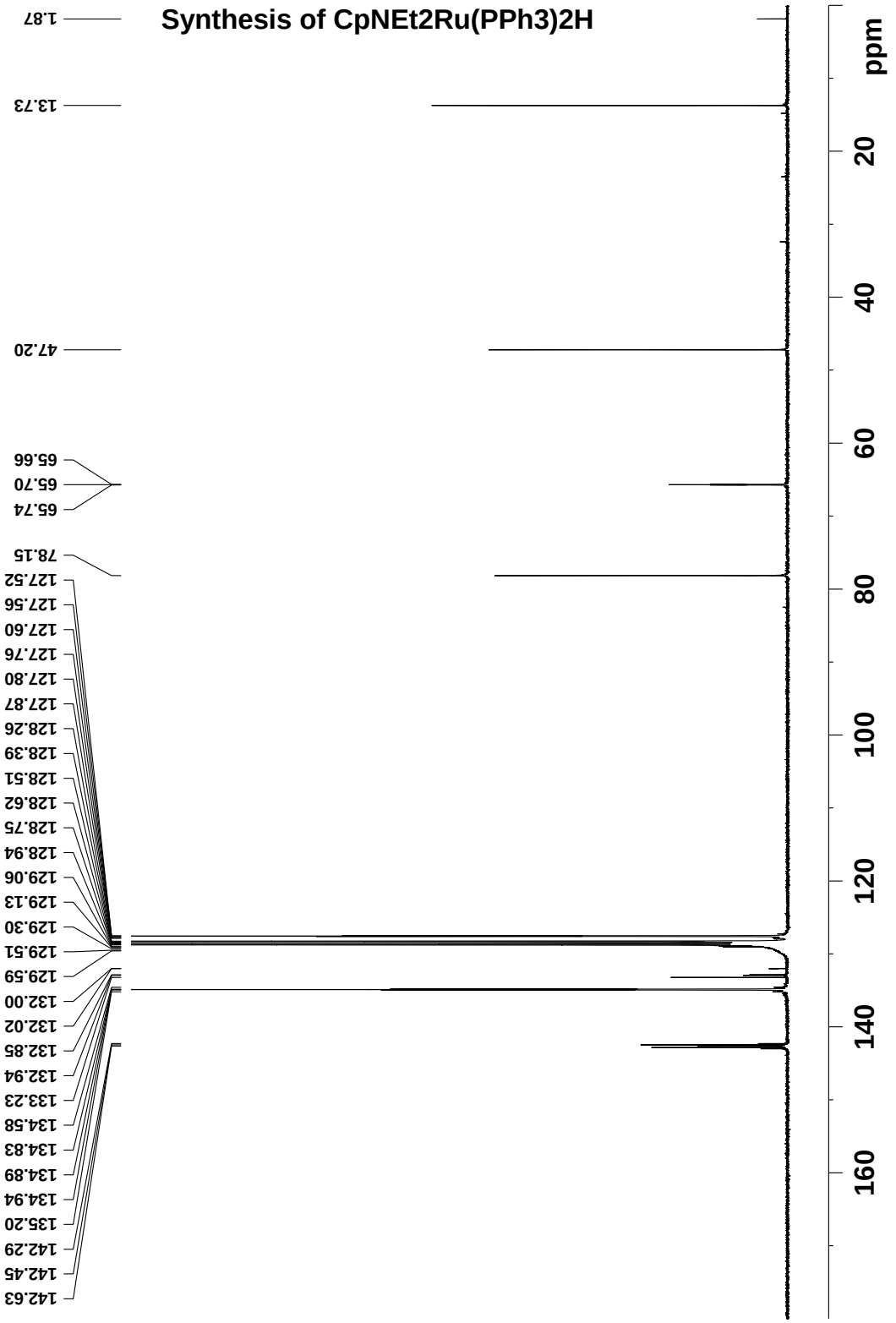

Figure 3.14 $^{13}C\{^{1}H\}$NMR spectrium of $(CpNEt_2)Ru(PPh_3)_2H$ (M15)

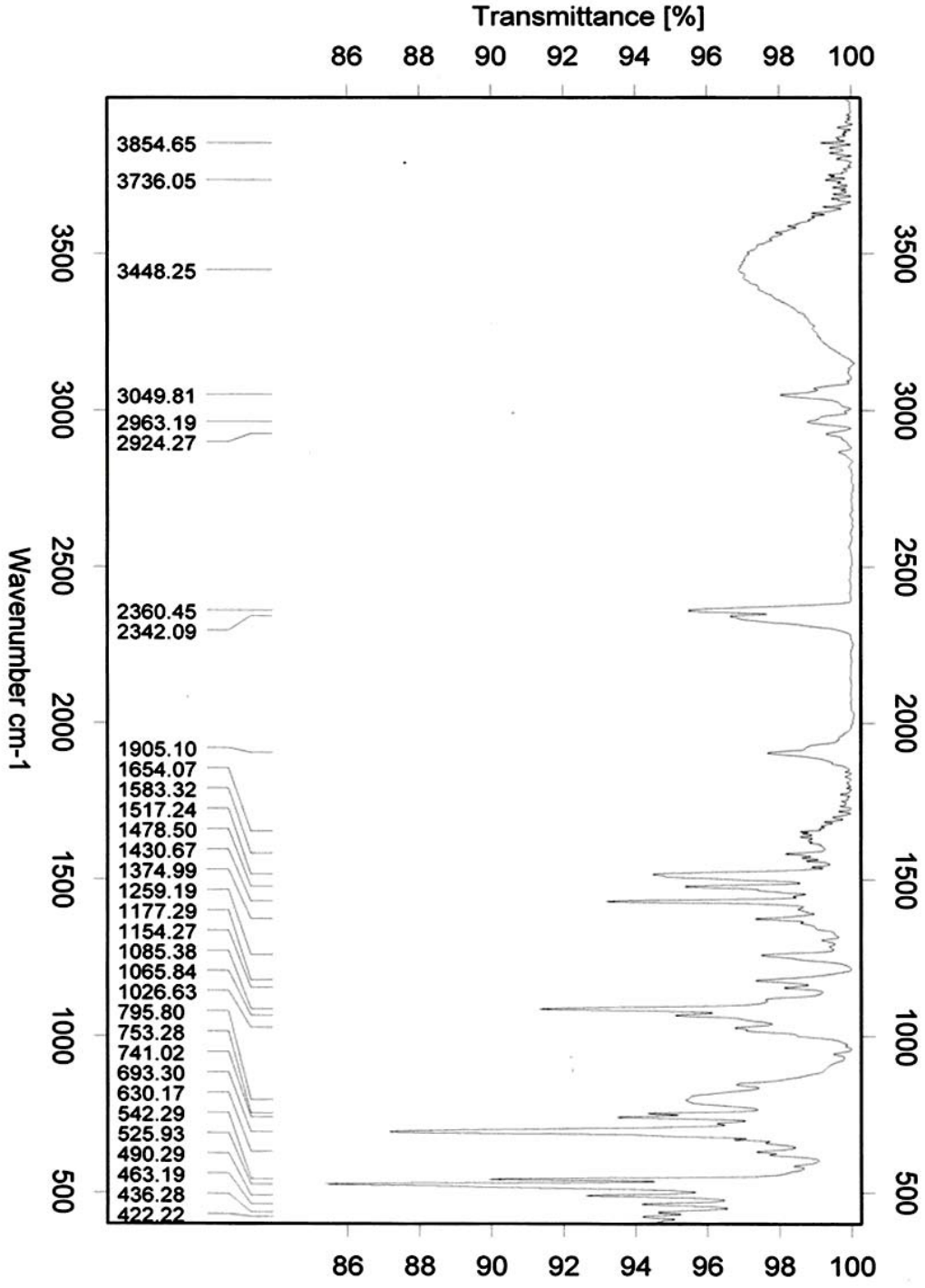

Figure 3.15 1Infra-red spectrium of $(CpNEt_2)Ru(PPh_3)_2H$ (M15)

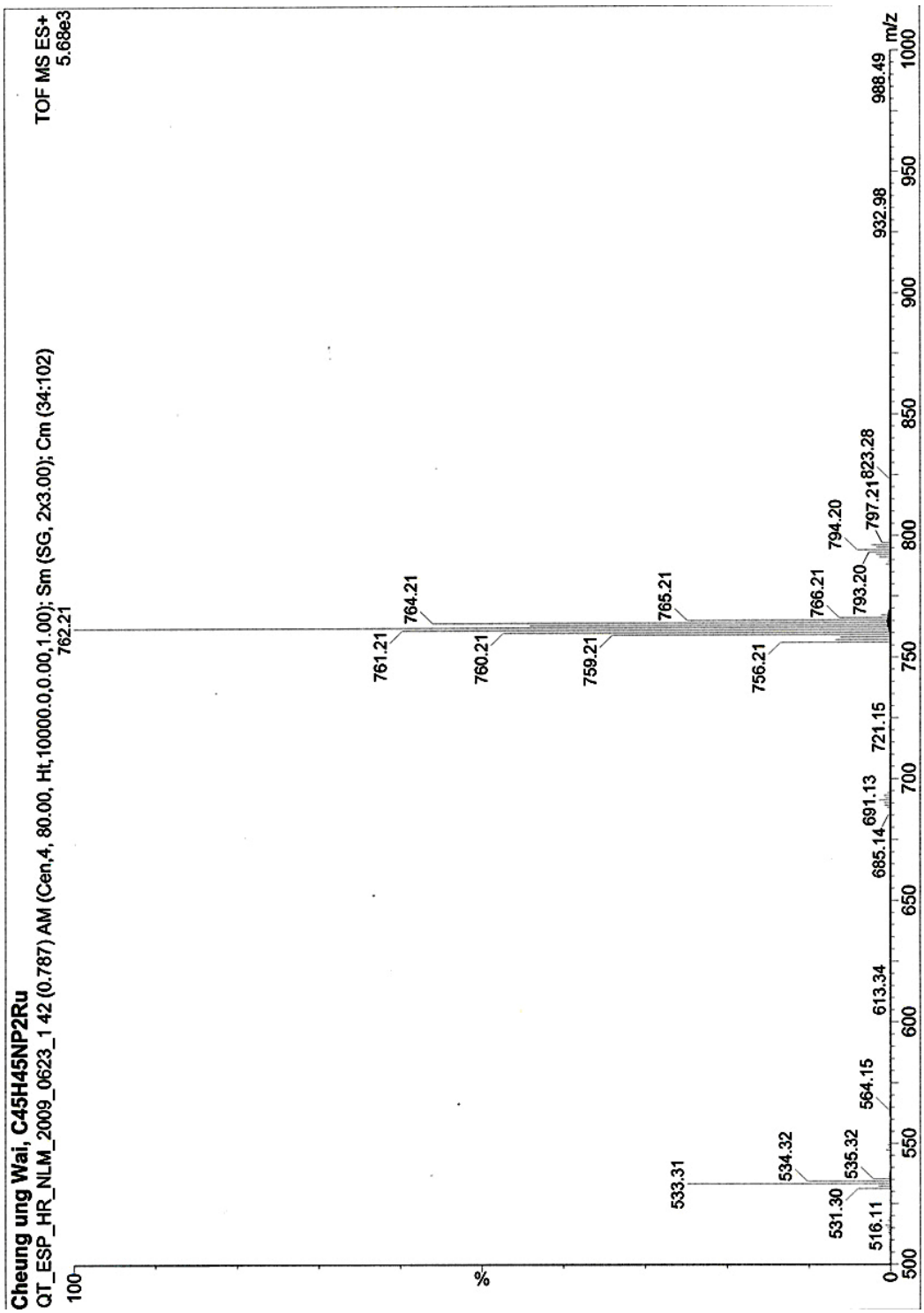

Figure 3.16 Mass spectrium of $(CpNEt_2)Ru(PPh_3)_2H$ (M15)

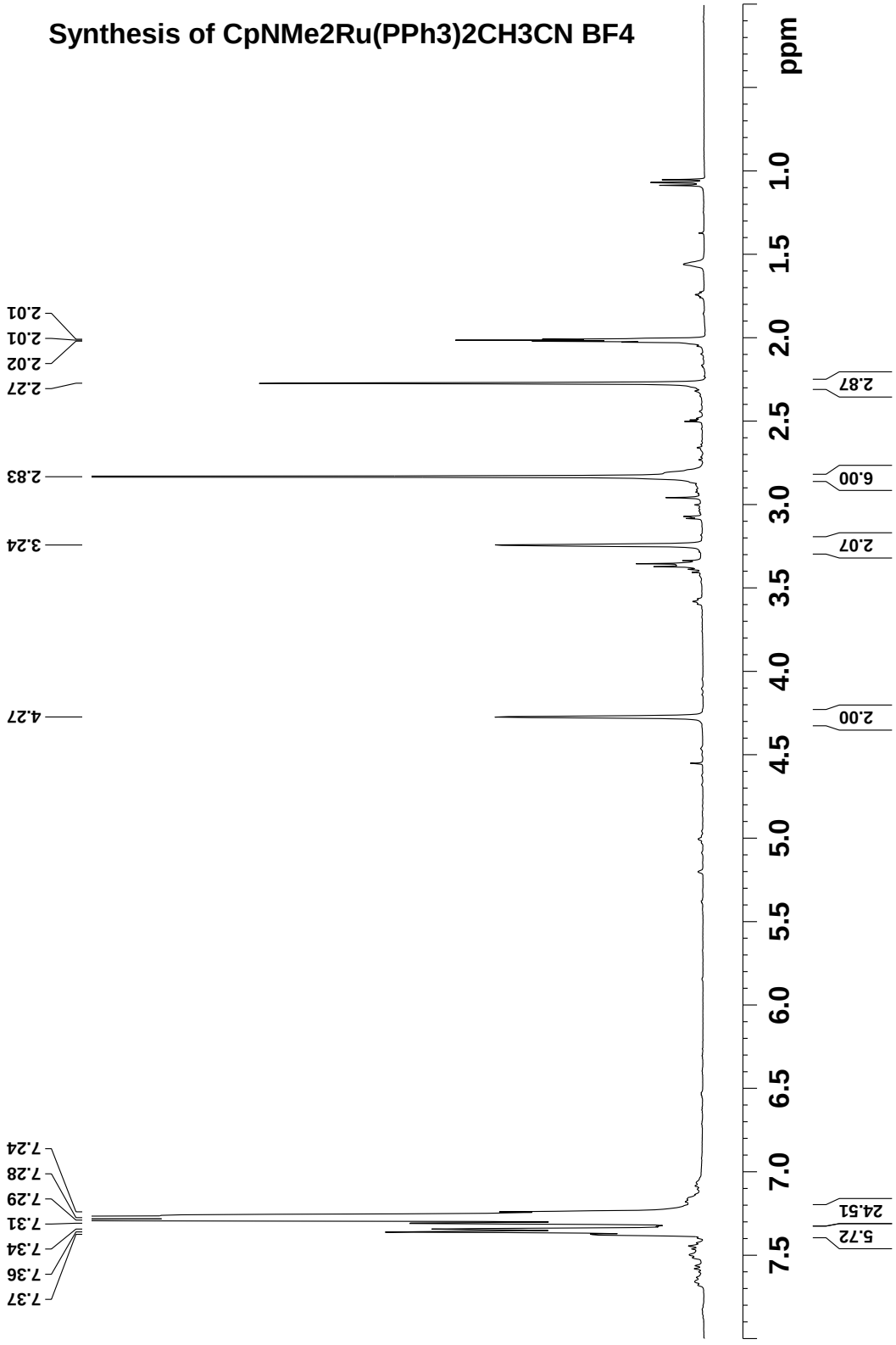

Figure 3.17 ^{1}H NMR spectrium of $[(CpNMe_2)Ru(PPh_3)_2(CH_3CN)]^+BF_4^-$ (M16)

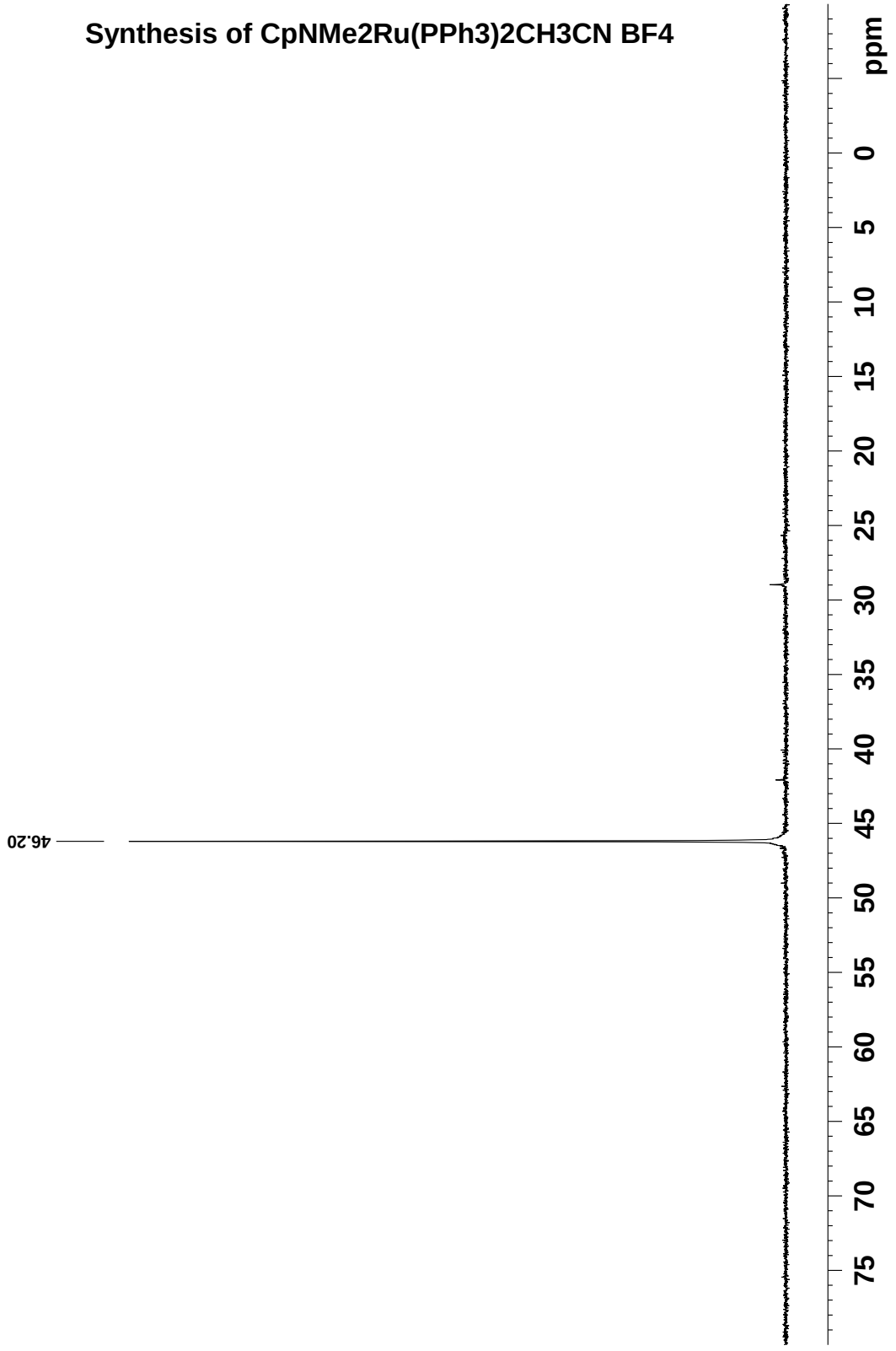

Figure 3.18 $^{31}P\{^{1}H\}$NMR spectrium of $[(CpNMe_2)Ru(PPh_3)_2(CH_3CN)]^{+}BF_4^{-}$ (M16)

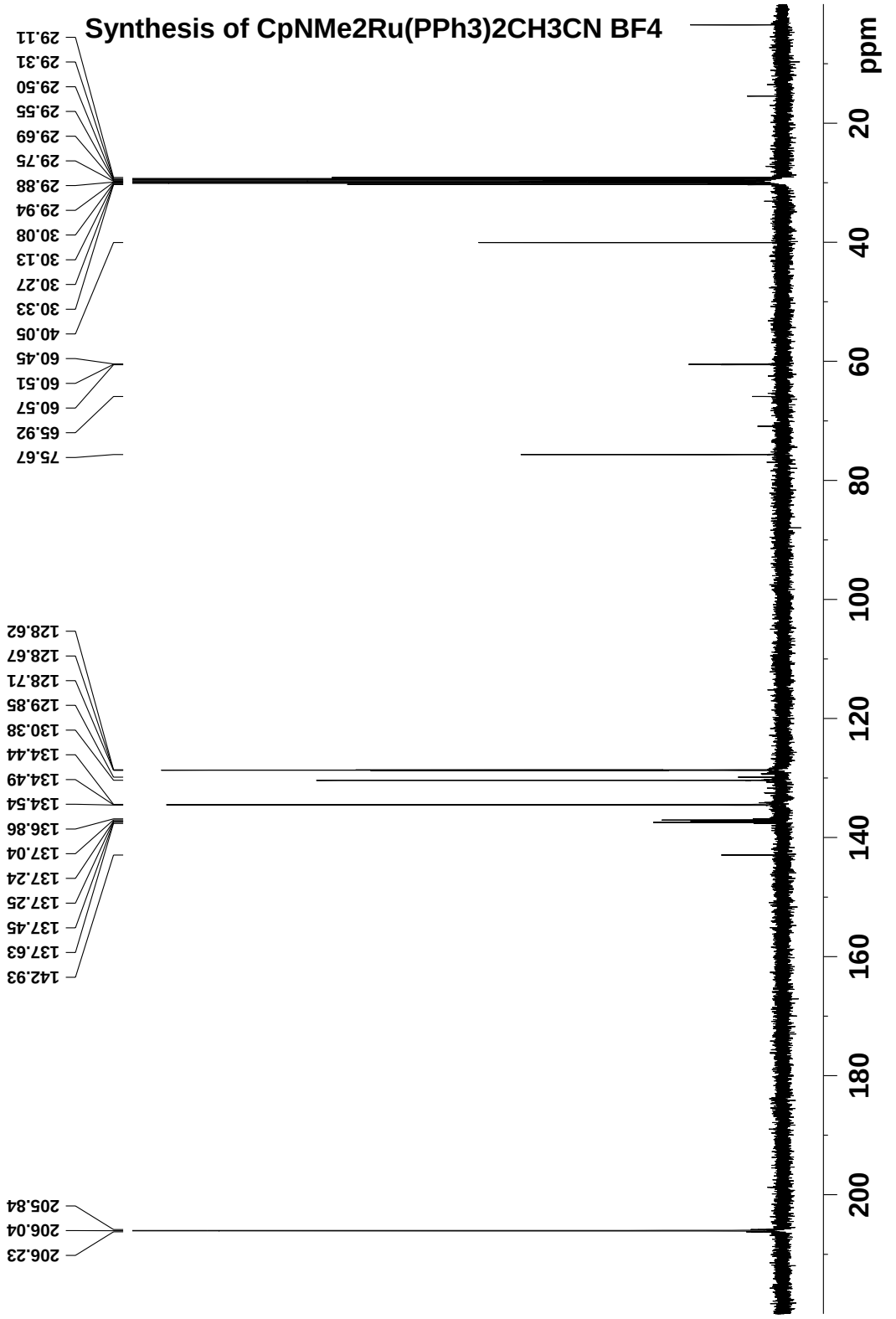

Figure 3.19 $^{13}C\{^{1}H\}$NMR spectrium of $[(CpNMe_2)Ru(PPh_3)_2(CH_3CN)]^+BF_4^-$ (M16)

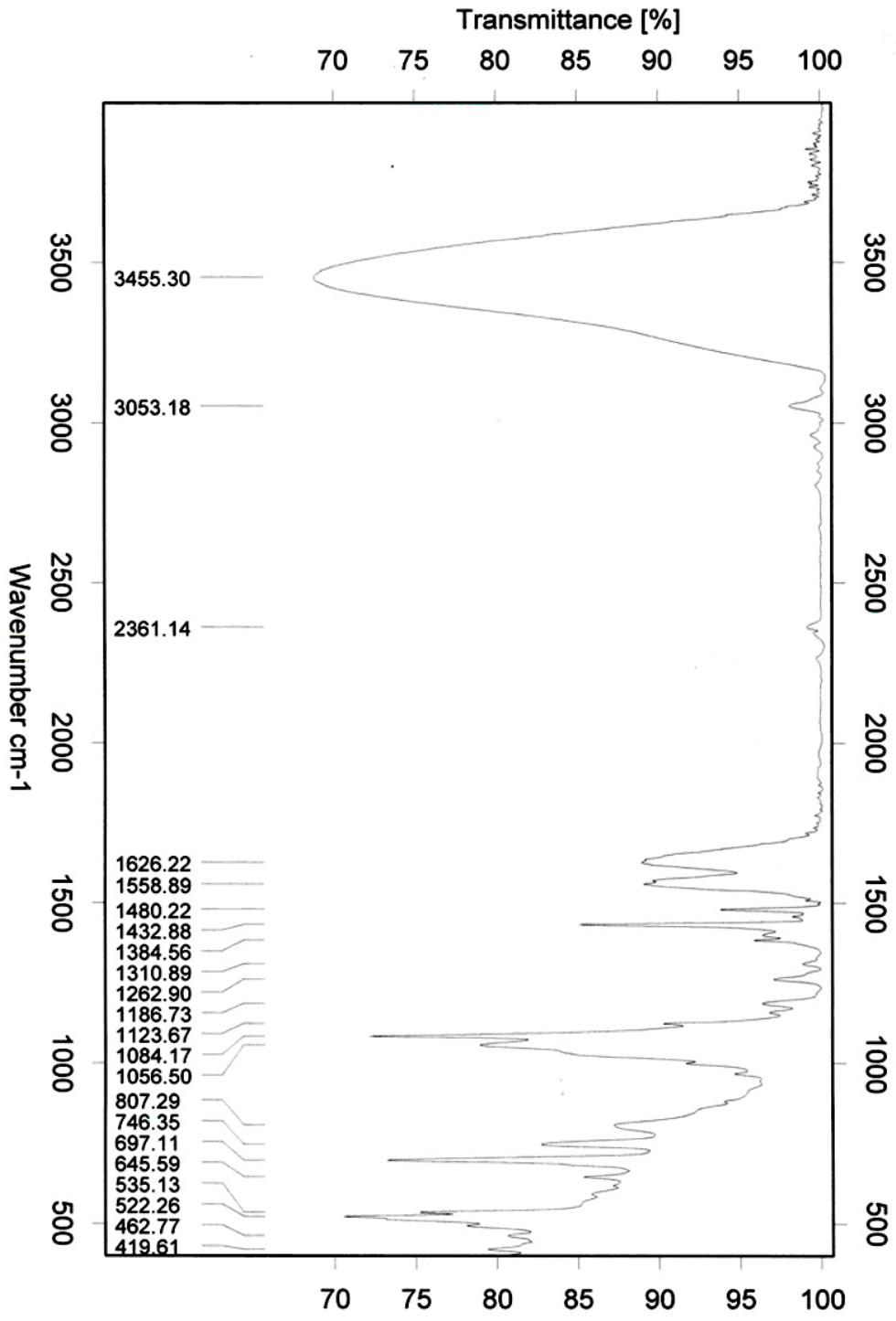

Figure 3.20 Infra-red spectrium of $[(CpNMe_2)Ru(PPh_3)_2(CH_3CN)]^+BF_4^-$ (M16)

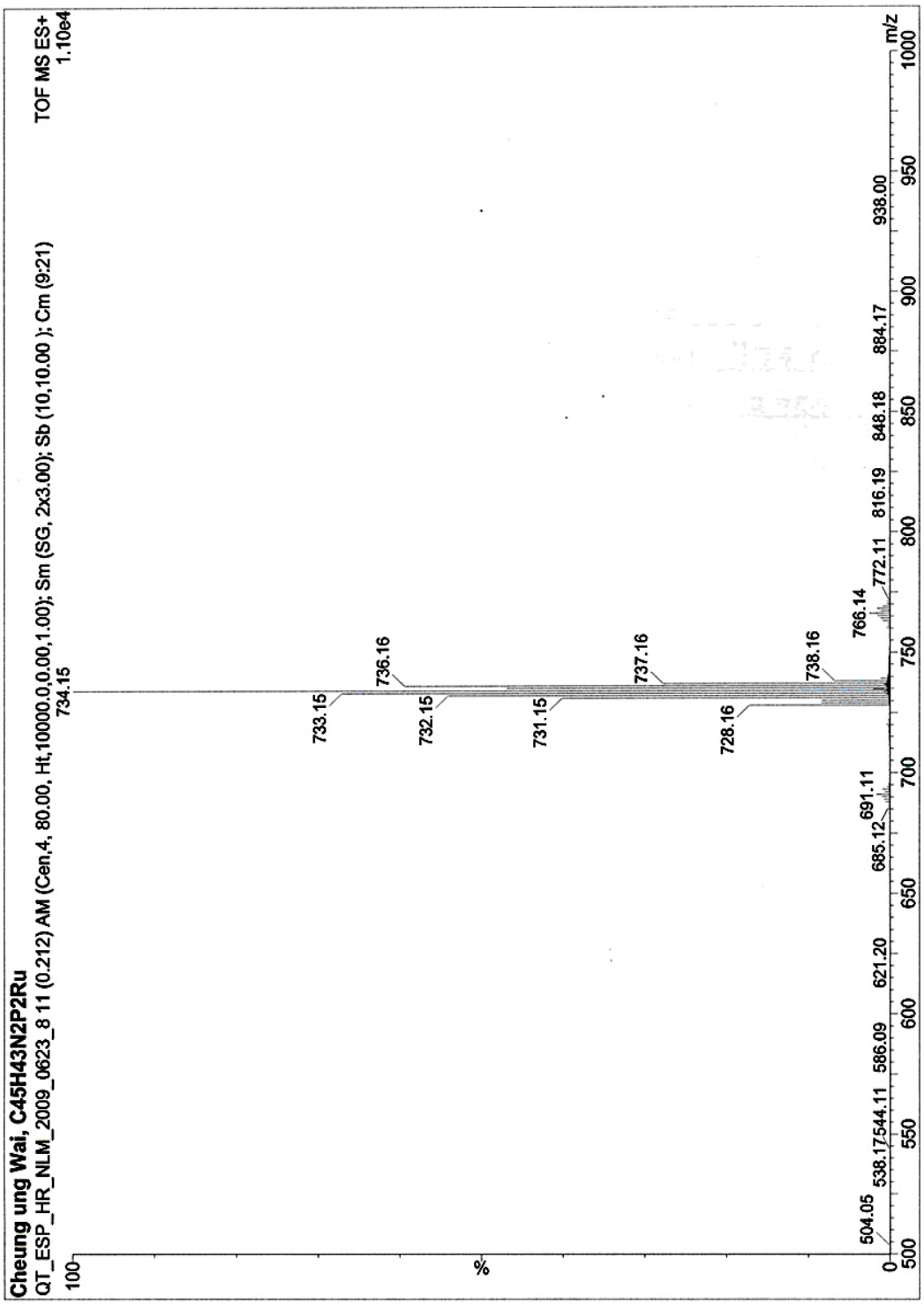

Figure 3.21 Mass spectrum of $[(CpNMe_2)Ru(PPh_3)_2(CH_3CN)]^+BF_4^-$ (M16)

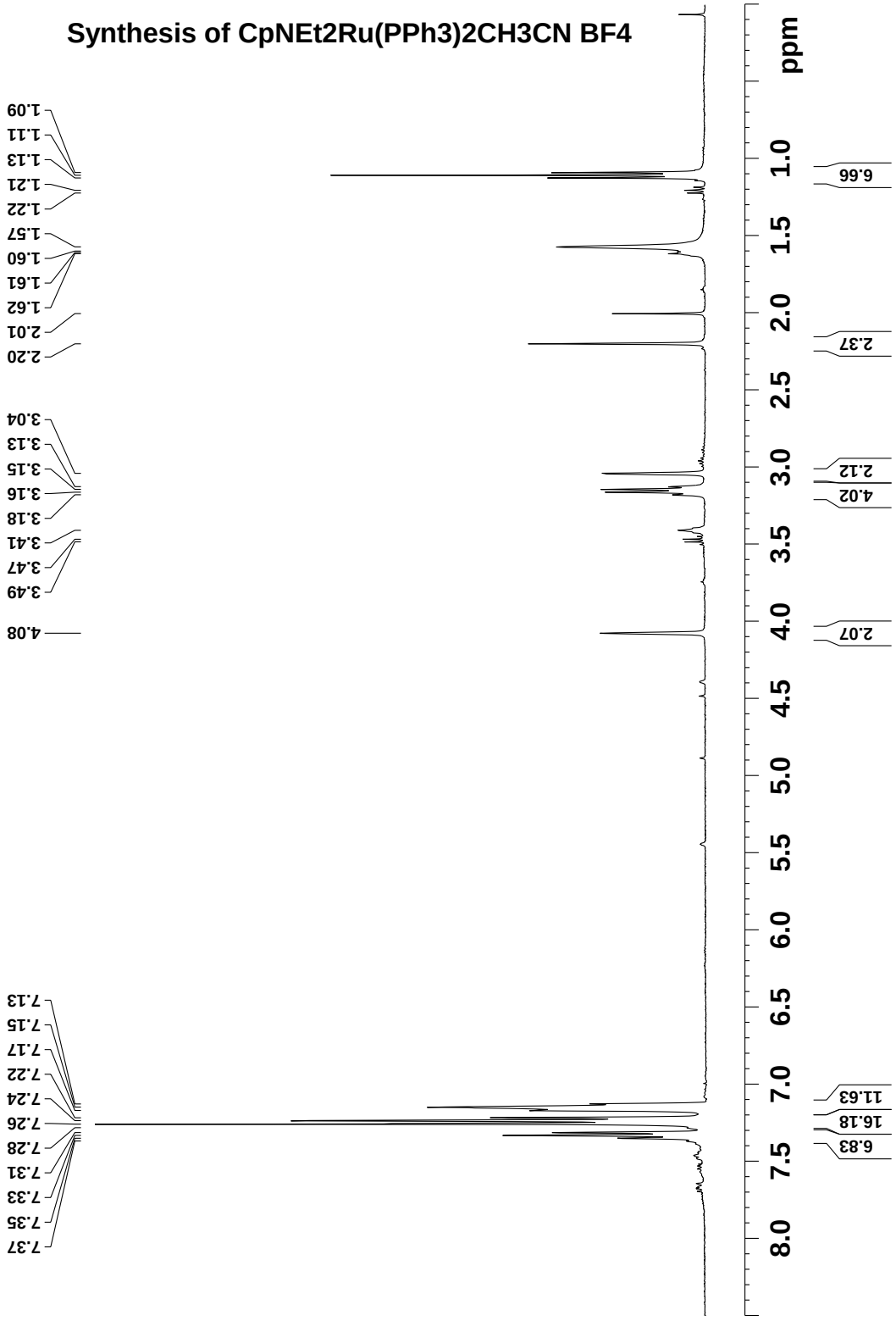

Figure 3.22 ^{1}H NMR spectrium of $[(CpNEt_2)Ru(PPh_3)_2(CH_3CN)]^+BF_4^-$ (M17)

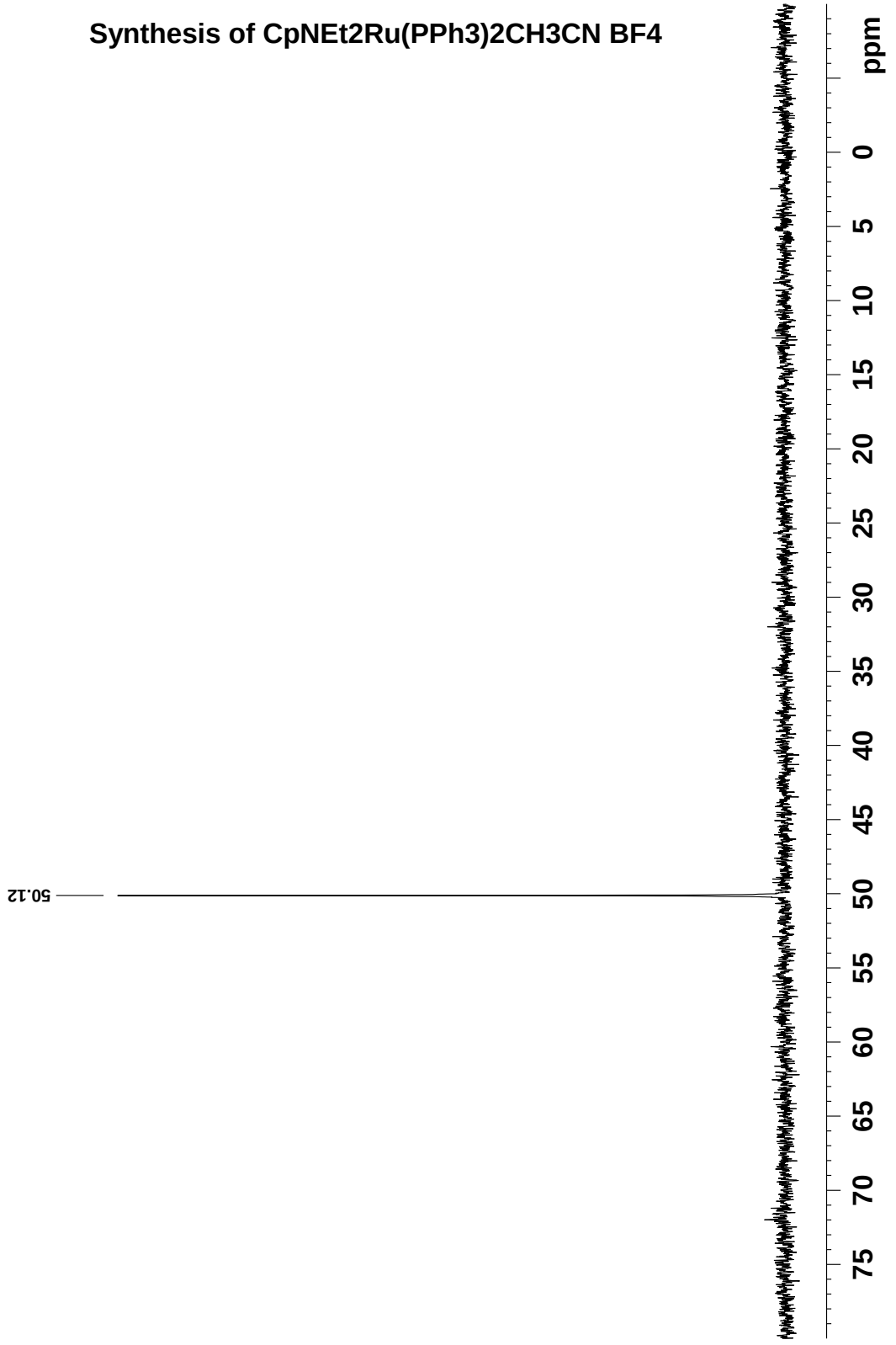

Figure 3.23 $^{31}P\{^{1}H\}$NMR spectrum of $[(CpNEt_2)Ru(PPh_3)_2(CH_3CN)]^{+}BF_4^{-}$ (M17)

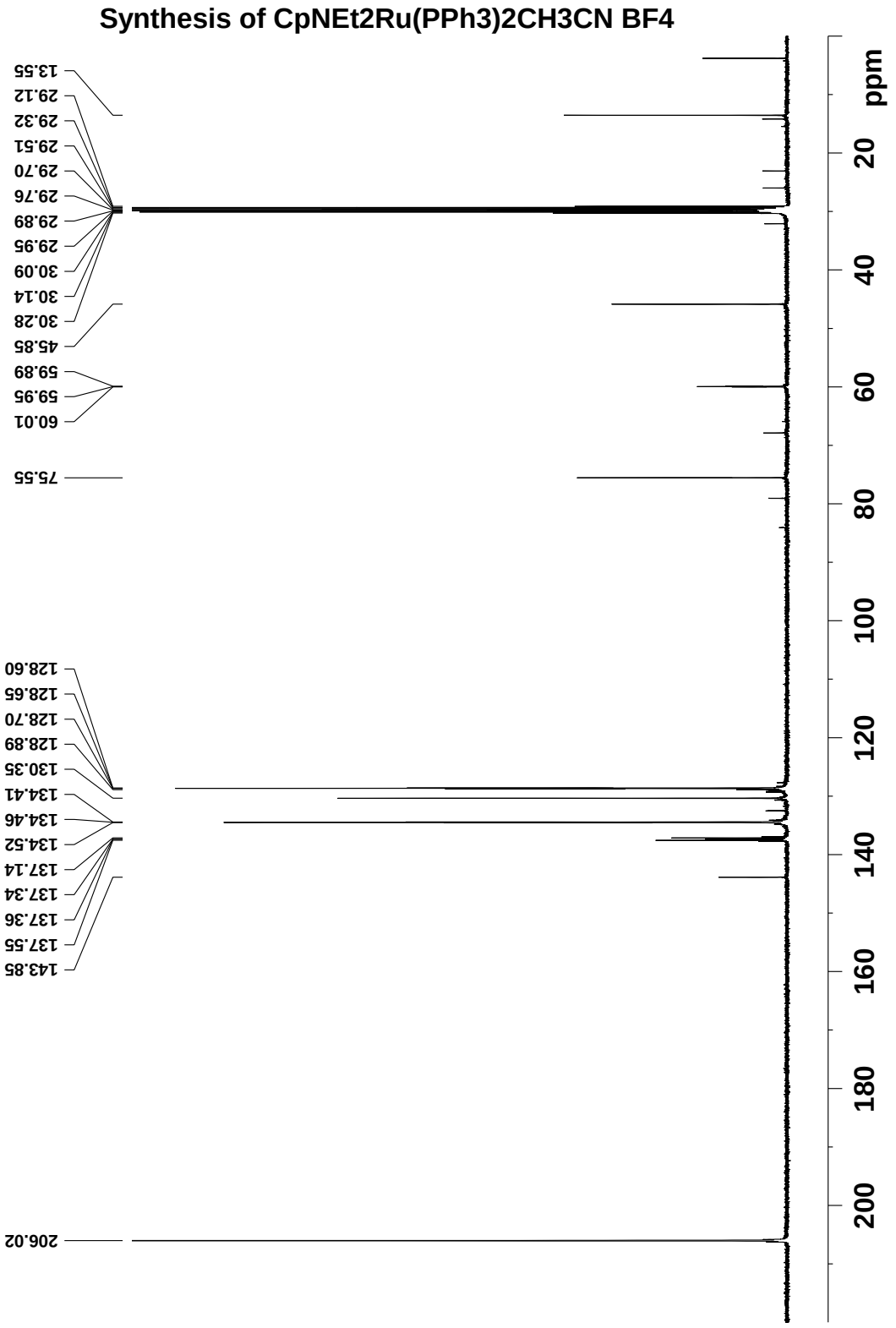

Figure 3.24 $^{13}C\{^{1}H\}$NMR spectrum of $[(CpNEt_2)Ru(PPh_3)_2(CH_3CN)]^+BF_4^-$ (M17)

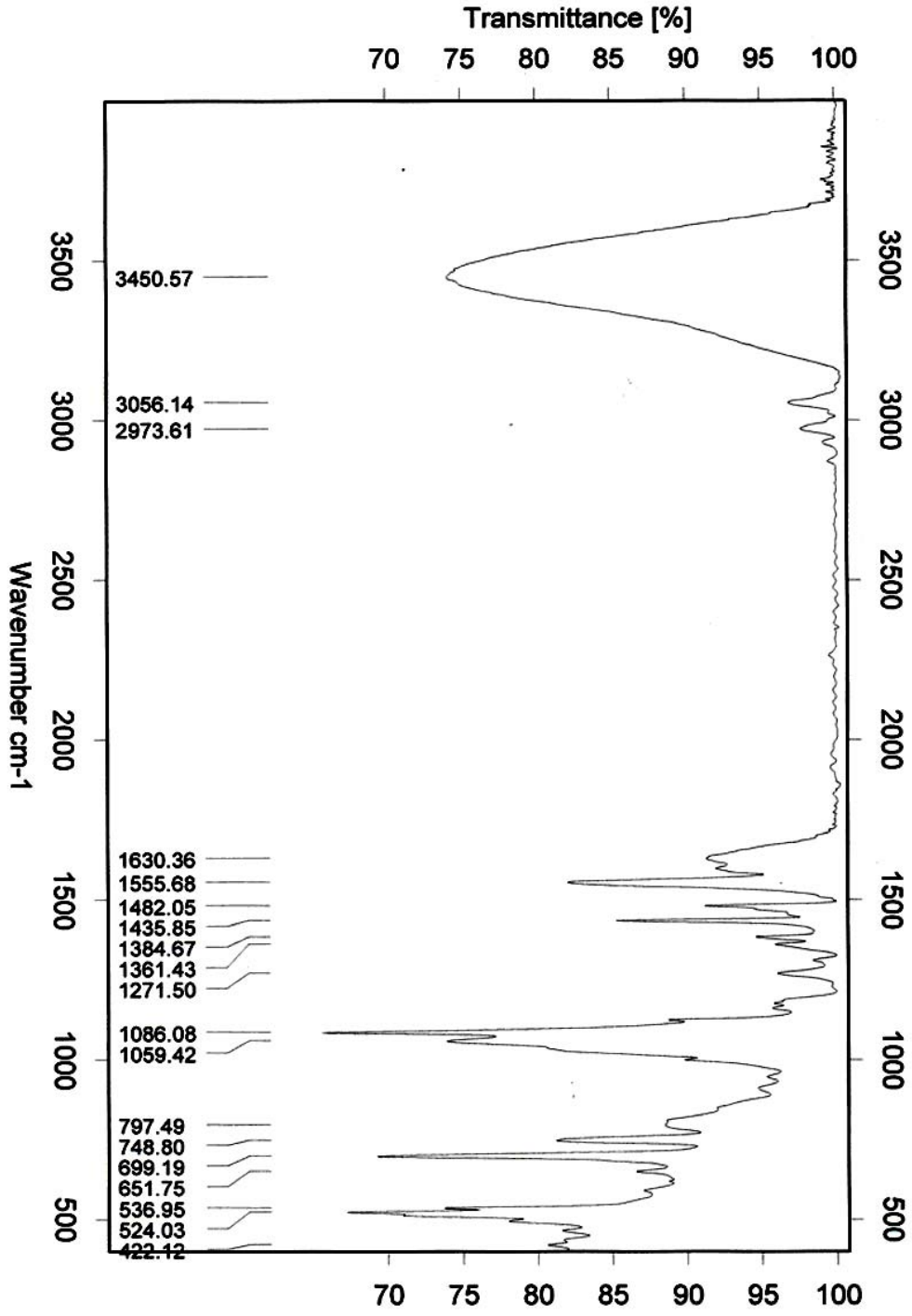

Figure 3.25 Infra-red spectrium of $[(CpNEt_2)Ru(PPh_3)_2(CH_3CN)]^+BF_4^-$ (M17)

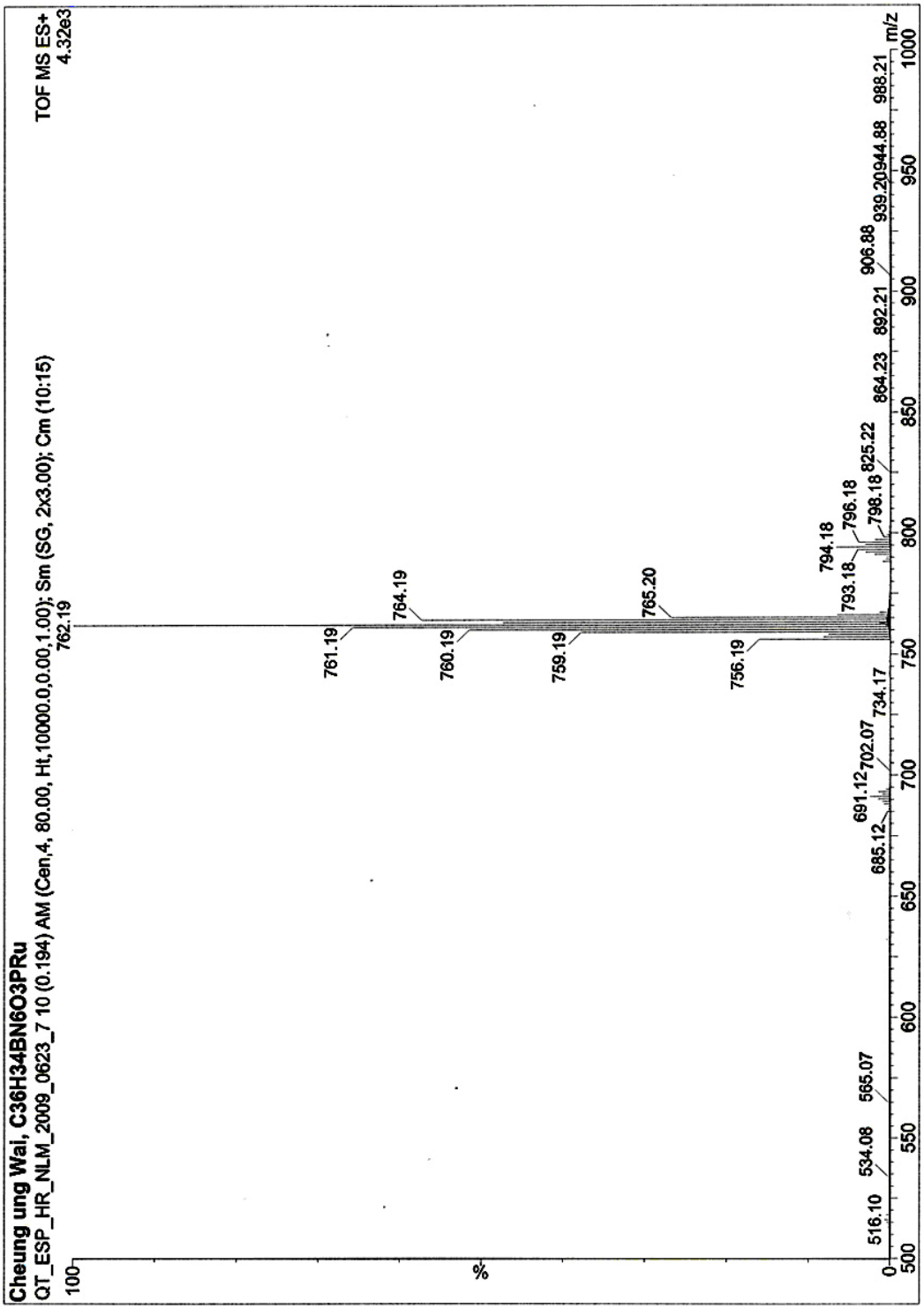

Figure 3.26 Mass spectrium of $[(CpNEt_2)Ru(PPh_3)_2(CH_3CN)]^+BF_4^-$ (M17)

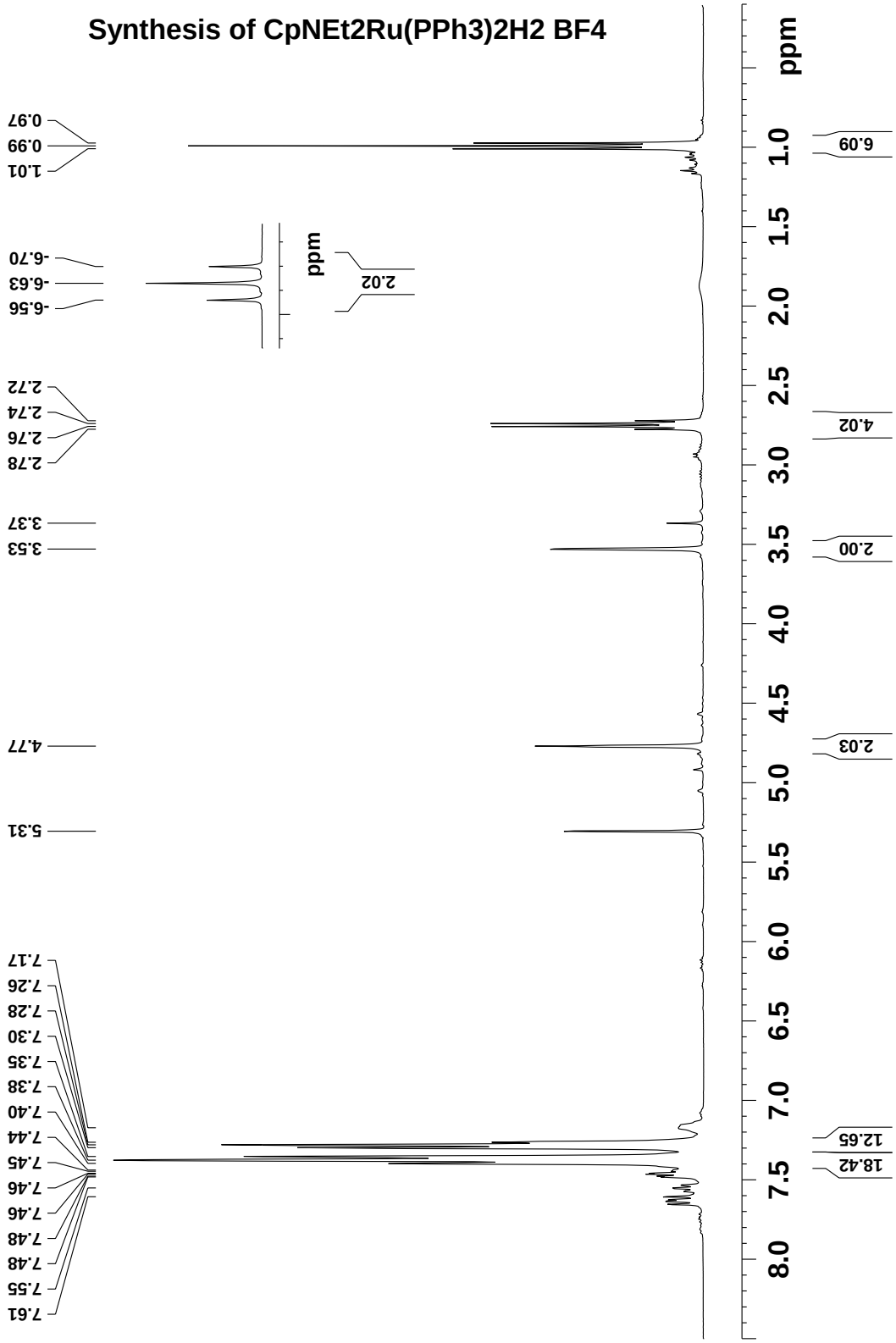

Figure 3.27 ^{1}H NMR spectrium of $[(CpNMe_2)Ru(PPh_3)_2H_2]^+BF_4^-$ (M19)

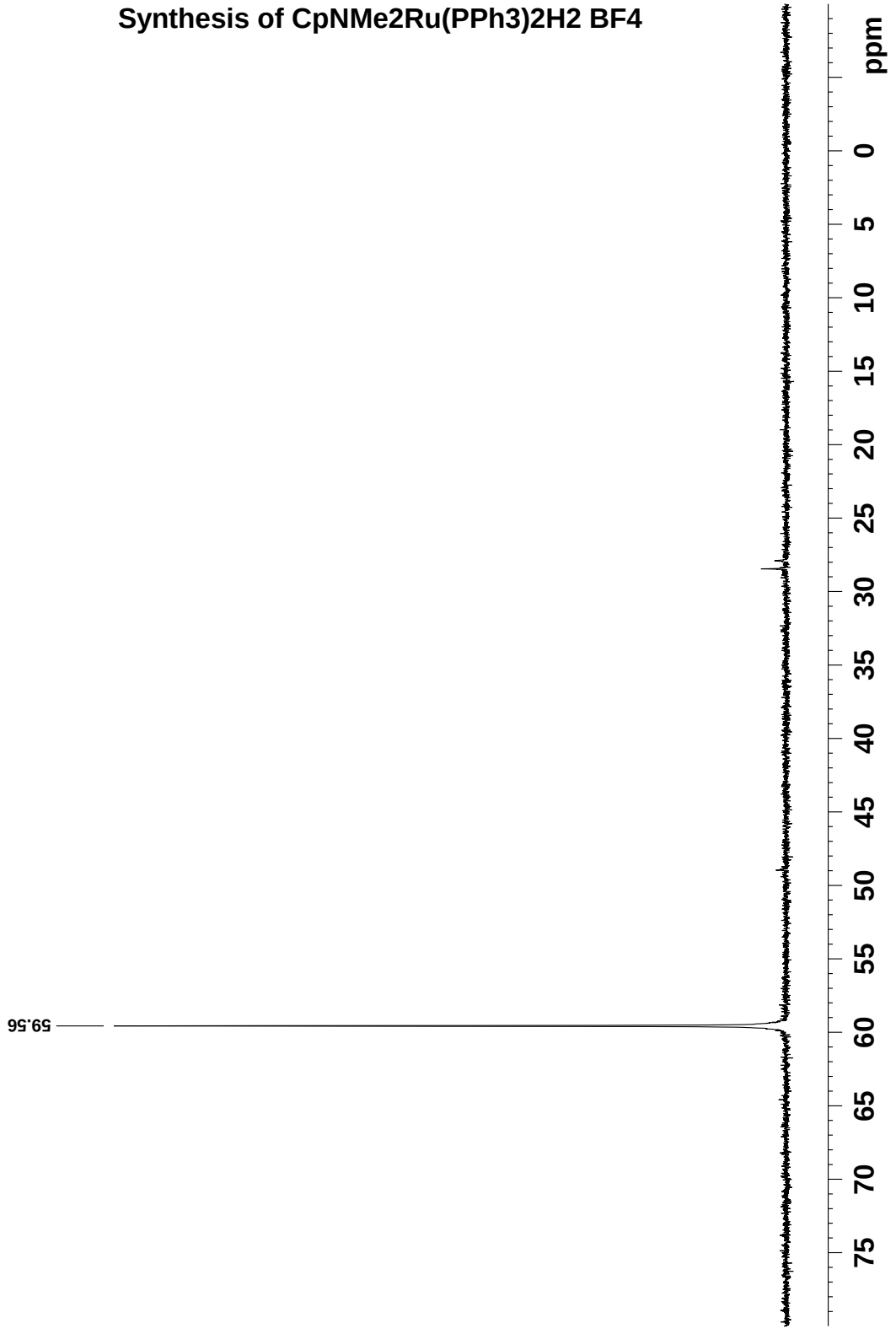

Figure 3.28 $^{31}P\{^{1}H\}$NMR spectrium of $[(CpNMe_2)Ru(PPh_3)_2H_2]^+BF_4^-$ (M19)

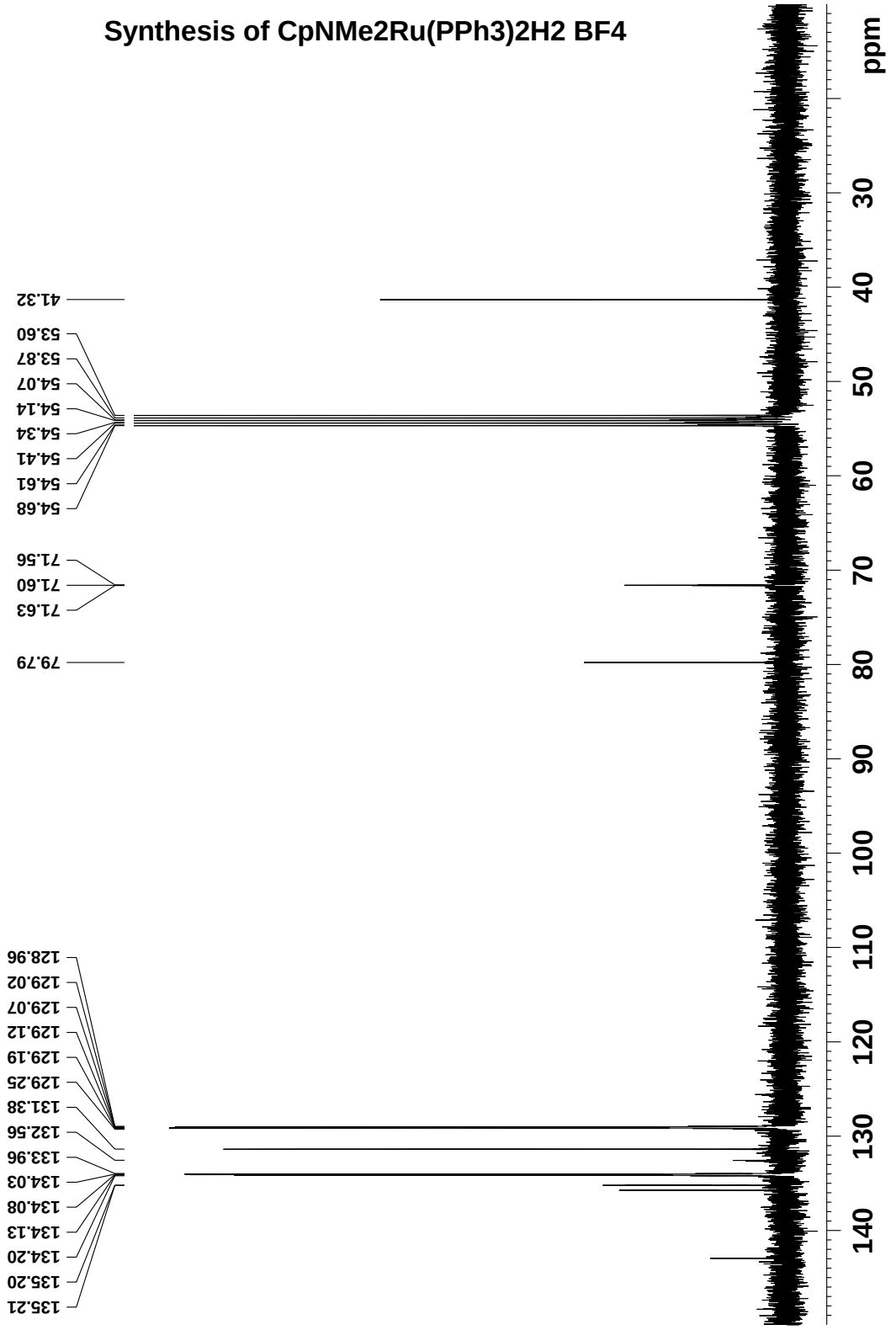

Figure 3.29 $^{13}C\{^{1}H\}$NMR spectrium of $[(CpNMe_2)Ru(PPh_3)_2H_2]^+BF_4^-$ (M19)

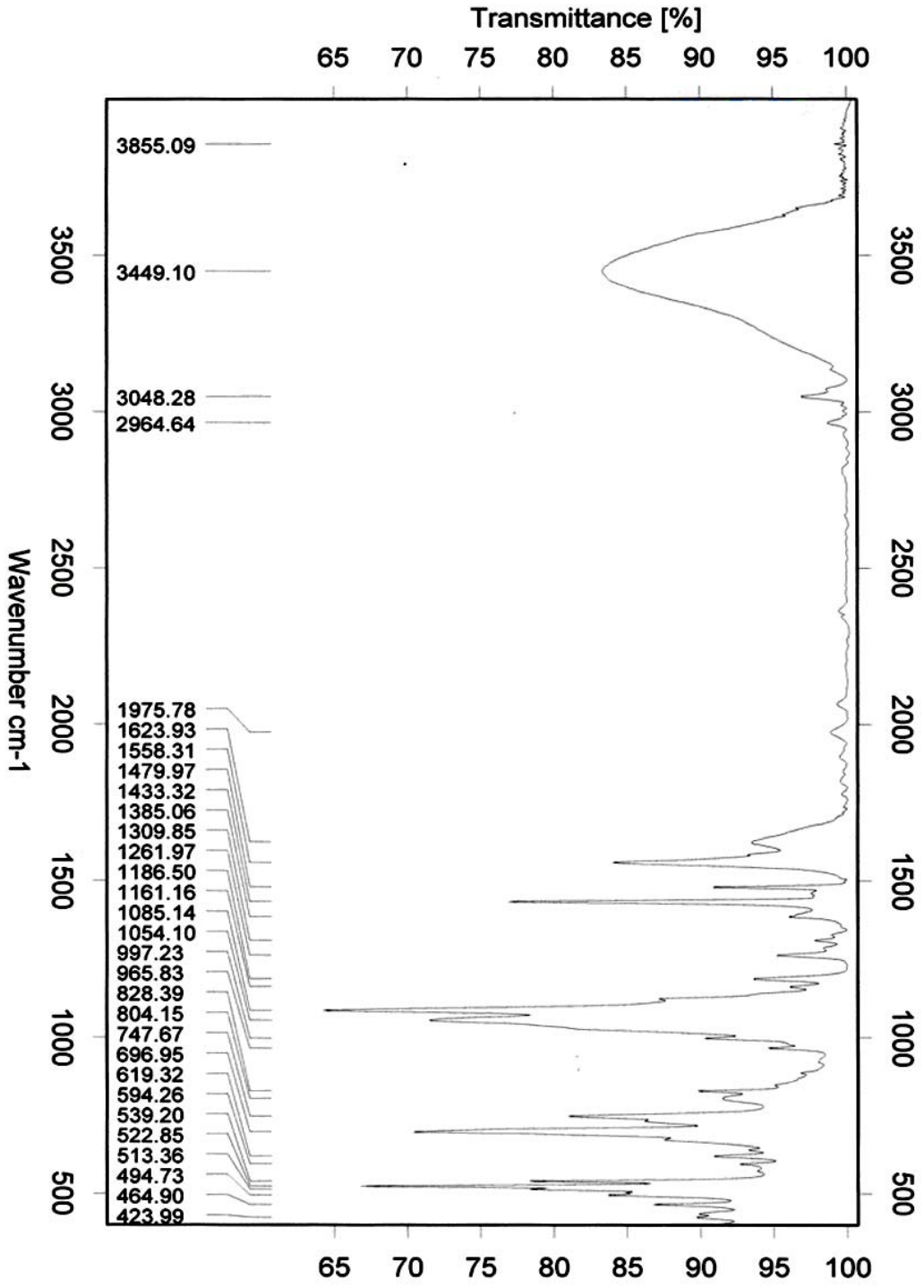

Figure 3.30 Infra-red spectrium of $[(CpNMe_2)Ru(PPh_3)_2H_2]^+BF_4^-$ (M19)

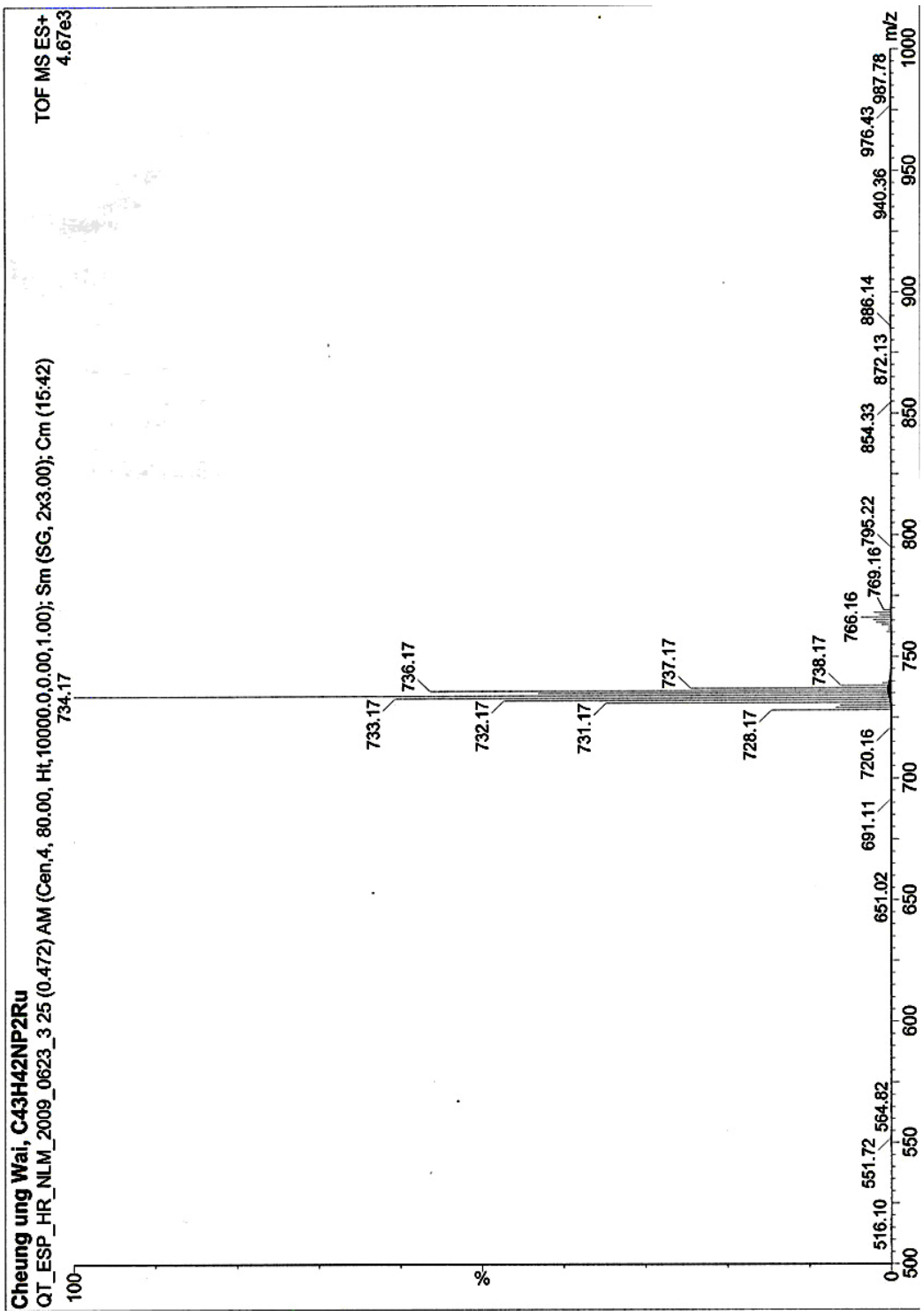

Figure 3.31 Mass spectrium of $[(CpNMe_2)Ru(PPh_3)_2H_2]^+BF_4^-$ (M19)

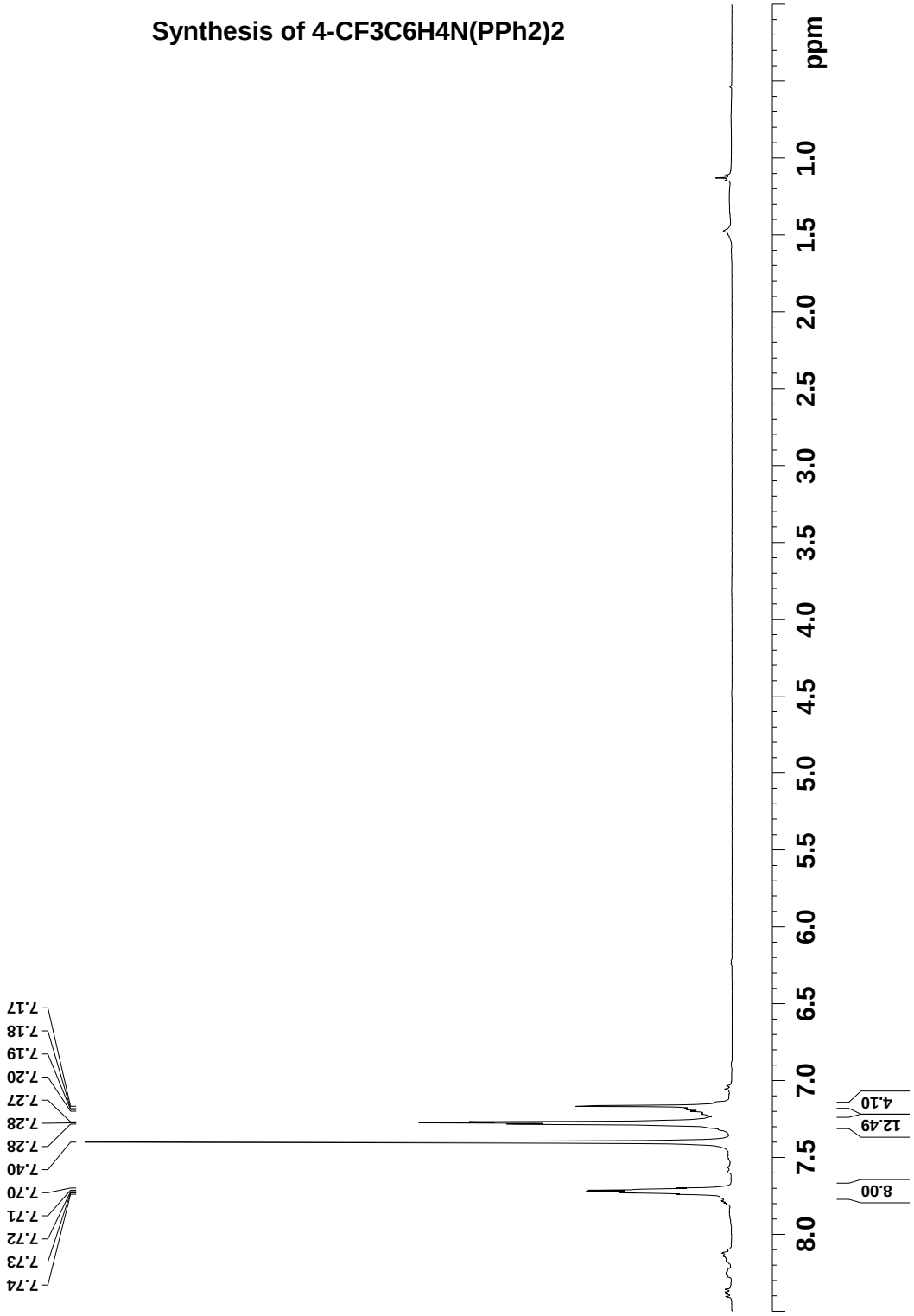

Figure 4.13 ^{1}H NMR spectrium of 4-$CF_3C_6H_4N(PPh_2)_2$

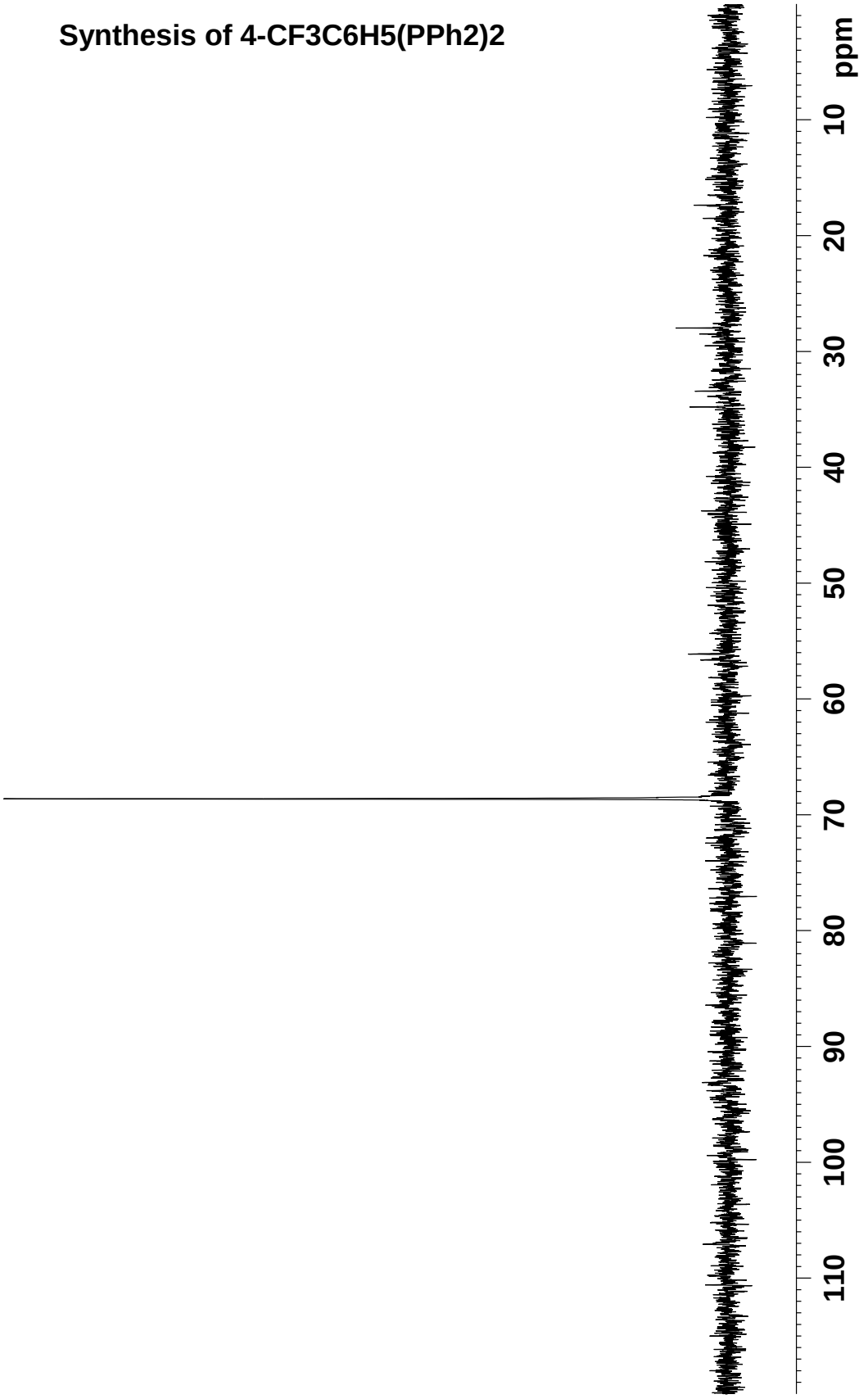

Figure 4.14 $^{31}P\{^{1}H\}$NMR spectrium of 4-$CF_3C_6H_4N(PPh_2)_2$

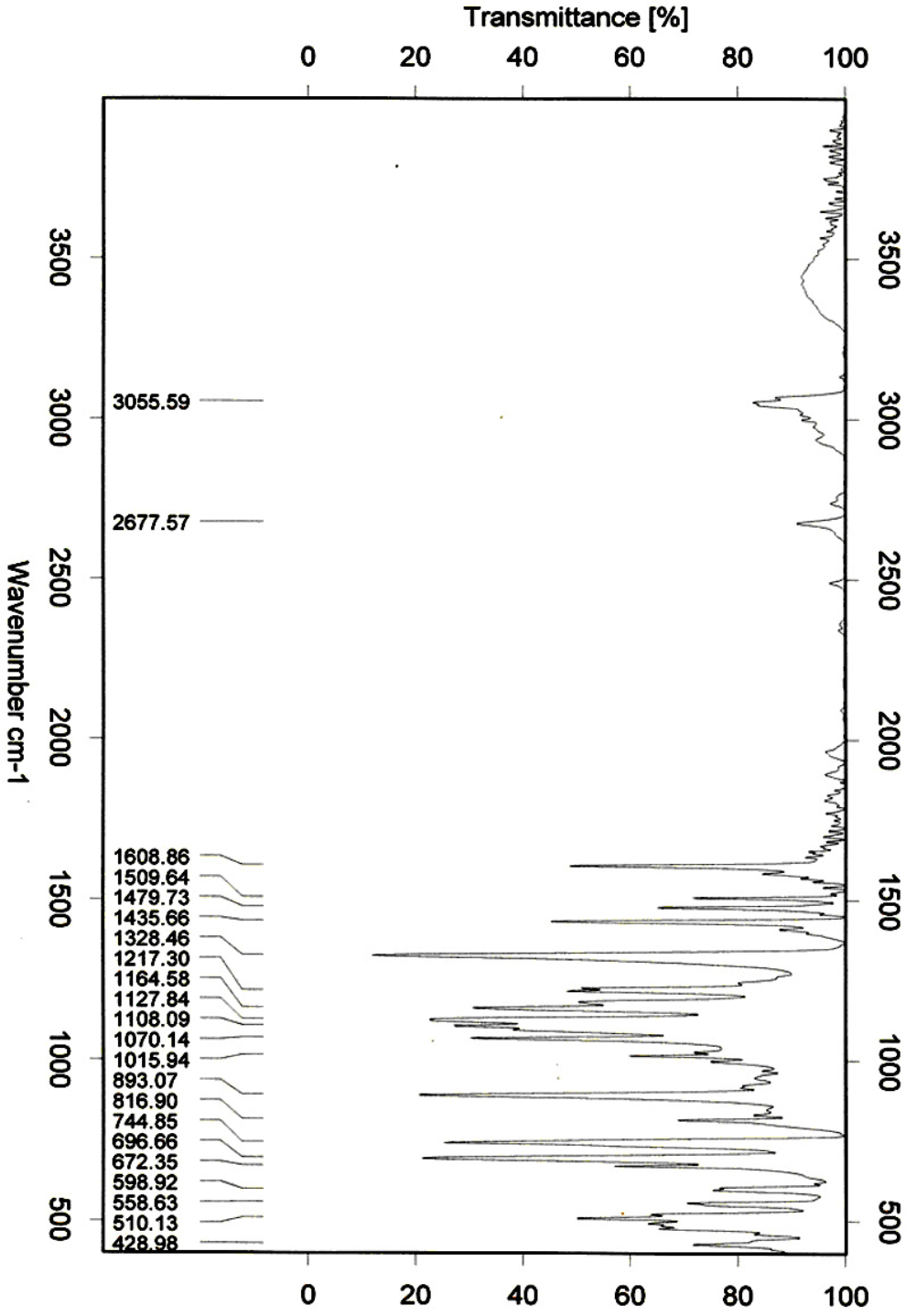

Figure 4.15 Infra-red spectrium of 4-$CF_3C_6H_4N(PPh_2)_2$

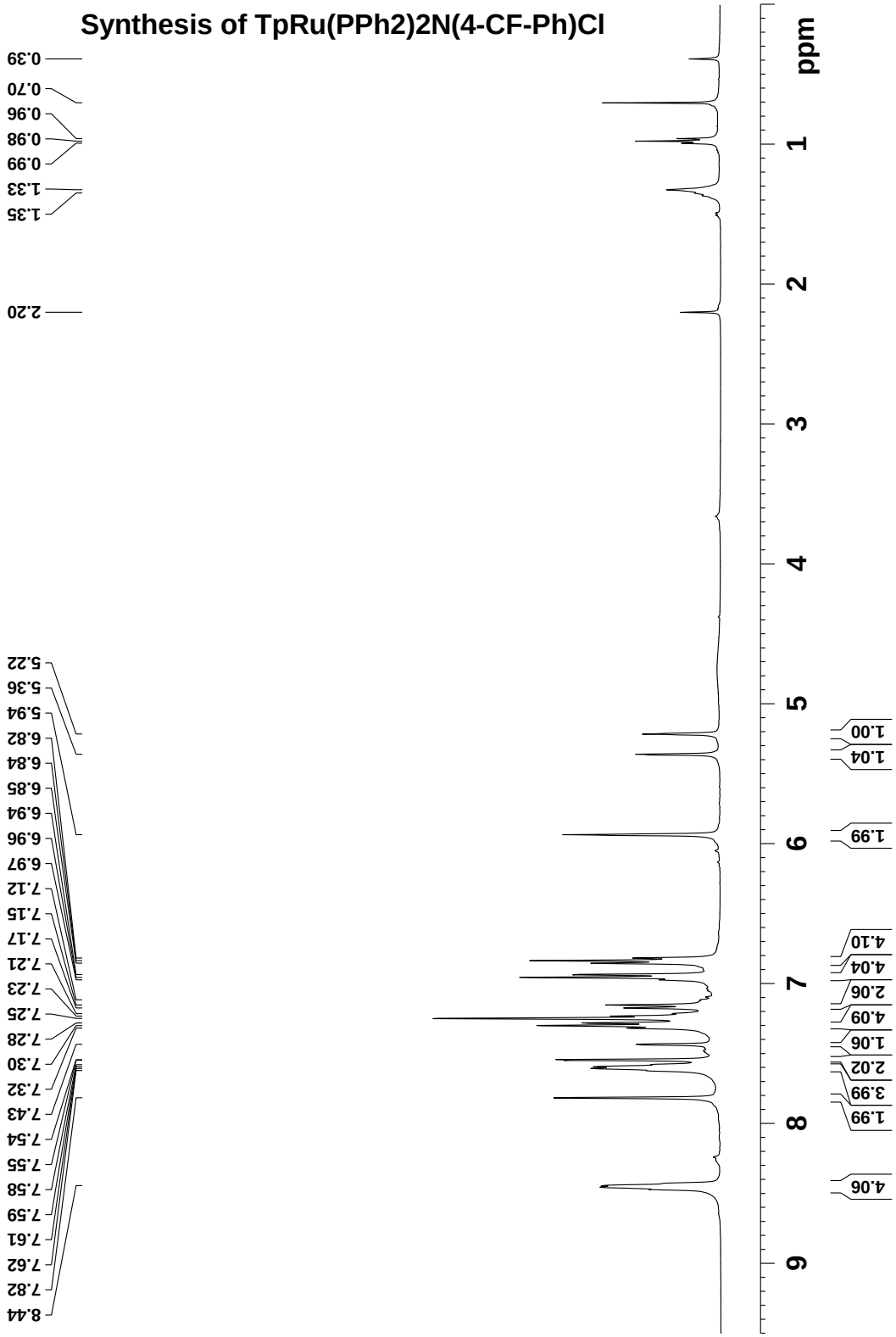

Figure 4.16 ^{1}H NMR spectrium of TpRu(4-$CF_3C_6H_4N(PPh_3)_2$)Cl (M21)

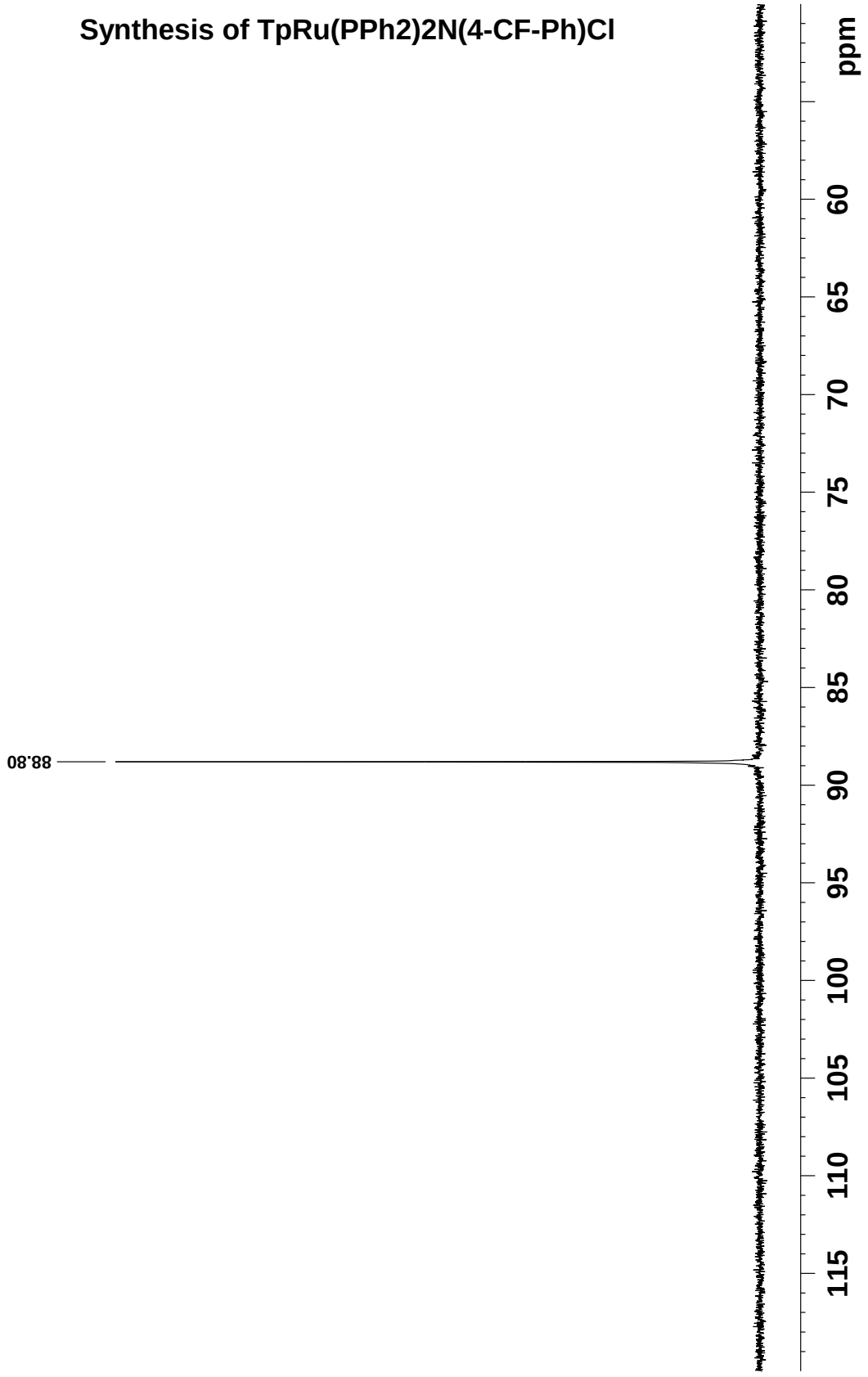

Figure 4.17 $^{31}P\{^{1}H\}$NMR spectrium of TpRu(4-$CF_3C_6H_4N(PPh_3)_2$)Cl (M21)

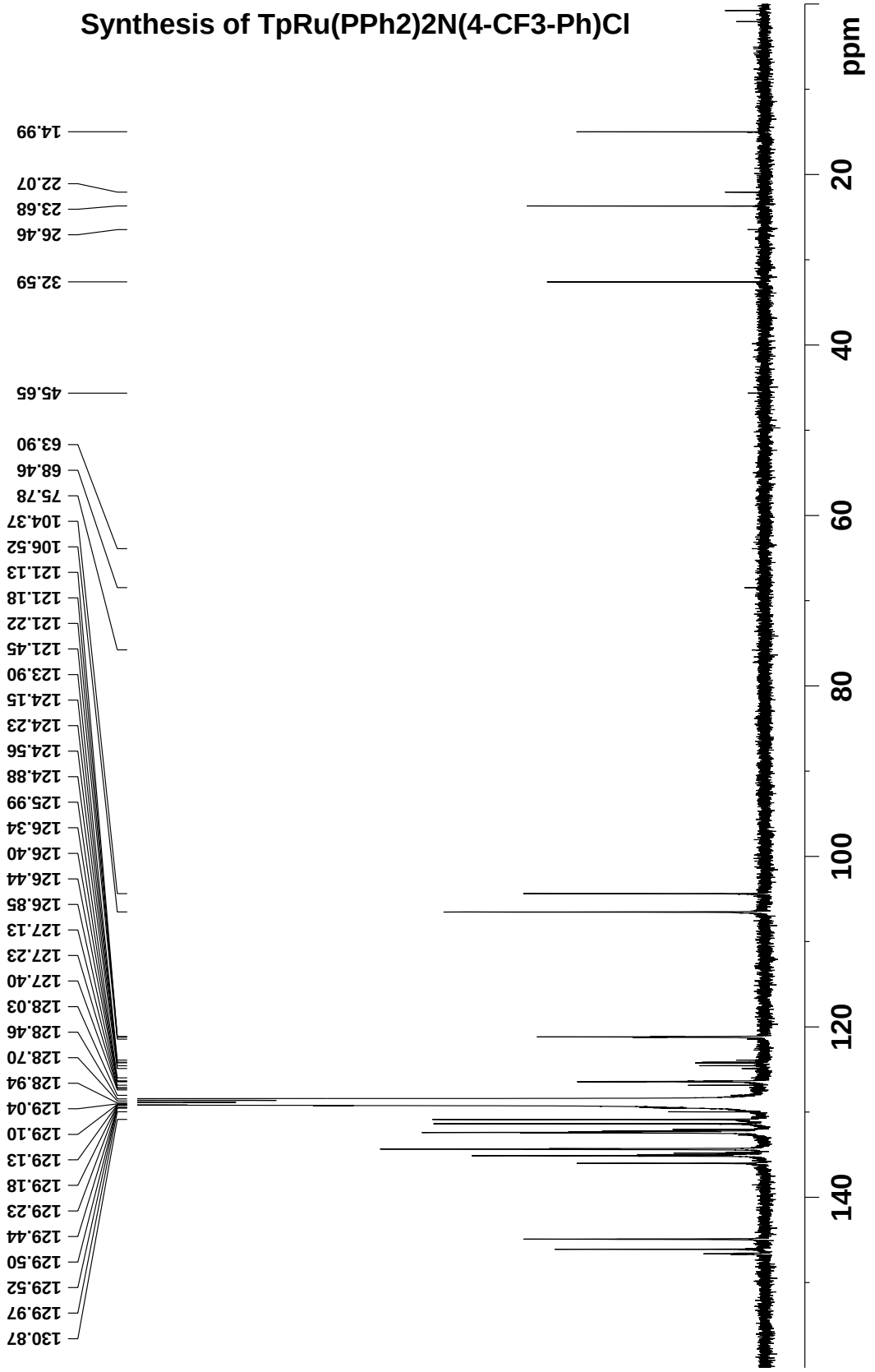

Figure 4.18 $^{13}C\{^{1}H\}$NMR spectrium of TpRu(4-$CF_3C_6H_4N(PPh_3)_2$)Cl (M21)

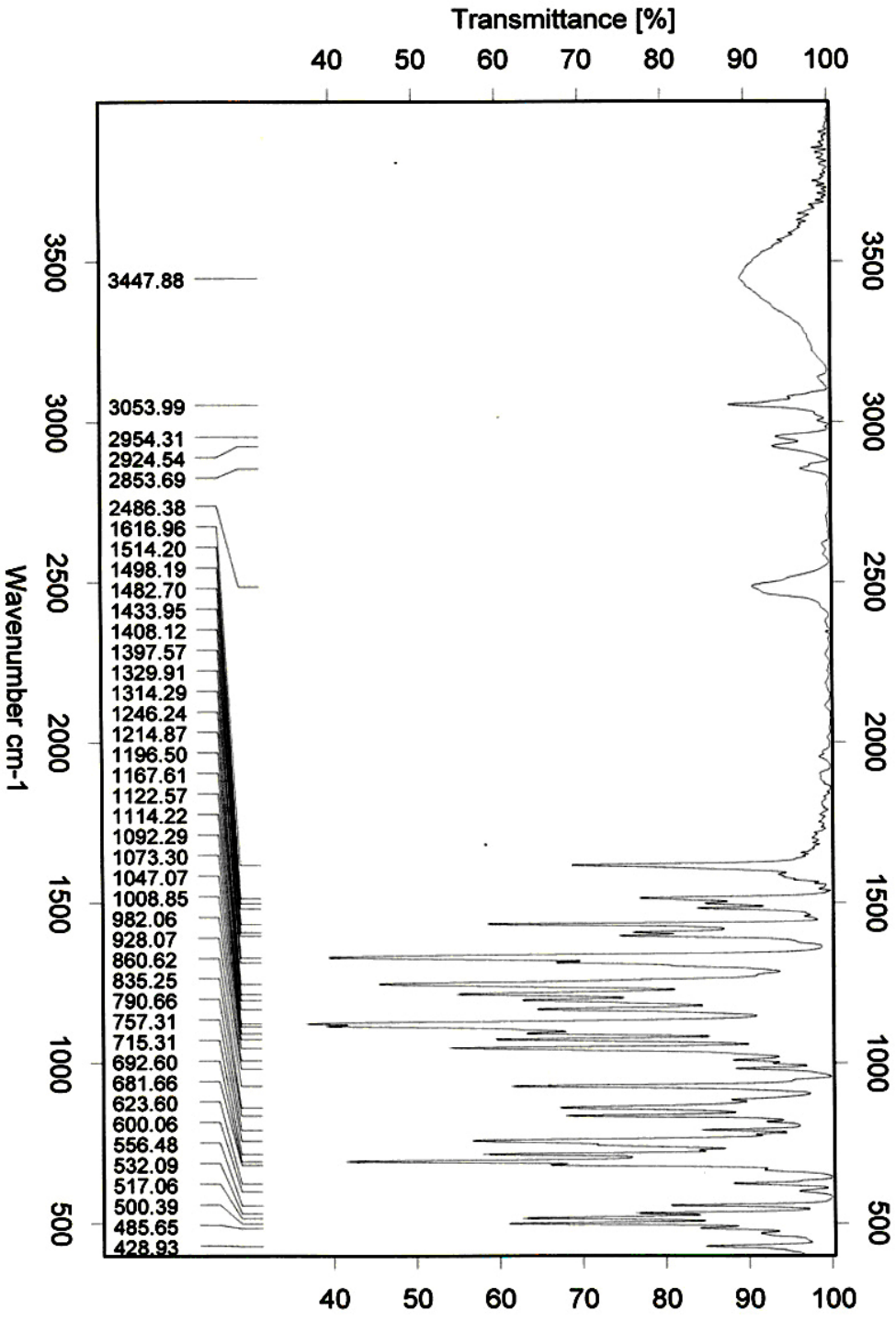

Figure 4.19 Infra-red spectrium of TpRu(4-$CF_3C_6H_4N(PPh_3)_2$)Cl (M21)

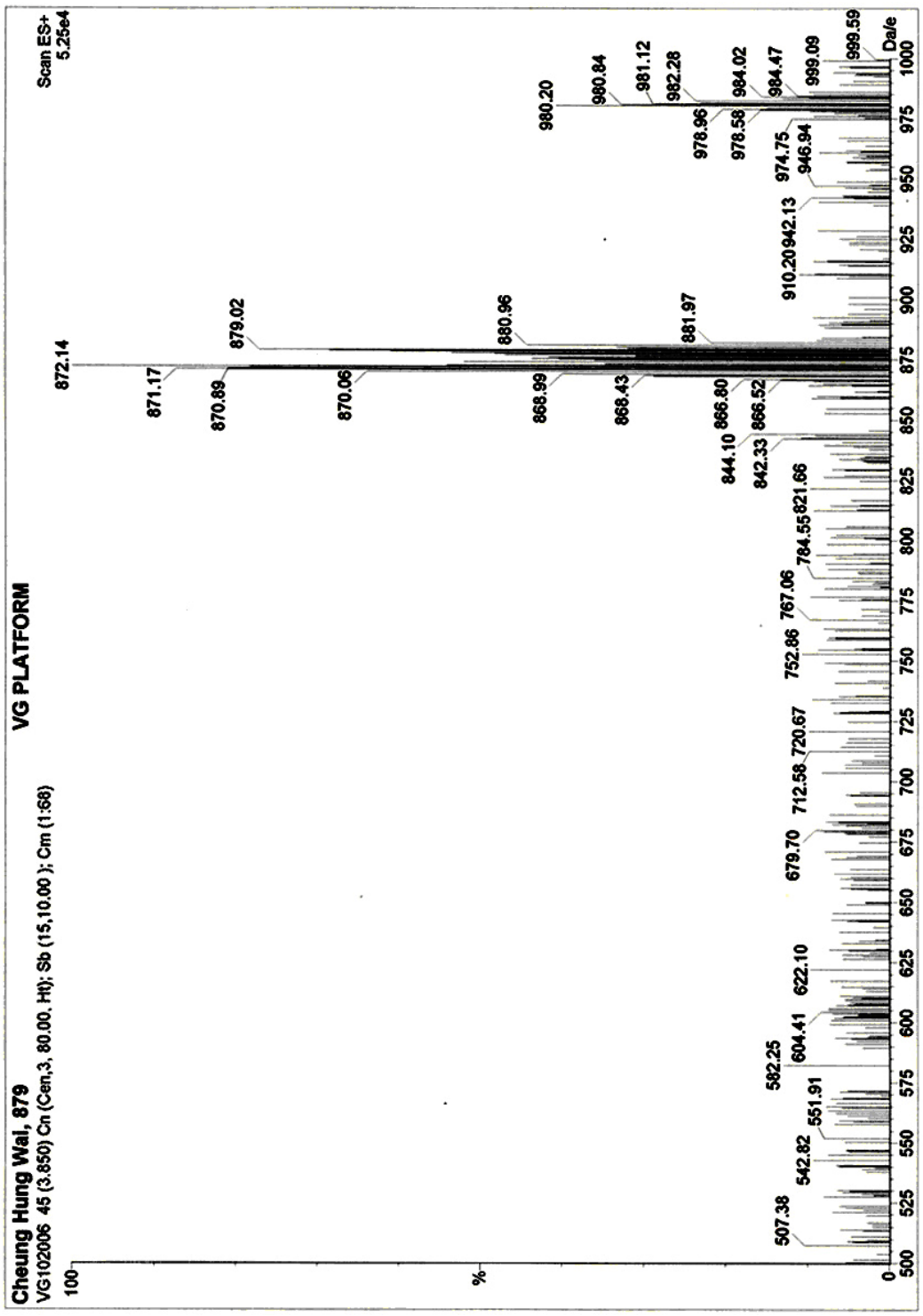

Figure 4.20 Mass spectrum of TpRu(4-$CF_3C_6H_4N(PPh_3)_2$)Cl (M21)

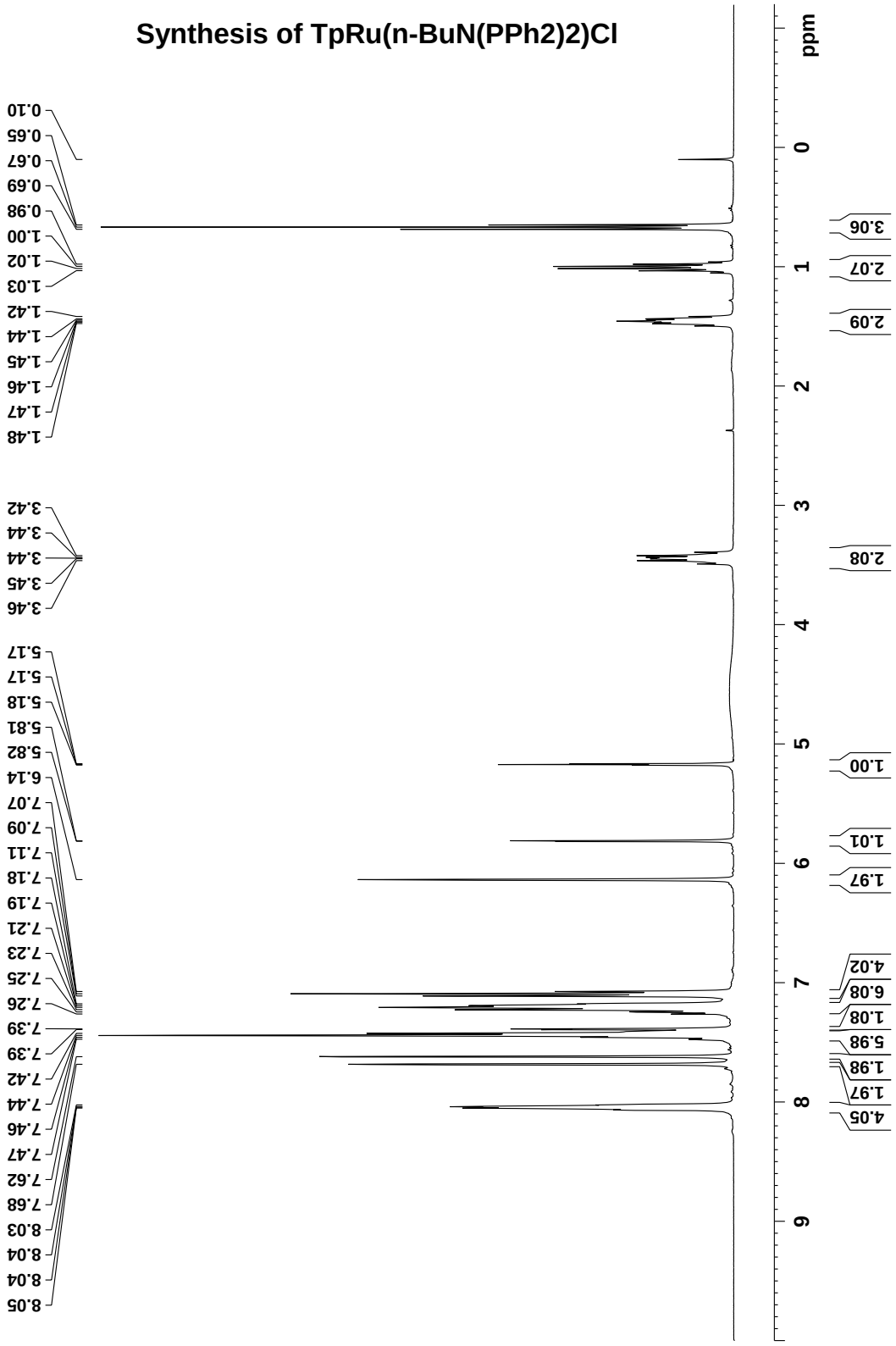

Figure 4.21 ^{1}H NMR spectrium of TpRu(^{n}BuN(PPh$_2$)$_2$)Cl (M22)

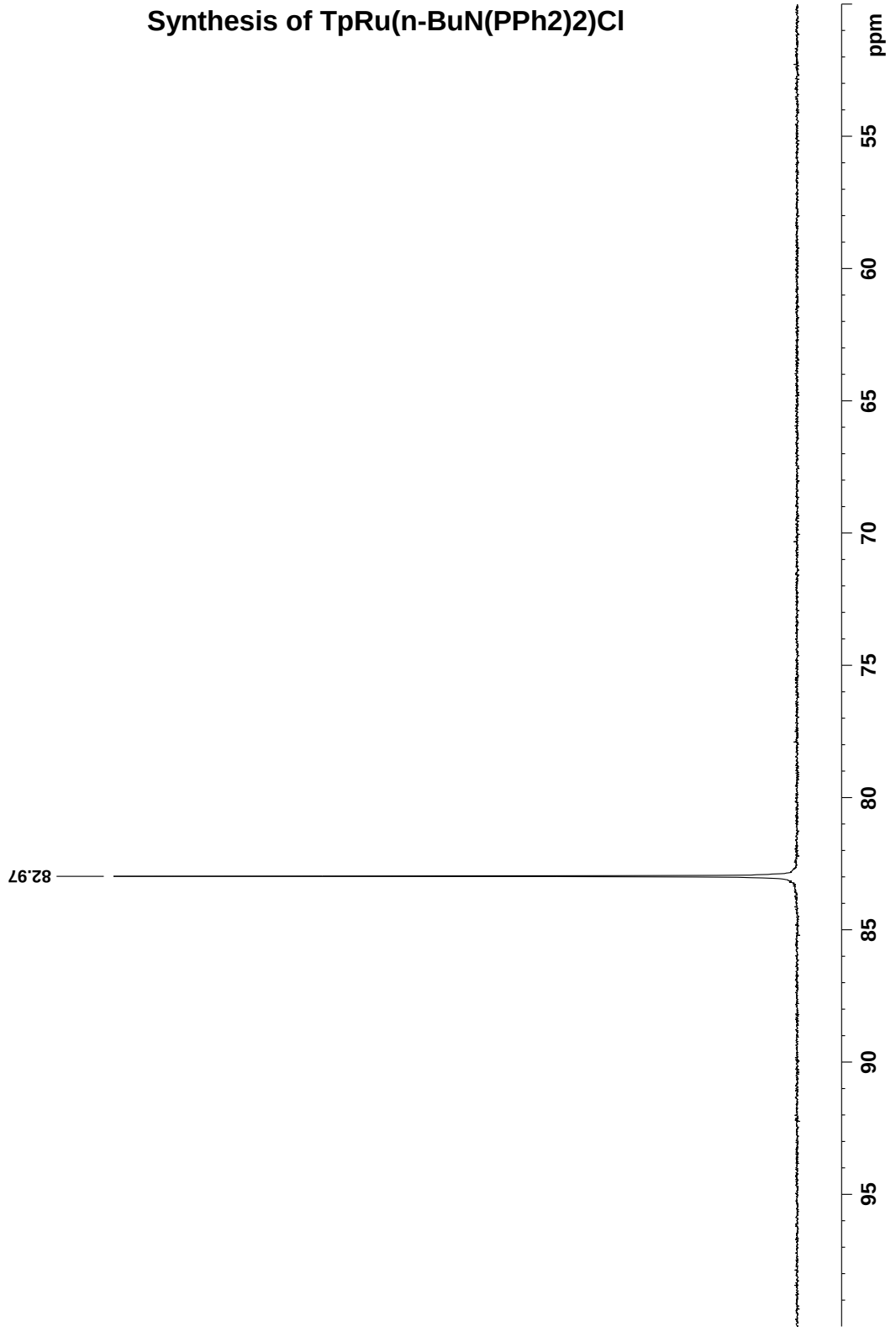

Figure 4.22 $^{31}P\{^{1}H\}$NMR spectrium of TpRu(^{n}BuN(PPh_2)$_2$)Cl (M22)

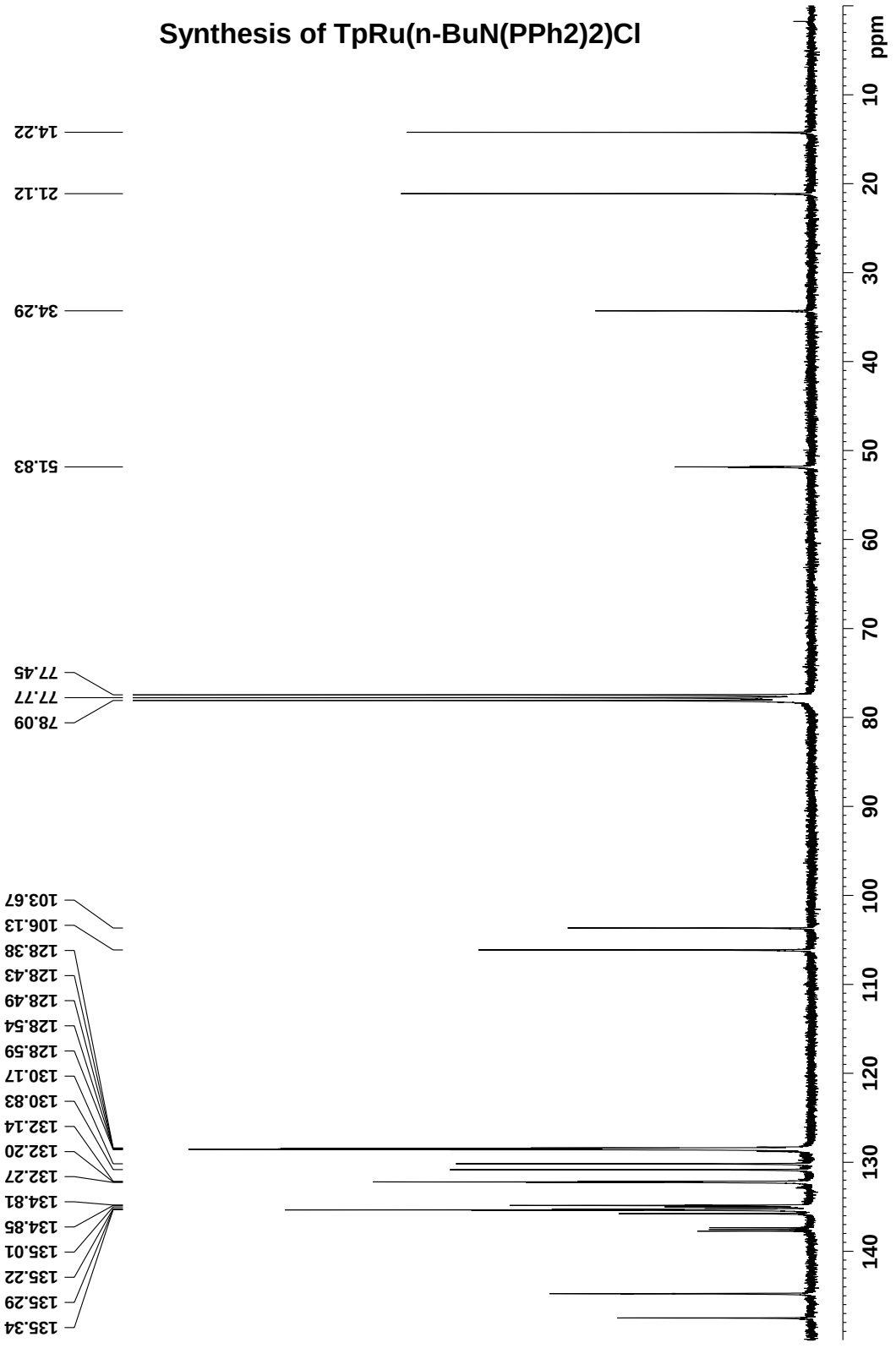

Figure 4.23 $^{13}C\{^{1}H\}$NMR spectrium of TpRu(^{n}BuN(PPh$_2$)$_2$)Cl (M22)

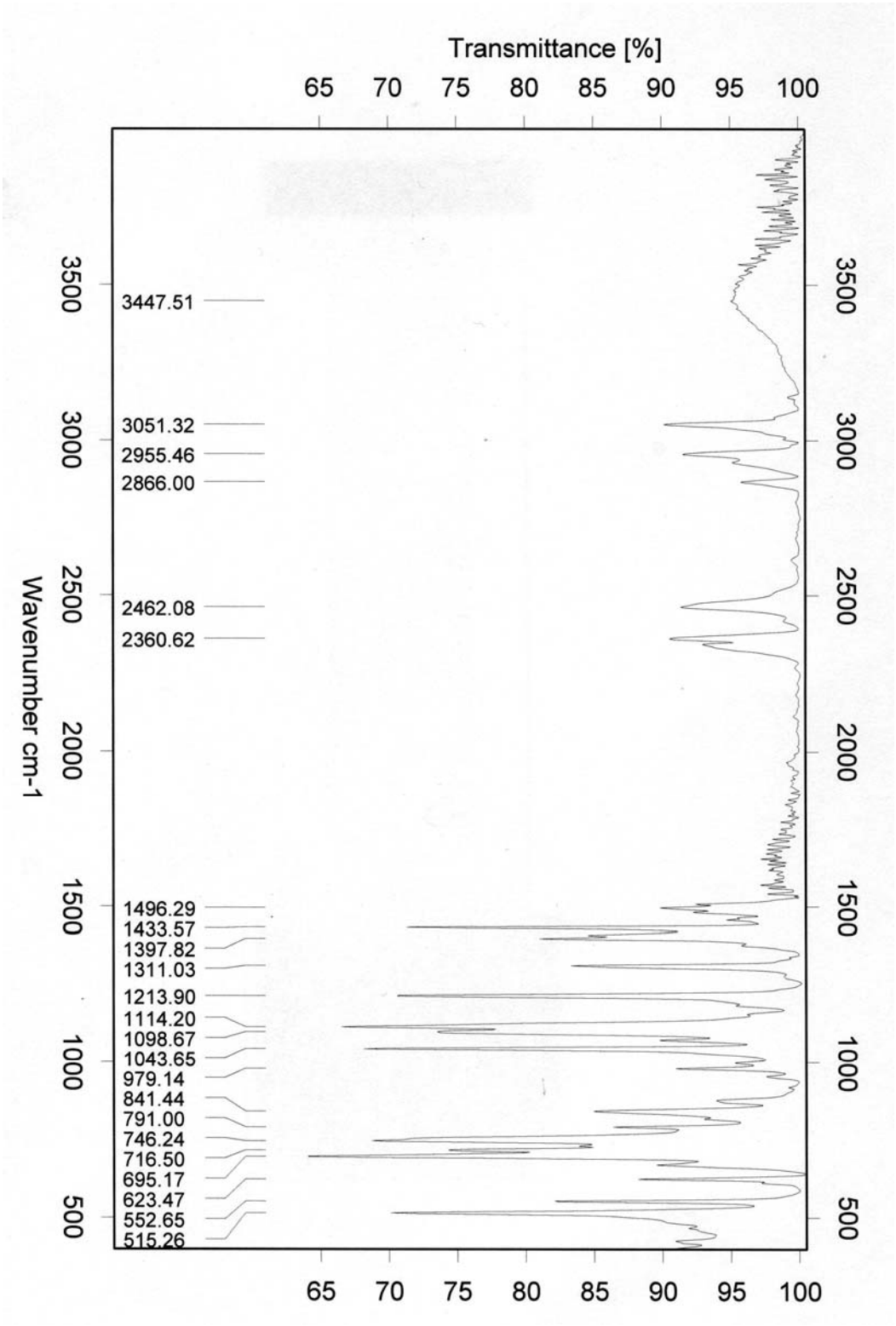

Figure 4.24 Infra-red spectrium of TpRu(^{n}BuN(PPh$_2$)$_2$)Cl (M22)

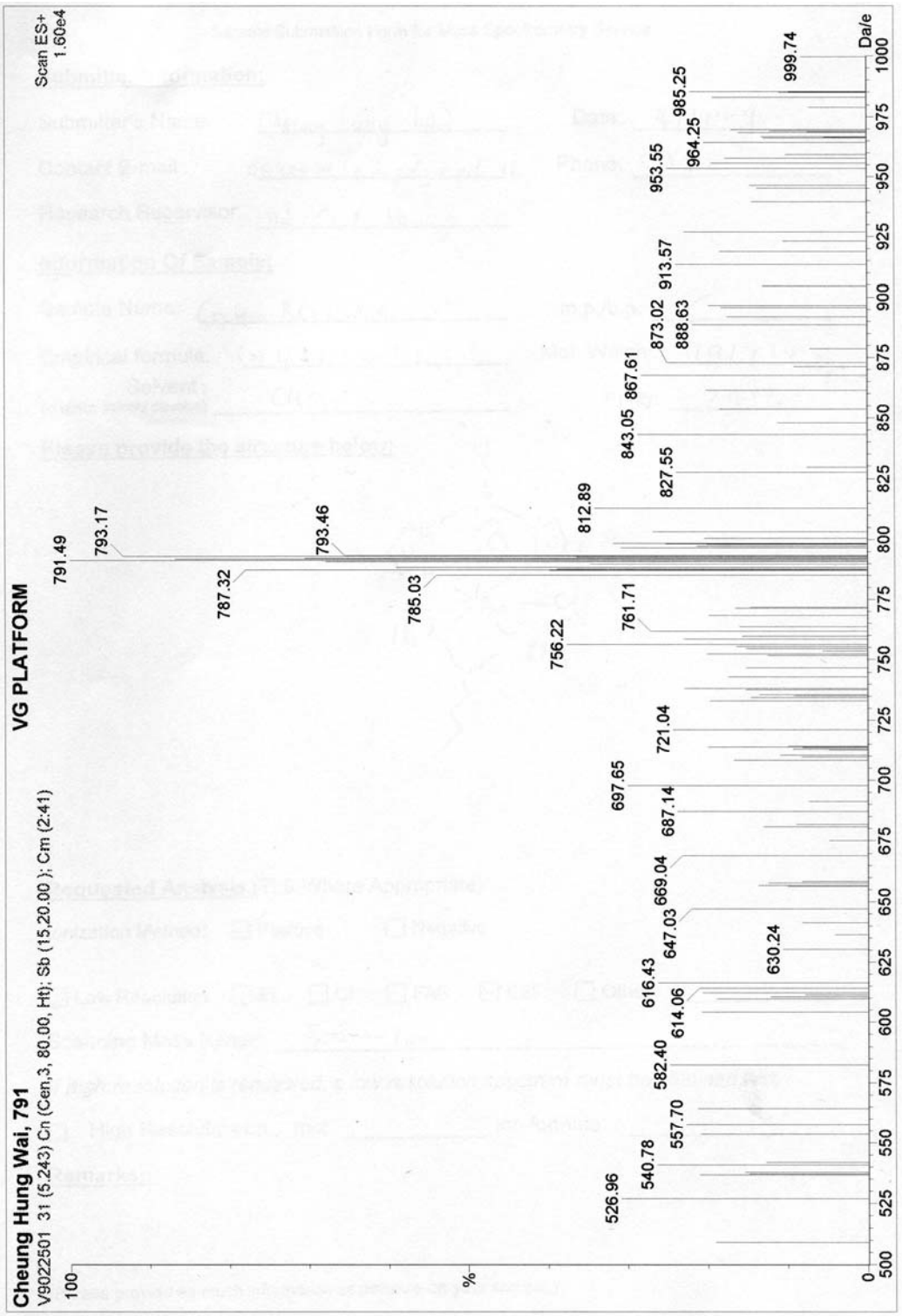

Figure 4.25 Mass spectrium of TpRu(^{n}BuN(PPh$_2$)$_2$)Cl (M22)

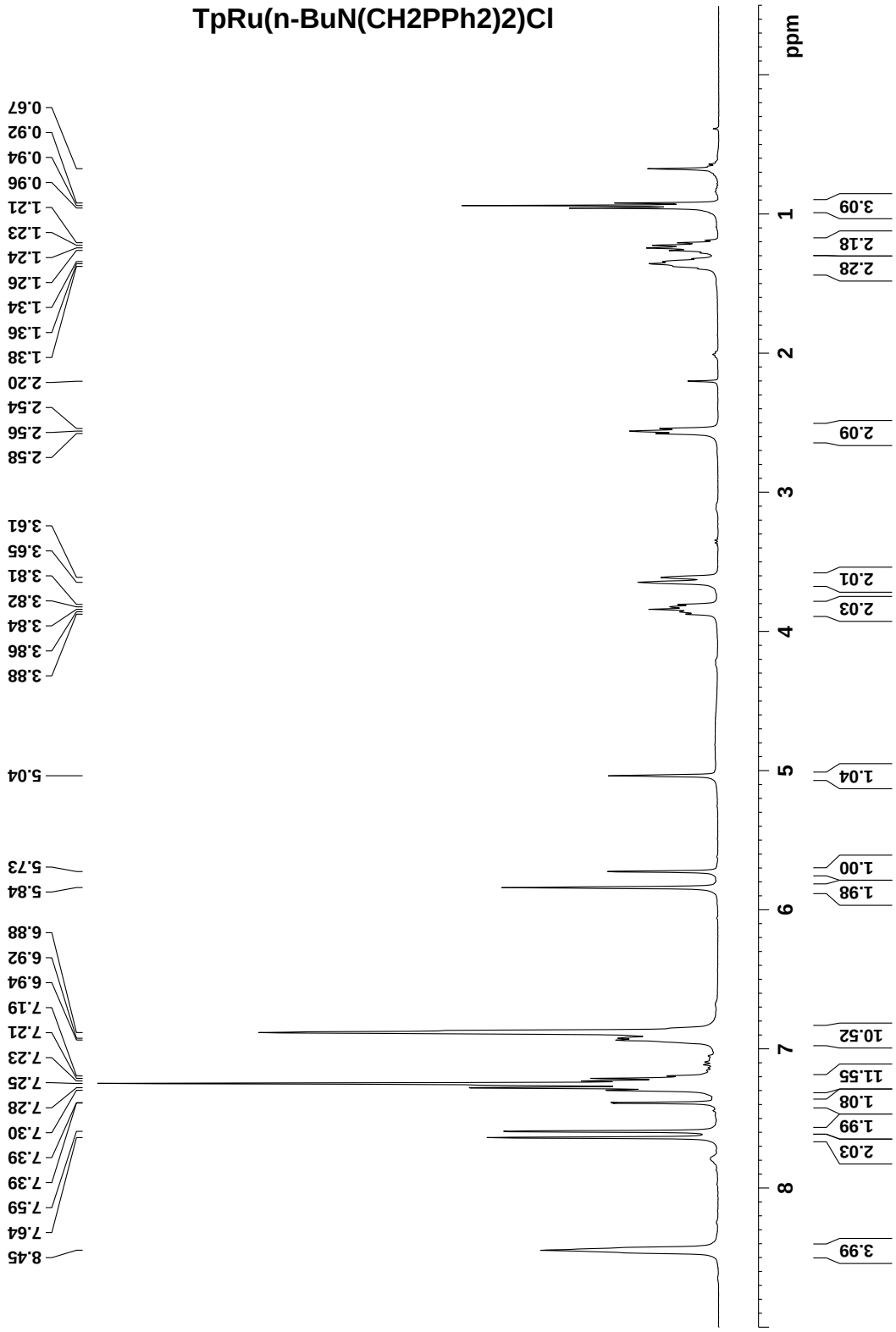

Figure 4.26 ^{1}H NMR spectrium of TpRu(^{n}BuN(CH_2PPh_2)$_2$)Cl (M23)

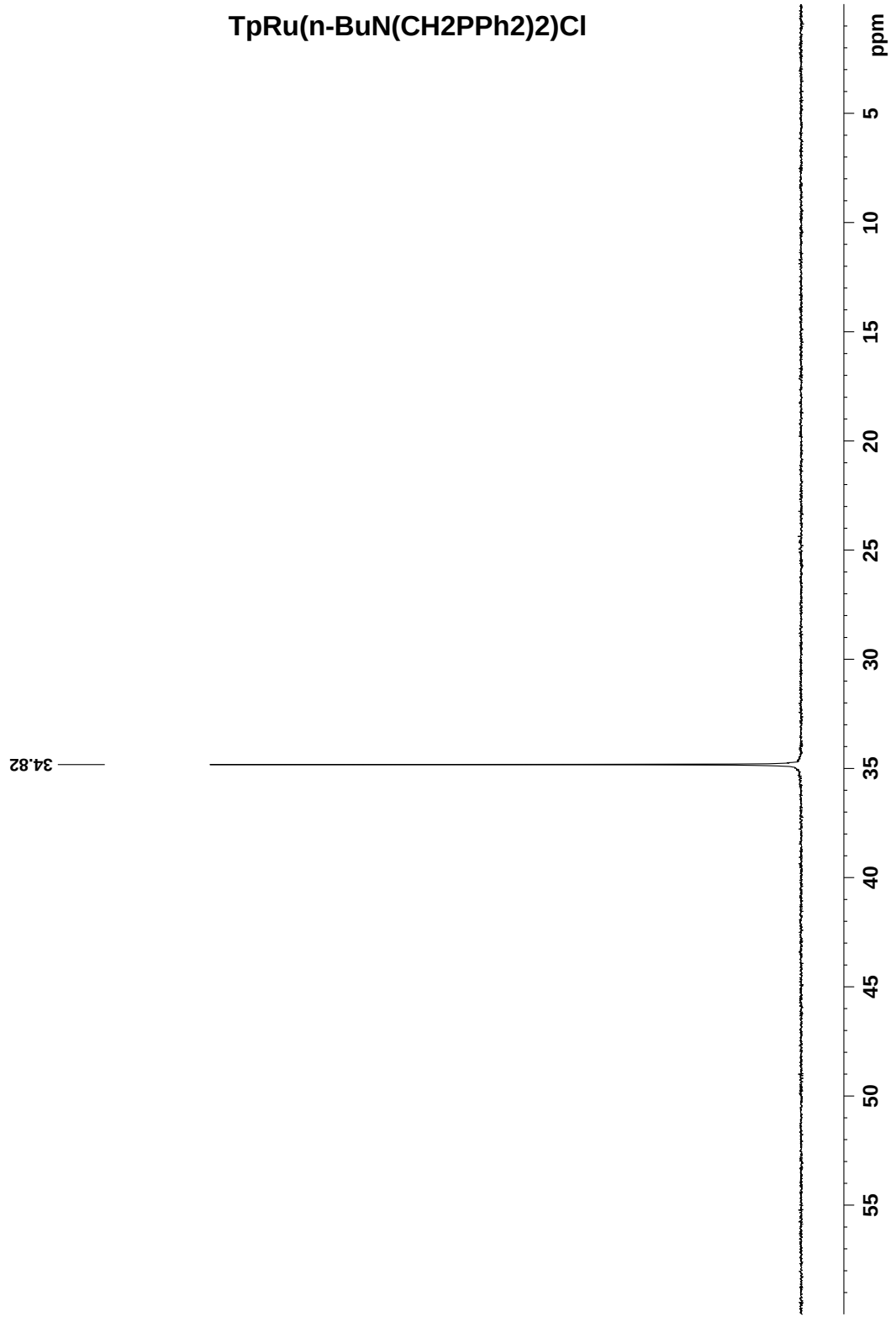

Figure 4.27 $^{31}P\{^{1}H\}$NMR spectrium of TpRu(^{n}BuN(CH_2PPh_2)$_2$)Cl (M23)

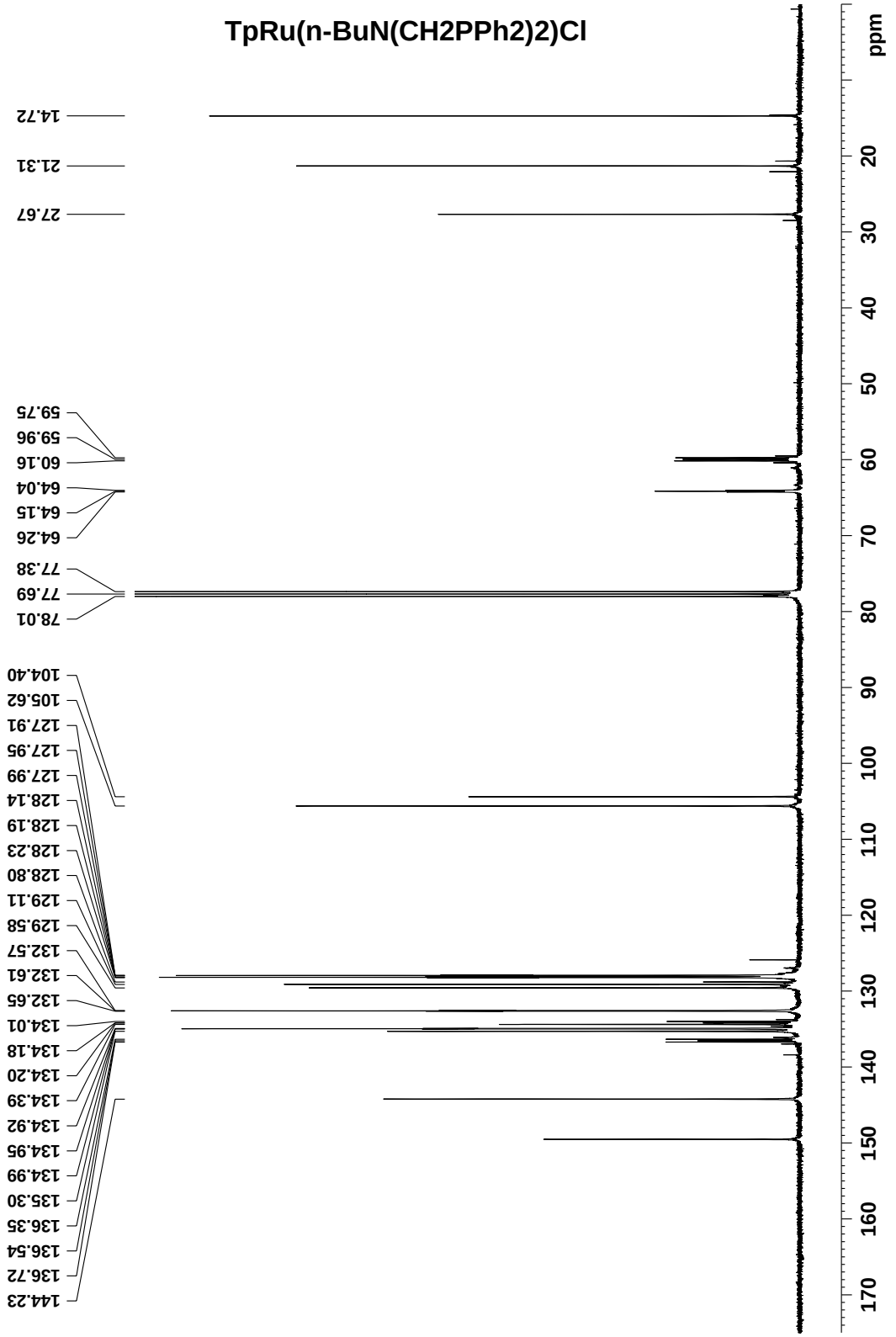

Figure 4.28 $^{13}C\{^{1}H\}$NMR spectrium of TpRu(^{n}BuN(CH_2PPh_2)$_2$)Cl (M23)

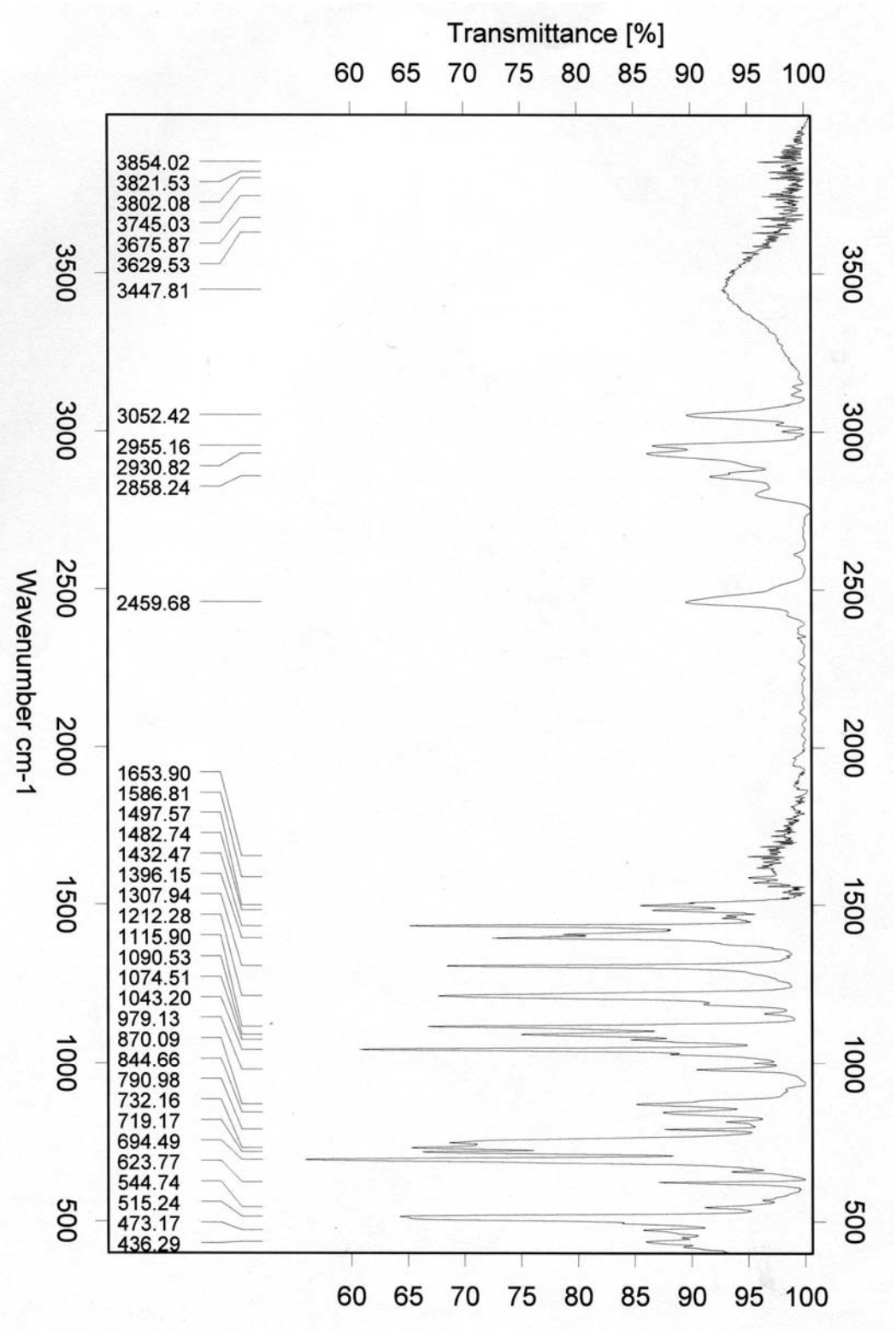

Figure 4.29 Infra-red spectrium of TpRu(^{n}BuN(CH_2PPh_2)$_2$)Cl (M23)

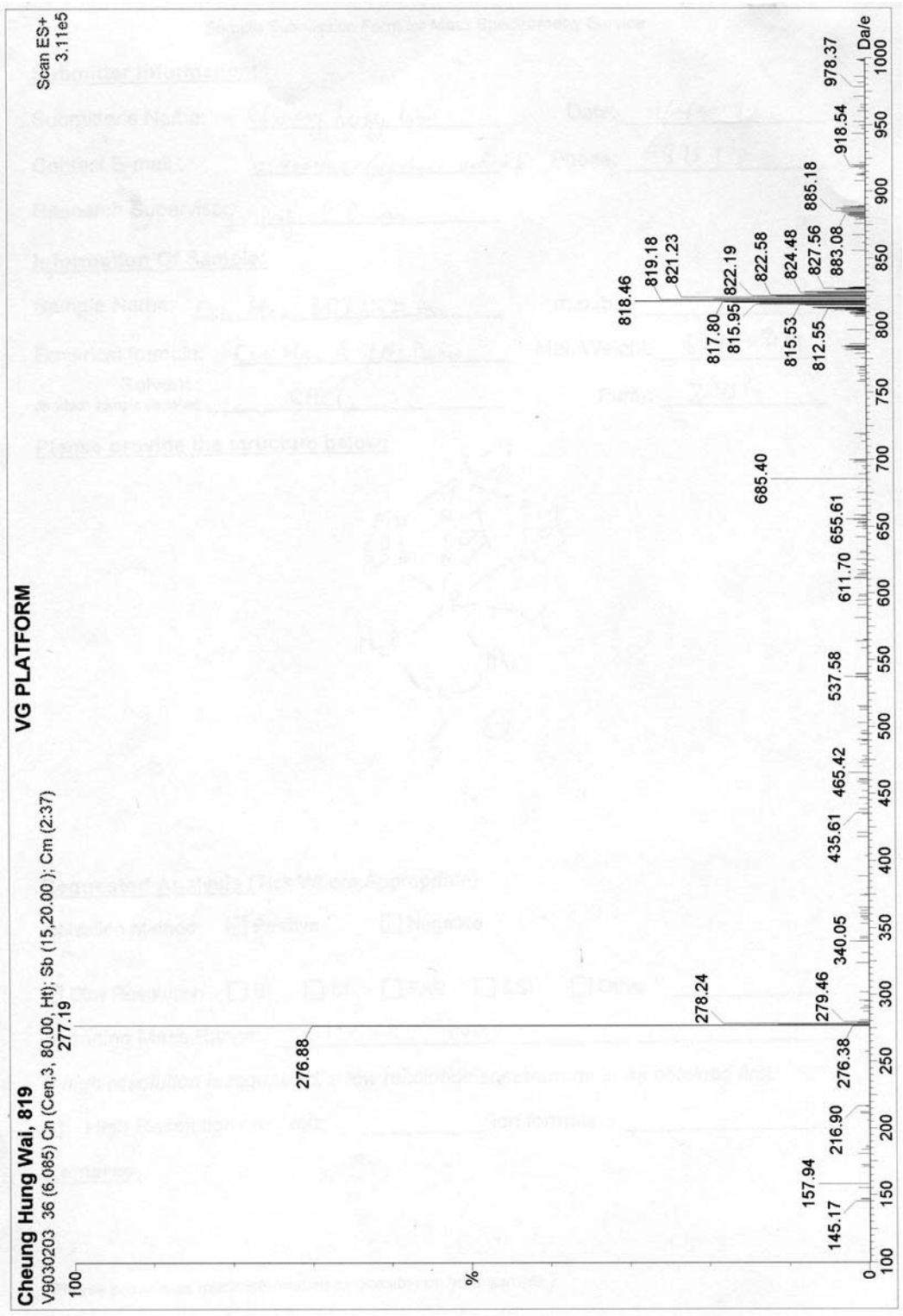

Figure 4.30 Mass spectrium of TpRu(^{n}BuN(CH_2PPh_2)$_2$)Cl (M23)

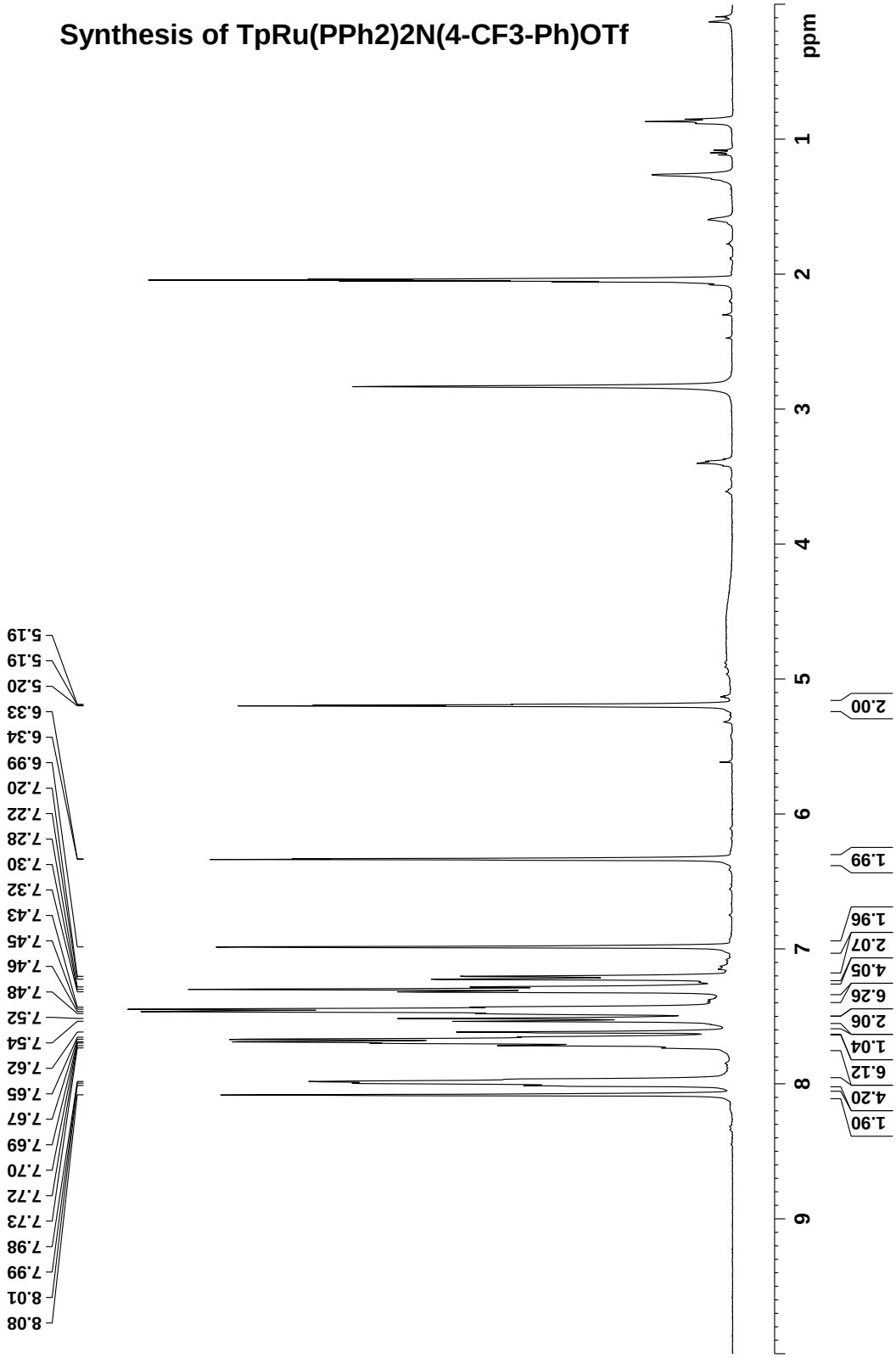

Figure 4.31 ^{1}H NMR spectrium of TpRu(4-$CF_3C_6H_4N(PPh_3)_2$)OTf (M24)

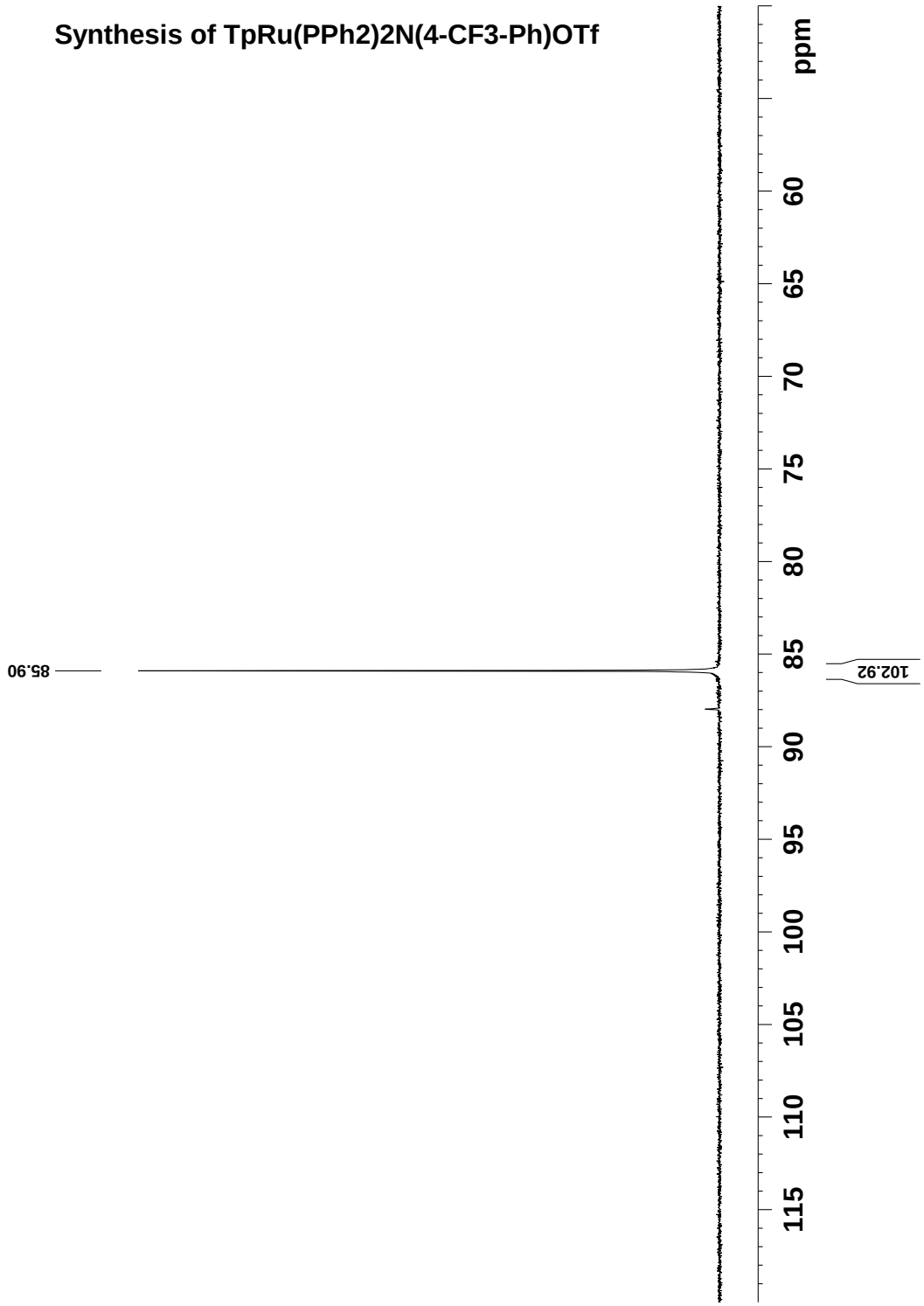

Figure 4.32 $^{31}P\{^{1}H\}$NMR spectrum of TpRu(4-$CF_3C_6H_4N(PPh_3)_2$)OTf (M24)

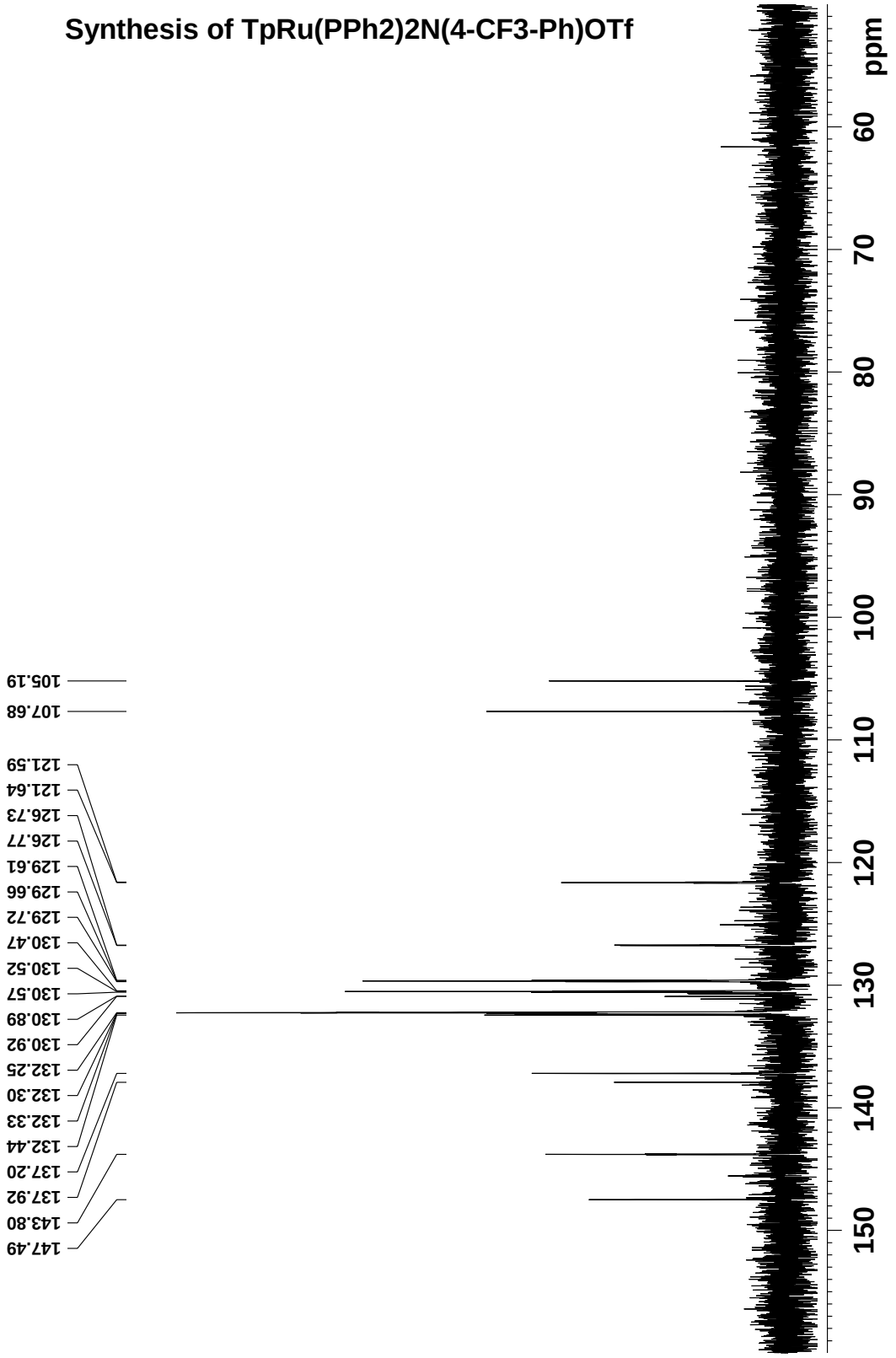

Figure 4.33 $^{13}C\{^{1}H\}$NMR spectrium of TpRu(4-$CF_3C_6H_4N(PPh_3)_2$)OTf (M24)

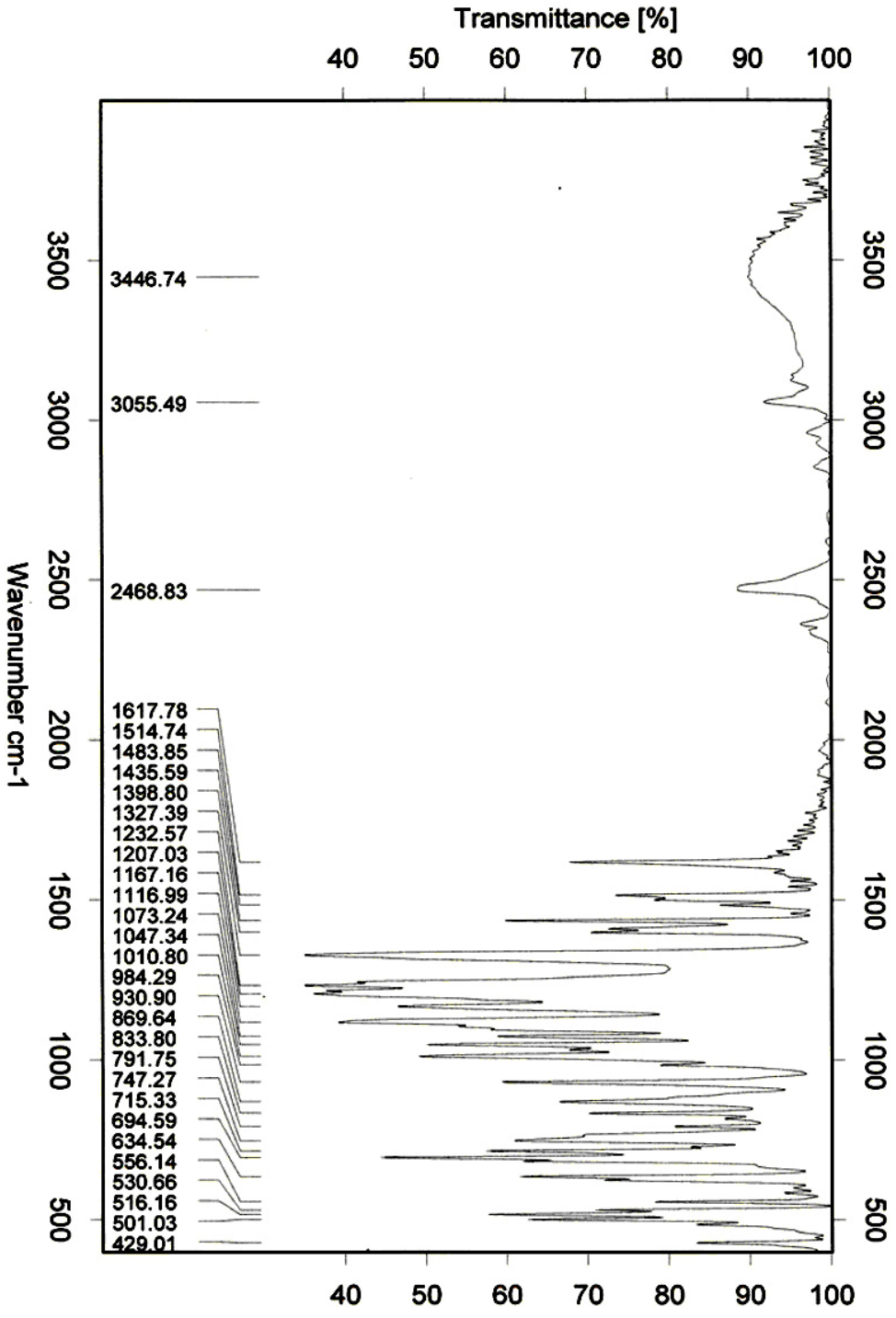

Figure 4.34 Infra-red spectrium of TpRu(4-$CF_3C_6H_4N(PPh_3)_2$)OTf (M24)

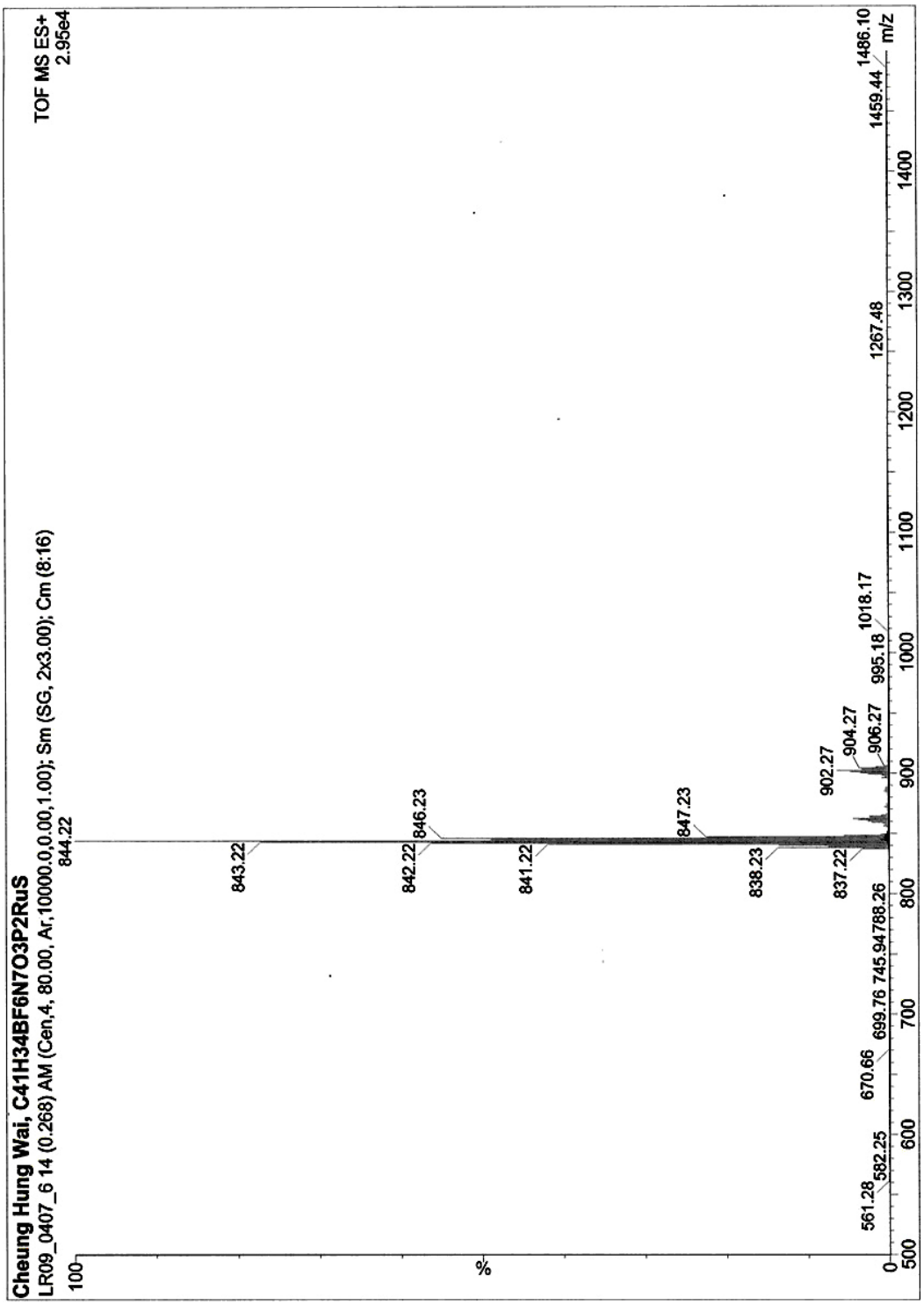

Figure 4.35 Mass spectrium of TpRu(4-$CF_3C_6H_4N(PPh_3)_2$)OTf (M24)

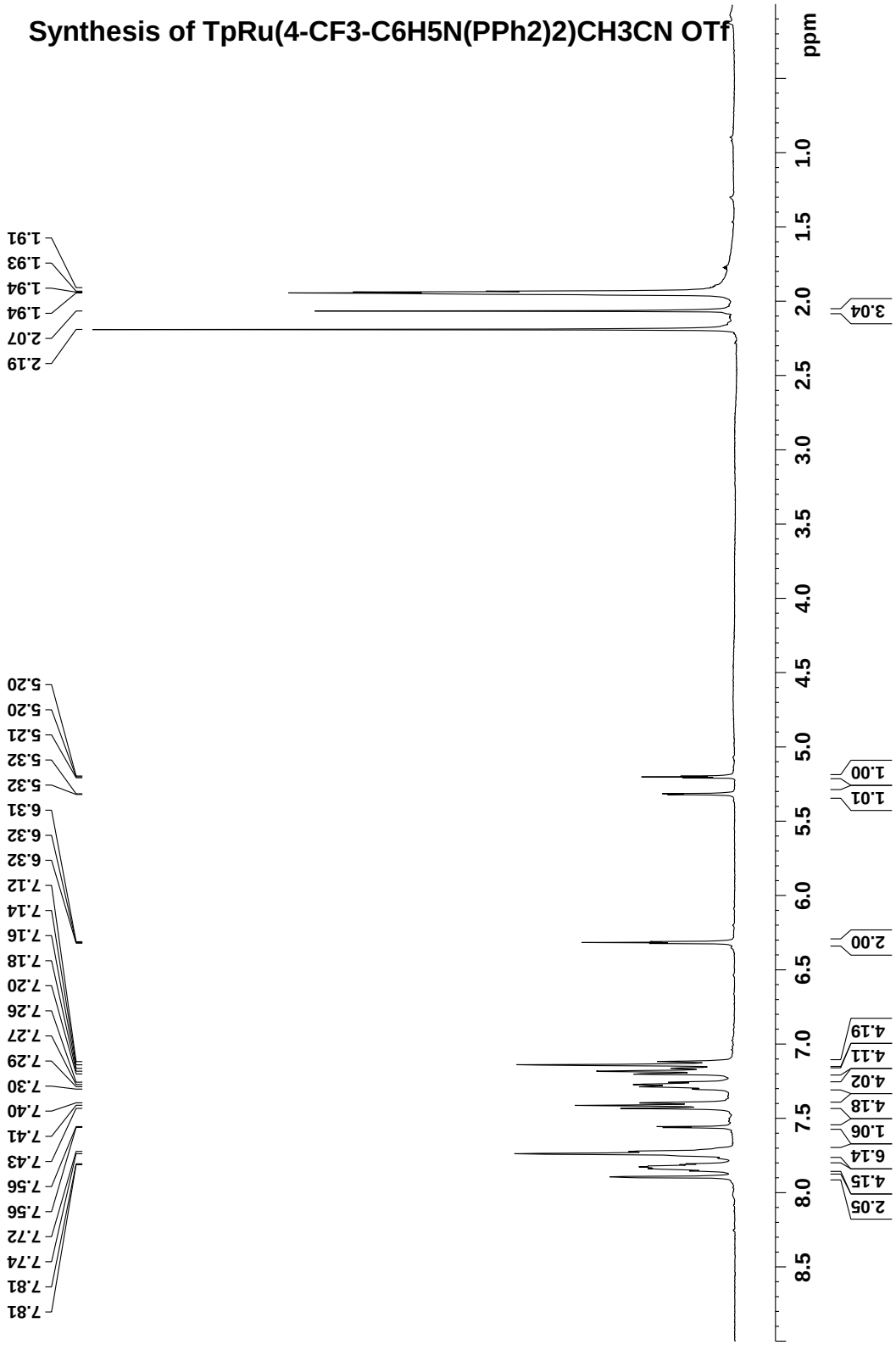

Figure 4.36 ^{1}H NMR spectrium of [TpRu(4-$CF_3C_6H_4N(PPh_2)_2$)CH_3CN]$^{+}$$OTf^{-}$ (M25)

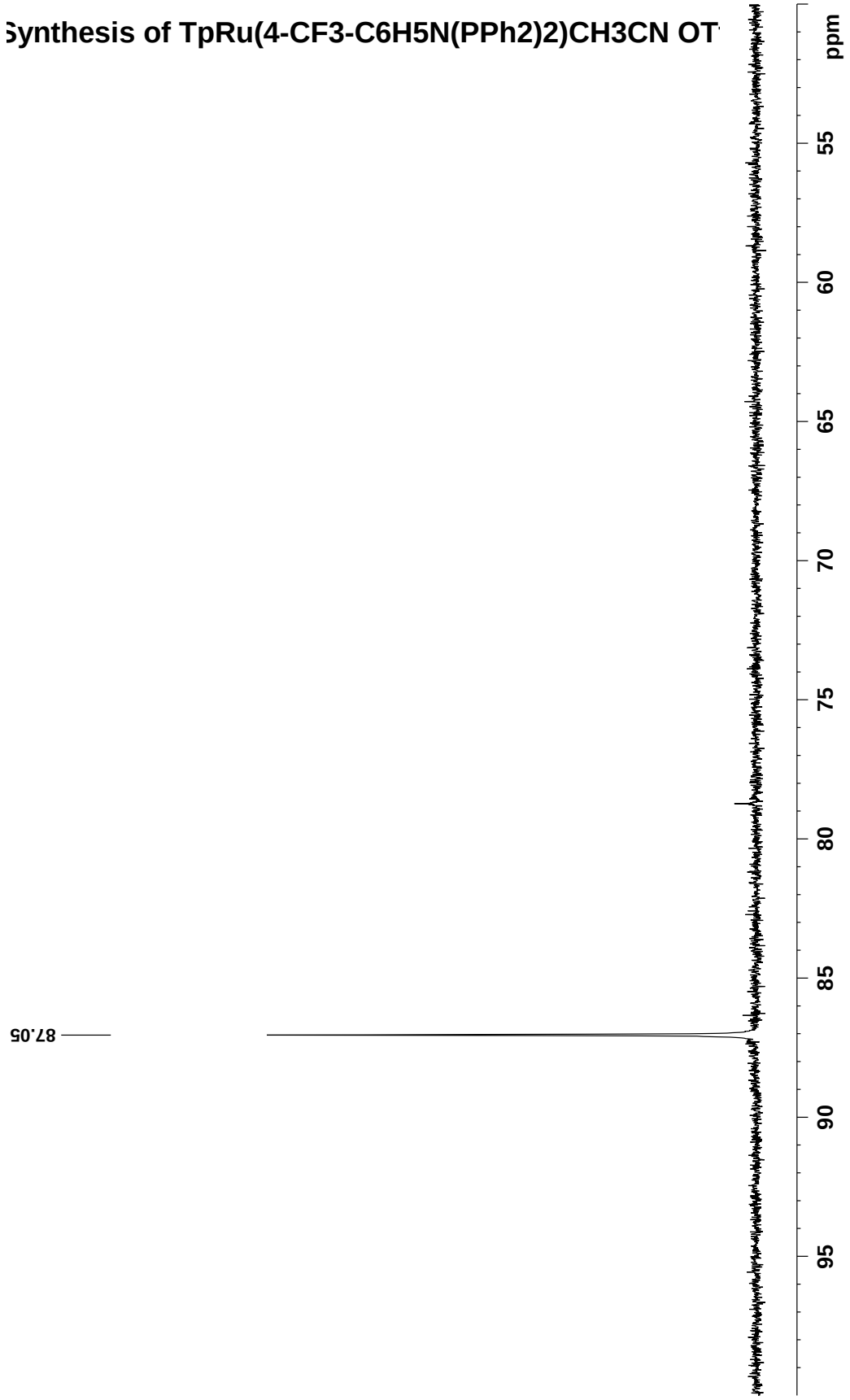

Figure 4.37 $^{31}P\{^{1}H\}$NMR spectrium of $[TpRu(4\text{-}CF_3C_6H_4N(PPh_2)_2)CH_3CN]^+OTf^-$ (M25)

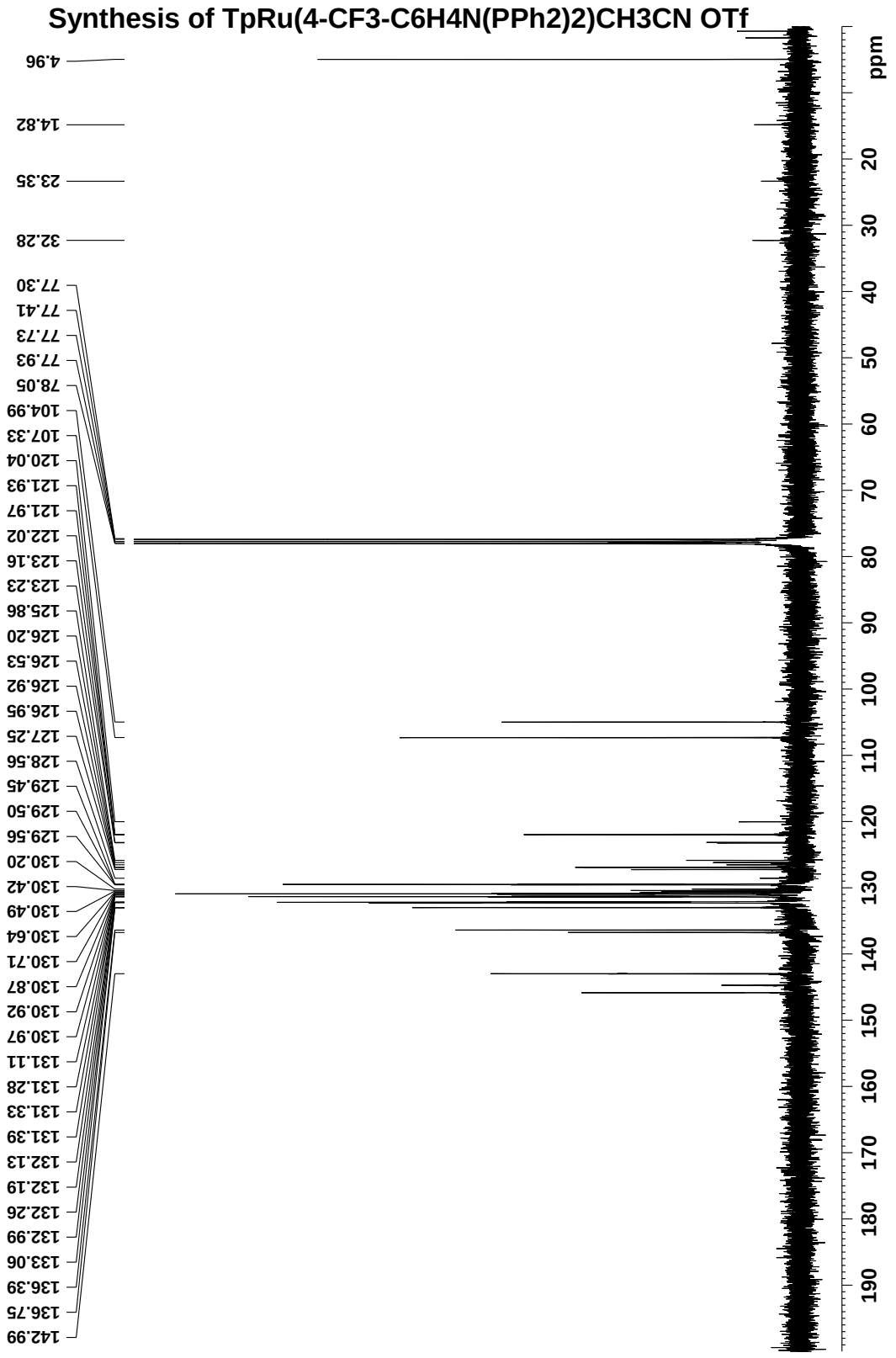

Figure 4.38 $^{13}C\{^{1}H\}$NMR spectrium of $[TpRu(4\text{-}CF_3C_6H_4N(PPh_2)_2)CH_3CN]^+OTf^-$ (M25)

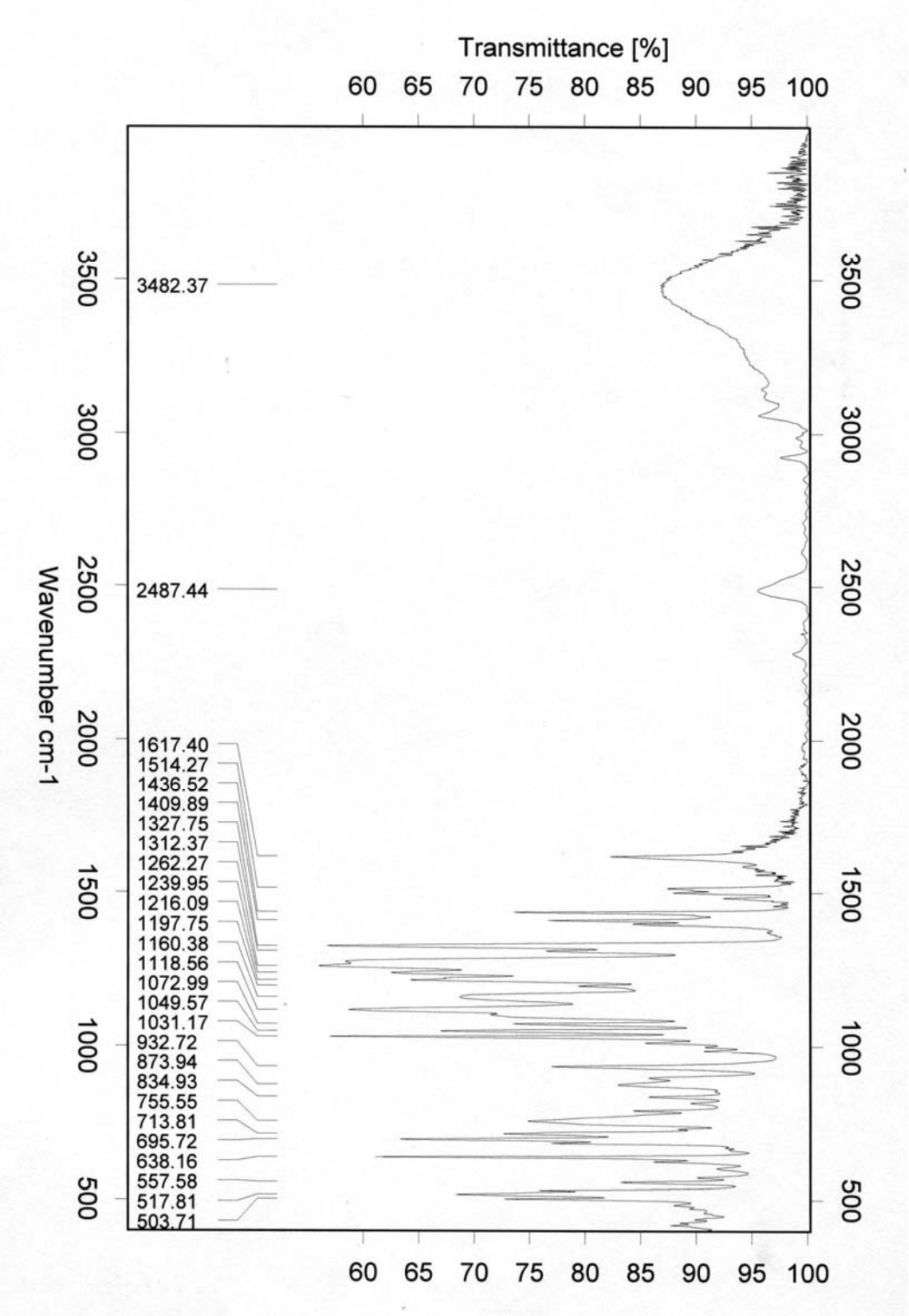

Figure 4.39 Infra-red spectrium of $[TpRu(4\text{-}CF_3C_6H_4N(PPh_2)_2)CH_3CN]^+OTf^-$ (M25)

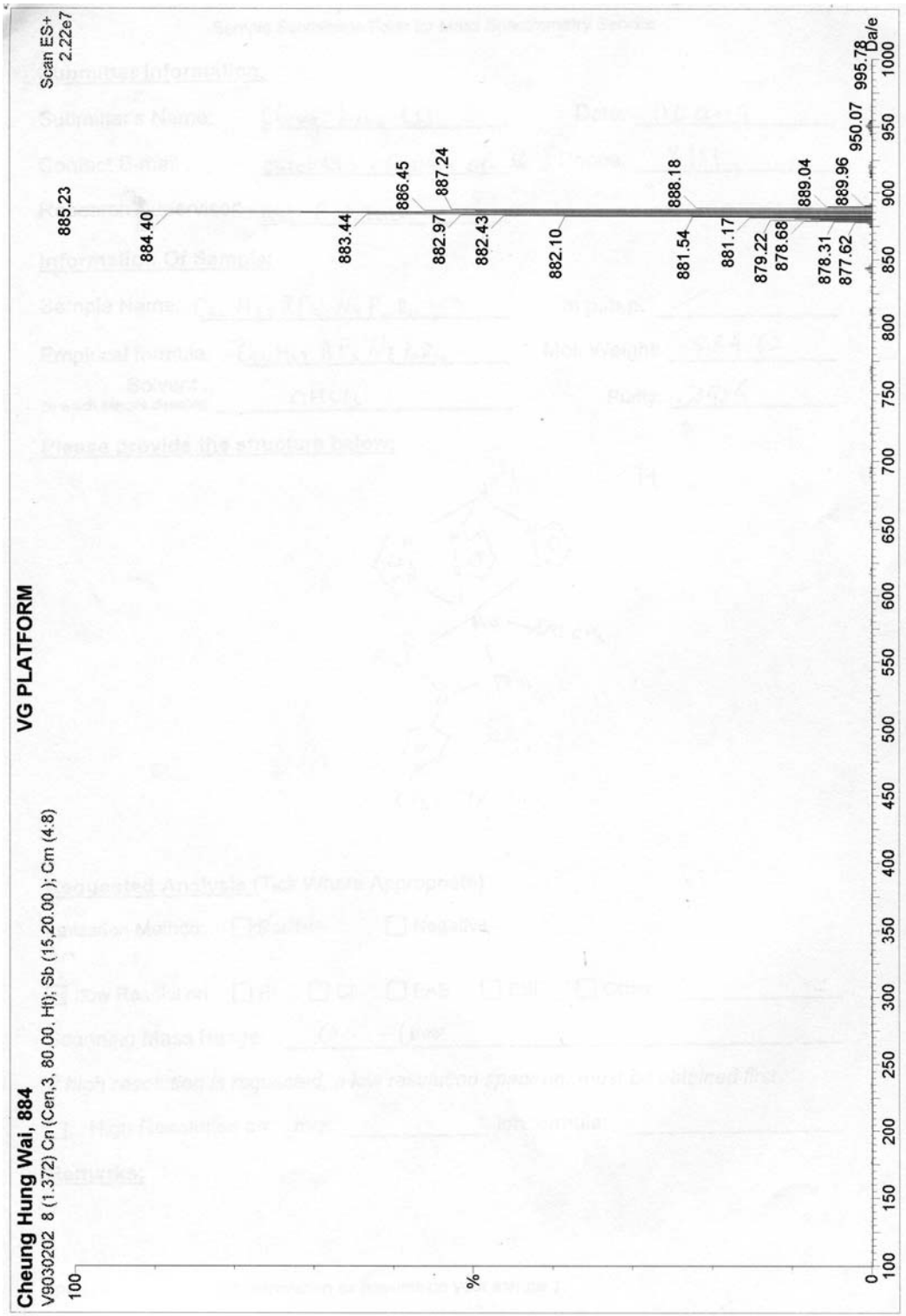

Figure 4.40 Mass spectrium of $[TpRu(4\text{-}CF_3C_6H_4N(PPh_2)_2)CH_3CN]^+OTf^-$ (M25)

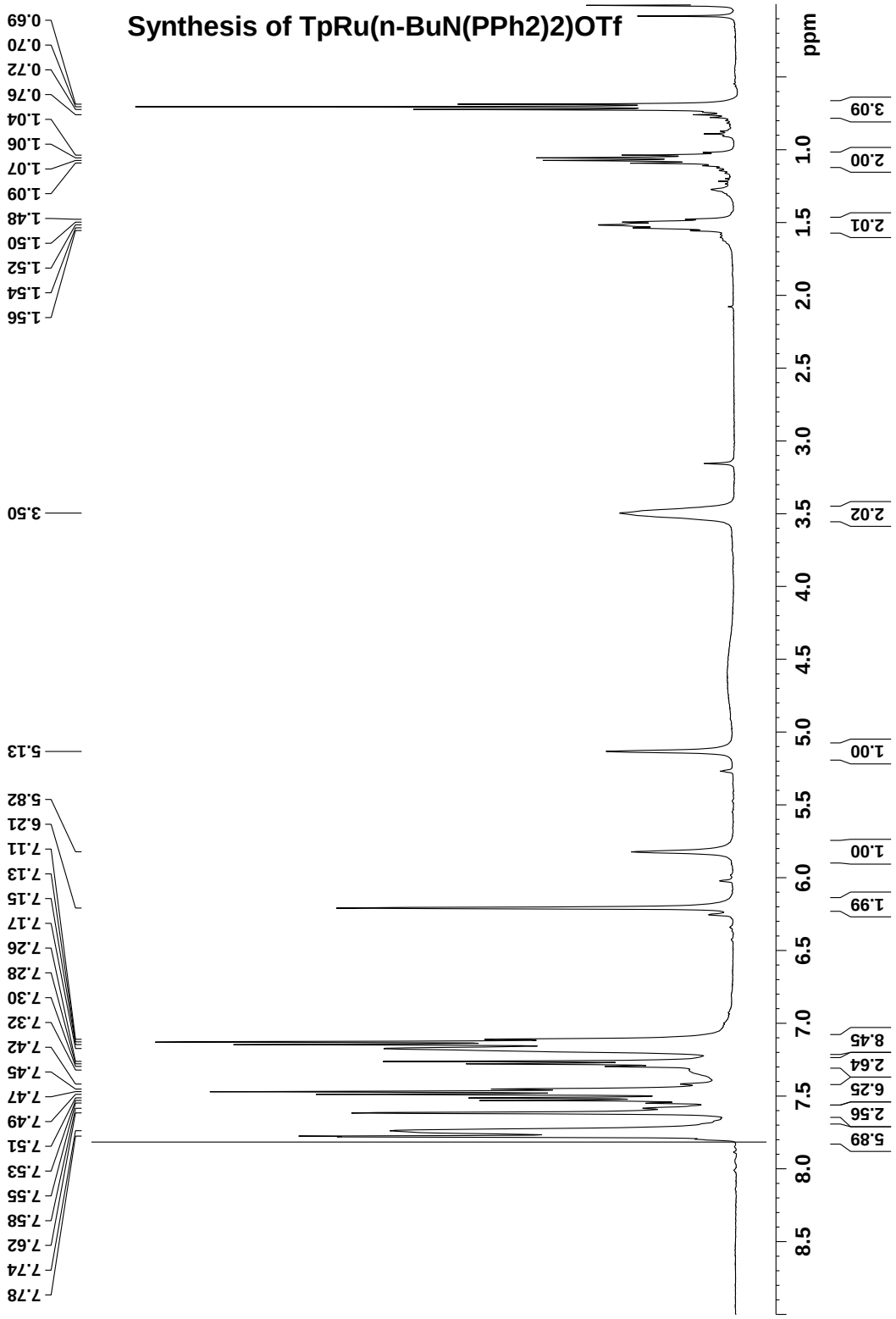

Figure 4.41 ^{1}H NMR spectrium of TpRu(^{n}BuN(PPh$_2$)$_2$) OTf (M26)

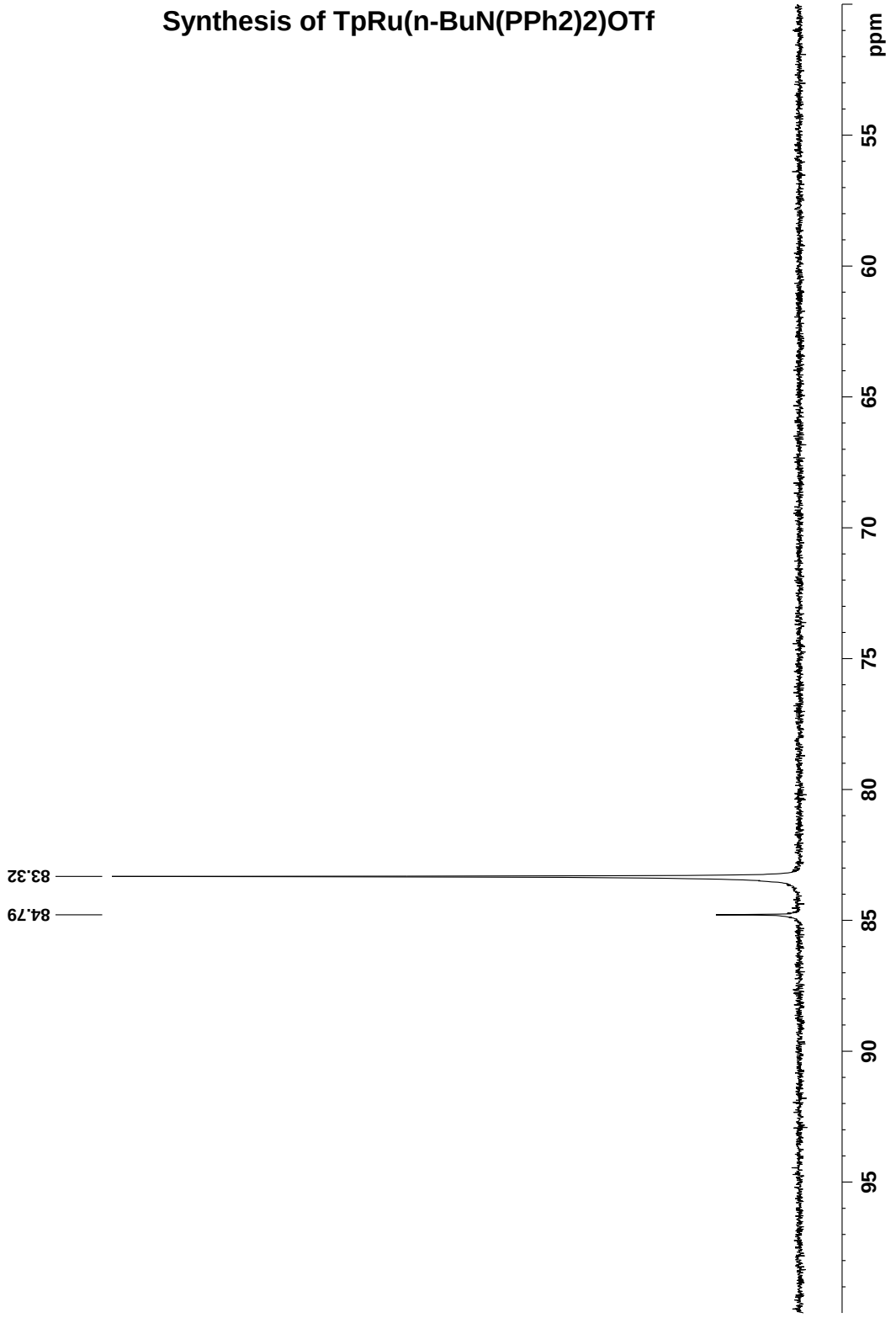

Figure 4.42 $^{31}P\{^{1}H\}$NMR spectrum of TpRu(^{n}BuN(PPh_2)$_2$) OTf (M26)

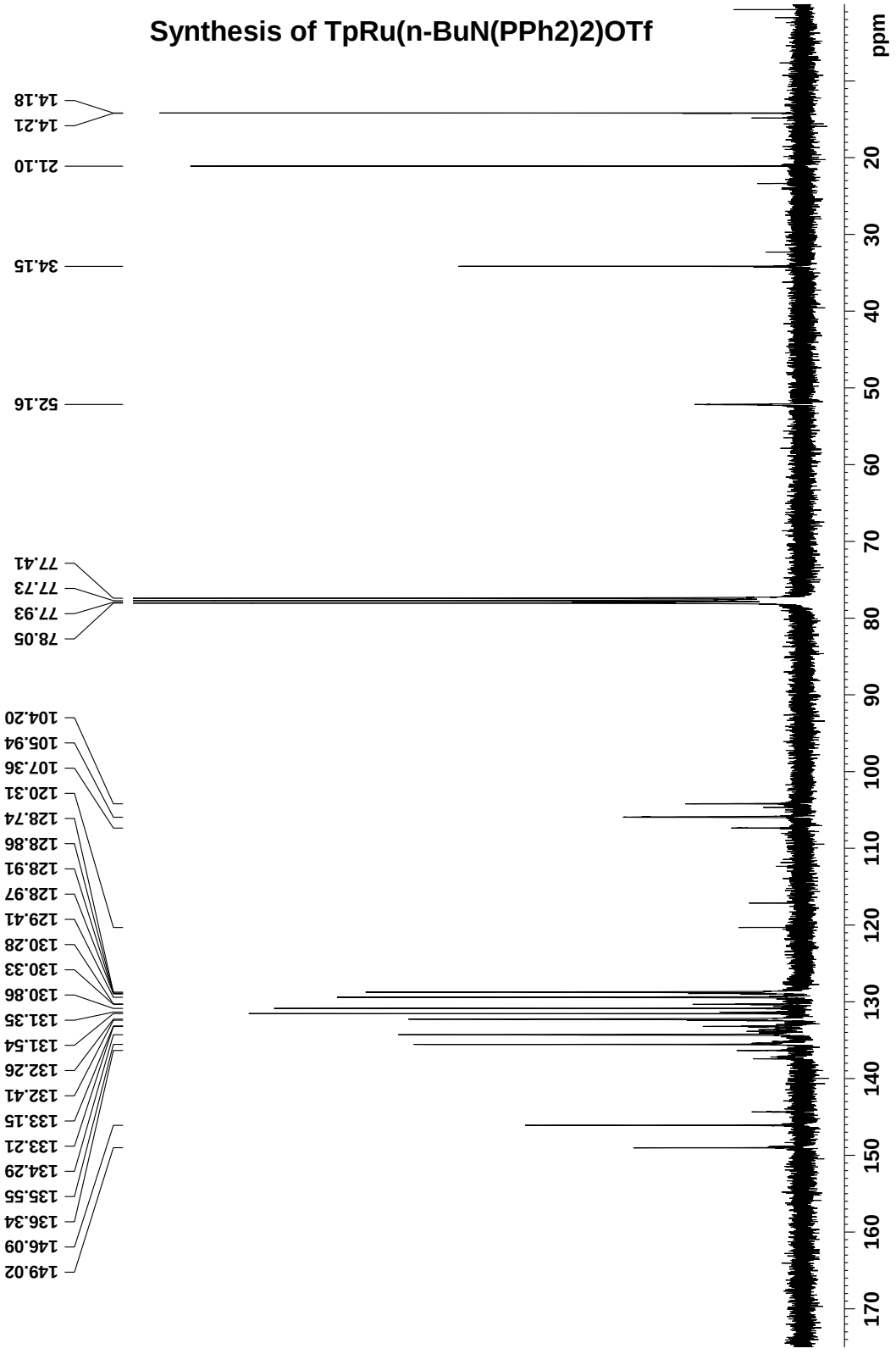

Figure 4.43 $^{13}C\{^{1}H\}$NMR spectrium of TpRu(^{n}BuN(PPh_2)$_2$) OTf (M26)

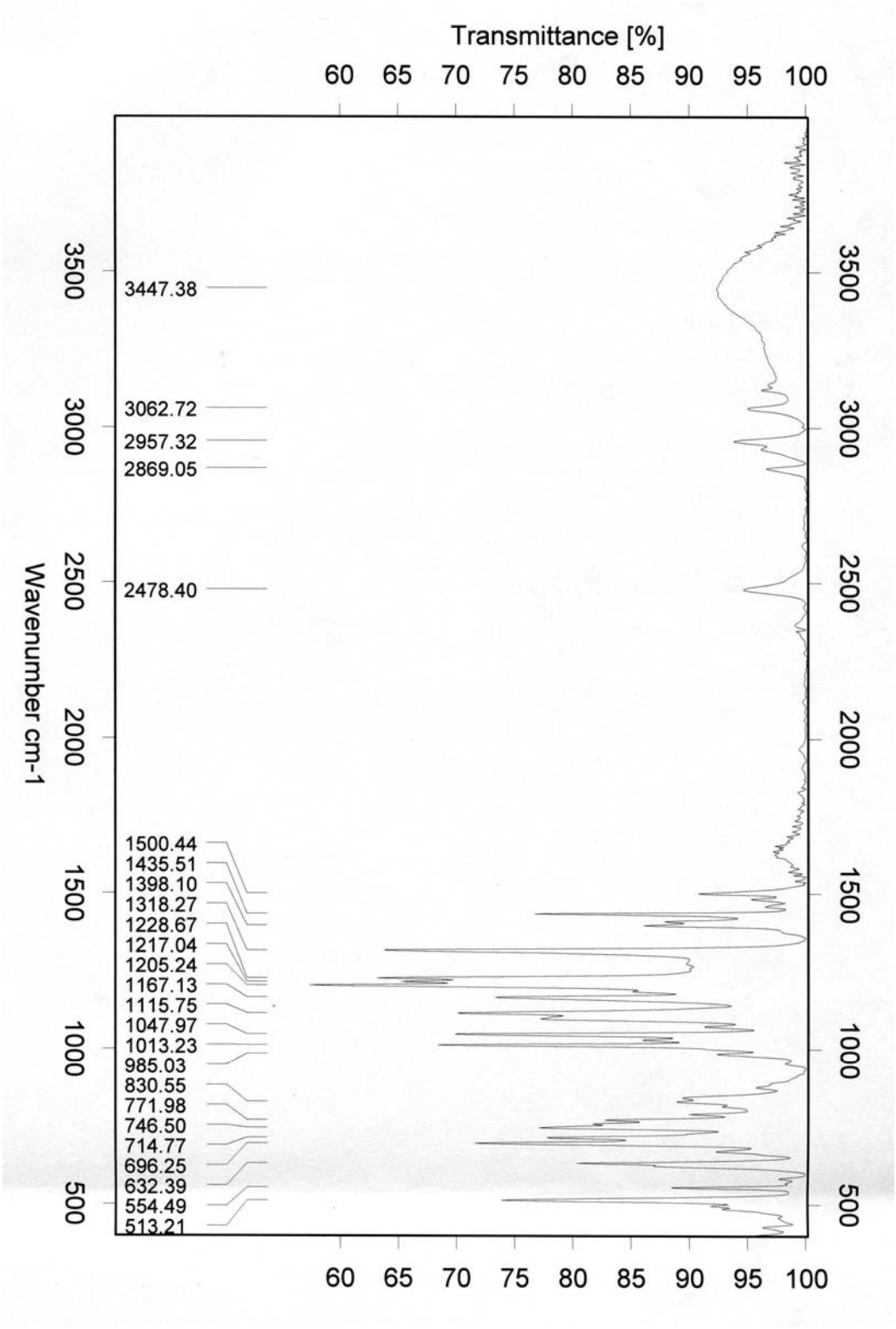

Figure 4.44 Infra-red spectrium of TpRu(^{n}BuN(PPh$_2$)$_2$) OTf (M26)

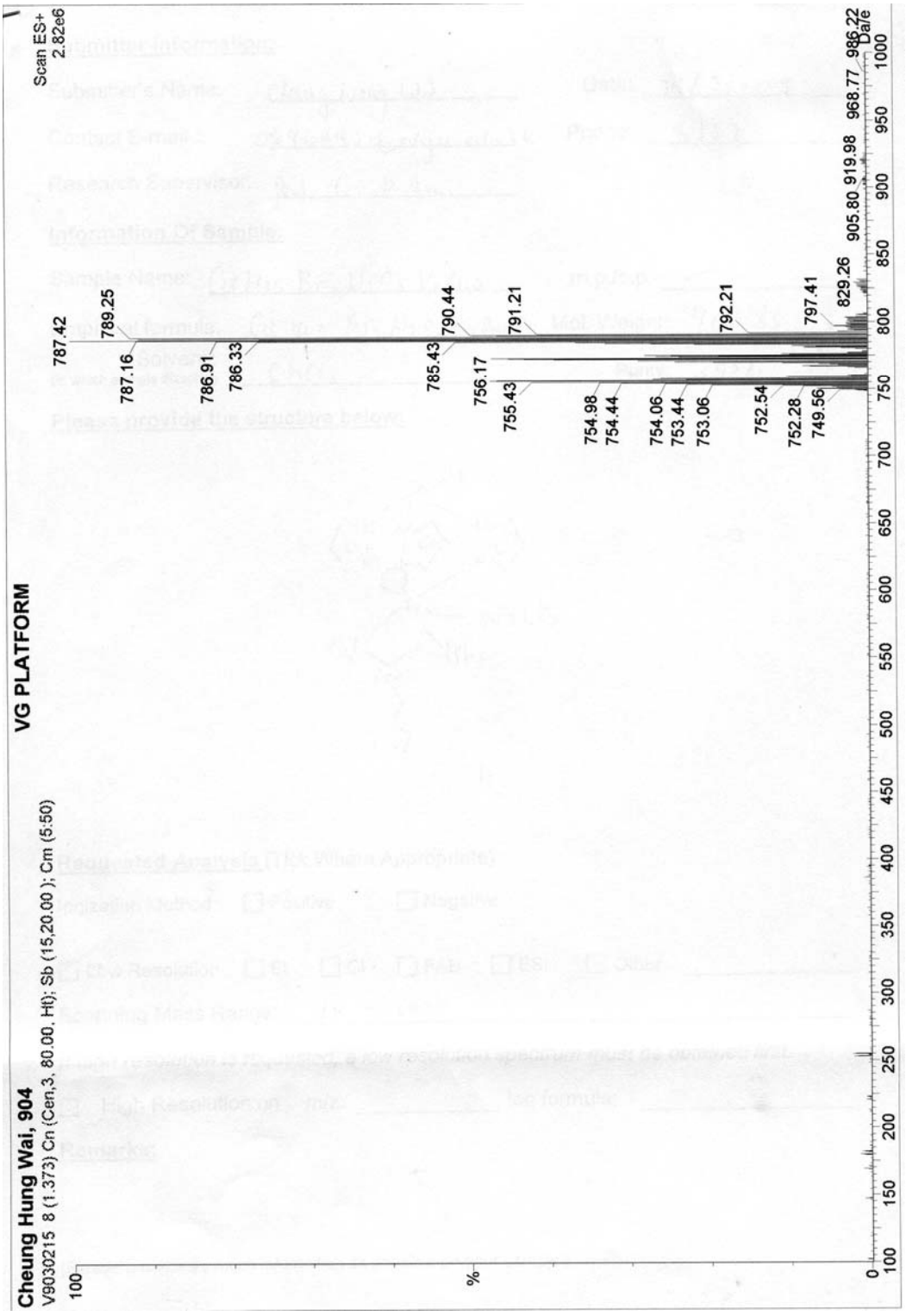

Figure 4.45 Mass spectrium of TpRu(^{n}BuN(PPh$_2$)$_2$) OTf (M26)

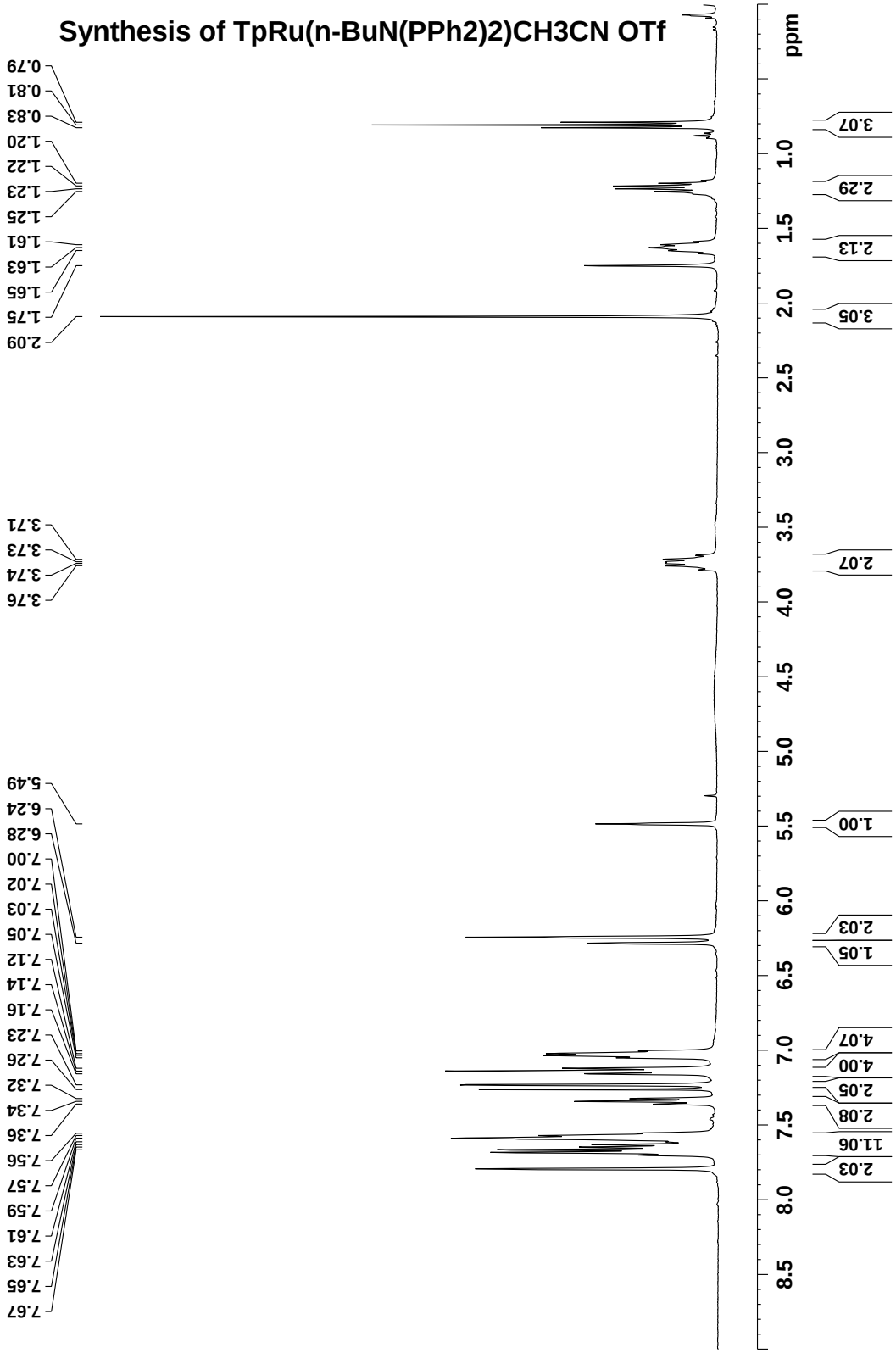

Figure 4.46 ^{1}H NMR spectrum of $[TpRu(^{n}BuN(PPh_2)_2)CH_3CN]^{+}OTf^{-}$ (M27)

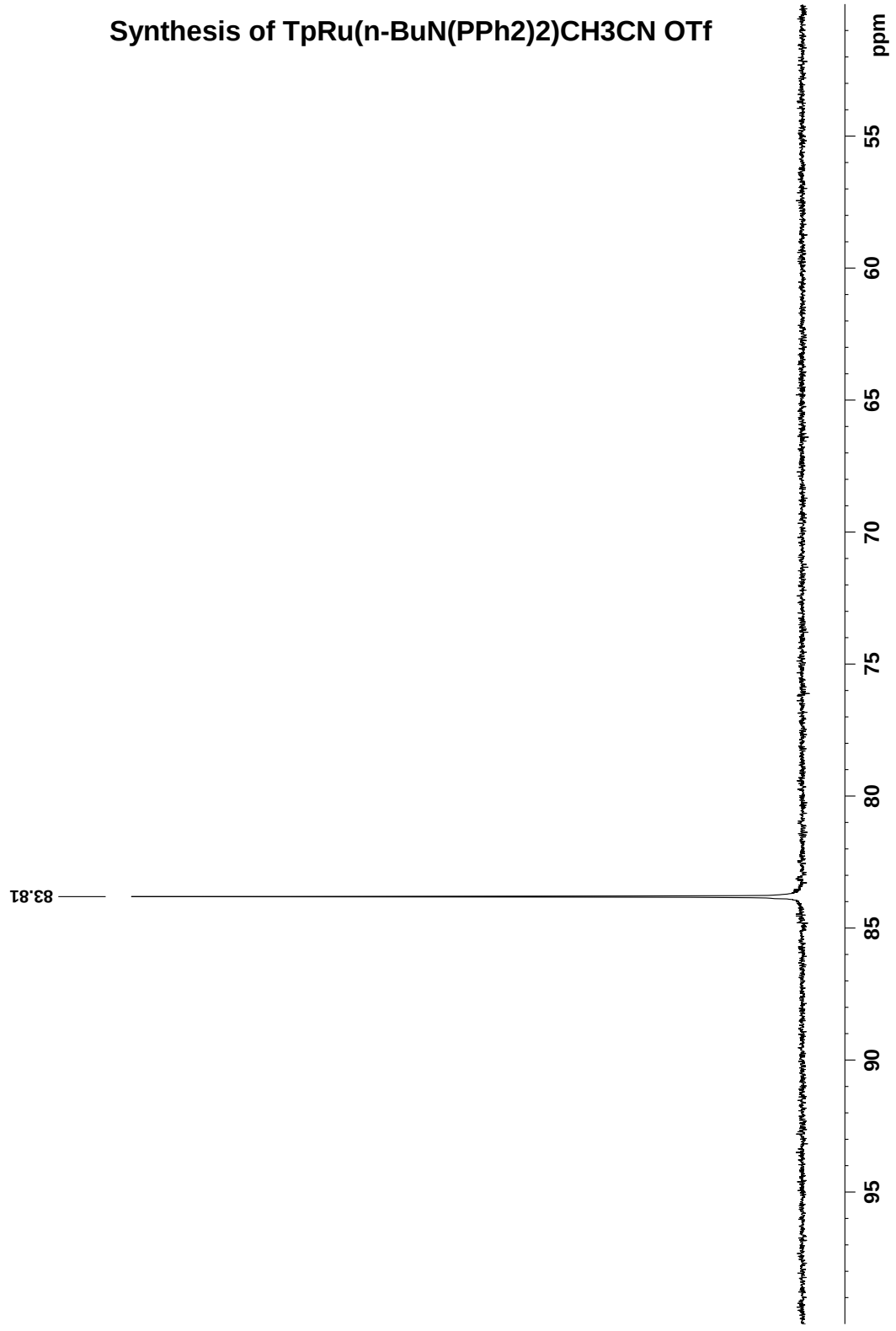

Figure 4.47 $^{31}P\{^{1}H\}$NMR spectrium of $[TpRu(^{n}BuN(PPh_2)_2)CH_3CN]^{+}OTf^{-}$ (M27)

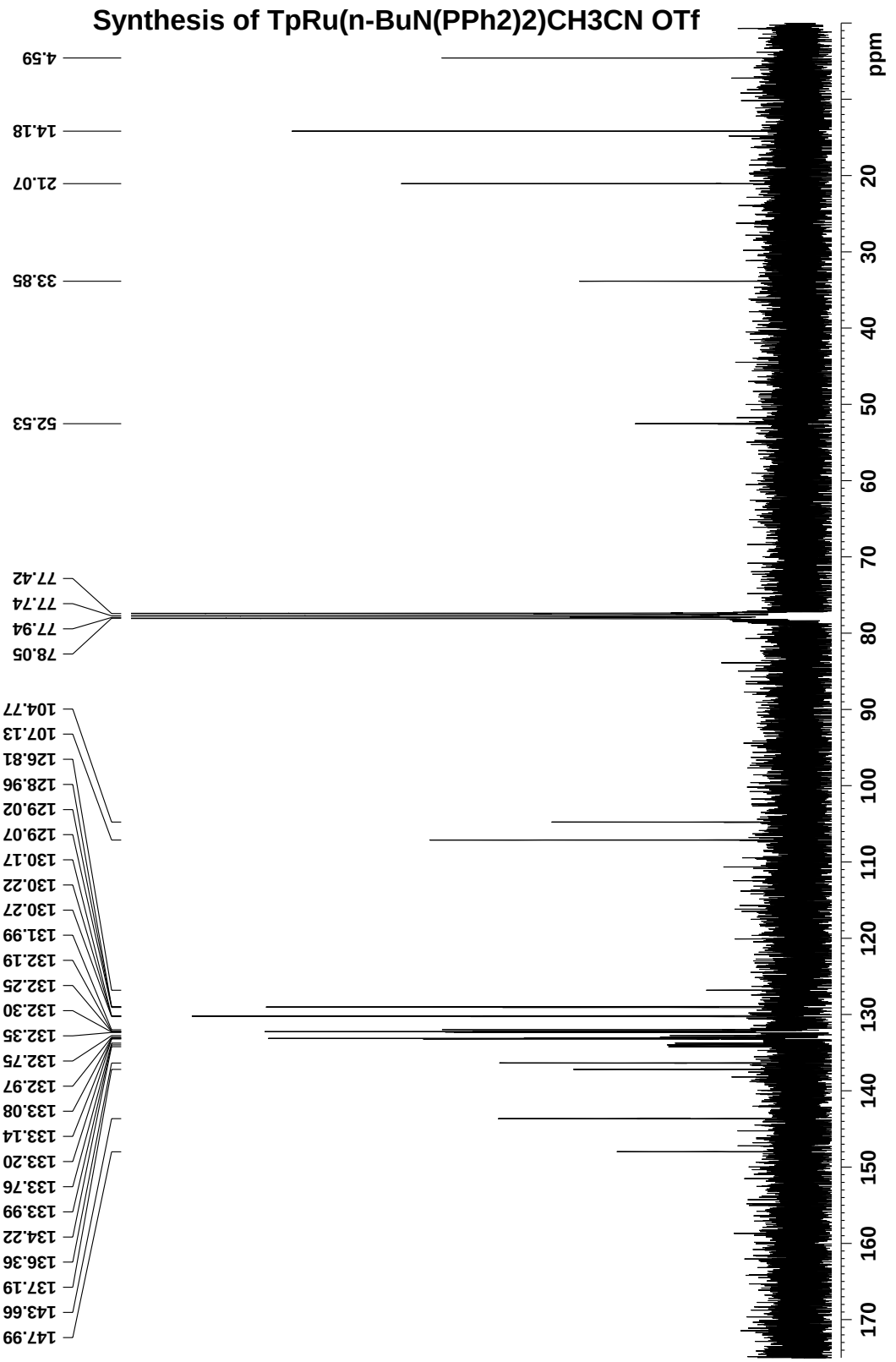

Figure 4.48 $^{13}C\{^{1}H\}$NMR spectrium of $[TpRu(^{n}BuN(PPh_2)_2)CH_3CN]^{+}OTf^{-}$ (M27)

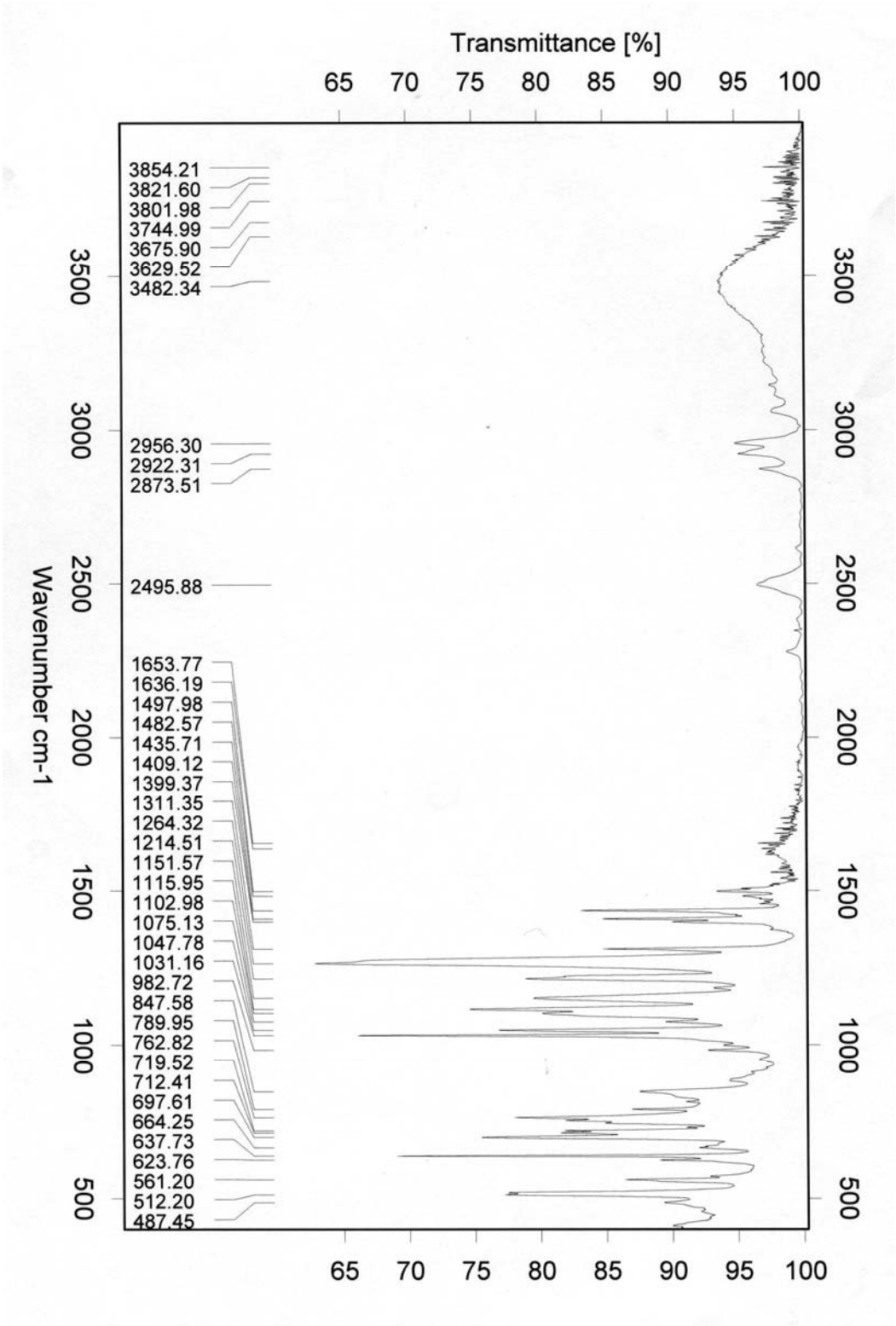

Figure 4.49 Infra-red spectrium of $[TpRu(^{n}BuN(PPh_2)_2)CH_3CN]^{+}OTf^{-}$ (M27)

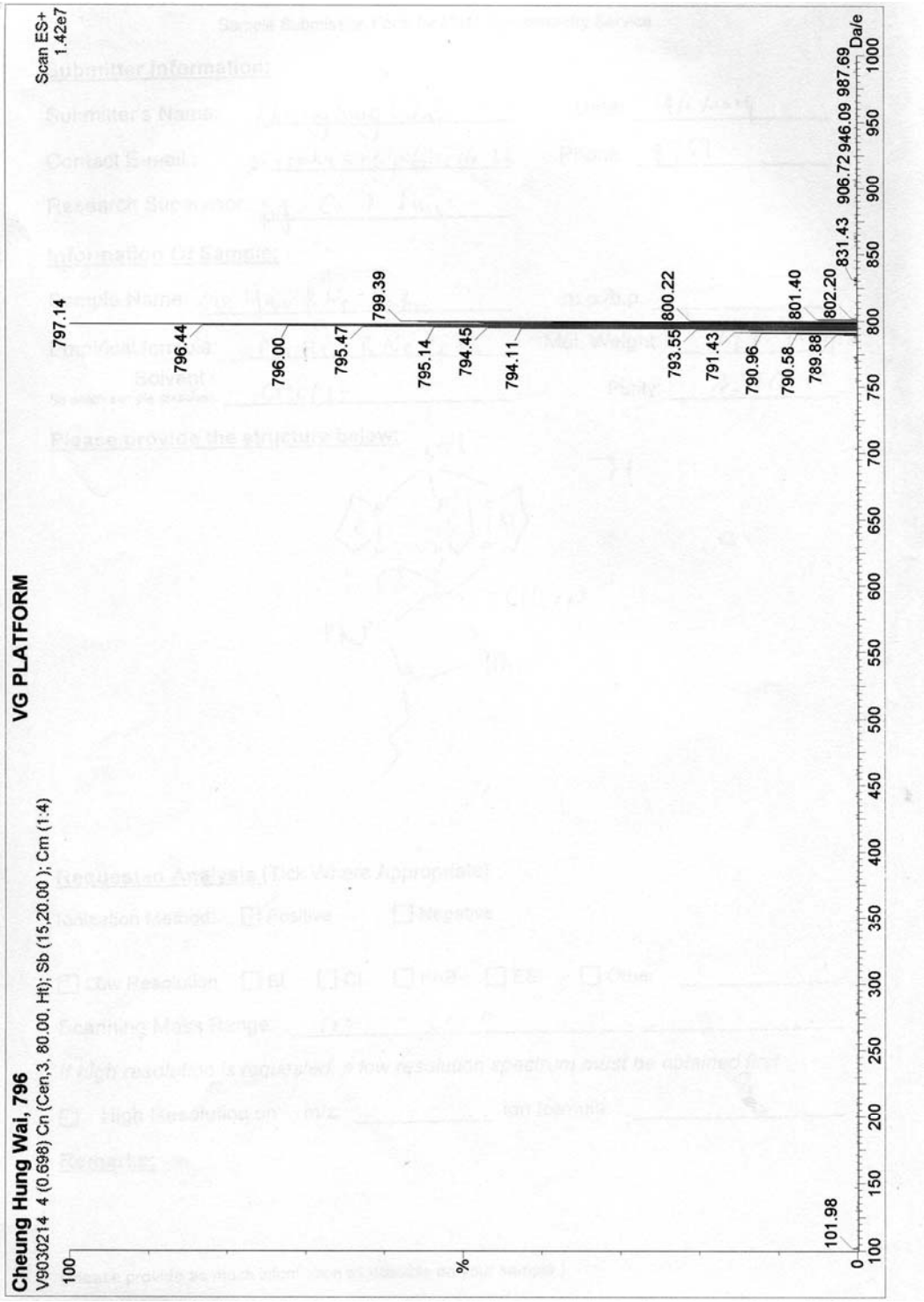

Figure 4.50 Mass spectrium of [TpRu(^{n}BuN(PPh$_2$)$_2$)CH$_3$CN]$^+$OTf$^-$ (M27)

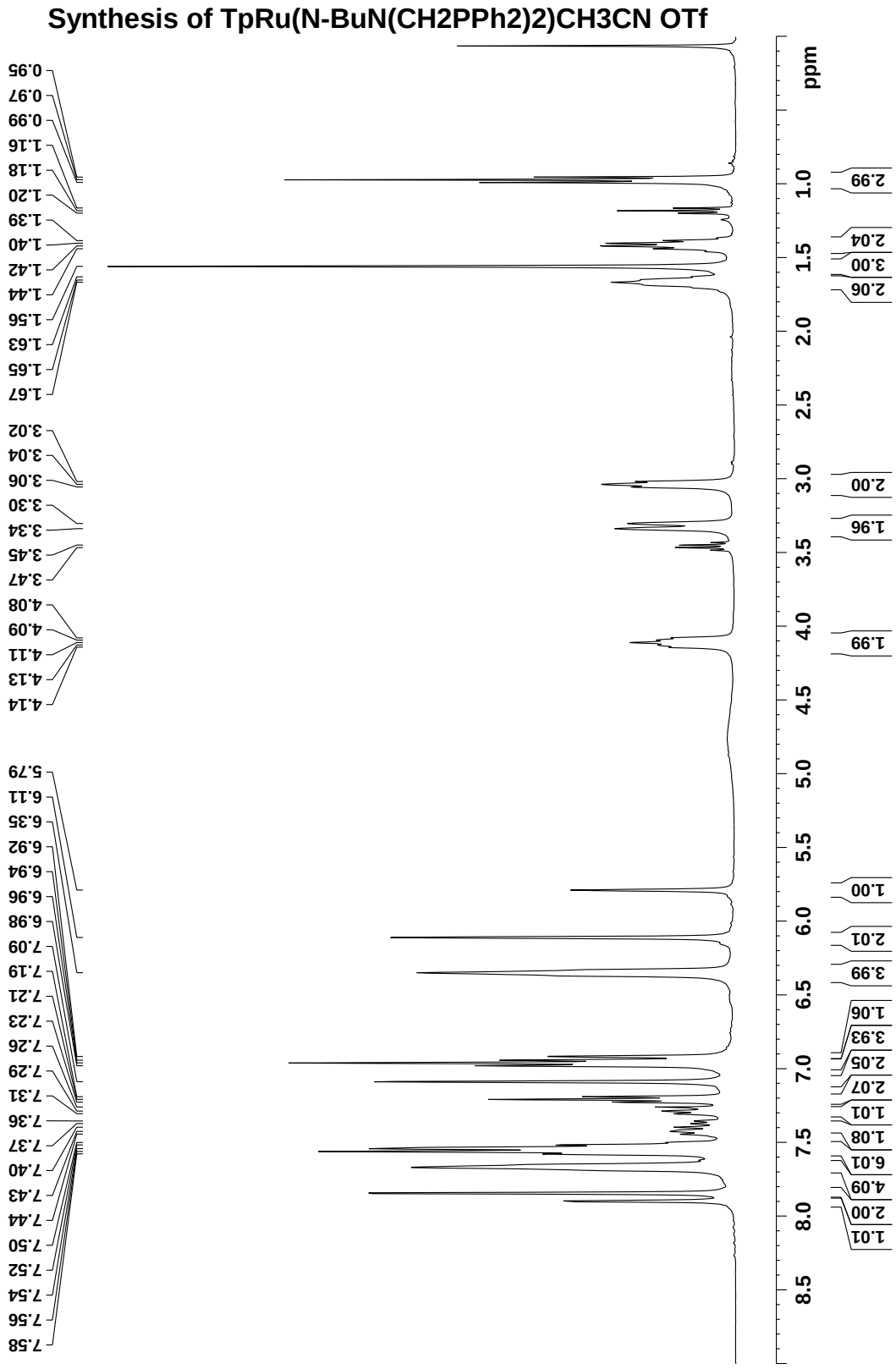

Figure 4.51 ^{1}H NMR spectrium of [TpRu(^{n}BuN(CH_2PPh_2)$_2$)CH_3CN]$^{+}$OTf^{-} (M28)

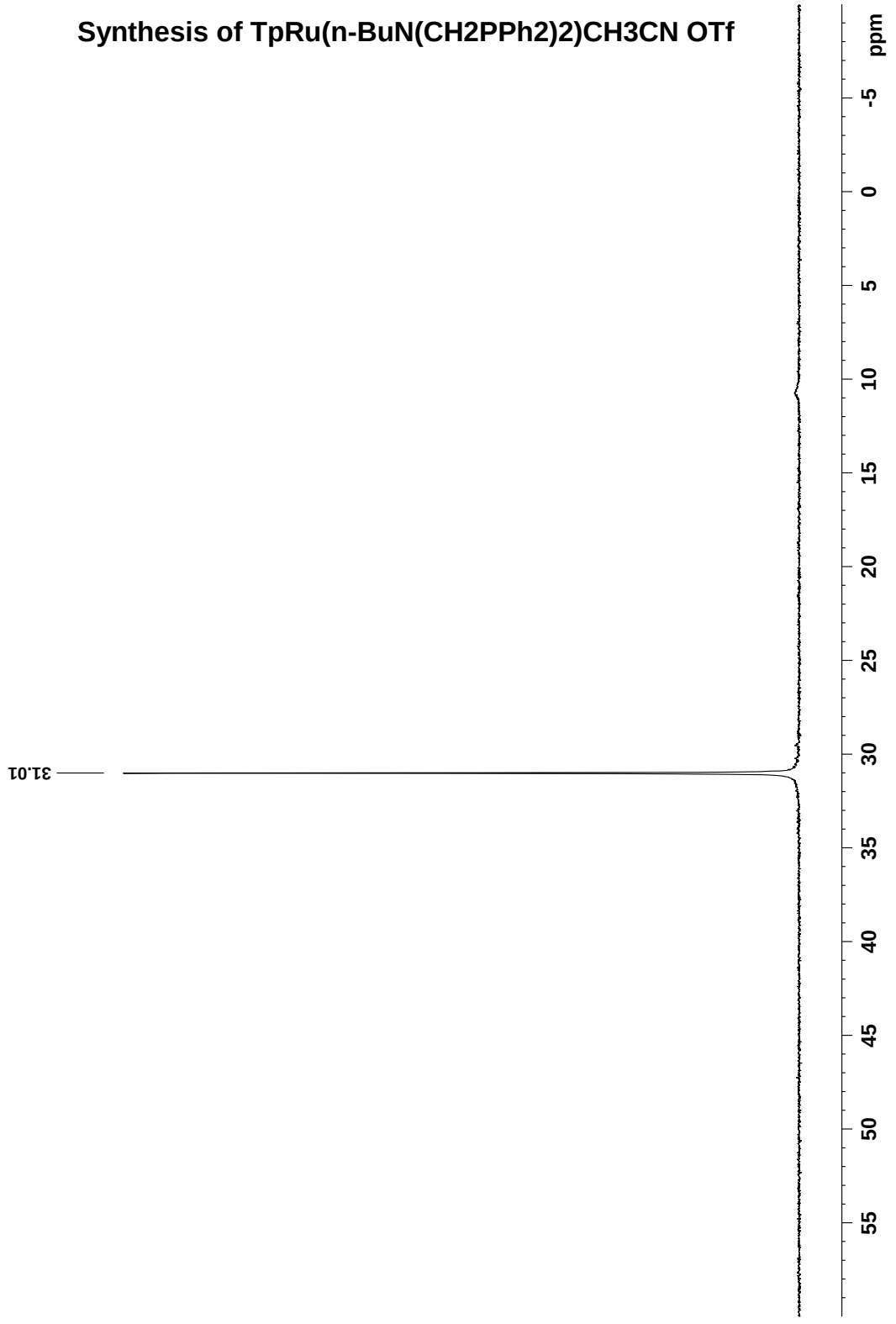

Figure 4.52 $^{31}P\{^{1}H\}$NMR spectrium of $[TpRu(^{n}BuN(CH_2PPh_2)_2)CH_3CN]^{+}OTf^{-}$ (M28)

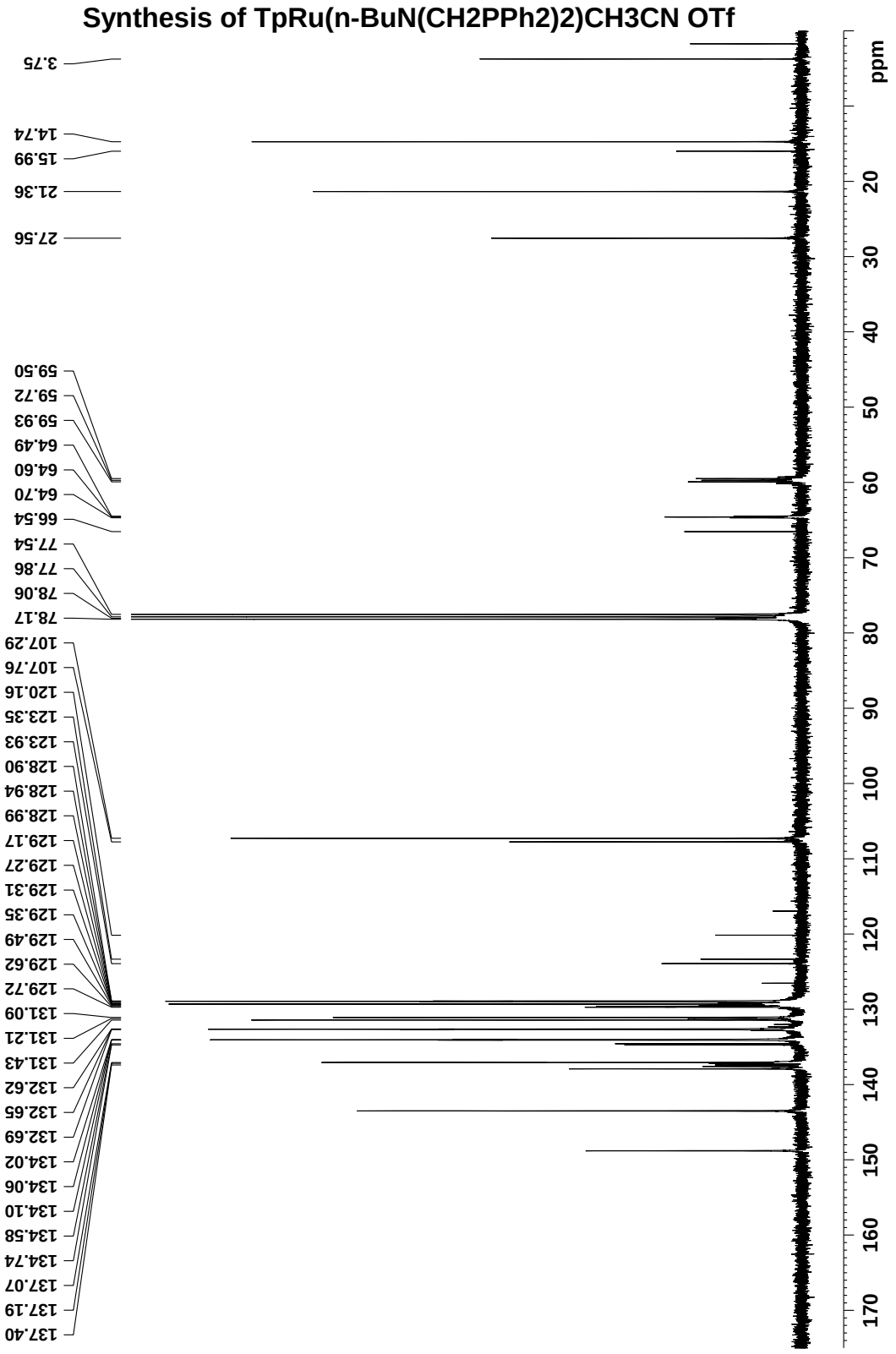

Figure 4.53 $^{13}C\{^{1}H\}$NMR spectrium of [TpRu(^{n}BuN($CH_2PPh_2)_2$)CH_3CN]$^{+}$OTf^{-} (M28)

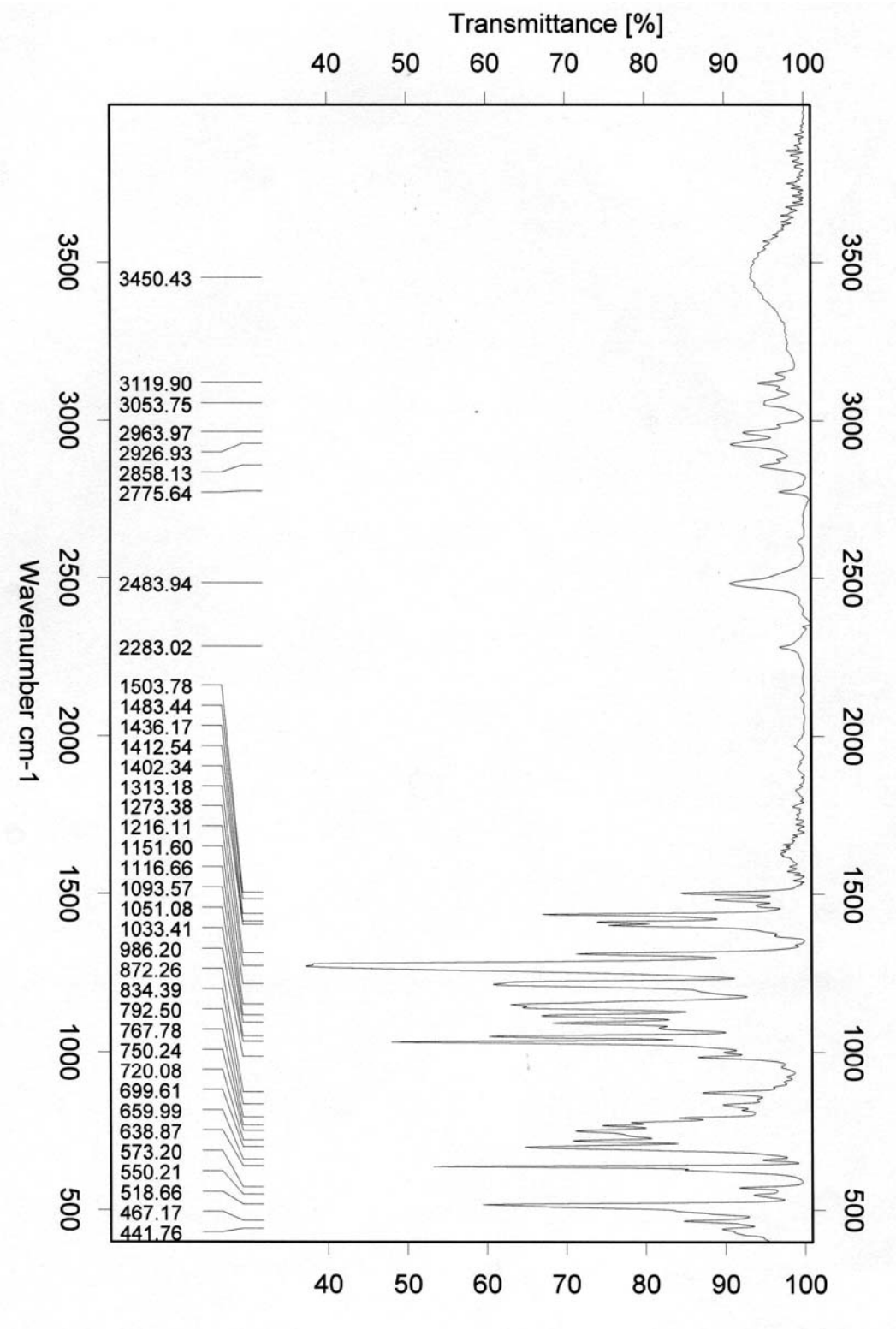

Figure 4.54 Infra-red spectrium of [TpRu(^{n}BuN(CH_2PPh_2)$_2$)CH_3CN]$^{+}$OTf^{-} (M28)

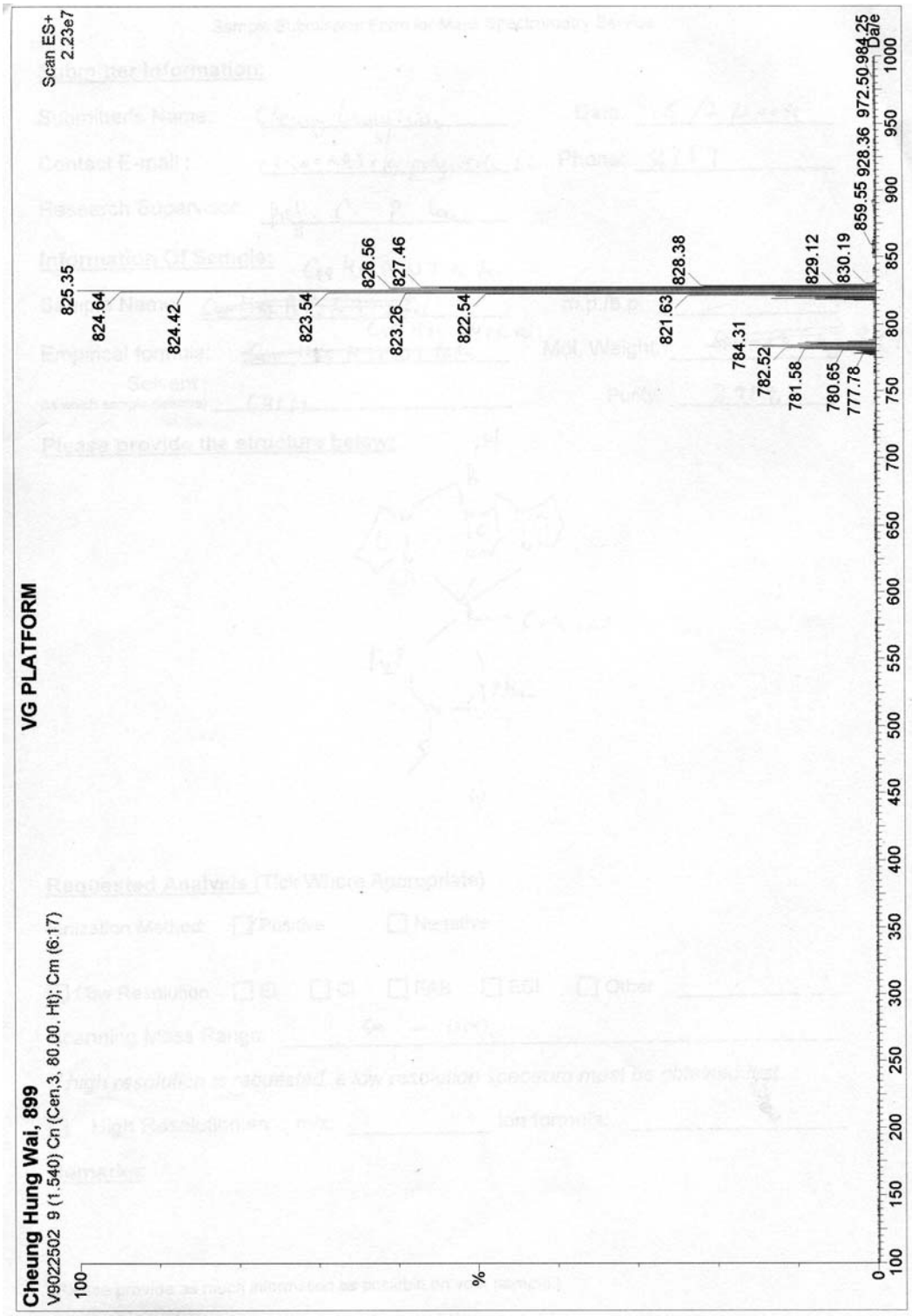

Figure 4.55 Mass spectrium of [TpRu(^{n}BuN(CH_2PPh_2)$_2$)CH_3CN]$^+$OTf$^-$ (M28)

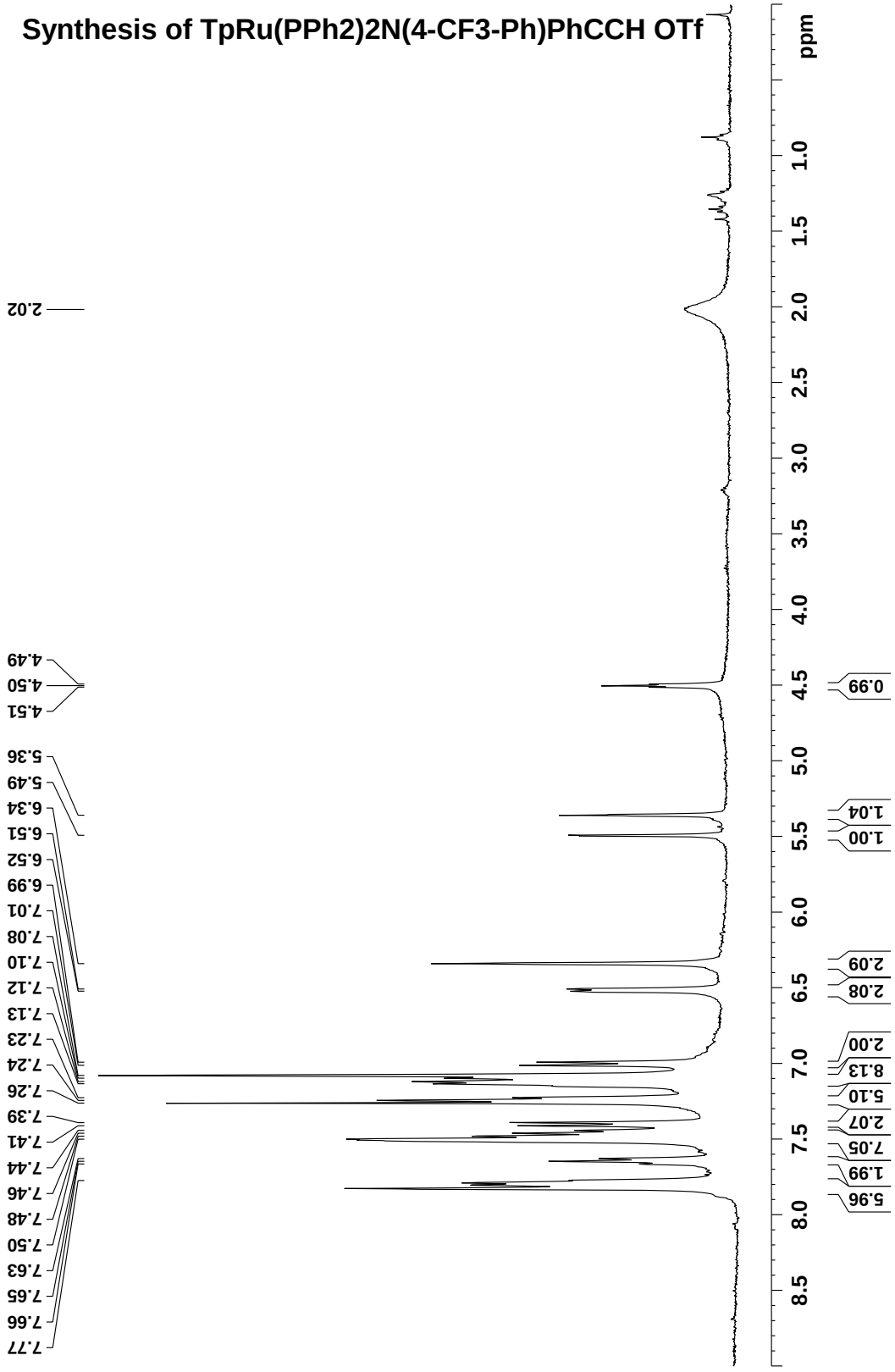

Figure 4.56 ^{1}H NMR spectrium of [TpRu(4-$CF_3C_6H_4N(PPh_2)_2$)(=C=CHPh)]$^{+}$OTf^{-} (M33)

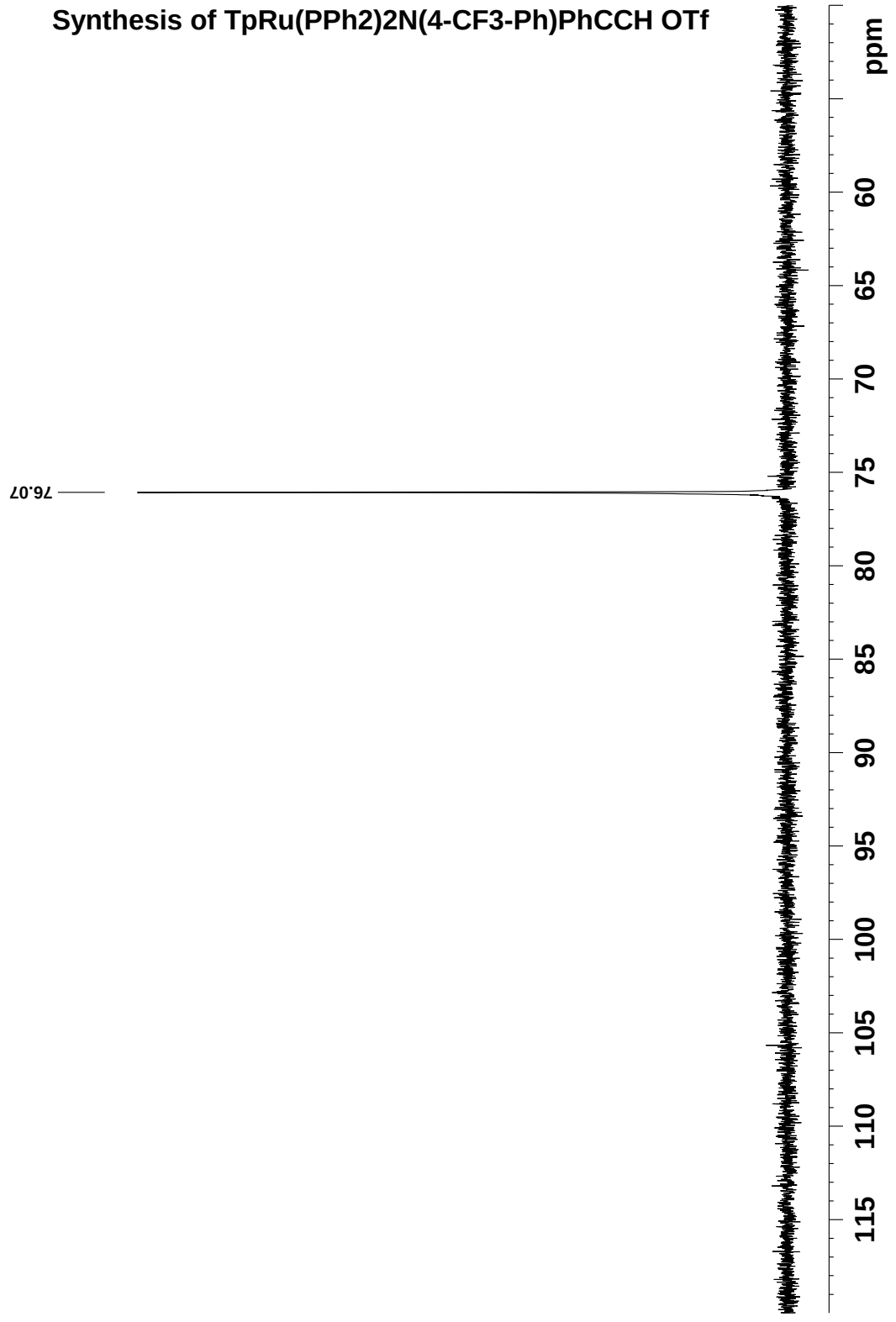

Figure 4.57 $^{31}P\{^{1}H\}$NMR spectrium of [TpRu(4-$CF_3C_6H_4N(PPh_2)_2)(=C=CHPh)]^+OTf^-$ (M33)

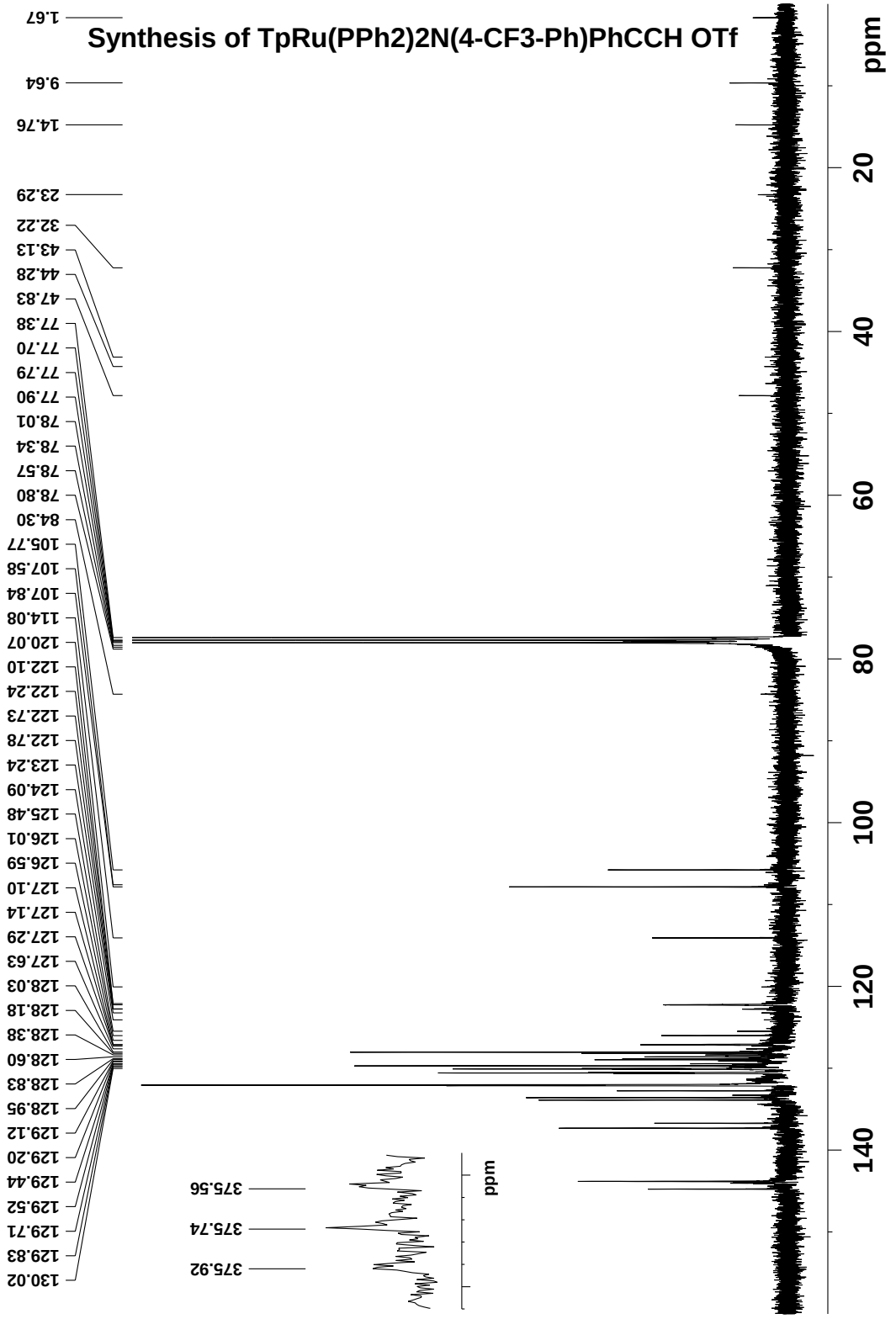

Figure 4.58 $^{13}C\{^{1}H\}$NMR spectrium of [TpRu(4-$CF_3C_6H_4N(PPh_2)_2)(=C=CHPh)]^+OTf^-$ (M33)

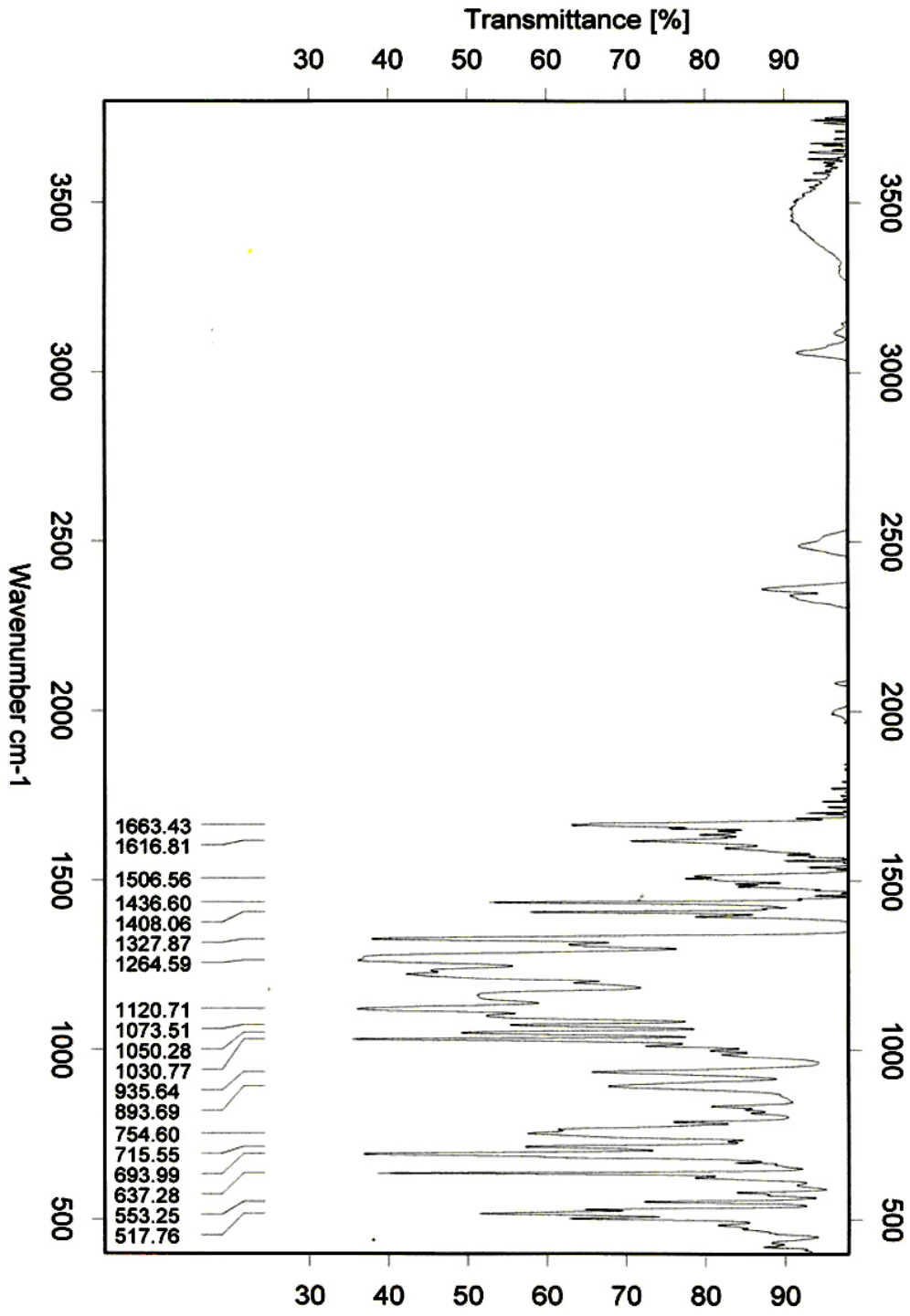

Figure 4.59 Infra-red spectrium of [TpRu(4-$CF_3C_6H_4N(PPh_2)_2$)(=C=CHPh)]$^+$OTf$^-$ (M33)

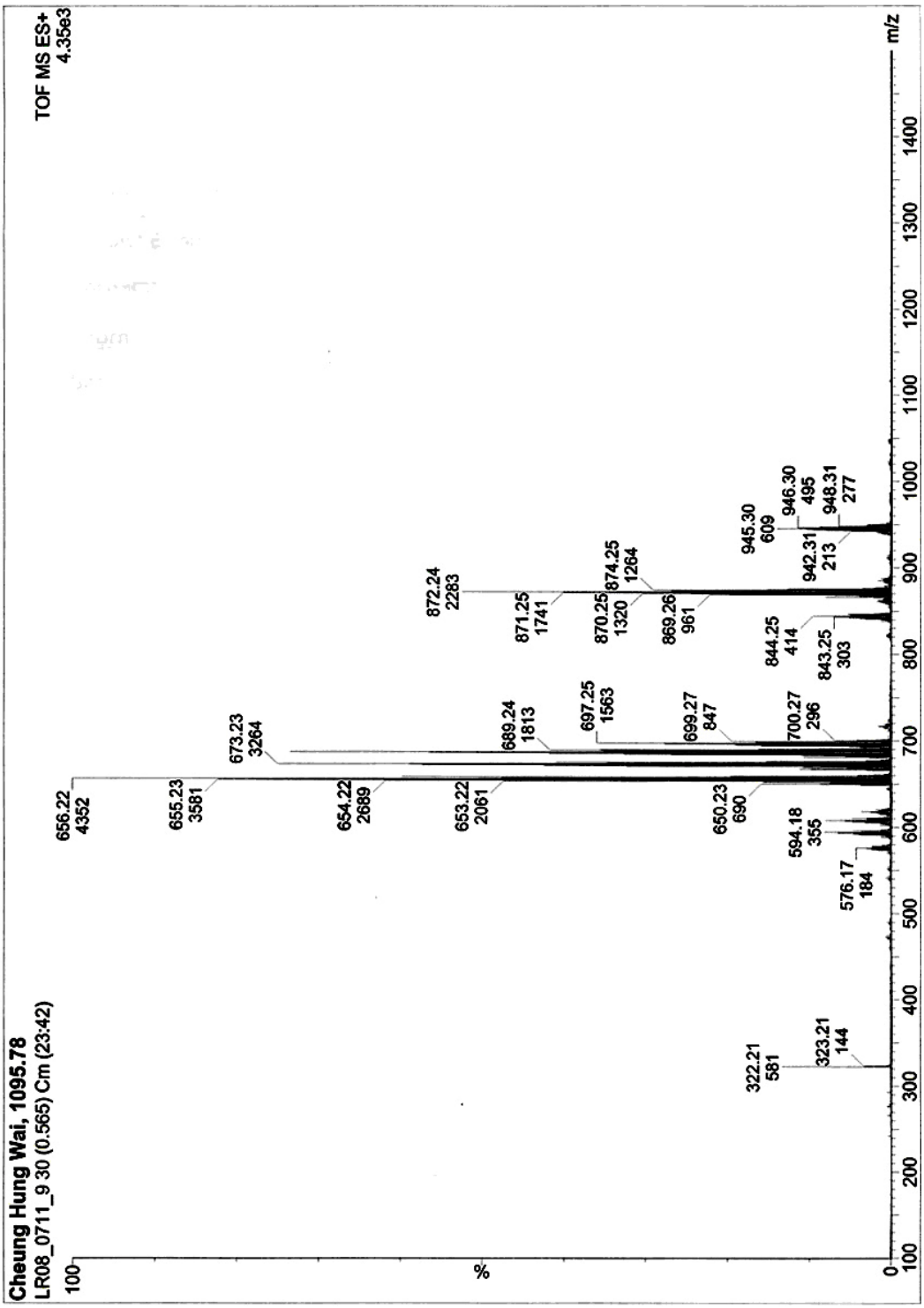

Figure 4.60 Mass spectrium of [TpRu(4-$CF_3C_6H_4N(PPh_2)_2$)(=C=CHPh)]$^+$OTf$^-$ (M33)

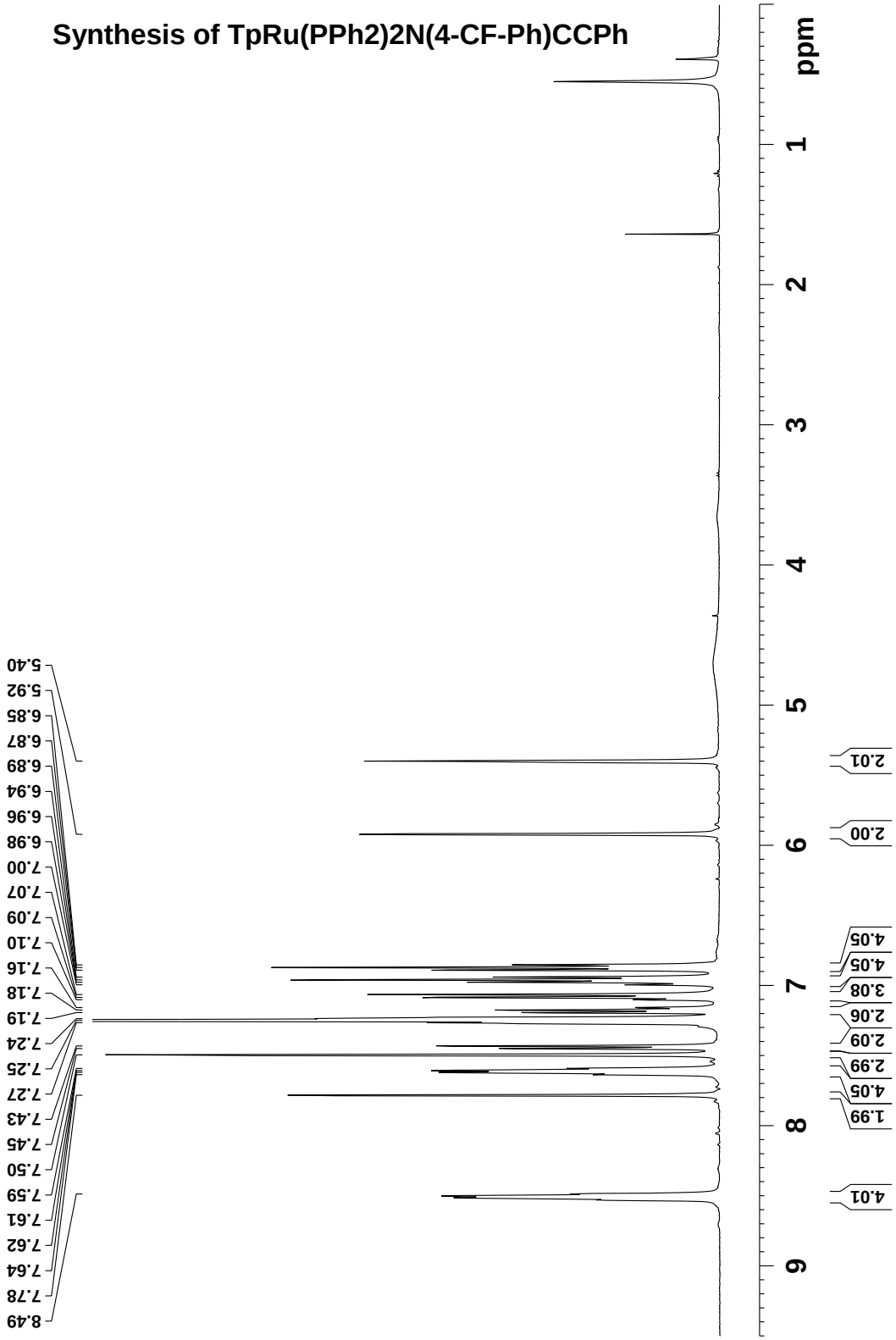

Figure 4.61 ^{1}H NMR spectrium of TpRu(4-$CF_3C_6H_4N(PPh_2)_2$)(C≡CPh) (M34)

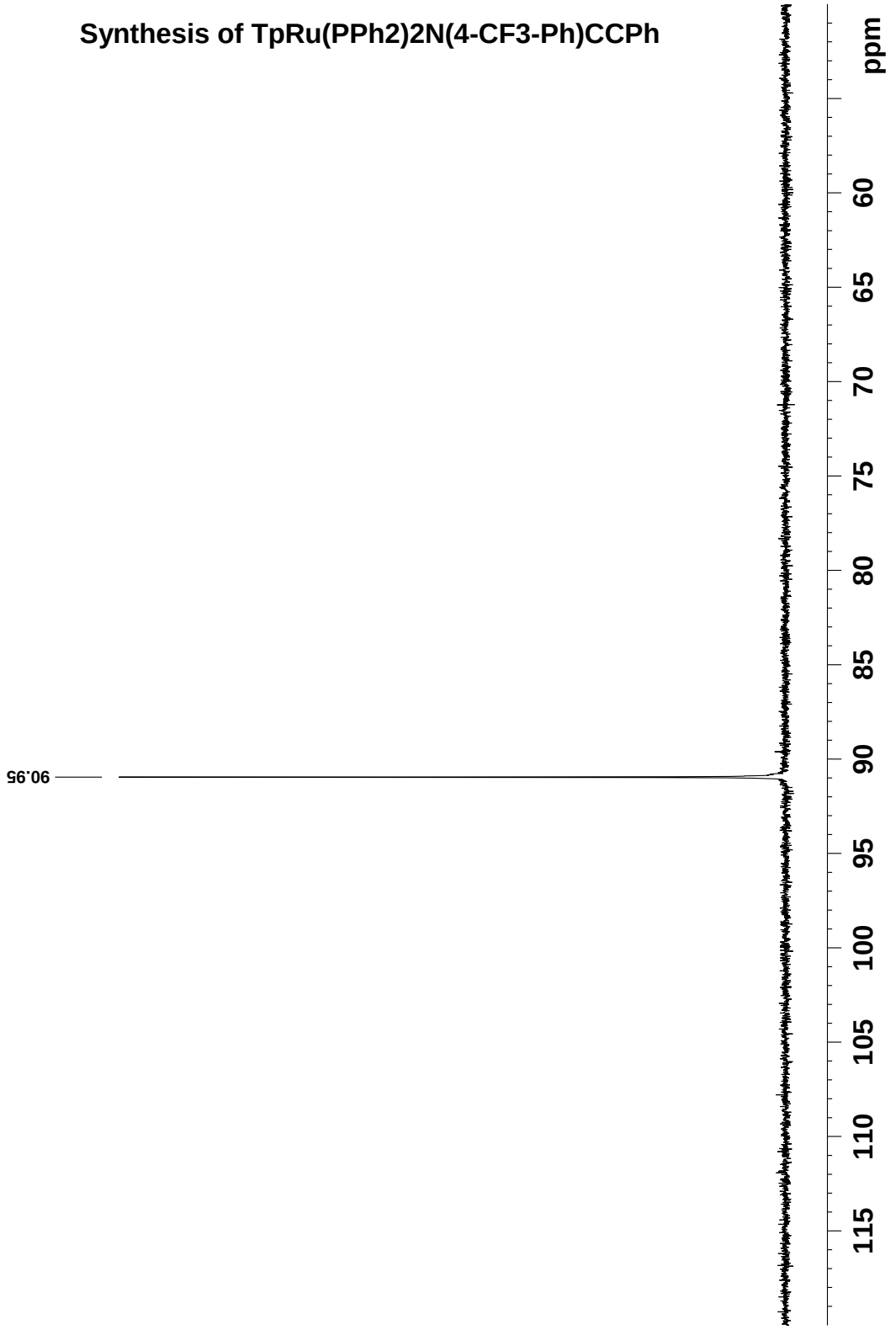

Figure 4.62 $^{31}P\{^{1}H\}$NMR spectrium of TpRu(4-$CF_3C_6H_4N(PPh_2)_2$)(C≡CPh) (M34)

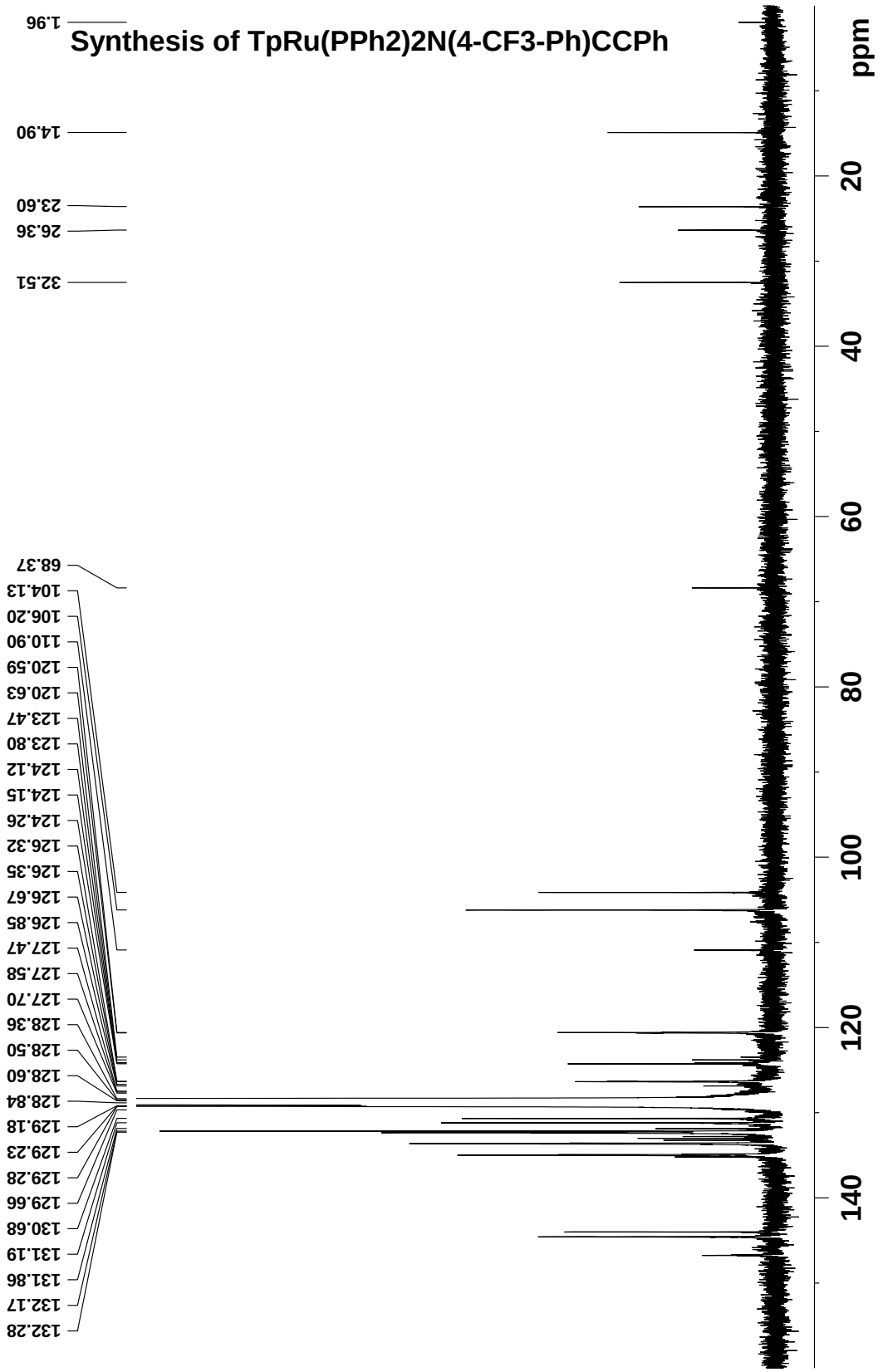

Figure 4.63 $^{13}C\{^{1}H\}$NMR spectrium of TpRu(4-$CF_3C_6H_4N(PPh_2)_2$)(C≡CPh) (M34)

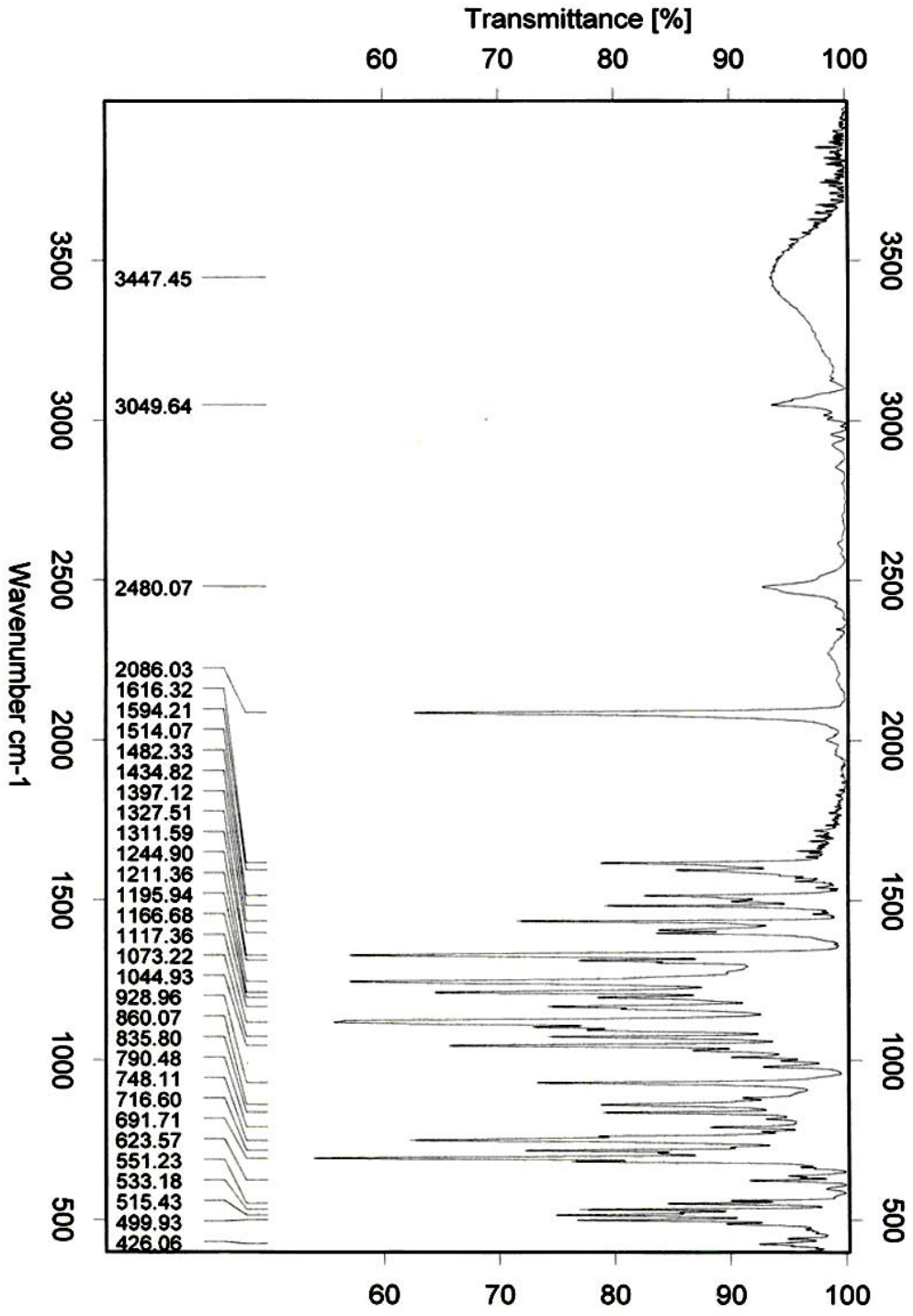

Figure 4.64 Infra-red spectrum of TpRu(4-$CF_3C_6H_4N(PPh_2)_2$)(C≡CPh) (M34)

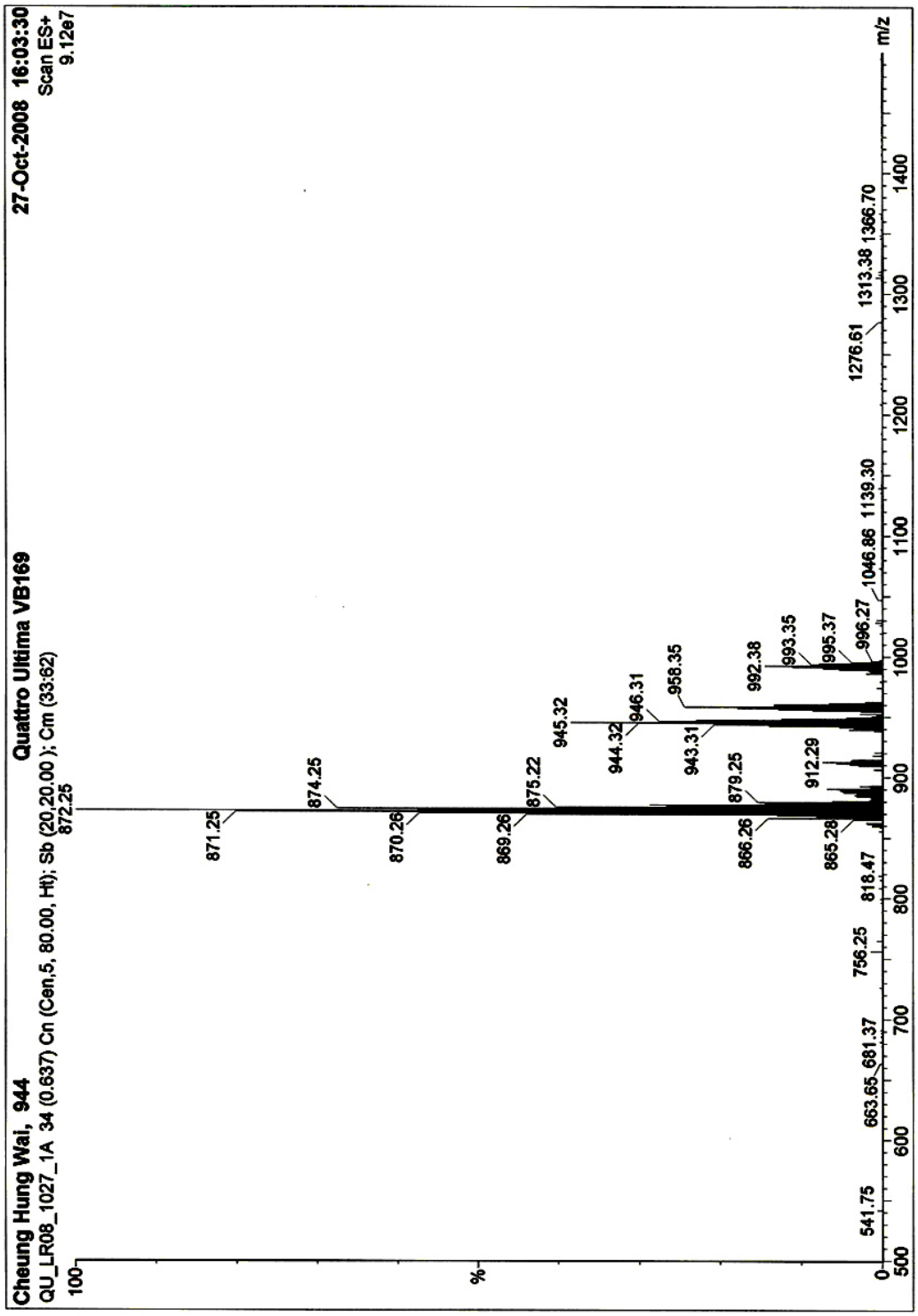

Figure 4.65 Mass spectrium of TpRu(4-$CF_3C_6H_4N(PPh_2)_2$)(C≡CPh) (M34)

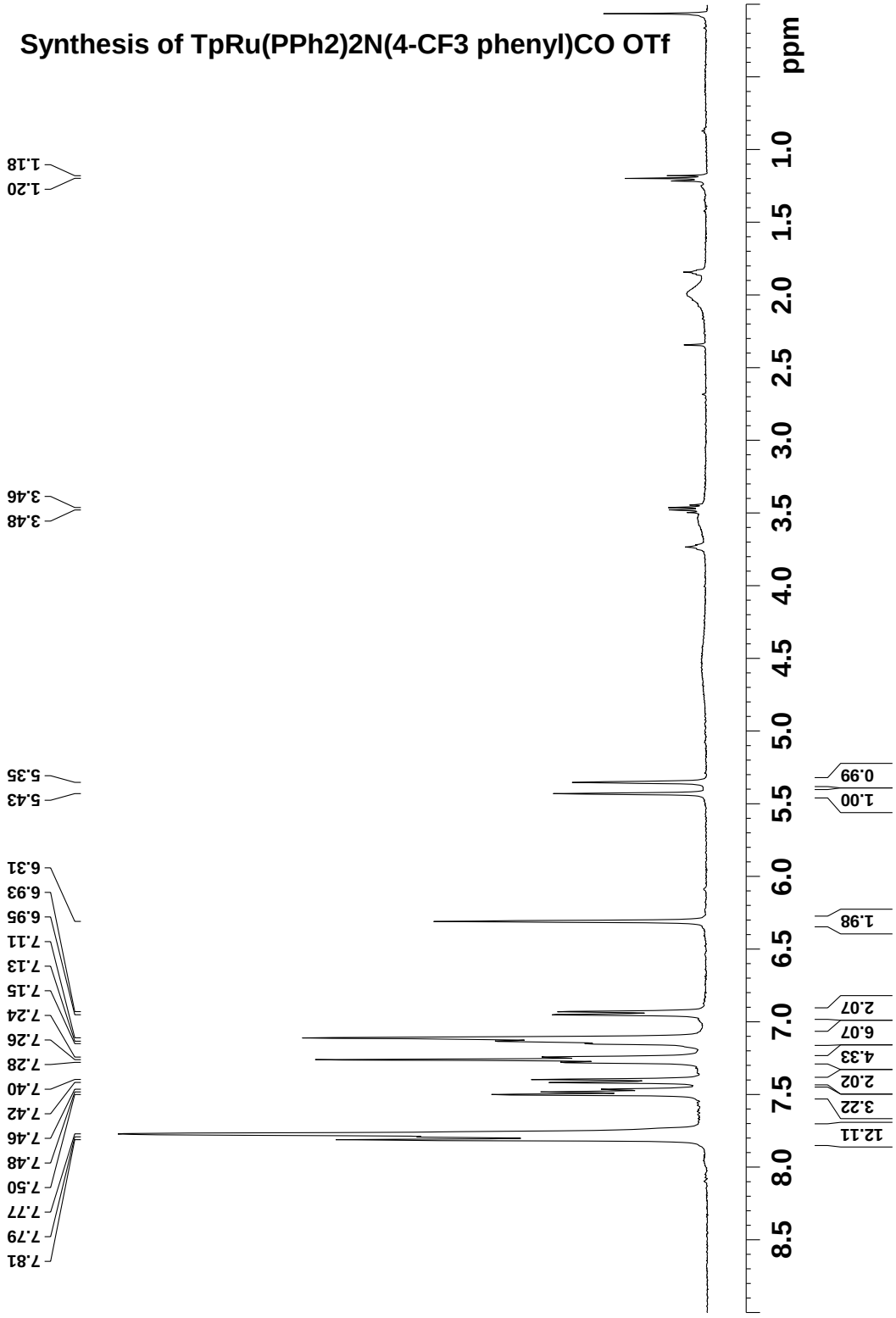

Figure 4.66 ^{1}H NMR spectrum of [TpRu(4-$CF_3C_6H_4N(PPh_2)_2$)(CO)]$^{+}$OTf^{-} (M35)

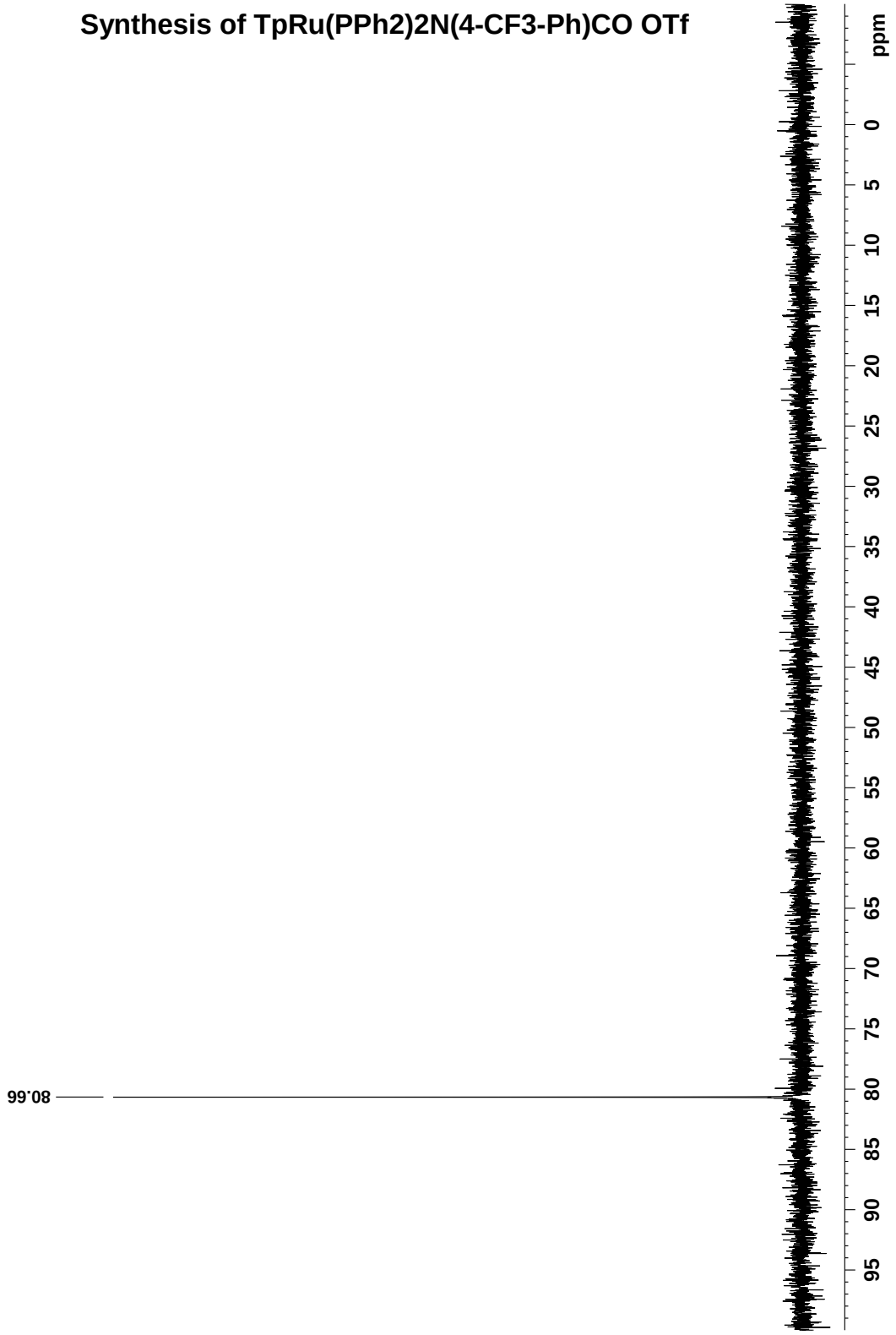

Figure 4.67 $^{31}P\{^{1}H\}$NMR spectrium of $[TpRu(4\text{-}CF_3C_6H_4N(PPh_2)_2)(CO)]^+OTf^-$ (M35)

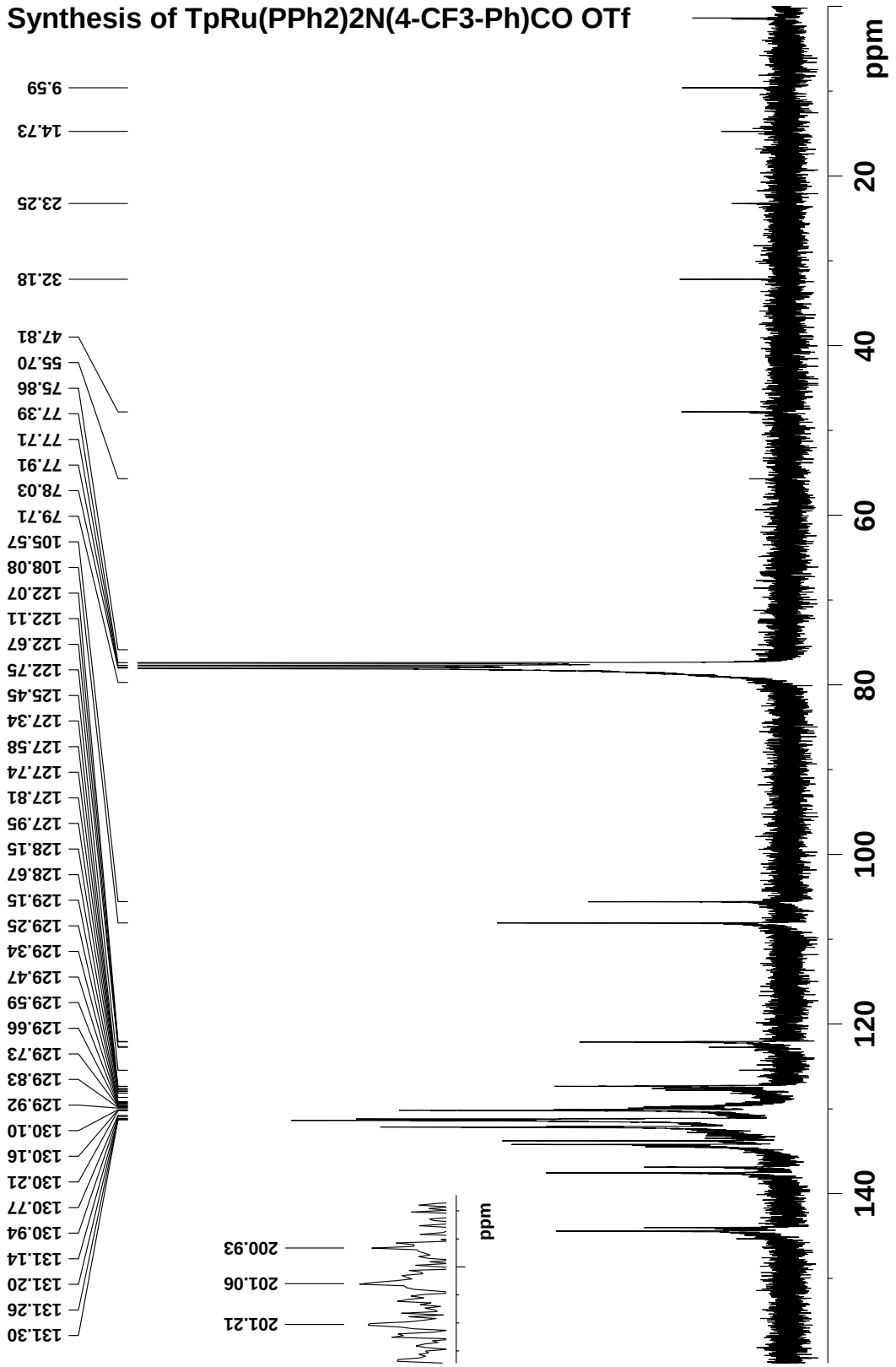

Figure 4.68 $^{13}C\{^{1}H\}$NMR spectrium of $[TpRu(4\text{-}CF_3C_6H_4N(PPh_2)_2)(CO)]^+OTf^-$ (M35)

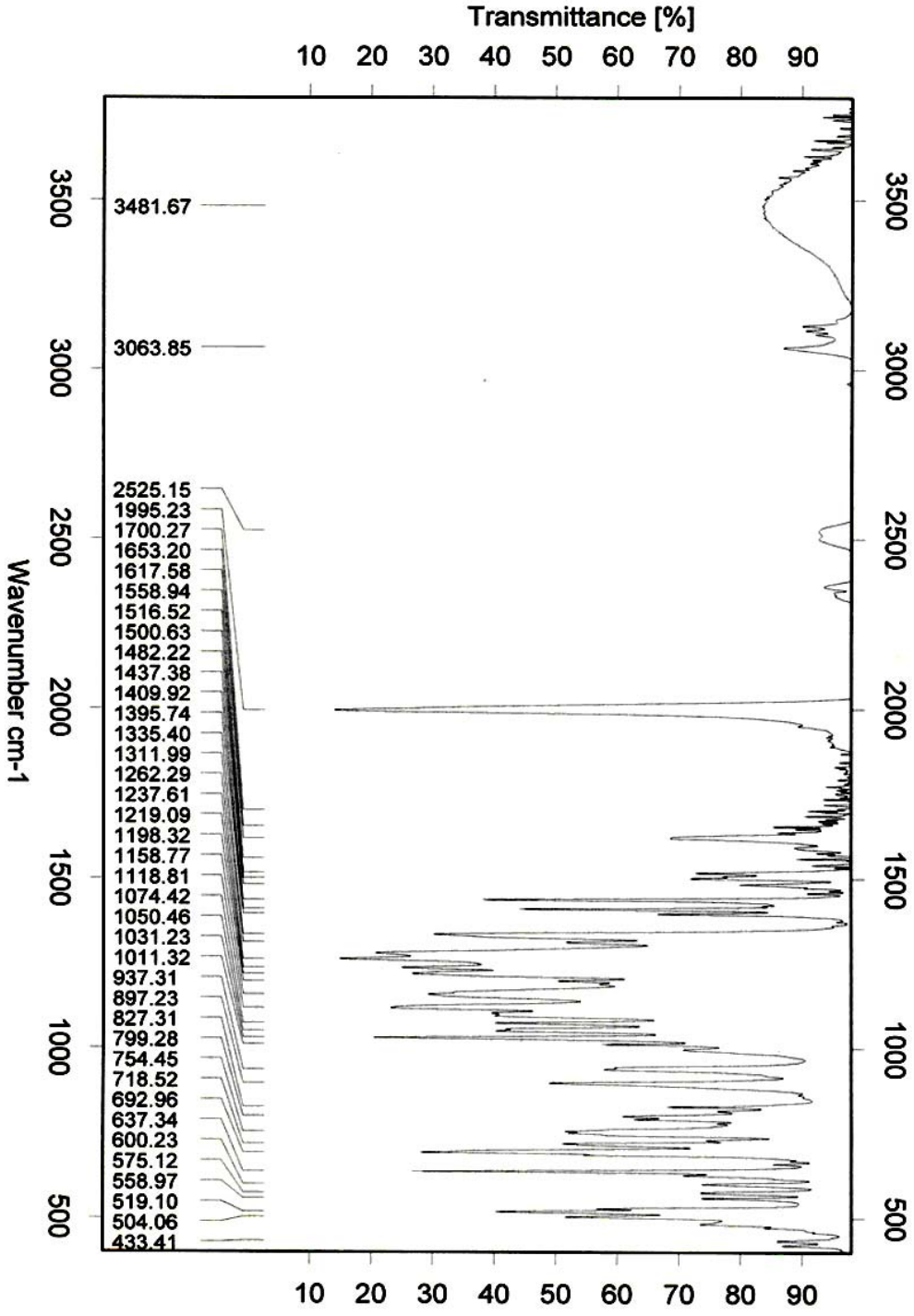

Figure 4.69 Infra-red spectrium of $[TpRu(4\text{-}CF_3C_6H_4N(PPh_2)_2)(CO)]^+OTf^-$ (M35)

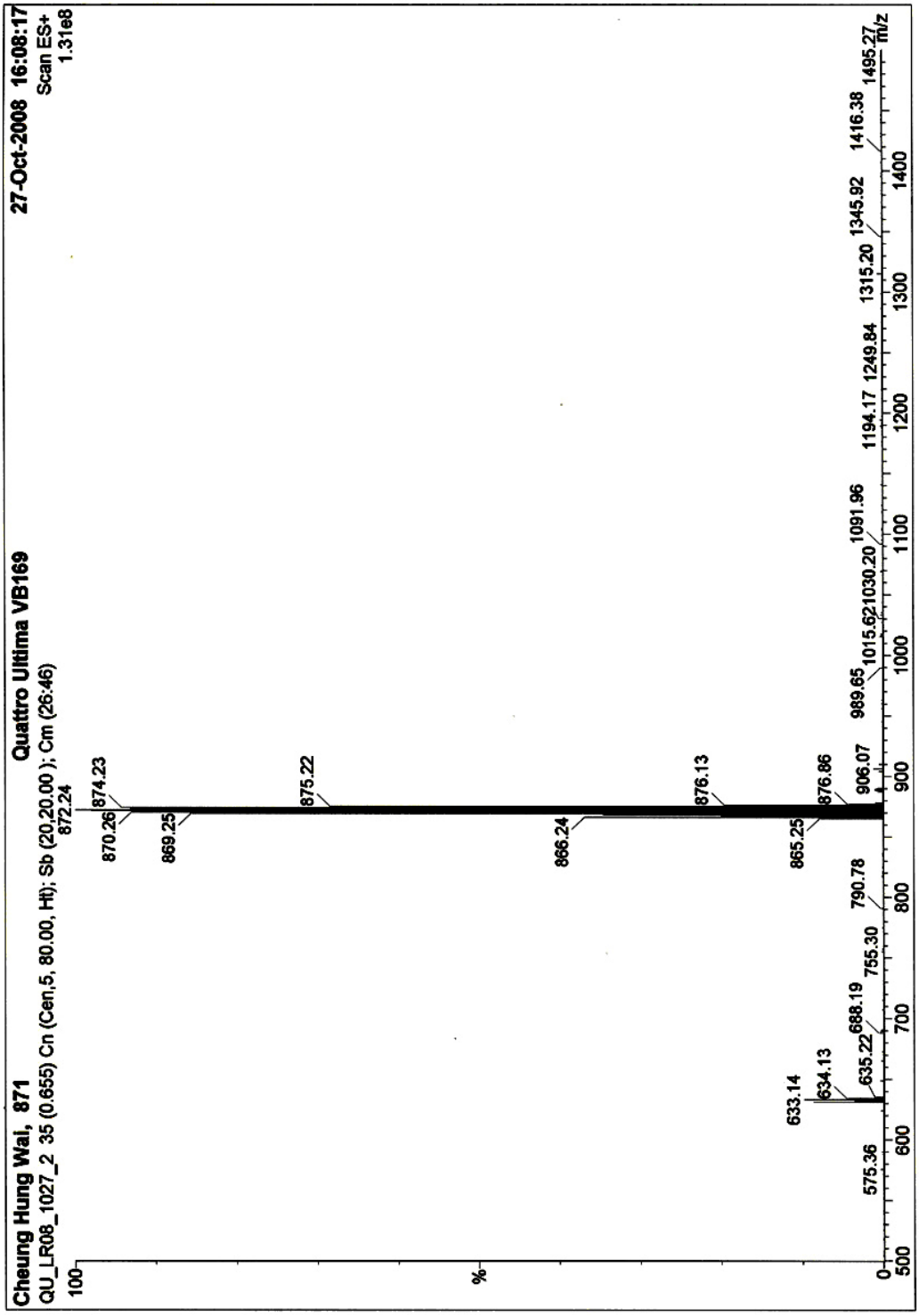

Figure 4.70 Mass spectrium of [TpRu(4-$CF_3C_6H_4N(PPh_2)_2$)(CO)]$^+$OTf$^-$ (M35)

References

1. Burling, S., Whittlesey, M. K., and Williams, J. M. J., Direct and transfer hydrogenation of ketones and imines with a ruthenium N-heterocyclic carbene complex, *Advanced Synthesis & Catalysis*, 2005, 347(4), 591-594.
2. Zassinovich, G., Mestroni, G., and Gladiali, S., Asymmetric Hydrogen Transfer-Reactions Promoted by Homogeneous Transition-Metal Catalysts, *Chemical Reviews*, 1992, 92(5), 1051-1069.
3. Gladiali, S. and Alberico, E., Asymmetric transfer hydrogenation: chiral ligands and applications, *Chemical Society Reviews*, 2006, 35(3), 226-236.
4. Samec, J. S. M., Bäckvall, J. E., Andersson, P. G., and Brandt, P., Mechanistic aspects of transition metal-catalyzed hydrogen transfer reactions, *Chemical Society Reviews*, 2006, 35(3), 237-248.
5. Motokura, K., Fujita, N., Mori, K., Mizugaki, T., Ebitani, K., and Kaneda, K., One-pot synthesis of alpha-alkylated nitriles with carbonyl compounds through consecutive aldol reaction/hydrogenation using a hydrotalcite-supported palladium nanoparticle as a multifunctional heterogeneous catalyst, *Tetrahedron Letters*, 2005, 46(33), 5507-5510.
6. Motokura, K., Fujita, N., Mori, K., Mizugaki, T., Ebitani, K., Htsukawa, K., and Kanedar, K., Environmentally friendly one-pot synthesis of alpha-alkylated nitriles using hydrotalcite-supported metal species as multifunctional solid catalysts, *Chemistry-a European Journal*, 2006, 12(32), 8228-8239.
7. Löfberg, C., Grigg, R., Whittaker, M. A., Keep, A., and Derrick, A., Efficient solvent-free selective monoalkylation of arylacetonitriles with mono-, bis-, and tris-primary alcohols catalyzed by a Cp*Ir complex, *Journal of Organic Chemistry*, 2006, 71(21), 8023-8027.

8. Edwards, M. G. and Williams, J. M. J., Catalytic electronic activation: Indirect "Wittig" reaction of alcohols, *Angewandte Chemie-International Edition*, 2002, 41(24), 4740-4743.

9. Cho, C. S., Kim, B. T., Kim, T. J., and Shim, S. C., An unusual type of ruthenium-catalyzed transfer hydrogenation of ketones with alcohols accompanied by C-C coupling, *Journal of Organic Chemistry*, 2001, 66(26), 9020-9022.

10. Cho, C. S., Kim, B. T., Kim, T. J., and Shim, S. C., Ruthenium-catalyzed regioselective alpha-alkylation of ketones with primary alcohols, *Tetrahedron Letters*, 2002, 43(44), 7987-7989.

11. Martínez, R., Brand, G. J., Ramón, D. J., and Yus, M., $[Ru(DMSO)_4]Cl_2$ catalyzes the alpha-alkylation of ketones by alcohols, *Tetrahedron Letters*, 2005, 46(21), 3683-3686.

12. Martínez, R., Ramón, D. J., and Yus, M., Easy alpha-alkylation of ketones with alcohols through a hydrogen autotransfer process catalyzed by $RuCl_2(DMSO)_4$, *Tetrahedron*, 2006, 62(38), 8988-9001.

13. Kwon, M. S., Khn, N., Seo, S. H., Park, I. S., Cheedrala, R. K., and Park, J., Recyclable palladium catalyst for highly selective alpha alkylation of ketones with alcohols, *Angewandte Chemie-International Edition*, 2005, 44(42), 6913-6915.

14. Taguchi, K., Nakagawa, H., Hirabayashi, T., Sakaguchi, S., and Ishii, Y., An efficient direct alpha-alkylation of ketones with primary alcohols catalyzed by $[Ir(cod)Cl]_2/PPh_3/KOH$ system without solvent, *Journal of the American Chemical Society*, 2004, 126(1), 72-73.

15. Cami-Kobeci, G. and Williams, J. M. J., Substrate activation: Indirect beta-bromination of alcohols, *Synlett*, 2003(1), 124-126.

16. Carlini, C., Di Girolamo, M., Macinai, A., Marchionna, M., Noviello, M., Galletti, A. M. R., and Sbrana, G., Synthesis of isobutanol by the Guerbet condensation of methanol with n-propanol in the presence of heterogeneous and homogeneous palladium-based catalytic systems, *Journal of Molecular Catalysis a-Chemical*, 2003, 204, 721-728.

17. Carlini, C., Macinai, A., Marchionna, M., Noviello, M., Galletti, A. M. R., and Sbrana, G., Selective synthesis of isobutanol by means of the Guerbet reaction - Part 3: Methanol/*n*-propanol condensation by using bifunctional catalytic systems based on nickel, rhodium and ruthenium species with basic components, *Journal of Molecular Catalysis a-Chemical*, 2003, 206(1-2), 409-418.

18. Cho, C. S., Kim, B. T., Kim, H. S., Kim, T. J., and Shim, S. C., Ruthenium-catalyzed one-pot beta-alkylation of secondary alcohols with primary alcohols, *Organometallics*, 2003, 22(17), 3608-3610.

19. Fujita, K., Asai, C., Yamaguchi, T., Hanasaka, F., and Yamaguchi, R., Direct beta-alkylation of secondary alcohols with primary alcohols catalyzed by a Cp*lr complex, *Organic Letters*, 2005, 7(18), 4017-4019.

20. Tolman, C. A., Steric Effects of Phosphorus Ligands in Organometallic Chemistry and Homogeneous Catalysis, *Chemical Reviews*, 1977, 77(3), 313-348.

21. Booth, G., Complexes of the Transition Metals with Phosphines, Arsines, and Stibines, *Advances in Inorganic Chemistry*, 1964, 6, 1-69.

22. Puddephatt, R. J., Chemistry of Bis(Diphenylphosphino)Methane, *Chemical Society Reviews*, 1983, 12(2), 99-127.

23. Chaudret, B., Delavaux, B., and Poilblanc, R., Bisdiphenylphosphinomethane in Dinuclear Complexes, *Coordination Chemistry Reviews*, 1988, 86, 191-243.

24. Wilkinson, G., Stone, F. G. A., and Abel, E. W., *Comprehensive organometallic chemistry : the synthesis, reactions, and structures of organometallic compounds*. 1st ed. 1982, Oxford [Oxfordshire] ; New York: Pergamon Press.

25. Pignolet, L. H., *Homogeneous catalysis with metal phosphine complexes*. Modern inorganic chemistry. 1983, New York: Plenum Press. xvi, 489 p.

26. Osborn, J. A., Jardine, F. H., Young, J. F., and Wilkinso.G, Preparation and Properties of Tris(Triphenylphosphine)Halogenorhodium(1) and Some Reactions Thereof Including Catalytic Homogeneous Hydrogenation of Olefins and Acetylenes and Their Derivatives, *Journal of the Chemical Society a -Inorganic Physical Theoretical*, 1966(12), 1711-1732.

27. Taqui Khan, M. M. and Martell, A. E., *Homogeneous catalysis by metal complexes*. 1974, New York,: Academic Press. 2 v.

28. King, R. B. and Lee, T. W., Metal-Complexes of Fluorophosphines .10. Mononuclear and Binuclear Chromium, Molybdenum, and Tungsten Carbonyl Derivatives of (Alkylamino)Bis(Difluorophosphines), *Inorganic Chemistry*, 1982, 21(1), 319-329.

29. Deleeuw, G., Field, J. S., Haines, R. J., Mcculloch, B., Meintjies, E., Monberg, C., Olivier, G. M., Ramdial, P., Sampson, C. N., Sigwarth, B., Steen, N. D., and Moodley, K. G., Stabilization of [$Fe_2(CO)_9$] and [$Ru_2(CO)_9$] by Substitution with Bridging Diphosphorus Ligands, *Journal of Organometallic Chemistry*, 1984, 275(1), 99-111.

30. Blagg, A., Carr, S. W., Cooper, G. R., Dobson, I. D., Gill, J. B., Goodall, D. C., Shaw, B. L., Taylor, N., and Boddington, T., A Mechanistic Study on Complexes of Type *Mer*-[$Cr(Co)_3(\eta^2$L-L)(σ-L-L)] (Where L-L = $Ph_2PCH_2PPh_2$, $Ph_2PNHPPh_2$, or $Ph_2PNMePPh_2$) Using Spectroscopic and Convolutive Electrochemical

Techniques, *Journal of the Chemical Society-Dalton Transactions*, 1985(6), 1213-1221.

31. Tarassoli, A., Chen, H. J., Thompson, M. L., Allured, V. S., Haltiwanger, R. C., and Norman, A. D., Syntheses of Secondary-Amine-Substituted Bis(Phosphino) Molybdenum Tetracarbonyl Complexes, *Inorganic Chemistry*, 1986, 25(23), 4152-4157.

32. Uson, R., Fornies, J., Navarro, R., and Cebollada, J. I., Mononuclear (Pd,Pt) and Binuclear (Pd,Pd-Pd,Ag-Pt,Ag) Complexes Containing the Bis(Diphenylphosphino)Amine Ligand, *Journal of Organometallic Chemistry*, 1986, 304(3), 381-390.

33. King, R. B., Alkylaminobis(Difluorophosphines) - Novel Bidentate Ligands for Stabilizing Low Metal Oxidation-States and Metal-Metal Bonded Systems, *Accounts of Chemical Research*, 1980, 13(7), 243-248.

34. Keat, R., Manojlovicmuir, L., Muir, K. W., and Rycroft, D. S., Conformations of Diphosphinoamines - Variable-Temperature Nuclear Magnetic-Resonance and X-Ray Crystallographic Studies, *Journal of the Chemical Society-Dalton Transactions*, 1981(11), 2192-2198.

35. Chen, H. J., Barendt, J. M., Haltiwanger, R. C., Hill, T. G., and Norman, A. D., Structural Studies of N-N-Bis(Dichlorophosphino)Phenylamines, *Phosphorus Sulfur and Silicon and the Related Elements*, 1986, 26(2), 155-162.

36. Field, J. S., Haines, R. J., and Sampson, C. N., Electrophilic Attack on a Series of Dinuclear Diphosphazane-Bridged Derivatives of Iron by Halogens - X-Ray Crystal-Structures of $[Fe_2I(CO)_5$-$(\mu$-$(MeO)_2PN(Et)P(OMe)_2)_2]PF_6$ and $[Fe_2(\mu$-$Br)(CO)_4$(Mu-$(PhO)_2PN(Et)$-$P(OPh)_2)_2]PF_6$, *Journal of the Chemical Society-Dalton Transactions*, 1987(8), 1933-1945.

37. Noth, H. and Meinel, L., Amino-Phosphane. VIII. Octaphenyltertraphosphor nitrid chlorid and Tetraphenyldiphosphin-N-Diphenylphosphino-Imid, *Zeitschrift Fur Anorganische Und Allgemeine Chemie*, 1967, 349(5-6), 225-240.

38. Ewart, G., Lane, A. P., Payne, D. S., and Mckechnie, J., Tervalent Phosphorus-Nitrogen Chemistry. II. Mono- and Bis-(Diphenylphosphino) Alkylamines, *Journal of the Chemical Society*, 1964(May), 1543-1547.

39. Nixon, J. F., Phosphorus-Fluorine Compounds .X. Alkylaminobisdichloro- and Alkylaminobisdifluoro-Phosphines, *Journal of the Chemical Society a -Inorganic Physical Theoretical*, 1968(11), 2689-2692.

40. Johnson, T. R. and Nixon, J. F., Phosphorus-Fluorine Chemistry .16. Phosphorus-Phosphorus Coupling Constants, 2j(PMP') in Ethylaminobisdifluorophosphine Complexes of Chromium, Molybdenum, and Tungsten Carbonyls, *Journal of the Chemical Society a -Inorganic Physical Theoretical*, 1969(17), 2518-2520.

41. Hedberg, E., Hedberg, L., and Hedberg, K., Electron-Diffraction Investigation of Molecular-Structure of Gaseous Methylaminobis(Difluorophosphine), $CH_3N(PF_2)_2$, *Journal of the American Chemical Society*, 1974, 96(14), 4417-4421.

42. King, R. B. and Chen, K. N., Cyclopentadienylbis[Methylaminobis(Difluorophosphine)] Vanadium - 1st Fully Substituted Cyclopentadienylteracarbonylvanadium Derivative, *Inorganica Chimica Acta*, 1977, 23(1), L19-L20.

43. Payne, D. S., Mokuolu, J. A. A., and Speakman, J. C., X-Ray Studies of Aminophosphine Complexes of Molybdenum and Palladium and of an Aminophosphonium Iodide, *Chemical Communications*, 1965(23), 599.

44. Payne, D. S. and Walker, A. P., Tervalent Phosphorus-Nitrogen Chemistry . Part III. Molybdenum Carbonyl Complexes of Bis(Diphenylphosphino)Alkylamines, *Journal of the Chemical Society C-Organic*, 1966(5), 498-499.

45. Balakrishna, M. S., Prakasha, T. K., Krishnamurthy, S. S., Siriwardane, U., and Hosmane, N. S., Organometallic Derivatives of Diphosphinoamines, $X_2PN(R)PX_2$ - Reactions with Carbonyl Derivatives of Group-6 Metals and Iron Pentacarbonyl - the Crystal-Structures of $[Mo(CO)_4PhN(P(OPh)_2)_2]$ and $[W(CO)_4$-$^{i}PrN(PPh_2)_2]$, *Journal of Organometallic Chemistry*, 1990, 390(2), 203-216.

46. King, R. B. and Gimeno, J., Tris[Methylaminobis(Difluorophosphine)]Metal(0) Derivatives of Chromium, Molybdenum, and Tungsten - New Volatile Carbonyl-Free Zerovalent Metal Derivatives of High Thermal and Oxidative Stabilities, *Journal of the Chemical Society-Chemical Communications*, 1977(5), 142-143.

47. King, R. B. and Gimeno, J., Metal-Complexes of Fluorophosphines .4. Reactions of Mononuclear Metal-Carbonyls with Methylaminobis(Difluorophosphine), *Inorganic Chemistry*, 1978, 17(9), 2390-2395.

48. King, R. B. and Gimeno, J., Metal-Complexes of Fluorophosphines .5. Reactions of Mononuclear Cyclopentadienylmetal Carbonyls with Methylaminobis(Difluorophosphine), *Inorganic Chemistry*, 1978, 17(9), 2396-2400.

49. Derringer, D. R., Fanwick, P. E., Moran, J., and Walton, R. A., Dirhenium Complexes Containing Pairs of Bridging Acetate and Bis(Diphenylphosphino)Amine Ligands. Cis and Trans Isomers of the Type $[Re_2(O_2CCH_3)_2X_2(Ph_2PNHPh_2)_2]^{n+}$ (X = Cl, Br-N = 0, 1), *Inorganic Chemistry*, 1989, 28(7), 1384-1389.

50. Costello, M. T., Derringer, D. R., Fanwick, P. E., Price, A. C., Rivera, M. I., Scheiber, E., Siurek, E. W., and Walton, R. A., Studies Directed Towards the Isolation and Characterization of the Paramagnetic Cations $[Re_2X_4(LL)_2]^+$ (X = Cl or Br; LL = $Ph_2PCH_2PPh_2$, $Ph_2As_2CH_2AsPh_2$ or $Ph_2PNHPPh_2$), and the Crystal-Structure of $Re_2Cl_4(Ph_2PNHPPh_2)_2.(CH_3)_2CO$, *Polyhedron*, 1990, 9(4), 573-580.

51. Haines, R. J. and Dupreez, A. L., Reactions of Metal Carbonyl Derivatives .II. Ditertiary Phosphine and Arsine Derivatives of Tetracarbonyldi-Pi-Cyclopentadienyldiiron, *Journal of Organometallic Chemistry*, 1970, 21(1), 181-193.

52. Deleeuw, G., Field, J. S., Haines, R. J., Mcculloch, B., Meintjies, E., Monberg, C., Moodley, K. G., Olivier, G. M., Sampson, C. N., and Steen, N. D., Substituted Derivatives of $[Fe_2(CO)_9]$ and $[Ru_2(CO)_9]$ and Their Susceptibility to Electrophilic Attack - X-Ray Crystal-Structure of $[Fe_2(\mu\text{-}Br)(CO)_4\{\mu\text{-}(C_6H_5O)_2PN(C_2H_5)P(OC_6H_5)_2\}_2]PF_6$, *Journal of Organometallic Chemistry*, 1982, 228(3), C66-C70.

53. Engel, D. W., Moodley, K. G., Subramony, L., and Haines, R. J., Reaction of Triruthenium Dodecacarbonyl with Bis(Dimethylphosphino) Methane, Bis(Diphenylphosphino) Methane and Bis(Diphenylphosphino)-Ethylamine under Photochemical Conditions, *Journal of Organometallic Chemistry*, 1988, 349(3), 393-403.

54. Sanchez-Cabrera, G., Garcia-Baez, E. V., and Rosales-Hoz, M. J., The reaction of $[Ru_3(CO)_{12}]$ with bis(diphenylphosphino)amine. The crystal and molecular structure of $[Ru_3(CO)_{10}(dppa)]$ and $[Ru_3(CO)_8(dppa)_2]$, *Journal of Organometallic Chemistry*, 2000, 599(2), 313-316.

55. Balakrishna, M. S., Ramaswamy, K., and Abhyankar, R. M., Transition metal chemistry of phosphorus based ligands. Ruthenium(II) chemistry of bis(phosphino)amines, $X_2PN(R)PX_2$ (R = H or Ph, X = Ph; R = Ph, $X_2 = O_2C_6H_4$), *Journal of Organometallic Chemistry*, 1998, 560(1-2), 131-136.

56. Brown, G. M., Finholt, J. E., King, R. B., and Bibber, J. W., Poly(tertiary phosphines and arsines).18. Preparation and Structure of Bis(μ-[(Methylamino)Bis(Dimethoxyphosphine)])-Bis(Dicarbonylcobalt), a Binuclear Complex with Approximate Square-Pyramidal and Trigonal-Bipyramidal Coordination of Cobalt Atoms in the Same Molecule, *Inorganic Chemistry*, 1982, 21(6), 2139-2145.

57. Deleeuw, G., Field, J. S., and Haines, R. J., $[Co_2(CO)_4\{\mu(CH_2O)_2PN(Et)P(OCH_2)_2\}_2]$ - a Molecule with a Symmetrical Formula but an Unsymmetrical Structure, *Journal of Organometallic Chemistry*, 1989, 359(2), 245-254.

58. Field, J. S., Haines, R. J., and Rix, L. A., Protonation of Electron-Rich Diphosphazane-Bridged Derivatives of Dicobalt Octacarbonyl - Crystal-Structure of $[Co_2(\mu\text{-}H)(Co)_4\{\mu\text{-}(MeO)2PN(Et)P(OMe)_2\}_2]BPh_4.CH_2Cl_2$, *Journal of the Chemical Society-Dalton Transactions*, 1990(7), 2311-2314.

59. Werner, H., Lippert, F., Peters, K., and Vonschnering, H. G., Synthesis and Reactions of the Metal Base $[(C_5Me_4H)Co(PMe_3)_2]$, *Chemische Berichte-Recueil*, 1992, 125(2), 347-352.

60. Haines, R. J. and Meintjies, E., Synthesis and Reactivity of Some 2-Ethyltetraphenoxydiphosphazane Derivatives of Rhodium, *Journal of the Chemical Society-Dalton Transactions*, 1979(2), 367-370.

61. Mague, J. T. and Lloyd, C. L., Cationic Complexes of Rhodium(I) and Iridium(I) with Methylbis and Phenylbis(Dimethoxyphosphino)Amine, *Organometallics*, 1988, 7(4), 983-993.

62. Mague, J. T. and Johnson, M. P., Chemistry of Bis(Dialkoxyphosphino)Methylamines - Monometallic and Bimetallic Complexes of Chromium(0), Molybdenum(0), Tungsten(0), Rhodium(I), and Ruthenium(II), *Organometallics*, 1990, 9(4), 1254-1269.

63. Mague, J. T., Heterobimetallic Complexes Derived from [(η^5-C_5H_5)FeCl{$CH_3N(PF_2)_2$}$_2$] - Crystal and Molecular-Structure of [(η^5-C_5H_5)Fe{μ-$CH_3N(PF_2)_2$}$_2$$IrCl_2${$P(CH_3)2C_6H_5$}], *Organometallics*, 1991, 10(2), 513-516.

64. Seidel, W. and Alexiev, M., Complex-Formation with Aminophosphines .9. Fourfold and Fivefold Coordinated Nickel(Ii) Complexes of Bidentate N,N-Bis(Diphenylphosphino)Phenylamine, *Zeitschrift Fur Anorganische Und Allgemeine Chemie*, 1978, 438(1), 68-74.

65. Kuhn, N. and Winter, M., Synthesis and Reactivity of Dienyl Metal-Compounds .III. Phosphinous-Acid Imides as Ligands in Cyclopentadienylnickel Complexes, *Journal of Organometallic Chemistry*, 1982, 229(3), C33-C36.

66. Mokuolu, J. A. A., Payne, D. S., and Speakman, J. C., Crystal and Molecular-Structure of Dichloro[Bis(Diphenylphosphino)-Ethylamine]Palladium(II), *Journal of the Chemical Society-Dalton Transactions*, 1973(14), 1443-1445.

67. Haines, R. J., Pidcock, A., and Safari, M., Complexes of Palladium and Platinum with Tetraethyl Diphosphite and Related Ligands, *Journal of the Chemical Society-Dalton Transactions*, 1977(8), 830-832.

68. Balakrishna, M. S., Krishnamurthy, S. S., Murugavel, R., Nethaji, M., and Mathews, I. I., Organometallic Chemistry of Diphosphazanes .7. Platinum(II),

Palladium(0), Palladium(I) and Palladium(II) Complexes of $RN[P(OPh)_2]_2$ (R = Me or Ph), *Journal of the Chemical Society-Dalton Transactions*, 1993(3), 477-482.

69. Dossett, S. J., Gillon, A., Orpen, A. G., Fleming, J. S., Pringle, P. G., Wass, D. F., and Jones, M. D., Steric activation of chelate catalysts: efficient polyketone catalysts based on four-membered palladium(II) diphosphine chelates, *Chemical Communications*, 2001(8), 699-700.

70. Cooley, N. A., Green, S. M., Wass, D. F., Heslop, K., Orpen, A. G., and Pringle, P. G., Nickel ethylene polymerization catalysts based on phosphorus ligands, *Organometallics*, 2001, 20(23), 4769-4771.

71. Carter, A., Cohen, S. A., Cooley, N. A., Murphy, A., Scutt, J., and Wass, D. F., High activity ethylene trimerisation catalysts based on diphosphine ligands, *Chemical Communications*, 2002(8), 858-859.

72. Bollmann, A., Blann, K., Dixon, J. T., Hess, F. M., Killian, E., Maumela, H., McGuinness, D. S., Morgan, D. H., Neveling, A., Otto, S., Overett, M., Slawin, A. M. Z., Wasserscheid, P., and Kuhlmann, S., Ethylene tetramerization: A new route to produce 1-octene in exceptionally high selectivities, *Journal of the American Chemical Society*, 2004, 126(45), 14712-14713.

73. Blann, K., Bollmann, A., Dixon, J. T., Hess, F. M., Killian, E., Maumela, H., Morgan, D. H., Neveling, A., Otto, S., and Overett, M. J., Highly selective chromium-based ethylene trimerisation catalysts with bulky diphosphinoamine ligands, *Chemical Communications*, 2005(5), 620-621.

74. Overett, M. J., Blann, K., Bollmann, A., Dixon, J. T., Hess, F., Killian, E., Maumela, H., Morgan, D. H., Neveling, A., and Otto, S., Ethylene trimerisation

and tetramerisation catalysts with polar-substituted diphosphinoamine ligands, *Chemical Communications*, 2005(5), 622-624.

75. Blann, K., Bollmann, A., de Bod, H., Dixon, J. T., Killian, E., Nongodlwana, P., Maumela, M. C., Maumela, H., McConnell, A. E., Morgan, D. H., Overett, M. J., Pretorius, M., Kuhlmann, S., and Wasserscheid, P., Ethylene tetramerisation: Subtle effects exhibited by *N*-substituted diphosphinoamine ligands, *Journal of Catalysis*, 2007, 249(2), 244-249.

76. Wakatsuki, Y., Koga, N., Yamazaki, H., and Morokuma, K., Acetylene π-Coordination, Slippage to Sigma-Coordination, and 1,2-Hydrogen Migration Taking Place on a Transition-Metal - the Case of a Ru(II) Complex as Studied by Experiment and Ab-Initio Molecular-Orbital Simulations, *Journal of the American Chemical Society*, 1994, 116(18), 8105-8111.

77. Touchard, D., Haquette, P., Pirio, N., Toupet, L., and Dixneuf, P. H., New Ruthenium Vinylidene Complexes as Intermediates for the Access to Sigma-Acetylide and Unsymmetrical Trans-Diynyl, Alkynyl Metal-Complexes - Crystal-Structures of $[(Ph_2PCH_2PPh_2)_2(Cl)Ru=C=CH_2]PF_6$ and $[(Ph_2PCH_2PPh_2)_2(Cl)RuC=CH]$ Complexes, *Organometallics*, 1993, 12(8), 3132-3139.

78. deLosRios, I., Tenorio, M. J., Puerta, M. C., and Valerga, P., Alternative mechanisms of the alkyne to vinylidene isomerization promoted by half-sandwich ruthenium complexes. X-ray crystal structures of $[Cp^*Ru=C=CHCOOMe(dippe)][BPh_4]$ and $[Cp^*RuH(C\equiv CCOOMe)(dippe)][BPh_4]$ (dippe=1,2-bis(diisopropylphosphino)ethane; Cp*=C5Me5), *Journal of the American Chemical Society*, 1997, 119(28), 6529-6538.

79. Antonova, A. B. and Ioganson, A. A., Complexes of Transition-Metals with Unsaturated Carbenes - Synthesis, Structure and Reactivity, *Uspekhi Khimii*, 1989, 58(7), 1197-1229.

80. Wakatsuki, Y., Mechanistic aspects regarding the formation of metal vinylidenes from alkynes and related reactions, *Journal of Organometallic Chemistry*, 2004, 689(24), 4092-4109.

81. Bustelo, E., Carbo, J. J., Lledos, A., Mereiter, K., Puerta, M. C., and Valerga, P., First X-ray characterization and theoretical study of π-alkyne, alkynyl-hydride, and vinylidene isomers for the same transition metal fragment [Cp*Ru(PEt_3)$_2$], *Journal of the American Chemical Society*, 2003, 125(11), 3311-3321.

82. Knifton, J. F., Alpha,Beta-Unsaturated Carboxylic Esters from Alkynes Catalyzed by Homogeneous Palladium Complexes, *Journal of Molecular Catalysis*, 1977, 2(4), 293-299.

83. Jayasree, S., Seayad, A., Gupte, S. P., and Chaudhari, R. V., A novel palladium complex catalyst for carbonylation of alkynes under mild conditions, *Catalysis Letters*, 1999, 58(4), 213-216.

84. Tsuji, Y., Kondo, T., and Watanabe, Y., Platinum Complex-Catalyzed Carbonylation of Acetylenic-Compounds, *Journal of Molecular Catalysis*, 1987, 40(3), 295-304.

85. Kennedy-Smith, J. J., Staben, S. T., and Toste, F. D., Gold(I)-catalyzed conia-ene reaction of beta-ketoesters with alkynes, *Journal of the American Chemical Society*, 2004, 126(14), 4526-4527.

86. Gao, Q., Zheng, B. F., Li, J. H., and Yang, D., Ni(II)-catalyzed conia-ene reaction of 1,3-dicarbonyl compounds with alkynes, *Organic Letters*, 2005, 7(11), 2185-2188.

87. Nakamura, M., Endo, K., and Nakamura, B., Indium-catalyzed addition of active methylene compounds to 1-alkynes, *Journal of the American Chemical Society*, 2003, 125(43), 13002-13003.

88. Endo, K., Hatakeyama, T., Nakamura, M., and Nakamura, E., Indium-catalyzed 2-alkenylation of 1,3-dicarbonyl compounds with unactivated alkynes, *Journal of the American Chemical Society*, 2007, 129(16), 5264-5271.

89. Kuninobu, Y., Kawata, A., and Takai, K., Rhenium-catalyzed insertion of terminal acetylenes into a C-H bond of active methylene compounds, *Organic Letters*, 2005, 7(22), 4823-4825.

90. Tokunaga, M., Eckert, M., and Wakatsuki, Y., Ruthenium-catalyzed intermolecular hydroamination of terminal alkynes with anilines: A practical synthesis of aromatic ketimines, *Angewandte Chemie-International Edition*, 1999, 38(21), 3222-3225.

91. Lingaiah, N., Babu, N. S., Reddy, K. M., Prasad, P. S. S., and Suryanarayana, I., An efficient reusable silver-exchanged tungstophosphoric acid heterogeneous catalyst for solvent-free intermolecular hydroamination of alkynes, *Chemical Communications*, 2007(3), 278-279.

92. Hartung, C. G., Tillack, A., Trauthwein, H., and Beller, M., A convenient rhodium-catalyzed intermolecular hydroamination procedure for terminal alkynes, *Journal of Organic Chemistry*, 2001, 66(19), 6339-6343.

93. Haskel, A., Straub, T., and Eisen, M. S., Organoactinide-catalyzed intermolecular hydroamination of terminal alkynes, *Organometallics*, 1996, 15(18), 3773-3775.

94. Straub, T., Haskel, A., Neyroud, T. G., Kapon, M., Botoshansky, M., and Eisen, M. S., Intermolecular hydroamination of terminal alkynes catalyzed by

organoactinide complexes. Scope and mechanistic studies, *Organometallics*, 2001, 20(24), 5017-5035.

95. Tillack, A., Castro, I. G., Hartung, C. G., and Beller, M., Anti-Markovnikov hydroamination of terminal alkynes, *Angewandte Chemie-International Edition*, 2002, 41(14), 2541-2543.

96. Tillack, A., Jiao, H. J., Castro, I. G., Hartung, C. G., and Beller, M., A general study of [(η^5-Cp')$_2$Ti(η^2-$Me_3SiC_2SiMe_3$)]-catalyzed hydroamination of terminal alkynes: Regioselective formation of Markovnikov and anti-Markovnikov products and mechanistic explanation (Cp' = C_5H_5, C_5H_4Et, C_5Me_5), *Chemistry-a European Journal*, 2004, 10(10), 2409-2420.

97. Zhang, Z. and Schafer, L. L., Anti-Markovnikov intermolecular hydroamination: A bis(amidate) titanium precatalyst for the preparation of reactive aldimines, *Organic Letters*, 2003, 5(24), 4733-4736.

98. Zhang, Z., Leitch, D. C., Lu, M., Patrick, B. O., and Schafer, L. L., An easy-to-use, regioselective, and robust bis(amidate) titanium hydroamination precatalyst: Mechanistic and synthetic investigations toward the preparation of tetrahydroisoquinolines and benzoquinolizine alkaloids, *Chemistry-a European Journal*, 2007, 13(7), 2012-2022.

99. Tzalis, D., Koradin, C., and Knochel, P., Cesium hydroxide catalyzed addition of alcohols and amine derivatives to alkynes and styrene, *Tetrahedron Letters*, 1999, 40(34), 6193-6195.

100. Park, Y. J., Kwon, B. I., Ahn, J. A., Lee, H., and Jun, C. H., Chelation-assisted hydrative dimerization of 1-alkyne forming α,β-enones by an Rh(I) catalyst, *Journal of the American Chemical Society*, 2004, 126(43), 13892-13893.

101. Fukumoto, Y., Asai, H., Shimizu, M., and Chatani, N., Anti-markovnikov addition of both primary and secondary Amines to terminal Alkynes catalyzed by the $TpRh(C_2H_4)_2/PPh_3$ system, *Journal of the American Chemical Society*, 2007, 129(45), 13792-13793.

102. Hiscox, W. and Jennings, P. W., Catalytic Hydration of Alkynes with Zeise Dimer, *Organometallics*, 1990, 9(7), 1997-1999.

103. Francisco, L. W., Moreno, D. A., and Atwood, J. D., Synthesis, characterization, and reaction chemistry of $PtCl_2[P(m\text{-}C_6H_4SO_3Na)_3]_2$, an alkyne hydration catalyst, *Organometallics*, 2001, 20(20), 4237-4245.

104. Suzuki, T., Tokunaga, M., and Wakatsuki, Y., Ruthenium complex-catalyzed anti-Markovnikov hydration of terminal alkynes, *Organic Letters*, 2001, 3(5), 735-737.

105. Grotjahn, D. B., Incarvito, C. D., and Rheingold, A. L., Combined effects of metal and ligand capable of accepting a proton or hydrogen bond catalyze anti-Markovnikov hydration of terminal alkynes, *Angewandte Chemie-International Edition*, 2001, 40(20), 3884-3887.

106. Grotjahn, D. B. and Lev, D. A., A general bifunctional catalyst for the anti-Markovnikov hydration of terminal alkynes to aldehydes gives enzyme-like rate and selectivity enhancements, *Journal of the American Chemical Society*, 2004, 126(39), 12232-12233.

107. Grotjahn, D. B., Kragulj, E. J., Zeinalipour-Yazdi, C. D., Miranda-Soto, V., Lev, D. A., and Cooksy, A. L., Finding the proton in a key intermediate of anti-Markovnikov alkyne hydration by a bifunctional catalyst, *Journal of the American Chemical Society*, 2008, 130(33), 10860-10861.

108. Guillena, G., Ramón, D. J., and Yus, M., Alcohols as electrophiles in C-C bond-forming reactions: The hydrogen autotransfer process, *Angewandte Chemie-International Edition*, 2007, 46(14), 2358-2364.

109. Hamid, M. H. S. A., Slatford, P. A., and Williams, J. M. J., Borrowing hydrogen in the activation of alcohols, *Advanced Synthesis & Catalysis*, 2007, 349(10), 1555-1575.

110. Adair, G. R. A. and Williams, J. M. J., Oxidant-free oxidation: ruthenium catalysed dehydrogenation of alcohols, *Tetrahedron Letters*, 2005, 46(47), 8233-8235.

111. Martínez, R., Ramón, D. J., and Yus, M., $RuCl_2(DMSO)_4$ catalyzes the beta-alkylation of secondary alcohols with primary alcohols through a hydrogen autotransfer process, *Tetrahedron*, 2006, 62(38), 8982-8987.

112. Viciano, M., Sanaú, M., and Peris, E., Ruthenium Janus-head complexes with a triazolediylidene ligand. structural features and catalytic applications, *Organometallics*, 2007, 26(24), 6050-6054.

113. Fan, L., Einstein, F. W. B., and Sutton, D., Ruthenium cyclopentadienyl aryldiazenido complexes. Synthesis of [Cp ' $Ru(PR_3)_2(N_2C_6H_4OMe)][BF4]_2$ and [Cp ' $RuCl(PPh_3)(N_2C_6H_4OMe)][BF4]$ (Cp ' = Cp, Cp*) and X-ray crystal structure of $[CpRu(PPh_3)_2(N_2C_6H_4OMe)][BF4]_2$, an aryldiazenido complex with a large N-N-C(aryl) angle and near-linear Ru-N-N-C(aryl) skeleton, *Organometallics*, 2000, 19(4), 684-694.

114. Bruce, M. I., Hameister, C., Swincer, A. G., and Wallis, R. C., Some η-5-Cyclopentadienylruthenium(II) Complexes Containing Triphenylphosphine, *Inorganic Syntheses*, 1982, 21, 78-84.

115. Ashby, G. S., Bruce, M. I., Tomkins, I. B., and Wallis, R. C., Cyclopentadienyl-Ruthenium and Cyclopentadienyl-Osmium Chemistry .7. Complexes Containing Nitriles, Tertiary Phosphines or Phosphites Formed by Addition or Displacement-Reactions, *Australian Journal of Chemistry*, 1979, 32(5), 1003-1016.

116. Alcock, N. W., Burns, I. D., Claire, K. S., and Hill, A. F., Ruthenatetraboranes - Synthesis of $[Ru(B_3H_8)(PPh_3)(HB(pz)_3)]$ and Crystal-Structure of $[RuCl(PPh_3)_2(HB(pz)_3)]$ (pz = Pyrazol-1-yl), *Inorganic Chemistry*, 1992, 31(13), 2906-2908.

117. Gemel, C., Trimmel, G., Slugovc, C., Kremel, S., Mereiter, K., Schmid, R., and Kirchner, K., Ruthenium tris(pyrazolyl)borate complexes .1. Synthesis and reactivity of $Ru(HB(pz)_3)(COD)X$ (X=Cl, Br) and $Ru(HB(pz)_3)(L_2)Cl$ (L=nitrogen and phosphorus donor ligands), *Organometallics*, 1996, 15(19), 3998-4004.

118. Chan, W. C., Lau, C. P., Chen, Y. Z., Fang, Y. Q., Ng, S. M., and Jia, G. C., Syntheses and characterization of hydrotris(1-pyrazolyl)borate dihydrogen complexes of ruthenium and their roles in catalytic hydrogenation reactions, *Organometallics*, 1997, 16(1), 34-44.

119. Khurana, J. M. and Kiran, Rapid reduction of chalcones to tetrahydrochalcones using nickel boride, *Journal of Chemical Research-S*, 2006(6), 374-375.

120. Blakemore, P. R. and Burge, M. S., Iterative stereospecific reagent-controlled homologation of pinacol boronates by enantioenriched alpha-chloroalkyllithium reagents, *Journal of the American Chemical Society*, 2007, 129(11), 3068-3069.

121. Shen, Z. L., Yeo, Y. L., and Loh, T. P., Indium-copper and indium-silver mediated Barbier-Grignard-type alkylation reaction of aldehydes using

unactivated alkyl halides in water, *Journal of Organic Chemistry*, 2008, 73(10), 3922-3924.

122. Tooley, P. A., Ovalles, C., Kao, S. C., Darensbourg, D. J., and Darensbourg, M. Y., Anionic Group-6 Hydrides and Carboxylates as Homogeneous Catalysts for Reduction of Aldehydes and Ketones, *Journal of the American Chemical Society*, 1986, 108(18), 5465-5470.

123. Grey, R. A., Pez, G. P., and Wallo, A., Anionic Metal Hydride Catalysts .2. Application to the Hydrogenation of Ketones, Aldehydes, Carboxylic-Acid Esters, and Nitriles, *Journal of the American Chemical Society*, 1981, 103(25), 7536-7542.

124. Gaus, P. L., Kao, S. C., Youngdahl, K., and Darensbourg, M. Y., Anionic Group-6 Transition-Metal Carbonyl Hydrides as Reducing Agents - Ketones, Aldehydes, and Epoxides, *Journal of the American Chemical Society*, 1985, 107(8), 2428-2434.

125. Kinney, R. J., Jones, W. D., and Bergman, R. G., Synthesis and Reactions of (η^5-Cyclopentadienyl)Tricarbonylhydridovanadate - a Comparative Mechanistic Study of Its Organic Halide Reduction Reactions with Those of Tri-Normal-Butyltin Hydride, *Journal of the American Chemical Society*, 1978, 100(25), 7902-7915.

126. Kao, S. C., Spillett, C. T., Ash, C., Lusk, R., Park, Y. K., and Darensbourg, M. Y., Relative Reactivity and Mechanistic Studies of the Hydride-Transfer Reagents $HM(CO)_4L^-$ (M = Cr, W ; L = CO, PR_3), *Organometallics*, 1985, 4(1), 83-91.

127. Esteruelas, M. A., Hernández, Y. A., Lopez, A. M., Oliván, M., and Rubio, L., Reactions of a dihydride-osmium(IV) complex with aldehydes: Influence of the substituent at the carbonyl group, *Organometallics*, 2008, 27(4), 799-802.

128. Bullock, R. M., Catalytic ionic Hydrogenations, *Chemistry-a European Journal*, 2004, 10(10), 2366-2374.

129. Trimmel, G., Slugovc, C., Wiede, P., Mereiter, K., Sapunov, V. N., Schmid, R., and Kirchner, K., Labile complexes of the $[RuTp(pn)]^+$ (Tp = tripyrazolylborate, pn = $Ph_2PCH_2CH_2NMe_2$) fragment including the dinitrogen ligand, *Inorganic Chemistry*, 1997, 36(6), 1076-1083.

130. Slugovc, C., Sapunov, V. N., Wiede, P., Mereiter, K., Schmid, R., and Kirchner, K., Ruthenium(II) tris(pyrazolyl)borate complexes. Reversible vinylidene complex formation, *Journal of the Chemical Society-Dalton Transactions*, 1997(22), 4209-4216.

131. Itagaki, H., Shinoda, S., and Saito, Y., Liquid-Phase Dehydrogenation of Methanol with Homogeneous Ruthenium Complex Catalysts, *Bulletin of the Chemical Society of Japan*, 1988, 61(7), 2291-2294.

132. Jung, C. W. and Garrou, P. E., Dehydrogenation of Alcohols and Hydrogenation of Aldehydes Using Homogeneous Ruthenium Catalysts, *Organometallics*, 1982, 1(4), 658-666.

133. Shinoda, S., Itagaki, H., and Saito, Y., Dehydrogenation of Methanol in the Liquid-Phase with a Homogeneous Ruthenium Complex Catalyst, *Journal of the Chemical Society-Chemical Communications*, 1985(13), 860-861.

134. Murahashi, S. I., Naota, T., Ito, K., Maeda, Y., and Taki, H., Ruthenium-Catalyzed Oxidative Transformation of Alcohols and Aldehydes to Esters and Lactones, *Journal of Organic Chemistry*, 1987, 52(19), 4319-4327.

135. Grigg, R., Hasakunpaisarn, A., Kilner, C., Kongkathip, B., Kongkathip, N., Pettman, A., and Sridharan, V., Catalytic processes for the functionalisation and

desymmetrisation of malononitrile derivatives, *Tetrahedron*, 2005, 61(39), 9356-9367.

136. Kulp, S. S. and Mcgee, M. J., Oxidative Decyanation of Benzyl and Benzhydryl Cyanides - a Simplified Procedure, *Journal of Organic Chemistry*, 1983, 48(22), 4097-4098.

137. Im, D. S., Cheong, C. S., Lee, S. H., Youn, B. H., and Kim, S. C., Chemoenzymatic synthesis of optically active 2-phenyl-2-(1H-1,2,4-triazol-1-ylmethyl)hexanenitrile, *Tetrahedron*, 2000, 56(10), 1309-1314.

138. Takaya, H., Yoshida, K., Isozaki, K., Terai, H., and Murahashi, S. I., Transition-metal-based Lewis acid and base ambiphilic catalysts of iridium hydride complexes: Multicomponent synthesis of glutarimides, *Angewandte Chemie-International Edition*, 2003, 42(28), 3302-3304.

139. Dei, S., Romanelli, M. N., Scapecchi, S., Teodori, E., Chiarini, A., and Gualtieri, F., Verapamil Analogs with Restricted Molecular Flexibility, *Journal of Medicinal Chemistry*, 1991, 34(7), 2219-2225.

140. Hartmann, R. W. and Batzl, C., Aromatase Inhibitors - Synthesis and Evaluation of Mammary-Tumor Inhibiting Activity of 3-Alkylated 3-(4-Aminophenyl) Piperidine-2,6-Diones, *Journal of Medicinal Chemistry*, 1986, 29(8), 1362-1369.

141. Wu, Z. L. and Li, Z. Y., Enantioselective hydrolysis of various racemic alpha-substituted arylacetonitriles using Rhodococcus sp CGMCC 0497, *Tetrahedron-Asymmetry*, 2001, 12(23), 3305-3312.

142. Grigg, R., Mitchell, T. R. B., Sutthivaiyakit, S., and Tongpenyai, N., Oxidation of Alcohols by Transition-Metal Complexes .5. Selective Catalytic Monoalkylation of Arylacetonitriles by Alcohols, *Tetrahedron Letters*, 1981, 22(41), 4107-4110.

143. Motokura, K., Nishimura, D., Mori, K., Mizugaki, T., Ebitani, K., and Kaneda, K., A ruthenium-grafted hydrotalcite as a multifunctional catalyst for direct alpha-alkylation of nitriles with primary alcohols, *Journal of the American Chemical Society*, 2004, 126(18), 5662-5663.

144. Kumagai, N., Matsunaga, S., and Shibasaki, M., Cooperative catalysis of a cationic ruthenium complex, amine base, and Na salt: Catalytic activation of acetonitrile as a nucleophile, *Journal of the American Chemical Society*, 2004, 126(42), 13632-13633.

145. Kumagai, N., Matsunaga, S., and Shibasaki, M., Catalytic chemoselective addition of acetonitrile to enolizable aldehydes with cationic Ru complex/DBU combination, *Chemical Communications*, 2005(28), 3600-3602.

146. Goto, A., Endo, K., Ukai, Y., Irle, S., and Saito, S., Rh-I-catalyzed aldol-type reaction of organonitriles under mild conditions, *Chemical Communications*, 2008(19), 2212-2214.

147. Ellis, G. P. and Romneyalexander, T. M., Cyanation of Aromatic Halides, *Chemical Reviews*, 1987, 87(4), 779-794.

148. Gregory, R. J. H., Cyanohydrins in nature and the laboratory: Biology, preparations, and synthetic applications, *Chemical Reviews*, 1999, 99(12), 3649-3682.

149. Cheung, H. W., Lee, T. Y., Lui, H. Y., Yeung, C. H., and Lau, C. P., Ruthenium-Catalyzed β-Alkylation of Secondary Alcohols with Primary Alcohols, *Advanced Synthesis & Catalysis*, 2008, 350(18), 2975-2983.

150. Fan, L. and Ozerov, O. V., Efficient nickel catalyst for coupling of acetonitrile with aldehydes, *Chemical Communications*, 2005(35), 4450-4452.

151. Velde, C. M. L. V., Blockhuys, F., Van Alsenoy, C., Lenstra, A. T. H., and Geise, H. J., Structural effects influencing *cis-trans* isomerisation in methoxy and cyano substituted stilbene derivatives, *Journal of the Chemical Society-Perkin Transactions 2*, 2002(7), 1345-1351.

152. Loupy, A., Pellet, M., Petit, A., and Vo-Thanh, G., Solvent-free condensation of phenylacetonitrile and nonanenitrile with 4-methoxybenzaldehyde: optimization and mechanistic studies, *Organic & Biomolecular Chemistry*, 2005, 3(8), 1534-1540.

153. Hwang, J., Yang, K., Koo, I. S., Sung, D. D., and Lee, I., Kinetic and mechanism of the addition of benzylamines to α-phenyl-β-thiophenylacrylonitriles in acetonitrile, *Bulletin of the Korean Chemical Society*, 2006, 27(5), 733-738.

154. Murahashi, S. I., Naota, T., Taki, H., Mizuno, M., Takaya, H., Komiya, S., Mizuho, Y., Oyasato, N., Hiraoka, M., Hirano, M., and Fukuoka, A., Ruthenium-catalyzed aldol and Michael reactions of nitriles. Carbon-carbon bond formation by alpha-C-H activation of nitriles, *Journal of the American Chemical Society*, 1995, 117(50), 12436-12451.

155. Becke, A. D., Density-Functional Thermochemistry .3. The Role of Exact Exchange, *Journal of Chemical Physics*, 1993, 98(7), 5648-5652.

156. Lee, C. T., Yang, W. T., and Parr, R. G., Development of the Colle-Salvetti Correlation-Energy Formula into a Functional of the Electron-Density, *Physical Review B*, 1988, 37(2), 785-789.

157. Stephens, P. J., Devlin, F. J., Chabalowski, C. F., and Frisch, M. J., Ab-Initio Calculation of Vibrational Absorption and Circular-Dichroism Spectra Using Density-Functional Force-Fields, *Journal of Physical Chemistry*, 1994, 98(45), 11623-11627.

158. Fukui, K., A Formulation of Reaction Coordinate, *Journal of Physical Chemistry*, 1970, 74(23), 4161.

159. Fukui, K., The Path of Chemical-Reactions - the Irc Approach, *Accounts of Chemical Research*, 1981, 14(12), 363-368.

160. Wadt, W. R. and Hay, P. J., Abinitio Effective Core Potentials for Molecular Calculations - Potentials for Main Group Elements Na to Bi, *Journal of Chemical Physics*, 1985, 82(1), 284-298.

161. Hay, P. J. and Wadt, W. R., Abinitio Effective Core Potentials for Molecular Calculations - Potentials for K to Au Including the Outermost Core Orbitals, *Journal of Chemical Physics*, 1985, 82(1), 299-310.

162. Harihara.Pc and Pople, J. A., Influence of Polarization Functions on Molecular-Orbital Hydrogenation Energies, *Theoretica Chimica Acta*, 1973, 28(3), 213-222.

163. Höllwarth, A., Böhme, M., Dapprich, S., Ehlers, A. W., Gobbi, A., Jonas, V., Kohler, K. F., Stegmann, R., Veldkamp, A., and Frenking, G., A Set of D-Polarization Functions for Pseudo-Potential Basis-Sets of the Main-Group Elements Al-Bi and F-Type Polarization Functions for Zn, Cd, Hg, *Chemical Physics Letters*, 1993, 208(3-4), 237-240.

164. Frisch, M. J. T., G. W.; Schlegel, H. B.; Scuseria, G. E.; Robb, M. A.; Cheeseman, J. R.; Zakrzewski, V. G.; Montgomery, J. A., Jr.; Stratmann, R. E.; Burant, J. C.; Dapprich, S.; Millam, J. M.; Daniels, A. D.; Kudin, K. N.; Strain, M. C.; Farkas, O.; Tomasi, J.; Barone, V.; Cossi, M.; Cammi, R.; Mennucci, B.; Pomelli, C.; Adamo, C.; Clifford, S.; Ochterski, J.; Petersson, G. A.; Ayala, P. Y.; Cui, Q.; Morokuma, K.; Malick, D. K.; Rabuck, A. D.; Raghavachari, K.; Foresman, J. B.; Cioslowski, J.; Ortiz, J. V.; Stefanov, B. B.; Liu, G.; Liashenko, A.; Piskorz, P.; Komaromi, I.; Gomperts, R.; Martin, R. L.; Fox, D. J.; Keith, T.; Al-Laham, M.

A.; Peng, C. Y.; Nanayakkara, A.; Gonzalez, C.; Challacombe, M.; Gill, P. m. W.; Johnson, B.; Chen, W.; Wong, M. W.; Andres, J. L.; Gonzalez, C.; Head-Gordon, M.; Replogle, E. S.; Pople, J. A. Gaussian 03, Revision B.05; Gaussian, Inc.: Pittsburgh, PA, 2003.

165. Brun, P., Vierling, P., Riess, J. G., and Leborgne, G., Study of the Amination Reaction of the Coordinated Cyclopentadienyl Ring in (η^5-Cp)Fe(II) Derivatives - Crystal and Molecular-Structure of (η^5-$C_5H_4NEt_2$)Fe(CO)[$PhP(OEt)_2$]Br, *Organometallics*, 1987, 6(5), 1032-1040.

166. Allman, R. in The Chemistry of the Hydrazo, Azo, and Azoxy Groups; Patai, S. Ed.; Wiley: New York 1975, 23.

167. Hammond, H. L. Acta Crystallogr., Sect. B.: Struct. Crystallogr. Cryst. Chem. , 1974(B30), 1731.

168. See Appendix for ORTEP view (30% probability), crystal data and structure refinement and selected bond distances (Å) and angles (˚)of **M1**.

169. Stahl, K. P., Boche, G., and Massa, W., 1,1'-Bis(N,N-Dimethylamino)Ferrocene, 1,1'-Bis(N,N-Dimethylamino)Cobaltocenium Hexafluorophosphate and 1,1'-Bis(N,N-Dimethylamino)Titanocene Dichloride - Crystal-Structure of 1,1'-Bis(N,N-Dimethylamino)Titanocene Dichloride, *Journal of Organometallic Chemistry*, 1984, 277(1), 113-125.

170. Castarlenas, R., Esteruelas, M. A., and Oñate, E., Preparation, X-ray structure, and reactivity of an osmium-hydroxo complex stabilized by an N-heterocyclic carbene ligand: A base-free catalytic precursor for hydrogen transfer from 2-propanol to aldehydes, *Organometallics*, 2008, 27(13), 3240-3247.

171. Zhao, J. and Hartwig, J. F., Acceptorless, neat, ruthenium-catalyzed dehydrogenative cyclization of diols to lactones, *Organometallics*, 2005, 24(10), 2441-2446.

172. Dinger, M. B. and Mol, J. C., Degradation of the first-generation Grubbs metathesis catalyst with primary alcohols, water, and oxygen. Formation and catalytic activity of ruthenium(II) monocarbonyl species, *Organometallics*, 2003, 22(5), 1089-1095.

173. Portnoy, M., Frolow, F., and Milstein, D., Methanol Reduces an Organopalladium(II) Complex to a Palladium(I) Hydride - Crystallographic Characterization of a Hydrido-Bridged Palladium Complex, *Organometallics*, 1991, 10(12), 3960-3962.

174. Esteruelas, M. A. and Werner, H., 5-Coordinate and 6-Coordinate Hydrido(Carbonyl)-Ruthenium(II) and Osmium(II) Complexes Containing Triisopropylphosphine as Ligand, *Journal of Organometallic Chemistry*, 1986, 303(2), 221-231.

175. Heinekey, D. M. and Oldham, W. J., Coordination Chemistry of Dihydrogen, *Chemical Reviews*, 1993, 93(3), 913-926 and references therein.

176. Shubina, E. S., Belkova, N. V., Krylov, A. N., Vorontsov, E. V., Epstein, L. M., Gusev, D. G., Niedermann, M., and Berke, H., Spectroscopic evidence for intermolecular M-H ··· H-OR hydrogen bonding: Interaction of $WH(CO)_2(NO)L_2$ hydrides with acidic alcohols, *Journal of the American Chemical Society*, 1996, 118(5), 1105-1112.

177. Ayllón, J. A., Gervaux, C., SaboEtienne, S., and Chaudret, B., First NMR observation of the intermolecular dynamic proton transfer equilibrium between a

hydride and coordinated dihydrogen: $(dppm)_2HRuH^{\cdots}H$-OR=$[(dppm)_2HRu(H_2)]^+(OR)^-$, *Organometallics*, 1997, 16(10), 2000-2002.

178. Gründemann, S., Ulrich, S., Limbach, H. H., Golubev, N. S., Denisov, G. S., Epstein, L. M., Sabo-Etienne, S., and Chaudret, B., Solvent-assisted reversible proton transfer within an intermolecular dihydrogen bond and characterization of an unstable dihydrogen complex, *Inorganic Chemistry*, 1999, 38(11), 2550-2551.

179. Chen, Y. Z., Chan, W. C., Lau, C. P., Chu, H. S., Lee, H. L., and Jia, G. C., Synthesis of alkyl- and aryl[hydrotris(pyrazolyl)borato]carbonylruthenium complexes by decarbonylation of alcohols. Synthesis of $TpRuH(H_2)(PPh_3)$ [Tp equals hydrotris(pyrazolyl)borate], an observable intermediate in the decarbonylation reaction, *Organometallics*, 1997, 16(6), 1241-1246.

180. Ng, S. M., Yin, C. Q., Yeung, C. H., Chan, T. C., and Lau, C. P., Ruthenium-catalyzed hydrogenation of carbon dioxide to formic acid in alcohols, *European Journal of Inorganic Chemistry*, 2004(9), 1788-1793.

181. Kubas, G. J., Fundamentals of H_2 binding and reactivity on transition metals underlying hydrogenase function and H_2 production and storage, *Chemical Reviews*, 2007, 107(10), 4152-4205.

182. Rerek, M. E., Ji, L. N., and Basolo, F., The Indenyl Ligand Effect on the Rate of Substitution-Reactions of $Rh(\eta\text{-}C_9H_7)(CO)_2$ and $Mn(\eta\text{-}C_9H_7)(CO)_3$, *Journal of the Chemical Society-Chemical Communications*, 1983(21), 1208-1209.

183. Kakkar, A. K., Taylor, N. J., Marder, T. B., Shen, J. K., Hallinan, N., and Basolo, F., Kinetics and Mechanism of Co Ligand Substitution in the Ring-Substituted Indenyl Rhodium Complexes $[(\eta^5\text{-}C_9R_nH_{7-n})Rh(CO)_2]$, *Inorganica Chimica Acta*, 1992, 200, 219-231.

184. Calhorda, M. J., Romaõ, C. C., and Veiros, L. F., The nature of the indenyl effect, *Chemistry-a European Journal*, 2002, 8(4), 868-875 and references therein.

185. Chang, S., Scharrer, E., and Brookhart, M., Catalytic silane alcoholysis based on the $C_5H_5(CO)(PPh_3)Fe^+$ moiety. NMR spectroscopic identification of key intermediates, *Journal of Molecular Catalysis a-Chemical*, 1998, 130(1-2), 107-119.

186. Bűhl, M. and Mauschick, F. T., Density functional study of catalytic silane alcoholysis at a $[Fe(Cp)(CO)(PR_3)^+$ center, *Organometallics*, 2003, 22(7), 1422-1431.

187. Trost, B. M. and Fleming, I., *Comprehensive organic synthesis: selectivity, strategy, and efficiency in modern organic chemistry*. 1st ed. 1991, Oxford, England ; New York: Pergamon Press.

188. Adams, J. P., Imines, enamines and oximes, *Journal of the Chemical Society-Perkin Transactions 1*, 2000(2), 125-139.

189. Odom, A. L., New C-N and C-C bond forming reactions catalyzed by titanium complexes, *Dalton Transactions*, 2005(2), 225-233.

190. Hultzsch, K. C., Transition metal-catalyzed asymmetric hydroamination of alkenes (AHA), *Advanced Synthesis & Catalysis*, 2005, 347(2-3), 367-391.

191. Roesky, P. W. and Müller, T. E., Enantioselective catalytic hydroamination of alkenes, *Angewandte Chemie-International Edition*, 2003, 42(24), 2708-2710.

192. Clemens, D. F. and Perkinso.We, Further Studies in Rearrangement of Bis(Diphenylphosphino)Amines Upon Chloramination, *Inorganic Chemistry*, 1974, 13(2), 333-339.

193. Wu, W. and Li, C. J., A highly regio- and stereoselective transition metal-catalyzed hydrosilylation of terminal alkynes under ambient conditions of air, water, and room temperature, *Chemical Communications*, 2003(14), 1668-1669.

194. Conner, D., Jayaprakash, K. N., Wells, M. B., Manzer, S., Gunnoe, T. B., and Boyle, P. D., Octahedral Ru(II) amido complexes TpRu(L)(L ')(NHR) (Tp = hydridotris(pyrazolyl)borate; L = L ' = $P(OMe)_3$ or PMe_3 or L = CO and L ' = PPh_3; R = H, Ph, or ^tBu): Synthesis, characterization, and reactions with weakly acidic C-H bonds, *Inorganic Chemistry*, 2003, 42(15), 4759-4772.

195. Chu, H. S., Xu, Z. T., Ng, S. M., Lau, C. P., and Lin, Z. Y., Protonation of $[tpmRu(PPh_3)_2H]BF_4$ [tpm = tris(pyrazolyl)methane] - Formation of unusual hydrogen-bonded species, *European Journal of Inorganic Chemistry*, 2000(5), 993-1000.

196. Badayan, S. O., Chobanyan, Z. A., Tirakyan, M. R., and Danielyan, A. O., Reaction properties of butyl- and phenylacetylenes with CH-acids, *Russian Journal of Organic Chemistry*, 1997, 33(1), 17-20.

197. Pei, L. and Qian, W. X., CuI/L-proline-catalyzed coupling reactions of vinyl bromides with activated methylene compounds, *Synlett*, 2006(11), 1719-1723.

198. Mickler, W., Uhlemann, E., and Herzchuh, R., By-Products of Classical Beta-Diketone Syntheses, *Journal Fur Praktische Chemie-Chemiker-Zeitung*, 1992, 334(5), 435-436.

199. Reddy, C., Reddy, V., Urgaonkar, S., and Verkade, J. G., A highly effective catalyst system for the Pd-catalyzed amination of vinyl bromides and chlorides, *Organic Letters*, 2005, 7(20), 4427-4430.

200. Bélanger, G., Doré, M., Ménard, F., and Darsigny, V., Highly chemoselective formation of aldehyde enamines under very mild reaction conditions, *Journal of Organic Chemistry*, 2006, 71(19), 7481-7484.

201. Costa, M., Chiusoli, G. P., Gaetti, R., Gabriele, B., and Salerno, G., Amination of aryl- and vinylacetylenic compounds catalyzed by rhodium(I) complexes, *Russian Chemical Bulletin*, 1998, 47(5), 936-940.

202. Beller, M., Eichberger, M., and Trauthwein, H., Anti-Markovnikov functionalization of olefins: Rhodium-catalyzed oxidative aminations of styrenes, *Angewandte Chemie-International Edition in English*, 1997, 36(20), 2225-2227.

203. Meilahn, M. K., Cox, B., and Munk, M. E., Polar [π4 + π2] Cycloaddition Reaction - Enamines as Dipolarophiles in 1,3-Dipolar Additions, *Journal of Organic Chemistry*, 1975, 40(7), 819-824.

204. Tillack, A., Trauthwein, H., Hartung, C. G., Eichberger, M., Pitter, S., Jansen, A., and Beller, M., Anti-Markovnikov Reactions, Part VIII - Rhodium-catalyzed amination of aromatic olefins, *Monatshefte Fur Chemie*, 2000, 131(12), 1327-1334.

205. Balakrishna, M. S., Reddy, V. S., Krishnamurthy, S. S., Nixon, J. F., and Stlaurent, J. C. T. R. B., Coordination Chemistry of Diphosphinoamine and Cyclodiphosphazane Ligands, *Coordination Chemistry Reviews*, 1994, 129(1-2), 1-90 and references therein.

206. Blosser, P. W., Gallucci, J. C., and Wojcicki, A., Synthesis, Characterization, and Reactivity of Ruthenium Carbonyl-Complexes Containing a Chelating Triphosphine Ligand and 2 Weakly Coordinated Anions, *Inorganic Chemistry*, 1992, 31(12), 2376-2384.

207. Kraakman, M. J. A., Deklerkengels, B., Delange, P. P. M., Vrieze, K., Smeets, W. J. J., and Spek, A. L., Carbonylation of the Ru-Me Bond of Ru(Me)(I)$(CO)_2$(^{i}Pr-N=CHCH=N-^{i}Pr) Catalyzed by $Ru(CO)_4(Pr_3)$, $ZnCl_2$, and H^+, *Organometallics*, 1992, 11(11), 3774-3784.

208. Sutter, J. P., James, S. L., Steenwinkel, P., Karlen, T., Grove, D. M., Veldman, N., Smeets, W. J. J., Spek, A. L., and vanKoten, G., Versatile *N*,*C*,*N* coordination behavior of a monoanionic aryldiamine ligand in ruthenium(II) complexes: Syntheses and crystal structures of [Ru-II(C6H3(CH(2)NMe(2))(2)-2,6)X(L)] (L equals norbornadiene, X=Cl, SO_3CF_3; L=PPh_3, X=I) and [Ru^{II}{$C_6H_3(CH_2NMe_2)_2$-2,6}(2,2':6:2"-terpyridine)]Cl, *Organometallics*, 1996, 15(3), 941-948.

209. Gemel, C., Wiede, P., Mereiter, K., Sapunov, V. N., Schmid, R., and Kirchner, K., Ruthenium tris(pyrazolyl)borate complexes. Formation and characterization of acetone, dimethylformamide and vinylidene complexes containing N,N-donor co-ligands, *Journal of the Chemical Society-Dalton Transactions*, 1996(21), 4071-4076.

210. Tenorio, M. A. J., Tenorio, M. J., Puerta, M. C., and Valerga, P., Alkyne coupling reactions mediated by tris(pyrazolyl)borate ruthenium vinylidene complexes: X-ray crystal structures of [TpRu=C=CHPh$(PEt_3)_2$][BPh_4] and [TpRu=C=C(COOMe)CH=CHCOOMe$(PEt_3)_2$][BPh_4], *Organometallics*, 2000, 19(7), 1333-1342.

211. Slugovc, C., Mereiter, K., Zobetz, E., Schmid, R., and Kirchner, K., Ruthenium-catalyzed dimerization of terminal alkynes initiated by a neutral vinylidene complex, *Organometallics*, 1996, 15(25), 5275-5277.

212. Menendez, C., Morales, D., Perez, J., Riera, V., and Miguel, D., New types of (Arene)ruthenium alkynyl complexes, *Organometallics*, 2001, 20(13), 2775-2781.

213. Pedersen, A., Tilset, M., Folting, K., and Caulton, K. G., Oxidatively Induced Reductive Elimination from $Ru(C_2Ph)_2(CO)(P^tBu_2Me)_2$ and $Ru(CHCHPh)(C_2Ph)(CO)(P^tBu_2Me)_2$, *Organometallics*, 1995, 14(2), 875-888.

214. Bianchini, C., Casares, J. A., Peruzzini, M., Romerosa, A., and Zanobini, F., The mechanism of the Ru-assisted C-C bond cleavage of terminal alkynes by water, *Journal of the American Chemical Society*, 1996, 118(19), 4585-4594.

215. Bassetti, M., Cadierno, V., Gimeno, J., and Pasquini, C., Rate studies on the release of terminal alkynes from indenylruthenium(II) vinylidene complexes. Implications on the mechanism of η^1-vinylidene into η^2-alkyne isomerization, *Organometallics*, 2008, 27(19), 5009-5016.

216. Frenna, V., Vivona, N., Consiglio, G., and Spinelli, D., Amine Basicities in Benzene and in Water, *Journal of the Chemical Society-Perkin Transactions 2*, 1985(12), 1865-1868.